FAP24

Government of the People's Republic of Bangladesh

Water Resources Planning Organization

European Commission

Delft Hydraulics

Danish Hydraulic Institute

Hydroland

Approtech

Osiris



# RIVER SURVEY PROJECT

## Special Report No.10

## Morphology of Gorai Off-take

October 1996

# Morphology of Gorai Off-take

**Special Report 10**

**River Survey Project (FAP24)**

**October 1996**

## List of contents

## Abbreviations

| | |
|---|---|
| ADCP | Acoustic Doppler Current Profiler |
| BRTS | River Training Studies of the Brahmaputra River (FAP1) |
| DANIDA | Danish International Development Assistance |
| EMF | Electro Magnetic Flowmeter |
| FAP | Flood Action Plan |
| FAP1 | River Training Studies of the Brahmaputra River |
| FAP24 | River Survey Project |
| FAP25 | Flood Modelling and Management Project |
| FPCO | Flood Plan Coordination Organisation |
| GM | General Model (of the main rivers in Bangladesh) |
| GoB | Government of Bangladesh |
| MIKE11 | DHI's one-dimensional modelling system |
| MIKE21 | DHI's two-dimensional modelling system |
| RSP | River Survey Project (FAP24) |
| SWMC | Surface Water Modelling Centre |
| SWSMP | Surface Water Simulation Modelling Programme |

# 1. Introduction

The distribution of discharge and sediment transport at river offtakes is a key factor for the long term morphological development of the distributaries of the main rivers.

The discharge distribution at an offtake is to a large extent determined by the hydraulic capacity along the entire offtake river branch and the relative discharge can therefore be stage dependant. The sediment transport distribution, in addition, may be influenced by the local planform and bathymetry at the offtake, which on the other hand are dependant on the planform and sediment transport conditions of the main river.

The presence of systems of moving bars (chars) further complicates conditions at offtake channels. A bar in front of the offtake may partly block the inflow to the distributary. This is the case at the Gorai offtake where inflow to the Gorai over the latest years has been blocked at low stages in the Ganges.

Main distributaries from the Jamuna, Ganges and Padma rivers are:

- Old Brahmaputra (Jamuna)
- Dhaleswari (Jamuna)
- Arial Khan (Padma)
- Gorai (Ganges)

Of these, the offtake of the Gorai has been selected for a detailed study. This distributary was selected because of the importance of the Gorai for the fresh water inflow to the Southwest region, but also because the Gorai is a well defined single channel without any tidal influence and therefore, in these respects, is less complex. The study area is shown in Figure 1.1.

The total isolation of the Gorai at the offtake from the Ganges every dry season during the latest years is a matter of great concern in Bangladesh. Several factors have been mentioned for being entirely or partly responsible for this development. These factors may be categorised according to their geographical origin:

- the overall morphological development of the Ganges
- the local morphological developments of the Ganges, such as changes of the curvature upstream of the offtake and bar formation patterns
- local morphological conditions of the Gorai at or near the offtake
- the developments downstream in the Gorai such as increased sinuosity and construction of groynes and other structures affecting the flow

In analyses of some of the phenomena that are observed it may be difficult clearly to distinguish between cause and effect. One external factor, the operations of the Farakka Barrage in India, is, however, often mentioned as a cause of the morphological changes which have now lead to the dry season closure of the Gorai mouth. The reasoning behind this is:

The faster decline of the Ganges flow and water levels at the end of the monsoon due to the operation of the Farakka Barrage to withhold water for the dry season does not provide sufficiently long time for the erosion of a dry season offtake channel at the Gorai mouth.

Extensive monitoring, data analyses and modelling may eventually improve the understanding of which phenomena are important. Such understanding is required in order to decide on actions to be taken to reopen the Gorai during dry seasons, if possible.

The present study has three main elements:

- Analysis of historical data in order to understand how the hydraulic conditions at Gorai offtake have changed over the last 30 years (Chapter 4).
- Collection and analysis of detailed data in special surveys of the RSP. The data are used to set up and calibrate a two-dimensional morphological model of the area (Chapter 5).
- Two-dimensional morphological modelling to improve the understanding of which processes are important for the development of the dry season flow to the Gorai (Chapter 6).

## 2. Objectives

The overall objective is to improve the understanding of the sediment transport distribution and the processes of erosion/deposition at an offtake channel, thereby gaining insight in the influence of various factors:

- the influence of hydraulic conditions downstream in the Gorai
- the influence of a bar in front of the offtake
- the influence of the hydraulic conditions of the Ganges
- the influence of various flow and sediment transport characteristics

The aims of the analyses, as initially set out in the study programme (FAP24, 1993) were to provide answers to questions like:

- how does the bathymetry of the offtake area develop from early monsoon when the offtake becomes active till late monsoon when it becomes inactive again?

- how does the bathymetry of the Ganges develop over the same period and is it possible to identify an interaction between the bathymetrical development in the Ganges and the development of flow conditions at the offtake?

- what is maintaining the two scour holes in the Ganges near Gorai offtake and which effect do they have on the discharge down the Gorai?

- how is the distribution of sediment transport at the offtake area?

- is it possible to estimate the effect of the incident angle of the Ganges flow on the discharge down the Gorai offtake?

- how is the relation between the geometry of the offtake channel(s) and the flow through it - is there a simple relation or are there other parameters involved?

- is it possible to understand/describe the erosion/deposition processes in the offtake channel using information on sediment and flow in the offtake area and upstream in the Ganges?

- to what extent is the discharge into the Gorai limited by local conditions at the offtake channel?

- how important are effects of physical phenomena that can be identified from the analysis of field data but are not yet embedded in a 2D morphological model like MIKE21-Curvilinear?

Most of these questions have been addressed in the following.

# 3. Approach and Methodologies

The objective is pursued through a detailed study of a selected location (the Gorai offtake) from which extensive data have been obtained from RSP surveys during the latest years.

First an analysis of the extensive historical data collected by BWDB is carried out in order to throw some light on how conditions have changed over the last 30 years and to find out if there are correlations between these changes and any major changes in planform or flow conditions.
Then the field data collected by the RSP are analysed and applied as the solid basis for establishing a two-dimensional model of the Gorai offtake area. The two-dimensional model is in itself a convenient analysis tool which combines and integrates the various kinds of information collected in the surveys, applying our present knowledge about isolated phenomena and the way they interact. RSP data provide detailed pictures of the actual bathymetrical changes and conditions of flow and sediment transport at selected locations for the recent years. The main tool for the analysis of data is the MIKE21-Curvilinear modelling system developed by Danish Hydraulic Institute.

**Field data analysis**

Detailed and accurate bathymetric surveys are applied to assess directly the morphological changes that have taken place between surveys, ie describe actual observed erosion/deposition patterns. The numerous ADCP/EMF measurements are applied to quantify the flow distribution pattern in the area at the times of measurements. The backscatter intensity from ADCP measurements has not been applied but they may in the future be used to give a qualitative assessment of patterns of concentrations of suspended sediment. The measurements of suspended sediment by sample collection may then be applied to quantify these.

Sediment transport measurements by the RSP downstream of Hardinge Bridge and at Kushtia have been applied to assess the sediment inflow and outflow to/from the study area at different stages.

**Analysis of satellite imageries**

In combination with water level data at the relevant times satellite imageries can be used for a qualitative assessment of the history of the morphological development leading up to the present situation. Satellite imageries are available back to 1973. The development of the offtake up to 1992 based on these has already been carried out by FAP4 (1993). Main changes since then, especially in terms of bank erosion, has been analysed as part of the present study.

**2-D Mathematical Modelling**

It is not practical to measure "everything" continuously and simultaneously. Field data may represent very closely the physical reality of the ongoing processes in the river. But, whatever the detailness and frequency of surveys, the representation will always be discrete in space and time. Especially during the monsoon period when the rate of change of bed levels is high, the bathymetry would in general not be expected to be in equilibrium with local flow conditions. In this case measurements of, say, sediment concentrations at a certain location would depend of course on local flow conditions, but also on conditions upstream and on the flow history. Field surveys with the purpose of understanding the processes would then include very large amounts of information. To collect the data and to

analyse it would be a very costly and time-consuming task. As mathematical models have their limitations, they cannot stand alone. Results should be assessed critically to assure that misleading conclusions are not drawn from a poorly designed and calibrated model. This was kept in mind during the study.

Mathematical modelling has been introduced as a tool to interpret the information provided by the field data in an integrated way. The mathematical model enables interpolation and extrapolation in space and time based on the observations from the field and on the understanding of the physical processes and their interaction to the extent that this has been incorporated in the model. The mathematical model further makes it possible to take into account conditions of non-equilibrium.

The DHI MIKE21-Curvilinear has been applied to model conditions of flow, sediment transport and morphological developments.

River bed bathymetry, boundary conditions, bed roughness and sediment grain size for model simulations has been established on the basis of field data analyses. The existence of extensive field data has made it possible to make a detailed calibration of the model, thereby improving the quality of the present model results. The model has been calibrated and validated using part of the measurements from within the area, only the extent it was necessary in order to meet the objectives.

The study area is morphologically very active and not expected at any time to be in equilibrium with the actual hydrodynamic conditions. This is likely to be more pronounced during the monsoon period than in the dry season. Continuous adjustment of the bed levels is taking place. The implication for the mathematical model is that a 'base run' would not at any time be in morphological equilibrium. Results of applications have been analysed by looking at the differences compared to the 'base run' results. The mathematical model executions start with dry season simulation and subsequently cover one monsoon period. The phenomena which have been studied in the 2D- model are:

- the development of the offtake channel from when it becomes active in the beginning of the monsoon until it again 'closes' at the end of the monsoon
- the development of the bar in front of the offtake during the monsoon period
- the effect of changes of the hydraulic conditions in the Ganges, downstream in Gorai and locally at Gorai mouth on the discharge, sediment transport and morphological changes in the offtake area.

The modelling tool has been applied to investigate the distribution of sediment transport and trends of morphological changes in the offtake area including the effects of changes in the discharge of the Ganges.

33

# 4. Development of Hydraulic Conditions and bed levels over the last 30 years

## 4.1 Objectives and approach

The objectives of the analysis of historical data are:

- to obtain information on bed level changes and changes of hydraulic conditions at Gorai mouth over the last 30 years by analysing existing water level and discharge data. The results are compared with present bed level information.

- to obtain information on changes in hydraulic conditions in the Ganges and the Gorai and, if possible, establish correlations with the performance of the Gorai offtake.

Water level data are analysed to provide information on local slopes near Gorai mouth. Together with the discharge data it is thereby possible to obtain an impression of the development with time of the bed levels at the Gorai mouth.

## 4.2 Available historical data

There is only little direct information about the bathymetry of the Gorai mouth from the past, and only from the most recent years. FAP4 (1993) carried out surveys of Gorai mouth in 1992, and BWDB also carried out cross section surveys in the 1990'es in relation with dredging of the offtake channel. The seasonal development of Gorai mouth bed levels before and after the Farakka Barrage became operational (1975) would of course have been very useful, but such data do not exist. Instead, existing water level and discharge data are applied to obtain information about changes in hydraulic conditions at the Gorai mouth and an attempt has been made to interpret the observed changes in terms of bed level changes.

Long time series of water level data are available from (see Figure 1.1):

- Hardinge Bridge in the Ganges 14.4 km upstream of Gorai offtake (Talbaria) (1964-1995) (except 1971)

- Talbaria in the Ganges immediately upstream of Gorai offtake (1986-1995)

- Sengram in the Ganges 27.9 km downstream of Gorai offtake (1964-1995) (except 1971)

- Gorai Railway Bridge in Gorai 16.1 km downstream of Gorai offtake (1964-1994) (Except 1971)

Discharge time series are available from:

- Gorai Railway Bridge (1964-1995) (except 1971/72,1982)
- Hardinge Bridge (not utilized in the present analysis)

Plots of water level and discharge data are in Appendix 1.

## 4.3 Ganges water levels

Water level time series are shown in Appendix 1 for Hardinge Bridge, Talbaria and Gorai Railway Bridge. Some corrections have been made to the data in cases where there were obvious typing mistakes. In a few cases some data have been deleted because they were clearly faulty for other reasons. The large variations in water levels at the falling stage of 1974 (hydrological year) can be seen both at Hardinge Bridge and at Gorai Railway Bridge and are due to operation trials at Farakka.

The minimum water level of the Ganges at Hardinge Bridge has clearly been falling since 1964 by more than 2.5 metres, see Figure 4.3.1. The drop has been particularly sharp after 1987 but seems to have been going on gradually over the entire period. A clear decrease in minimum water level is seen to take place in the second half of the 1970'es - coinciding with the commissioning of the Farakka Barrage. The maximum water level does not show any decreasing or increasing trends.

A simple analysis of the rate at which the water level drops in the Ganges (Hardinge Bridge) after the peak of the monsoon flow has been carried out. The results of the analysis are presented in Figures 4.3.2 and 4.3.3. The average hydrographs for Hardinge Bridge for three consecutive 10-year periods (1964-73, 1974-84, 1985-94) are shown in Figure 4.3.2. It is quite clear that the average rate of water level decrease at the end of the monsoon period has increased considerably from the first to the latest 10-year period. The changes from the first to the second 10-year period are far less pronounced. This can be illustrated by the time it takes the water level to fall from 11 to 7 m PWD: For the period 1964-73 it took on average approximately 5 months, whereas for the period 1985-94 it took only 2½ months. The level range 11 to 7 m PWD is chosen because it would be the water level range where a major part of the erosion of a dry season flow channel would take place. The time available for the erosion of such a channel has roughly been halved during a 20-year period. The plot in Figure 4.3.3 shows the time span between 11 m and 7 m PWD at Hardinge Bridge. It shows an apparent sharp drop in the 1960'es, again in 1974 and then a more gradual decrease.

## 4.4 Gorai discharges

During the latest years (since 1988) the water level at Gorai Railway Bridge stops falling at a certain Ganges water level - which may change from year to year. This indication of closure of Gorai mouth is more clearly illustrated by the variation in local slopes (Sec. 4.5).

The closure is also indicated by the discharges at Gorai Railway Bridge which falls to near zero (the small remaining flow may be due to a slight ground water seepage from Ganges to the Gorai).

26

Discharge time series at Gorai Railway Bridge are shown in Appendix 1 and annual extremes and averages are shown in Figure 4.4.1.

Two phenomena may cause the Gorai offtake to be closed for a longer period of time every year:

- dropping dry season water levels in the Ganges (in combination with increased fall rates).
- increasing threshold bed levels at the Gorai mouth.

Figure 4.3.1 shows that the first factor has been effective, especially since 1988, which happens to be the first year closure could be clearly detected from analysis of water levels. Whether the reasons for changes in threshold bed levels at the Gorai mouth are actually to be found locally near the offtake, in the Ganges or further downstream in the Gorai is another matter. FAP4 (1993) found by studying the discharge rating curves of Gorai Railway Bridge that low flow water levels (for given discharge) had increased significantly over a 45-year period (1947-92) by more than 1 metre. This could in fact worsen the conditions at the mouth because the water level gradient would have become smaller and thereby also the sediment transport capacity and the capability of the flow to erode a low flow offtake channel at the Gorai mouth.

In the following it will be investigated how the geometric conditions of the Gorai mouth have been changing.

## 4.5 Local slopes of upper Gorai

The water level slopes in the Ganges are approximately $5 \cdot 10^{-5}$ during the monsoon, falling to near zero in places during the dry season. The slope in the Upper Gorai behaves quite differently. It is high during the rising and falling stage and drops to a minimum in between, at maximum stage in the Ganges.

Figure 4.5.1 illustrates the difference in Ganges and Gorai mouth water level slopes over the year, taking 1993 as an example. It should be mentioned that in 1993 the Gorai was closed during the dry season (before day 50 and after day 270) during which period the slope of course has no hydraulic meaning.

It is more illustrative to show the annual variation of the slope at Gorai mouth (Talbaria to Gorai Railway Bridge) as a function of the Ganges water level at Talbaria. Appendix 2 shows such graphs for the period 1986-94. They clearly illustrate both the opening in the beginning of the monsoon and the closure at the end of the monsoon. The Talbaria water levels at the times of opening/closure, which is also the threshold bed level at Gorai mouth, can be read from these graphs. The difference in the shape of the curves from one year to the next is striking. If we assume that the Gorai flow is mainly controlled by conditions locally at or near the mouth and far less by the conditions downstream of Gorai Railway Bridge then the observed development in local slope can be related to the overall resistance to flow represented by changes in a representative cross section.

The water level at Talbaria which would have a direct relation to the conditions at Gorai mouth was not recorded before 1986. By plotting the water level difference between Hardinge Bridge and Gorai

Railway Bridge a similar set of curves is obtained (Appendix 2) also indicating that the annual variation of the slopes at Gorai mouth differ from year to year.

The next step is to estimate the water levels at Talbaria before 1986 from the water levels at Hardinge Bridge and Sengram. On the basis of 6 years of water level time series (1987-89 and 1992-94) the following relation was found to give the best estimate:

$$WL(Talbaria) = [\,27.9 \cdot WL(Hardinge) + 14.4 \cdot WL(Sengram)]/42.3 - 0.18m$$

The water level gradients based on estimated Talbaria water levels are not shown, but they are used in the following assessments of changes in conveyance factor for Gorai mouth.

## 4.6 Bed level changes at Gorai mouth

The water level gradient at Gorai mouth would depend both on the cross section characteristics and on characteristics of the flow. It is, however possible to split the two effects with some simplifying assumptions:

- the Upper Gorai from the mouth to Gorai Railway Bridge may be represented by the same flow cross section.
- the flow is considered quasi-steady.

Under these not very restrictive assumptions the discharge is related to the energy gradient and cross section parameters by

$$Q = M \cdot K \cdot I^{1/2}$$

where M is the Manning number and K is the conveyance factor calculated by

$$K = A \cdot R_*^{2/3}$$

Here A is the cross section area and $R_*$ is the resistance radius of the cross section. It should be noted that this approach is one-dimensional, which means that possible 2D and 3D effects are not taken into account.

The energy gradient is in this case well represented by the water level gradient, which is known. The discharge, which is known at Gorai Railway Bridge, is taken to be valid up to Gorai mouth. The conveyance factor, K, which is purely dependent on the cross section geometry can thus be determined if we guess a suitable Manning number; M=55 is selected based on results of 1D-modelling carried out at SWMC, (SWMC/DHI, 1996). The Manning number is less dependent on water depth than the Chezy number. This is important for Gorai mouth where the water level is highly variable over the year. It is less important to select a correct value of M since the main purpose of this analysis is to see relative changes from one year to another, rather than to quantify in absolute terms.

The simplistic conveyance method outlined above, which interprets changes in discharge and slope in terms of changes of a representative bed level is naturally rather crude. One of the assumptions is

that the slope is constant between Talbaria and Gorai Railway Bridge, which it is not. The additional water level measurements by the RSP during the 1995 monsoon clearly shows that the slope is highly variable along this distance, but more so in the early and late monsoon than during the peak of the monsoon, see section 6.3. Lag effects in channel formation and possible bedform formation can explain this behaviour in the local slope. The 2D model also visualizes the variation in slope, see Figure 7.5.6. The strength of the conveyance method is that, although it does not provide a detailed interpretation of the morphological development at the offtake, it does relate observed changes in hydraulic conditions to readily comprehendible quantified changes of the morphology, which can be used in a relative evaluation of the development that has taken place in the past.

The conveyance factor vs. Talbaria water level for each hydrological year from 1964 to 1995 is shown in Appendix 3. For the period 1964-86 when water levels were not recorded at Talbaria, this water level has been estimated as explained in Sec. 4.4. To check the error involved in use of estimated instead of measured Talbaria water levels, the conveyance vs. water level is shown both with use of estimated levels and actual levels for 1988, see Figure 4.6.1 showing the conveyance variation for 1988 both using the measured water levels at Talbaria and the Talbaria water levels estimated by the above relation. The uncertainty is expected to increase the further back in time from 1986 the relation is used. The following observations can be made from the conveyance curves:

- some years the conveyance factor is very low before and/or after the monsoon period indicating closure or near closure of Gorai mouth at those times. The Ganges water levels when this condition occurs can be read from the curves.

- some years the development of the conveyance factor with decreasing depth after the monsoon follows almost the same curve as during the rise of the monsoon indicating that hydraulic conditions were almost uniquely identified by the water level. It cannot immediately be argued that this indicates no change in overall bed levels during the monsoon. However, with the time lag involved it is likely that if bed levels did change during the monsoon the conveyance factor for the rising and for the falling stage of the monsoon would have been different along rising and falling limbs.

  some years the development of the conveyance factor with decreasing depth after the monsoon follows a curve distinctly different from the one it followed during the rise of the monsoon, indicating that hydraulic conditions were different. This may be due to differences in overall bed levels or differences in the Manning number. Since the difference goes both ways (sometimes higher conveyance during the rising, sometimes lower) it is most likely that this difference is affected by bed level changes rather than changes in Manning number.

Gorai mouth water levels at selected conveyance factors can be read from the above plots and are shown as time series (Figure 4.6.2). Two points are shown for each hydrological year, corresponding to rising and falling stage. These two points have been shown with half year intervals, ie they do not represent actual time intervals. This is a minor inaccuracy which does not affect the overall picture of this graph. The range of levels covered is restricted to the range of Ganges water levels experienced each year. By extrapolating the conveyance curves downwards for those years when closure did not occur, the levels of lower conveyance factors can be estimated also for these years. In Figure 4.6.3 is shown the levels of the lower conveyance factors together with minimum water level at Talbaria. Figures 4.6.2 and 4.6.3 show that:

27

- over the period from 1964 to 1993 the minimum water level at Talbaria has fallen by more than 2.5 m from 6.2 m PWD to 3.6 m PWD. The decrease has occurred gradually although a sharper drop seems to have taken place since 1989.

- the threshold bed level at the Gorai mouth (represented by the 10 $m^{8/3}$ conveyance factor level) has been varying by up to more than 3 metres from below 4 m PWD in the sixties and again in the late seventies (estimated, because the minimum water level was higher) to 7.2 m PWD in 1995. A sharp increase appears to have taken place at the high floods of 1987 and the high level was maintained and even increased further in 1988. Before 1987 the bed level varied by approximately 1.5 m in a seemingly periodic way (period 6 to 12 years).

- closure or near-closure of the offtake during the dry season has occurred now and again during the 30-year period. The tendency to close every year was initiated by a sharp bed level rise at the Gorai mouth in 1987 which continued in 1988. The sharp drop in the minimum water level in the Ganges after 1988 has made it increasingly likely that closure in the future will take place every year.

- increasing trends after 1987 can be seen for all the plotted conveyance levels.

Dredging at Gorai offtake was carried out in 1977. This corresponds well with a drop in threshold bed level estimated from the conveyance level plots (Figures 4.6.2 and 4.6.3). After 1977 the bed level conditions deteriorated in 1980. Also this is clearly illustrated in Figures 4.6.2 and 4.6.3. Dredging was again carried out in 1982-83 and 1984-85. The minimum flow rate at Gorai Railway Bridge increased slightly in 1984 (Figure 4.3.2) but dropped again in 1985. Dredging was again carried out in 1992-93, but the Gorai still closed in the dry season.

The best indication of bed level changes taking place is the one mentioned above, where a threshold level is indicated by cessation of flow. Apart from that, the conveyance factor profiles in Appendix 3 do contain some information about the cross section shape. Each conveyance factor profile can be considered as measured over a period of some months, ie changes of the profile may have taken place during this period. Analyses of bed level changes during a year would have to be based on the assumption that the basic shape function of the cross section does not change. When a certain cross section shape is assumed, for instance based on some measured cross sections, then it is possible for each conveyance curve to estimate a width factor and a bottom level. In this way it is possible to determine changes in the width/depth ratio of the governing characteristic cross section at Gorai mouth and also get a less subjective estimate of the bottom level of the cross section.

This exercise has not been carried out. Only a qualitative interpretation of conveyance factor levels in terms of cross section widening/narrowing has been made based on the variation in level gaps between the conveyance levels shown in Figure 4.6.2. The following trends are found:

- there is a tendency of narrowing of the lower part of the cross section, initially in 1982 and increased from 1989. This may be due to the dredging of narrow channels.

- the intermediate part of the cross section, and to some extent also the upper part, shows a tendency to widen since 1987.

## 4.7 Conclusions

- The minimum water level of the Ganges has clearly fallen since 1964 by more than 2.5 metres. The drop has been particularly sharp after 1987, but seems to have been going on gradually over the entire period. A clear decrease in minimum water level took place in the second half of the 1970's - which coincides with the beginning operation of the Farakka Barrage. The maximum water level does not show any decreasing or increasing trends.

- On average the water level of the Ganges at the end of the monsoon period has clearly been falling much faster during the latest 10-year period (1985-95) than it did 1964-73. The fall time has gradually decreased over the last 30 years. The water level fall from 11 m PWD to 7 m PWD now takes only half as long time as it did 20 years ago. This implies that a dry season flow channel on average has roughly only half as long time to develop by erosion than it had 20 years ago.

- The threshold bed level at the Gorai mouth (represented by the 10 $m^{8/3}$ conveyance factor level) has been varying by up to more than 3 metres from 4.0 m PWD in 1966 (estimated, because the minimum water level was 5.6 m PWD) to 7.2 m PWD in 1989. A sharp increase appears to have taken place at the high floods of 1987 and 1988. Before 1987 the bed level varied by approximately 1.5 m in a seemingly periodic way (period 6 to 12 years).

- Two factors may separately or in combination cause the closure of the Gorai offtake: Dropping dry season water levels in the Ganges, and increasing threshold bed levels at the Gorai mouth. It was found that both factors have been effective.

- Closure or near-closure of the offtake during the dry season has occurred now and again during the 30-year period. The tendency to close every year was initiated by a sharp bed level rise at the Gorai mouth in 1987 which continued in 1988. The sharp drop in the minimum water level in the Ganges after 1988 has made it increasingly likely that closure in the future will take place every year.

- The increasing bed level after 1987 seem to have reduced the conveyance factor for all stages of the flow.

- There is a tendency of narrowing of the lower part of the cross section, initially in 1982 and increased from 1989. This may be due to the dredging of narrow channels. The intermediate part of the cross section, and to some extent also the upper part, shows a tendency to widen since 1987.

# 5. Routine and special surveys by RSP

## 5.1 Bathymetric surveys

A total of four routine bathymetric surveys of the entire area shown in Figure 1.1 have been carried out. In addition to these, three special bathymetric surveys covered a more limited area of the upper Gorai. This area is also shown in Figure 1.1. One topographic land survey of char areas in the upper Gorai was carried out to supplement the available bathymetric data. Table 5.1 below gives details of these eight surveys.

| Type | Extent | Start date | End date | Bulletin no. |
|---|---|---|---|---|
| Bathymetry | full | 13-Oct-94 | 23-Oct-94 | 8009 |
| Bathymetry | full | 6-Jan-95 | 20-Jan-95 | 8014 |
| Topography | partial | 15-Jan-95 | 14-Feb-95 | 9044 |
| Bathymetry | full | 28-May-95 | 12-Jun-95 | 8022 |
| Bathymetry | partial | 24-Jun-95 | 30-Jun-95 | 8023 |
| Bathymetry | partial | 8-Aug-95 | 14-Aug-95 | 8025 |
| Bathymetry | full | 8-Sep-95 | 24-Sep-95 | 8027 |
| Bathymetry | partial | 16-Oct-95 | 20-Oct-95 | 8028 |

Table 5.1 Ganges-Gorai bathymetric and topographic surveys carried out by the RSP.

## 5.2 Transect line surveys

A transect line survey is a survey which covers the entire cross section at a selected location with measurements of cross section geometry, flow and sediments. Such surveys are carried out as part of all routine gaugings and most often also in special surveys. Two routine survey locations are of interest for the present study: The one downstream of Hardinge Bridge in the Ganges and the one at Kushtia (at the downstream groyne) in the Gorai. In addition, a number of special surveys were carried out near the Gorai offtake, including transects both in the Ganges and the Gorai. A list of the surveys performed by the RSP which are relevant for the present study of the Gorai offtake is given in Table 5.2.

22

| Location | Start date | End date | Survey type | Final Bulletin |
|---|---|---|---|---|
| Hardinge Bridge | 26-Sep-93 | 29-Sep-93 | routine gauging | No. 15 |
| Hardinge Bridge | 16-Feb-94 | 18-Feb-94 | routine gauging | No. 36 |
| Hardinge Bridge | 07-Mar-94 | 07-Mar-94 | routine gauging | No. 39 |
| Hardinge Bridge | 27-Mar-94 | 29-Mar-94 | routine gauging | No. 47 |
| Hardinge Bridge | 08-Apr-94 | 08-Apr-94 | routine gauging | No. 50 |
| Hardinge Bridge | 12-May-94 | 12-May-94 | routine gauging | No. 58 |
| Hardinge Bridge | 05-Jun-94 | 06-Jun-94 | routine gauging | No. 61 |
| Hardinge Bridge | 20-Jun-94 | 21-Jun-94 | routine gauging | No. 67 |
| Hardinge Bridge | 14-Jul-94 | 15-Jul-94 | routine gauging | No. 79 |
| Hardinge Bridge | 31-Jul-94 | 01-Aug-94 | routine gauging | No. 87 |
| Hardinge Bridge | 11-Oct-94 | 12-Oct-94 | routine gauging | No. 104 |
| Hardinge Bridge | 20-Oct-94 | 20-Oct-94 | routine gauging | No. 108 |
| Hardinge Bridge | 31-Oct-94 | 01-Nov-94 | routine gauging | No. 115 |
| Hardinge Bridge | 02-Dec-94 | 04-Dec-94 | routine gauging | No. 125 |
| Hardinge Bridge | 03-Jan-95 | 04-Jan-95 | routine gauging | No. 129 |
| Hardinge Bridge | 03-Feb-95 | 04-Feb-95 | routine gauging | No. 131 |
| Hardinge Bridge | 27-Mar-95 | 30-Mar-95 | routine gauging | No. 143 |
| Hardinge Bridge | 27-Apr-95 | 30-Apr-95 | routine gauging | No. 150 |
| Hardinge Bridge | 25-May-95 | 26-May-95 | routine gauging | No. 157 |
| Hardinge Bridge | 27-Jun-95 | 29-Jun-95 | routine gauging | No. 169 |
| Hardinge Bridge | 09-Aug-95 | 10-Aug-95 | routine gauging | No. 180 |
| Hardinge Bridge | 05-Sep-95 | 05-Sep-95 | routine gauging | No. 189 |
| Hardinge Bridge | 26-Sep-95 | 28-Sep-95 | routine gauging | No. 197 |
| Hardinge Bridge | 02-Oct-95 | 02-Oct-95 | routine gauging | No. 203 |
| Hardinge Bridge | 12-Oct-95 | 13-Oct-95 | routine gauging | No. 209 |
| Hardinge Bridge | 29-Oct-95 | 29-Oct-95 | routine gauging | No. 218 |
| Hardinge Bridge | 29-Oct-95 | 29-Oct-95 | routine gauging | No. 220 |
| Hardinge Bridge | 18-Nov-95 | 19-Nov-95 | routine gauging | No. 227 |
| Hardinge Bridge | 13-Dec-95 | 13-Dec-95 | routine gauging | No. 238 |
| Hardinge Bridge | 26-Dec-95 | 26-Dec-95 | routine gauging | No. 243 |
| Hardinge Bridge | 20-Jan-96 | 20-Jan-96 | routine gauging | No. 250 |

20

| Location | Start date | End date | Survey type | Final Bulletin |
|---|---|---|---|---|
| Kushtia/Gorai | 14-Feb-94 | 15-Feb-94 | routine gauging | No. 35 |
| Kushtia/Gorai | 05-Mar-94 | 06-Mar-94 | routine gauging | No. 38 |
| Kushtia/Gorai | 11-May-94 | 11-May-94 | routine gauging | No. 57 |
| Kushtia/Gorai | 19-Jun-94 | 19-Jun-94 | routine gauging | No. 66 |
| Kushtia/Gorai | 03-Aug-94 | 03-Aug-94 | routine gauging | No. 88 |
| Kushtia/Gorai | 16-Oct-94 | 16-Oct-94 | routine gauging | No. 106 |
| Kushtia/Gorai | 24-Oct-94 | 24-Oct-94 | routine gauging | No. 109 |
| Kushtia/Gorai | 05-Dec-94 | 05-Dec-94 | routine gauging | No. 126 |
| Kushtia/Gorai | 05-Jan-95 | 05-Jan-95 | routine gauging | No. 130 |
| Kushtia/Gorai | 27-May-95 | 27-May-95 | routine gauging | No. 158 |
| Kushtia/Gorai | 21-Jun-95 | 22-Jun-95 | routine gauging | No. 166 |
| Kushtia/Gorai | 12-Aug-95 | 12-Aug-95 | routine gauging | No. 181 |
| Kushtia/Gorai | 06-Sep-95 | 06-Sep-95 | routine gauging | No. 190 |
| Kushtia/Gorai | 28-Sep-95 | 28-Sep-95 | routine gauging | No. 200 |
| Kushtia/Gorai | 12-Oct-95 | 12-Oct-95 | routine gauging | No. 208 |
| Kushtia/Gorai | 09-Nov-95 | 09-Nov-95 | routine gauging | No. 224 |
| Kushtia/Gorai | 20-Nov-95 | 20-Nov-95 | routine gauging | No. 229 |
| Kushtia/Gorai | 12-Dec-95 | 12-Dec-95 | routine gauging | No. 237 |
| Ganges/Gorai | 21-Oct-94 | 21-Oct-94 | offtake study survey | No. 9034 |
| Gorai Offtake | 27-Jun-95 | 28-Jun-95 | offtake study survey | No. 9065 |
| Gorai Offtake | 11-Aug-95 | 14-Aug-95 | offtake study survey | No. 9077 |
| Gorai Offtake | 07-Sep-95 | 12-Sep-95 | offtake study survey | No. 9078 |
| Hardinge Bridge | 03-Oct-95 | 03-Oct-95 | joint BWDB survey | No. 9086 |
| Gorai Offtake | 13-Oct-95 | 16-Oct-95 | offtake study survey | No. 9088 |

Table 5.2 List of transect line surveys in the study area.

The routine gaugings from 1994-96 have been used in analyses for the present study, together with the data from special surveys. The data analyses are described in Secs. 6.4 and 6.5. The special offtake study surveys were planned in such a way that they can supply the necessary data for the 2D modelling (Chapter 7). The planning of these special surveys has taken into account results from pilot 2D modelling as well as the findings from analyses of historical data.

Apart from the above discharge measurement at the routine cross section downstream of Hardinge Bridge, a few discharge measurements were made at other locations near the study area:

22

- near the sharp bend upstream of Hardinge Bridge
  - 2 August 1994 (Bull. 9010)
  - 19 October 1994 (Bull. 9033)

- near the BWDB cross section 700 m upstream of Hardinge Bridge 3 October 1995
  - 2-3 October 1995 (Bull. 9086)

These surveys may become useful in future studies of the Gorai offtake, for instance if the 2D model area should be extended further upstream as recommended in Chapter 9.

## 5.3 Bed material surveys

Bed material samples have been obtained from the study area from three different collection campaigns which were dedicated to bed sample collection. Some additional samples were collected during transect surveys. A total of 106 samples were collected within the study area.

About 10 percent of the samples, usually collected near the river banks, had a high silt content and a $d_{50}$ within the silt fraction. For the remaining samples it was found that typical grain diameters are:

Ganges: $d_{50} = 0.15$ mm
Gorai mouth: $d_{50} = 0.17$ mm

## 5.4 Float trackings

A large float tracking survey covering the entire study area was carried out 11-15 October 1995, and a few smaller float tracks were done near the Gorai mouth in connection with the Gorai offtake study surveys. The float tracking was carried out using near surface floats which are followed and positioned frequently during their journey. A main purpose of the float trackings at the Gorai mouth was to determine a 'separating flow path', ie the flow path for which a float to the left of it would be going down the Ganges and a float to the right of it would go to the Gorai. The results of these surveys have not been applied in the modelling of the present study, but will be well suited for future study applications of the model.

## 5.5 Water level gaugings

Both BWDB and the RSP have water level stations at Hardinge Bridge and Gorai Railway Bridge. The RSP collected data only for the most recent years while BWDB has been maintaining the stations for many years. At Bheramara, Talbaria and Shelaidah, 2.6 km, 14 km and 30 km, respectively, downstream of Hardinge Bridge the RSP collected water levels during the monsoon period of 1995.

# 6. Data Analyses

## 6.1 Bank erosion from satellite imageries

In particular two reaches of the Ganges river within the study area are exposed to significant bank erosion. Only the erosion in these two reaches has been analysed further:

**The right bank of Ganges between Hardinge Bridge and Gorai mouth**

The development over the last 6 years, 1989-95, indicates erosion of up to 100 m/year on average over this period; highest where the curvature is presently highest, see Figure 6.1.1 The erosion at Talbaria point where the bank line takes the direction down the Gorai has been small, only about 50 metres total over the entire period.

There is no sign that the 'hard point' at Talbaria is increasingly exposed to erosion, neither is there any indication that the erosion of the bend as a whole has been decreasing over the 6 year period. The curvature of the bend has, however, increased significantly during the period, especially for the downstream part immediately upstream of the 'hard point'.

**The left bank of Ganges downstream of Gorai mouth**

The erosion here has been somewhat higher, up to 125 m/year on average over the 6 year period, see Figure 6.1.2. Although the considered reach has been eroding at a similar rate on average over the entire period, the erosion started at the upstream part in 1992 and proceeded further downstream thereafter.

Of these two eroding banks the most interesting in relation to the development of the Gorai offtake is undoubtedly the right bank upstream of the Gorai. The ongoing bend erosion gradually changes the angle between the Ganges flow and the flow to the Gorai. Looking back in time, the curvature of this bend has been 'fluctuating': The analysis of historical information carried out by FAP4 (1993) shows that the bend was sharper in 1914 and 1957 than it is now. The planform to day is gradually becoming similar to the planforms in 1914 and 1957. In the periods in between it has on the other hand been much gentler. From this we may conclude:

- the development of the curvature of the bend upstream of Gorai offtake is cyclic in time, with a period of the order of 40-50 years according to the above observations.

- at present we are in a development towards a sharp bend situation which is not yet extreme compared to past records. It is likely that this development will continue some years ahead.

The annual erosion volumes for the right bank upstream of the offtake have been estimated based on bank levels and near bank bed levels from the nearest BWDB cross sections (surveyed annually). The total volume has been estimated to be in the order of 10 mill. $m^3$/year (deposited volume). With an estimated porosity of 0.4 this corresponds to an average contribution to the sediment transport balance of this area of approximately 0.2 $m^3/s$ (grain volume). This contribution would of course not be distributed uniformly over the year, but be concentrated during high discharge periods of the monsoon. Compared to the total transport of the Ganges at Hardinge Bridge the contribution from bank erosion

is only a few percent. Compared with deposition volumes at the Gorai offtake the bank erosion represents a volume which is considerably larger than the volumes corresponding to annual variations in bed levels in the upper Gorai. The erosion upstream of the Gorai offtake may, therefore, have a significant effect on the morphology at the offtake.

## 6.2 Development in bed levels from bathymetric data

The frequent bathymetric surveys carried out during the monsoon period of 1995 (Table 5.1) makes it possible to follow the detailed morphological development during a monsoon. The full bathymetric surveys cover the entire study area, while the partial surveys cover only the upper Gorai. The full bathymetries are shown in the Figures 6.2.1 to 6.2.5. The main developments in the Ganges river can be summarized as follows:

- the deep scour hole near the offtake is maintained without major developments
- the main channel of the Ganges downstream of Talbaria is narrow and curved during the dry season, whereas it is wider and more straight during the monsoon

Detailed bathymetries of the upper Gorai are shown in Figures 6.2.6 to 6.2.9, including both full and partial bathymetric measurements. The 'full' bathymetric survey of January 1996 is not included because the upper Gorai was dry at the time and therefore not surveyed. The main features and developments can be summarized as follows:

- the deepest channel becomes more shallow and wider at the peak of the monsoon as it was before the monsoon; the channel deposition of the order of 1 metre takes place within a 1 kilometre reach at the Gorai mouth
- the deepest channel again becomes deeper and more narrow (more well defined on the bathymetry maps) towards the end of the monsoon period (October)
- the changes in position and direction of the deepest channel seem to be minor, although there seem to be a tendency that the main offtake channel moves towards the left bank of Gorai. This tendency is seen most clearly in the September 1995 survey where a second channel is more prominent than the one first developed.

Figure 6.2.10 shows a comparison of the bathymetry of September 1995 with a bathymetry of 1992 surveyed by FAP4 (1993). It was not possible to obtain the raw survey data that formed the basis for the 1992 bathymetry, so no detailed comparison could be made. Figure 6.2.10 does, however, show some interesting features.

- the large scour hole near Talbaria was present in 1992 and has not moved much since
- the 1992 bathymetry shows the presence of two offtake channels. The tendency of formation of a two-channel system was also observed from the 1995 bathymetries.

18

## 6.3 Analysis of water level data

Extensive analysis of historical data is presented in Chapter 4. The following presents observations made from the water level data collected during the monsoon of 1995. Figure 6.3.1 shows water level measurements within the study area in 1995 from both BWDB gauges and RSP gauging stations. The levels given by BWDB have been corrected according to the findings of FAP24 (1993a). The corrections for Hardinge Bridge and Gorai Railway Bridge are minor, while the corrections for Talbaria and Sengram are +0.45 m and -0.52 m, respectively. Figure 6.3.2 shows time series of water level slopes for different reaches of the Ganges, calculated from the water level records. It shows that the water level slope rises from near zero in the dry season to around $6 \cdot 10^{-5}$ during the peak of the monsoon; even somewhat higher at the downstream reach between Talbaria and Shelaidah.

The water level slope of the Gorai was studied in detail in Chapter 4. For the 1995 monsoon we have one additional staff gauge at Kushtia, approximately halfway between Talbaria and Gorai Railway Bridge, which gives an opportunity to investigate differences in the slope very near Gorai mouth and further downstream and how a difference develops in time. Figure 6.3.3 shows the time series of measured slopes in the Gorai. As it was observed for previous years, the slope is generally high in the beginning and at the end of the monsoon, while it decreases to nearly the same level as for the Ganges during the peak of the monsoon. In addition, the new measurements show that the slopes along the two reaches, Talbaria to Kushtia and Kushtia to Gorai Railway Bridge are almost the same during the peak of the monsoon, but in the beginning and towards the end the slope near the mouth is much larger than further downstream. This indicates that the geological controls of the upper Gorai change during the monsoon: At the lower stages in the Ganges the Gorai mouth is clearly a controlling section, but as the discharge to the Gorai increases at higher stages of the Ganges, this control vanishes. It may have been replaced by a control further downstream.

In Figure 6.3.4 the slopes have been plotted against the water level of Ganges at Talbaria. It is interesting to see that the loop is far more distinct for the upper Gorai than further downstream. This is not surprising, since the loop is related to the seasonal changes in morphology, which are expectedly higher close to the offtake than further downstream. The higher slope at decreasing flow in comparison with increasing flow seem to develop during high stages: Gradually during the peak of the monsoon the slope of the upper Gorai is becoming higher and higher. This tendency could be caused by deposition somewhere along the first 5 kilometres of the Gorai. The measured bathymetries do actually indicate that the Gorai mouth becomes shallower during the monsoon, see Section 6.3. Future analyses using simulation results of a two-dimensional model, observations of bathymetric changes and detailed water level and discharge data may be able to relate information about the loop in local slope to seasonal variations in erosion/deposition at the offtake.

## 6.4 Analysis of flow data

Hardinge Bridge has been a routine discharge measurement station for BWDB for many years. The RSP measured the discharge at the station approximately monthly since September 1993 (except for some months in the dry season). The total number of discharge measurements by the RSP is approximately 30. A two-stage rating curve for 1994 and 1995 has been established for Hardinge Bridge using the measured discharge of the RSP and measured water level of BWDB (the water level data of the RSP for that period were not available at the time of the analysis). The rating curve is shown in Figure 6.4.1 and the segment equations are as follows:

$$Q = 69.599 ( H - 4.407 )^{2.729} \quad H < 11.77$$

$$Q = 3.080 ( H - 4.084 )^{4.200} \quad H > 11.77$$

where Q = Discharge, and H = Stage (m PWD)

This rating curve has been used for generating a continuous discharge time series for the upper boundary of the 2D model (see Chapter 7). The validity of the rating curve is limited to the range of water levels/discharges which occurred in 1994-95. The monsoon discharges these years were not above average (up to approximately 45,000 $m^3/s$).

The discharge and water level data of BWDB from the period 1987-89 are shown together with the RSP data in Figure 6.4.2 for comparison. 1987-88 were extreme years with a highest measured discharge of 76,000 $m^3/s$ on 19 September 1987. The corresponding water level at Hardinge Bridge was 14.8 m PWD. The 1987-89 data agree well with the rating curve developed for 1994-95, although the Hardinge Bridge area experience large annual variations in bed level (constriction scour), see Figure 6.4.2.

## 6.5 Analysis of sediment transport data

The results of laboratory analyses distinguish between wash load and bed material load. The wash load is the transport of fine material (silt and finer), which is not usually taking part in the morphological developments of the river bed. The transport of bed material is the most transport component. Figures 6.5.1 and 6.5.2 show the measured sediment transport components against measured discharges at the routine transects downstream of Hardinge Bridge and at Kushtia, respectively. The transport of bed material (grain diameters larger than 0.063 mm) is shown together with the total transport.

# 7. Two-dimensional Morphological Modelling

## 7.1 Introduction

A two-dimensional mathematical model was applied for the morphological analysis of the Gorai offtake. It provides means of exploring the governing morphodynamic processes in more detail. Furthermore, it is possible to make predictions of the effects of various measures to improve the conditions for flow into the Gorai river.

Extensive measurements and analyses of data have been carried out by the RSP, see previous chapters and other Special Reports of RSP. The Surface Water Modelling Centre, SWMC, was commissioned by the RSP to carry out the modelling work supported by local and expatriate staff members of the RSP. The SWMC has experience in two-dimensional modelling from similar studies of Bangladeshi rivers, see DHI/SWMC (1996), DHI/SWMC (1996a), SWMC (1996).

The applied modelling system is a two-dimensional (2D), morphological and dynamic system. One-dimensional (1D) modelling of the Gorai has also been carried out at SWMC in connection with another project (SWMC/DHI,1996). A 1D model cannot, however, automatically simulate bifurcations and offtakes as it requires explicit specification of the sediment distribution at the bifurcation. Thus, a 2D modelling approach has to be adopted. Substantial changes of the river bed take place over the monsoon season. It is therefore essential that the modelling system is based on a movable model bathymetry, ie with continuous update of the bed levels as well as the model flow resistance. Furthermore, the conditions during rising and falling stage, respectively, are not the same. Therefore, a dynamic simulation is required, with modelling of real time series of discharge and water levels.

The overall objective of the mathematical model study as described in the RSP report, 1993, and later elaborated in RSP report, 1995, is:

- to improve the understanding of sediment transport distribution and the processes of erosion and deposition at an offtake channel, thereby gaining insigth in the influence of bar formation in front of the offtake.

More specifically, the study will address the following:

- the development of the offtake channel from when it becomes active in the beginning of the monsoon until it closes at the end of the monsoon period
- the development of the bar in front of the offtake during the monsoon period the effect of changes of the bar on the discharge, sediment transport and morphological changes in the offtake area
- training of local staff in using a 2D hydrodynamic and morphological model on a rectangular and curvilinear grid, as a study tool

The proposed approach has been followed with the only exception that less resources of the mathematical modelling expert (1.5 man months against the 6 man months as proposed) have been used. Thus, fine calibration of the model has not been carried out.

29

The intention of the modelling study is to develop an analysis tool for extending the data analyses discussed in the previous chapters and to explore existing conditions rather than to develop a predictive tool. It is the first time advanced two-dimensional morphological modelling is used to simulate the complex processes of an important offtake in Bangladesh. In that sense the entire modelling exercise should be regarded as pilot modelling. The main outcome of the modelling is to learn as much possible about the importance of the various factors that affect the performance of the offtake and thereby be able to make recommendations regarding how to proceed. Therefore, the potential for further use of 2D mathematical morphological modelling of offtakes should also be evaluated from the present study.

## 7.2 Modelling System

The MIKE21-Curvilinear (MIKE21C) from Danish Hydraulic Institute has been used. A short description is given in Appendix 4. The modelling system has been used extensively in connection with the Brahmaputra River Training Studies in 1991-92, see FAP1 (1993), Enggrob et al (1994), the Jamuna Multipurpose Bridge Project for morphological forecast simulations in 1995-96, DHI/SWMC (1996), and for several minor studies of Bangladeshi rivers, see e.g. DHI/SWMC (1996a) and SWMC (1996). MIKE21C comprises computational modules to describe:

- Flow hydrodynamics, ie water levels and flow velocities over a curvilinear or a rectangular computational grid covering the study area by solving the vertically integrated equations of continuity and conservation of momentum

- Helical flow (secondary currents) developing in channel bends due to curved stream lines. The time and space lag in the development of the helical flow is included.

- Sediment transport, based on different model types (van Rijn, Engelund-Hansen, Engelund–Fredsøe, or user-defined empirical formulas). The effect of helical flow, gravity on a sloping river bed, shapes of concentration and velocity profiles are taken into account in separate bed load and suspended load sub-models based on the theories by Galappatti (1986).

- Hydraulic resistance due to bed material and bed forms (calculation of skin friction from the grain sizes and form drag friction from the bed forms). The model is based on the bed-form model developed by Fredsøe (1979). A less complicated depth dependant alluvial resistance model was applied for the present study.

- Large-scale movement of bed material due to scour or deposition causing changes to the bathymetry. The continuity equation for sediment is solved for determining changes in bed elevations at each grid cell and at every time step.

- Large-scale movement of bank lines. The bank erosion is computed from a formula relating near-bank conditions to bank erosion rates. The accumulated bank erosion can be used for updating the bank lines, and for updating the curvilinear grid (extent of modelling area) at every time step.

The modules can be run interactively, incorporating feedback from variations in the hydraulic resistance, bed topography and bank line geometry to the flow hydrodynamics and sediment transport.

২৮

## 7.3 Modelling Approach

Most morphological developments take place during the monsoon period. In particular for the Gorai offtake, the low stage conditions of the Ganges are of very little interest. This is because there is no flow to Gorai when the Ganges water level is below around 6-7 m PWD. Therefore, all model simulations (calibration/verification, sensitivity and applications) are carried out for one monsoon flood period from June to October.

A phased approach has been adopted by which the level of detailness increases gradually. In this way it has been possible to revise the modelling activities in the desired direction in the course of the data collection period and as more experience was gained with the model. Furthermore, a smooth training programme could be designed by which the trainees gradually became acquainted with the modelling technology and procedures as the models became increasingly more advanced.

For the design of a field survey programme, pilot modelling was carried out. The results are presented in a working paper (FAP24, 1995e). The pilot model has been further refined and calibrated and is in the following referred to as the 'overall model'. This model has been used to assess the hydrodynamics and to provide boundary conditions for the local model, Figure 7.4.1.

The 'local model', which is based on a curvilinear grid, see Figure 7.4.3, covers a smaller area, and is set up to give a finer resolution of the morphological changes at the offtake and in the Gorai river. Unlike the overall model, this model is fully morphological, ie with a continuous feedback to the hydrodynamics during calculation of bed level changes. The extent of the modelling areas is shown in Figure 7.3.1.

For both models, the bathymetry setup is based on pre-monsoon conditions from 1995. Calibration and verification of hydrodynamics are done against measurements from the monsoon 1995. Calibration of the sediment transport model is based on sediment rating curves developed from measurements near Hardinge Bridge and at Kushtia.

The models have been calibrated to the extent it was found necessary for providing sufficiently precise information to meet the objectives of the model study of the Gorai offtake. Thus, a best possible calibration has not been achieved with respect to every detail as this would have been a labourious and time-consuming task in light of the allocated resources.

Once the calibration of the hydrodynamics and sediment transport is done, the calibration is completed. There is no separate calibration for the morphological model. Comparison of observed and simulated bed level changes over the monsoon of 1995 from June to October therefore serves as a verification of the morphological model. The sensitivity of the simulated bed level changes at the offtake has been tested by varying the flow resistance and the boundary conditions.

Subsequently, the model was applied for four different scenarios:

- a higher sand bar elevation (+ 2m) in front of the offtake at the beginning of the monsoon
- narrowing of the Gorai river at the offtake
- an extreme flood event (the 1987 monsoon)

২৯

- lowering of the water level in the Gorai (- 0.3m)

The sensitivity tests and applications have been selected from the point of view that we want to learn which processes are important and how they interact. Although the presentation of the results focus on the performance of the offtake with respect to dry season flow to the Gorai, it has not been the objective to test specific scenarios (structural etc.) for possible improvements of the offtake performance.

## 7.4 Model Bathymetry and Setup

The overall model covers a 23 km x 21 km area from Hardinge Bridge to Shelaidah approximately 10 km downstream of the Gorai mouth and down to Gorai Railway bridge, see Figure 7.4.1. The model is based on a rectangular cartesian grid with a grid cell spacing of 100 m in each horizontal direction.

Measurements of bed levels have been carried out regularly within the modelling area, see Table 5.1. The bathymetry from May 1995 has been chosen as the basis for the model calibration for the monsoon of 1995. The echo sounder data cannot be applied directly in the model because of the grid resolution. Therefore, the model bathymetry is smoothened slightly compared to the raw bathymetry. Some areas were not flooded in May, and therefore the data does not cover the entire area. Bed levels from such missing areas were taken from the bathymetric survey of October 1994, and the land survey of January 1995.

The local model is based on a curvilinear grid prepared before the bathymetry data is entered into the model. The grid generation uses specified boundary lines (extracted from satellite imageries) and specification of number of computational points (density) in the modelling area as input. The grid generator can also adjust the local density of grid lines so that it is possible to have a higher density of grid lines in areas which require a higher resolution, eg. near the thalweg.

The generated curvilinear grid is shown in Figure 7.4.2. Except from the separation zone downstream of Talbaria at the Gorai river mouth, the grid lines follow the bank lines. It was not possible to let the grid lines follow the banks at this particular location due to the requirement of orthogonality of the grid lines. This area is, however, not critical with respect to a good resolution of the bank lines due to the flow separation here.

The model bathymetry of the local morphological model is, like the overall model, based on the May 1995 survey, see Figure 7.4.3. The morphological model provides a.o. information about the bed levels at different times. Simulated bed levels are compared with measured bed levels as part of the verification of the model.

For both models, the hydrodynamic boundary conditions consist of a discharge boundary upstream based on the derived discharge rating curve at Hardinge Bridge, time series of water levels downstream in the Ganges (Shelaidah) and in the Gorai (Gorai Railway Bridge). Water levels and discharges (boundary conditions) for the local model are extracted from the overall model. Only for one application (extreme flood event) a 1D model was used to supply the downstream water level boundaries (more about this in section 7.9).

## 7.5 Hydrodynamic model calibration and verification

The objective of the hydrodynamic calibration is to determine the flow resistance and the eddy viscosity, to find an appropriate computational time step, and to specify how land flooding and drying should be handled by the model. The monsoon of 1995 has been chosen as the calibration period, see Figure 7.5.1.

The time step (20 s) and the flooding/drying facility (drying when less than 0.2 m water depth, flooding when more than 0.5 m) has been chosen in such a way that the model remains stable during the simulation and satisfactory accuracy is obtained.

Lateral exchange of flow momentum is modelled by adjusting the so-called eddy viscosity which was set to 10 $m^2/s$. Sensitivity analyses showed only minor influence of this parameter on the overall hydrodynamics. For further fine-tuning of the simulated flow field at the offtake, this parameter should, however, be investigated further: Flow separation takes place in this region and high lateral velocity gradients occur close to the bank.

The flow resistance is an important parameter affecting the simulation results in various ways:

- The simulated hydrodynamics is governed by the specified flow resistance. The overall water surface slope of the Ganges is controlled by the mean resistance number.
- The difference in flow resistance and conveyance in the Ganges and the Gorai, respectively, determines the flow distribution at the bifurcation/offtake.
- The flow over submerged chars depends on how the flow resistance over deep and shallow parts of the cross-section is specified. For reproduction of the braiding intensity of the river during the morphological simulation, the variation of model resistance from shallow to deep parts is very important as discussed in section 7.8.
- The sediment transport formulas use the bed resistance as input parameter. Small changes in model bed resistance have a high influence on the simulated transport.

Since the flow resistance is a main calibration parameter it is important to determine it quite accurately through measurements of high quality of not only hydrodynamic data but also sediment transport data.

The following relationship has been used for the Chezy number

$$C = C_0 \cdot h^{0.5}$$

with $C_0 = 31\ s^{-1}$ for the Ganges and $C_0 = 26\ s^{-1}$ for the Gorai. Thus the Chezy number varies with the depth, ie with stage and also bed level, since the Chezy number is updated throughout the simulation.

The water surface slope is depicted in Figures 7.5.2 and 7.5.6. The slope is approximately $3 \cdot 10^{-5}$ for June conditions and $8 \cdot 10^{-5}$ for August conditions. In the latter case, for high flow, the local slope immediately upstream of Gorai offtake is high, indicating a natural constriction at this location, see also section 7.10.

92

Observed and simulated flow velocity fields in June and August 1995 are shown in Figures 7.5.3-7.5.4 and 7.5.7-7.5.8. Comparison of simulated and observed velocities in selected cross-sections are shown in Figures 7.5.5 and 7.5.9. In general, there is a good agreement between simulated and measured values except in the Ganges downstream of the offtake along the right bank. Here, the simulated velocities are higher than observed values.

The discharge rating curve for Gorai depends on the morphological development at the mouth; therefore a fixed bed model may not be fully representative. Nevertheless, the simulated rating curve from the fixed bed model is shown together with the observed data in Figure 7.5.10. Except for very low water stages, there is a satisfactory agreement between observed and simulated discharges. For low water levels, the width of the thalweg channel in the Gorai river is much less than during the monsoon. Consequently, the model resolution with a fixed horizontal grid of the bathymetry becomes less detailed as fewer computational points cover the same channel. The simulated rating curves from the movable bed model are shown in Figure 7.10.5.

Verification of the calibrated hydrodynamic model has been carried out by simulating (without changing the model calibration parameters) the flow conditions over a period which is different from the calibration period, but with data available for comparison. Figures 7.5.11-7.5.14 show results of such a verification of the model. From the figures it is concluded that the model calibration is satisfactory, given the objectives of the present study. More accurate calibration is, however, recommended if design studies are to be carried out with the model in the future.

## 7.6 Sediment Transport Model Calibration

Different sediment transport formulas have been used in mathematical model studies of the Ganges and the Jamuna rivers in the past. The most commonly used are Engelund-Hansen and van Rijn. During the RSP, attempts have been made to derive a sediment transport formula specifically designed for conditions prevailing in the Jamuna and in the Ganges river, respectively, see FAP24 (1995f). The formulas were, however, not fully available at the time calibration of the 2D morphological model was carried out.

Based on the experience from previous studies and findings from RSP regarding analysis of the power 'n' on the velocity, the van Rijn formula was chosen for the initial calibration runs. The formula gave a satisfactory representation of the sediment rating curve as measured near Hardinge Bridge (Figure 7.6.1) assuming a grain size of 0.16 mm, which is in accordance with the results of bed sediment sampling in the study area, see section 5.3. For high discharges, the sediment transport rate is a strongly nonlinear function of the discharge, and the natural scatter in measurements of suspended sediment is substantial. The simulated and observed sediment rating curves at Kushtia in the Gorai are shown in Figure 7.6.6, and also here the agreement is satisfactory taking into consideration the inherent natural scatter of measurements.

As mentioned above, a uniform grain size was used. In reality, some sorting of the sediment takes place and the grain size can be non-uniformly distributed both in space and in time. For the conditions prevailing in the Ganges where most of the sediment is transported in suspension, the effect of sediment sorting is negligible.

Most of the sediment is transported as suspended load. The concentration of suspended sediment is depicted in Figure 7.6.2. The suspended sediment transport vector field is shown in Figure 7.6.4 and the corresponding bed load vector field is shown in Figure 7.6.3. The sediment transport exhibits large differences, partly due to the natural migration of major bed forms, partly because the results are based on a fixed bed model. The same results but from a movable bed model (i.e. when model bathymetry is continuously being updated according to the simulated erosion/deposition) are shown in Figures 7.7.1 - 7.7.3.

The direction of the bed load transport, the suspended load transport, and the water flux, respectively, do not coincide which can be seen from Figure 7.6.7. The reason for this is the helical flow, which is taken into consideration in computation of the sediment transport directions. Figure 7.6.5 shows the helical flow intensity simulated by the model. It should be noted in Figure 7.6.5, that the direction (ie the sign) of helical flow is not the same along the entire right bank upstream the offtake, which may be the reason for simulated deposition here, see later.

## 7.7 Morphological Model Verification

For verification of the morphological model, the bed level changes from 20 June to 18 October 1995 were simulated. The computational time step between each sediment transport computation and model bathymetry update was 80 min.

### Initial and Boundary Conditions

The bathymetry applied at the beginning of the simulation is based on measurements from May/June 1995. The simulated bathymetry after four months (120 days) is compared with the bathymetry observed at the same time in September 1995. At the upstream boundary, a bed level profile was specified: It was assumed that the upstream bed elevation would be constant, ie that the actual sediment transport at the boundary equals the prevailing sediment transport capacity.

In principle, simulated sediment transport rates from a 1D morphological model could have been used to obtain boundary conditions thereby reflecting the morphodynamics of the Ganges channel more accurately. As there is evidence from measurements that bed levels change considerably during the monsoon, especially near Hardinge Bridge, it would have been necessary to use a coupled morphological 1D model, ie. with continuous bed level update. Use of 1D modelling was not part of the present study, but combined use of 1D and 2D modelling for morphological studies of offtakes is highly recommended.

The specified boundary conditions are expected to influence the simulation results for most of the Ganges river, but to a far less extent for the offtake area itself as this is located in the middle of the modelling area.

### Comparison of Ganges bed levels

The simulated and measured morphological changes over the monsoon period are compared in Figures 7.7.5 and 7.7.6. As expected, the reproduction of bed level changes in the Ganges is not that accurate,

see Figure 7.7.5, whereas the simulated and measured bed level changes at the offtake are quite similar (Figure 7.7.6).

According to measurements from May and September, the main channel has become more straight, wide and shallow compared to pre-monsoon. The simulated Ganges river after the monsoon also shows a more straight channel than the start bathymetry, but unfortunately the model simulates the channel becoming more narrow and deep compared to measurements. The reason is the inaccuracy in the applied hydrodynamic boundary conditions: A time series of horizontal water level boundary is assumed along the downstream boundary at Shelaidah. According to the definition of a boundary condition, it remains unaffected by the changes inside the modelling area. Thus, when the model simulates concentration of the flow along the left bank, the water level does not respond by a corresponding increase at that side of the cross-section creating a water level gradient across the river. If this was the case, the concentration of flow in a channel with the shortest distance to the boundary would be avoided. It should be noted, though, that this lack of feedback from morphological developments to the downstream boundary condition is unable to attract a higher discharge, since the discharge is specified at the upstream boundary.

Other factors may also influence the formation of a narrow/deep Ganges channel. It has been shown in sensitivity tests (section 7.8) that the use of an alluvial resistance number (continuously updated according to instantaneous depth) tends to develop a narrower/deeper channel than if there is no depth dependency of the model resistance. Finally, it is possible that use of a sediment transport formula with a different relation between transport and Chezy number would have a significant effect. The fact that the van Rijn sediment transport formula fitted quite well with measurements, does not mean that it represents the best possible relation for this part of the Ganges. Seasonal bed level changes at the cross section where measurements have been taken may have affected the sediment rating curve in a systematic way, which has not been taken into account.

Upstream of the offtake in the Ganges, a scour hole has been observed and bank erosion has taken place further upstream during the last few years. The model simulates deposition of sediment along the right bank which is in contradiction to measurements. Again the reason is the boundary conditions, which are not sufficiently accurate: By changing the computed discharge distributions (from the overall model) along the upstream boundary significant changes in the simulated bed levels in the Ganges occurred, see Figure 7.8.7. Furthermore, the intensity of the helical flow at the upstream boundary was assumed to be zero although the boundary is located in the middle of a major river bend extending from Hardinge bridge down to Gorai. Inaccuracy of the boundary conditions was compensated for by locally increasing the model flow resistance along the left side of the main channel at the upstream boundary. Thus, it was accepted that the Ganges morphology was poorly reproduced as long as the model was able to reproduce the scour hole at Talbaria and the concentration of flow along the right bank.

**Comparison of Gorai offtake bed levels**

Comparison of observed and simulated bed levels at the offtake (Figure 7.7.6), shows that despite major discrepancies in the description of the Ganges bathymetry, the model is capable of reproducing the morphological changes over the monsoon at the offtake: During low stages, the channel which goes through the middle of the bar at the offtake is narrow and deep. With rising stage, the channel becomes shallow and wide, and during falling stage the channel erodes and becomes more narrow

again. The animations enclosed on a diskette at the back cover of the present report clearly illustrate the morphodynamics.

At the downstream side of the offtake, the bar is slowly growing higher throughout the monsoon period. This has caused some concern during model calibration, because it means the bed level before the monsoon in June and after the monsoon in October are somewhat different whereas dynamic equilibrium in the sand bar elevation at this location was expected. Unfortunately, only one set of survey data (from the January 1995 land survey) covers this area, so simulated bed level changes in this area could not be evaluated.

A bar is also present at the upstream side of the offtake. In the initial stage of the calibration, the flow along the right bank downstream of the corner point at Talbaria was too high, whereas observations at the site have revealed a very high flow gradient, with the flow nearly reversing close to the bank. Due to the finite resolution in the numerical model, there is a limit to how steep the simulated flow gradient can be, using the same resistance number all over. Thus, the problem was overcome in the model by locally increasing the model resistance along the bank. If time allowed, a more detailed calibration could have been done. As it was anticipated, that the planform geometry is very important for the development of the offtake and a relative coarse calibration was done, a sensitivity run was carried out to assess the importance of inaccurate calibration. The results, see section 7.8, showed only a modest effect outside the Gorai mouth of changing the simulated shape of the bar.

The lateral diffusion of sediment (ie due to turbulence and secondary currents) is described mathematically in the model in the following ways: 1. A diffusion coefficient (calibration parameter) in the advection-dispersion model calculating the concentration of suspended sediment represents the turbulent diffusion, 2. The helical flow is computed explicitly from the main flow field and is used for calculating deviations between the directions of bed load and suspended load, 3. the dispersion of suspended sediment due to non-uniform vertical profiles of velocity and concentration is computed by applying Galappatti's (1986) model of primary as well as secondary (due to helical flow) profile functions in the integration routines at every time step. The 3D flow pattern is therefore to some extent taken into consideration. For fine-tuning of the model performance in this area, it is recommended to adjust the calibration parameters on diffusion, helical flow and profile functions, respectively, together with the hydrodynamic parameters governing the flow field.

Observations of changes of the channel through the bar at the offtake are crucial for understanding the behaviour of the morphodynamics. Comparison with measurements shows satisfactory agreement. Thus, the model provides a convenient tool for analysing the combined effects of a number of different processes in a more integrated way, although it is recommended to improve the model calibration at the offtake.

## 7.8 Sensitivity of Model Results

As mentioned in the above section, the simulated morphology is quite sensitive to a number of parameters. During the calibration period, various simulations were carried out to evaluate the sensitivity of the model against small changes in the input parameters. The most important simulations are described below. In addition to these, also the sensitivity to bank erosion along the right bank of the Ganges upstream of Gorai offtake was tested in a schematized model with a movable bed as well as movable bank description. Since it was not possible, however, to simulate bank erosion along this

bank in the local model without forcing the model parameters excessively, this sensitivity test was left out from this presentation.

**Boundary conditions**

Figure 7.8.7 illustrates the effect of using two different distributions of discharges at the upstream boundary. In the upper figure, it was assumed that most of the discharge entered along the right bank whereas in the lower figure, the discharge was distributed according to the local depth. Due to the applied sediment transport boundary condition, the inflow of sediment will also be high where the water inflow is high. Therefore, sediment is being deposited further downstream from the boundary where high inflow rates occur.

Water level simulations from the overall model have been used to establish the downstream boundary condition in the Gorai. The sensitivity to this boundary condition was evaluated by reducing the established water level boundary by 0.3 m throughout the simulation. The simulated bathymetry is shown in Figure 7.9.5 and 7.9.6. There is evidence from the historical data, see section 4.4, that the water level has been lower years ago for the same discharges, although this seemed to be only for the lower discharges.

A significant change of the Gorai occurs with this modest decrease in the water level at the downstream boundary. The offtake channel becomes much deeper and a substantial part of the total discharge is conveyed into the Gorai. Part of the reason for this sudden development is, however, to be found in the specification of the boundary condition: To specify a water level boundary is associated with some difficulties. As the model simulates a deeper and deeper channel in the Gorai and consequently a higher and higher discharge in the Gorai, one would expect that the water level in the Gorai would begin to rise. But by explicitly applying a water level boundary, this feedback is 'ruled out'. Combined use of 2D morphological modelling and 1D hydrodynamic modelling or simply using a discharge rating curve as a downstream boundary would have solved this problem. Still, the simulation shows that the development of the Gorai offtake is very sensitive to the applied downstream boundary conditions in the Gorai.

The boundary conditions upstream and downstream the Ganges govern to a large extent the simulated bathymetry. A change in the upstream discharge distribution (but not the total magnitude) resulted in a different bathymetry in the Ganges where the scour hole upstream of the offtake disappeared. The conditions in the Gorai were however less affected. The problem with high sensitivity to the boundary conditions can only be effectively solved by extending the modelling area. Thus, the predictability of the present model is relatively low when the scenarios which are being simulated are not pretty close to the conditions from the calibration event. If the same boundary conditions are used (i.e. the 1995 monsoon) the highest degree of reliability is obtained.

**Flow resistance**

The flow resistance in the Ganges and the Gorai was assumed to be a little different. This can be easily justified: The flow regime of the two rivers is very different, dunes may be present in the Gorai and not in the Ganges. Furthermore, man-made structures (groynes, bridges) add to the flow resistance of the Gorai. Two additional simulations were carried out to see the effect of variations in the flow resistance of Gorai.

The flow resistance in the Gorai river for the base run is assumed to be (h is depth, C is the Chezy number):

$$C = 26 \cdot h^{0.5}$$

In the model run with reduced resistance:

$$C = 29 \cdot h^{0.5}$$

In the model run with increased resistance:

$$C = 20 \cdot h^{0.5}$$

The simulated bathymetries at the end of each model run are depicted in Figures 7.8.3-7.8.4 (increased flow resistance in Gorai) and in Figures 7.8.5-7.8.6 (reduced flow resistance in Gorai). Significant differences in the development of the Gorai are found: With increased flow resistance, the Gorai becomes more shallow whereas with a decrease in flow resistance, the Gorai channel gets much deeper, and the opening through the upstream bar at the mouth becomes larger.

The model simulates a complex braiding pattern in the right side of Ganges downstream of the Gorai offtake: Several minor chars and a number of channels connecting the main channel with a small channel near the right bank are formed. The depth-dependency of the flow resistance (the exponent on the depth h) governs the deflection of the flow approaching more shallow areas. With a high depth-dependency (high value of the exponent), the flow tends to become deflected and braided channels (narrow and deep) form easily. With a low depth-dependency (low value of the exponent), the flow will tend to continue less diverted by bars and chars on its way, and will thereby tend to smoothen the bathymetry. This is demonstrated in a simulation with a constant flow resistance, in the Ganges $C=71\ m^{0.5}/s$ and in the Gorai $C=51\ m^{0.5}/s$, see Figure 7.8.8. The main channel is clearly wider and shallower, and the braided channels along the right bank have not emerged in this simulation. In the Gorai, the simulated braiding intensity is less important because the river flow is confined to a more narrow channel with other width/depth/slope relations than in the Ganges.

As discussed in section 7.7, a local increase in the flow resistance was necessary in the model setup to reproduce the minor bar at the Western side of the offtake. A simulation was carried out without this adjustment (extent shown in Figure 7.8.10) to see the effect both on the planform geometry of the offtake and on the water and sediment flow into the Gorai. Figure 7.8.9 and 7.8.10 shows the bathymetry after 2 and 4 months. The angle of incidence of the offtake channel is clearly different from the base run in Figure 7.8.2. Looking at the sediment transport and discharge into Gorai, a little difference (less than 10%) is noticed, Figure 7.10.13. The computed sediment transport and discharge ratios between Ganges and Gorai (Figures 7.10.16 and 7.10.26) are also quite similar to the base run although the discharge and sediment transport is in general higher after the monsoon. Compared to the other inherent uncertainties (boundary conditions and flow resistance), the model indicates that the reproduction of the development of the Gorai offtake is not that sensitive to the uncertainty in simulating the bar along the western bank.

## 7.9 Model Applications

Four scenarios were simulated with the model:

- Increase of the initial bar elevation in front of the offtake
- Narrowing of the offtake mouth
- Lowering of the water level in Gorai (through e. g. bend-cuts)
- Effect of extreme flood (1987)

The third simulation is also partly described in section 7.8 under sensitivity to boundary conditions.

Bar in front of the offtake

The simulation of the increased bar height in front of the offtake was carried out to give information about the impact of previous years heavy sedimentation (for instance 1987): Would a fairly average monsoon flood (1995) be able to reestablish the river bed levels at the offtake as if the bar level had not been increased initially?

The initial bed levels were increased by 2 m within an area of about 1 $km^2$ (indicated on Figure 7.9.1), but keeping the bed levels everywhere lower than 11 m PWD. Simulated bed levels are depicted in Figures 7.9.1-7.9.2. Compared to the base run, flow into the Gorai naturally starts later. A very narrow channel is being formed from the beginning and this channel even at some stage (early August) gets deeper than the channel of the base run, see Figure 7.10.3. The cross-section area, however, remains much lower than for the base run and at the end of the monsoon the cross section area remains lower than it was in the base run.

The recovery during one monsoon is clearly only partial. It remains an open question how long time full recovery would take.

Narrowing of the offtake mouth

A simulation was carried out with part of the Gorai offtake (the shallow part) artificially closed, see Figure 7.9.3-7.9.4. The part closure only becomes effective during high flow where the whole bar in front of the offtake is submerged. The idea of the narrowing would be to concentrate the flow into the Gorai along the western side of the offtake and thereby enhancing erosion of the channel through the bar.

It is difficult to see any significant difference in the developed bed levels compared to the base run in Figure 7.8.1. Close to the constriction, a local scour hole is noticed. The narrowing does, however, have a small but favourable effect on low stage flow to the Gorai, as the channel has become a little wider, see Figure 7.9.4.

The fact that the base run indicates considerable (and probably not realistic) growth of the bar immediately upstream of the applied narrowing may have reduced the simulated effect of the narrowing.

### Lowering of Gorai water level

The various river training works, other structures (e.g. bridges) as well as dredging activities in the Gorai affect the water levels. Furthermore, the river sinuosity is in some places rather high, and a bend-cut would cause significant changes in the water levels, at least locally, but after some years also along a longer stretch. As discussed in section 4.4, the low flow water level for a given discharge has increased by more than 1 m since the late 1940'es. To see the short-term effect on the bar development at the offtake of a modest change in the water level in Gorai, a simulation was carried out where the water level was lowered by 0.3 m constantly throughout the monsoon period. The simulation must be interpreted with caution as the uncertainty in using a water level boundary in this simulation is high (see previous section). Still, a remarkable change in the development of the offtake is noticed in Figures 7.9.5-7.9.6 indicating that downstream conditions have a large influence on the development of the offtake.

### Extreme flood event

The 1987 flood event was simulated to see the short-term effect of a high discharge event. Historical data indicate that high deposition took place in front of the offtake this year, see Chapter 4. The simulation, however, predicts heavy erosion. The reason for this is to be found in the way the downstream boundary condition in Gorai is established. For this particular application, this boundary condition could not be determined with any accuracy by the 2D overall model. Instead, a 1D model was used. Although the calibration of the 1D model at Gorai Railway Bridge was fairly good, some uncertainty in the downstream water level boundary condition remained. With a modest change in the water level boundary, the local model would have simulated deposition at the offtake instead of erosion, which is in line with the findings in section 7.7 regarding uncertainty of downstream water level boundary. Still, the modelling results show how big changes take place over the monsoon, Figures 7.9.7-7.9.8.

### Short-term effect of angle of incidence

A sensitivity run was carried out as discussed in section 7.8 to see the short-term effect of inaccurate calibration of the bar at the western side of the offtake, see Figure 7.8.9-7.8.10. The simulation also serves as a test of the effect of a different angle of incidence, as the model gave another slightly different angle of the channel through the bar at the offtake. As mentioned previously, the short-term effect was modest outside the river mouth area, see Figures 7.10.16 and 7.10.26. Still, there is a tendency towards higher discharge and sediment transport in Gorai if the angle between the main channel and the offtake channel is less.

## 7.10 Further Morphological Interpretations

The results of 2D morphological simulations contain a large amount of information. A user may have particular interests in certain parts of this information, communicated in the form of questions to the model(ler). Answering such questions can be done through extraction of certain results and presenting them in different ways. In the following such selected extracts of results are presented to ease the comprehension.

The dynamic response of the bed levels at the Gorai offtake to the variations taking place in the Ganges is crucial for understanding how and why the offtake conditions change. Time series plots of the development of a threshold cross section profile indicated in Figure 7.10.1 have therefore been produced together with computer animations, by which the simulated results can be displayed on a PC (attached on a diskette).

Another way of presenting the modelling results, which is convenient for interpretations, is to plot water levels, discharges, and sediment transport rates against each others. Especially the simulated rating curves at the Gorai Railway Bridge give an indication of the morphological development of the Gorai. But also the distribution of sediment at the offtake is important because this result is vital for developing a 1D morphological model.

**Dynamic response of the offtake to varying river discharge**

The elevation of the bar in front of the offtake as a function of time is shown in two different ways in Figures 7.10.2-7.10.4 for all the reported simulations: 1. The minimum bed level (i.e. bed level of the channel through the bar), and 2. the cross-section area below the elevation 10 m PWD. The discharge in the Ganges at the same time is also displayed. The exact location of the considered cross-section is indicated in Figure 7.10.1.

With a higher resistance in the Gorai, the bed level at the mouth is generally higher than in the base run. With a lower resistance in the Gorai, the bed level is below the base run. An important feature is, that the elevation of the bar follows the variations in the river discharge. The bar is growing during rising flood and decaying during receding flood. As mentioned in section 7.5, there seems to be a natural constriction of the Ganges just upstream the offtake. In a study of the morphological conditions at the Hardinge/Paksey Bridge sites (DHI/SWMC, 1996a), it was shown that the bed levels follow the stage of the river: Erosion during rising stage, deposition during falling stage. Thus, the eroded material just upstream the offtake may deposit here during rising stage. During falling stage, there may be a relative deficit of sediment transport, and erosion can take place at the offtake. This explanation does, however, for the time being remain a hypothesis, which could not be properly tested during the present study.

The implication of the apparent relation between the flood dynamics and bar development is that upstream control of the river flow in the Ganges may have a significant impact on the bed level development at the Gorai.

The animation (on a diskette at the back of this report) clearly shows the dynamics with a channel opening and closing in response to the discharge conditions in the Ganges. Both a 2D horizontal plan view and a 2D cross-section view are displayed.

**Rating curves**

The base run presented as discharge against water level at Gorai Railway Bridge in Figure 7.10.5 (full line) shows that the rating curve starts and ends approximately at the same point indicating that the Gorai river is in equilibrium (although it is known that in the long term, it is changing). Compared to the base run, the increased flow resistance in the Gorai is seen to have the short-term effect that the discharges for the same water levels are smaller and also that the rating curve ends further down

compared to where it started at the beginning of the monsoon (dotted line). This indicates a slow closure of the Gorai.

In the same figure, the short-term effect of reduced resistance in the Gorai is depicted (dashed line). Expectedly, the results compared to the baseline simulation are opposite to the results of increased resistance: The discharges are much higher and the rating curve is changing significantly, especially after the peak of the flood.

The implication of the findings with the two different simulations with varying flow resistance in the Gorai, is that the flow resistance has a significant influence on the development of the offtake. Contributions to increased flow resistance in the Gorai near the mouth are river training works (groynes) for bank protection at Kushtia, and constrictions of the river, for instance at Gorai Railway Bridge as well as increased sinuosity. It is important to note, however, that the findings with the present model is only valid considering a short period (few years). For evaluating long term effects, other study tools must be applied, see later.

In the simulation with a bar height increase initially by two metres, the flow into Gorai starts later compared to the base run. The maximum discharge is only 3,400 $m^3/s$ compared to 4,200 $m^3/s$ in the base run. Furthermore, the rating curve ends significantly lower than in the base run.

The short-term effect of narrowing the offtake mouth is seen in Figure 7.10.7. Although, only small differences from the base line simulation are seen, they are quite interesting: During high flow, the discharge with the constriction is less. That is because the effective flow area is reduced when the whole bar is submerged. During low flow, after the monsoon, the discharge is a little higher instead. This is because more scouring takes place during receding flood at the offtake due to concentration of the flow. So, even though the narrowing has been made within a shallow area, it is in fact having a positive effect on dry season flow to the Gorai.

Change in the downstream boundary condition in Gorai has a significant impact according to the model, see Figure 7.10.8. The discharge gets very high, up to 7,500 $m^3/s$. Although, the applied boundary condition may be unrealistic, the simulation demonstrates an important fact: The flow into the Gorai will be enhanced by lowering the water level in the Gorai. By increasing the water level, the reverse would happen: The discharge into Gorai would become less. Over the last decades the rating curve at Gorai Railway Bridge has changed in a way which would worsen the performance of the offtake: For the lower discharges, the corresponding water level has risen significantly.

The conveyance factor in the Gorai mouth was calculated from the base simulation and compared with the conveyance factor calculated from measurements, see section 4.6. The comparison which is depicted in Figure 7.10.9 is fairly good.

**Sediment distribution at an offtake**

One-dimensional modelling is required for simulating the long-term developments in river morphology. The major constraint of a 1D model is, however, that it cannot predict the distribution of sediment at an offtake or a bifurcation. This shortcoming is inherent in a one-dimensional model, and the distribution has to be specified explicitly by the model user. The present two-dimensional model constitutes a convenient tool for determining the sediment distribution at offtakes.

For analysing the distribution of discharge and sediment, the integrated discharge and sediment transport over two cross-sections have been extracted: Upstream of the offtake and downstream of the offtake in the Gorai. The discharge has simply been extracted in a line whereas a mean value of sediment transport over 30 grid lines (ie 2-3 km) at the two locations has been computed for every time step, see Figure 7.10.1. This was done in order to filter out bed form perturbations which would otherwise disturb the picture.

The following modelling results are plotted:

- Time series of $Q_a$, $Q_b$, $S_a$ and $S_b$, Figures 7.10.10-7.10.13
- Time series of $Q_b/Q_a$, $S_b/S_a$ and $(S_b/S_a)/(Q_b/Q_a)$, Figures 7.10.14-7.10.16
- Diagrammes of $S_a/S_b$ against $Q_a/Q_b$ , Figures 7.10.17-7.10.28

where Q denotes water discharge ($m^3/s$), S denotes sediment transport rate (kg/s); subscript 'a' refers to the Ganges 'b' to the Gorai.

The time series plot show that the times when the sediment transport peaks do not match completely the times of peaks in discharge. Therefore, loops appear in the sediment rating curves.

Time series of the sediment transport ratio between Ganges and Gorai reveal that the first 14 days up to 4 July is very different from the last 3½ months. It could be due to specific conditions just after opening of the Gorai but it is more likely due to the effect of inaccurate initial conditions (bed levels). Except from the first 14 days, there is a clear correlation with the discharge distribution between Ganges and Gorai.

**Long-term versus short-term effects**

Throughout this presentation, it has been emphasized that the 2D model simulates short-term developments (ie one monsoon). For evaluating long-term trends, other study tools such as 1D modelling or river regime equations have to be used. The essential basic information required for any long-term analysis is the distribution of discharge and sediment between the Ganges and the Gorai as discussed by Wang et al., 1995, who tested various assumptions in a 1D model of a bifurcation. This information could be obtained from field measurements (in this case the sediment and discharge rating curves from Hardinge Bridge and Kushtia). With a well calibrated 2D model, more detailed information can be provided from the model results. Moreover, the 2D model shows the dynamic behaviour of the sediment and discharge distributions and the inherent loops in the ratios as discussed below.

The sediment transport ratio is plotted against the discharge ratio in Figures 7.10.18 to 7.10.21. The previously mentioned 14 days at the beginning of the period are seen here as a horizontal line for large discharge ratios. The loops in the diagrammes indicate that there is no simple relationship between the sediment transport ratios and the discharges ratios by which sediment and flow is shared between the two rivers.

For a more clear impression of the seasonal variations in sediment transport ratios, moving averages of these curves are presented: Figure 7.10.22 shows the effect of using different filters (14, 42 and 120 days moving average). Certain dates are indicated along the curves to indicate times when significant changes occur. The total number of simulated days is 120. With the 14 days filter, sudden changes in the discharge and sediment ratios occur on 2 August when the second flood of that monsoon

starts to rise, and on 2 September, which is at the peak of the third flood. In between periods seem to experience more stable developments in sediment and discharge ratios. Similar sudden changes are seen for the other model runs as well, see Figures 7.10.23 to 7.10.24, although the curves may have quite different shapes. The reason may be found in the imposed boundary conditions, which are the same except for all simulations except for the 1987 flood simulation.

The (unrealistic) simulations of substantial erosion of the offtake channel are interesting to plot in these diagrammes as well because they show the behaviour of the channels when the offtake develops towards a bifurcation, see Figure 7.10.25. Due to limited time of the present study, further investigation of these characteristics have not been carried out.

For rough estimates of the long-term morphological state of equilibrium of a river, the simple expression by Lane (1955) may be used:

$$S \cdot D \sim Q \cdot i$$

where S is sediment transport ($m^3/s$), $D$ is grain size (mm), $Q$ is discharge ($m^3/s$), $I$ is energy slope of the river (m/m) and $\sim$ means 'proportional to'. Assuming a time-constant grain size and proportionality factor, the following expression for long-term equilibrium is obtained:

$$\frac{S_{Gorai}}{S_{Ganges}} = k \cdot \left[\frac{i_{Gorai}}{i_{Ganges}}\right] \cdot \left[\frac{Q_{Gorai}}{Q_{Ganges}}\right]$$

Klaassen (1995) investigated Lanes balance further and used it to assess the state of equilibrium of the main rivers in Bangladesh. He improved the balance relation by combining a flow formula (Chezy formula $u = C \cdot h^{0.5} \cdot I^{0.5}$) and a sediment transport formula ($S = D^{-p} \cdot m \cdot u^{n}$). With p, m, n and the Chezy number, C, being constants, he obtained:

$$\frac{S_{Gorai}}{S_{Ganges}} = k \cdot \left[\frac{i_{Gorai}}{i_{Ganges}}\right]^{\frac{n}{3}} \cdot \left[\frac{Q_{Gorai}}{Q_{Ganges}}\right]^{\frac{n+3}{6}}$$

If the Chezy number is not a constant but is depth-dependent as it is in the model simulations ($C \sim h^{1/2}$), or a constant Manning number had been applied ($C \sim h^{1/6}$), the powers of the two ratios of the above formula are somewhat different. The powers in the three cases are shown in the table below.

| CASE | Q-power | | i-power | |
|---|---|---|---|---|
| | General | n=5 | General | n=5 |
| Constant Chezy number | (n+3)/6 | 1.33 | n/3 | 1.67 |
| Constant Manning number ($C \sim h^{1/6}$) | (5+2n)/10 | 1.50 | 3n/10 | 1.50 |
| Depth-dependent Chezy as in simulations ($C \sim h^{1/2}$) | (n+1)/3 | 2.00 | n/4 | 1.25 |

The modified Lane relation is presented together with the average sediment transport and discharge ratios in Figures 7.10.27-7.10.28 assuming a constant slope, n=5 and with k selected in such a way that the modified Lane matches with the results of the base run. Points on the line representing the modified Lanes equation (called Lane line hereafter) are according to this theory in equilibrium. Roughly interpreted, points above the Lane line may represent a situation where the river is overloaded with sediment, and it will therefore try to increase its slope, I. Similarly, points below may represent an underloading situation, where the river would respond by developing towards a more gentle slope. The large seasonal variations predicted by the 2D model including the upper Gorai where for instance the slope is highly variable, see Figure 7.10.22, gives an impression of the simplifications inherent in the modified Lane's expression, which should therefore only be used for long-term predictions. The various scenarios simulated with the 2D model is also depicted together with the Lane line in Figure 7.10.27. According to the above interpretations, the scenarios apparently have long-term effects which are opposite to their short-term effects: With higher resistance in the Gorai, the river becomes underloaded with sediment. With lower flow resistance in Gorai, it becomes overloaded with sediment. With lowering of the downstream water level in Gorai, the river becomes overloaded with sediment.

The above comparisons show the importance of assessing both long-term and short-term developments. Jansen et al (1979, p. 410) briefly discusses the time aspects of the design of a diversion channel. Increase of the slope (lowering of downstream water level scenario) was mentioned as a possibility for increasing the ratio of the flow diverted to the Gorai, but at the same time the sediment inflow would become much higher and eventually lead to sedimentation.

These initial reflections on the long term development of the Gorai were using a modified Lanes balance with a number of inherent simplifications: A rectangular cross section was assumed and also a simple empirical relation between width and discharge. A one-dimensional morphological model will be able to provide similar evaluations but with better quantifications, because less simplifications are required. Furthermore, the 1D model can be used to investigate the time scale of long term developments.

A combination of 1D (long-term balance) and 2D (short-term) morphological modelling would be a very convenient method. Wang et al (1995) demonstrated the applicability of 1D morphodynamic models to investigate the overall response of bifurcating channels as a function of the sediment distribution at the bifurcation. Morphological modelling with a 1D model of the Ganges-Gorai river system is on-going at SWMC, where the results from the present 2D model is being used (SWMC/D-HI, 1996).

## 7.11 Conclusions

Two models, an overall hydrodynamic model and a local fully morphological model, have been set up, calibrated and applied for investigation of the offtake mechanisms. The overall model was used for pilot modelling in the beginning of the study and gave important information for setting up a field measurement programme. The overall model also supplied boundary conditions for the local model.

Hydrodynamics and sediment transport rates were reproduced to a satisfactory degree in the two models. The aim of the morphological modelling was to simulate the dynamic (short-term) equilibrium of bed levels at the offtake. The simulated and measured bed level changes in the Ganges river showed some discrepancies with respect to location and extent of erosion and deposition. From various sensitivity analyses it was concluded that the model could be tuned to reproduce the right pattern in

the Ganges, had time been available, but also that the model area would be too small if the objective was to assess the morphology in the Ganges. For further studies it is recommended to extend the local model instead of using boundary conditions from the overall model.

For the Gorai, the performance of the morphological model was assessed to be satisfactory based on comparisons between simulated and observed discharge rating curves, sediment transport rating curves, and bed level changes as well as planform changes at the offtake. Sensitivity tests were carried out where the model exhibited both general accretion and erosion of the bar in front of the offtake as well as different shapes of the offtake channel. Valuable information was extracted from these simulations. The flow resistance in the Gorai river appeared to be of major importance for the morphology at the offtake: With a modest increase in flow resistance, the offtake would close and with a similar modest decrease in resistance the offtake would develop and become larger on a short-term basis.

A full dynamic flood (1995) was simulated in all cases which gave the opportunity to investigate the dynamic response in bed levels. The simulations showed that deposition takes place during rising stage in Ganges. During falling stage, the bar in front of the offtake is being eroded. Accordingly, it can be concluded that a change in the flood dynamics by upstream discharge control has an influence on the deposition-erosion balance at the Gorai mouth.

Four different scenarios were simulated. The 1987 extreme flood event was simulated. According to measurements heavy deposition at the entrance was expected. However, the model showed the opposite. By varying the downstream boundary condition slightly it was concluded that the uncertainty in determining the downstream water level for this case was the reason for the discrepancy.

The flow conditions in the Gorai are subject to continuous changes due to man-made regulations of the river as well as natural morphological processes such as bend-cuts of river bends. To evaluate the sensitivity of such changes to the development of bed levels at the offtake, one application simulated flow and morphology with the water level lowered by 0.3 m at the downstream model boundary between Kushtia and Gorai Railway Bridge. The simulation showed a large increase in the discharge to Gorai over the monsoon. Thus, changes in downstream conditions in the Gorai, for instance from river training structures, bridges etc. seem to be quite important.

A scenario with narrowing of the river mouth was included in the model setup to see the short-term effects of a change at the offtake location itself. By narrowing the river, one might expect that the flow would be more concentrated and therefore be able to erode a deeper channel through the bar. The simulation showed a weak tendency towards less deposition during rising stage and more erosion during falling stage.

Finally the short-term effect of a higher elevation of the bar in front of the offtake at the beginning of the monsoon was investigated to see whether an ordinary monsoon flow would be able to reestablish the offtake geometry after a year with substantial deposition. The answer was negative according to the 2D model. A channel would be eroded through the bar, but not sufficiently deep and wide to avoid slow accretion of the bed levels around the offtake. The future developments during monsoons to come remain an open question.

The offtake mechanisms were demonstrated, but no long-term development was simulated. For this, a one-dimensional model is required. The constraint of a one-dimensional model is, however that the distribution of sediment transport at offtakes and bifurcations has to be given as an input parameter.

The present two-dimensional model was applied for calculating these sediment transport distribution ratios. Often it was found that combination of 2D and 1D modelling would have been beneficial. None of the two types of models are able to stand alone in a detailed analysis of the complex hydrodynamics and morphology of an offtake, but they would indeed complement each other very well.

To summarize, the following points were learnt or confirmed from the 2D modelling

- the flood dynamics (rate of water level changes) is important for the development of the offtake
  - during rising stage, the bed level at the offtake raises and the channel becomes wider
  - during falling stage, the bed level drops and the channel becomes more narrow
- development of the bar in front of the offtake is quite sensitive to the flow resistance in the downstream reach of the Gorai
- by careful calibration of the flow and sediment transport at the entrance, it is possible to reproduce the shape of the offtake channel, which has some effect on the river development further downstream.
- a sudden increase in bed levels at the offtake (due to for instance one year of severe flood) would remain in the following year after a normal flood event
- the 2D model provided valuable information about distribution of sediment at an offtake, which can be used in a 1D model for long-term predictions.
- the chosen modelling area was too small to allow for accurate model predictions as the boundary conditions had significant effect on the results. Thus, the same flood event (1995) had to be used for calibration and application of the present model.

As it was the intention to develop a pilot model of the Gorai Offtake by which morphological processes could be demonstrated and investigated in more details, the objectives of the present mathematical modelling study have been well covered.

The main limitation of the 2D model is that it is basically 2D, and therefore not capable of simulating 3D effects (other than helical flow). The study indicated that 3D effects may be important within a limited area near the western bank at Gorai mouth. For the present simulations, it is also a limitation that bank erosion effects were not included. Simulation of bank erosion is, however, included in the software and it has been applied in another study, DHI/SWMC (1996).

# 8. Main Conclusions

Detailed conclusions for the study of historical data, RSP data and two-dimensional morphological modelling are given in section 4.7, Chapter 6 and section 7.11, respectively. The present Chapter presents the main conclusions of the study.

**Historical changes of hydraulic conditions**

- The minimum water level of the Ganges has clearly fallen since 1964 by more than 2 metres. The drop has been particularly sharp after 1987, but seems to have been going on gradually over the entire period. The maximum water level does not show any decreasing or increasing trends.

- The time it takes for the Ganges water level to fall from 11 m to 7 m PWD has reduced to half over the last 20 years. This may be critical for the erosion of a dry season offtake channel.

- The bed levels at the controlling cross section at Gorai mouth have increased in the last decade by on average 1-1.5 metre. The high flood of 1987 initiated this increase. The increasing bed level after 1987 seem to have caused reduced conveyance for the flow to Gorai for all stages. Repeated dredging seem to have provided only a short term solution.

- There is a tendency of narrowing of the lower part of the controlling cross section at Gorai mouth since 1982 and increased from 1989 (may be due to the dredging of narrow channels). The intermediate part of the cross section, and to some extent also the upper part, shows a tendency to widen since 1987.

**Analysis of RSP data**

- The development of the curvature of the bend upstream of Gorai offtake is cyclic in time (period of the order of 40-50 years). Presently the development is towards a sharper bend, and it is likely this will continue some years ahead.

- Typical grain diameters are:
  Ganges: $d_{50}$ = 0.15 mm
  Gorai mouth: $d_{50}$ = 0.17 mm

- The total volume of erosion upstream of Gorai offtake has been estimated to be in the order of 10 mill. $m^3$/year (deposited volume), corresponding to an average contribution to the sediment transport balance of this area of approximately 0.2 $m^3$/s (grain volume).

- The main features and developments of the bathymetry locally at and near Gorai mouth over a monsoon period are as follows:

  - the deepest channel becomes more shallow and wider at the peak of the monsoon as it was before the monsoon; after the monsoon it again becomes deeper and more narrow

- the changes in position and direction of the deepest channel seem to be minor, although there seem to be a tendency that the main offtake channel moves towards the left bank of Gorai

- the large scour hole near Talbaria was there also in 1992 and has not moved significantly since

- the 1992 bathymetry shows the presence of two offtake channels. The tendency of formation of a two-channel system was also observed from the 1995 bathymetries

- Water level slopes in the upper Gorai (down to Gorai Railway Bridge) indicate that the controlling cross section moves during the monsoon: At the lower stages in the Ganges the Gorai mouth is clearly a controlling section, but as the discharge to the Gorai increases at higher stages of the Ganges, this control vanishes; it may have been replaced by a control further downstream.

The set of data collected by the RSP from within the study area is very extensive and detailed. It has only been partly utilised in the present study. This data set will be very useful in possible future studies including modelling of the Gorai offtake.

**Morphological modelling**

In summary, the following points were learnt or confirmed from the 2D modelling (for details see section 7.11):

- The flood dynamics (rate of water level changes) is important for the development of the offtake

  - during rising stage, the bed level at the offtake raises and the channel becomes wider

  - during falling stage, the bed level drops and the channel becomes more narrow

- Development of the bar in front of the offtake is quite sensitive to the flow resistance in the downstream reach of the Gorai. The sensitivity of the bar development to the sediment transport in the Ganges may be high, but needs to be tested further.

- By careful calibration of the flow and sediment transport at the entrance, it is possible to reproduce the shape of the offtake channel, which has some effect on the river development further downstream.

- A sudden increase in bed levels at the offtake (due to for instance one year of severe flood) would remain in the following year after a normal flood event

- The 2D model provided valuable information about distribution of sediment at an offtake, which can be used in a 1D model for long-term predictions.

- The chosen modelling area was too small to allow for accurate model predictions as the boundary conditions had significant effect on the results. Thus, the same flood event (1995) had to be used for calibration and application of the present model.

The pilot morphological model of the Gorai offtake has provided valuable information about the morphological nature of offtakes. It has contributed to a scientific explanation for the closure of the Gorai river, and it has highlighted the complexity of the morphological developments of offtakes. Some indications regarding measures to change the ongoing development have been obtained from the model applications and the potential of using 2D modelling for this kind of investigations has been demonstrated although it is stressed that 2D modelling cannot stand alone; other study tools are required to study long-term effects. The importance of distinguishing between long-term and short-term effects has been discussed and comparison between 2D model results and a simple analytical long-term predictor was done.

Local engineers at the Surface Water Modelling Centre have received initial training in the use of the present modelling technology.

# 9. Recommendations

The complexity of the morphology of offtakes implies that future analyses should rely on more than a single tool. Different analytical and modelling tools should be combined and the extensive data base collected by the RSP should be utilised fully. For the Gorai, especially the ADCP backscatter data and float tracking data should be utilised fully to contribute to a more complete description.

It is recommended to use the experience in mathematical modelling gained by the modelling engineers at Surface Water Modelling Centre to further explore the morphological developments of offtakes, the Gorai offtake in particular. Such further modelling should at least initially be guided by the modelling system developers to avoid misinterpretations. For improvement of the model performance, the following should be considered:

- Extension of the modelling area
- Combination of 2D and 1D morphological modelling
- Improvement of the calibration, in particular the flow field pattern at the Gorai mouth
- Carry out more sensitivity tests (especially resistance and sediment transport relation)
- Include the effect of bank erosion

Results of the present 2D modelling should be used to optimize the choice of modelling area, the coupling with a 1D model, choice of type of boundary conditions as well as optimization of the calibration. The present pilot modelling gives some ideas regarding selection of scenarios to be investigated, but more may be added.

For other offtakes it is recommended to carry out analyses of the historical development of the offtake in line with the analyses presented for Gorai, if availability of data allows. The analysis may, however, be more complex in case of multiple and/or shifting channels and in case of tidal influence. Such analyses should be carried out prior to or in connection with modelling.

# 10. References

Danish Hydraulic Institute, 1996
Short Description, MIKE21C Curvilinear 2D Modelling System.

Danish Hydraulic Institute/ Surface Water Modelling Centre, 1996.
Mathematical Morphological Modelling of the Jamuna Bridge Site.
First Forecast Report, March 1996. Second Forecast Report, October 1996.
Jamuna Multipurpose Bridge Authority.

Danish Hydraulic Institute/Surface Water Modelling Centre, 1996a
Paksey Bridge Two-Dimensional Model Study, Final Report, July 1996.

Enggrob, H. G. and von Lany, P. H, 1994
An Application of 2D Mathematical Modelling on the Brahmaputra River, 2nd Int. Conf. River Flood Hydraulics, 22-25 March 1994

Engelund, F., Hansen, E., 1967
A Monograph on Sediment Transport in Alluvial Streams
Teknisk Forlag, Copenhagen, Denmark

FAP1 River Training Studies of the Brahmaputra River, 1993.
Final Report, Mathematical Modelling.
Sir William Halcrow & Partners Ltd. in association with Danish Hydraulic Institute, Engineering & Planning Consultants Ltd., Design Innovations Group.

FAP4 Southwest Area Water Resources Management Project, 1993
Final Report. Volume 3, Morphological Studies.
By Sir William Halcrow & Partners in association with Danish Hydraulic Institute, Engineering and Planning Consultants Ltd., Sthapati Sangshad Limited. August 1993.

FAP24 River Survey Project, 1993.
Selection of Study Topics for Phase 2. September 1993.
GoB/FPCO. Donor: Commission of the European Communities (CEC)
Delft Hydraulics, Danish Hydraulic Institute, Osiris, Hydroland, Approtech.

FAP24 River Survey Project, 1993a.
Report on Land Survey: Water Level Gauging. Special Report 1, June 1993.
GoB/FPCO. Donor: Commission of the European Communities (CEC)
Delft Hydraulics, Danish Hydraulic Institute, Osiris, Hydroland, Approtech.

FAP24 River Survey Project, 1995.
Study Programme, February 1995. Annex 3.
GoB/FPCO. Donor: Commission of the European Communities (CEC)
Delft Hydraulics, Danish Hydraulic Institute, Osiris, Hydroland, Approtech.

FAP24 River Survey Project, 1995a.
2D Morphological modelling. Internal Note.
Hans Enggrob, 28 January 1995

FAP24 River Survey Project, 1995b.
1D-modelling for Gorai offtake. Internal Note.
Carsten Staub, 28 March 1995

FAP24 River Survey Project, 1995c.
2D-modelling for Gorai offtake. Internal Note.
Carsten Staub, 29 March 1995

FAP24 River Survey Project, 1995d.
Development of Hydraulic Conditions and Bed Levels at Gorai Mouth over the last 30 years. Working paper 6, March 1995.
GoB/FPCO. Donor: Commission of the European Communities (CEC)
Delft Hydraulics, Danish Hydraulic Institute, Osiris, Hydroland, Approtech.

FAP24 River Survey Project, 1995e.
2D Morphological Modelling of Gorai offtake.
Draft Work Report, 1 June 1995

FAP24 River Survey Project, 1995f.
Sediment Transport Predictors. Working paper.
GoB/FPCO. Donor: Commission of the European Communities (CEC)
Delft Hydraulics, Danish Hydraulic Institute, Osiris, Hydroland, Approtech.

Fredsøe, J., 1978
Meandering and Braiding of Rivers
J. of Fluid Mech., Vol 84, part 4

Fredsøe, J., 1979
Unsteady Flow in Straight Alluvial Streams: Modifications of Individual Dunes.
J. of Fluid Mech., Vol. 91, pp 497-512.

Galappatti, R., 1986
A Depth Integrated Model for Suspended Sediment Transport. Journal of Hydraulic Research, Vol. 23, No. 4, pp 359- 377

Jansen, P. P.; van Bendegom, L.; van den Berg, J.; de Vries, M.; Zanen, A., 1979
Principles of River Engineering

Klaassen, G.J., 1995
Lane's Balance Revisited, 6th International Symposium on River Sedimentation, New Delhi,India,7-11 November 1995

Lane, E.W., 1955
The Importance of Fluvial Morphology in Hydraulic Engineering, Transactions Am. Soc. of Civil Engineers, Paper 745, 17pp

Olesen, K.W., 1987
Bed Topography in Shallow River Bends
Faculty of Civ. Eng.,Delft Univ. of Tech., Report 87-1

Struiksma, N.; Olesen, K.W.; Flokstra, C.;de Vriend, H.J., 1985
Bed Deformation in Curved Alluvial Channels,
J. of Hydraulic Res., Vol. 23, no.1

Rijn, L.C. van, 1984
Part I: Bed load transport, J. of Hyd. Engrg., no.110, Oct. 1984
Part II: Suspended load transport, J. of Hyd. Engrg., no.110, Nov. 1984

Surface Water Modelling Centre, 1996
Bridge Improvement and Maintenance Project, Phase 2 (BIMP2).
Hydraulic Model Study for Seven Bridges, April 1996.

Surface Water Modelling Centre/ Danish Hydraulic Institute, 1996
Surface Water Simulation Modelling Programme, Phase III
One-dimensional Morphological Modelling of the Gorai
GoB/DANIDA, July 1996.

Wang, Z.B; de Vries, M.; Fokking, R.J.; Langerak, A., 1995
Stability of River Bifurcations in 1D Morphodynamic Models,
J. of Hydraulic Res., Vol.33, no.6

## List of Figures

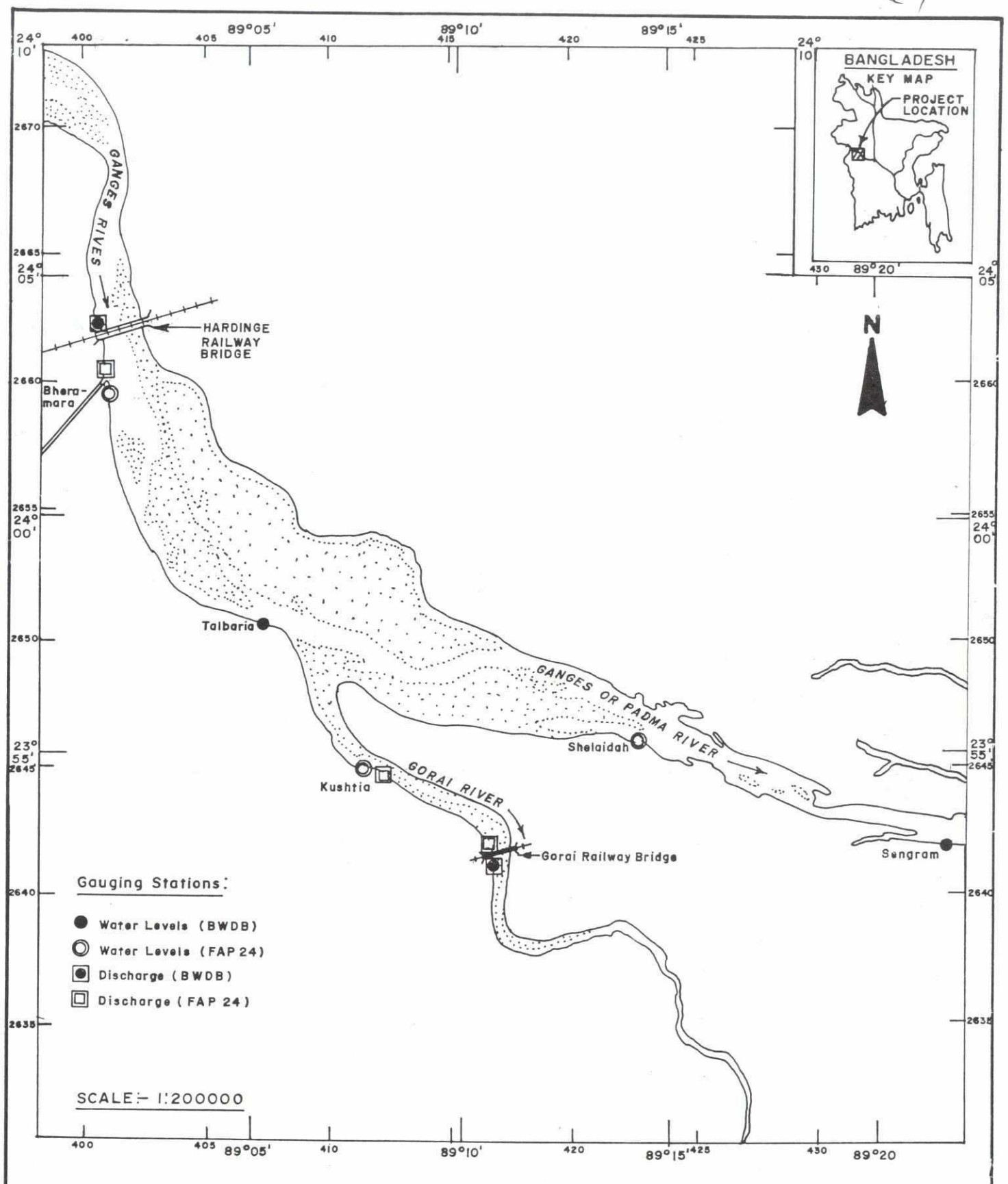


**Gorai Offtake Morphological Study**

Fig. 1.1 Hydrometric Stations

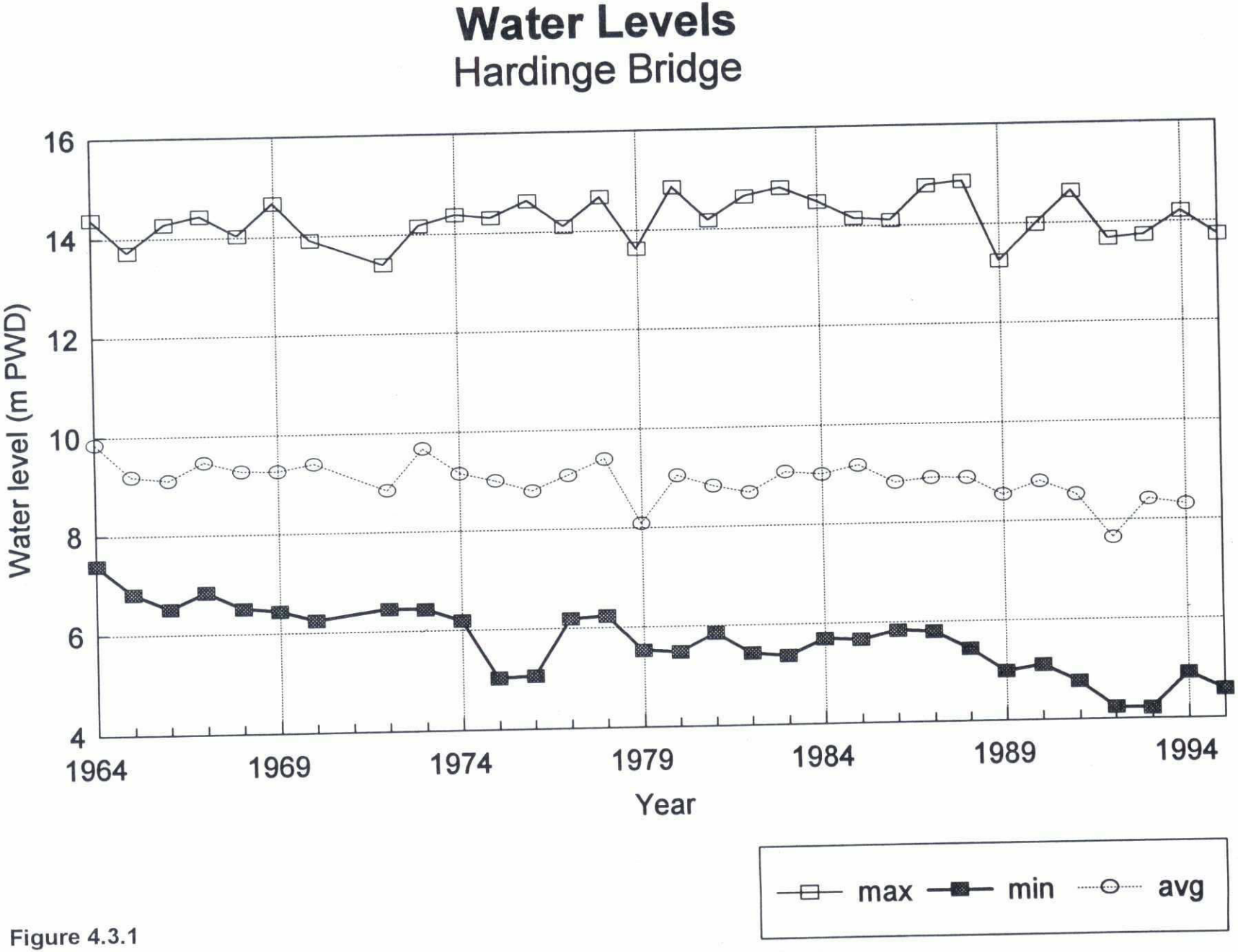
Water Levels
Hardinge Bridge
Water level (m PWD)
16
14
12
10
8
6
4
1964
1969
1974
1979
1984
1989
1994
Year
max
min
avg

Figure 4.3.1

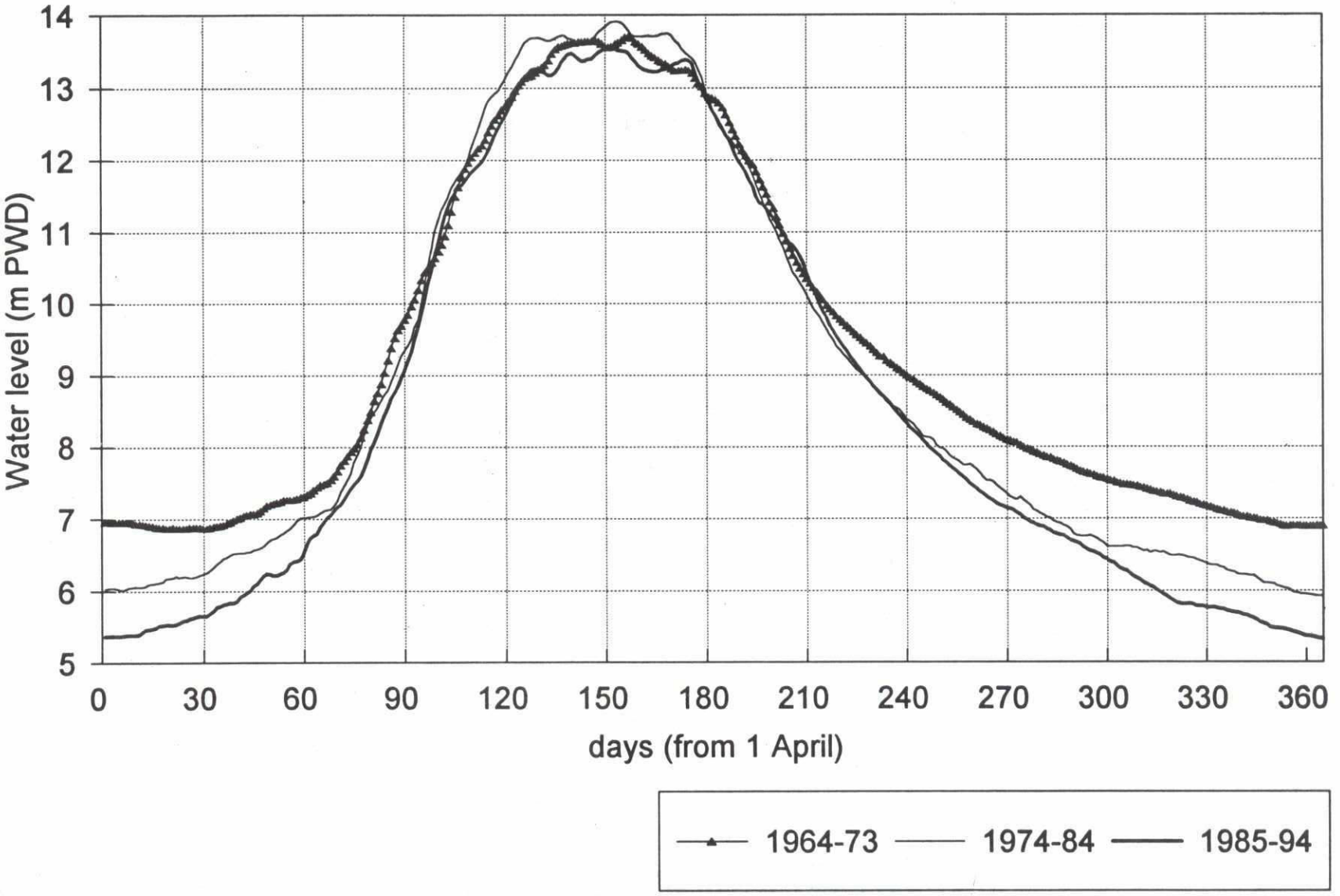
Hardinge Bridge
10-year averages of water levels
Water level (m PWD)
14
13
12
11
10
9
8
7
6
5
0
30
60
90
120
150
180
210
240
270
300
330
360
days (from 1 April)
1964-73
1974-84
1985-94

Figure 4.3.2

# Water level fall time (Ganges)
## 11 to 7 m PWD at Hardinge Bridge

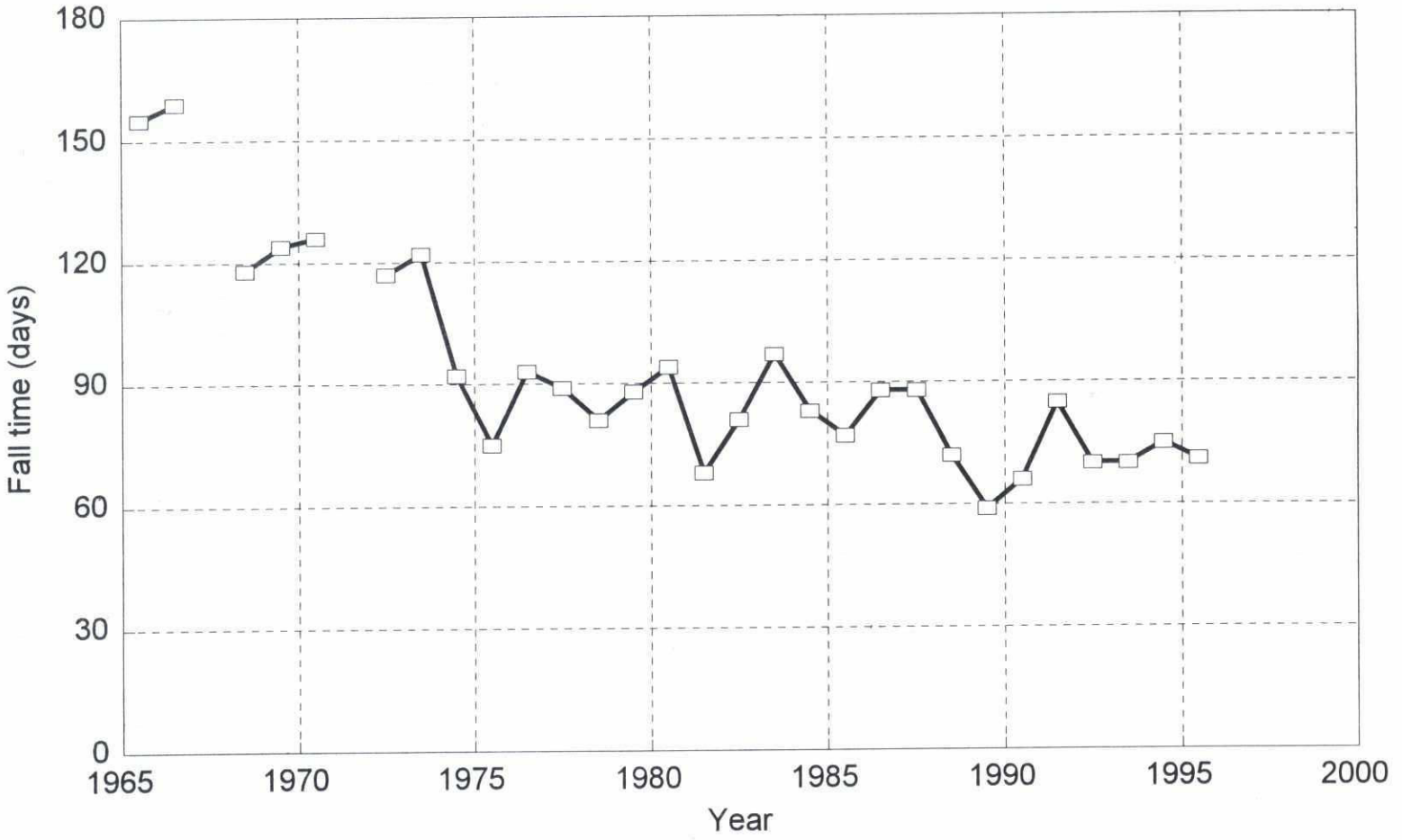


**Figure 4.3.3**

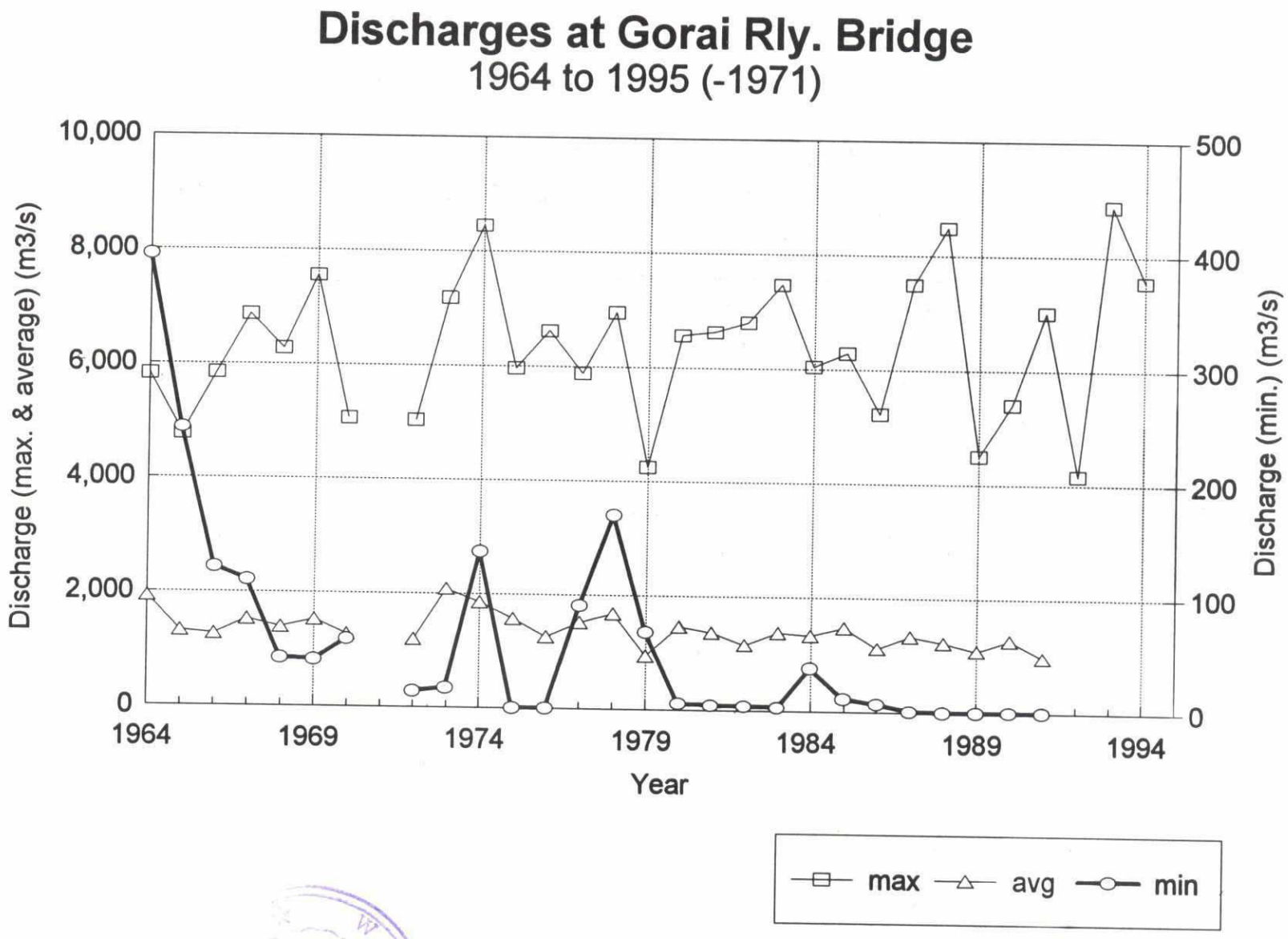
Discharges at Gorai Rly. Bridge
1964 to 1995 (-1971)
Discharge (max. & average) (m3/s)
Discharge (min.) (m3/s)
10,000
8,000
6,000
4,000
2,000
0
500
400
300
200
100
0
1964
1969
1974
1979
1984
1989
1994
Year
max
avg
min

Figure 4.4.1

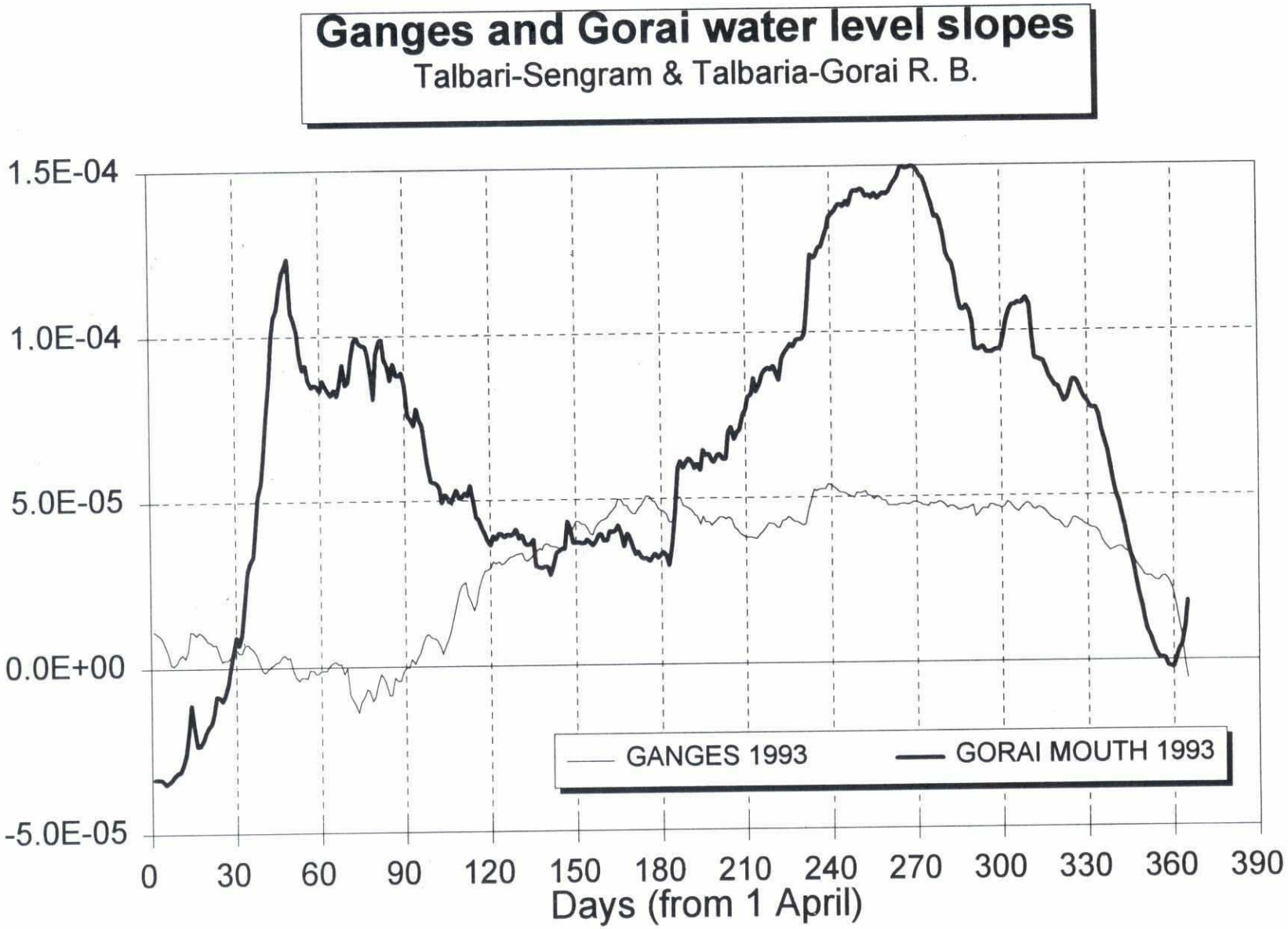
Ganges and Gorai water level slopes
Talbari-Sengram & Talbaria-Gorai R. B.
1.5E-04
1.0E-04
5.0E-05
0.0E+00
-5.0E-05
0
30
60
90
120
150
180
210
240
270
300
330
360
390
Days (from 1 April)
GANGES 1993
GORAI MOUTH 1993

Figure 4.5.1

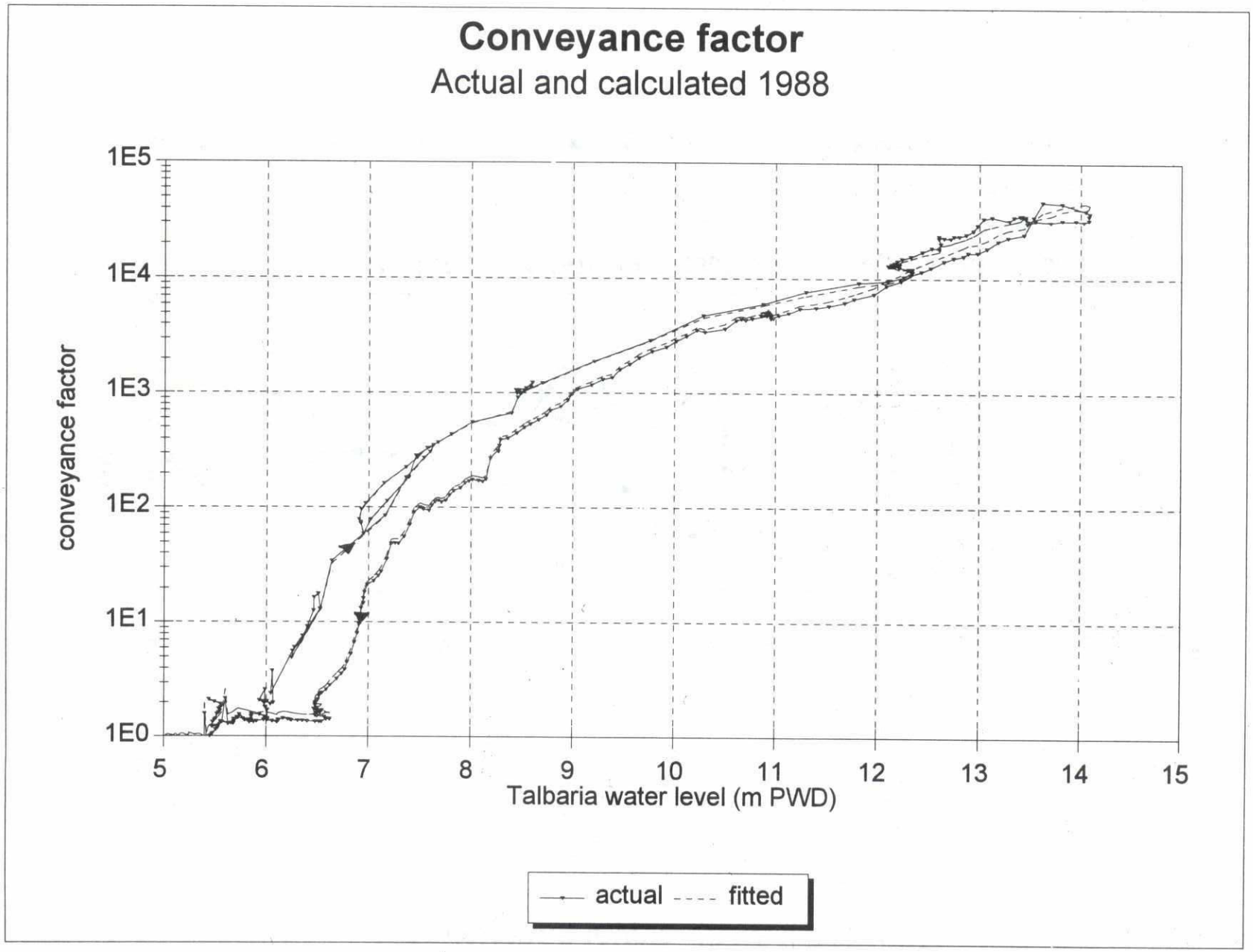
Conveyance factor
Actual and calculated 1988
conveyance factor
1E5
1E4
1E3
1E2
1E1
1E0
5
6
7
8
9
10
11
12
13
14
15
Talbaria water level (m PWD)
actual
fitted



Figure 4.6.1

# Gorai offtake

## Conveyance levels (K=A*R*^(2/3))

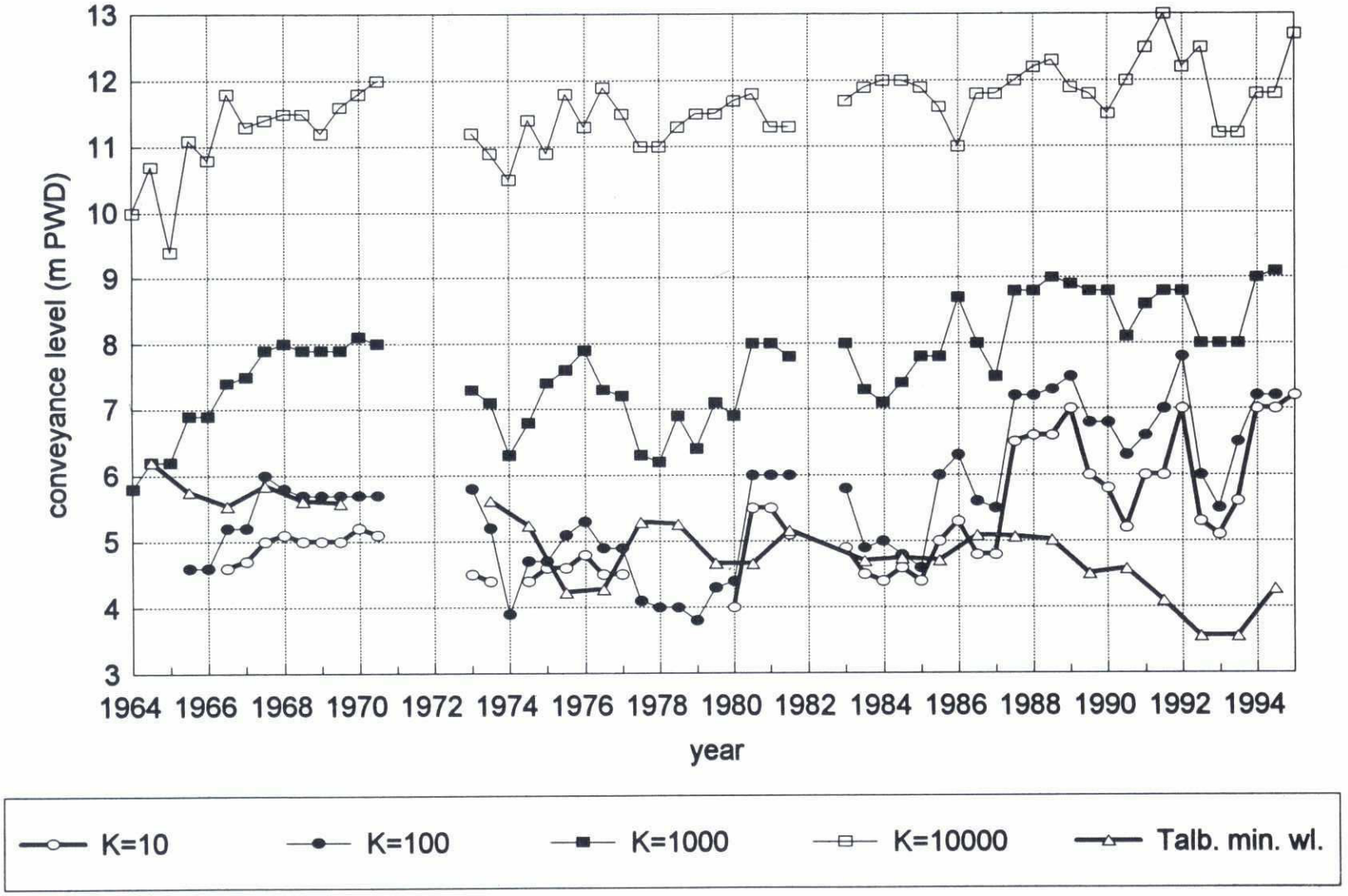


Figure 4.6.2

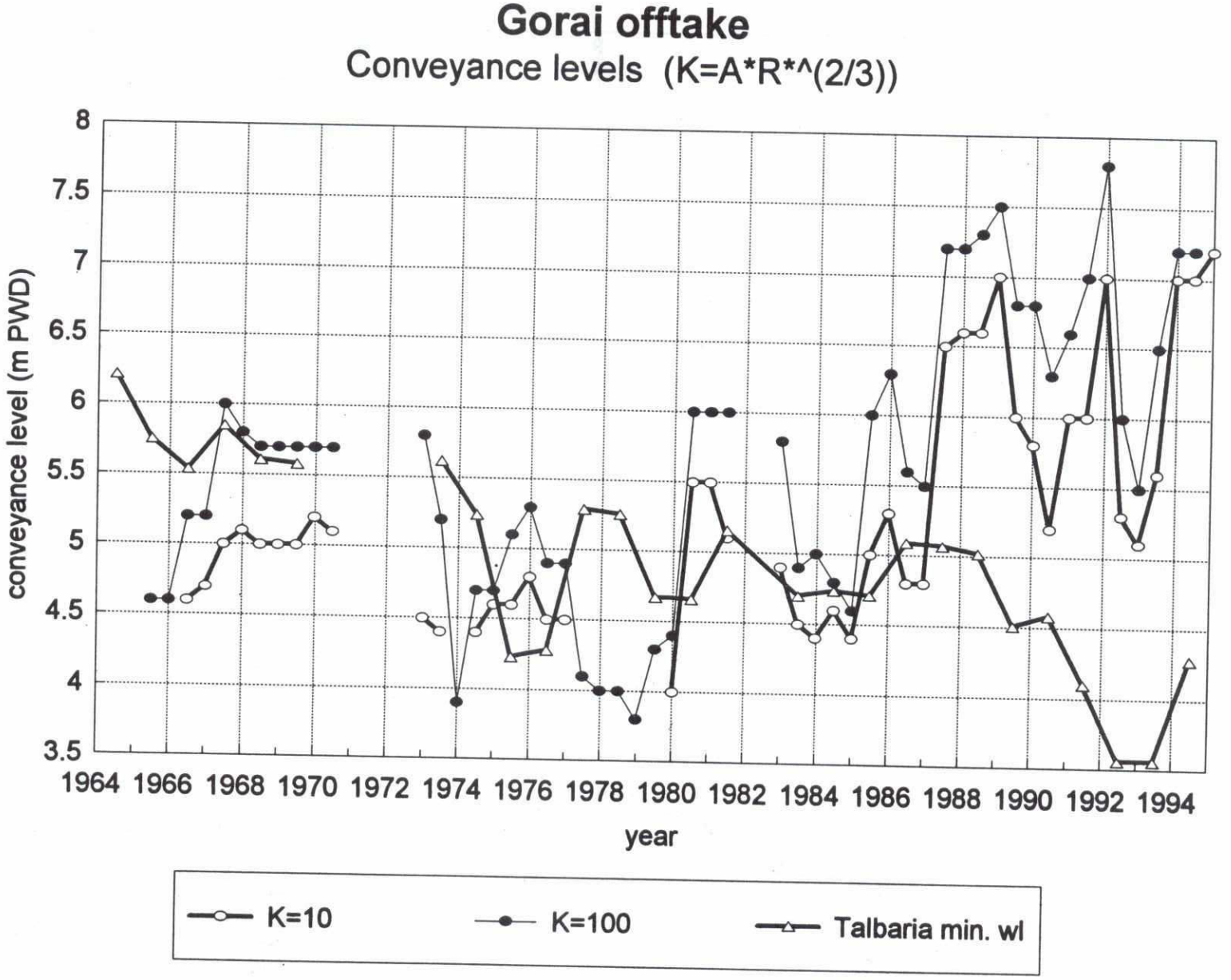
Gorai offtake
Conveyance levels (K=A*R*^(2/3))
conveyance level (m PWD)
8
7.5
7
6.5
6
5.5
5
4.5
4
3.5
1964 1966 1968 1970 1972 1974 1976 1978 1980 1982 1984 1986 1988 1990 1992 1994
year
K=10
K=100
Talbaria min. wl

Figure 4.6.3

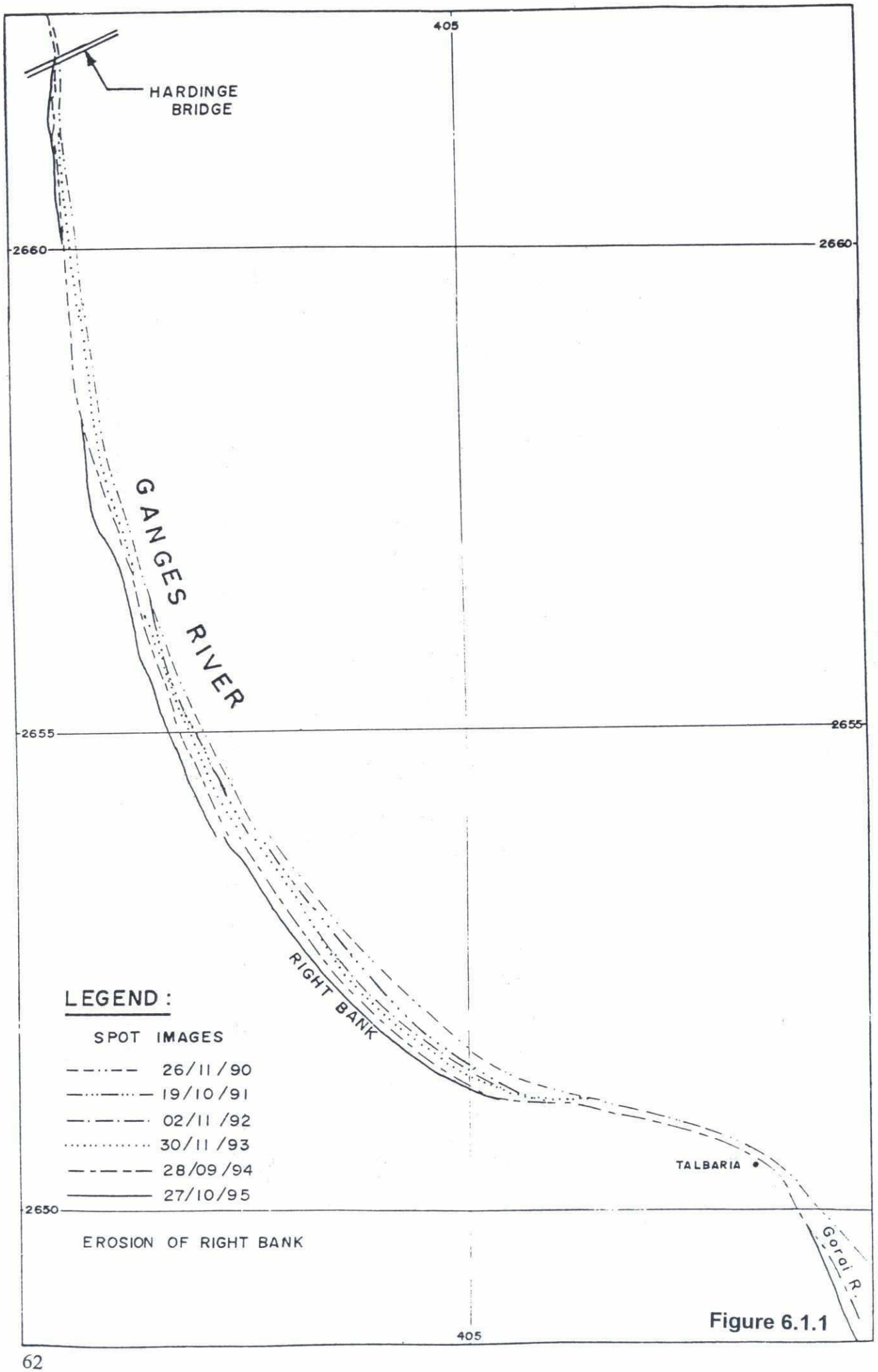
405
HARDINGE BRIDGE
2660
2660
GANGES RIVER
2655
2655
RIGHT BANK
LEGEND :
SPOT IMAGES
26/11/90
19/10/91
02/11/92
30/11/93
28/09/94
27/10/95
TALBARIA
2650
EROSION OF RIGHT BANK
Gorai R.
405

Figure 6.1.1

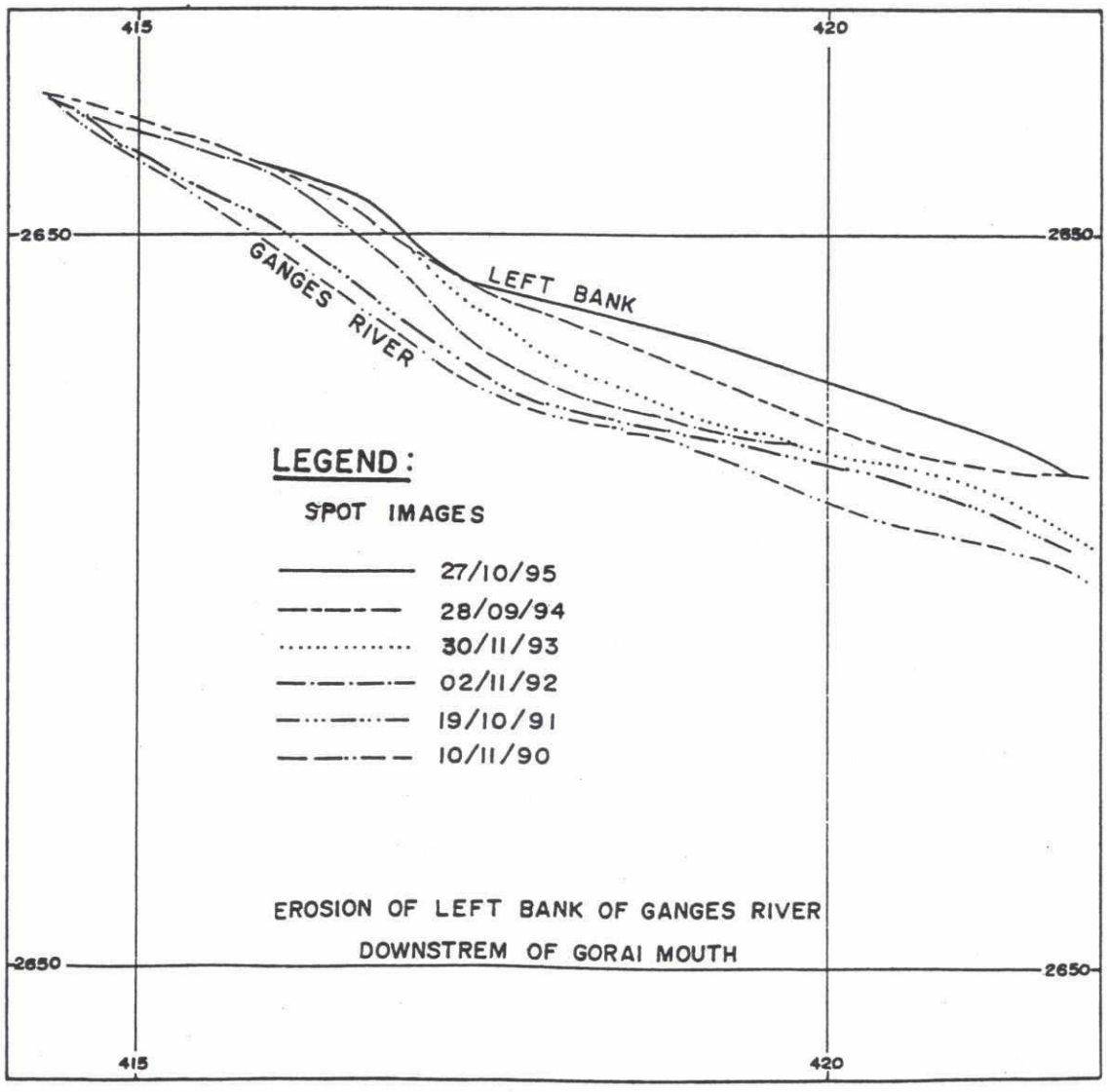
415
420
2650
2650
GANGES RIVER
LEFT BANK
LEGEND:
SPOT IMAGES
27/10/95
28/09/94
30/11/93
02/11/92
19/10/91
10/11/90
EROSION OF LEFT BANK OF GANGES RIVER
DOWNSTREM OF GORAI MOUTH
2650
2650
415
420

Figure 6.1.2

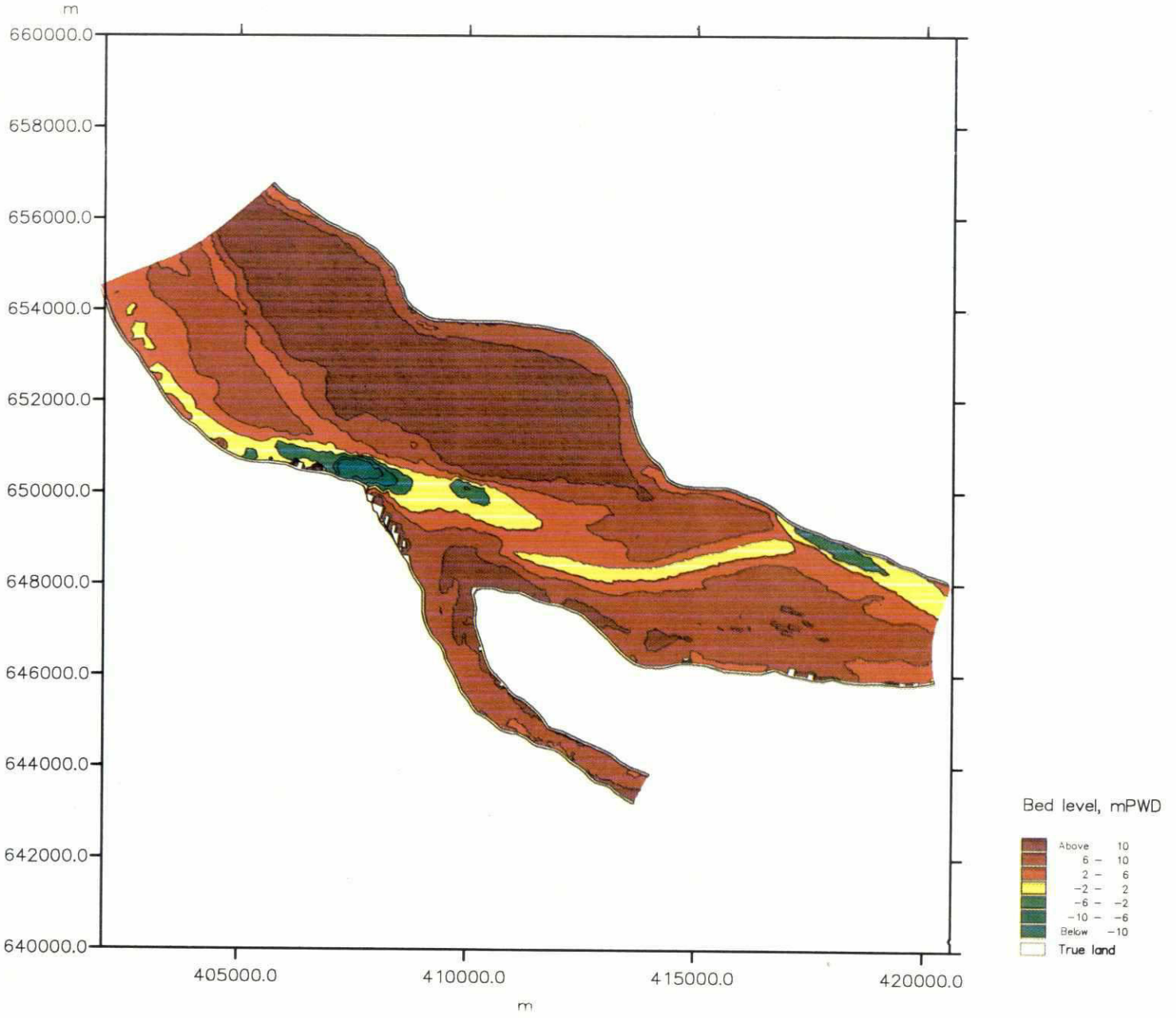


| SWMC | Client: River Survey Project FAP24 | MIKE 21 |
|---|---|---|
| | Project: Gorai Offtake Mathematical Modelling | |
| File: | Date: Sat Oct 5 1996 | Surveyed bathymetry<br>Ganges and Gorai river<br>October 1994 |
| Scale: 1:130000 | Init: p5015 | Drawing no.<br>**Figure 6·2·1** |

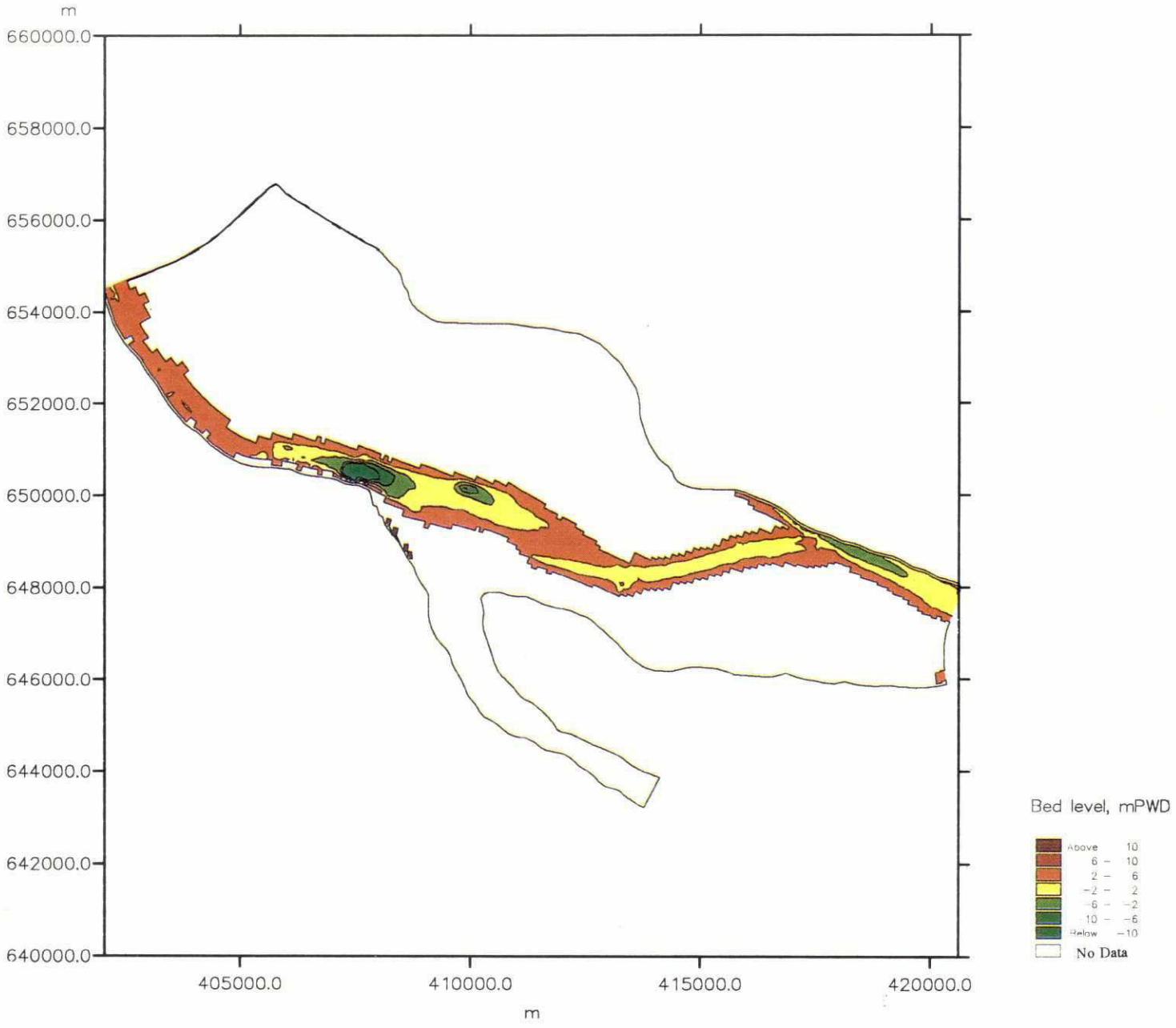


| | | | |
|---|---|---|---|
| SWMC | | Client: River Survey Project FAP24 | MIKE 21 |
| | | Project: Gorai Offtake Mathematical Modelling | |
| File: | Date: Wed Oct 2 1996 | Surveyed bathymetry (not complete)<br>Ganges and Gorai river<br>January 1995 | Drawing no. |
| Scale: 1:130000 | Init: p5015 | | Figure 6·2·2 |

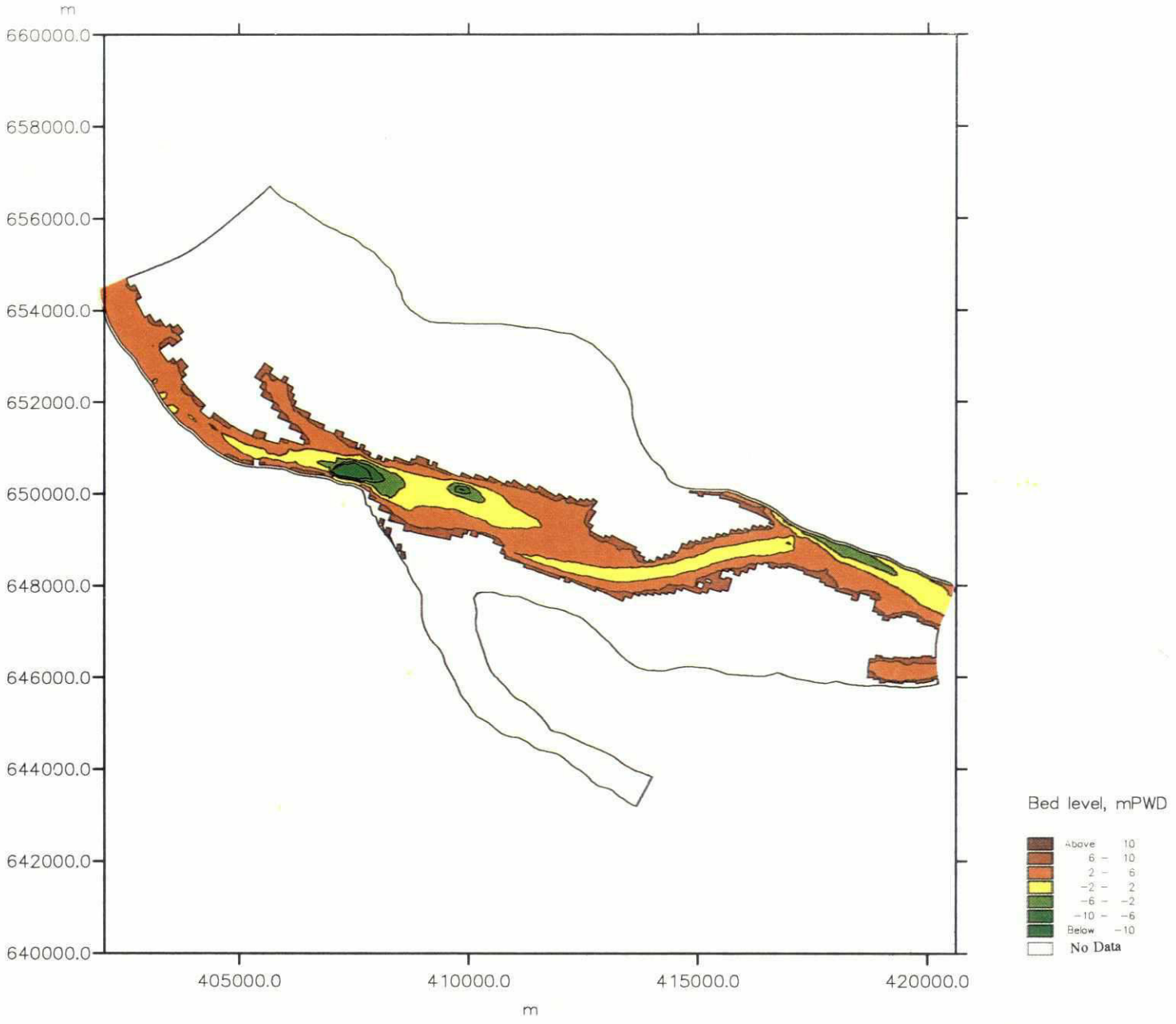


| | | | |
|---|---|---|---|
| SWMC | | Client: River Survey Project FAP24 | MIKE 21 |
| | | Project: Gorai Offtake Mathematical Modelling | |
| File: | Date: Wed Oct 2 1996 | Surveyed bathymetry (not complete)<br>Ganges and Gorai river<br>May/June 1995 | Drawing no. |
| Scale: 1:130000 | Init: p5015 | | Figure 6·2·3 |

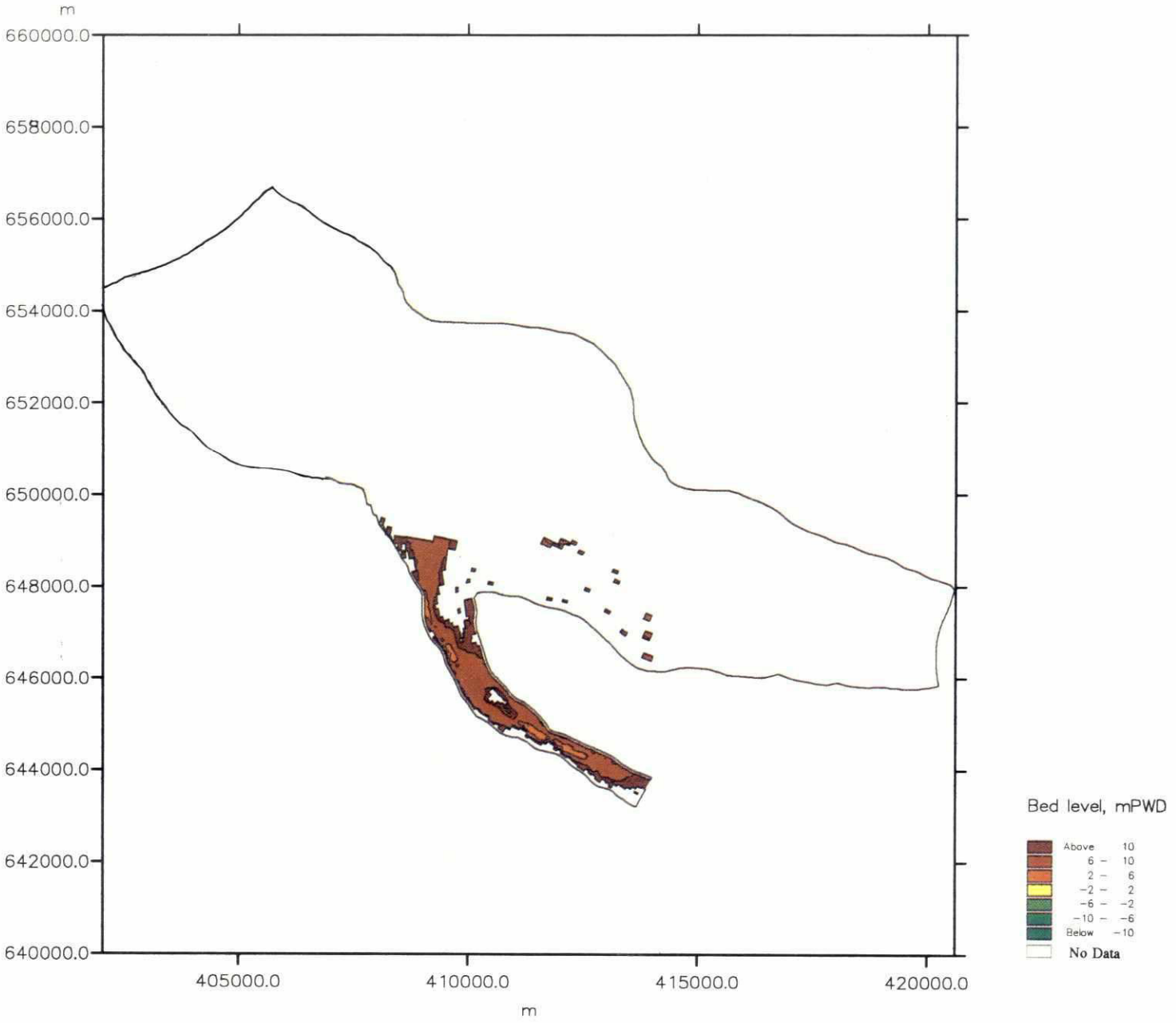


| | | | |
|---|---|---|---|
| SWMC | | Client: River Survey Project FAP24 | MIKE 21 |
| | | Project: Gorai Offtake Mathematical Modelling | |
| File: | Date: Wed Oct 2 1996 | Surveyed bathymetry (not complete)<br>Ganges and Gorai river<br>August 1995 | Drawing no.<br>**Figure 6·2·4** |
| Scale: 1:130000 | Init: p5015 | | |

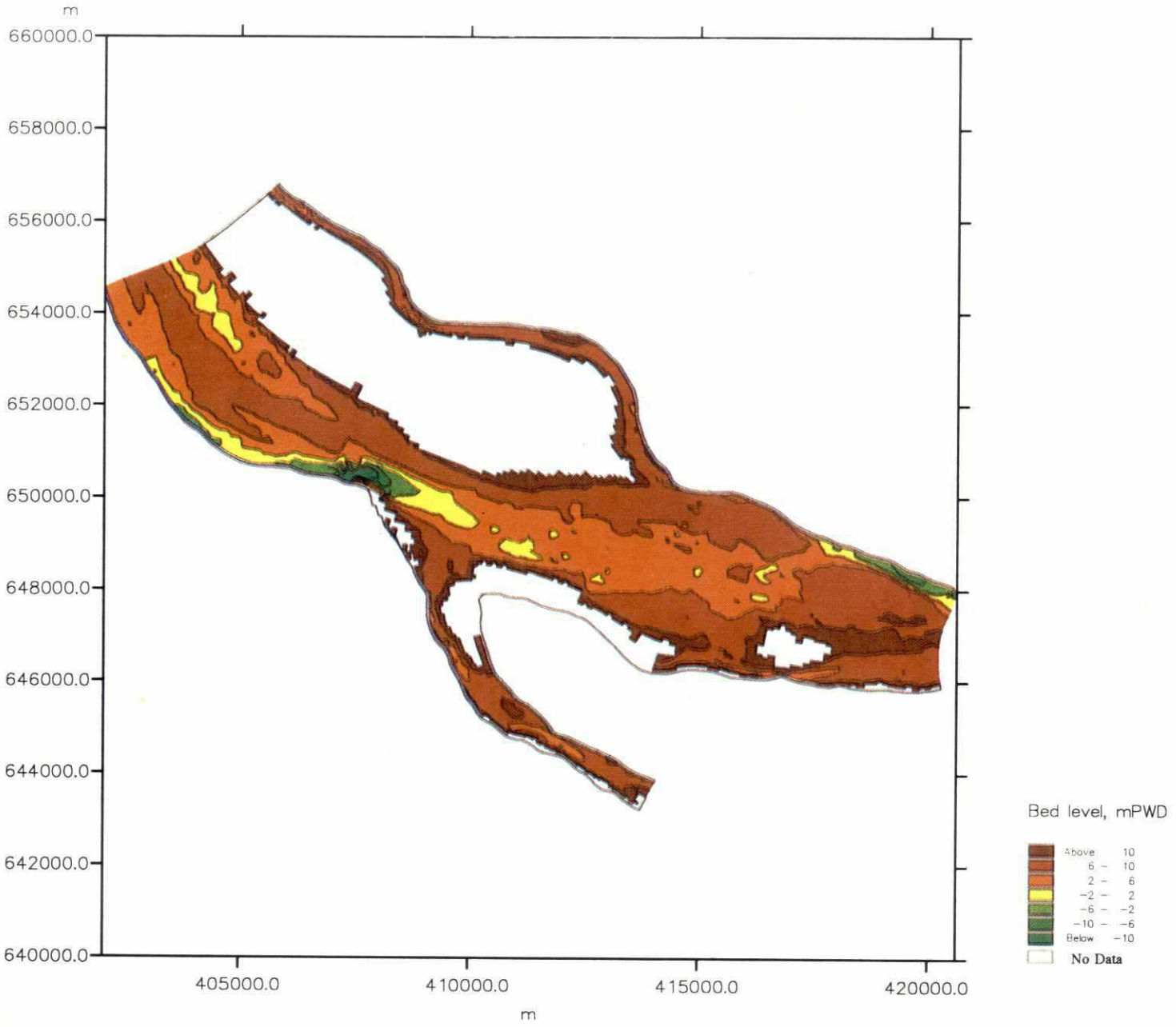


| | | | |
|---|---|---|---|
| SWMC | | Client: River Survey Project FAP24 | MIKE 21 |
| | | Project: Gorai Offtake Mathematical Modelling | |
| File: | Date: Wed Oct 2 1996 | Surveyed bathymetry (not complete)<br>Ganges and Gorai river<br>September 1995 | Drawing no.<br>Figure 6·2·5 |
| Scale: 1:130000 | Init: p5015 | | |

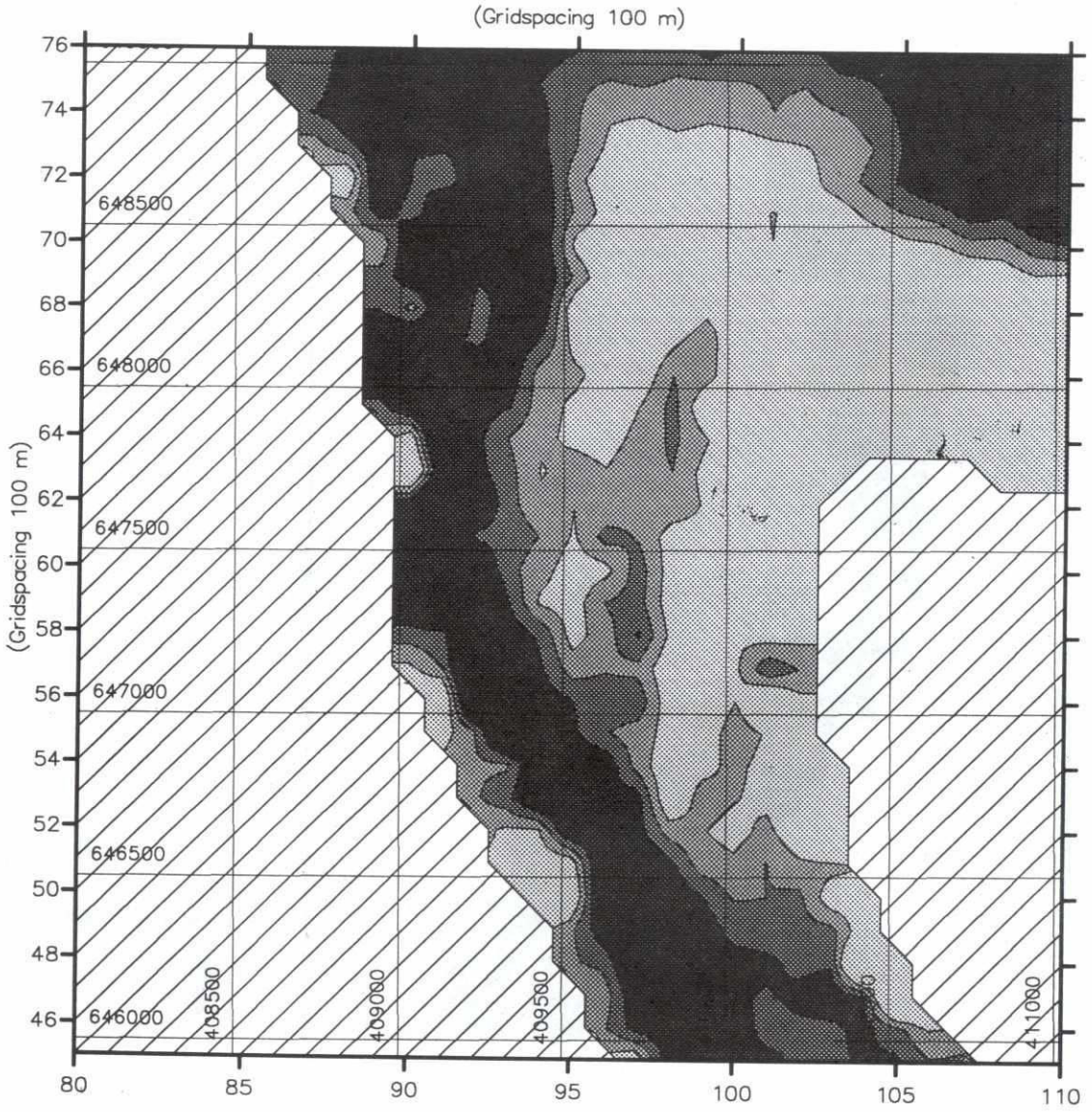




| SWMC | River Survey Project FAP24 | MIKE 21 |
|---|---|---|
| | Gorai Offtake Mathematical Modelling | |
| File: / Date: Sat Jul 6 1996 | Gorai mouth bathymetry measured from 13 to 23 October 1994 with land survey January 1995. Hatched : not surveyed | dwg. no. **Figure 6.2.6** |
| Scale: 1:22000 / Init: p5015 | | |

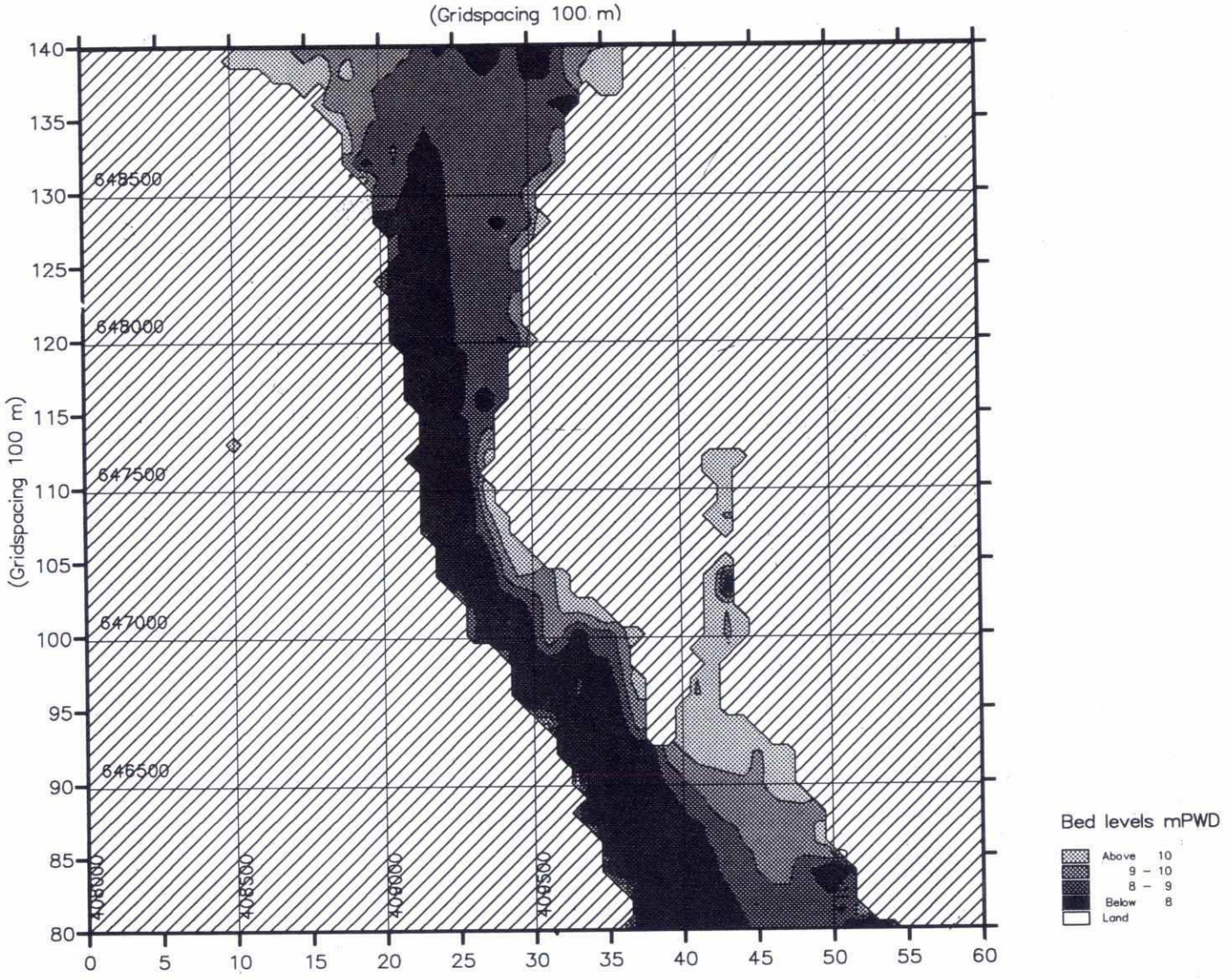


| SWMC | | River Survey Project FAP24 | MIKE 21 |
|---|---|---|---|
| | | Gorai Offtake Mathematical Modelling | |
| File: | Date: Sat Jul 6 1996 | Gorai mouth bathymetry measured from 8 to 14 August 1995. Hatched : not surveyed | dwg. no. Figure 6.2.7 |
| Scale: 1:22000 | Init: p5015 | | |

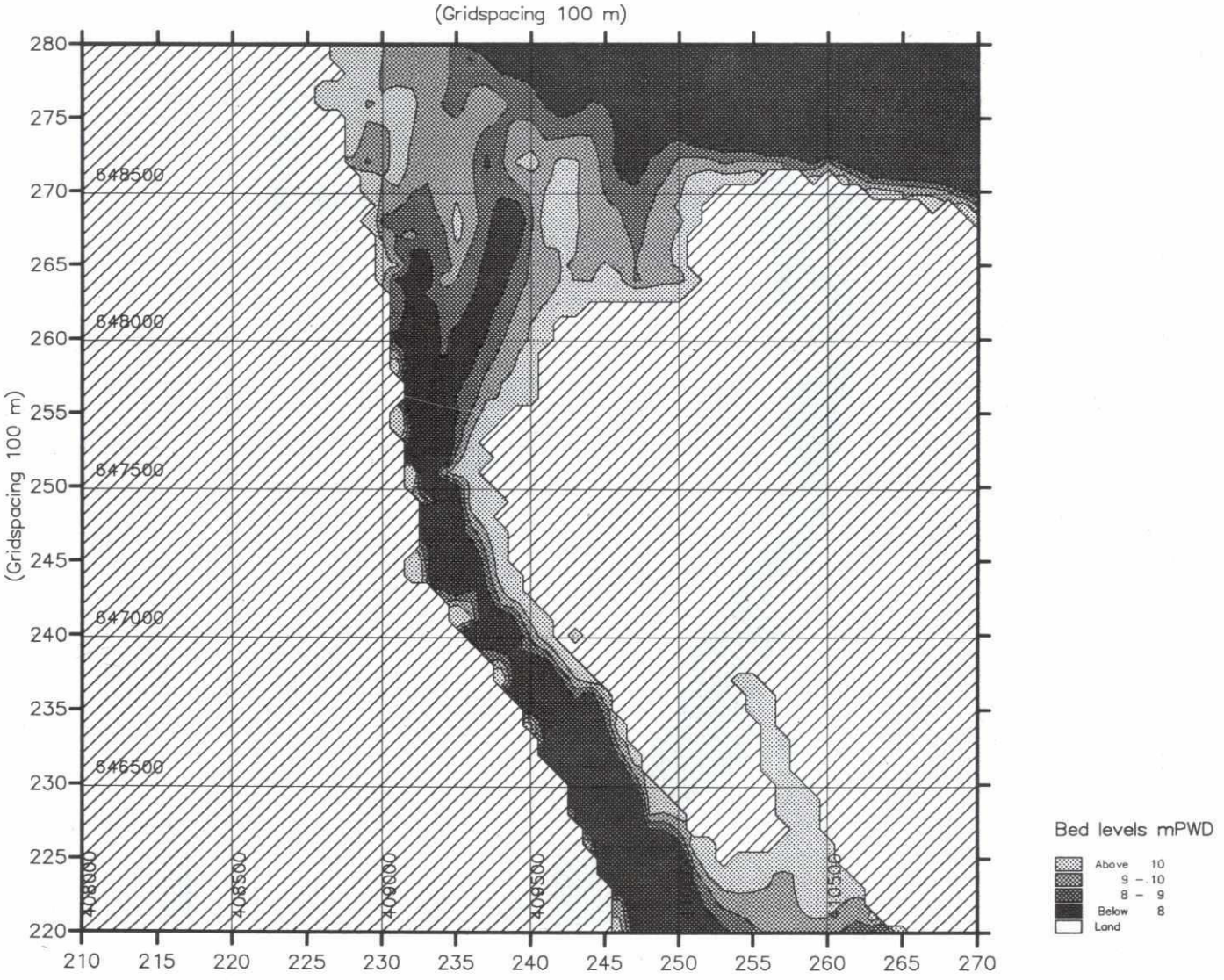


| SWMC | River Survey Project FAP24 | MIKE 21 |
|---|---|---|
| | Gorai Offtake Mathematical Modelling | |
| File: | Date: Sat Jul 6 1996 | Gorai mouth bathymetry measured from 8 to 24 September 1995. Hatched : not surveyed |
| Scale: 1:22000 | Init: p5015 | dwg. no. **Figure 6.2.8** |

8028.gorai oct95pwd

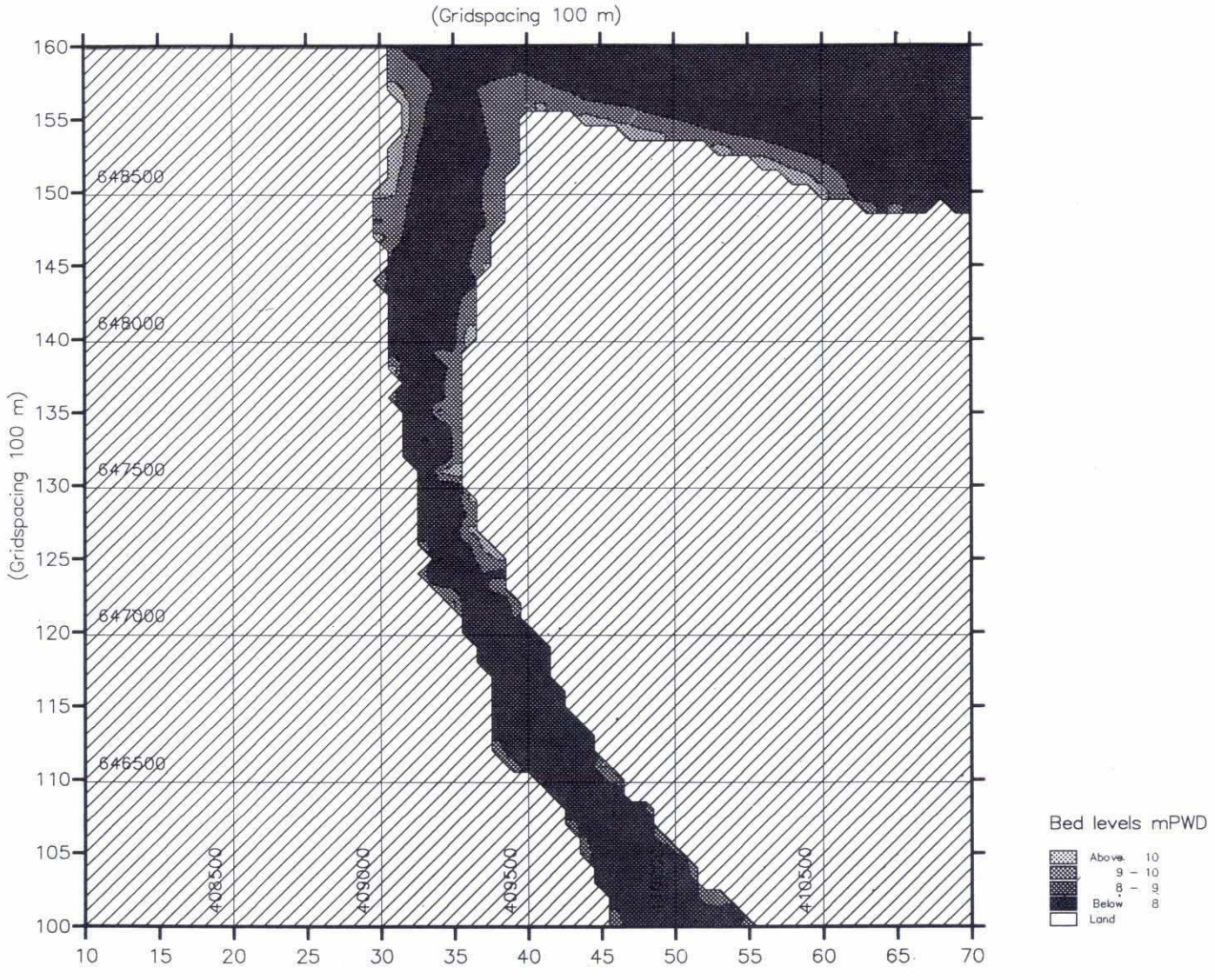


| SWMC | River Survey Project FAP24 | MIKE 21 |
|---|---|---|
| | Gorai Offtake Mathematical Modelling | |
| File: | Date: Sat Jul 6 1996 | Gorai mouth bathymetry measured from 16 to 20 October 1995. Hatched : not surveyed |
| Scale: 1:22000 | Init: p5015 | dwg. no. **Figure 6.2.9** |

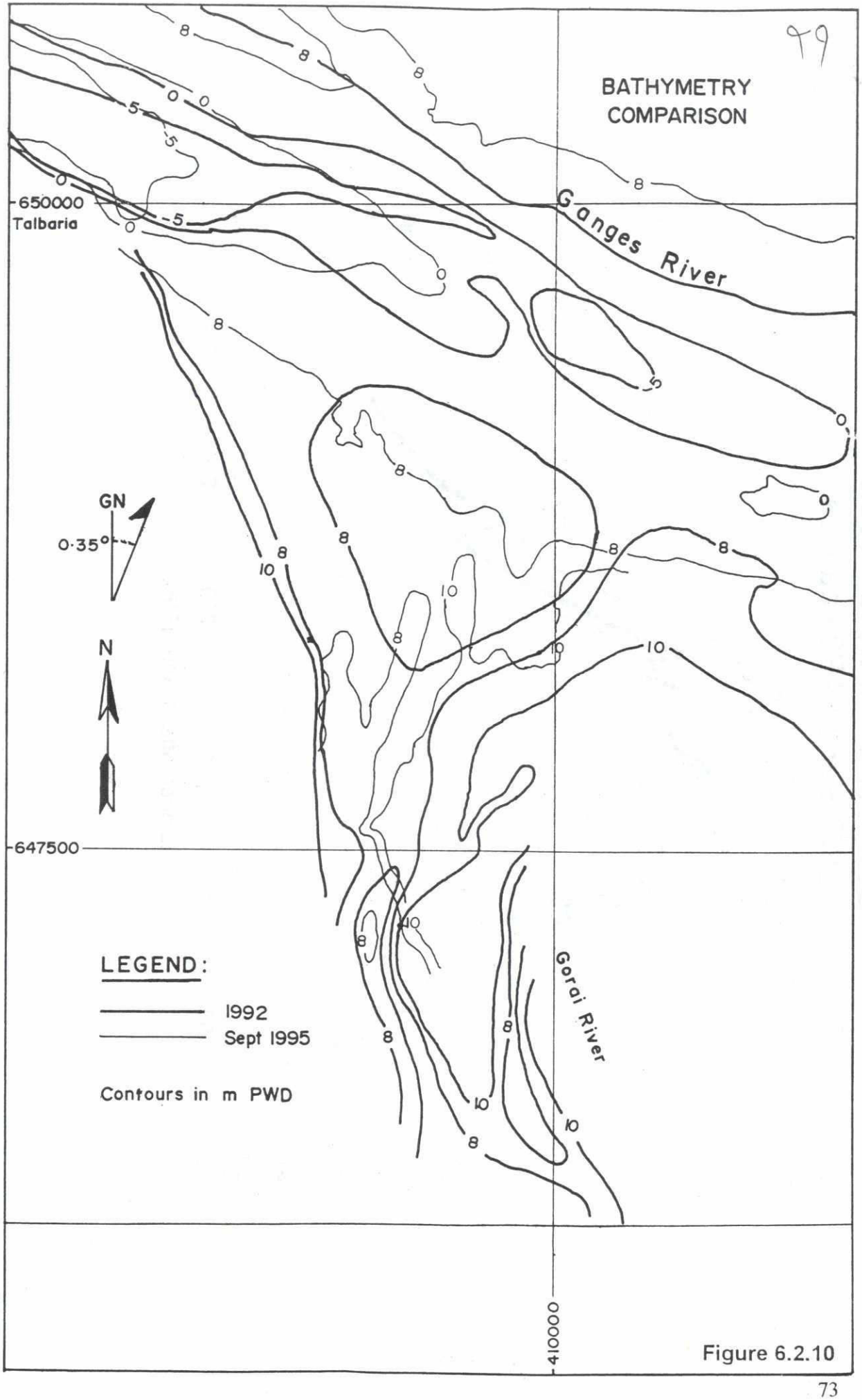
BATHYMETRY
COMPARISON
Ganges River
650000
Talbaria
647500
410000
GN
0·35°
N
LEGEND:
1992
Sept 1995
Contours in m PWD
Gorai River

Figure 6.2.10

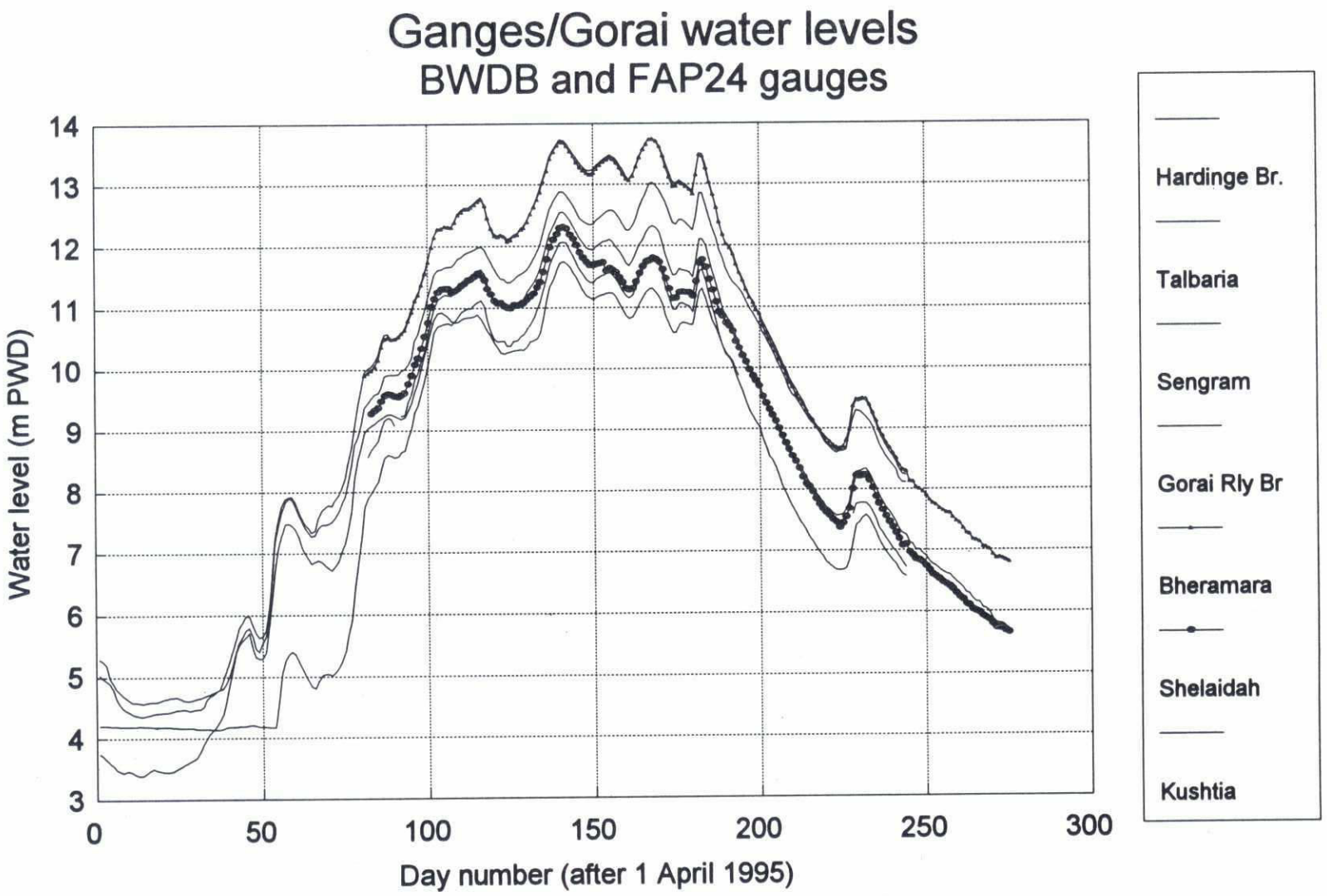
Ganges/Gorai water levels
BWDB and FAP24 gauges
Water level (m PWD)
14
13
12
11
10
9
8
7
6
5
4
3
0
50
100
150
200
250
300
Day number (after 1 April 1995)
Hardinge Br.
Talbaria
Sengram
Gorai Rly Br
Bheramara
Shelaidah
Kushtia

Figure 6.3.1

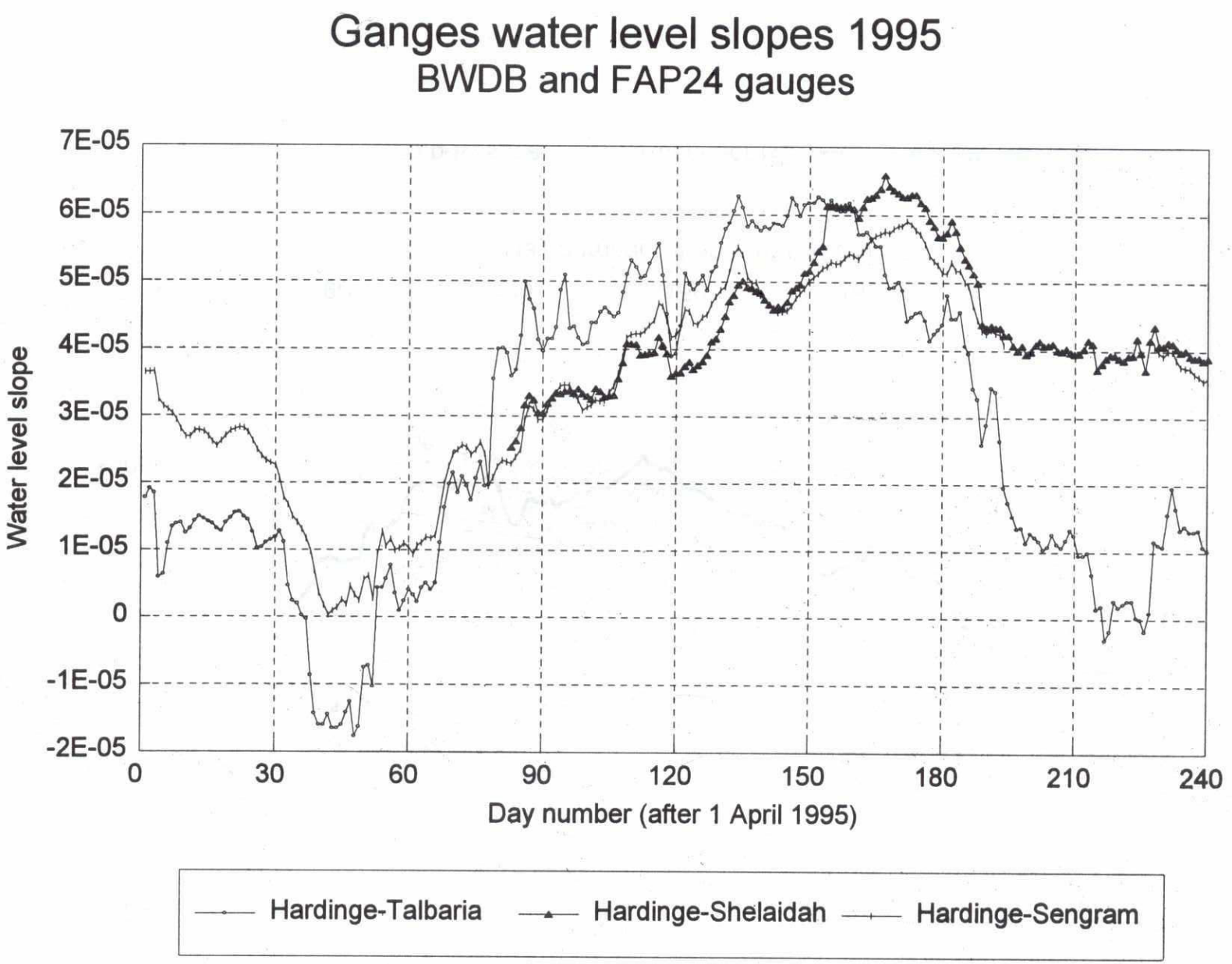
Ganges water level slopes 1995
BWDB and FAP24 gauges
Water level slope
7E-05
6E-05
5E-05
4E-05
3E-05
2E-05
1E-05
0
-1E-05
-2E-05
0
30
60
90
120
150
180
210
240
Day number (after 1 April 1995)
Hardinge-Talbaria
Hardinge-Shelaidah
Hardinge-Sengram



Figure 6.3.2

# Ganges/Gorai water levels
## BWDB and FAP24 gauges

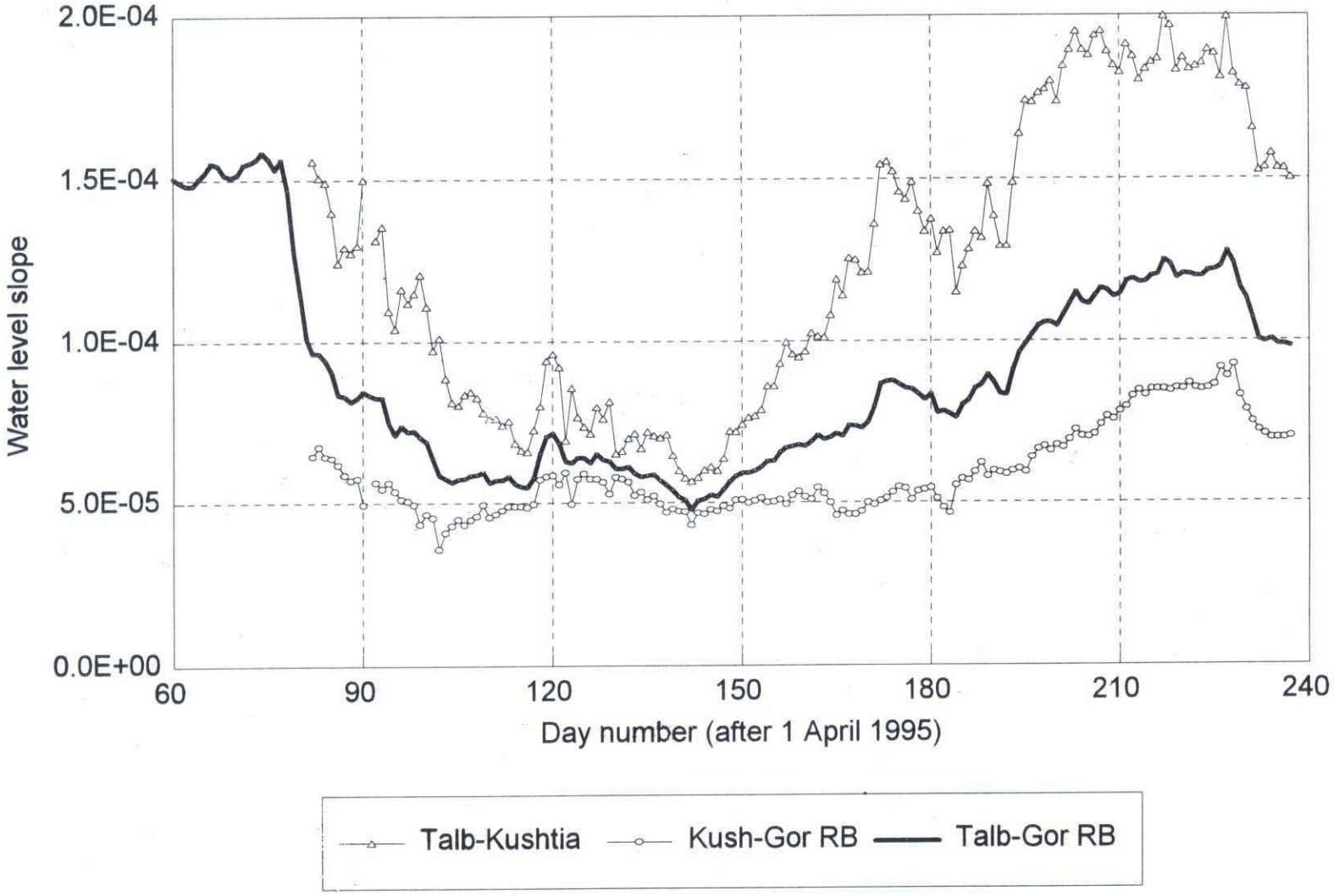


Figure 6.3.3

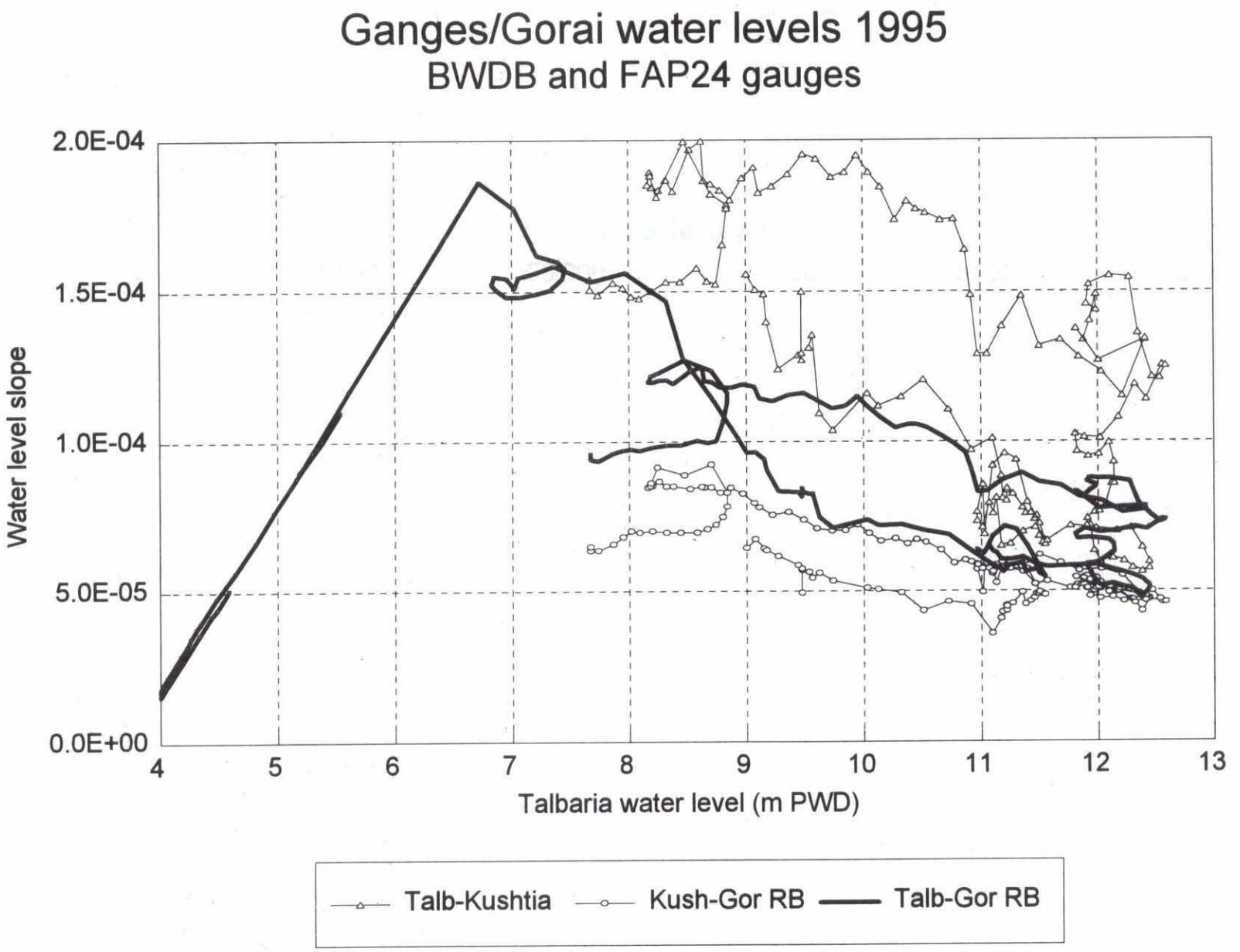
Ganges/Gorai water levels 1995
BWDB and FAP24 gauges
Water level slope
2.0E-04
1.5E-04
1.0E-04
5.0E-05
0.0E+00
4
5
6
7
8
9
10
11
12
13
Talbaria water level (m PWD)
Talb-Kushtia
Kush-Gor RB
Talb-Gor RB

Figure 6.3.4

# Hardinge Bridge rating curve
## FAP24 1994-95 data

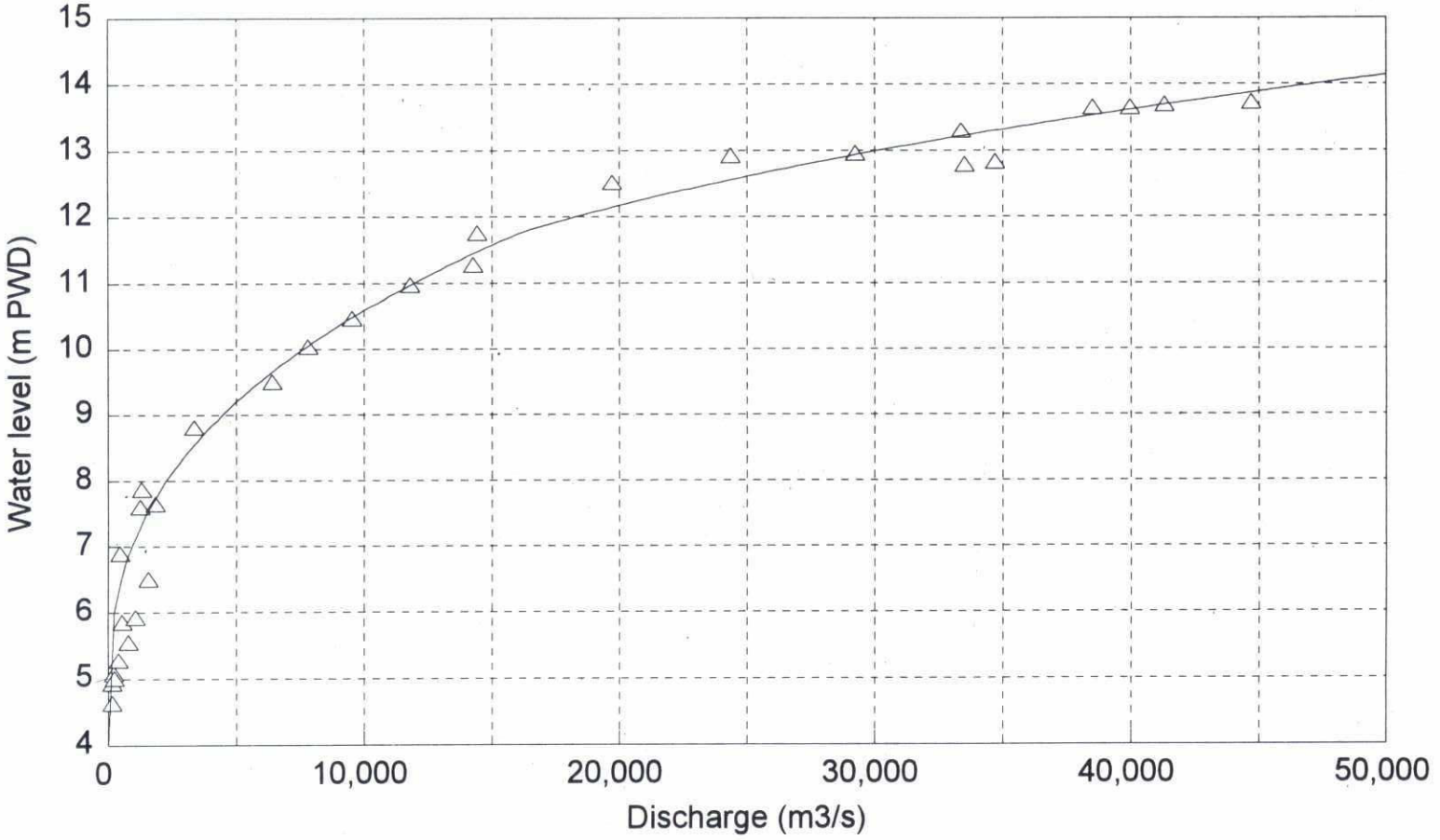


**Figure 6.4.1**

# Hardinge Bridge rating curve
## FAP24 1994-95 and BWDB 1987-89 data

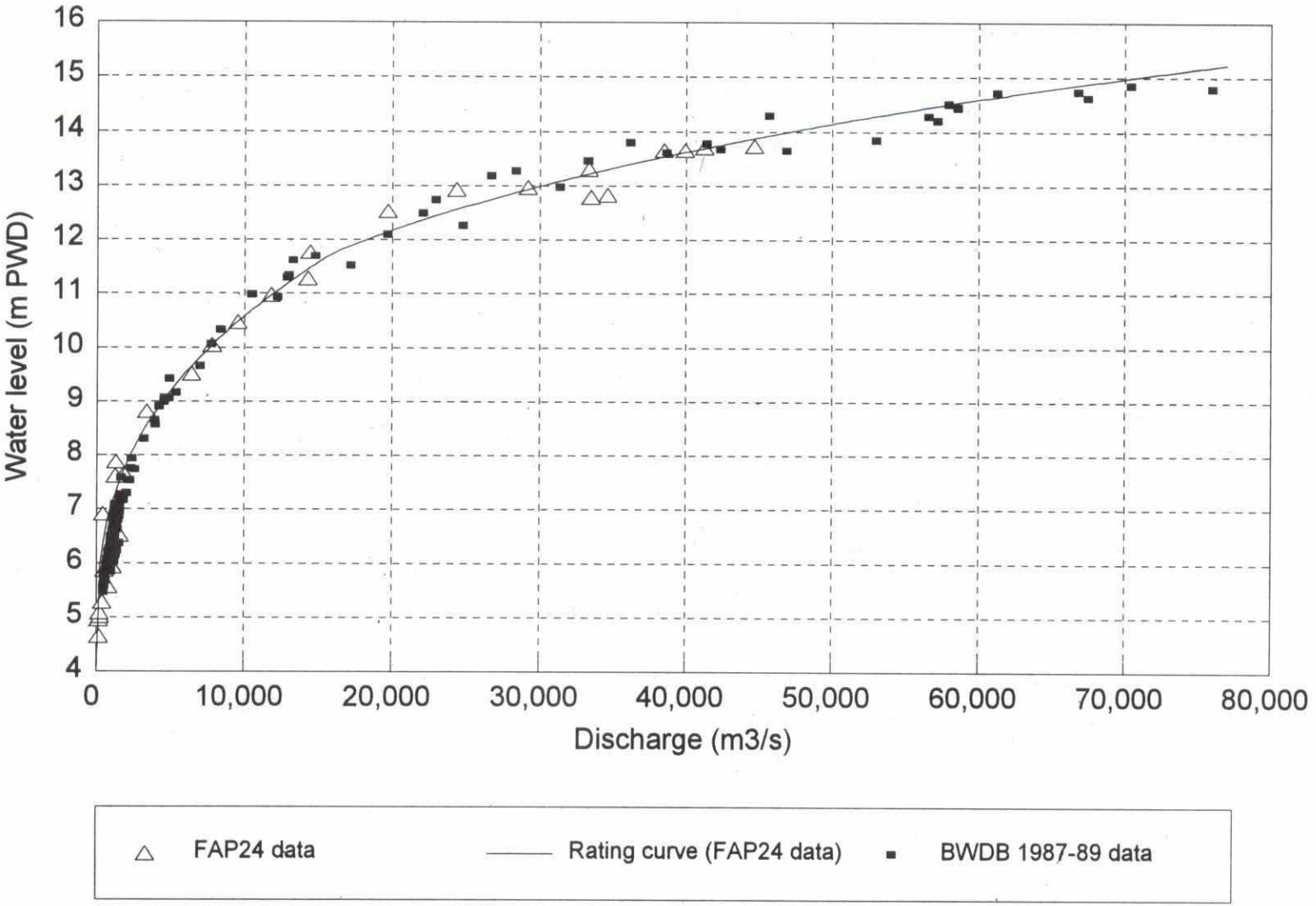




Figure 6.4.2

# Hardinge Bridge sediment rating curve
## 1994-95 data

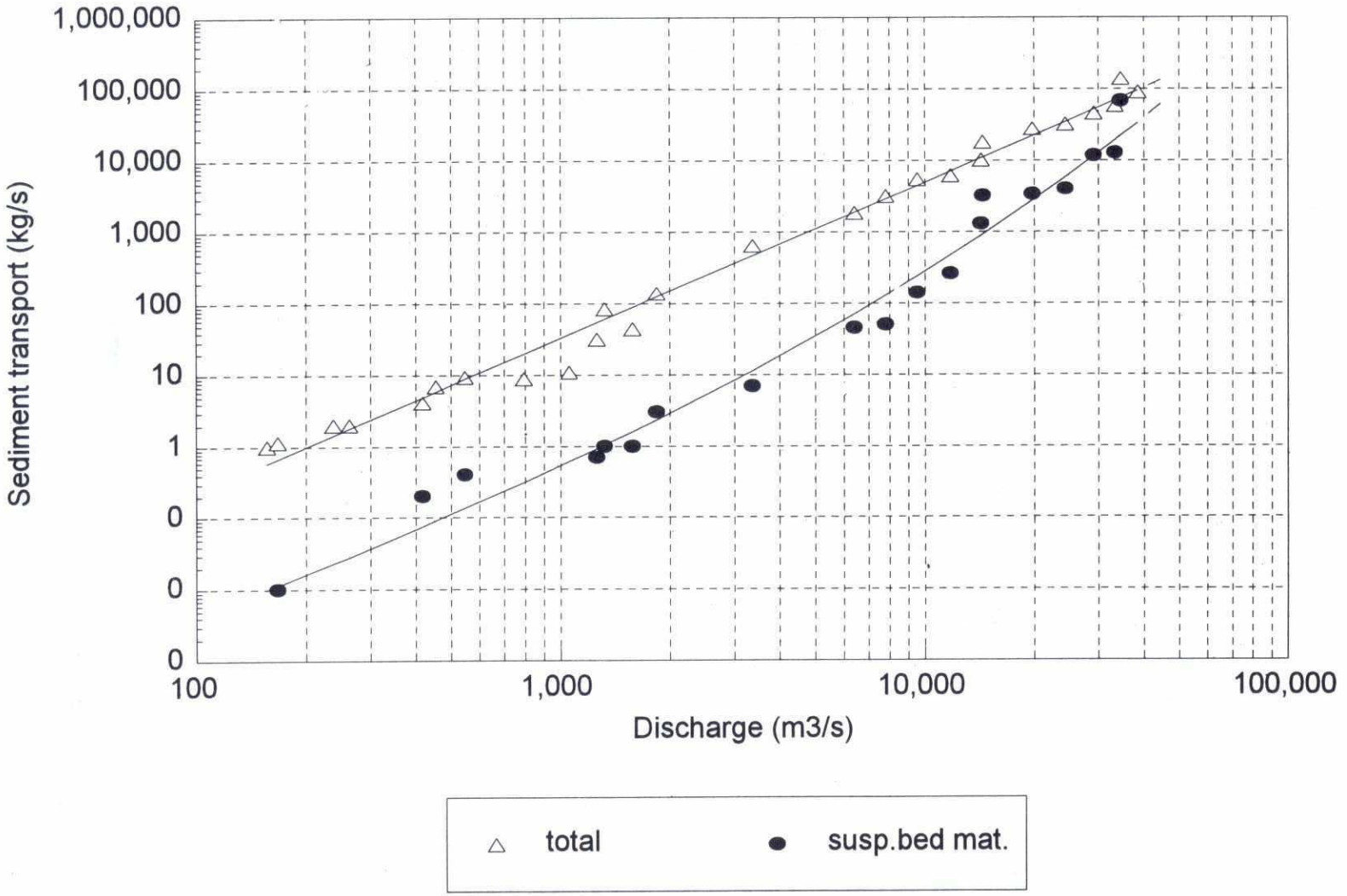


**Figure 6.5.1**

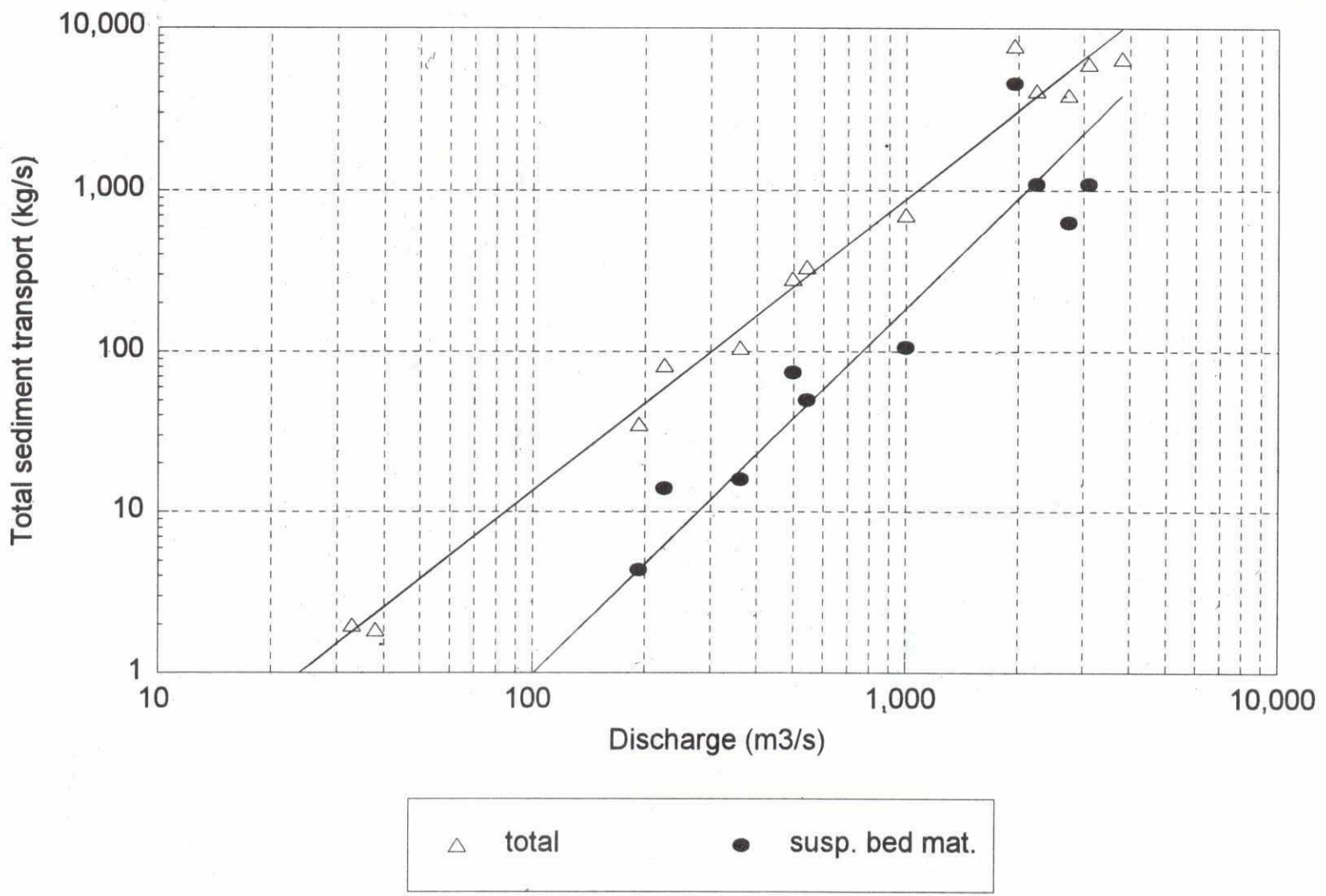
Gorai Kushtia sediment rating curve
1994-95 data
Total sediment transport (kg/s)
10,000
1,000
100
10
1
10
100
1,000
10,000
Discharge (m3/s)
total
susp. bed mat.

Figure 6.5.2

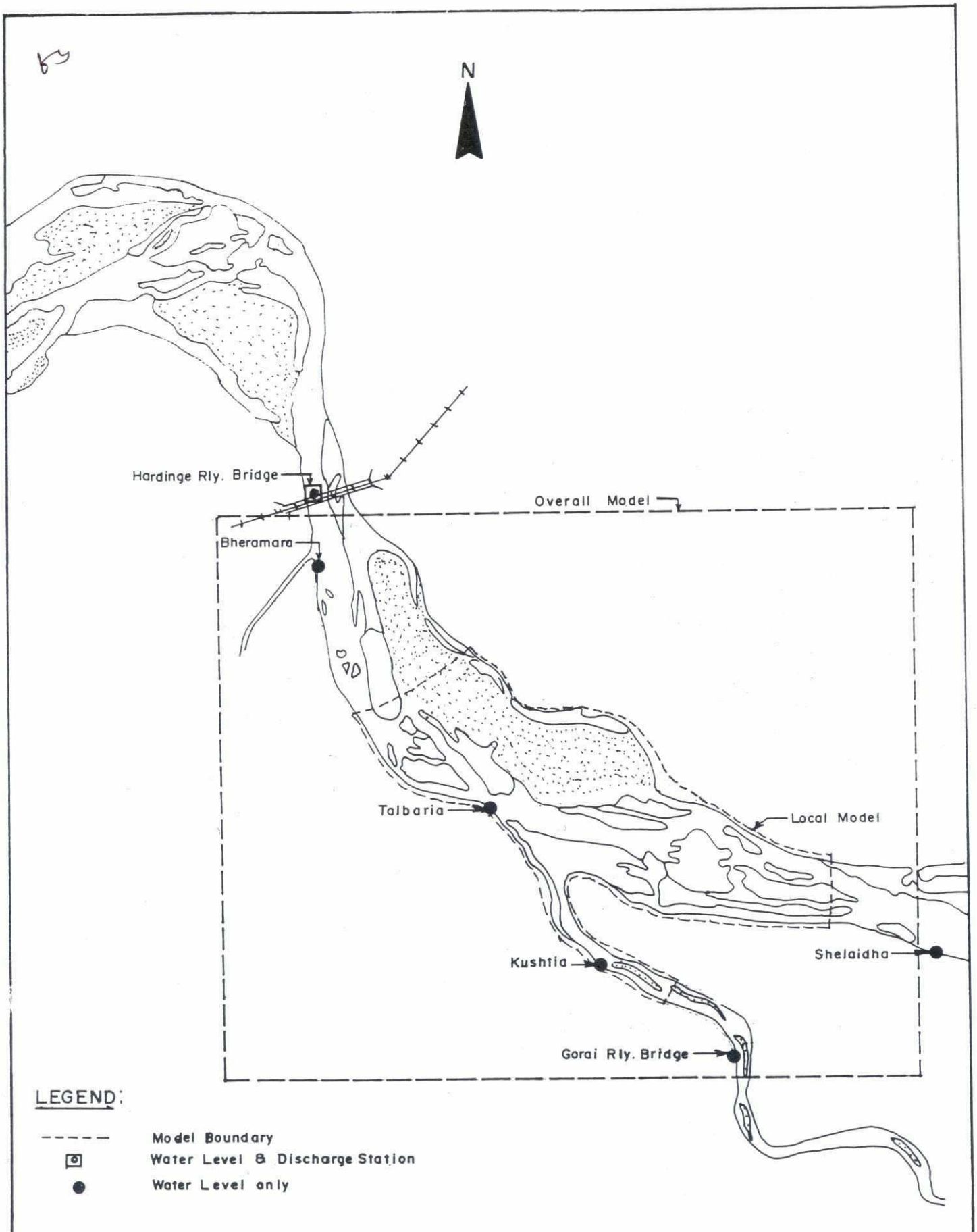


Figure 7.3.1 Location map, Hydrometric Survey Locations

69

bathy95 gorai-new

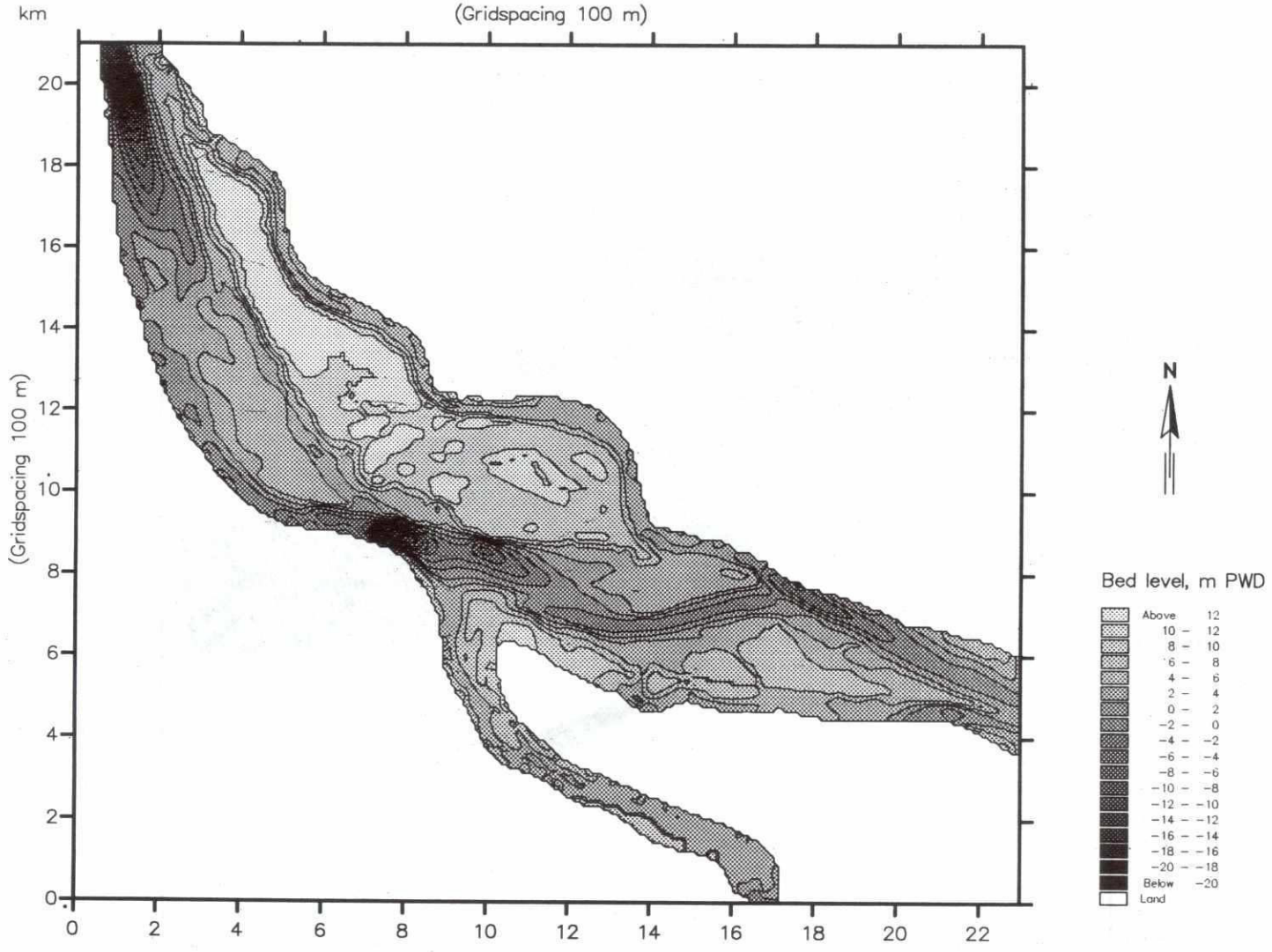


| SWMC | River Survey Project FAP24 | MIKE 21 |
|---|---|---|
| | Gorai Offtake Mathematical Modelling | |
| File: | Date: Sun Jun 9 1996 | Model Bathymetry<br>Overall Model<br>Based on May 1995 survey |
| Scale: 1:160000 | Init: hge | dwg. no.<br>**Figure 7.4.1** |

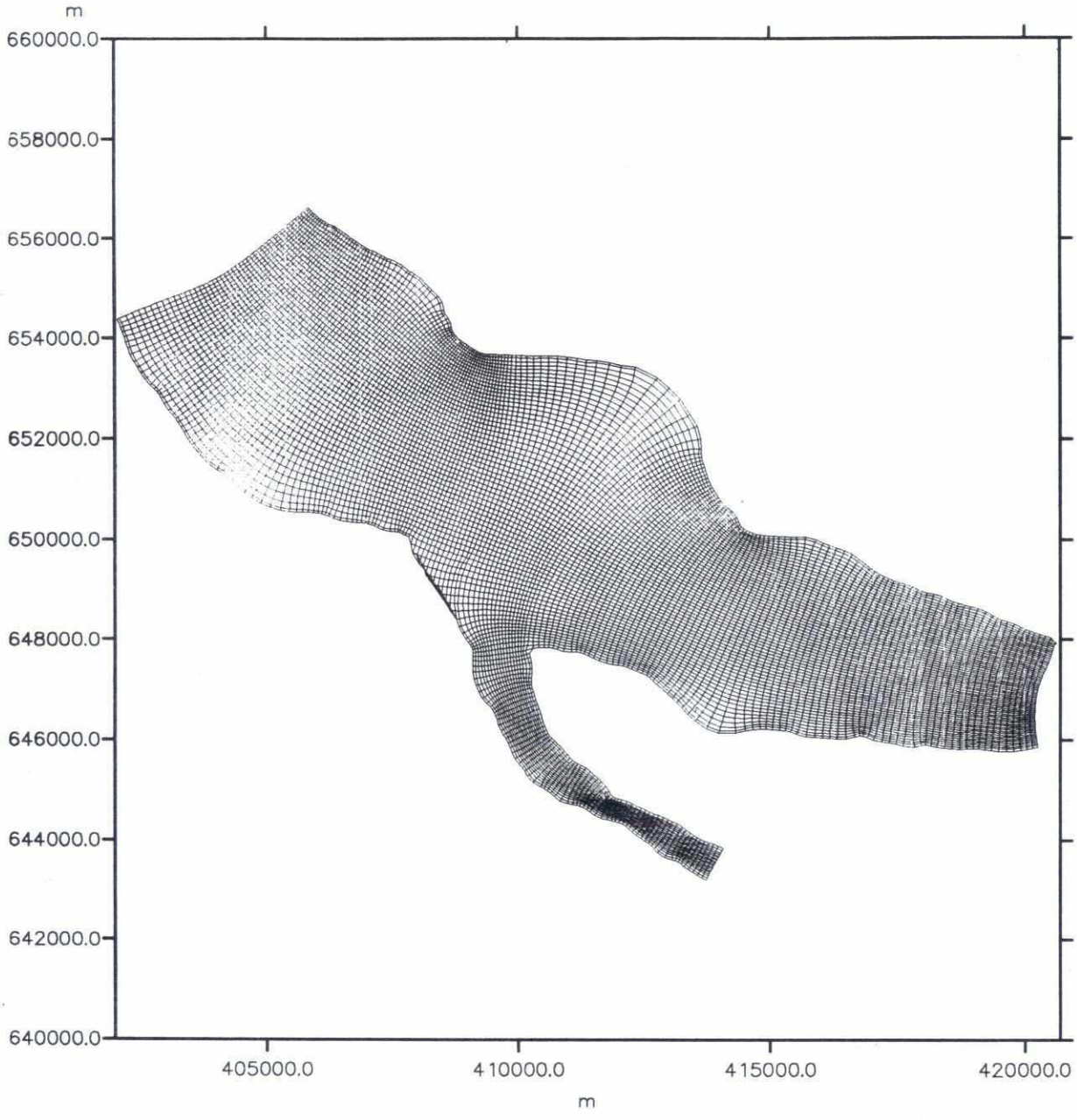


| | | | |
|---|---|---|---|
| SWMC | | Client: River Survey Project FAP24 | MIKE 21 |
| | | Project: Gorai Offtake Mathematical Modelling | |
| File: | Date: Sun Jun 9 1996 | Curvilinear Computational Grid<br>Local Model of Gorai Offtake | Drawing no.<br>**Figure 7.4.2** |
| Scale: 1:130000 | Init: hge | | |

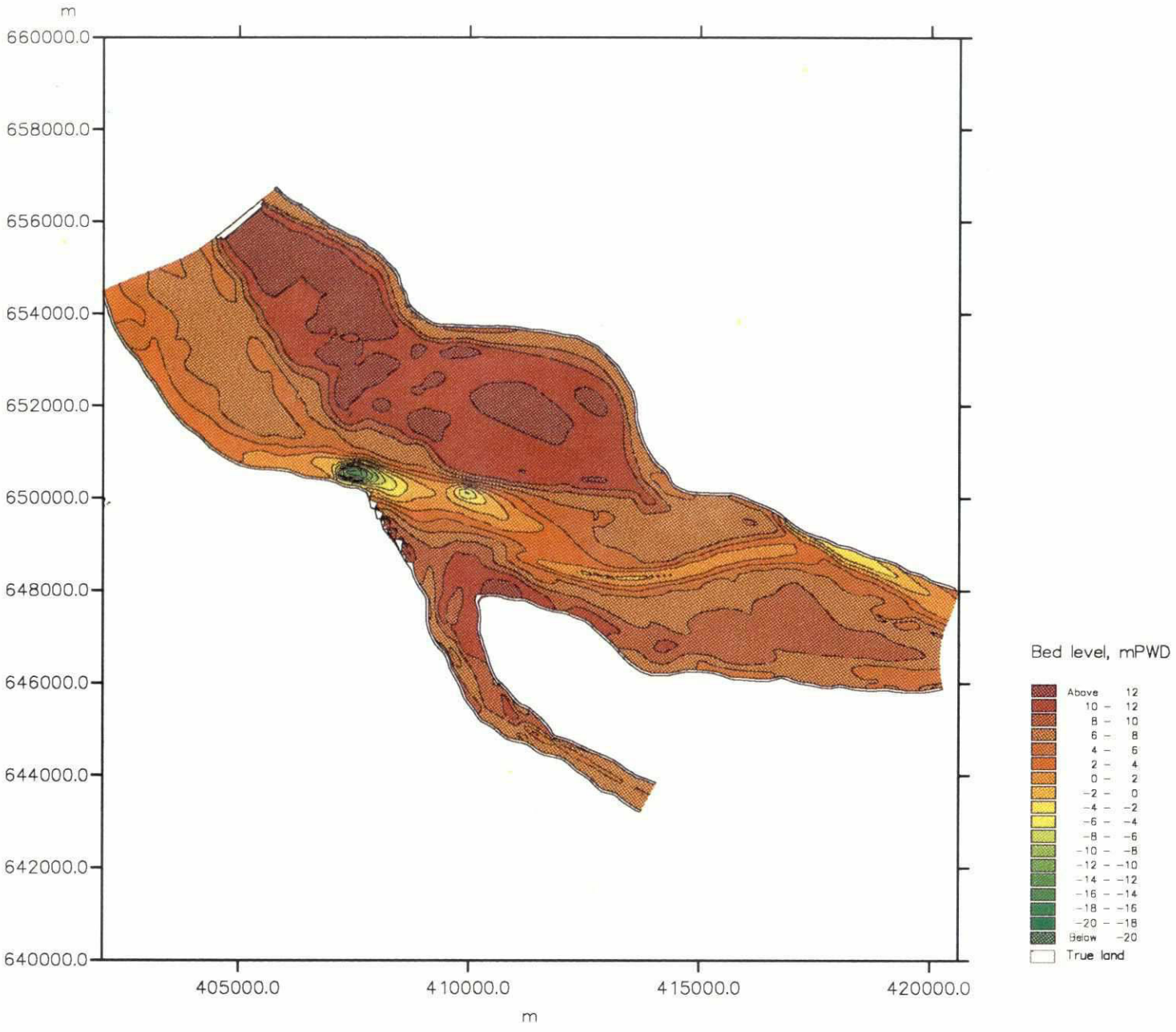


| | | | |
|---|---|---|---|
| SWMC | | Client: River Survey Project FAP24 | MIKE 21 |
| | | Project: Gorai Offtake Mathematical Modelling | |
| File: | Date: Sat Oct 5 1996 | Model bathymetry (smoothened data)<br>Local model<br>based on May 1995 measurement | Drawing no. |
| Scale: 1:130000 | Init: p5015 | | Figure 7·4·3 |

data95 boundary

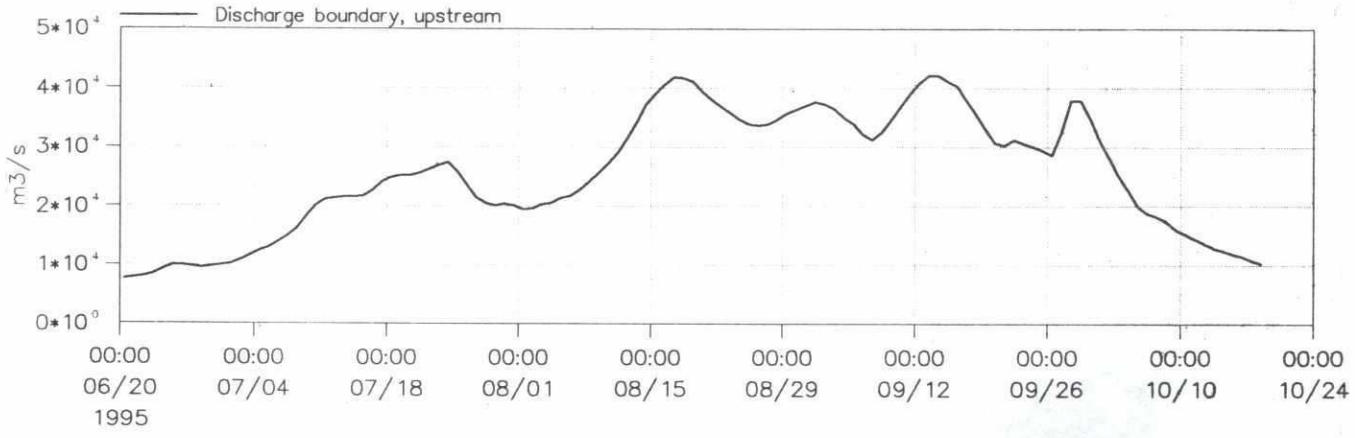


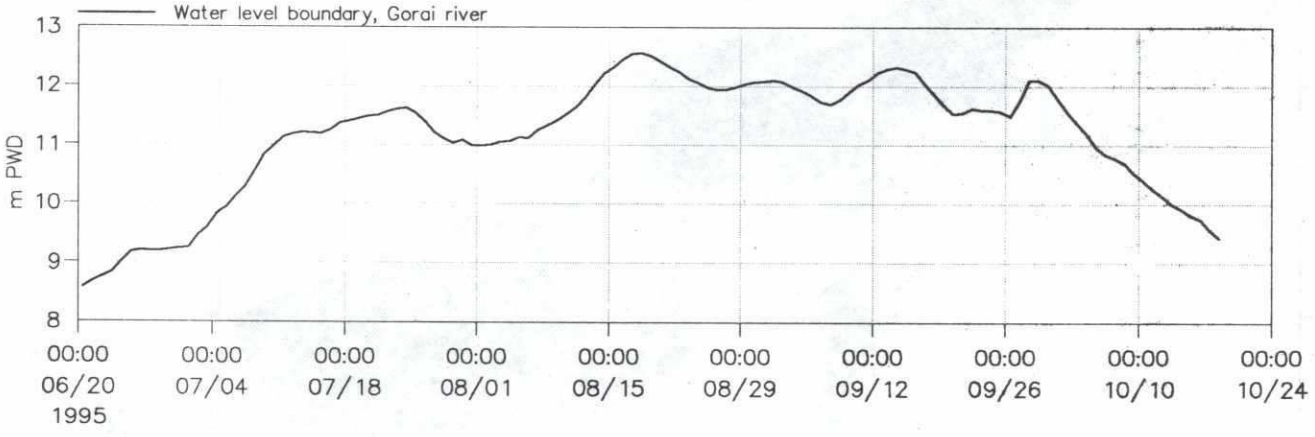


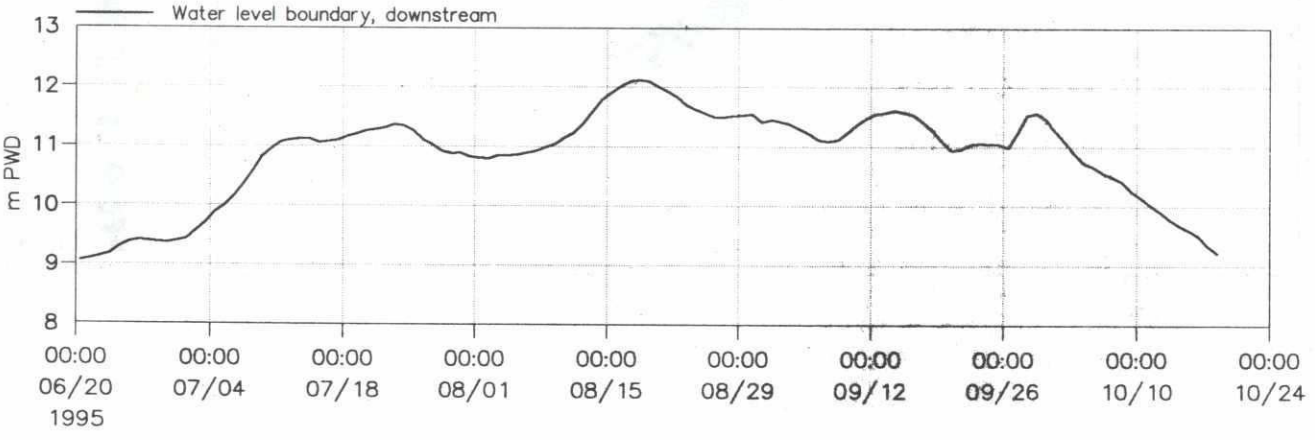


| SWMC | River Survey Project FAP24 | MIKE 21 |
|---|---|---|
| | Gorai Offtake Mathematical Modelling | |
| File: | Date: Mon Jun 10 1996 | Boundary conditions for local curvilinear model |
| Scale: | Init: hge | dwg. no. Figure 7.5.1 |

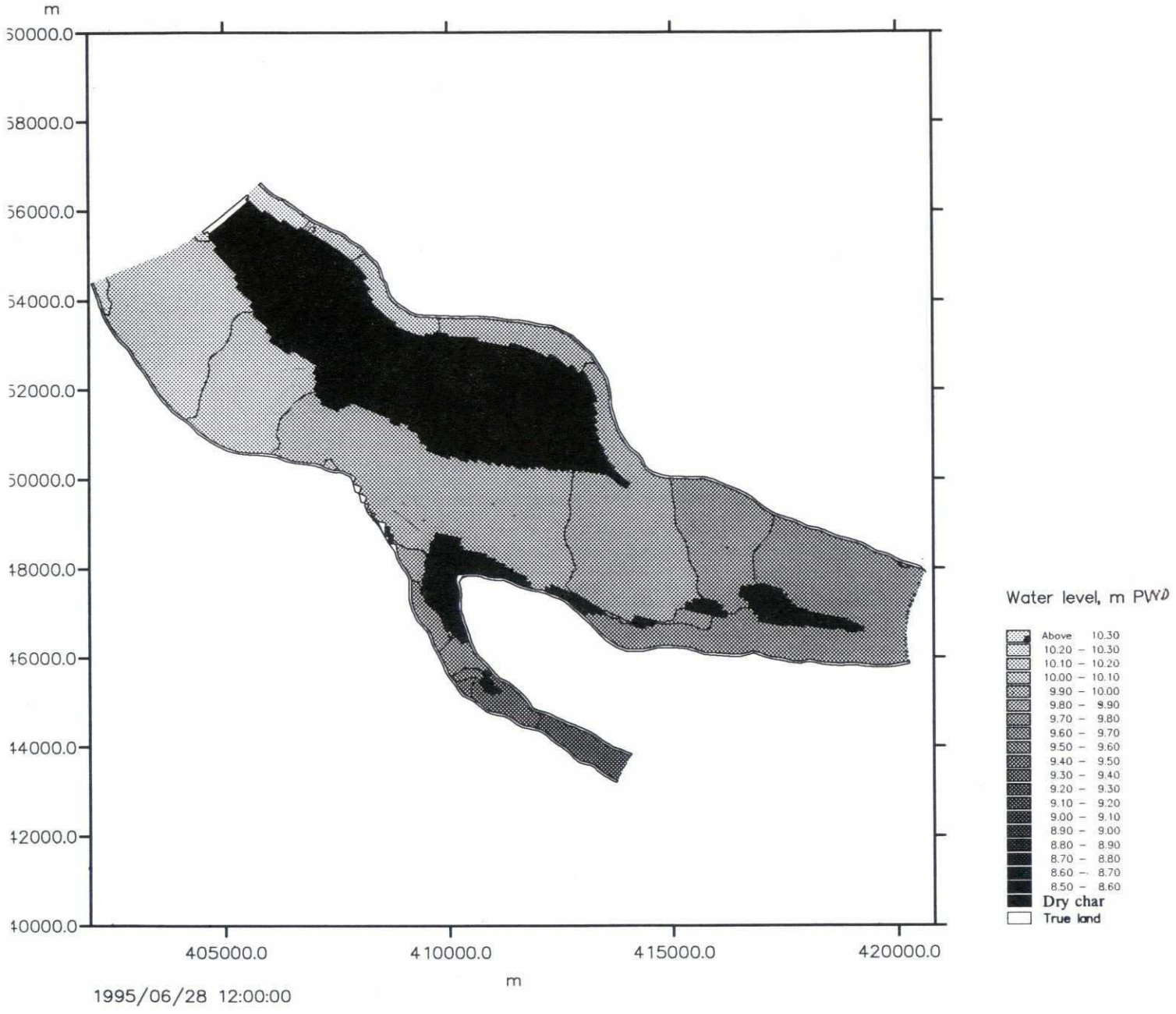


| SWMC | | Client: River Survey Project FAP24 | MIKE 21 |
|---|---|---|---|
| | | Project: Gorai Offtake Mathematical Modelling | |
| File: | Date: Thu Jun 13 1996 | Simulated water level<br>June 20, 1995<br>Local model | Drawing no.<br>**Figure 7.5.2** |
| Scale: 1:130000 | Init: hge | | |

D2

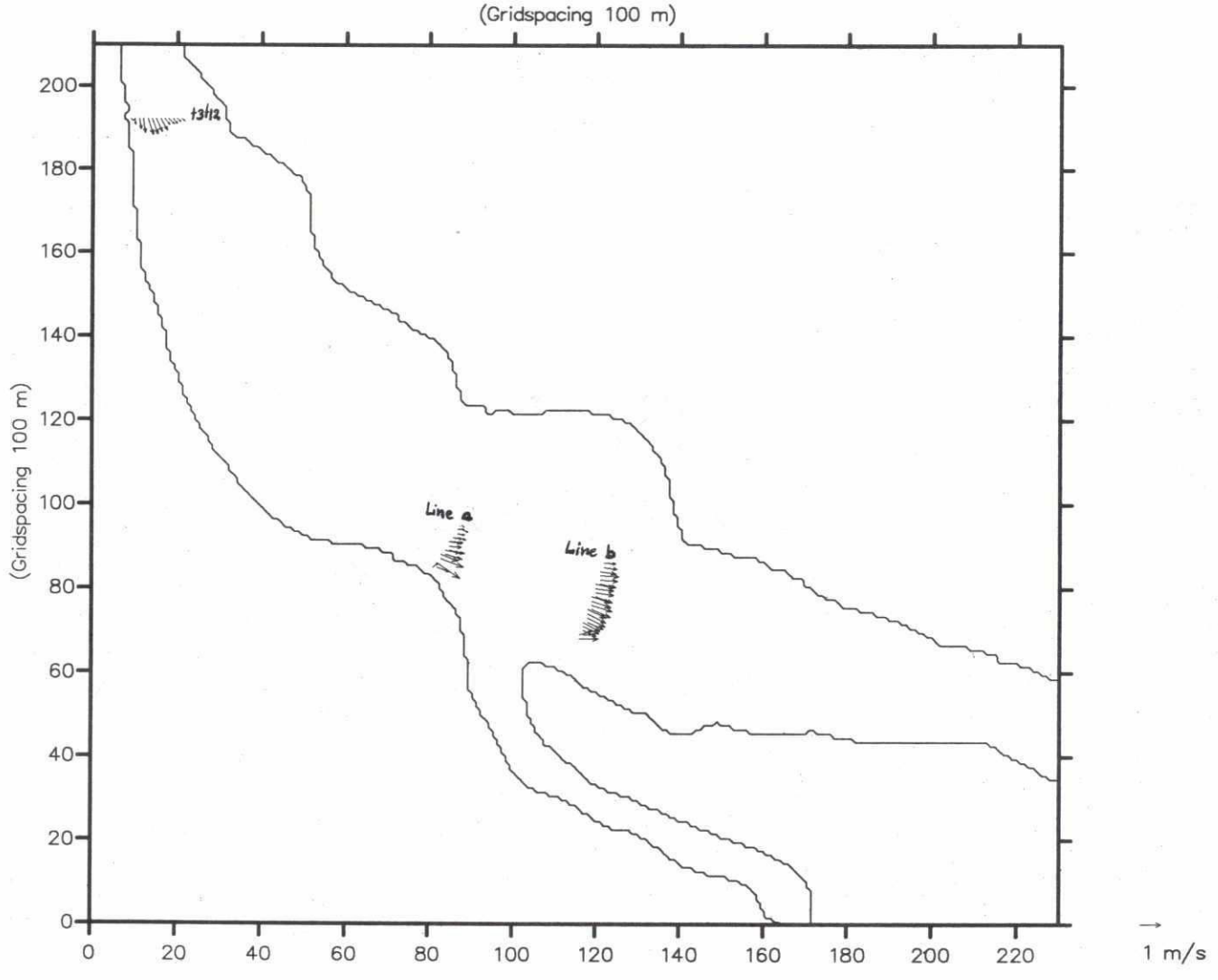


| SWMC | River Survey Project FAP24 | MIKE 21 |
|---|---|---|
| | Gorai Offtake Mathematical Modelling | |
| File: | Date: Mon Jun 10 1996 | Measured flow velocity field<br>June 28, 1995 |
| Scale: 1:160000 | Init: hge | dwg. no.<br>**Figure 7.5.3** |

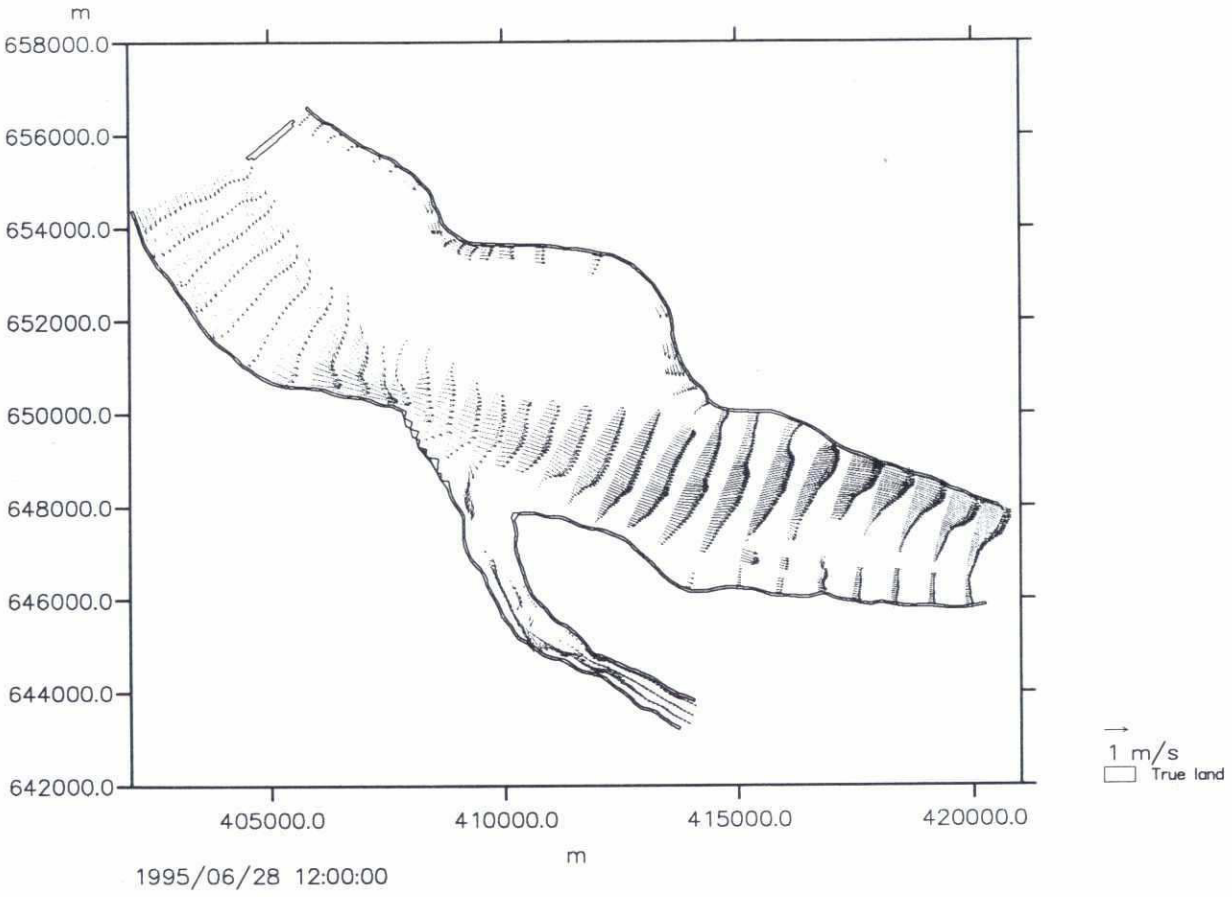


| | | | |
|---|---|---|---|
| SWMC | | Client: River Survey Project FAP24 | MIKE 21 |
| | | Project: Gorai Offtake Mathematical Modelling | |
| File: | Date: Mon Jun 10 1996 | Simulated flow velocity field<br>Local curvilinear model<br>June 28, 1995 | Drawing no.<br>**Figure 7.5.4** |
| Scale: 1:160000 | Init: p5015 | | |

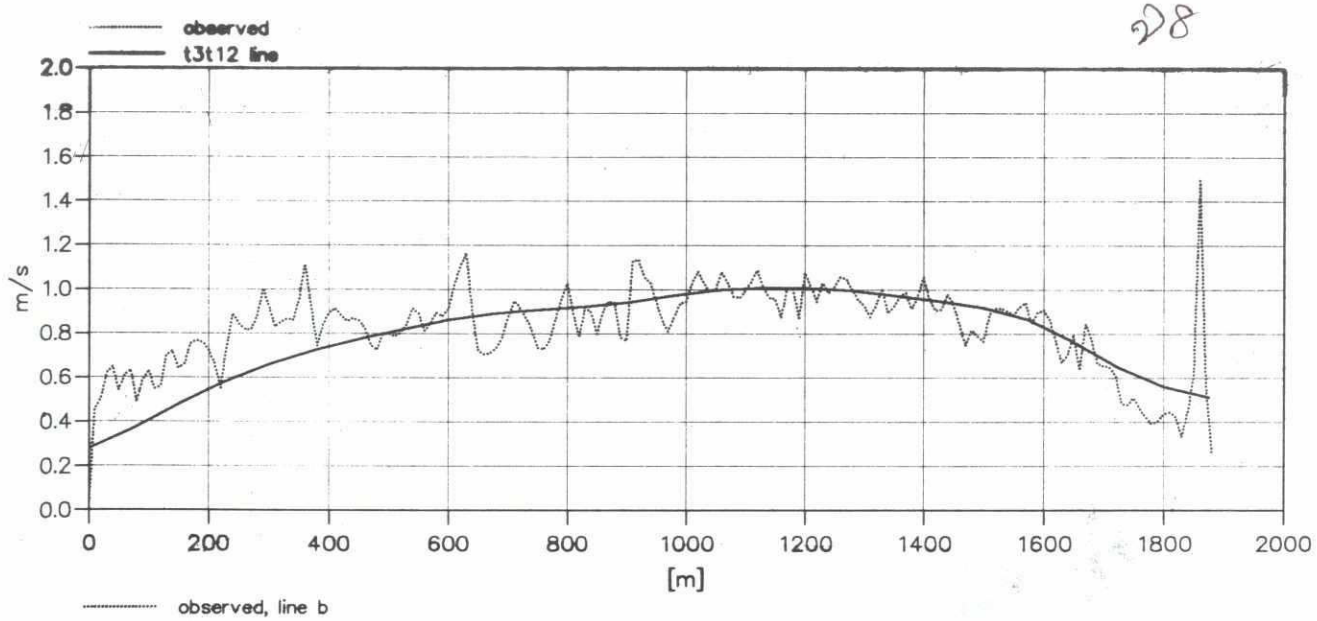


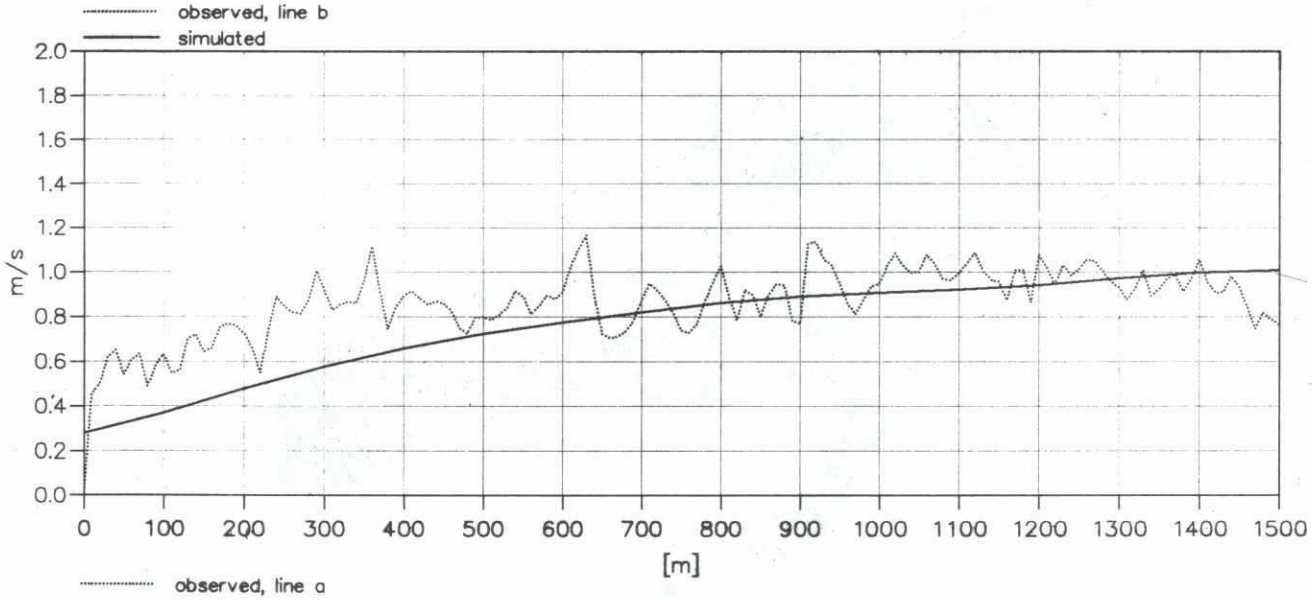


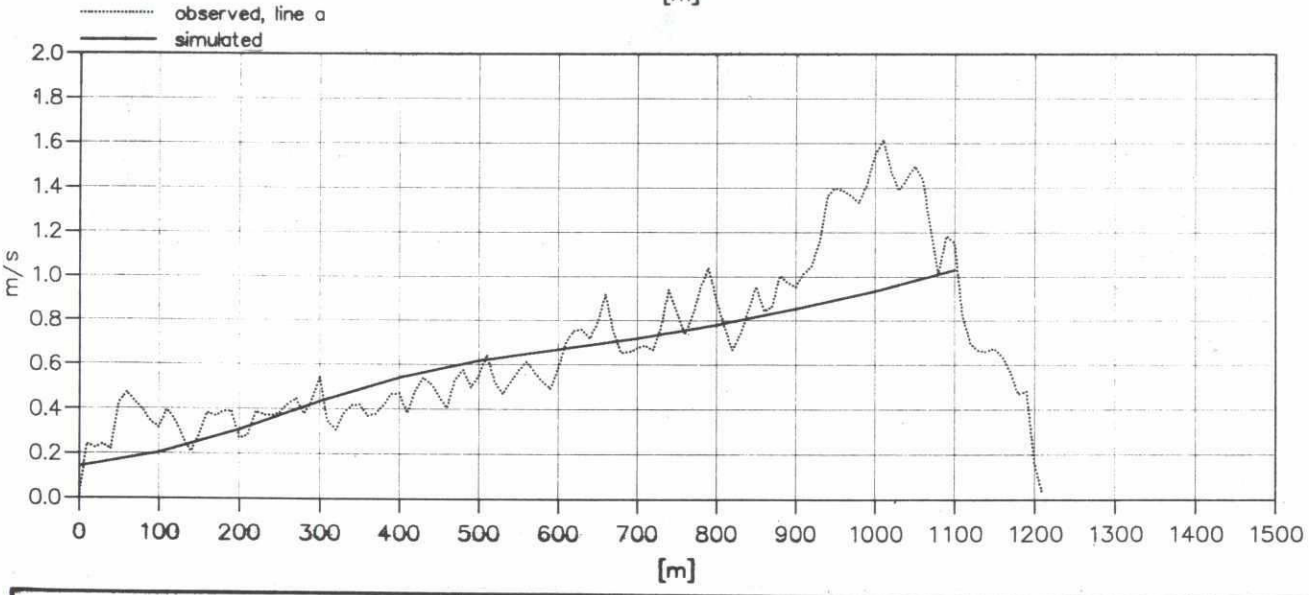


| SWMC | River Survey Project FAP24 | MIKE 21 |
|---|---|---|
| | Gorai Offtake Mathematical Modelling | |
| File: / Date: Mon Jun 10 1996 | Simulated and observed flow velocity<br>Different cross-sections<br>June 28, 1995 | dwg. no.<br>Figure 7.5.5 |
| Scale: / Init: hge | | |

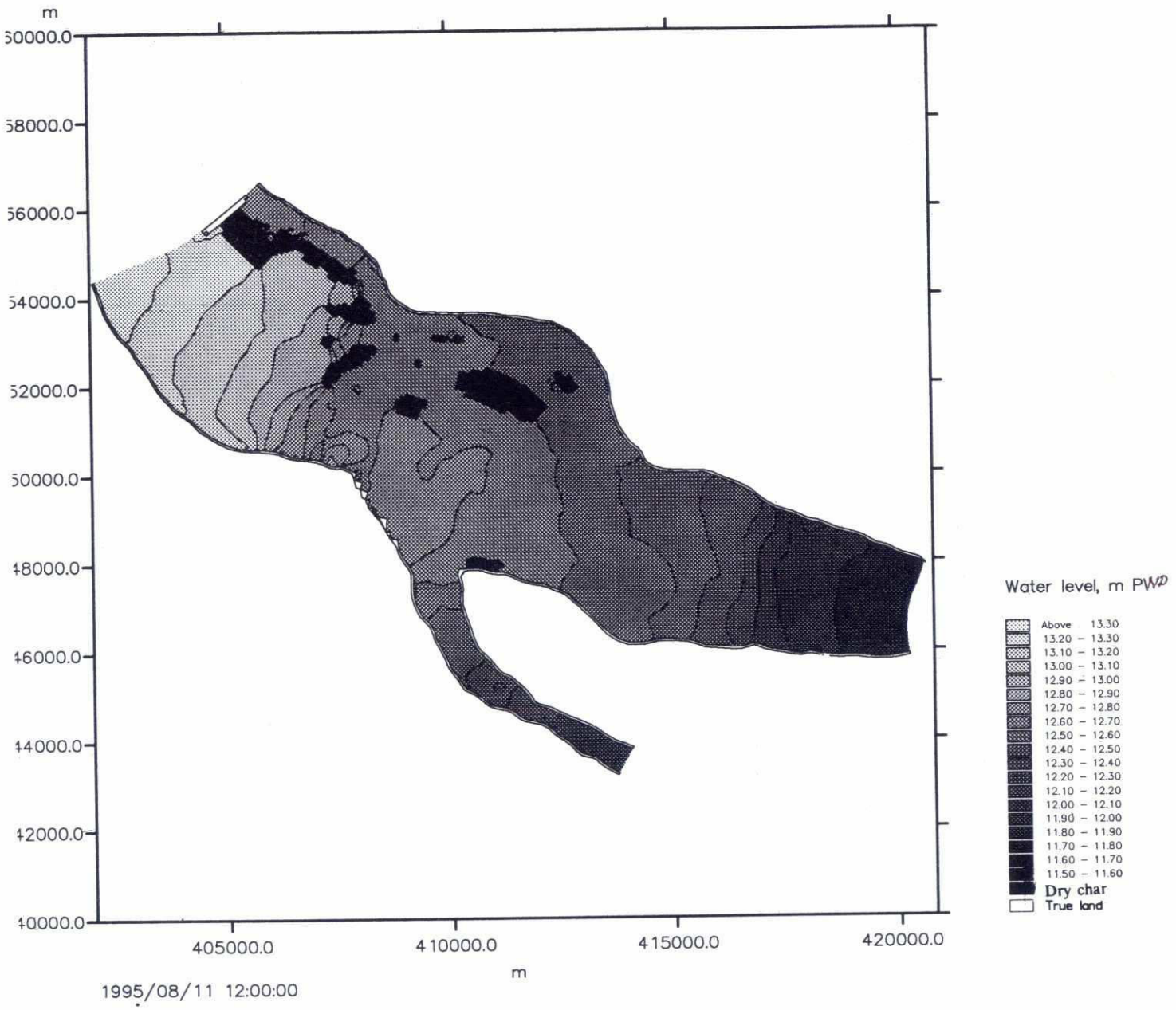


| | | | |
|---|---|---|---|
| SWMC | | Client: River Survey Project FAP24 | MIKE 21 |
| | | Project: Gorai Offtake Mathematical Modelling | |
| File: | Date: Thu Jun 13 1996 | Simulated water level<br>August 11, 1995<br>Local model | Drawing no.<br>**Figure 7.5.6** |
| Scale: 1:130000 | Init: hge | | |

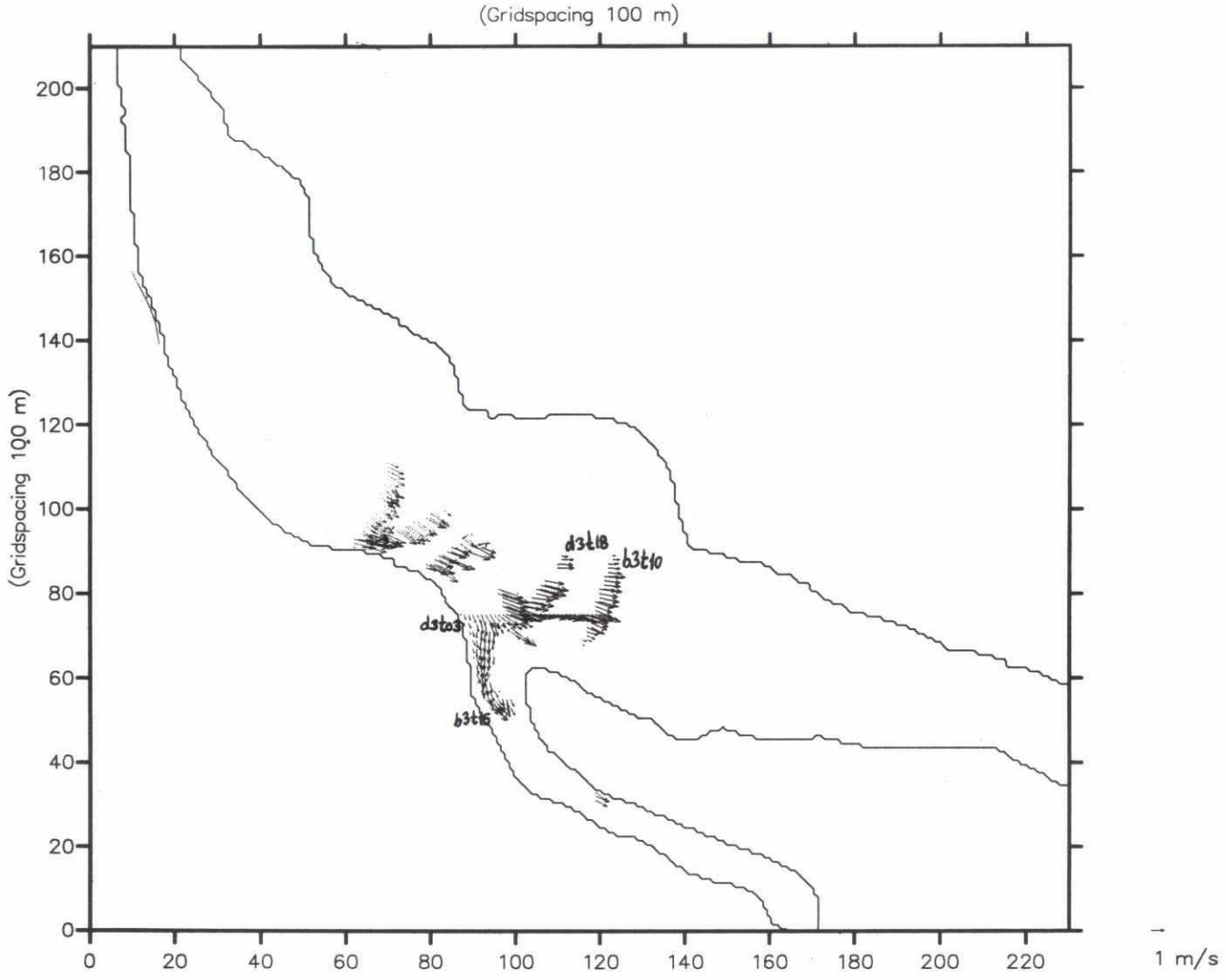


| SWMC | River Survey Project FAP24 | MIKE 21 |
|---|---|---|
| | Gorai Offtake Mathematical Modelling | |
| File: | Date: Mon Jun 10 1996 | Measured flow velocity field<br>August 11, 1995 |
| Scale: 1:160000 | Init: hge | dwg. no.<br>**Figure 7.5.7** |

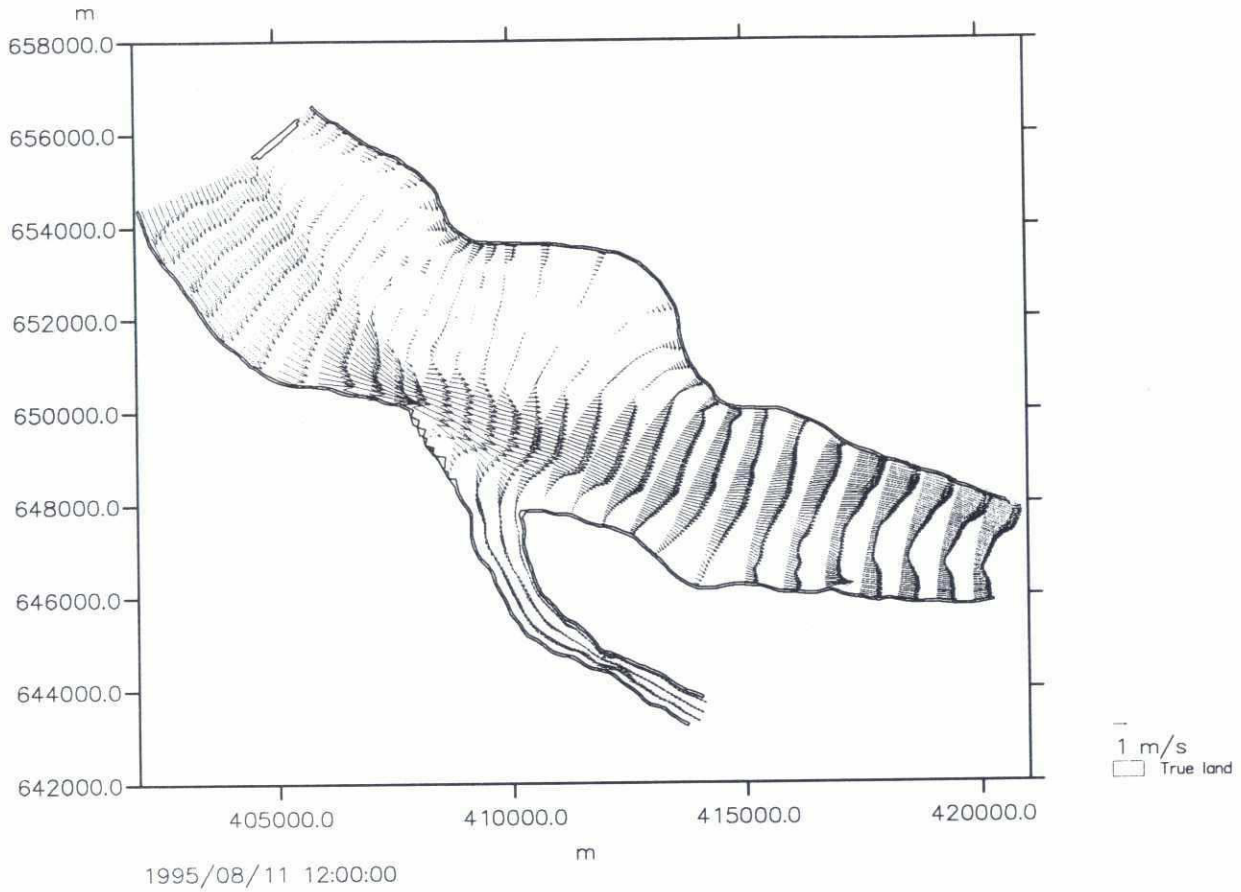


| | | | |
|---|---|---|---|
| SWMC | | Client: River Survey Project FAP24 | MIKE 21 |
| | | Project: Gorai Offtake Mathematical Modelling | |
| File: | Date: Mon Jun 10 1996 | Simulated flow velocity field<br>Local curvilinear model<br>August 11, 1995 | Drawing no.<br>**Figure 7.5.8** |
| Scale: 1:160000 | Init: p5015 | | |

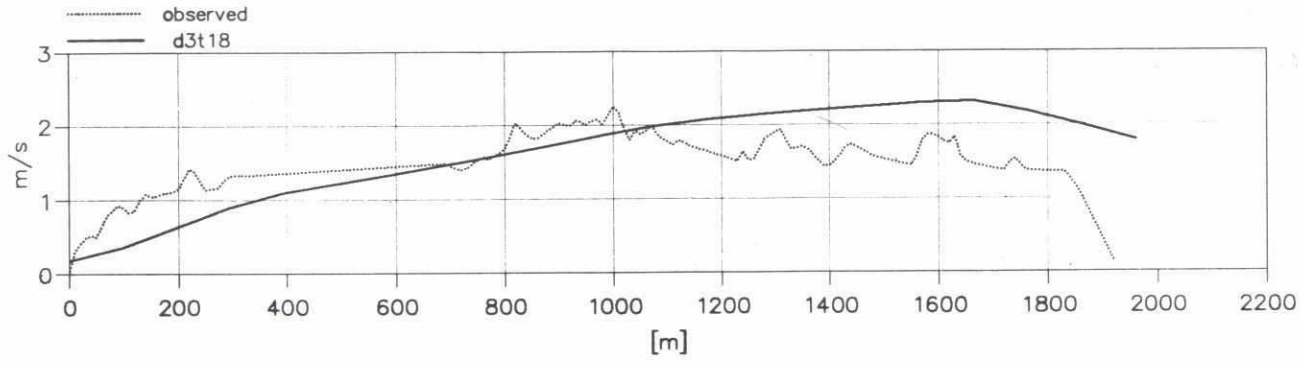


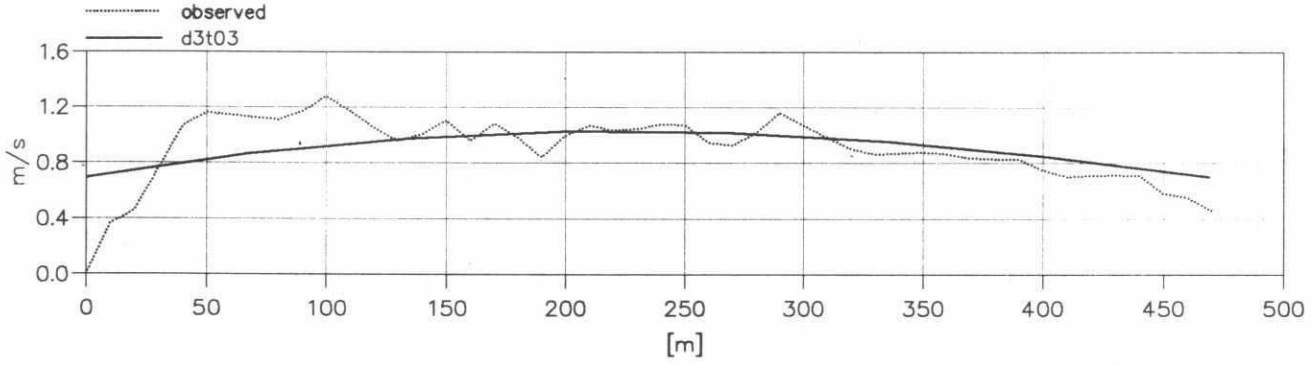


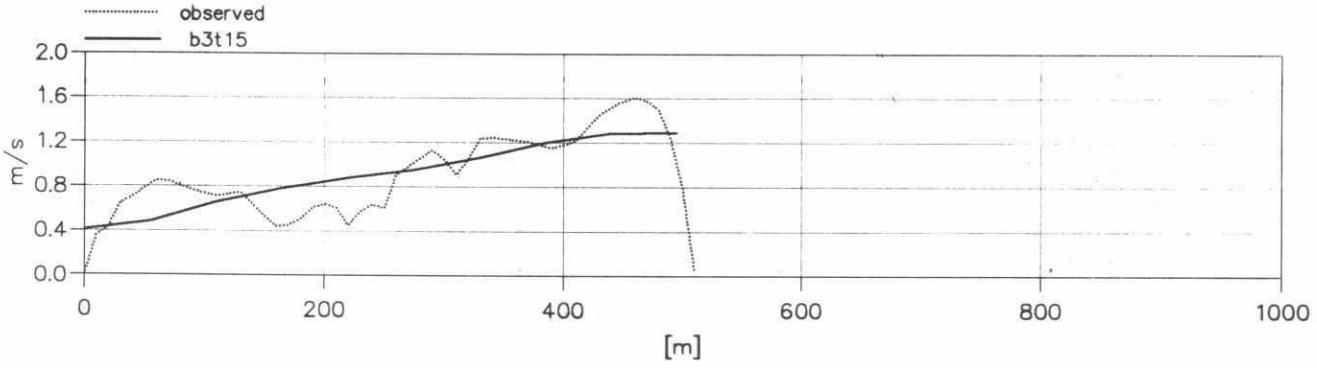


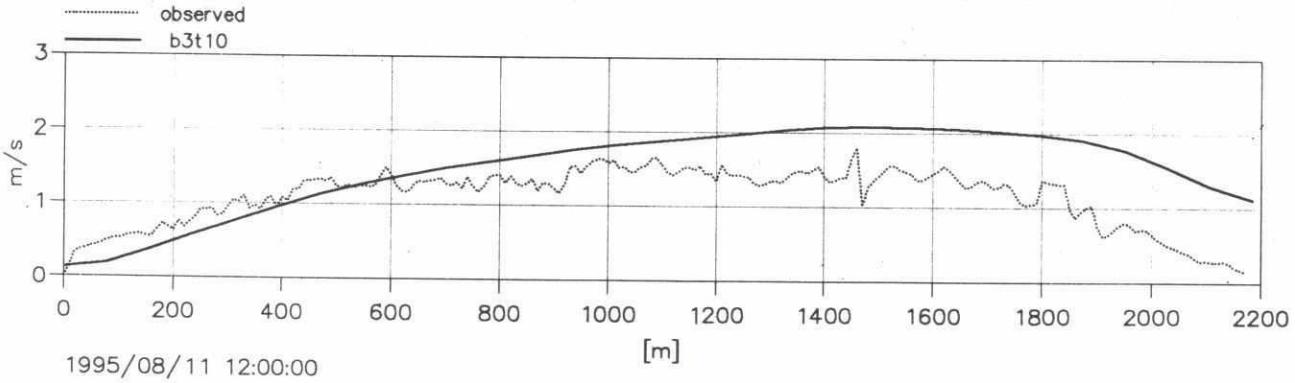


| SWMC | River Survey Project FAP24 | MIKE 21 |
|---|---|---|
| | Gorai Offtake Mathematical Modelling | |
| File: / Date: Mon Jun 10 1996 | Simulated and observed flow velocity<br>Different cross-sections<br>August 11, 1995 | dwg. no.<br>**Figure 7.5.9** |
| Scale: / Init: hge | | |

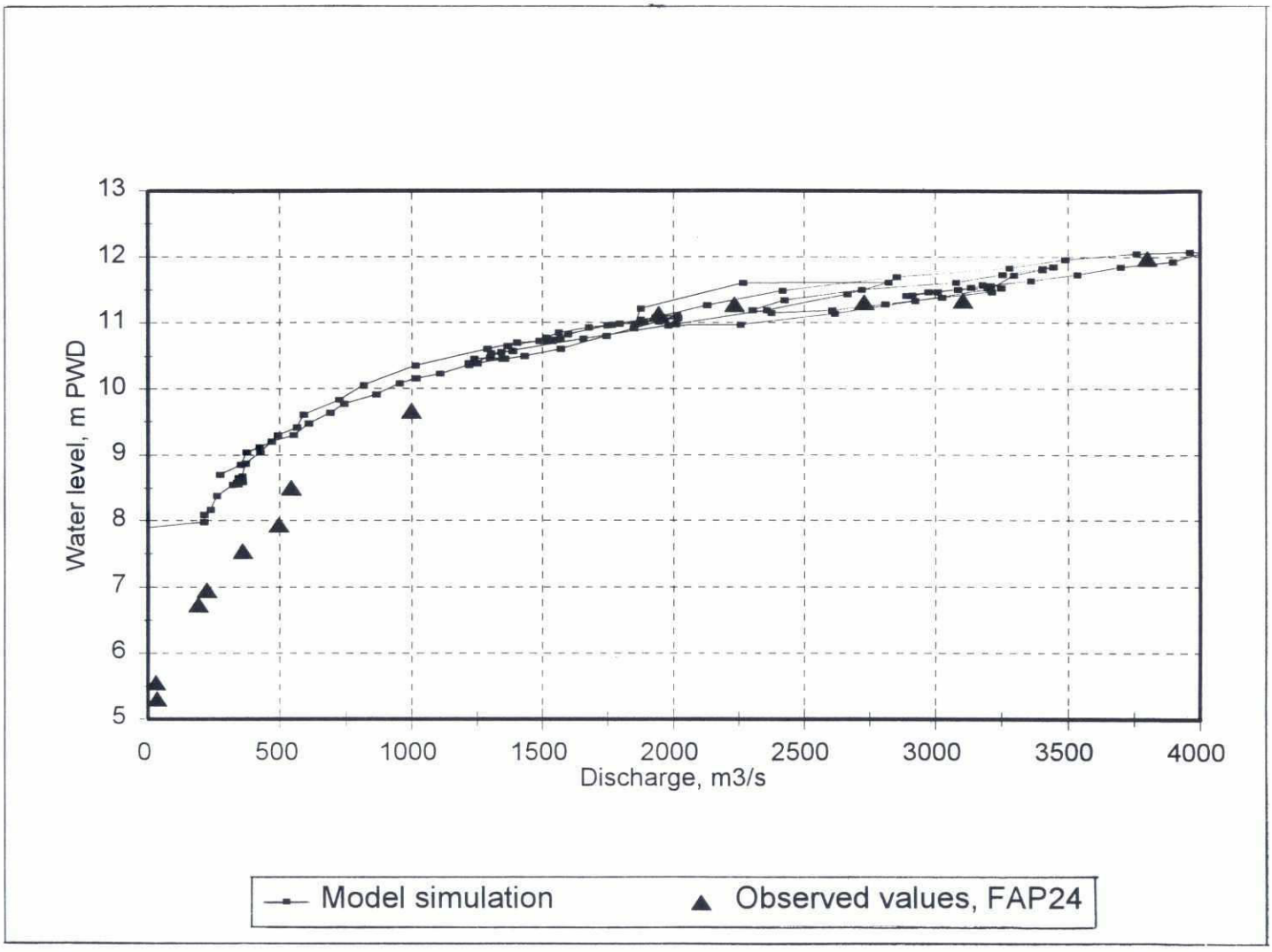


| | | | |
|---|---|---|---|
| SWMC | | Client: River Survey Project FAP24 | MIKE 21 |
| | | Project: Gorai Offtake Mathematical Modelling | |
| File: | Date: Thu Jun 13 1996 | Simulated and observed discharge rating curve Kushtia, Gorai River | Drawing no. Figure 7.5.10 |
| Scale: 1:110000 | Init: p5015 | | |

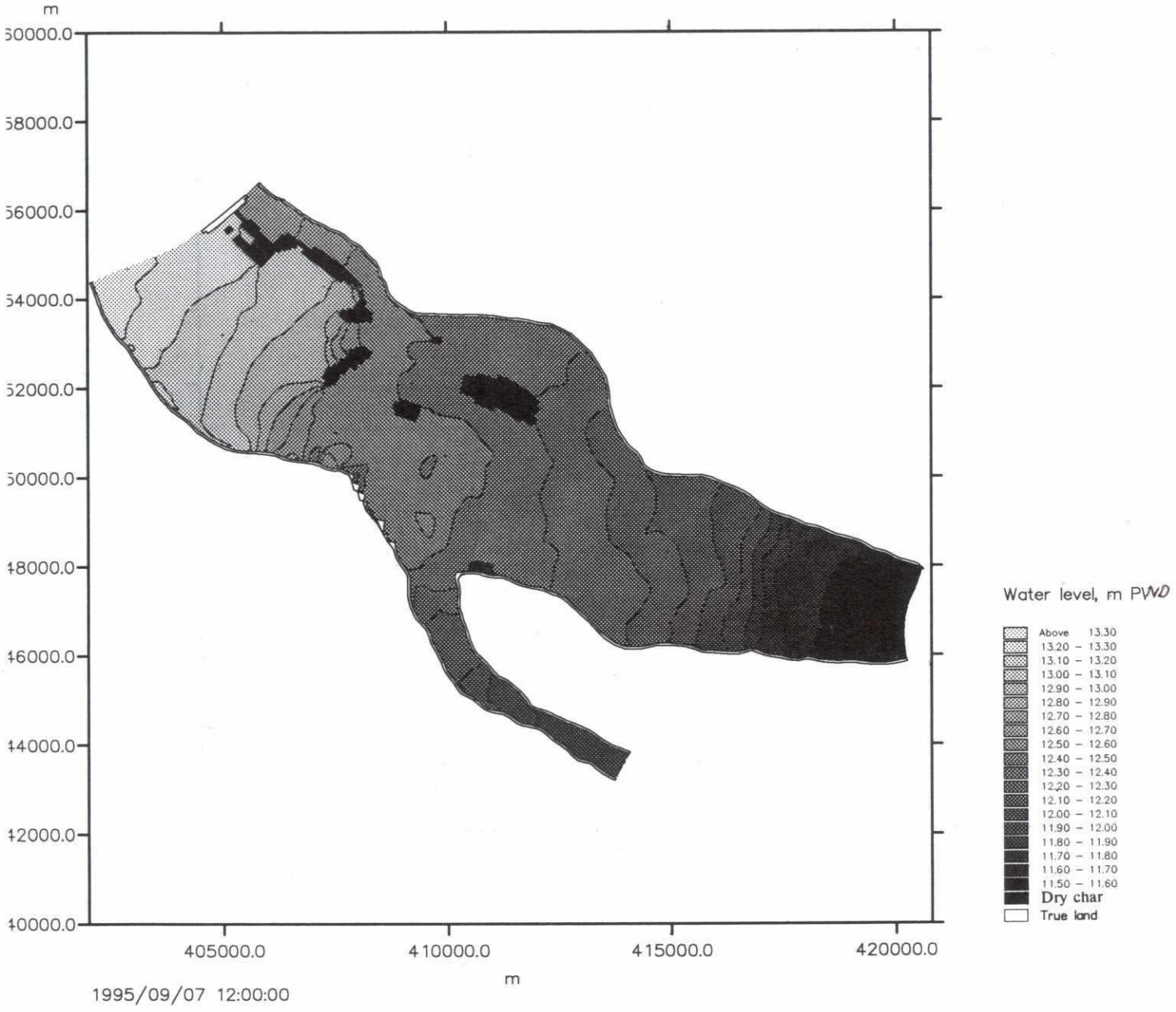


| | | | |
|---|---|---|---|
| SWMC | | Client: River Survey Project FAP24 | MIKE 21 |
| | | Project: Gorai Offtake Mathematical Modelling | |
| File: | Date: Thu Jun 13 1996 | Simulated water level<br>September 7, 1995<br>Local model | Drawing no.<br>**Figure 7.5.11** |
| Scale: 1:130000 | Init: hge | | |

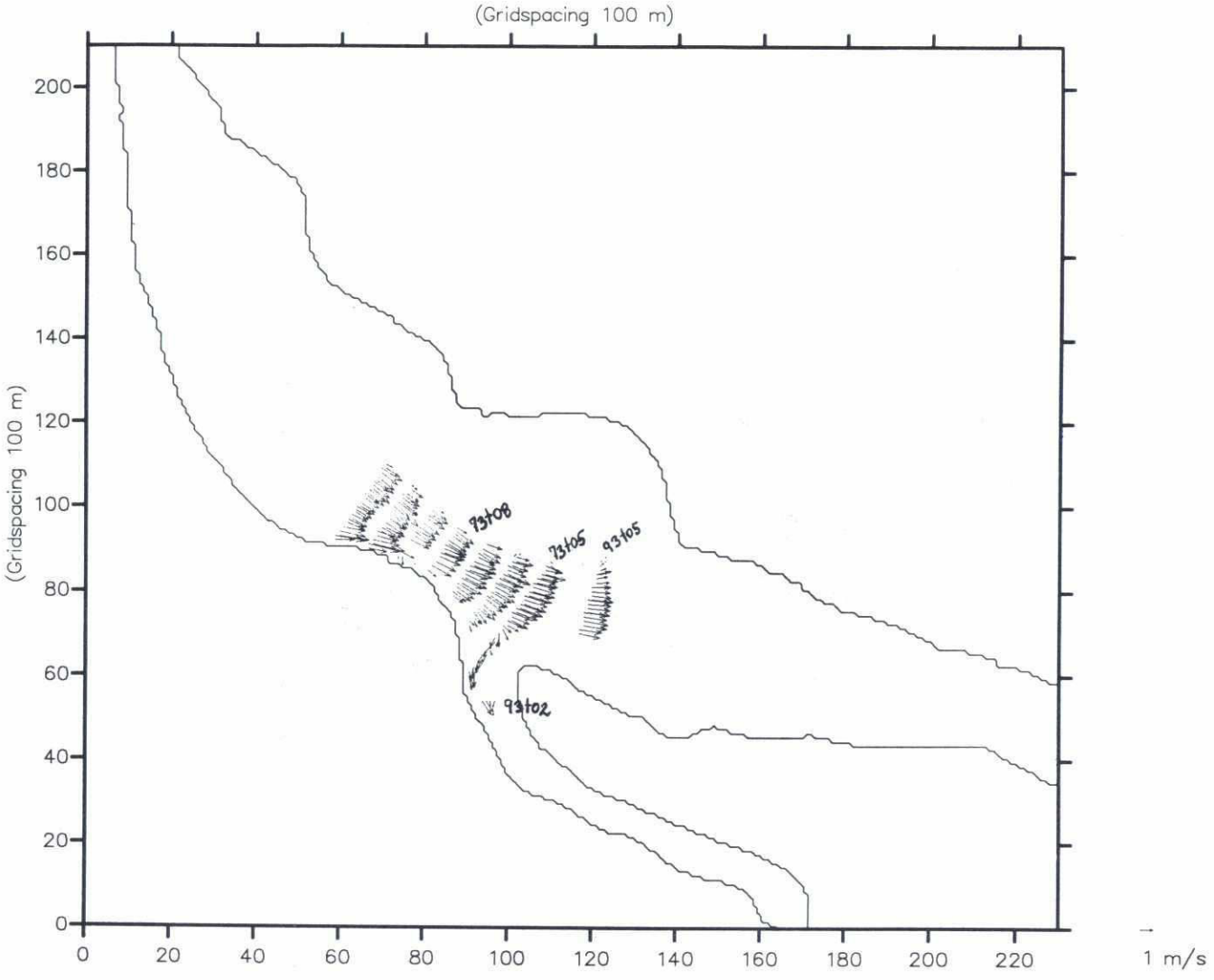


| SWMC | River Survey Project FAP24 | MIKE 21 |
|---|---|---|
| | Gorai Offtake Mathematical Modelling | |
| File: | Date: Mon Jun 10 1996 | Measured flow velocity field<br>September 7, 1995 |
| Scale: 1:160000 | Init: hge | dwg. no.<br>**Figure 7.5.12** |

202

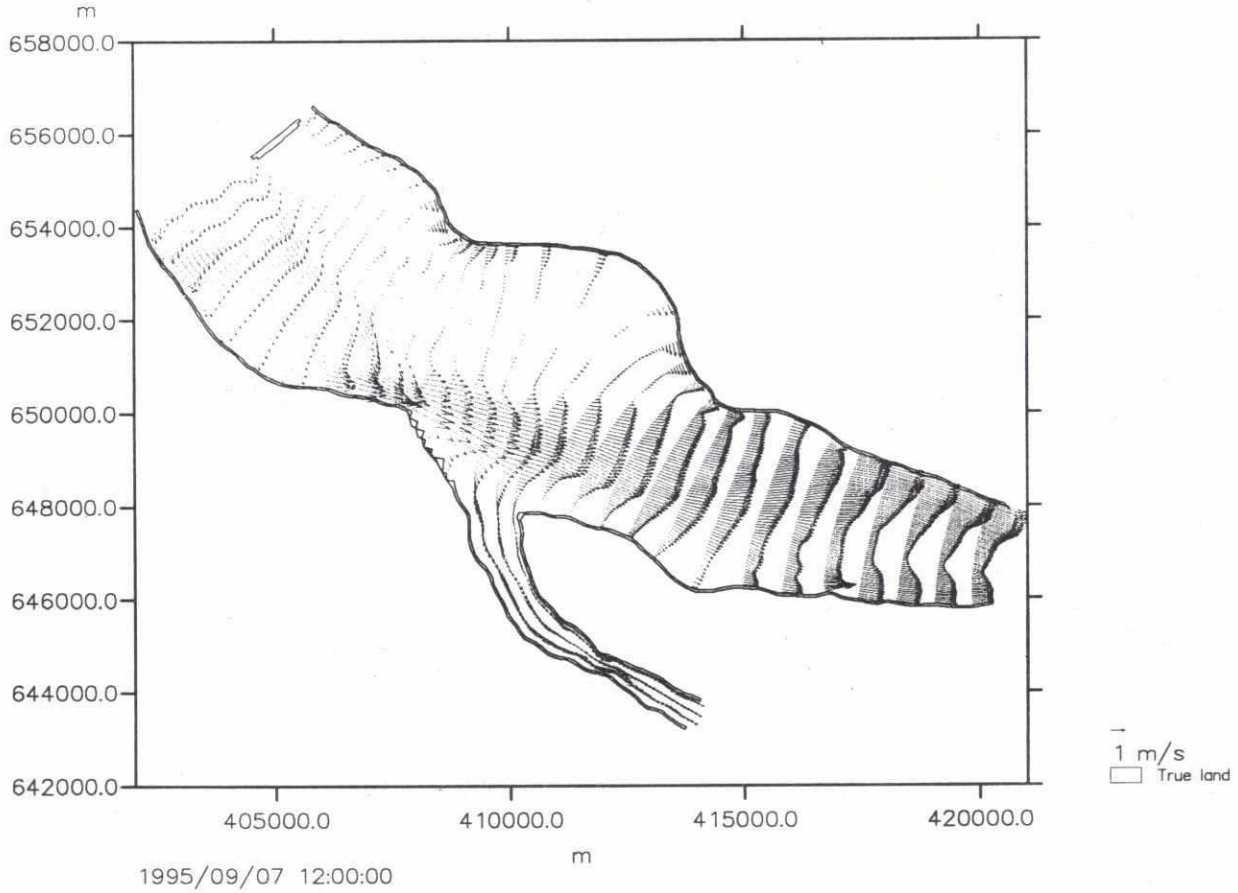


| SWMC | | Client: River Survey Project FAP24 | MIKE 21 |
|---|---|---|---|
| | | Project: Gorai Offtake Mathematical Modelling | |
| File: | Date: Mon Jun 10 1996 | Simulated flow velocity field<br>Local curvilinear model<br>September 7, 1995 | Drawing no.<br>**Figure 7.5.13** |
| Scale: 1:160000 | Init: p5015 | | |

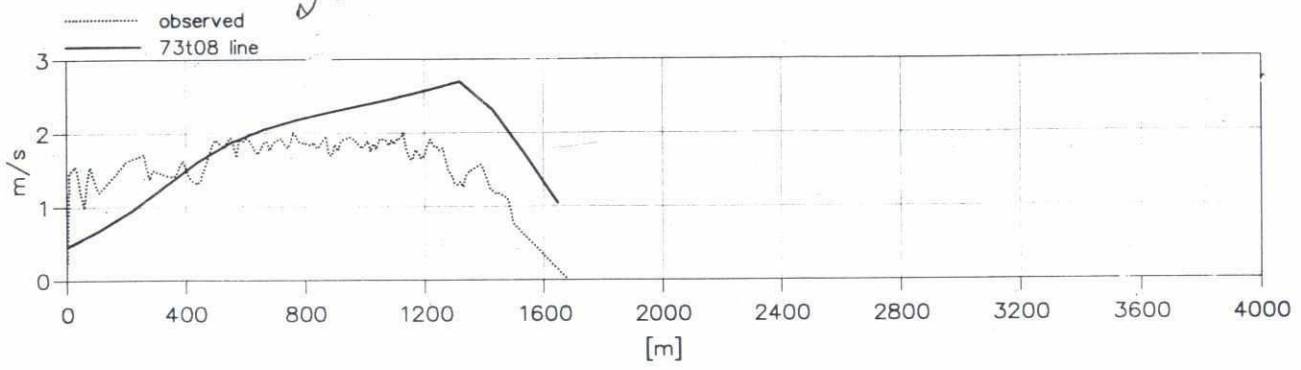


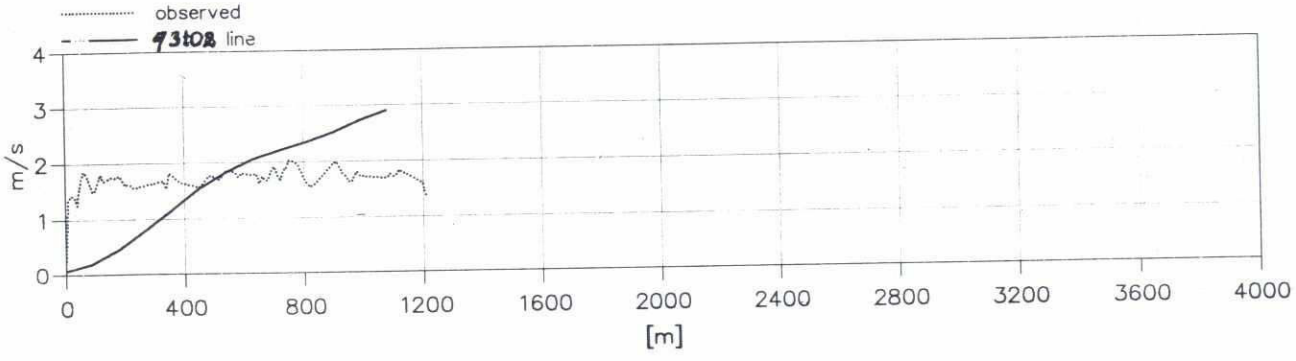


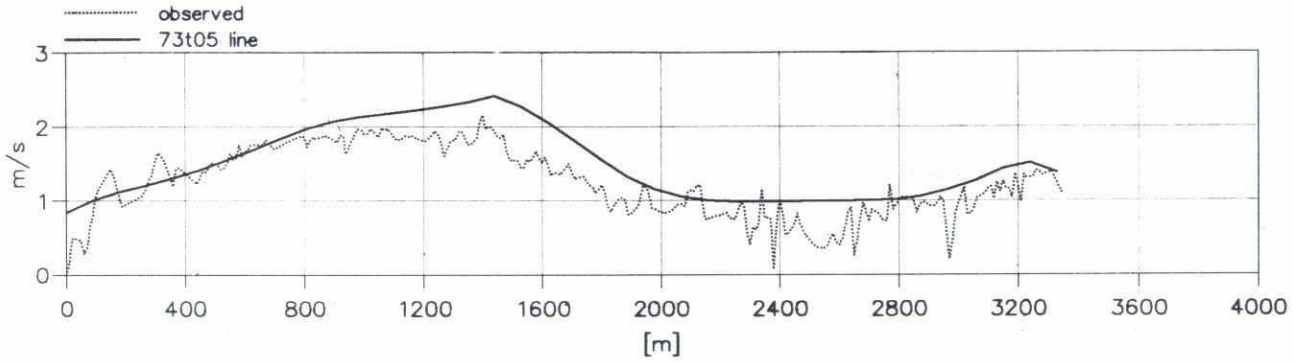


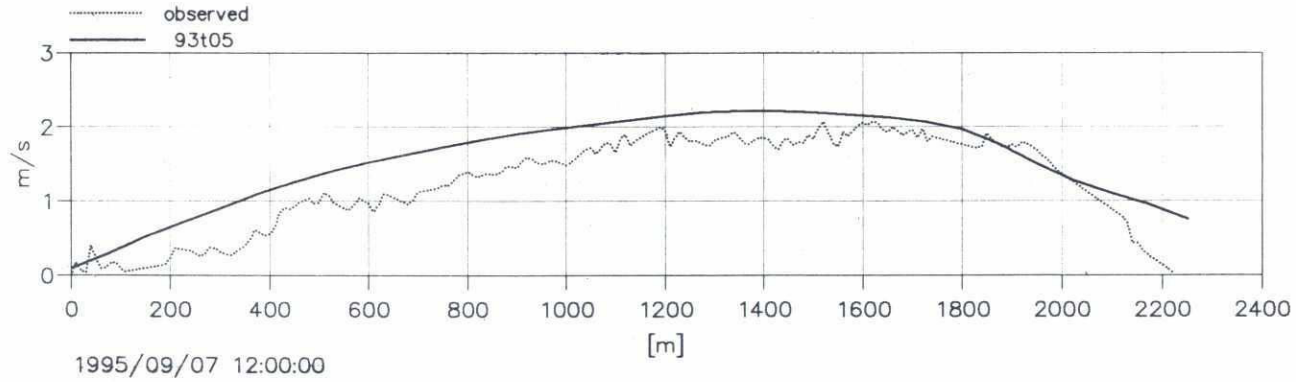


| SWMC | River Survey Project FAP24 | MIKE 21 |
|---|---|---|
| | Gorai Offtake Mathematical Modelling | |
| File: | Date: Mon Jun 10 1996 | Simulated and observed flow velocity<br>Different cross-sections<br>September 7, 1995 |
| $cale: | Init: hge | dwg. no.<br>**Figure 7.5.14** |

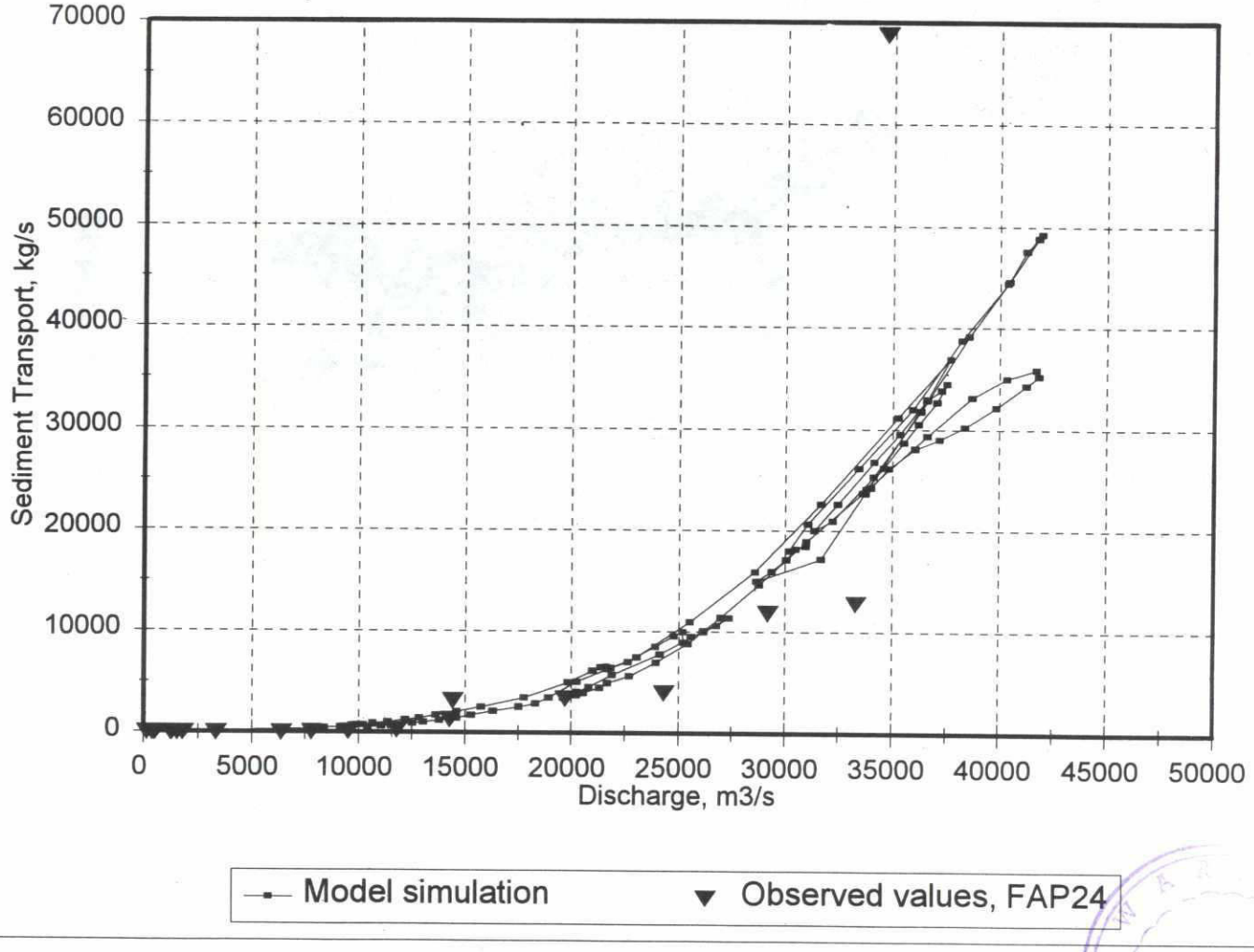




| | | | |
|---|---|---|---|
| SWMC | | Client: River Survey Project FAP24 | MIKE 21 |
| | | Project: Gorai Offtake Mathematical Modelling | |
| File: | Date: Thu Jun 13 1996 | Simulated and observed sediment transport rating curve Hardinge Bridge/Upstream Gorai Offtake | Drawing no. Figure 7.6.1 |
| Scale: 1:110000 | Init: p5015 | | |

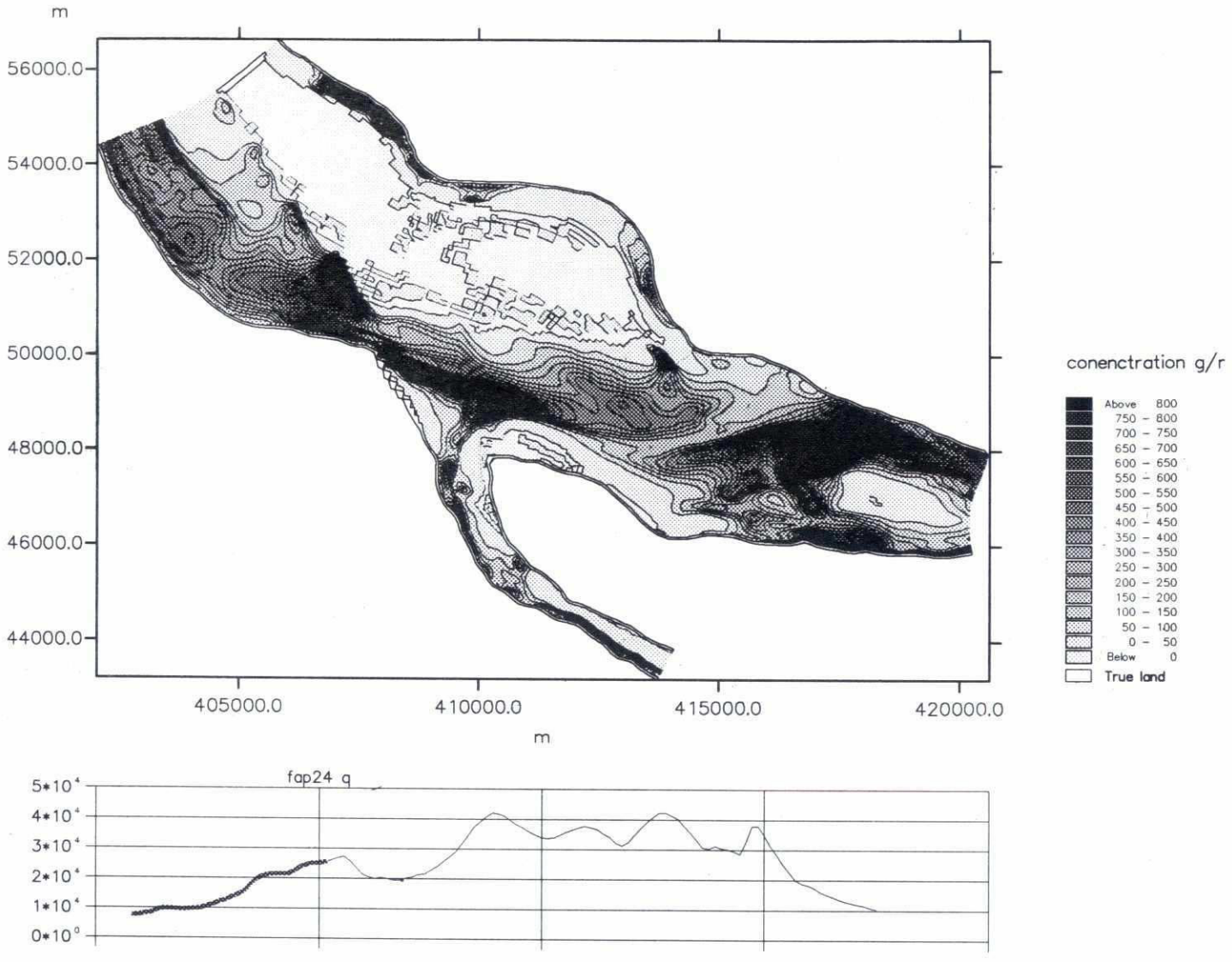


| | | | |
|---|---|---|---|
| SWMC | | Client: River Survey Project FAP24 | MIKE 21 |
| | | Project: Gorai Offtake Mathematical Modelling | |
| File: | Date: Mon Jun 10 1996 | Simulated concentration suspended sediment from fixed bed model | Drawing no. **Figure 7.6.2** |
| Scale: 1:130000 | Init: hge | | |

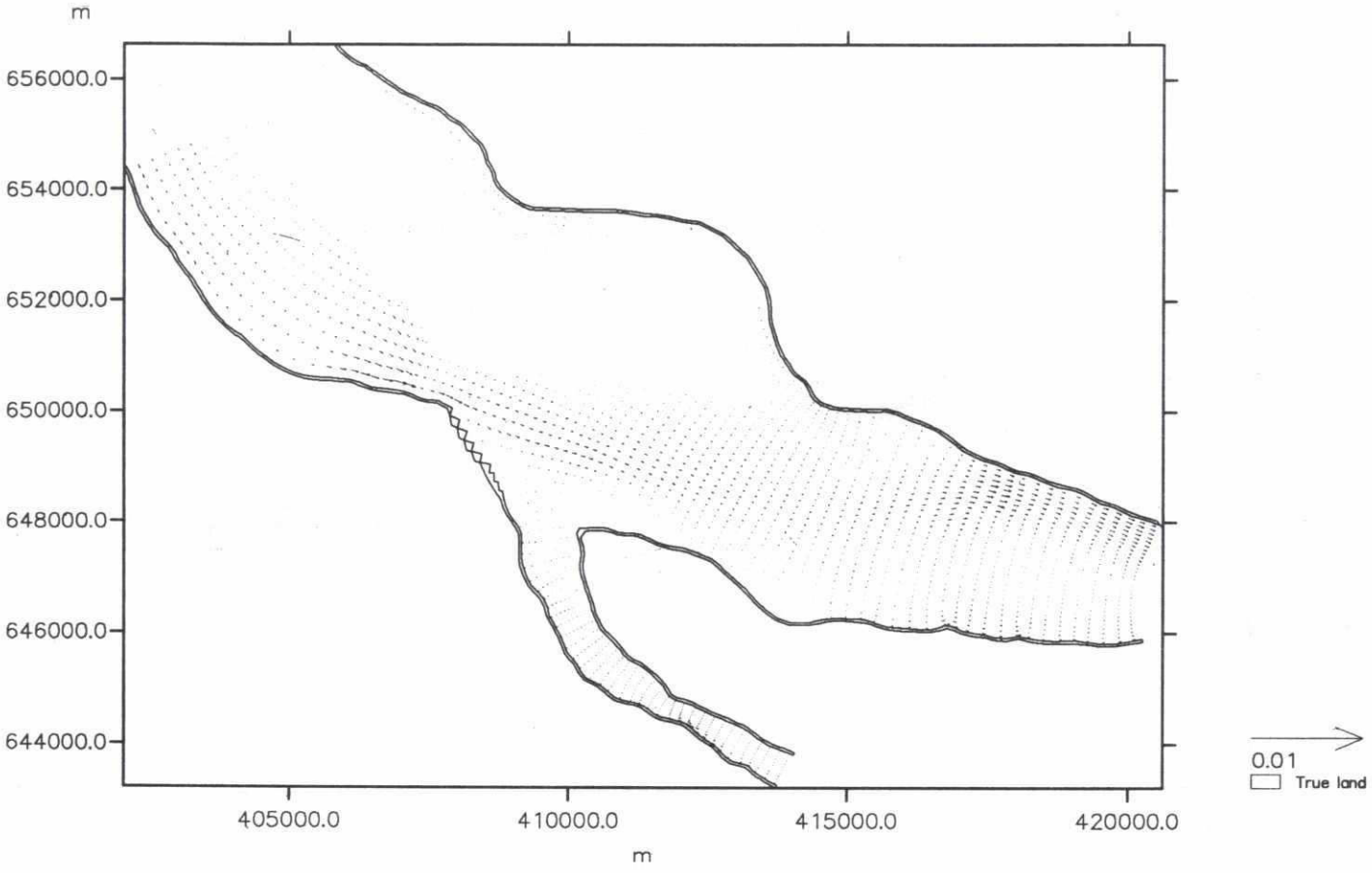


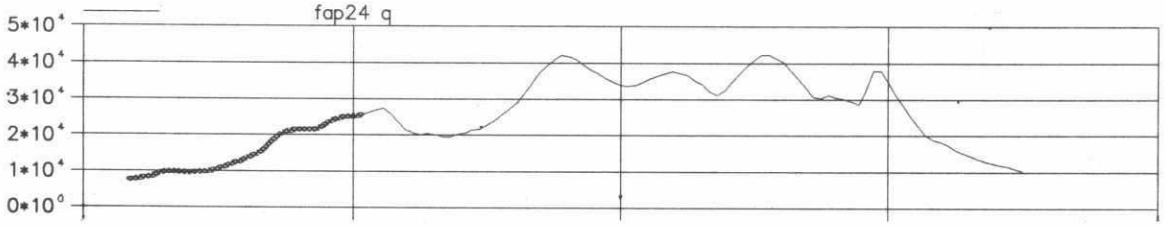


| | | | |
|---|---|---|---|
| SWMC | Client: River Survey Project FAP24 | | MIKE 21 |
| | Project: Gorai Offtake Mathematical Modelling | | |
| File: | Date: Sun Jun 9 1996 | Simulated bed load sediment transport<br>Vector field<br>from fixed bed model | Drawing no. **Figure 7.6.3** |
| Scale: 1:130000 | Init: hge | | |

207

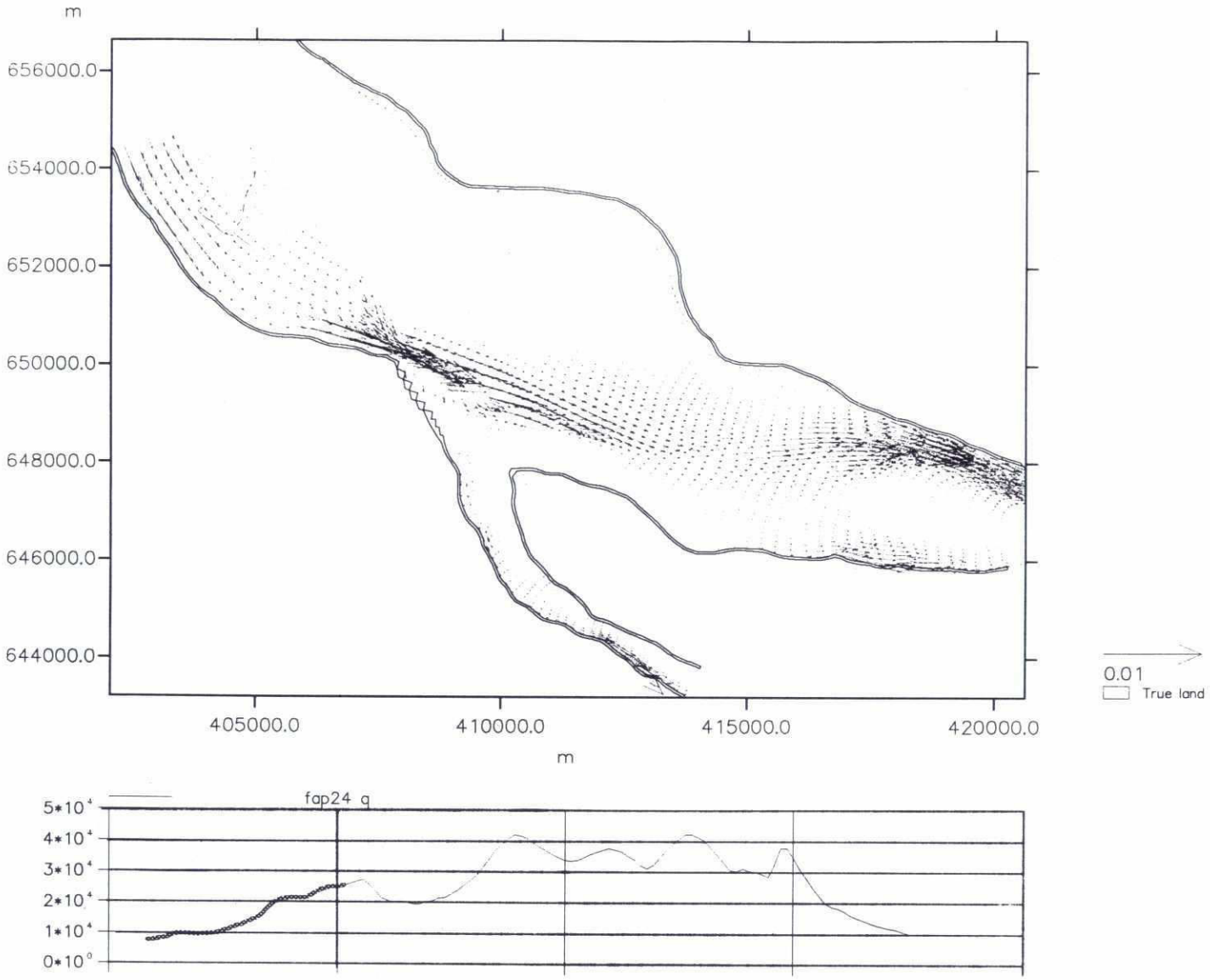


| | | | |
|---|---|---|---|
| SWMC | Client: River Survey Project FAP24 | | MIKE 21 |
| | Project: Gorai Offtake Mathematical Modelling | | |
| File: | Date: Sun Jun 9 1996 | Simulated suspended sediment transport<br>Vector field<br>from fixed bed model | Drawing no.<br>**Figure 7.6.4** |
| Scale: 1:130000 | Init: hge | | |

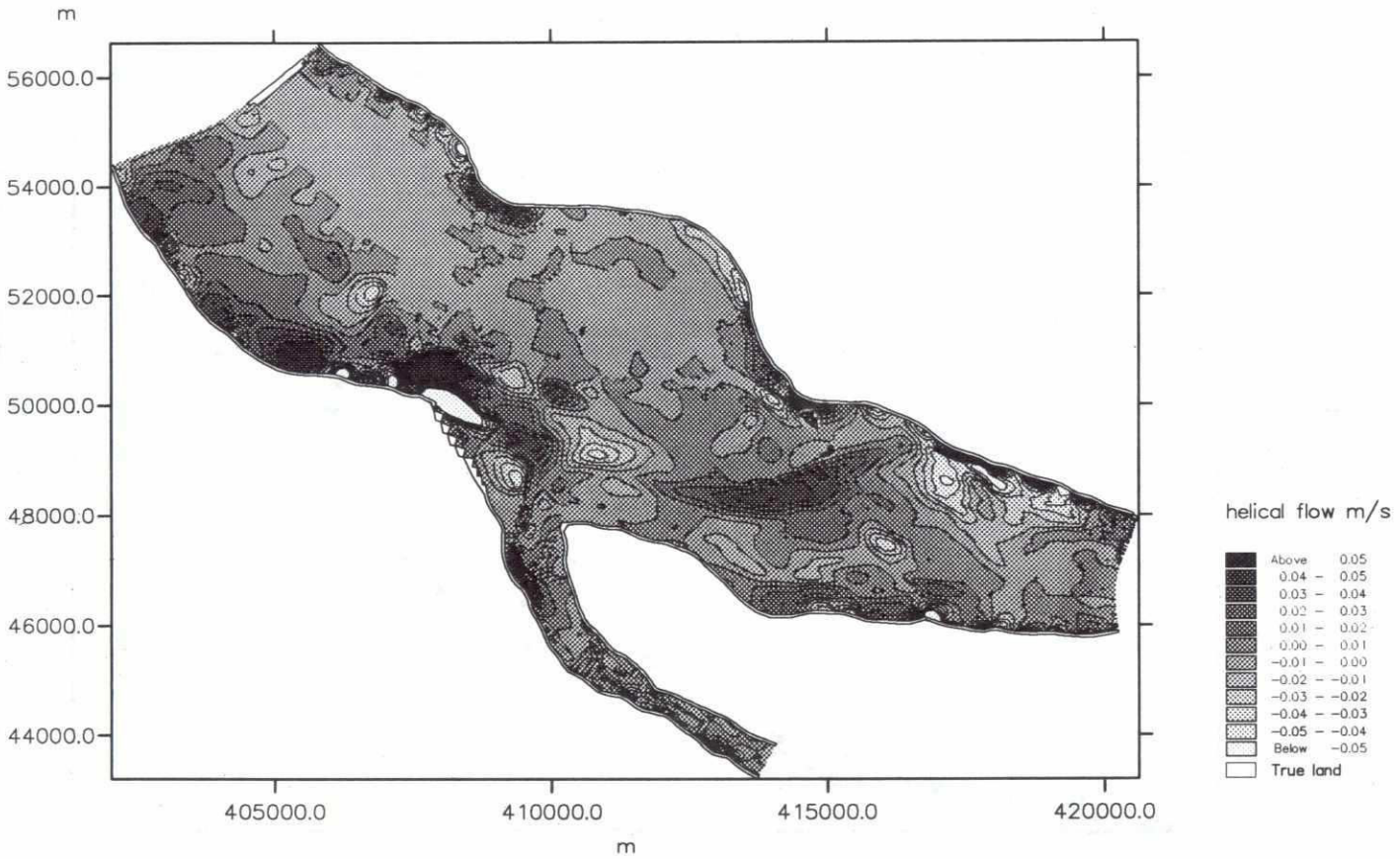


| SWMC | Client: River Survey Project FAP24 | MIKE 21 |
|---|---|---|
| | Project: Gorai Offtake Mathematical Modelling | |
| File: | Date: Mon Jun 10 1996 | Helical flow intensity<br>neg/pos depends on flow curvature<br>from fixed bed model |
| Scale: 1:130000 | Init: hge | Drawing no.<br>**Figure 7.6.5** |

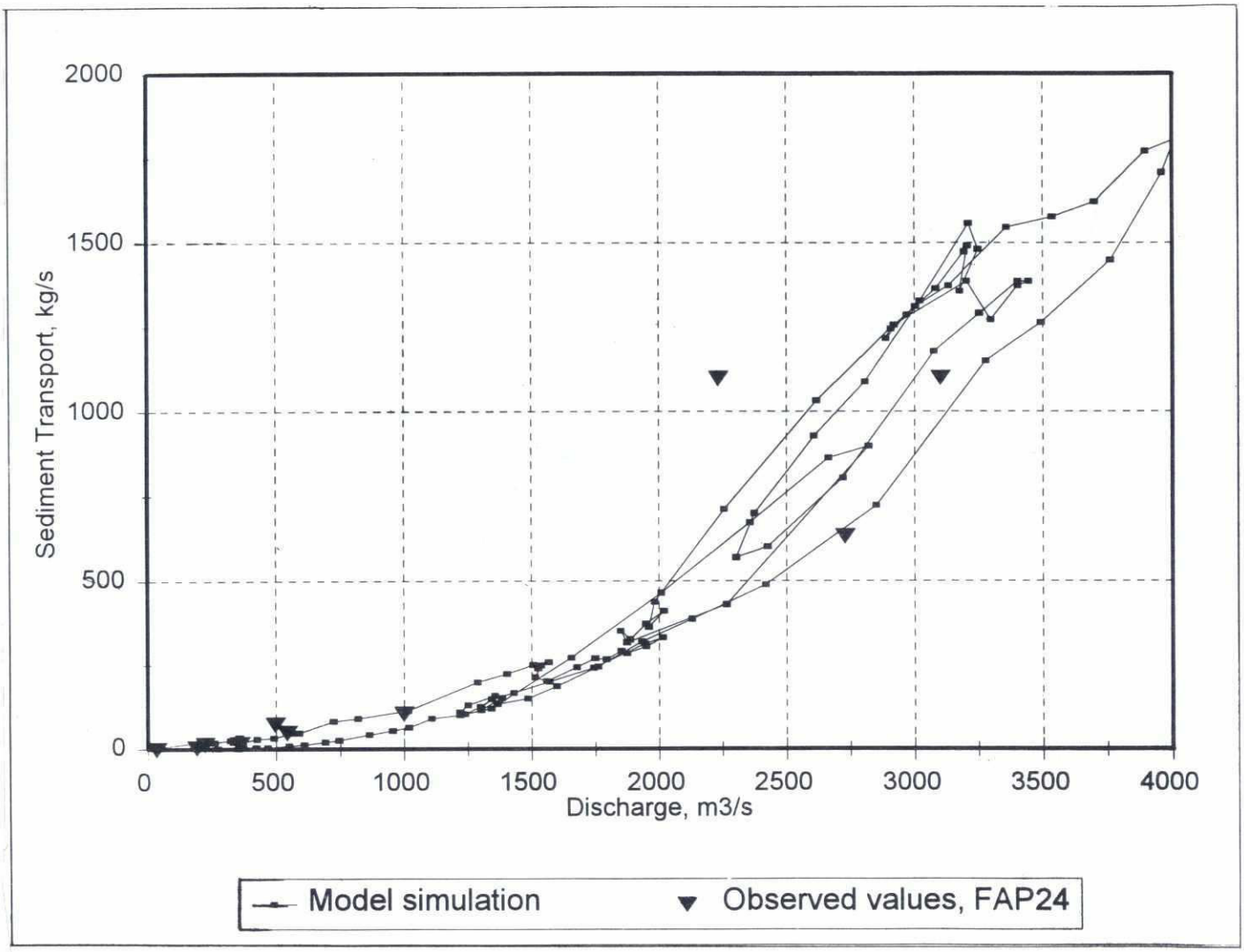


| SWMC | Client: River Survey Project FAP24 | MIKE 21 |
|---|---|---|
| | Project: Gorai Offtake Mathematical Modelling | |
| File: | Date: Thu Jun 13 1996 | Simulated and observed sediment transport rating curve Kushtia, Gorai River |
| Scale: 1:110000 | Init: p5015 | Drawing no. Figure 7.6.6 |

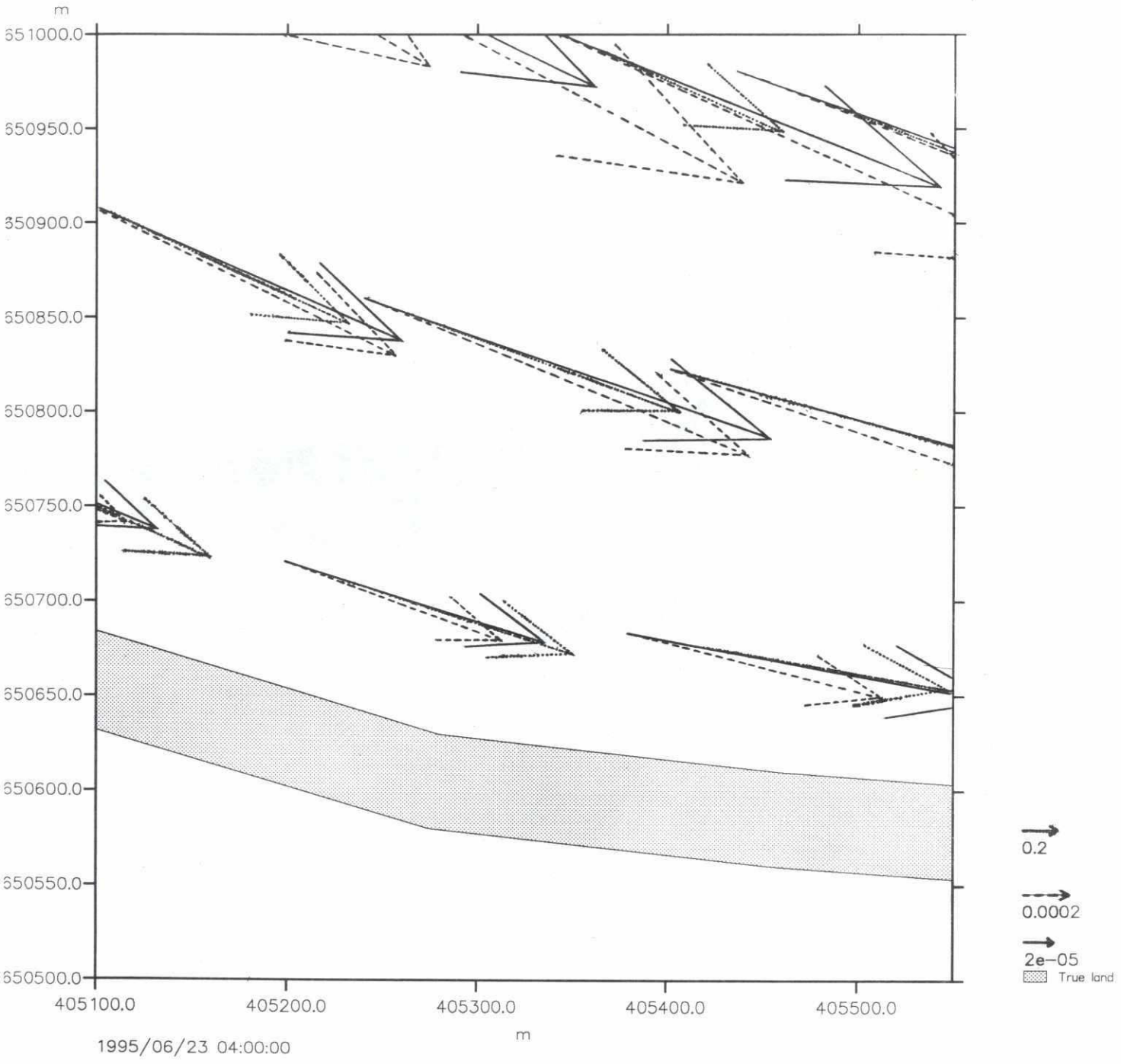


| | | | |
|---|---|---|---|
| SWMC | | Client: River Survey Project FAP24 | MIKE 21 |
| | | Project: Gorai Offtake Mathematical Modelling | |
| File: | Date: Fri Jul 5 1996 | Effect of helical flow in curved flow<br>Suspended load: dashed line<br>Bed load: full line flow velocity: dotted line | Drawing no. |
| Scale: 1:3000 | Init: hge | | Figure 7.6.7 |

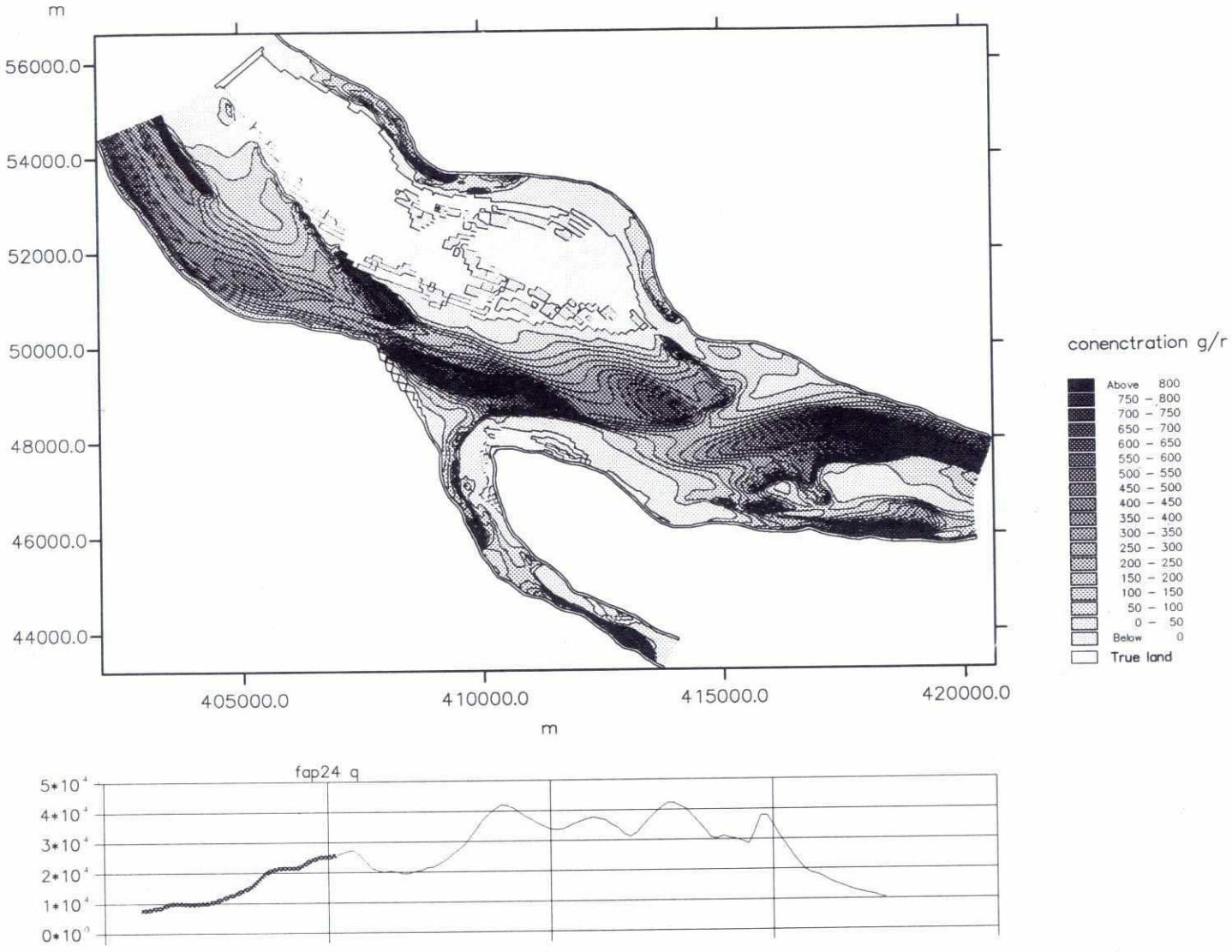


| | | | |
|---|---|---|---|
| SWMC | Client: River Survey Project FAP24 | | MIKE 21 |
| | Project: Gorai Offtake Mathematical Modelling | | |
| File: | Date: Mon Jun 10 1996 | Simulated concentration suspended sediment from movable bed model | Drawing no. **Figure 7.7.1** |
| Scale: 1:130000 | Init: hge | | |

222

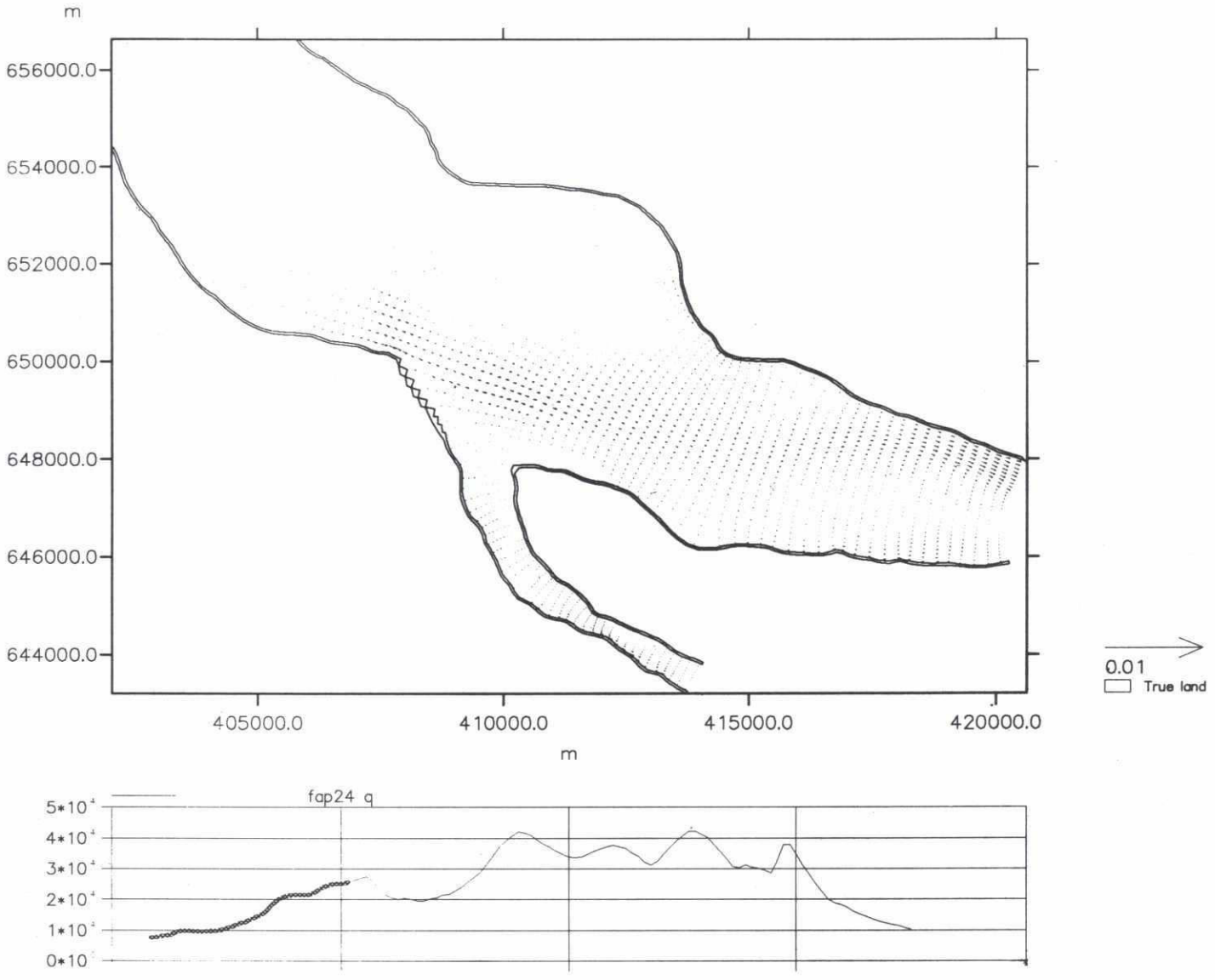


| | | | |
|---|---|---|---|
| SWMC | | Client: River Survey Project FAP24 | MIKE 21 |
| | | Project: Gorai Offtake Mathematical Modelling | |
| File: | Date: Sun Jun 9 1996 | Simulated bed load sediment transport<br>Vector field<br>from movable bed model | Drawing no.<br>**Figure 7.7.2** |
| Scale: 1:130000 | Init: hge | | |

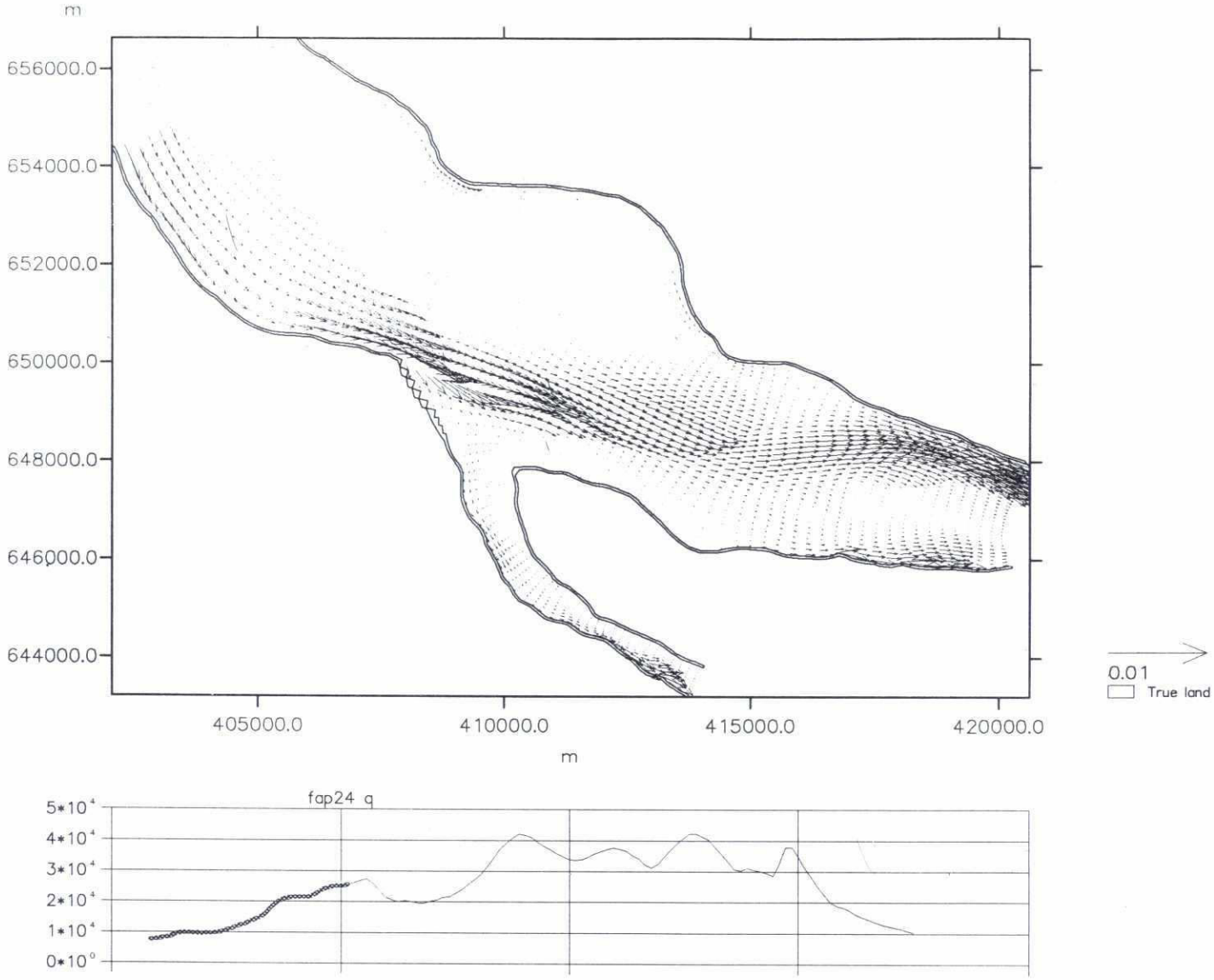


| | | | |
|---|---|---|---|
| SWMC | | Client: River Survey Project FAP24 | MIKE 21 |
| | | Project: Gorai Offtake Mathematical Modelling | |
| File: | Date: Sun Jun 9 1996 | Simulated suspended sediment transport<br>Vector field<br>from movable bed model | Drawing no.<br>**Figure 7.7.3** |
| Scale: 1:130000 | Init: hge | | |

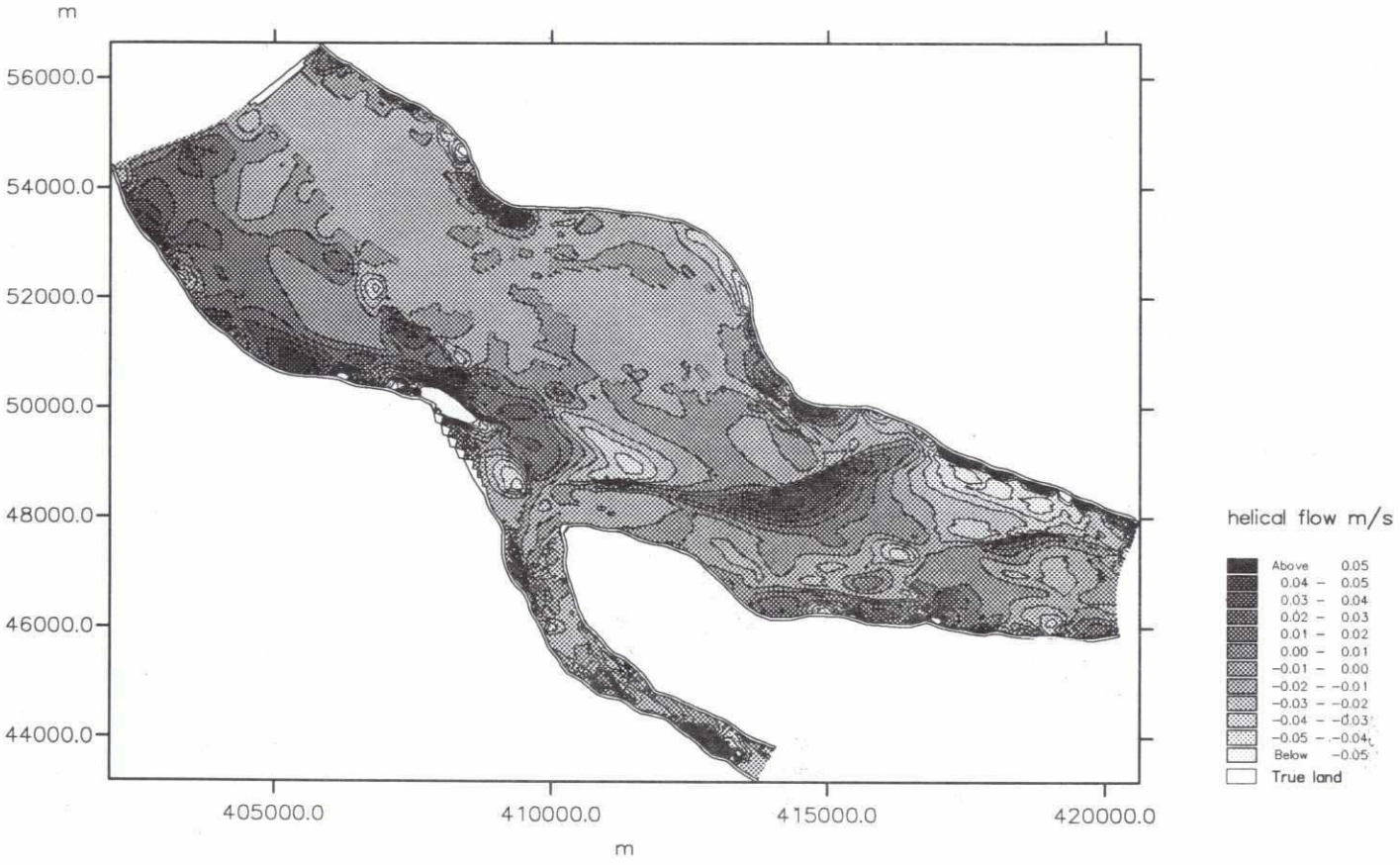


| | | | |
|---|---|---|---|
| SWMC | | Client: River Survey Project FAP24 | MIKE 21 |
| | | Project: Gorai Offtake Mathematical Modelling | |
| File: | Date: Mon Jun 10 1996 | Helical flow intensity<br>neg/pos depends on flow curvature<br>from movable bed model | Drawing no. **Figure 7.7.4** |
| Scale: 1:130000 | Init: hge | | |

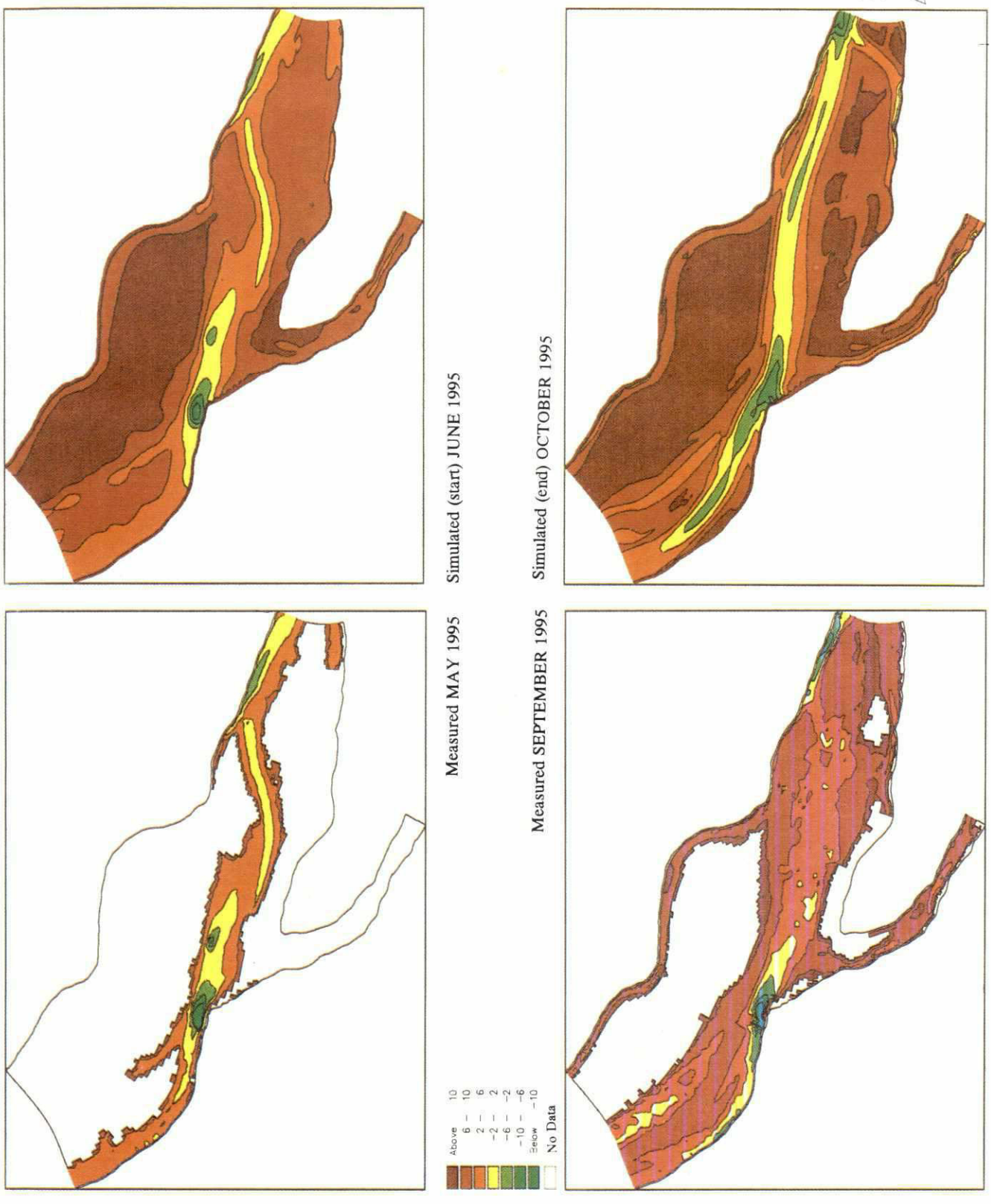


| | | | |
|---|---|---|---|
| SWMC | | Client: River Survey Project FAP24 | MIKE 21 |
| | | Project: Gorai Offtake Mathematical Modelling | |
| File: | Date: Wed Oct 2 1996 | Simulated and observed bathymetry<br>May/June 1995<br>September/October 1995 | Drawing no.<br>Figure 7·7·5 |
| Scale: 1:180000 | Init: p5015 | | |

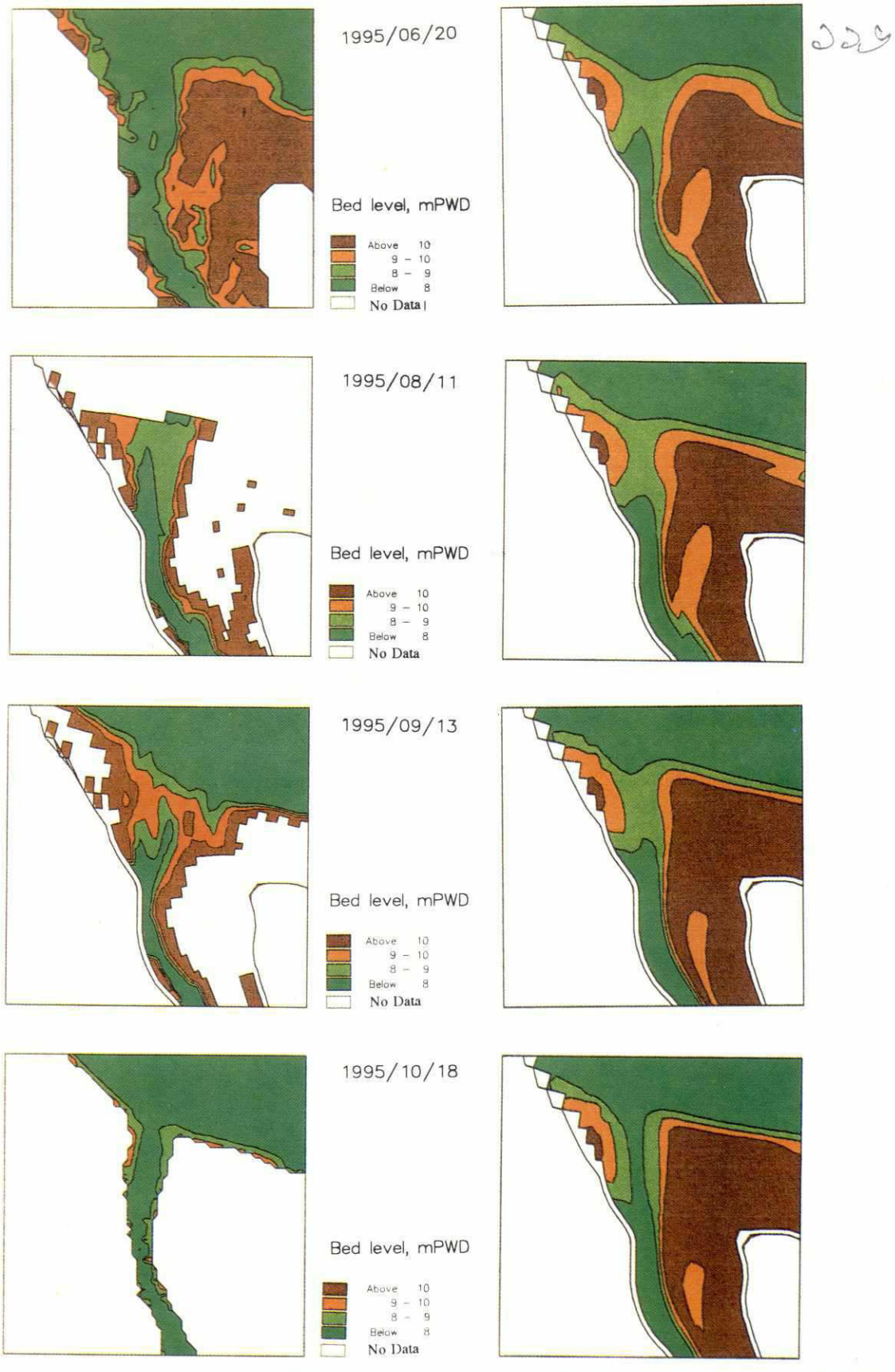


| | | | |
|---|---|---|---|
| SWMC | | Client: River Survey Project FAP24 | MIKE 21 |
| | | Project: Gorai Offtake Mathematical Modelling | |
| File: | Date: Wed Oct 2 1996 | Measured (left) and simulated (right) bed levels at offtake at different time of the monsoon | Drawing no. Figure 7·7·6 |
| Scale: 1:60000 | Init: p5015 | | |

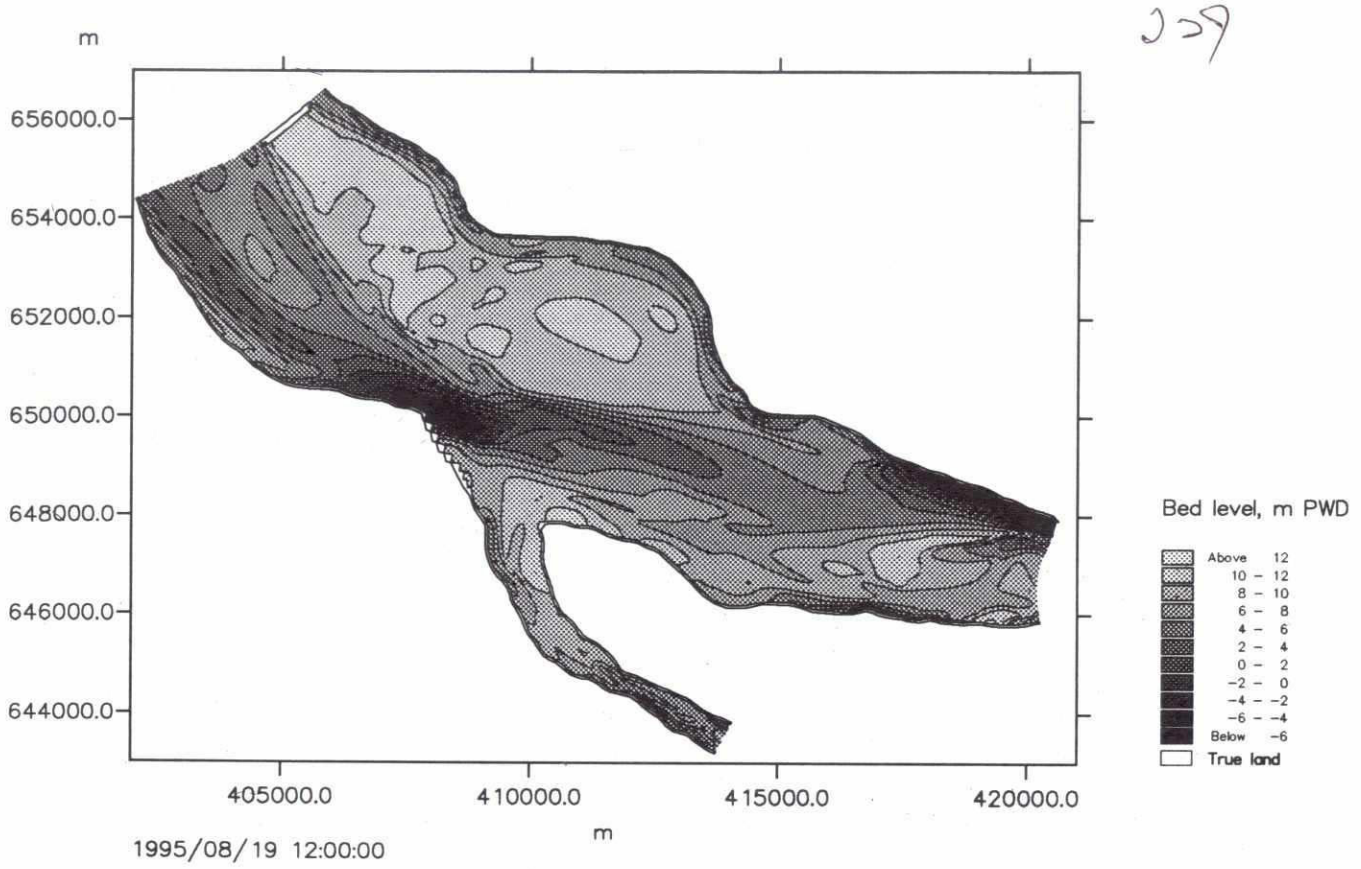


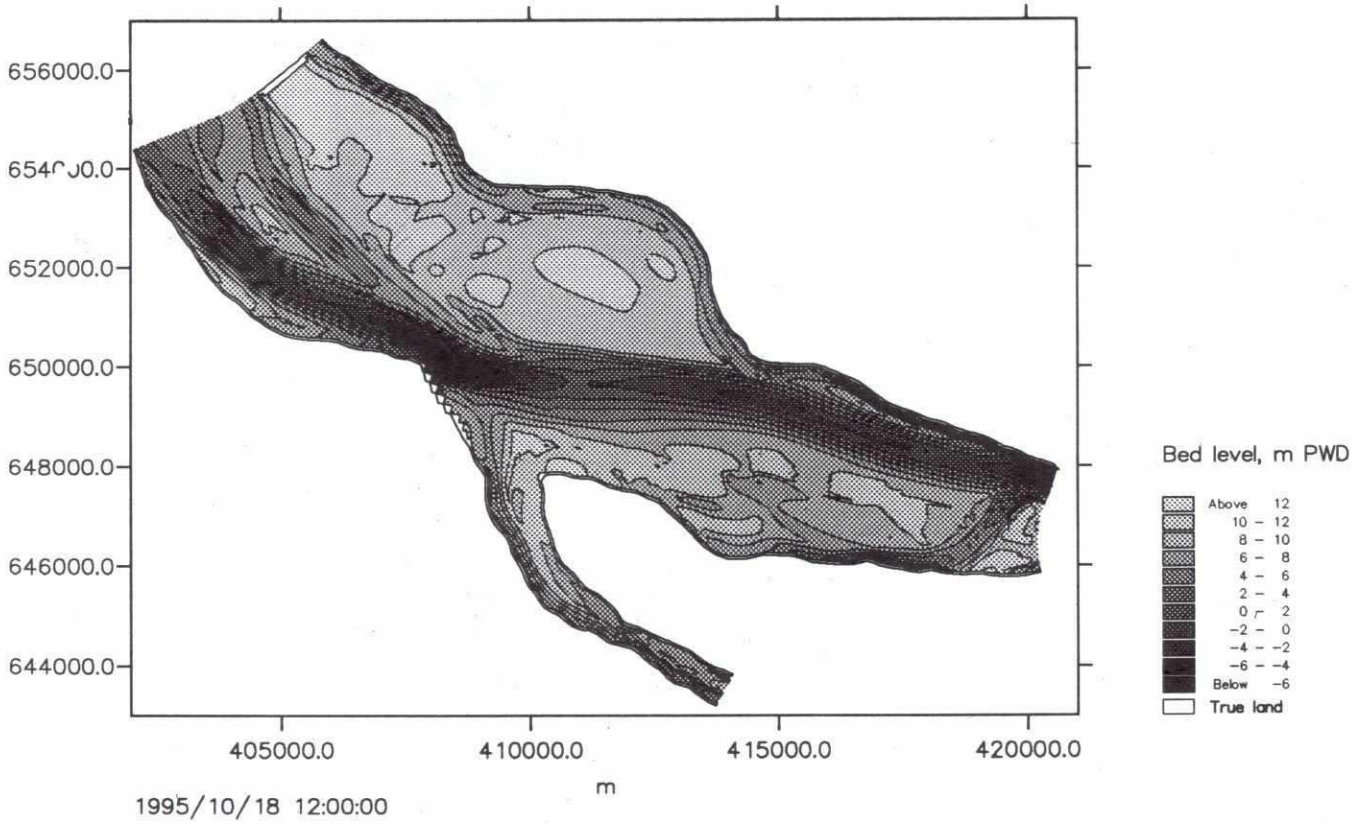


| | | | |
|---|---|---|---|
| SWMC | Client: River Survey Project FAP24 | | MIKE 21 |
| | Project: Gorai Offtake Mathematical Modelling | | |
| File: | Date: Thu Jul 4 1996 | Simulated bathymetry after 2 and 4 mths<br>Ganges and Gorai<br>Base run | Drawing no. **Figure 7.8.1** |
| Scale: 1:150000 | Init: hge | | |

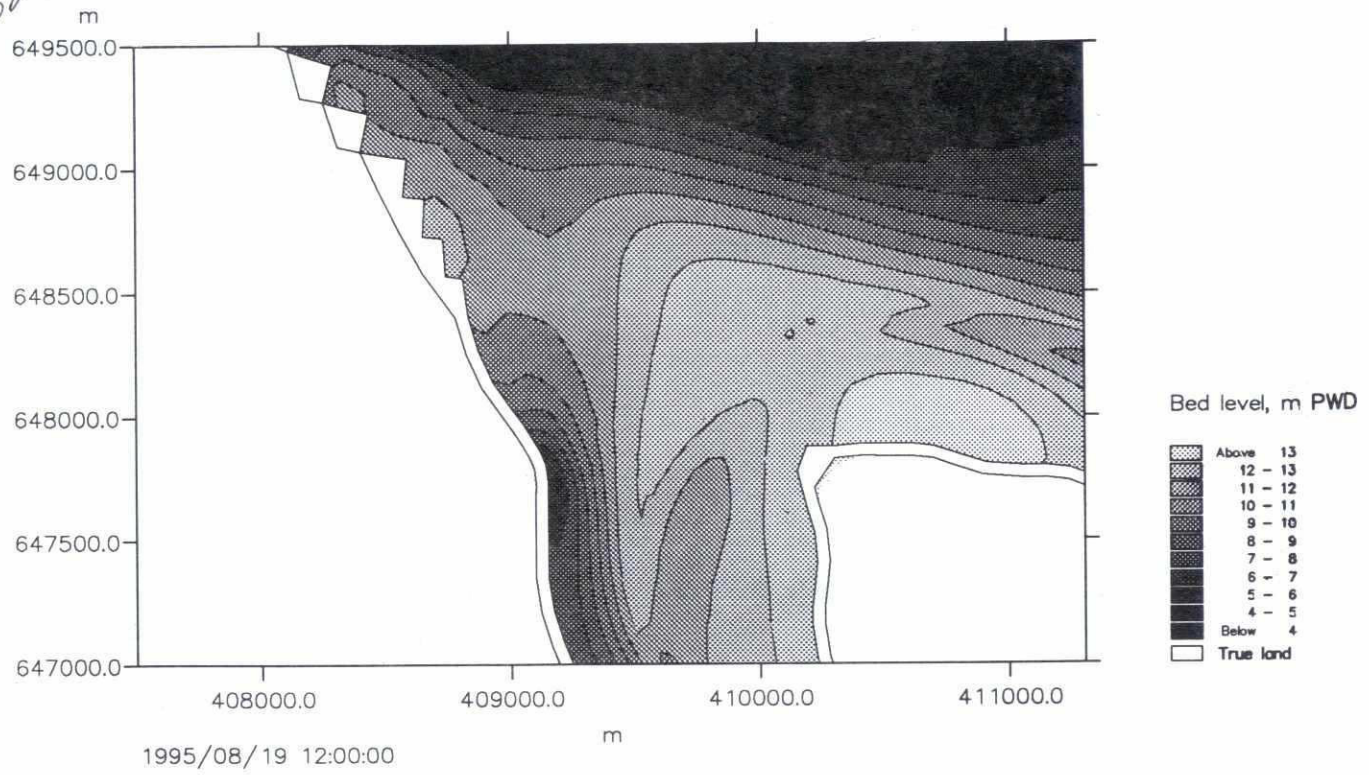


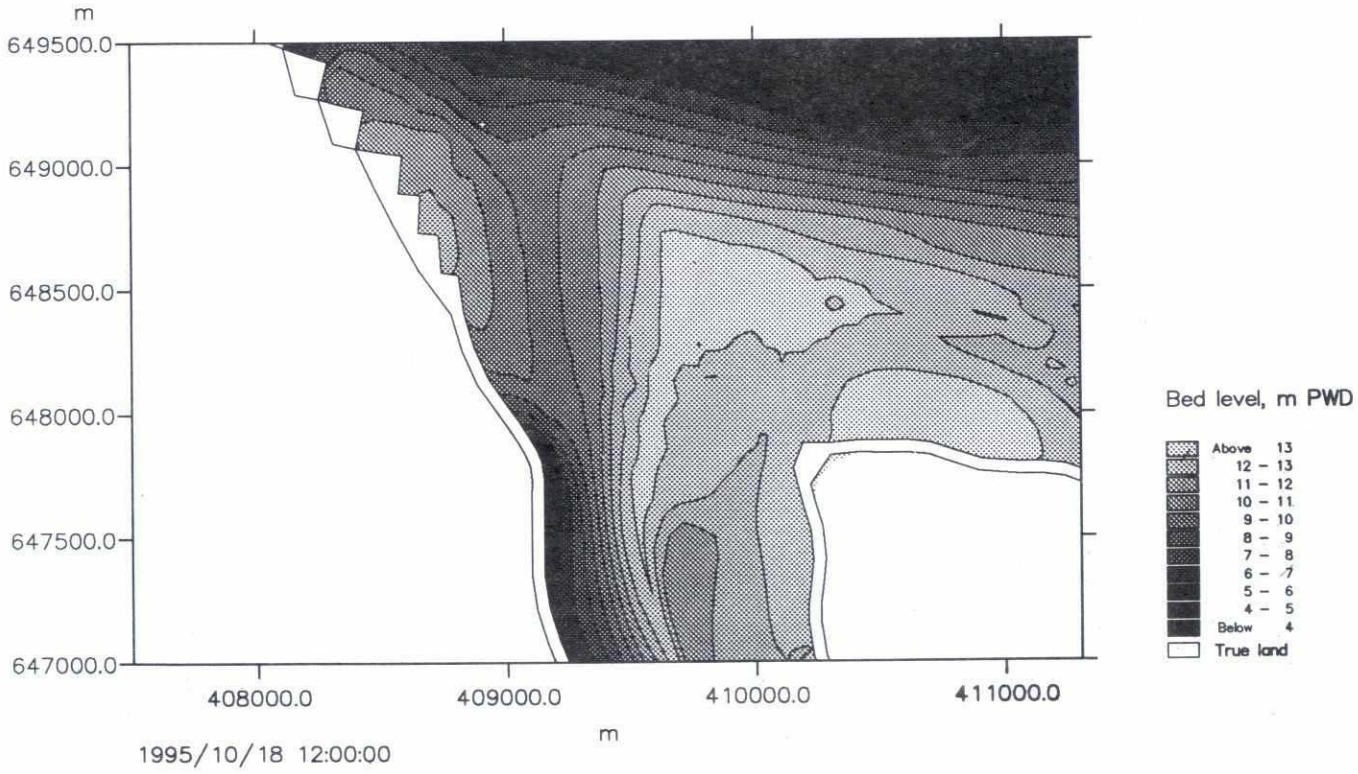


| | | | |
|---|---|---|---|
| SWMC | | Client: River Survey Project FAP24 | MIKE 21 |
| | | Project: Gorai Offtake Mathematical Modelling | |
| File: | Date: Thu Jul 4 1996 | Simulated bathymetry after 2 and 4 mths<br>Gorai Offtake<br>Base Run | Drawing no.<br>**Figure 7.8.2** |
| Scale: 1:30000 | Init: hge | | |

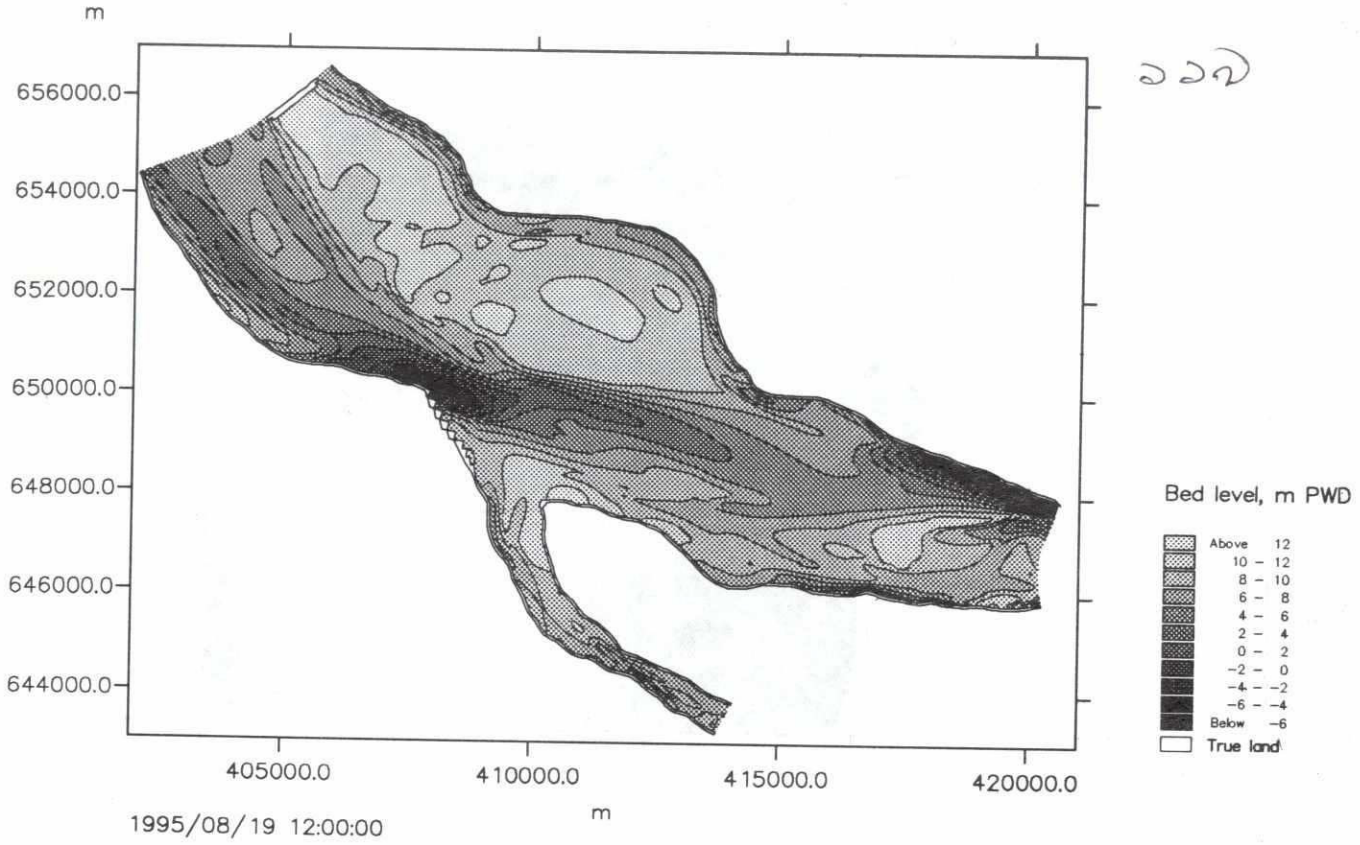


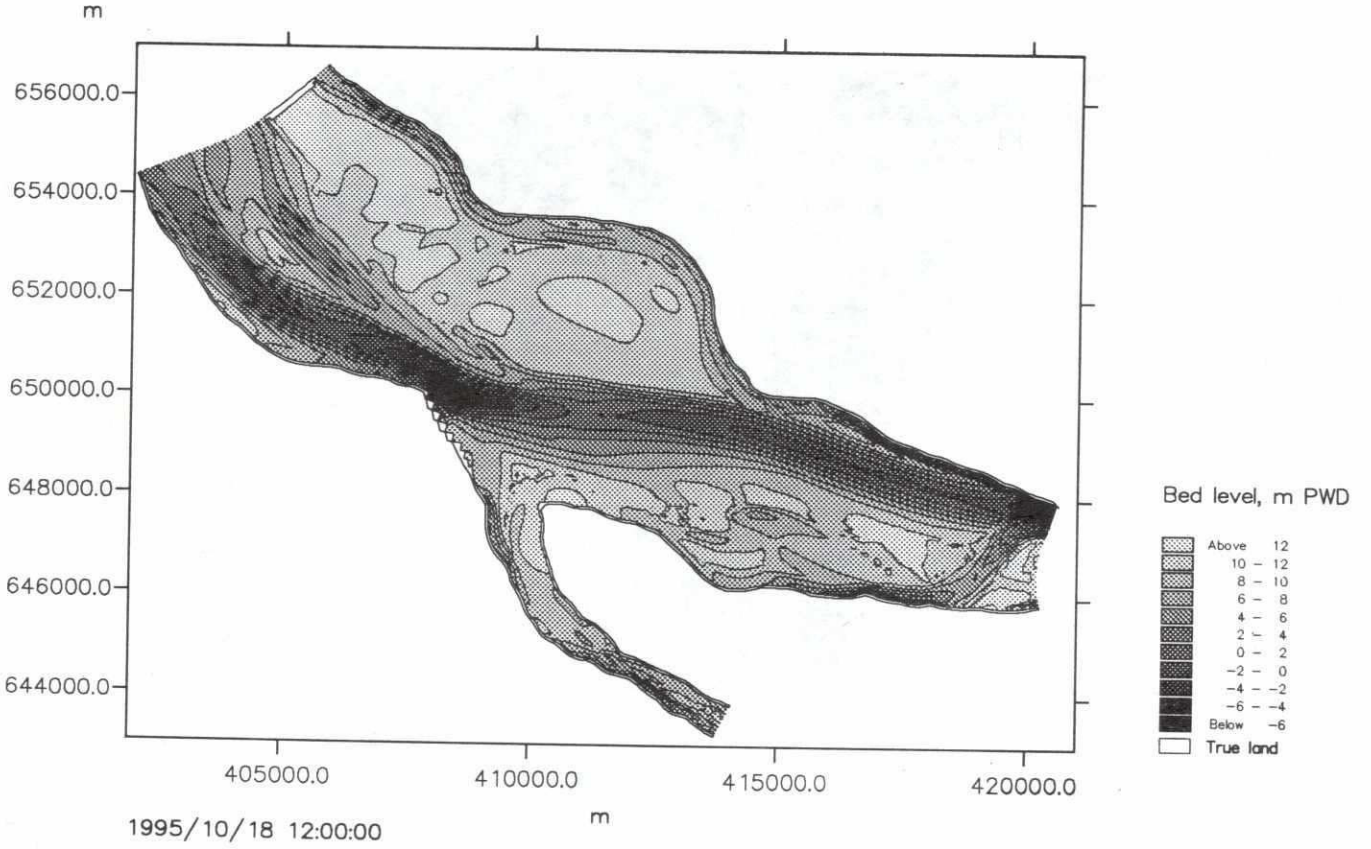


| SWMC | Client: River Survey Project FAP24 | MIKE 21 |
|---|---|---|
| | Project: Gorai Offtake Mathematical Modelling | |
| File: | Date: Thu Jul 4 1996 | Simulated bathymetry after 2 and 4 mths<br>Ganges and Gorai<br>Higher resistance in the Gorai river |
| Scale: 1:150000 | Init: hge | Drawing no. **Figure 7.8.3** |

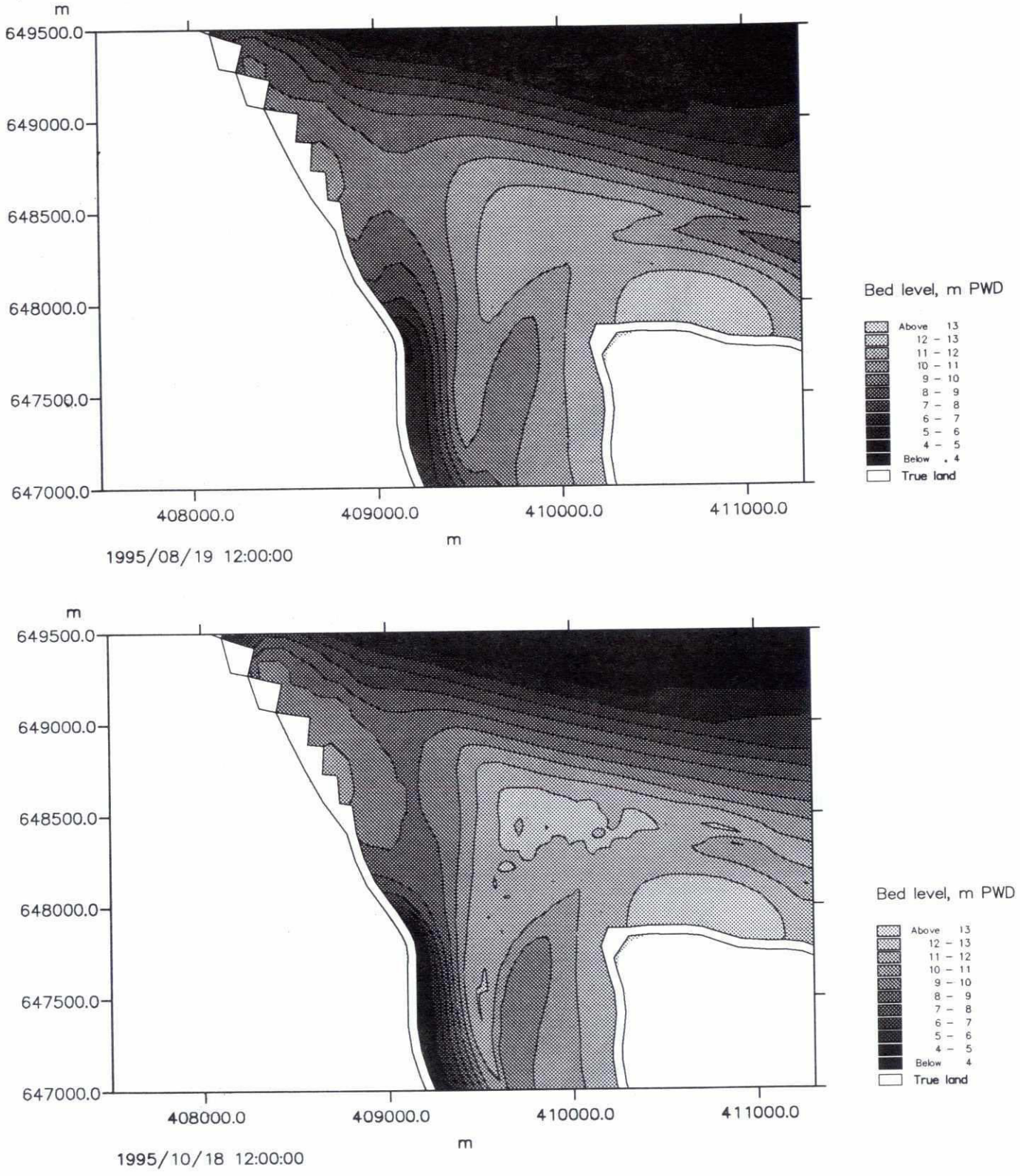


| | | | |
|---|---|---|---|
| SWMC | Client: River Survey Project FAP24 | | MIKE 21 |
| | Project: Gorai Offtake Mathematical Modelling | | |
| File: | Date: Thu Jul 4 1996 | Simulated bathymetry after 2 and 4 mths<br>Gorai Offtake<br>Higher resistance in the 'Gorai River | Drawing no.<br>**Figure 7.8.4** |
| Scale: 1:30000 | Init: hge | | |

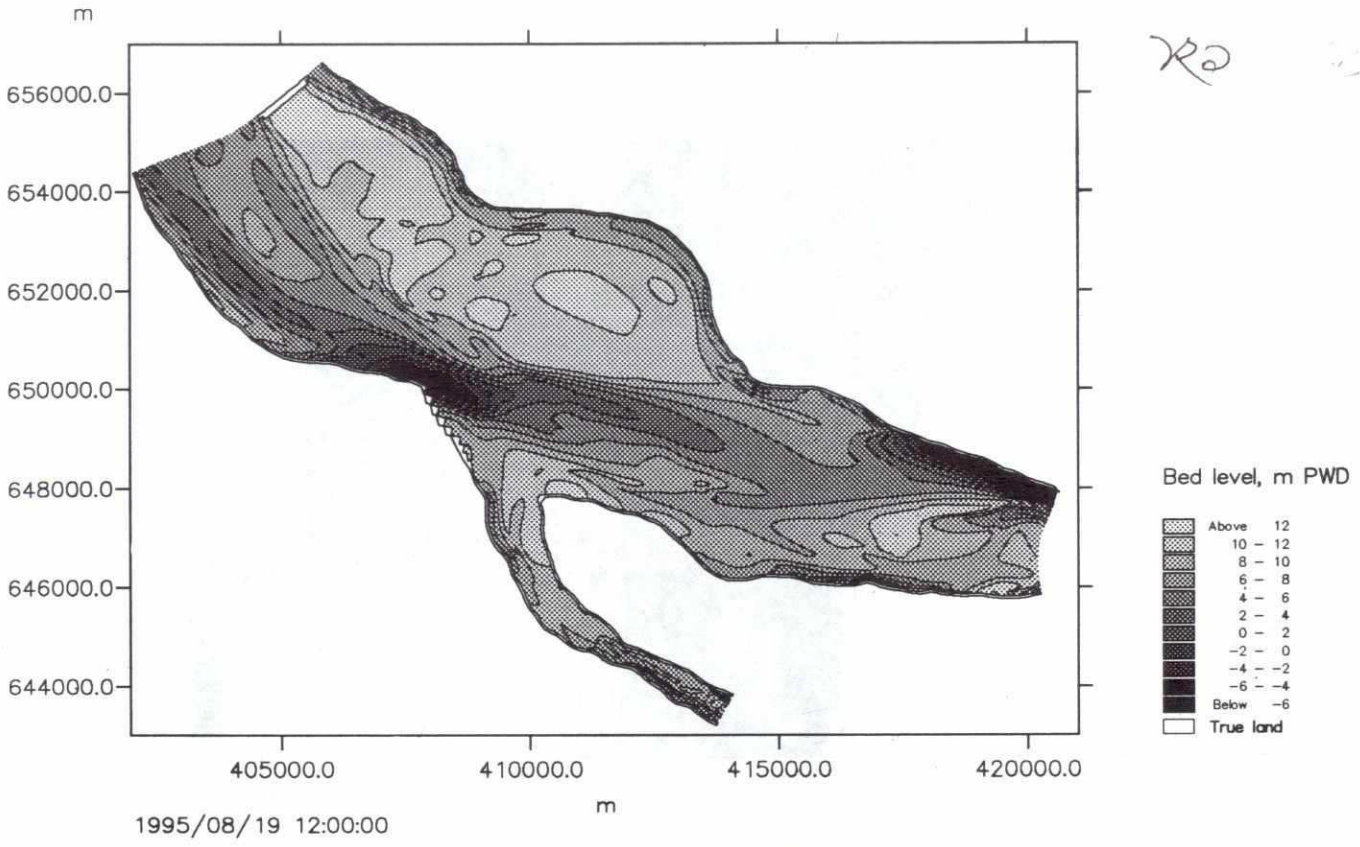


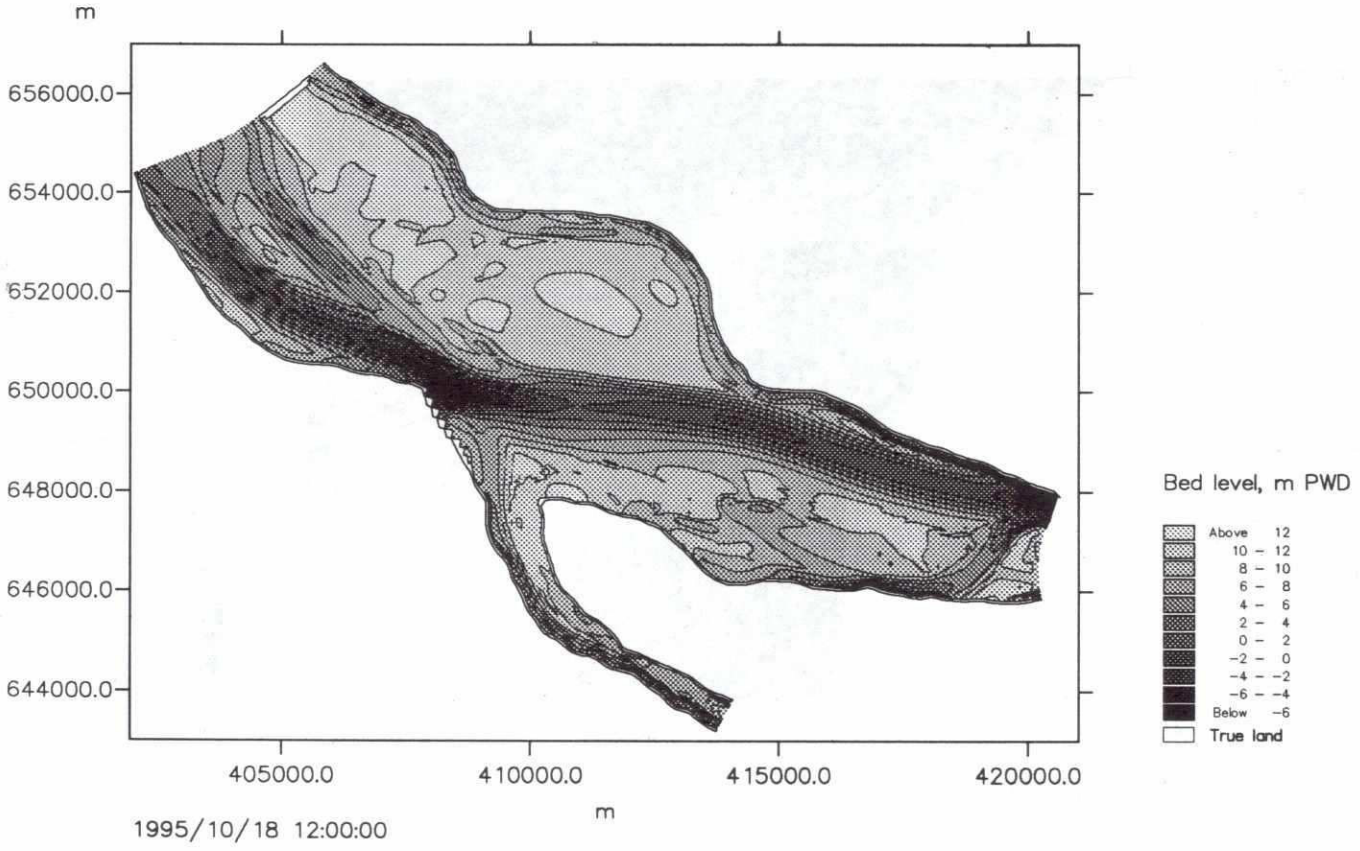


| SWMC | Client: River Survey Project FAP24 | MIKE 21 |
|---|---|---|
| | Project: Gorai Offtake Mathematical Modelling | |
| File: | Date: Thu Jul 4 1996 | Simulated bathymetry after 2 and 4 mths<br>Ganges and Gorai<br>Lower resistance in the Gorai river |
| Scale: 1:150000 | Init: hge | Drawing no. **Figure 7.8.5** |

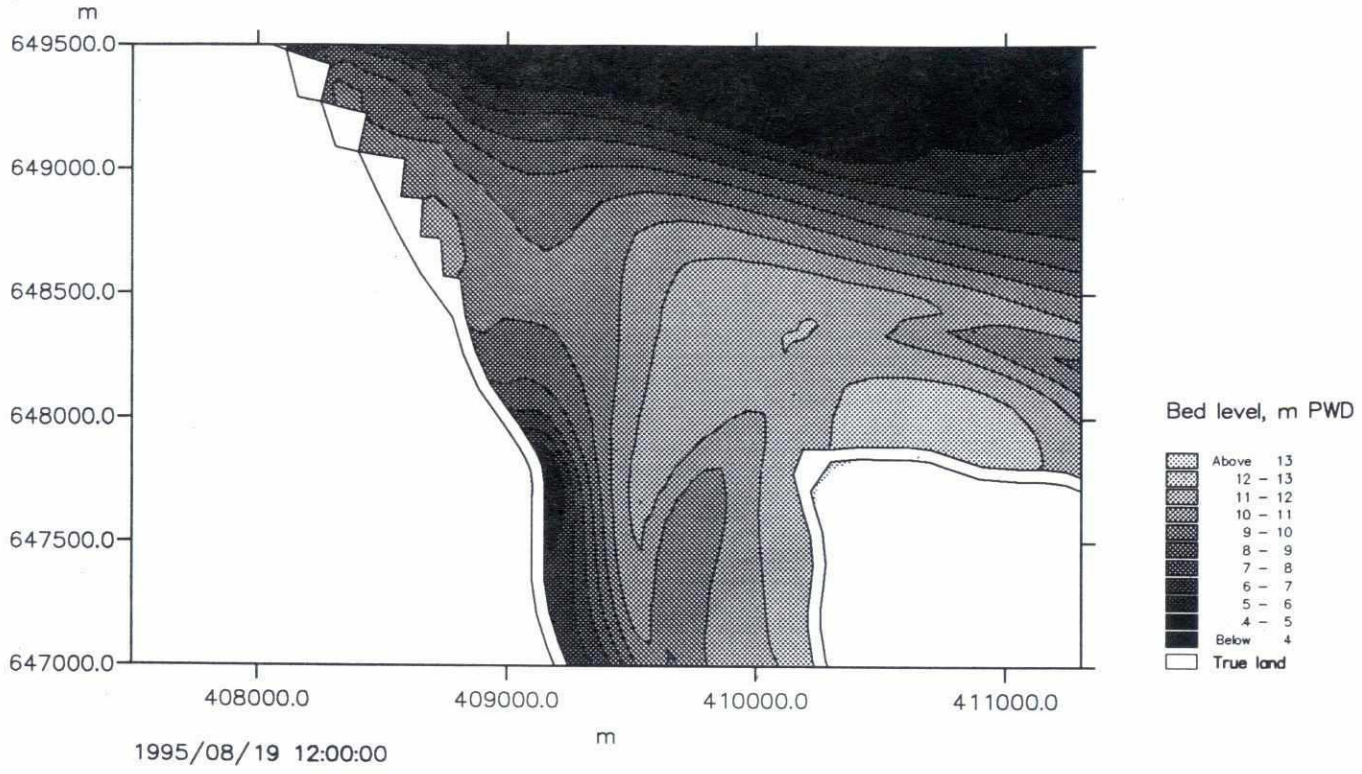


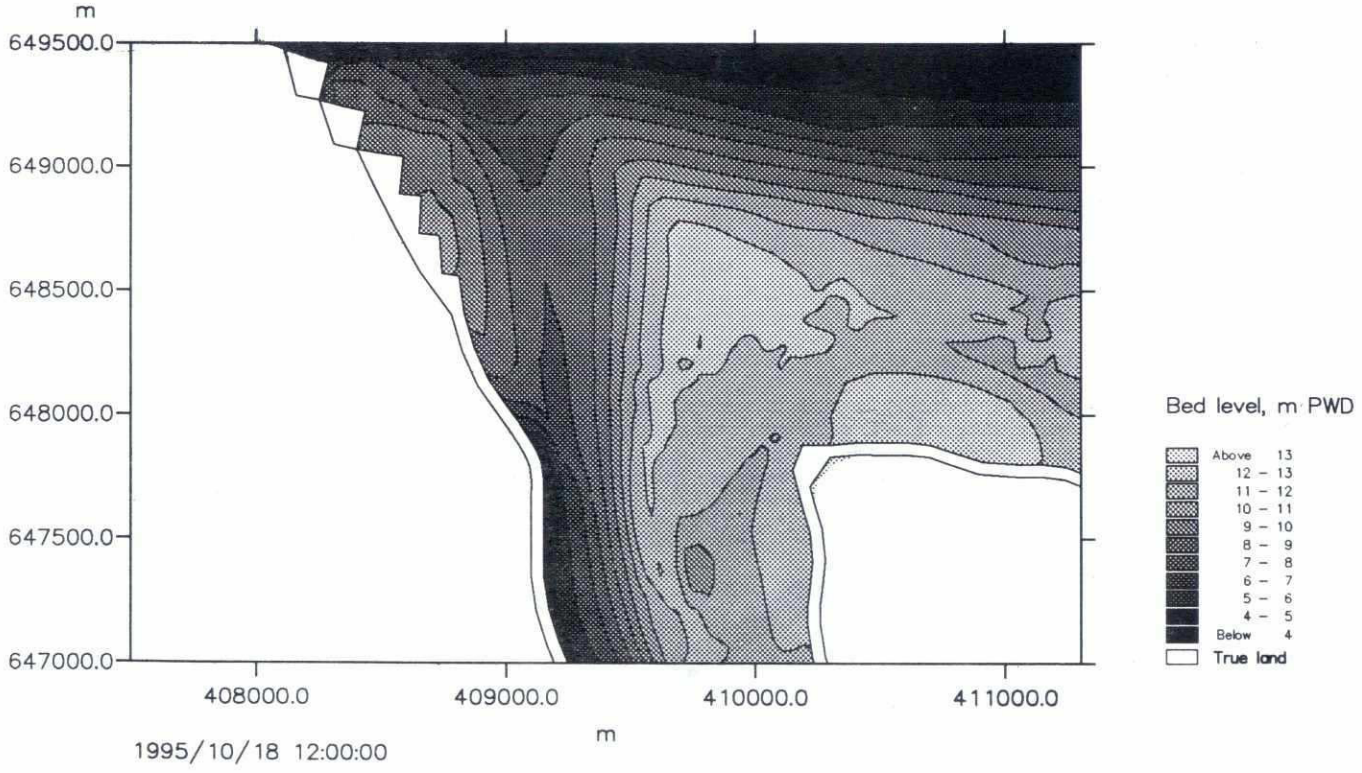


| SWMC | Client: River Survey Project FAP24 | MIKE 21 |
|---|---|---|
| | Project: Gorai Offtake Mathematical Modelling | |
| File: | Date: Thu Jul 4 1996 | Simulated bathymetry after 2 and 4 mths<br>Gorai Offtake<br>Lower resistance in the Gorai River |
| Scale: 1:30000 | Init: hge | Drawing no.<br>**Figure 7.8.6** |

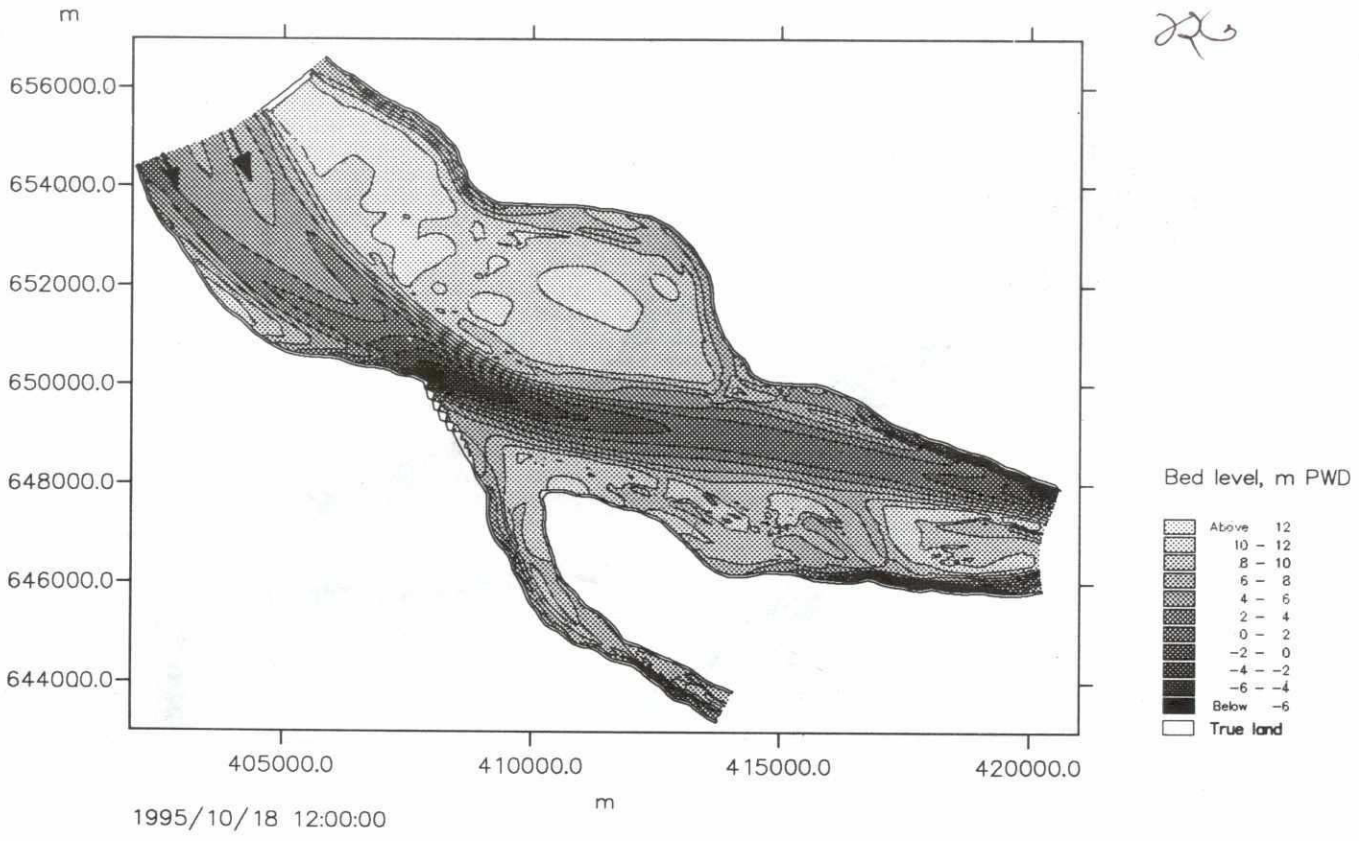


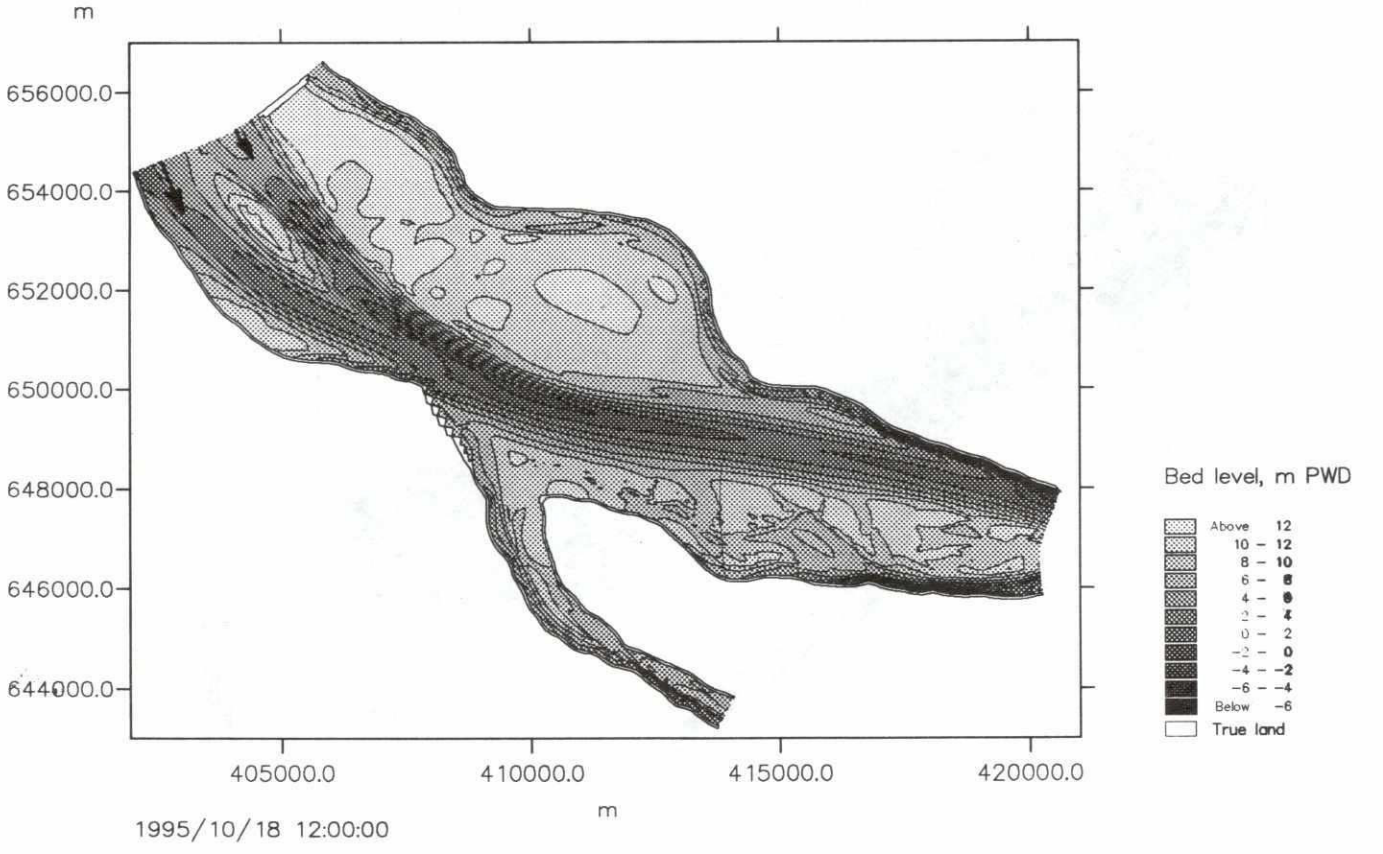


| | | | |
|---|---|---|---|
| SWMC | Client: River Survey Project FAP24 | | MIKE 21 |
| | Project: Gorai Offtake Mathematical Modelling | | |
| File: | Date: Sat Jul 6 1996 | Simulated bathymetry with different upstream discharge distribution | Drawing no. Figure 7.8.7 |
| Scale: 1:150000 | Init: hge | | |

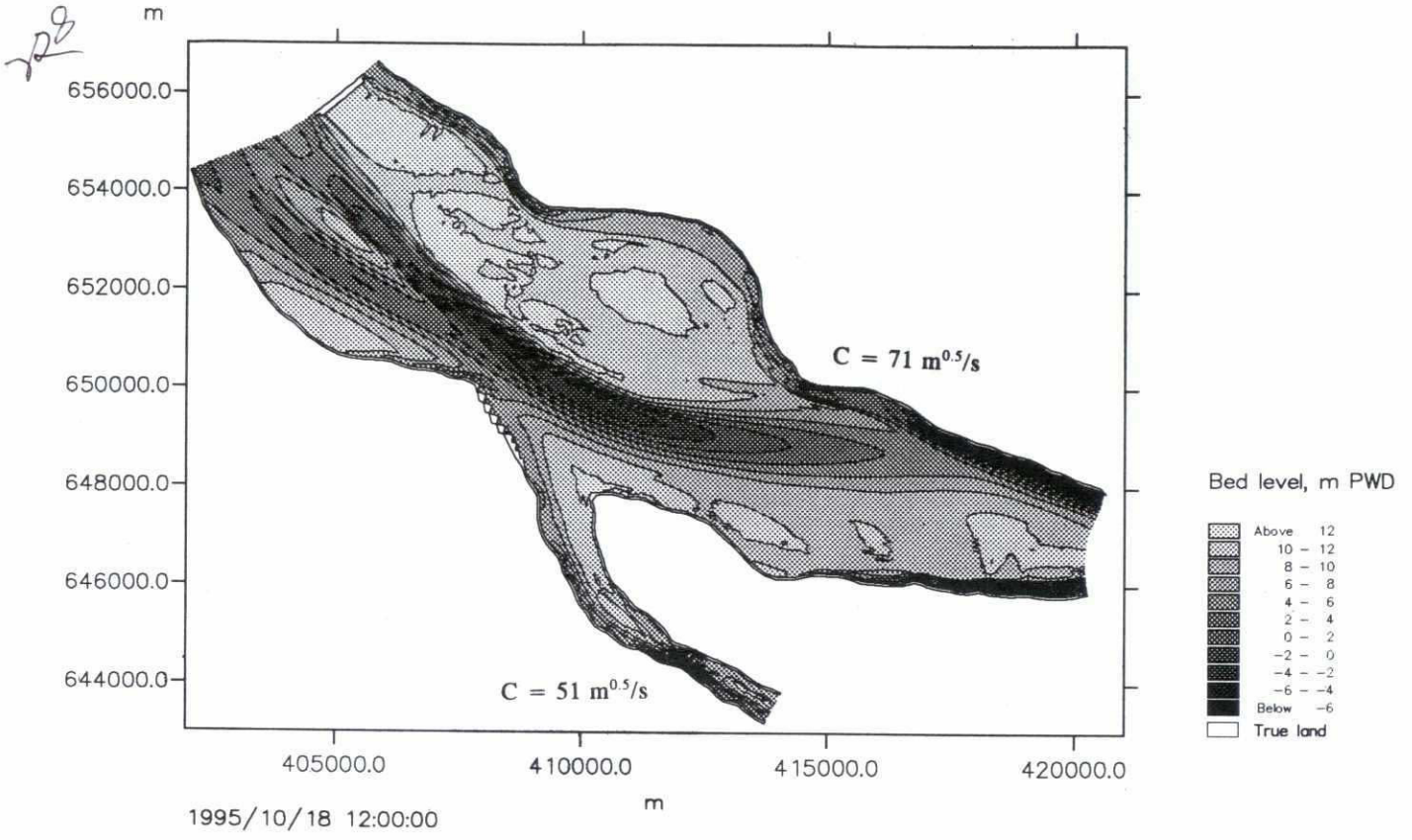


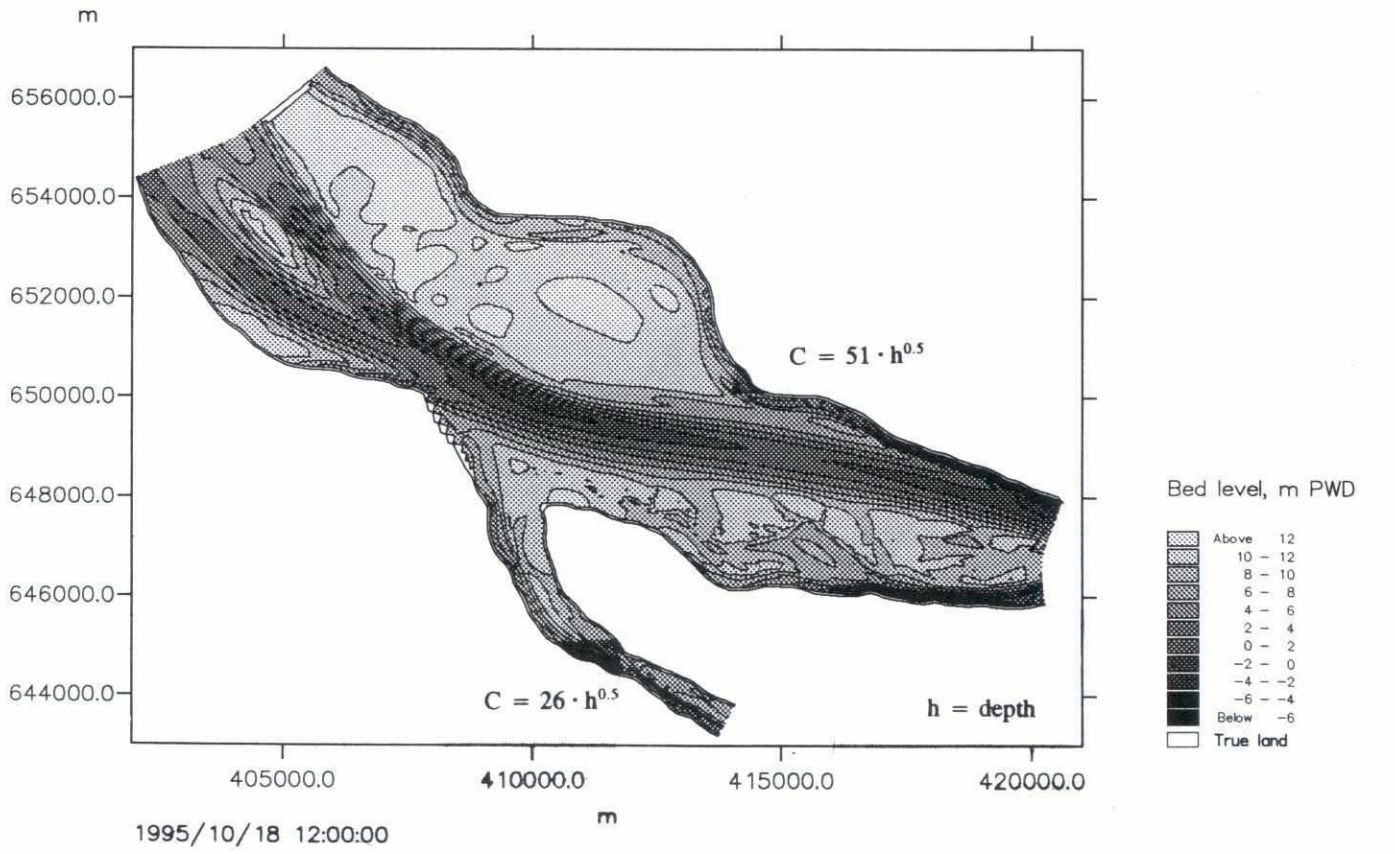


| SWMC | Client: River Survey Project FAP24 | MIKE 21 |
|---|---|---|
| | Project: Gorai Offtake Mathematical Modelling | |
| File: | Date: Sat Jul 6 1996 | Simulated bathymetry with depth–dependent alluvial resistance (bottom) and constant model resistance (top) |
| Scale: 1:150000 | Init: hge | Drawing no. **Figure 7.8.8** |

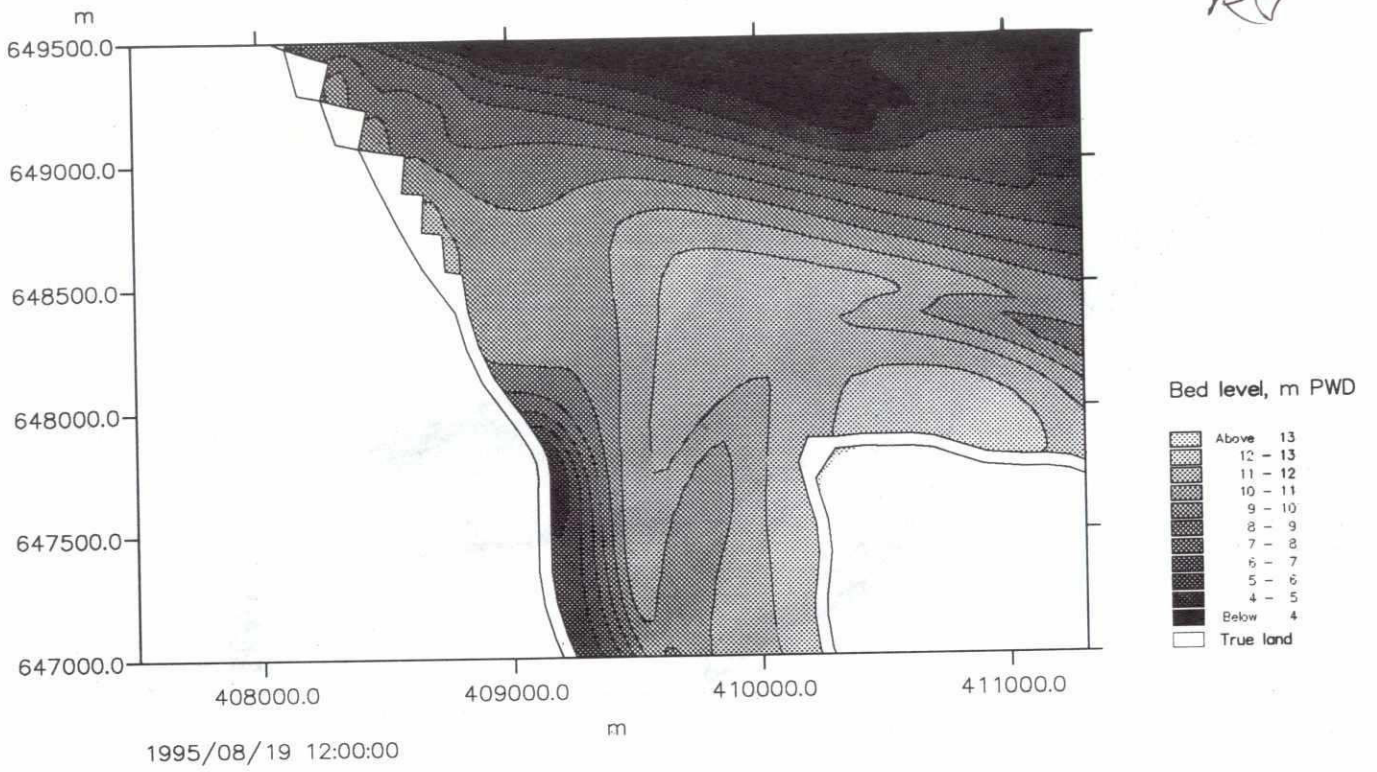


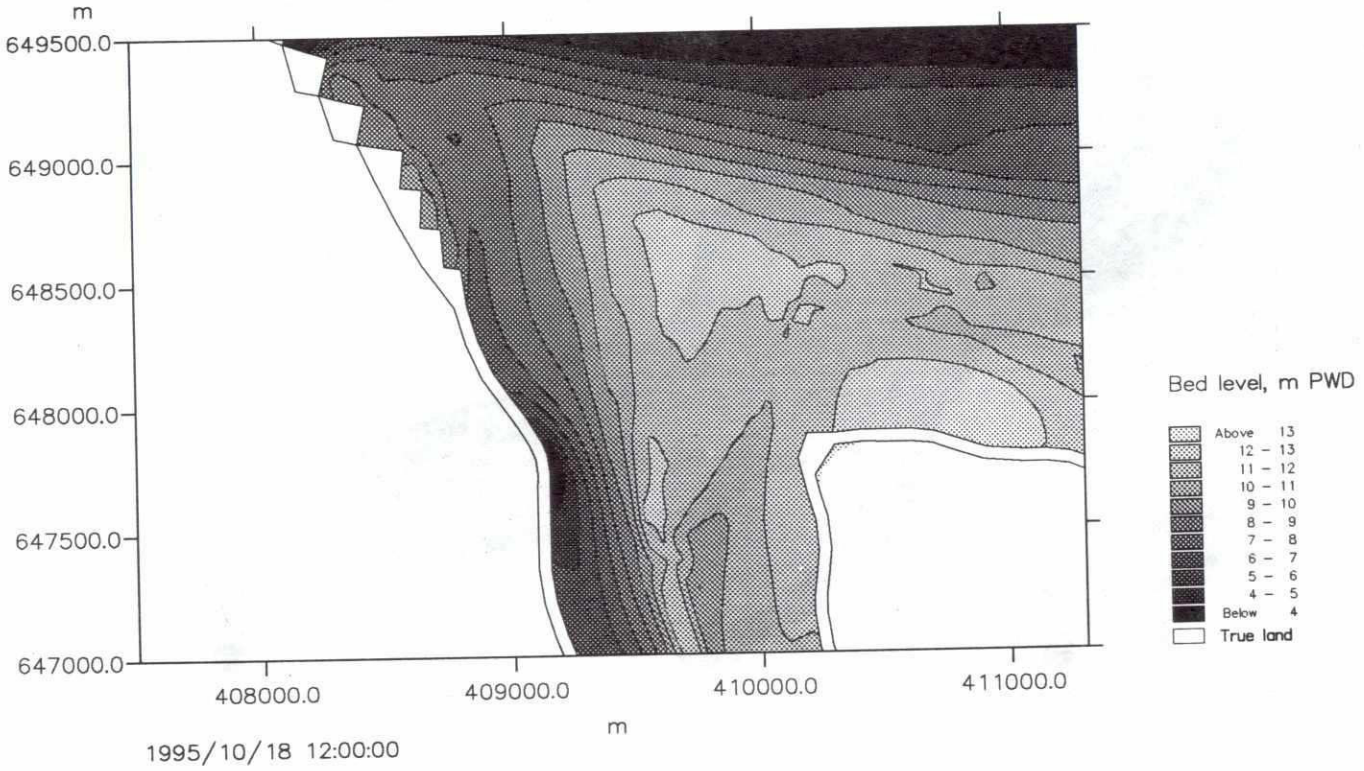


| SWMC | Client: River Survey Project FAP24 | MIKE 21 |
|---|---|---|
| | Project: Gorai Offtake Mathematical Modelling | |
| File: | Date: Thu Jul 11 1996 | Simulated bathymetry after 2 and 4 mths<br>Gorai offtake<br>No correction of resistance at Talbari |
| Scale: 1:30000 | Init: hge | Drawing no. **Figure 7.8.9** |

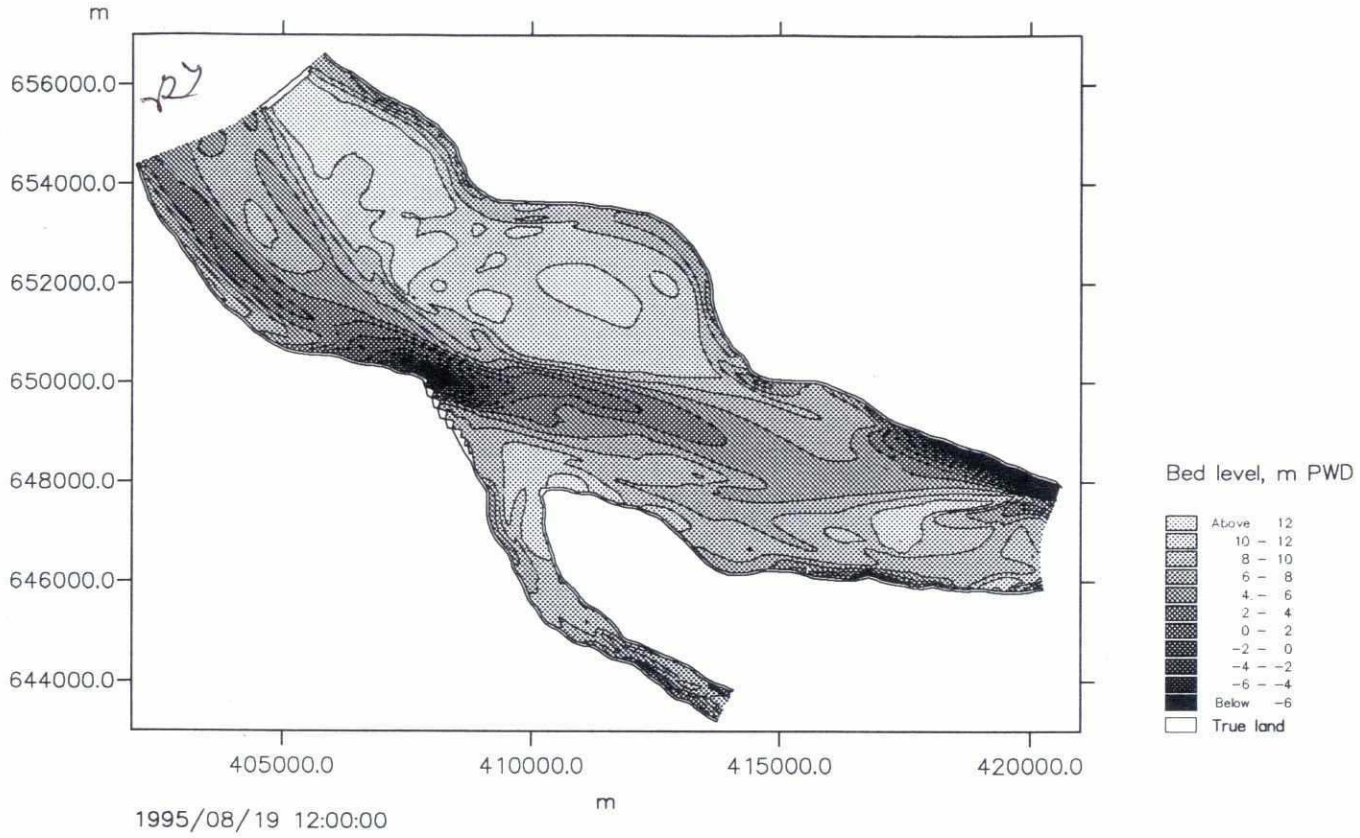


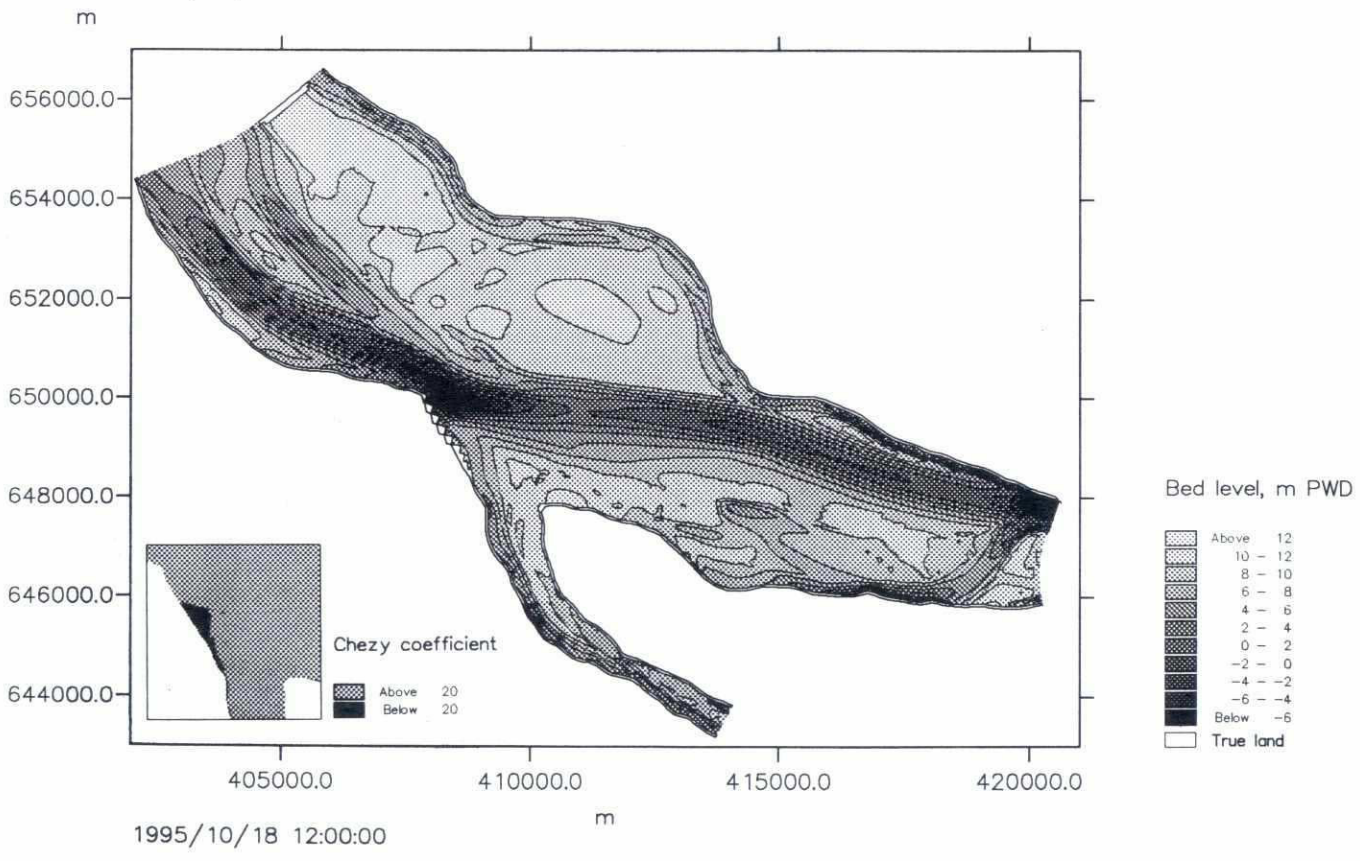


| | | | |
|---|---|---|---|
| SWMC | Client: River Survey Project FAP24 | | MIKE 21 |
| | Project: Gorai Offtake Mathematical Modelling | | |
| File: | Date: Sat Jul 6 1996 | Simulated bathymetry after 2 and 4 mths<br>Ganges and Gorai<br>No correction of resistance at Talbari | Drawing no.<br>**Figure 7.8.10** |
| Scale: 1:150000 | Init: hge | | |

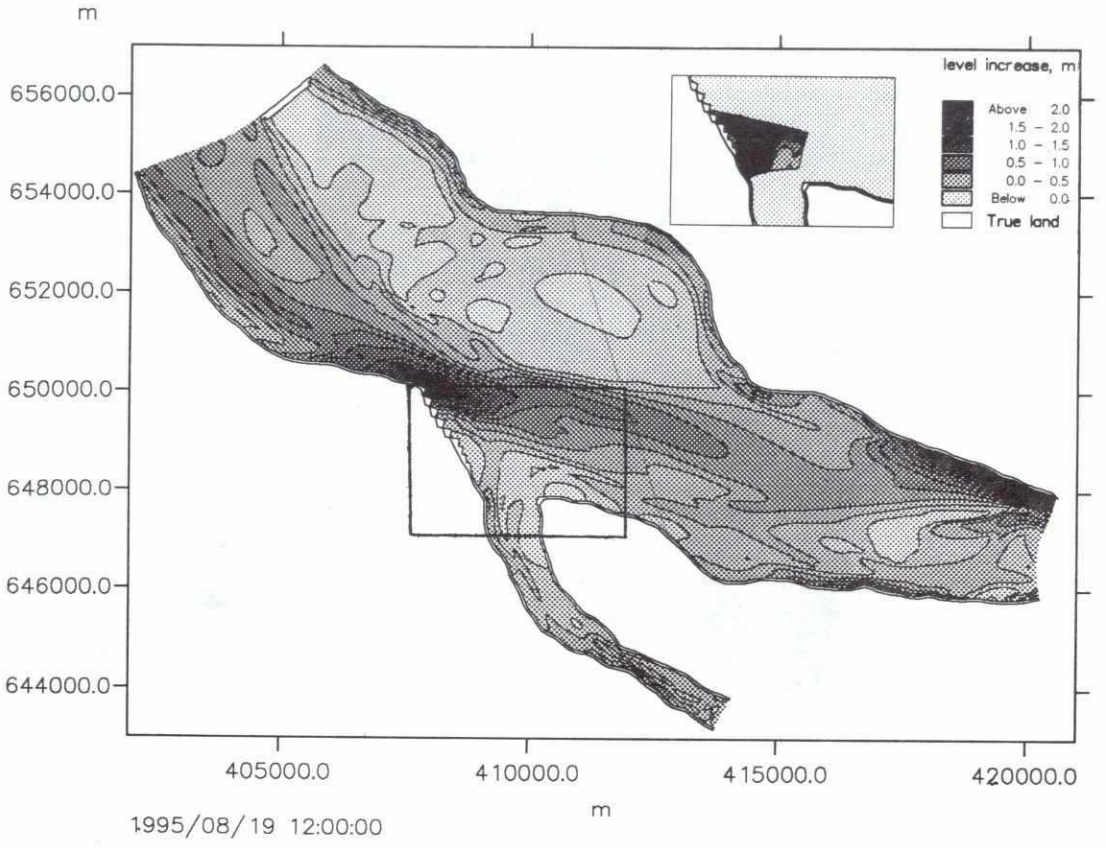


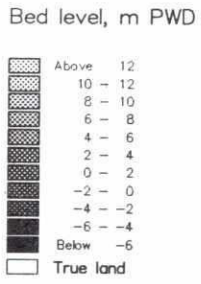


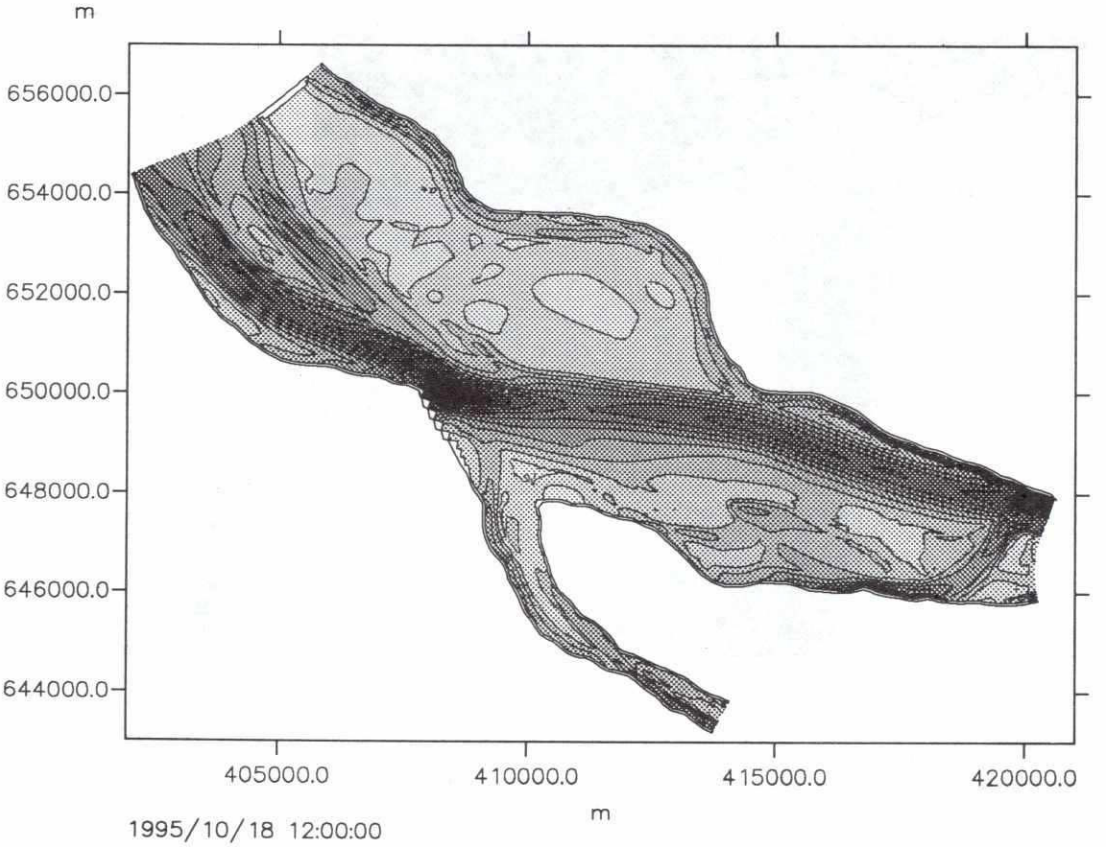


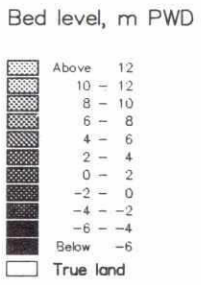


| | | | |
|---|---|---|---|
| SWMC | Client: River Survey Project FAP24 | | MIKE 21 |
| | Project: Gorai Offtake Mathematical Modelling | | |
| File: | Date: Thu Jul 4 1996 | Simulated bathymetry after 2 and 4 mths<br>Ganges and Gorai<br>Bar in front of offtake initially | Drawing no.<br>**Figure 7.9.1** |
| Scale: 1:150000 | Init: hge | | |

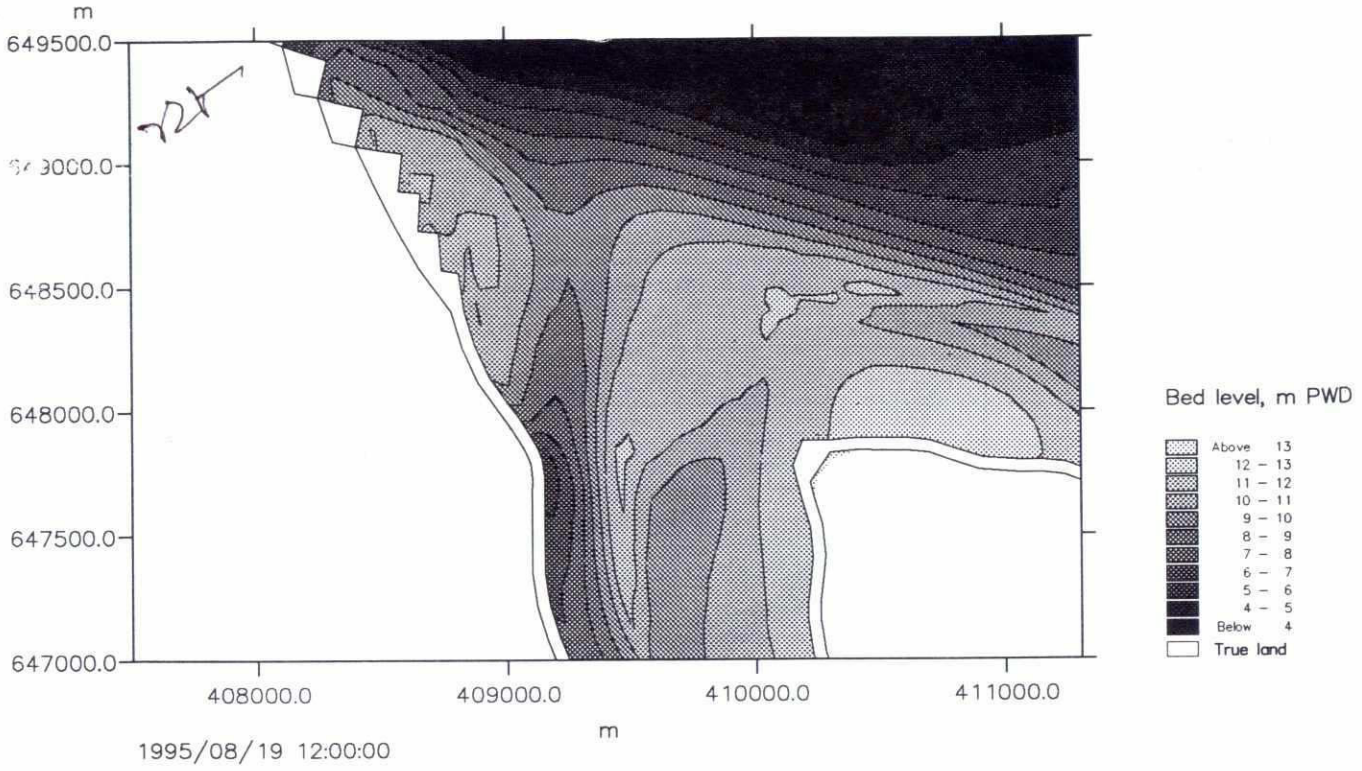


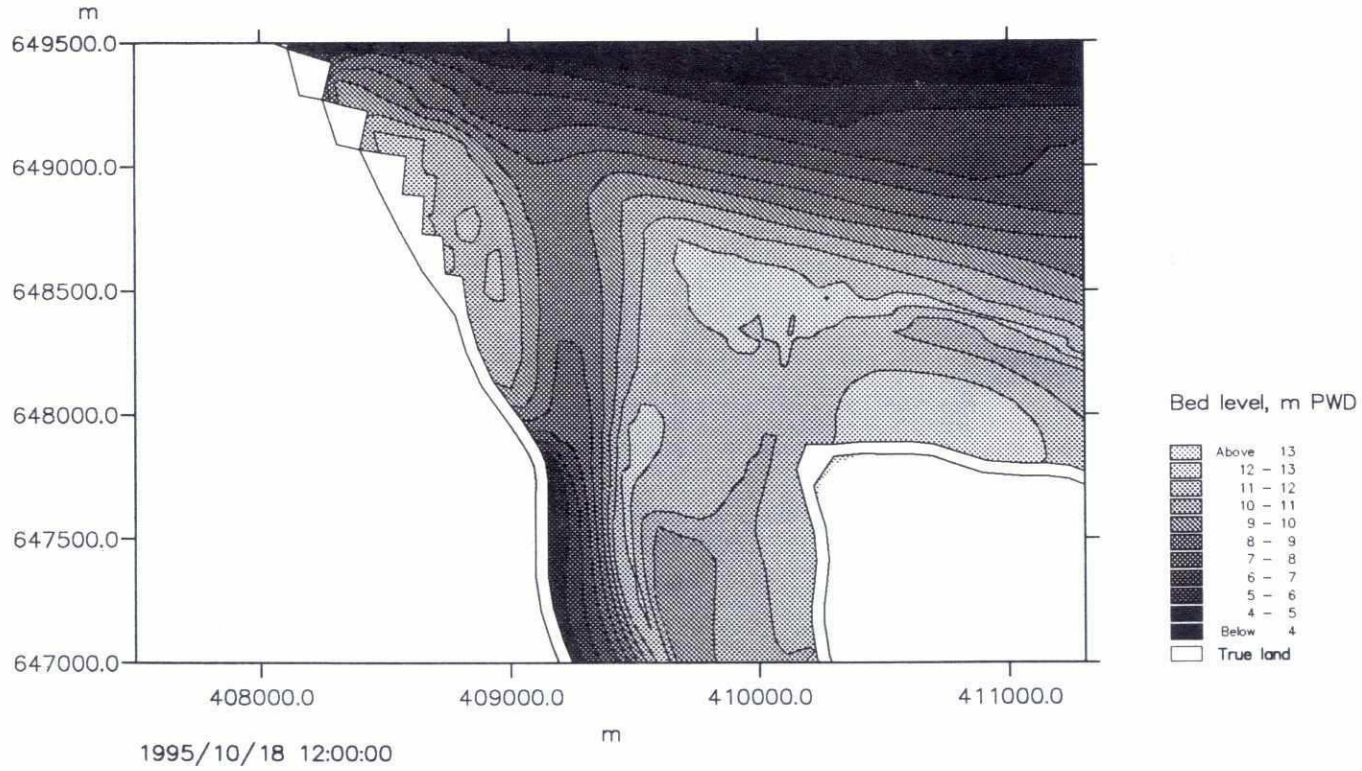


| SWMC | Client: River Survey Project FAP24 | MIKE 21 |
|---|---|---|
| | Project: Gorai Offtake Mathematical Modelling | |
| File: | Date: Thu Jul 4 1996 | Simulated bathymetry after 2 and 4 mths<br>Gorai Offtake<br>Bar in front of offtake initially |
| Scale: 1:30000 | Init: hge | Drawing no. **Figure 7.9.2** |

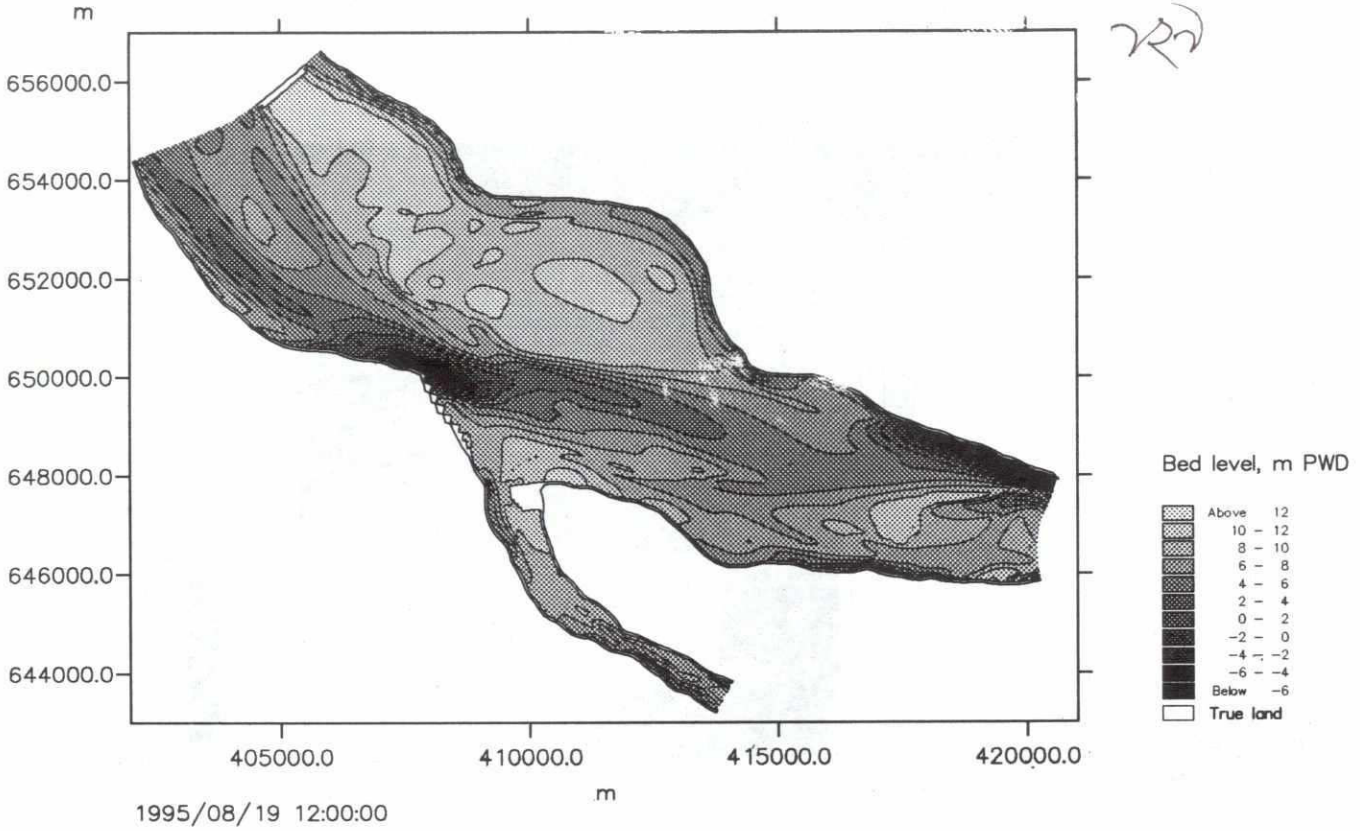


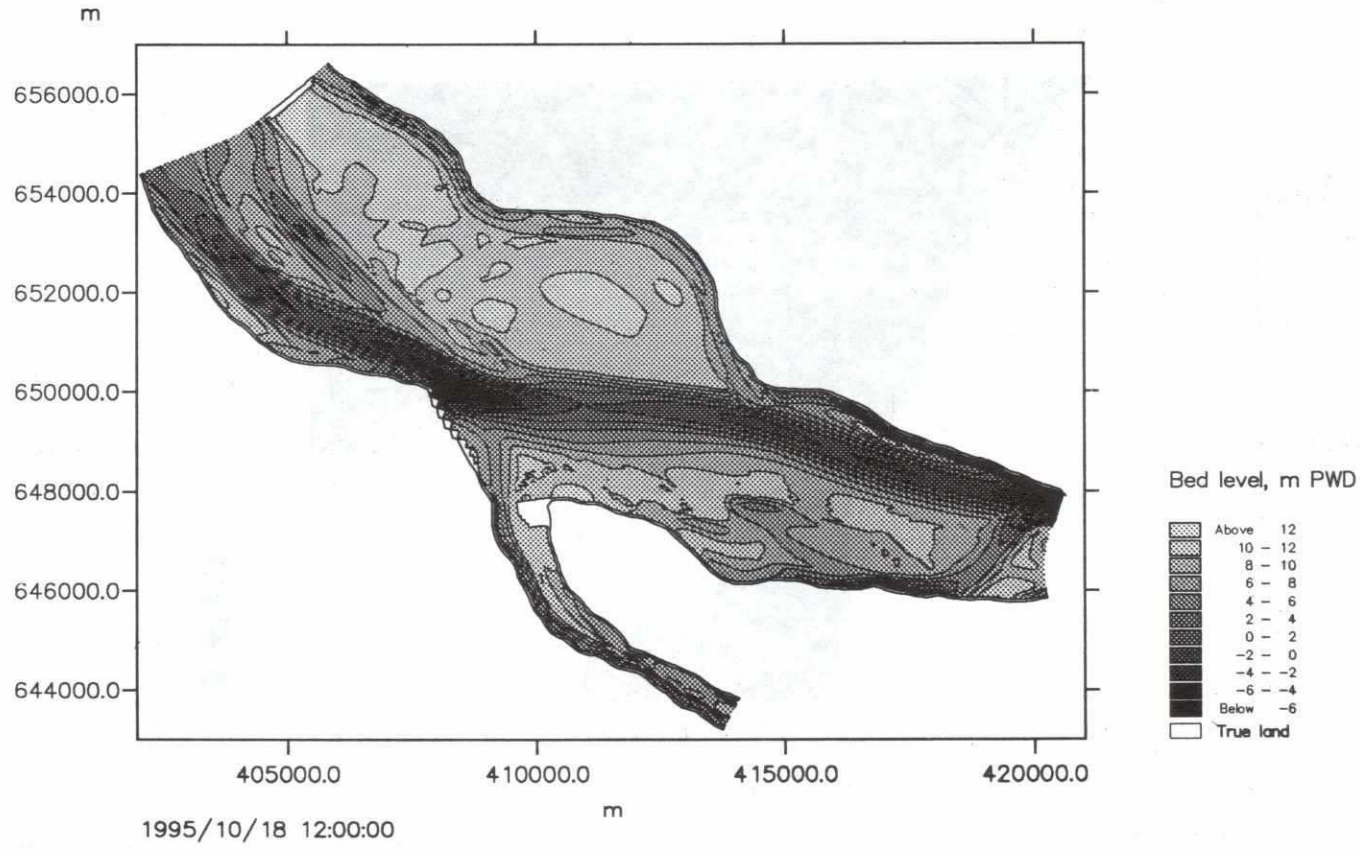


| | | | |
|---|---|---|---|
| SWMC | | Client: River Survey Project FAP24 | MIKE 21 |
| | | Project: Gorai Offtake Mathematical Modelling | |
| File: | Date: Thu Jul 4 1996 | Simulated bathymetry after 2 and 4 mths<br>Ganges and Gorai<br>Narrowing of Gorai river mouth | Drawing no.<br>**Figure 7.9.3** |
| Scale: 1:150000 | Init: hge | | |

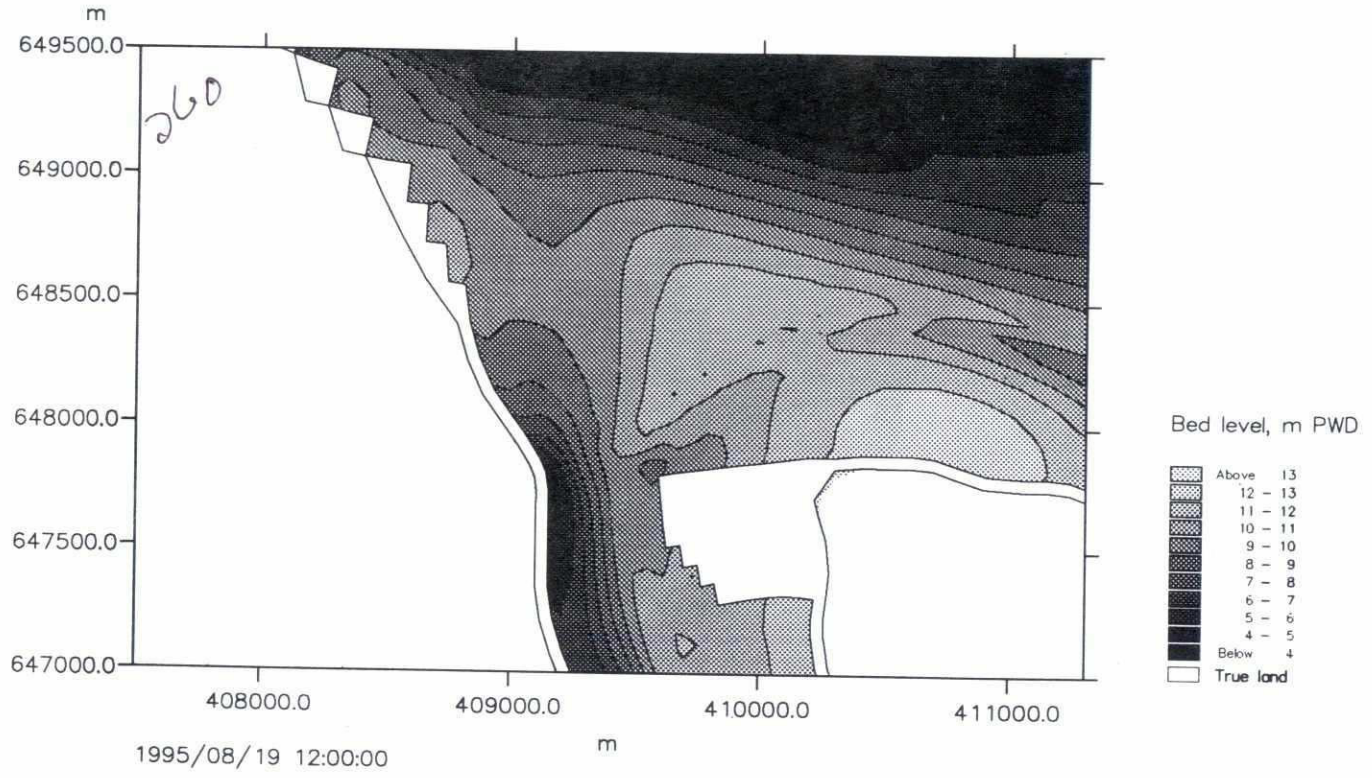


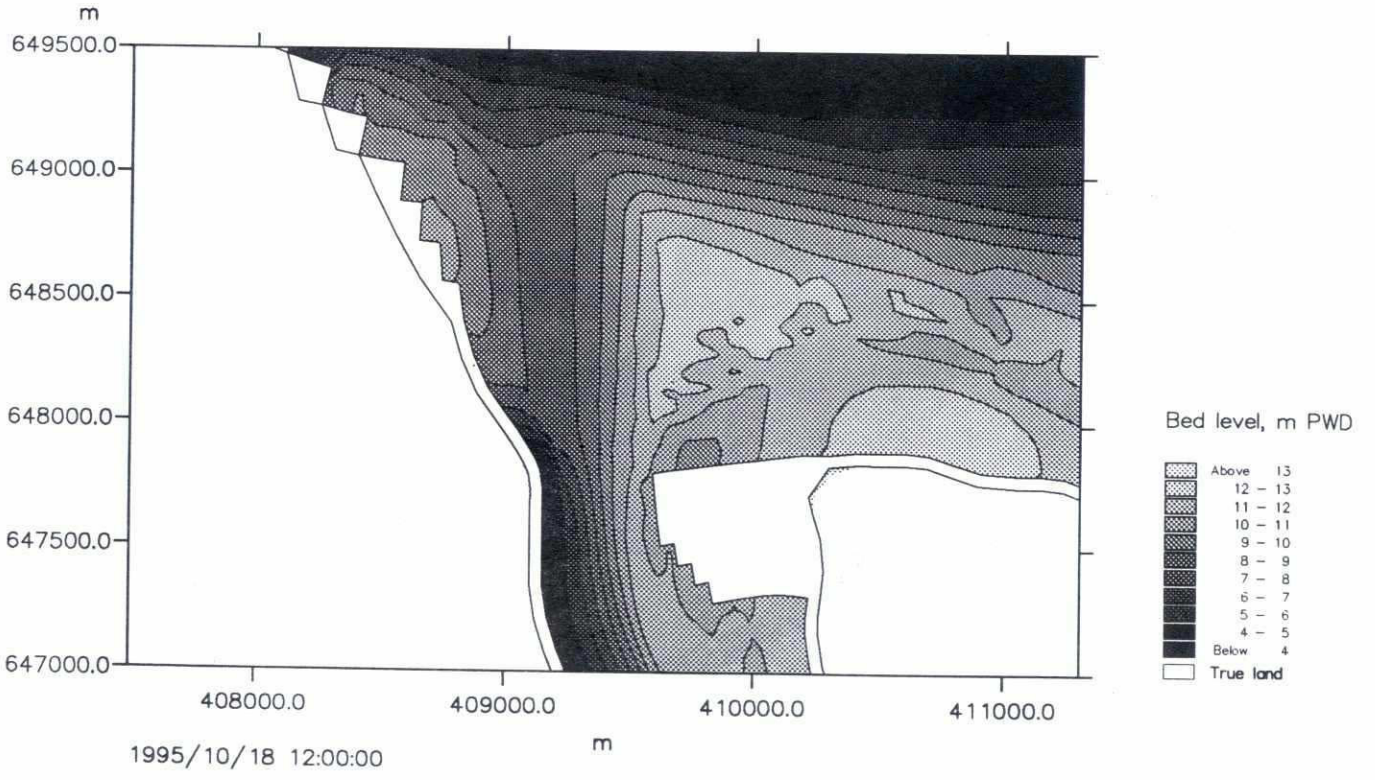


| SWMC | Client: River Survey Project FAP24 | | MIKE 21 |
|---|---|---|---|
| | Project: Gorai Offtake Mathematical Modelling | | |
| File: | Date: Thu Jul 4 1996 | Simulated bathymetry after 2 and 4 mths<br>Gorai Offtake<br>Narrowing of Gorai river mouth | Drawing no. |
| Scale: 1:30000 | Init: hge | | **Figure 7.9.4** |

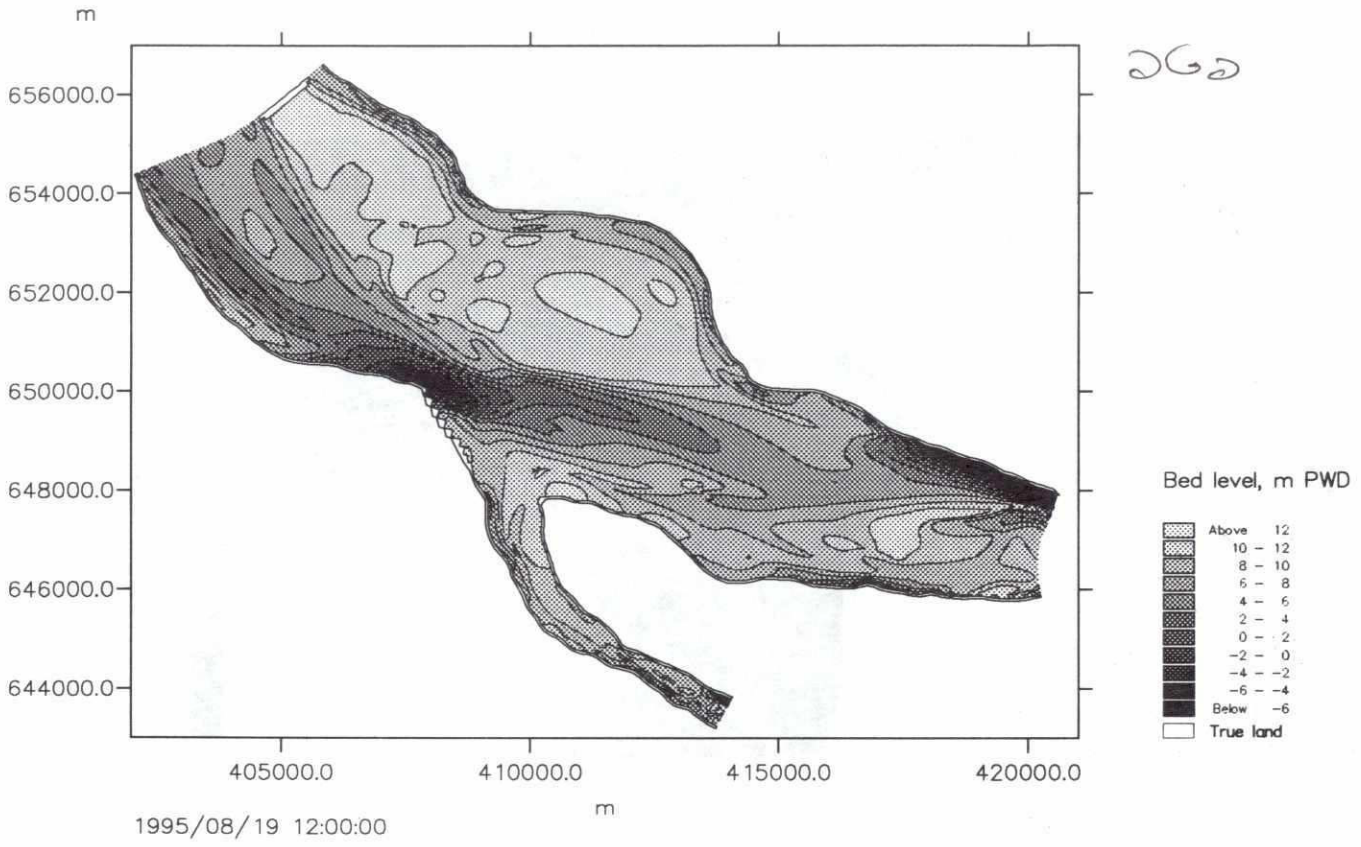


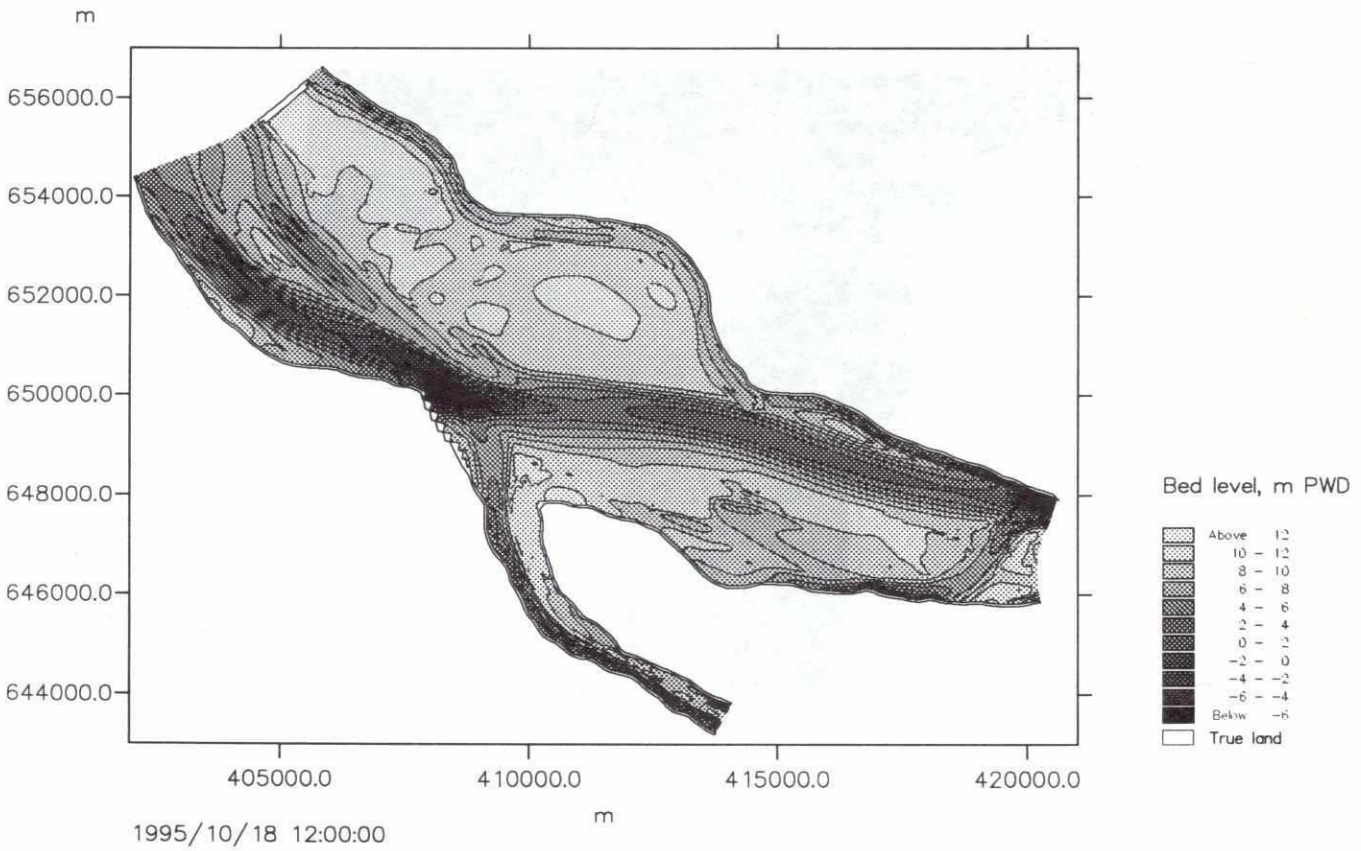


| SWMC | Client: River Survey Project FAP24 | MIKE 21 |
|---|---|---|
| | Project: Gorai Offtake Mathematical Modelling | |
| File: | Date: Thu Jul 4 1996 | Simulated bathymetry after 2 and 4 mths<br>Ganges and Gorai<br>Lowering of water level in Gorai |
| Scale: 1:150000 | Init: hge | Drawing no. **Figure 7.9.5** |

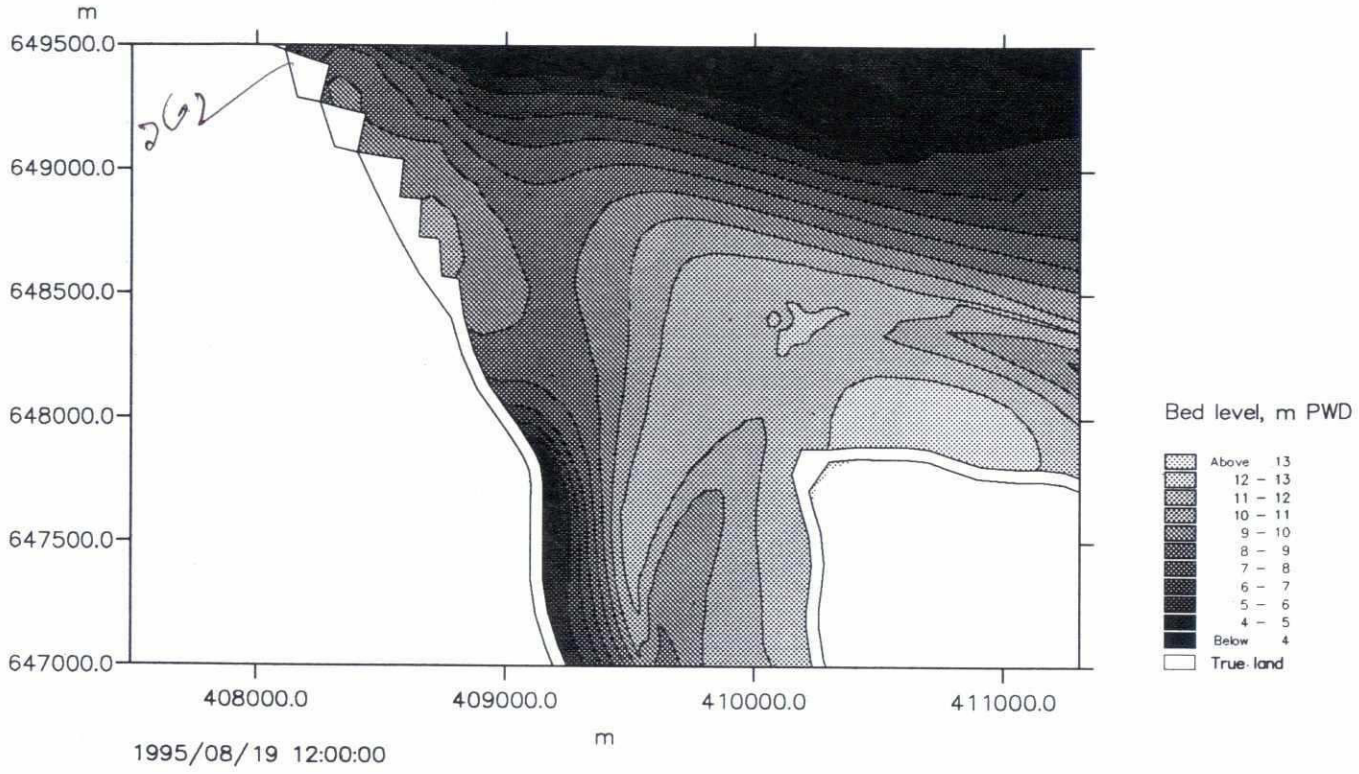


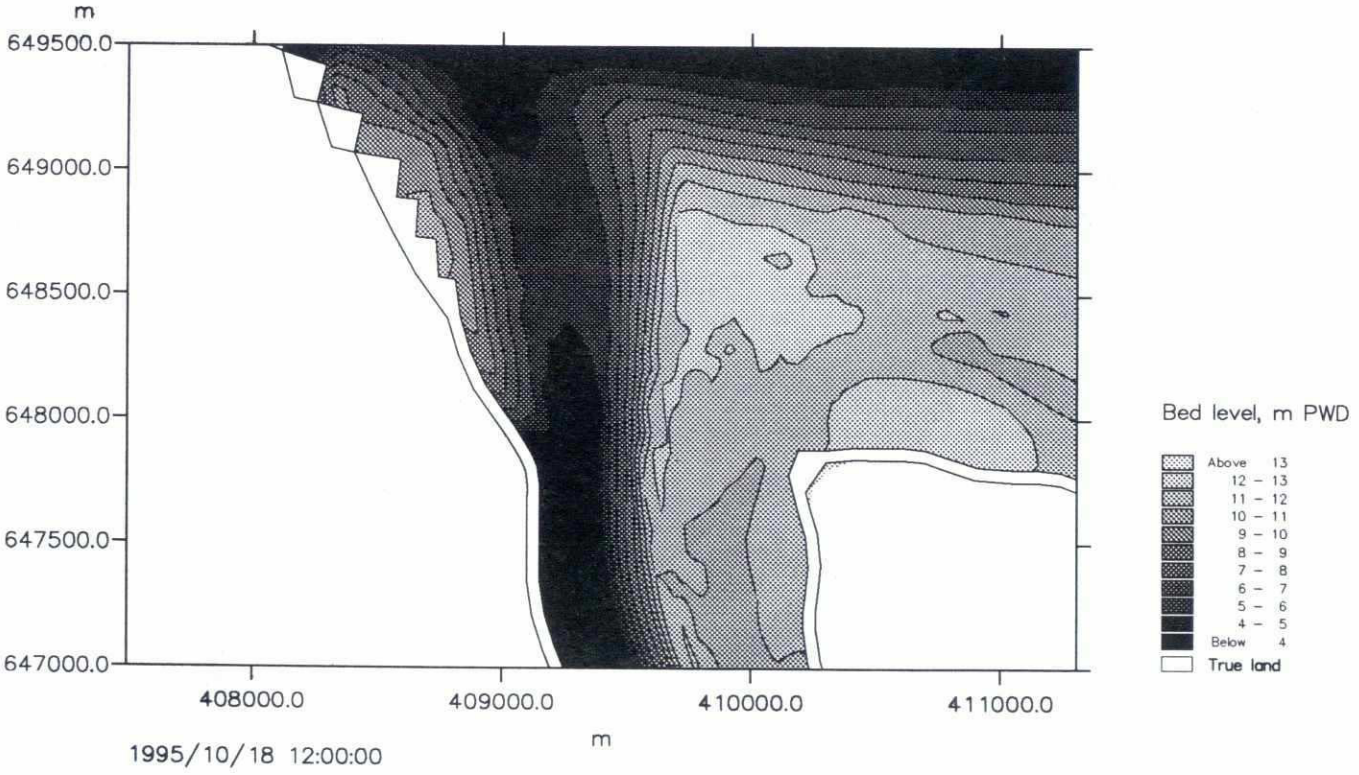


| | | | |
|---|---|---|---|
| SWMC | Client: River Survey Project FAP24 | | MIKE 21 |
| | Project: Gorai Offtake Mathematical Modelling | | |
| File: | Date: Thu Jul 4 1996 | Simulated bathymetry after 2 and 4 mths<br>Gorai Offtake<br>Lowering of water level in Gorai | Drawing no.<br>**Figure 7.9.6** |
| Scale: 1:30000 | Init: hge | | |

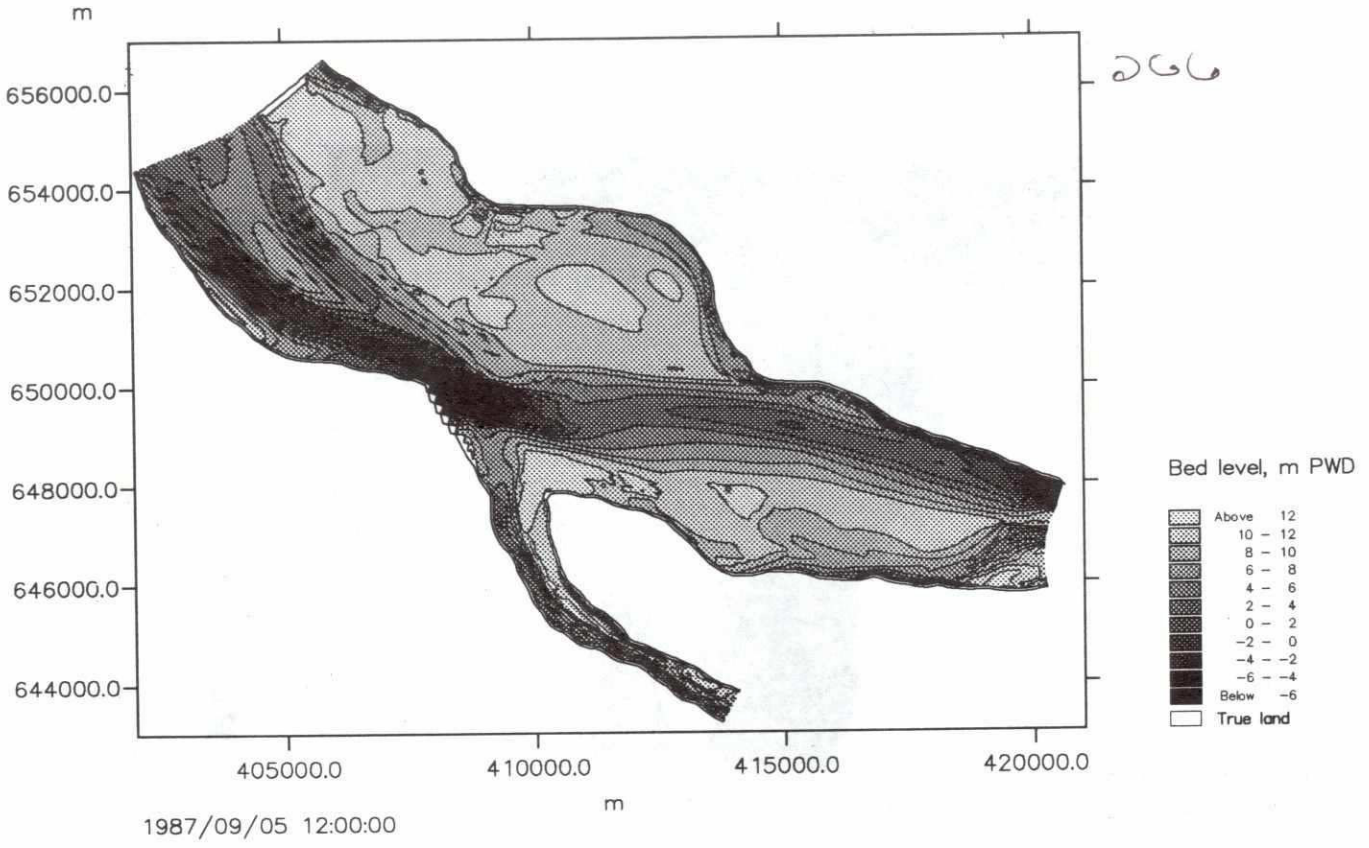


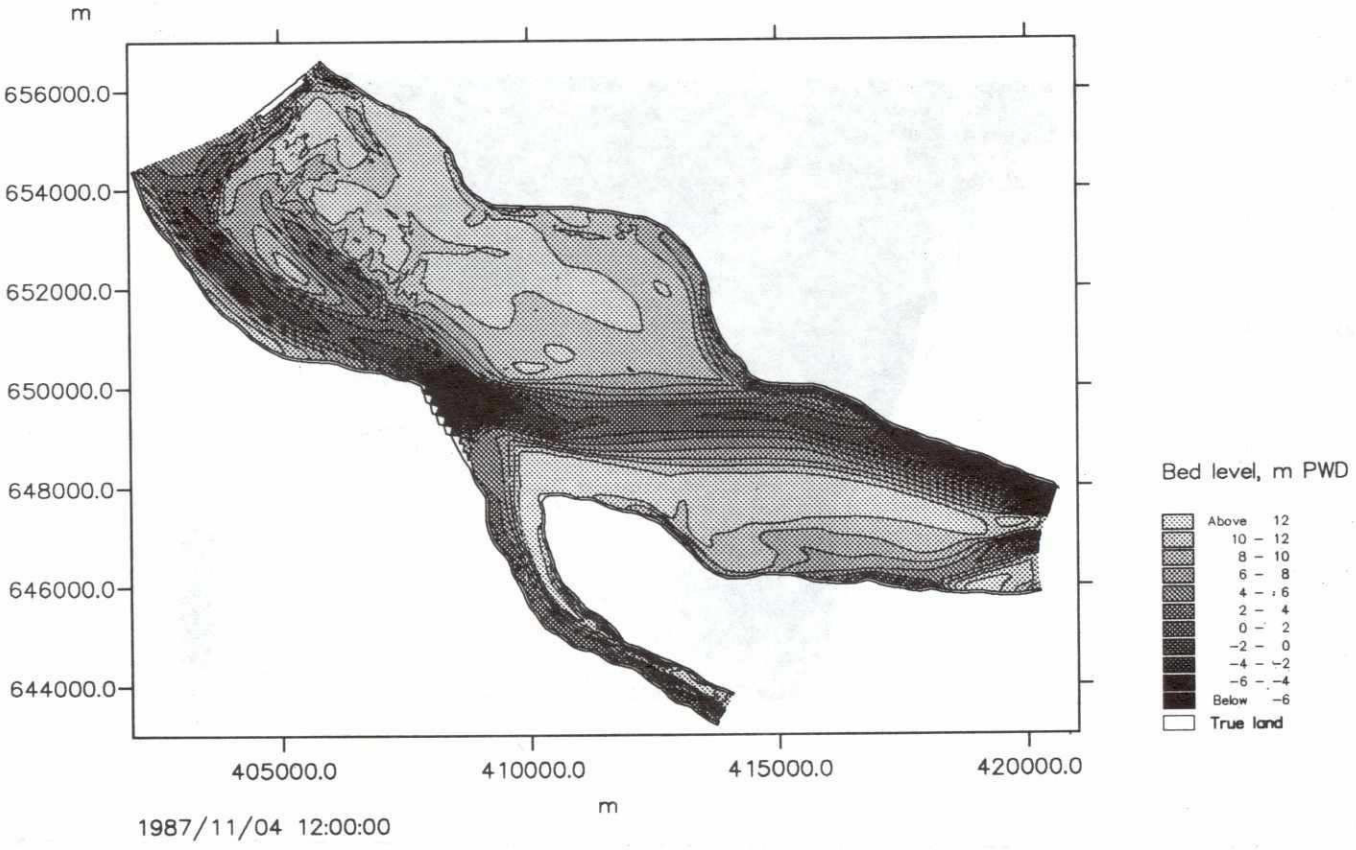


| | | | |
|---|---|---|---|
| SWMC | Client: River Survey Project FAP24 | | MIKE 21 |
| | Project: Gorai Offtake Mathematical Modelling | | |
| File: | Date: Thu Jul 4 1996 | Simulated bathymetry after 2 and 4 mths<br>Ganges and Gorai<br>1987 flood event | Drawing no.<br>**Figure 7.9.7** |
| Scale: 1:150000 | Init: hge | | |

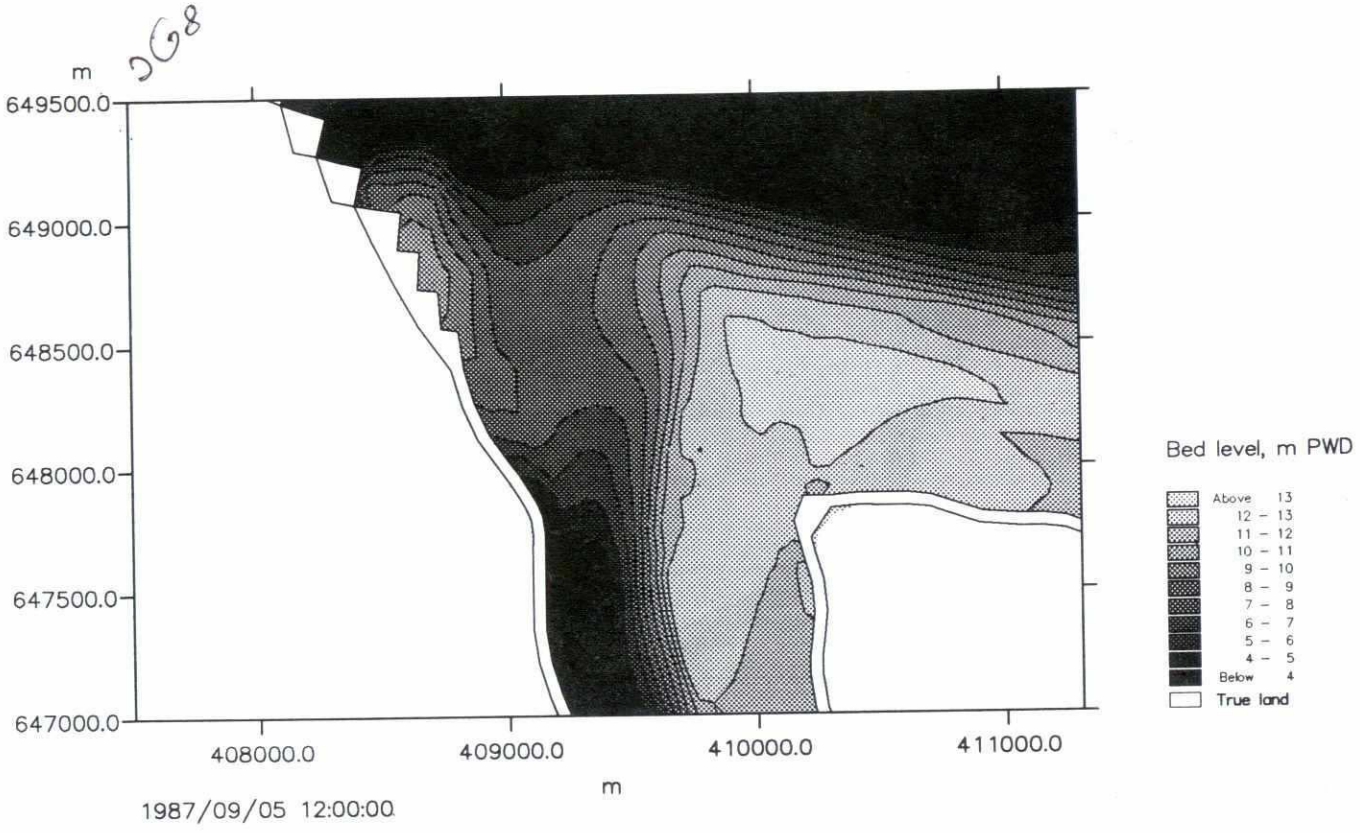


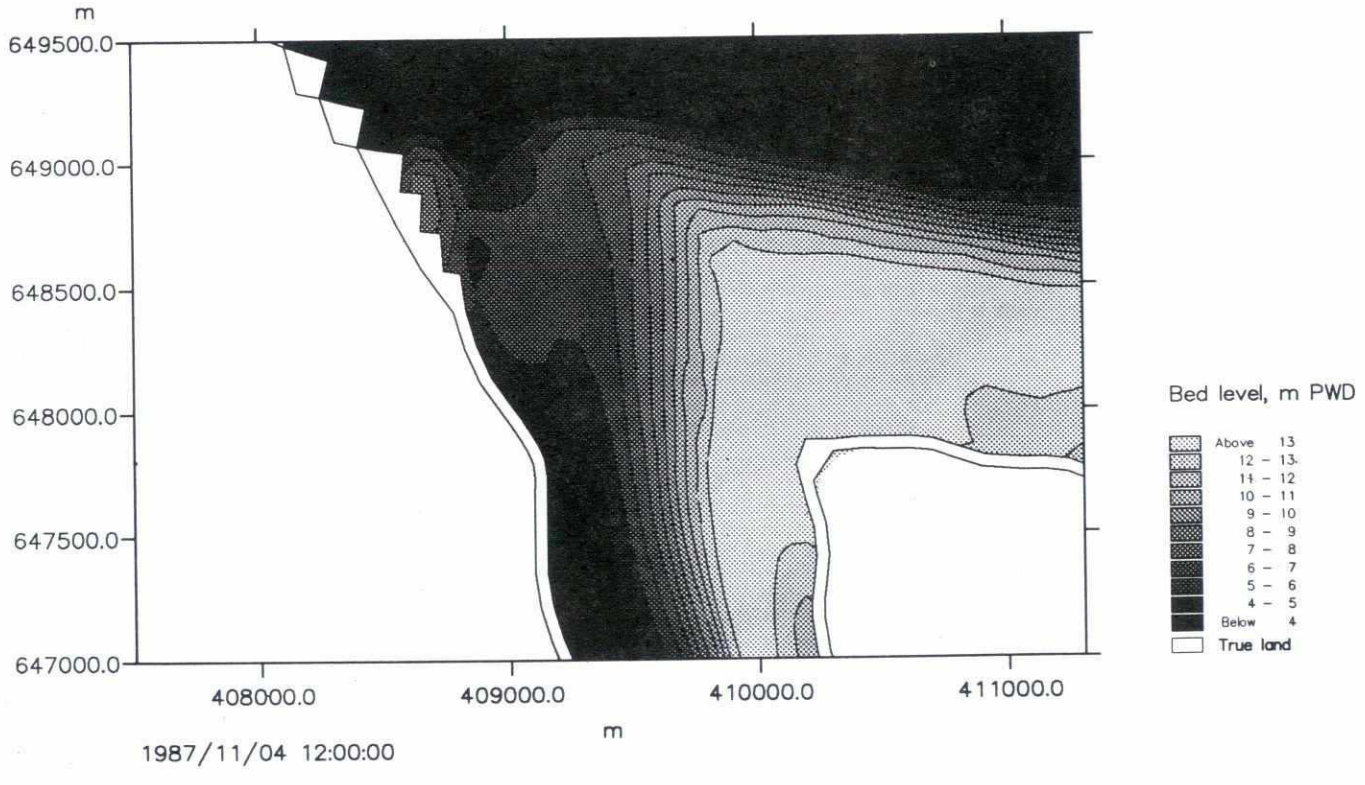


| | | | |
|---|---|---|---|
| SWMC | Client: River Survey Project FAP24 | | MIKE 21 |
| | Project: Gorai Offtake Mathematical Modelling | | |
| File: | Date: Thu Jul 4 1996 | Simulated bathymetry after 2 and 4 mths<br>Gorai Offtake<br>1987 flood event | Drawing no.<br>**Figure 7.9.8** |
| Scale: 1:30000 | Init: hge | | |

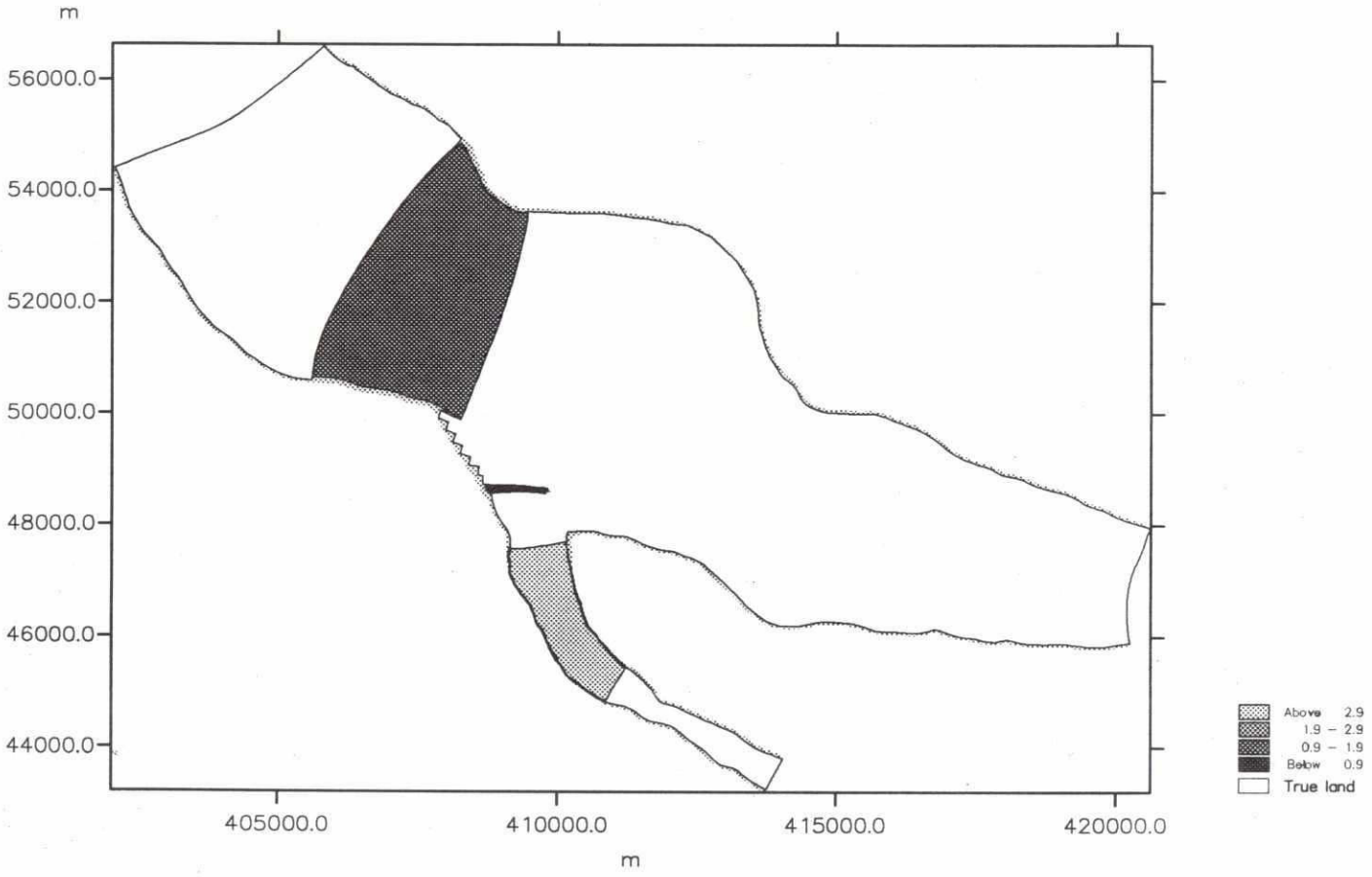


| | | | |
|---|---|---|---|
| SWMC | | Client: River Survey Project FAP24 | MIKE 21 |
| | | Project: Gorai Offtake Mathematical Modelling | |
| File: | Date: Thu Jul 4 1996 | Considered areas for averaging sediment transport rates from 2D model. Considered cross–section at Offtake. | Drawing no. **Figure 7.10.1** |
| Scale: 1:130000 | Init: hge | | |

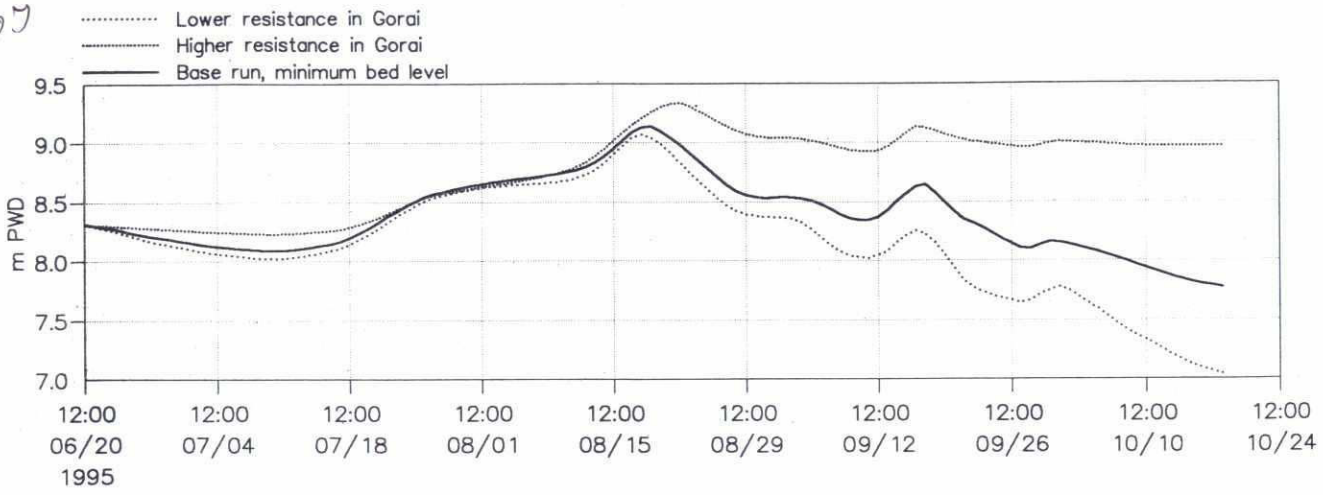


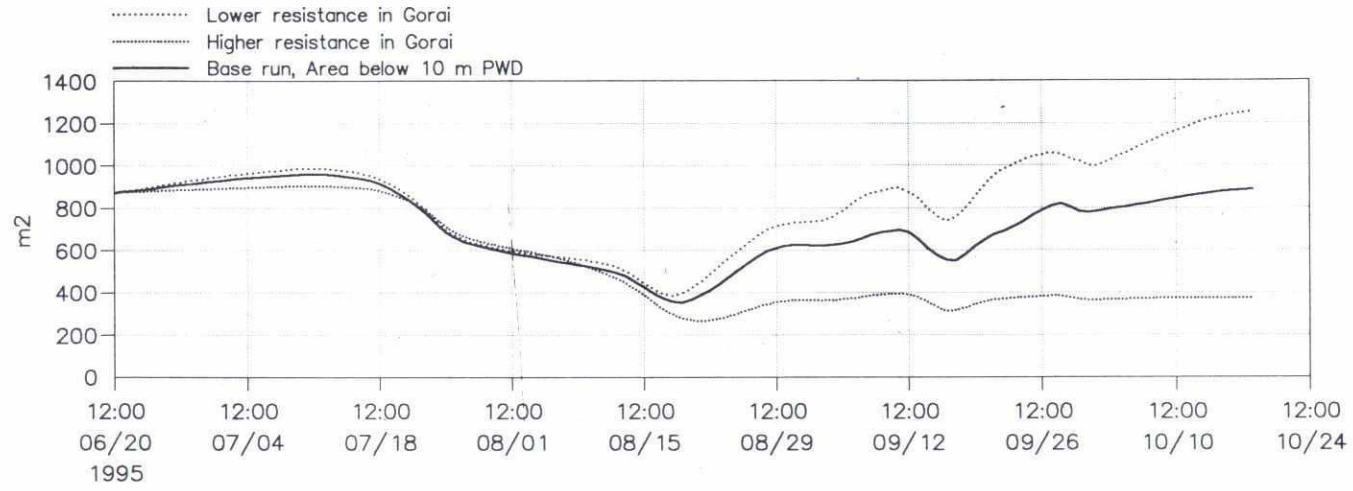


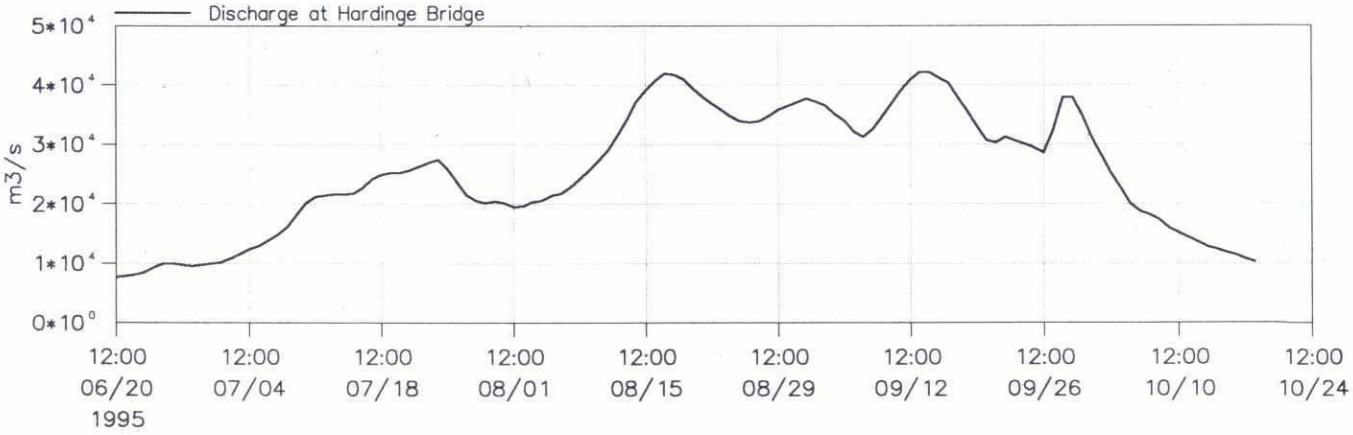


| SWMC | River Survey Project FAP24 | MIKE 21 |
|---|---|---|
| | Gorai Offtake Mathematical Modelling | |
| File: Date: Thu Jul 4 1996 | Simulated minimum bed level and cross-section area below 10 m PWD at the Offtake | dwg. no. Figure 7.10.2 |
| Scale: Init: hge | | |

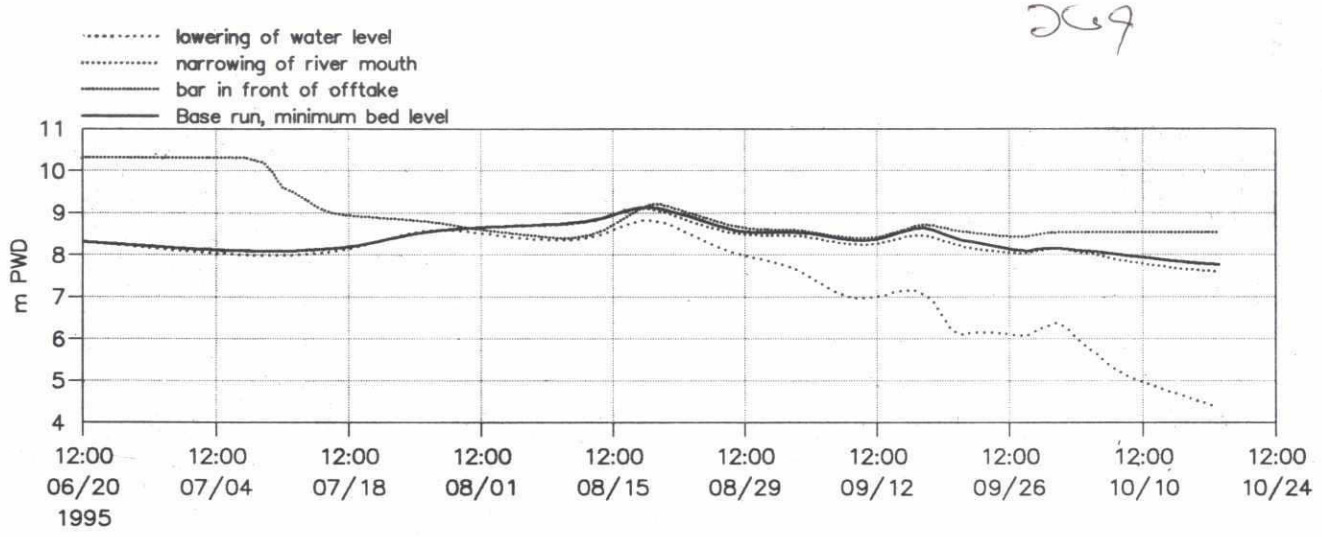


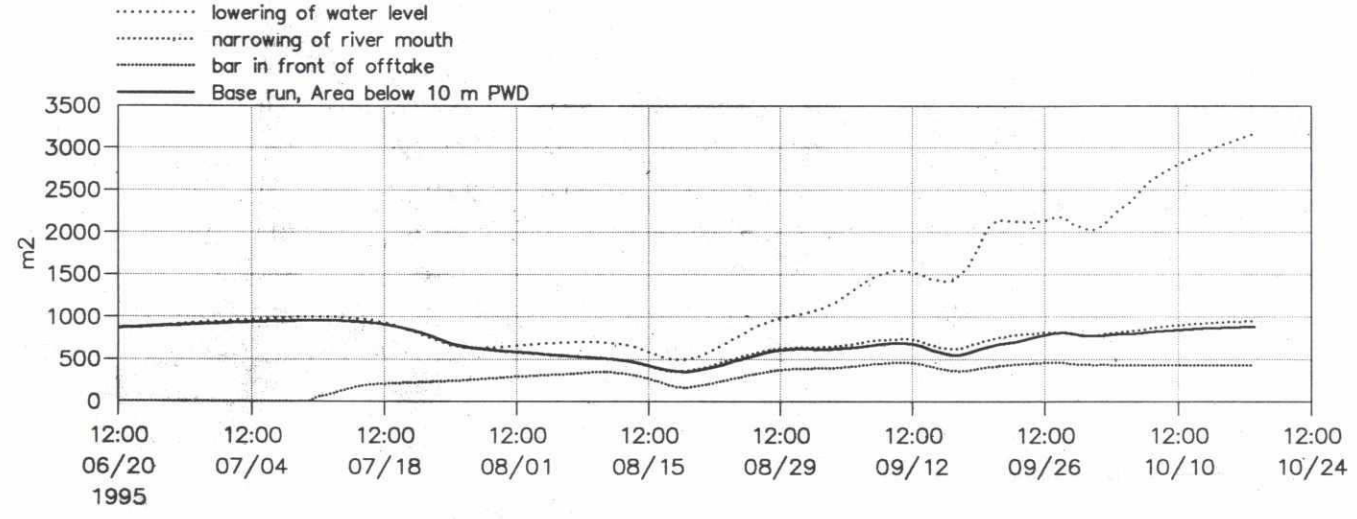


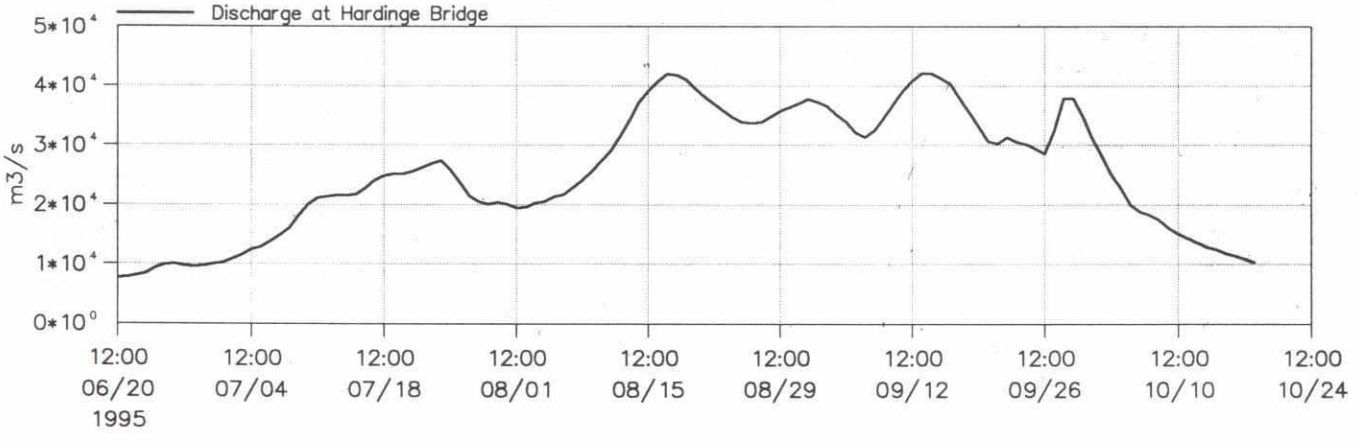


| SWMC | River Survey Project FAP24 | MIKE 21 |
|---|---|---|
| | Gorai Offtake Mathematical Modelling | |
| File: | Date: Thu Jul 4 1996 | Simulated minimum bed level and cross-section area below 10 m PWD at the Offtake |
| Scale: | Init: hge | dwg. no. **Figure 7.10.3** |

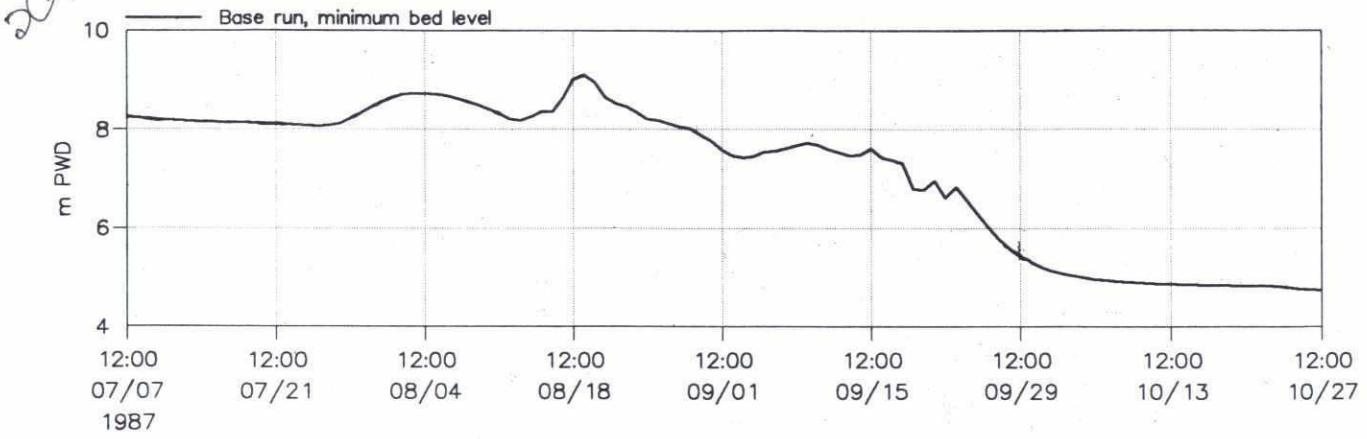


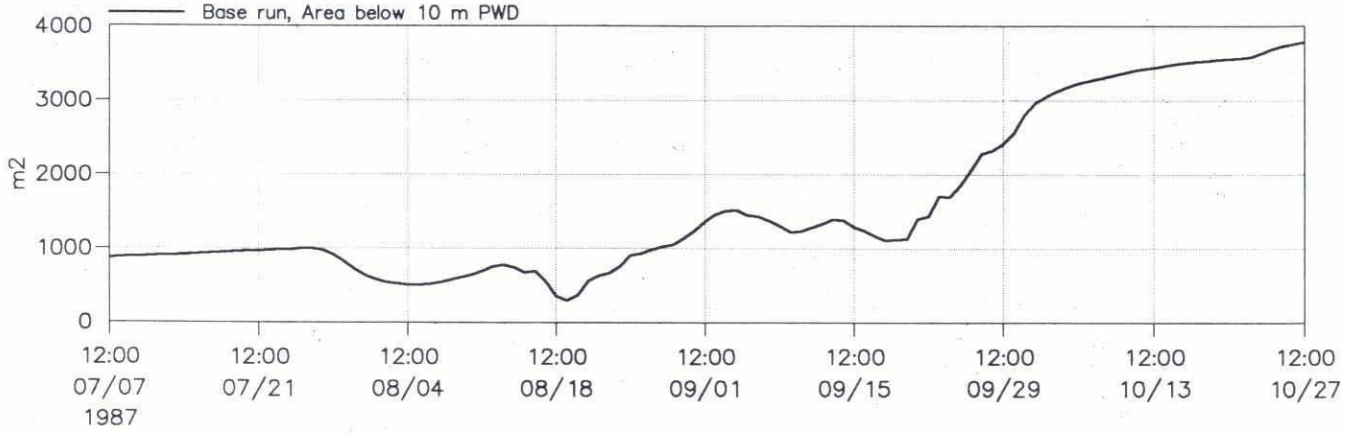


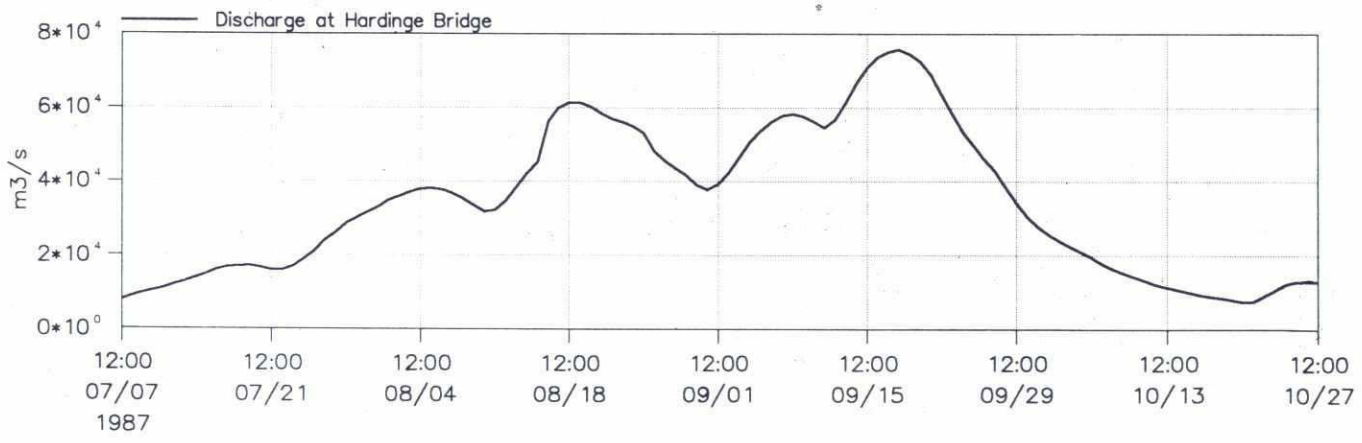


| SWMC | River Survey Project FAP24 | MIKE 21 |
|---|---|---|
| | Gorai Offtake Mathematical Modelling | |
| File: / Date: Thu Jul 4 1996 | Simulated minimum bed level and cross-section area below 10 m PWD at the Offtake using 1987 event | dwg. no. **Figure 7.10.4** |
| Scale: / Init: hge | | |

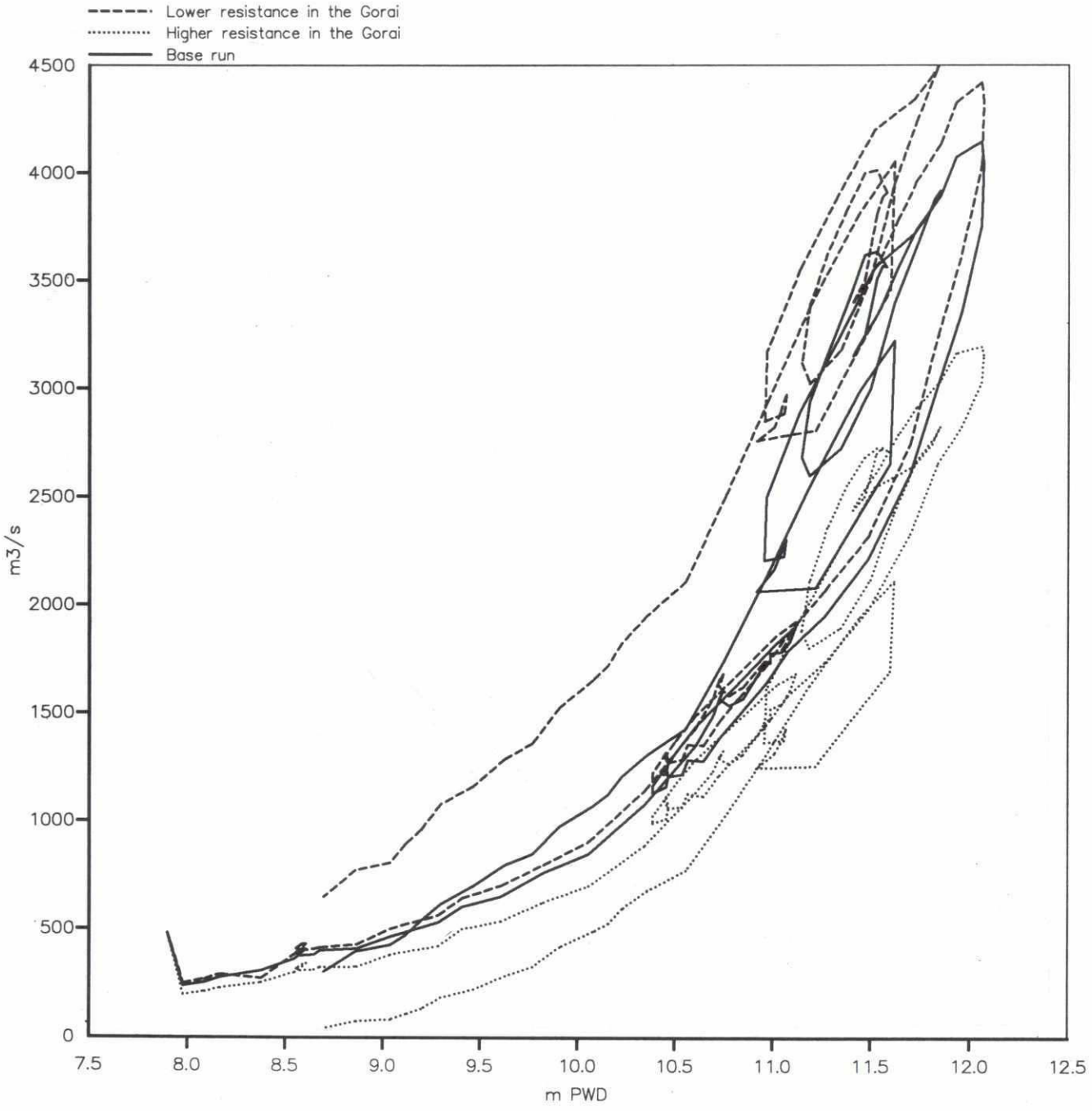


| SWMC | River Survey Project FAP24 | MIKE 21 |
|---|---|---|
| | Gorai Offtake Mathematical Modelling | |
| File: | Date: Thu Jul 4 1996 | Simulated Discharge Rating Curve<br>Gorai Railway Bridge<br>base run and two sensitivity runs |
| Scale: | Init: hge | dwg. no.<br>**Figure 7.10.5** |

280

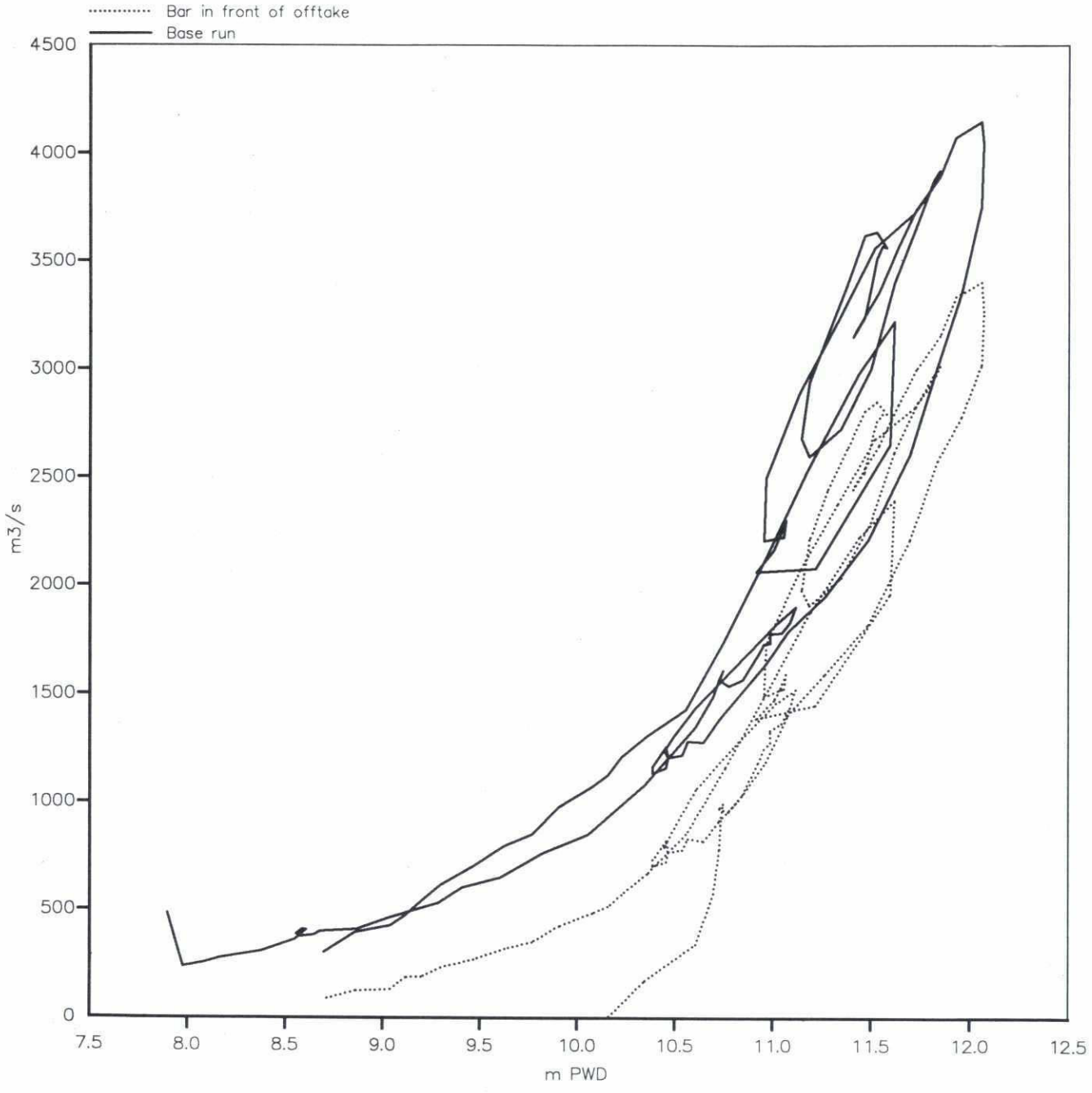


| SWMC | River Survey Project FAP24 | MIKE 21 |
|---|---|---|
| | Gorai Offtake Mathematical Modelling | |
| File: | Date: Fri Jul 5 1996 | Simulated Discharge Rating Curve<br>Gorai Railway Bridge<br>base run and bar in front of offtake |
| Scale: | Init: hge | dwg. no.<br>**Figure 7.10.6** |

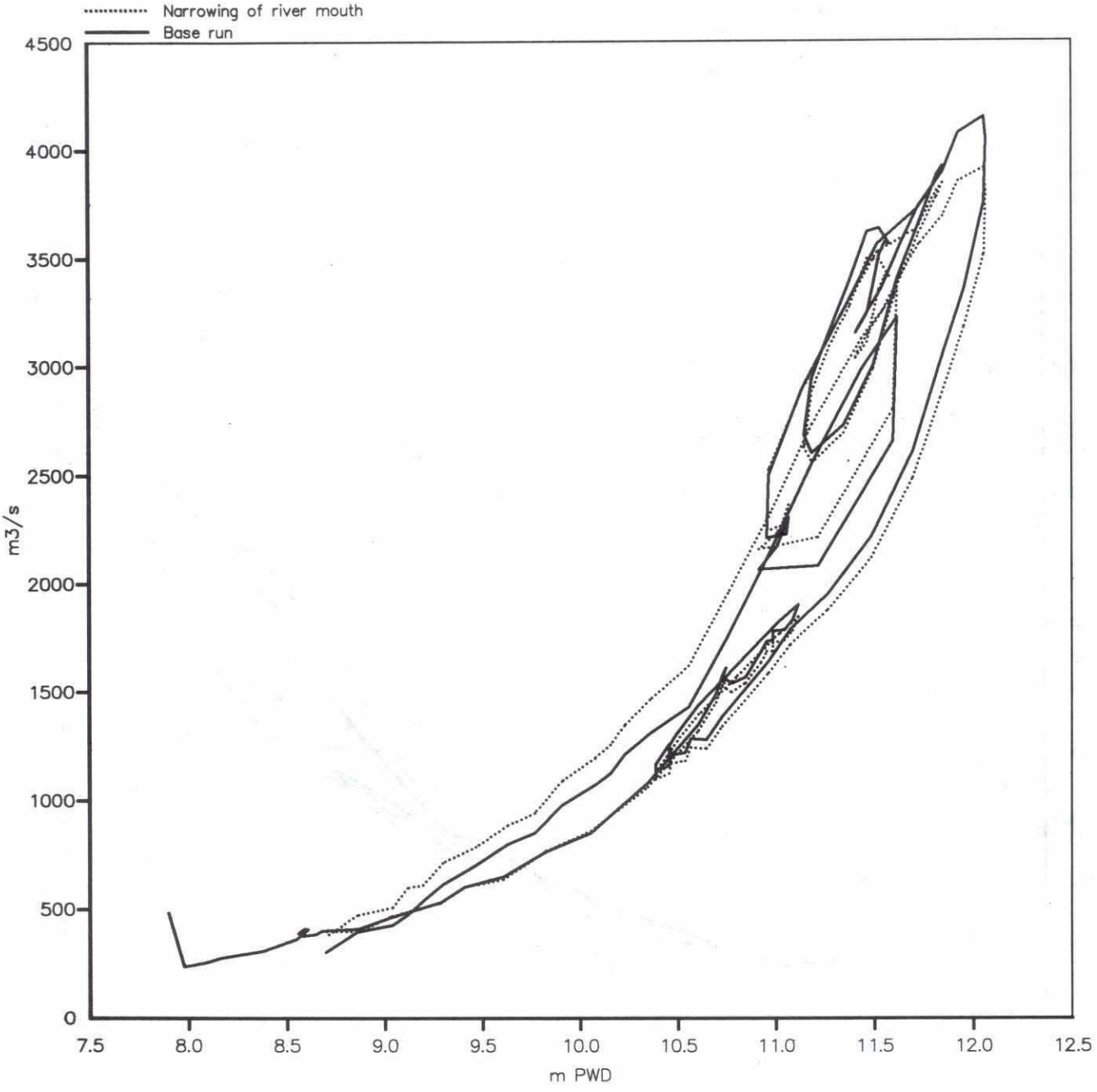


| SWMC | River Survey Project FAP24 | MIKE 21 |
|---|---|---|
| | Gorai Offtake Mathematical Modelling | |
| File: Date: Fri Jul 5 1996 | Simulated Discharge Rating Curve<br>Gorai Railway Bridge<br>narrowing of river mouth | dwg. no.<br>Figure 7.10.7 |
| Scale: Init: hge | | |

292

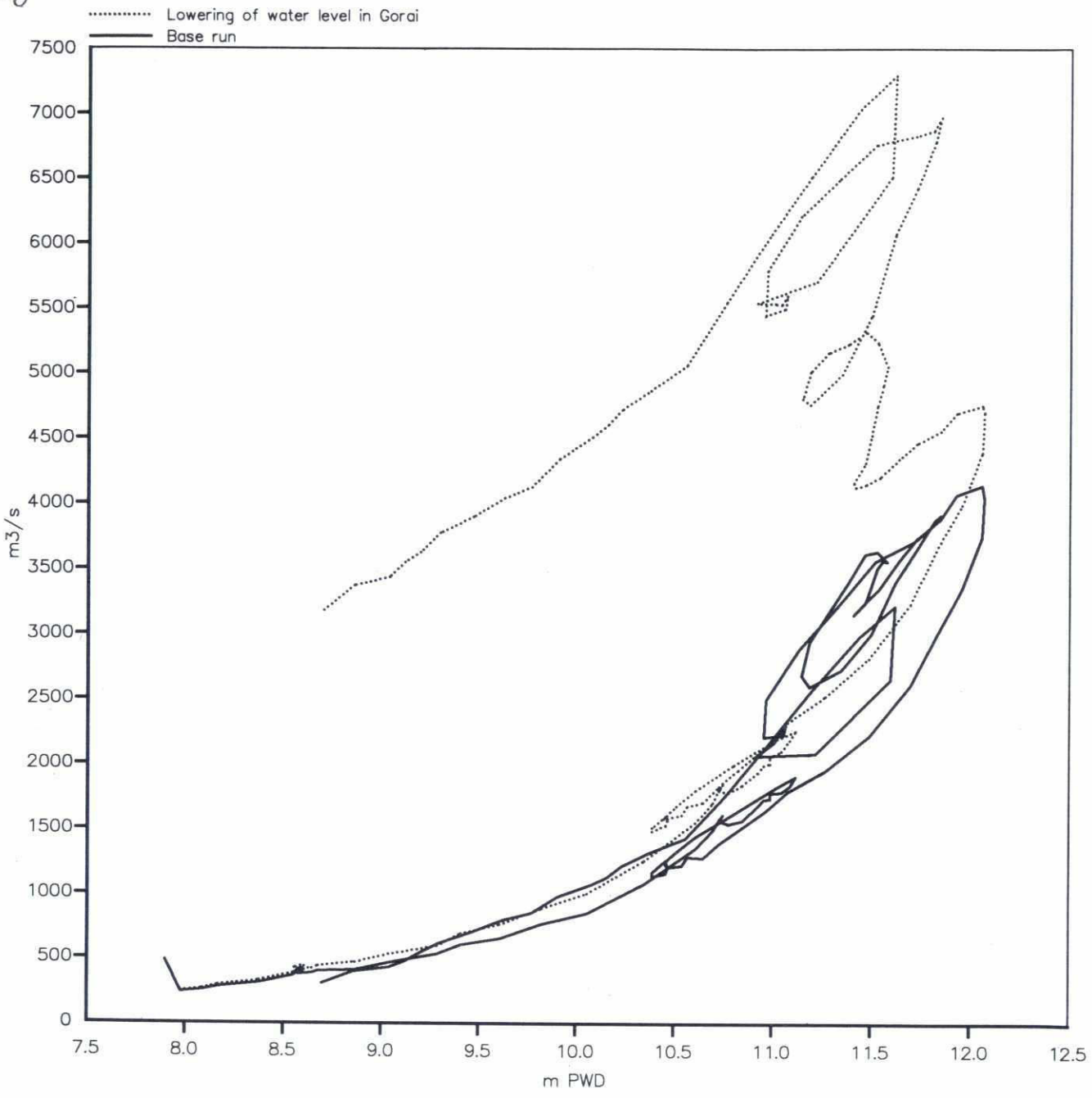


| SWMC | | River Survey Project FAP24 | MIKE 21 |
|---|---|---|---|
| | | Gorai Offtake Mathematical Modelling | |
| File: | Date: Thu Jul 4 1996 | Simulated Discharge Rating Curve<br>Gorai Railway Bridge<br>base run and water level lowering run | dwg. no.<br>**Figure 7.10.8** |
| Scale: | Init: hge | | |

| SWMC | Client: River Survey Project FAP24 | MIKE 21 |
|---|---|---|
| | Project: Gorai Offtake Mathematical Modelling | |
| File: | Date: Sat Jul 6 1996 | Simulated and calculated (from observations) conveyance factors at Gorai river mouth |
| Scale: 1:150000 | Init: hge | Drawing no. Figure 7.10.9 |

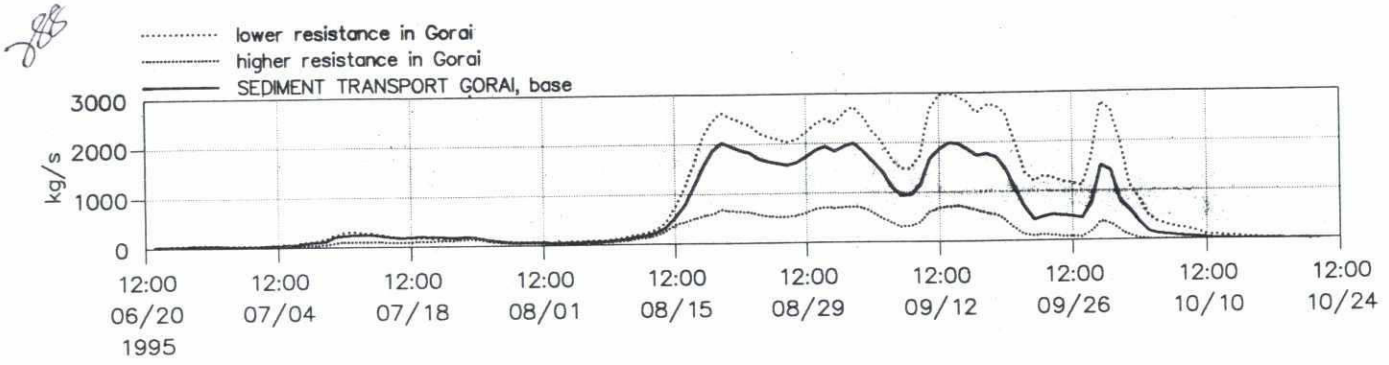


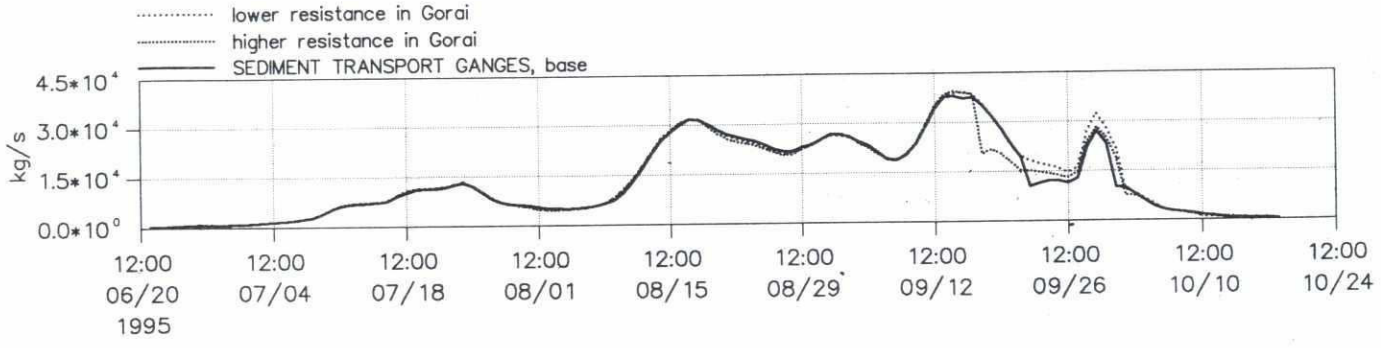


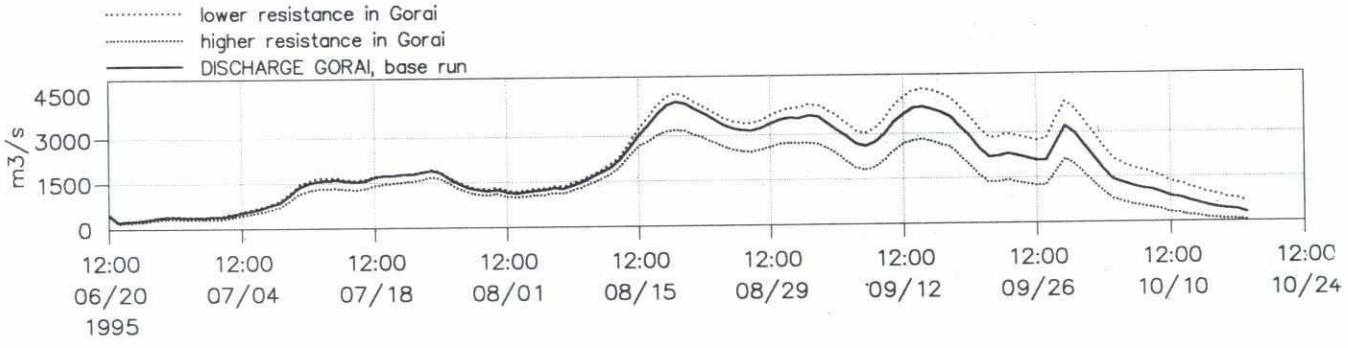


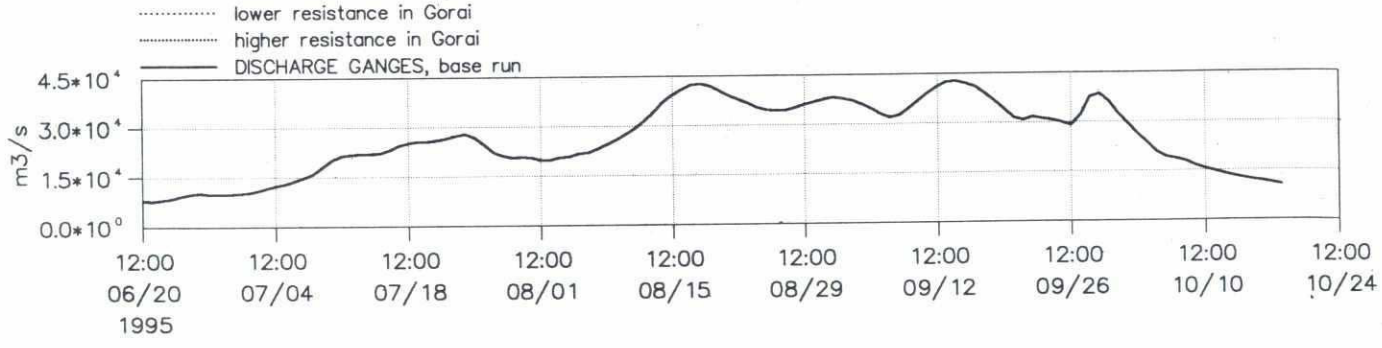


| SWMC | River Survey Project FAP24 | MIKE 21 |
|---|---|---|
| | Gorai Offtake Mathematical Modelling | |
| File: | Date: Fri Jul 5 1996 | Simulated Discharge and Sediment transport in Gorai and Ganges, 1. base 2. high resist 3. low resist |
| Scale: | Init: hge | dwg. no. **Figure 7.10.10** |

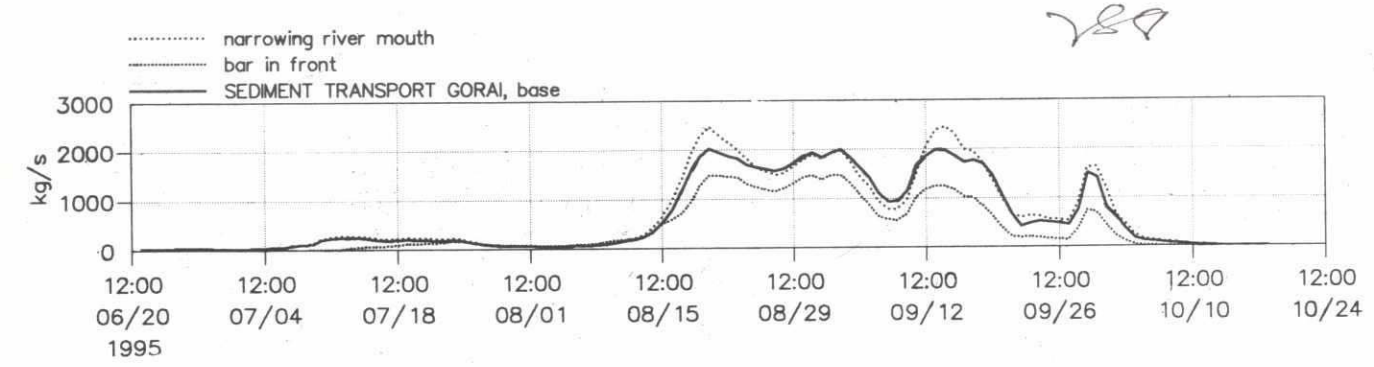


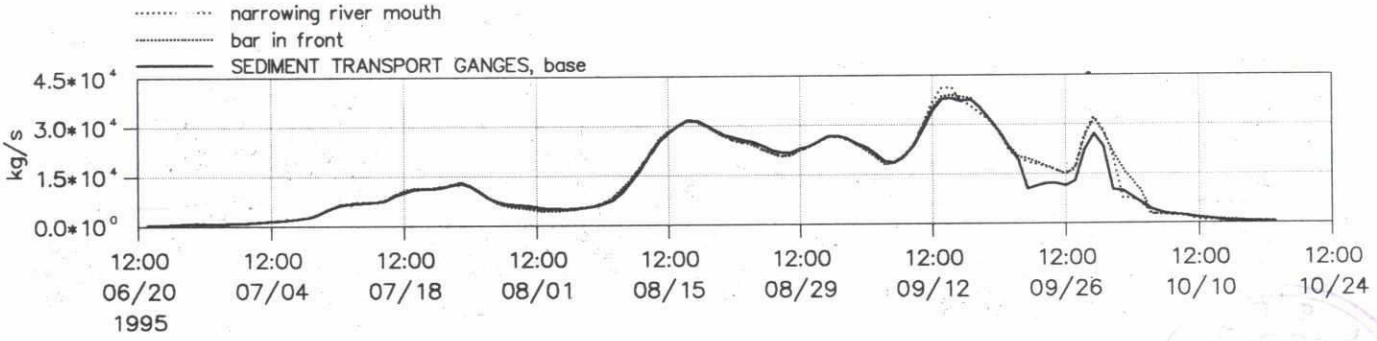


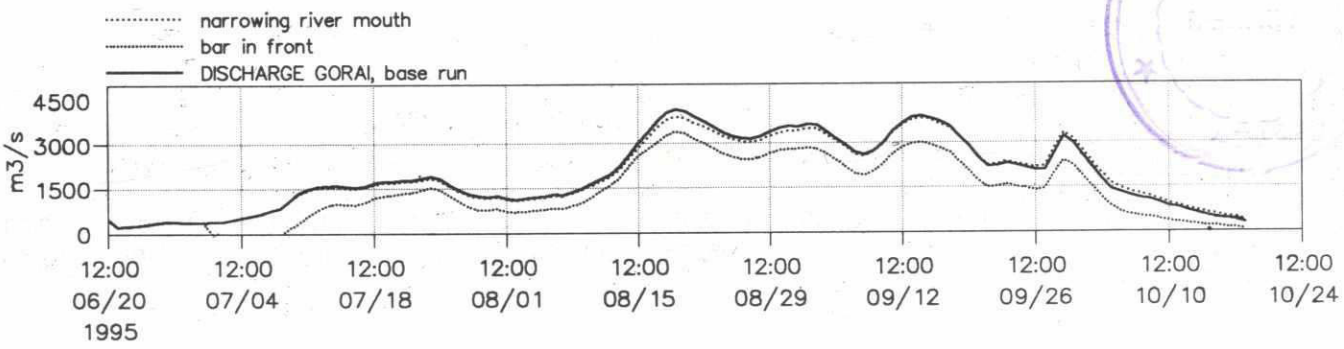


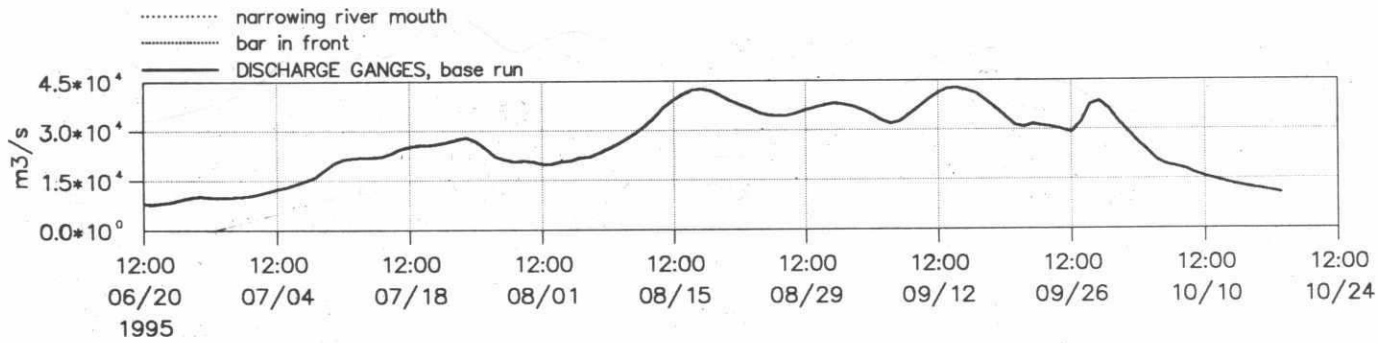


| SWMC | River Survey Project FAP24 | MIKE 21 |
|---|---|---|
| | Gorai Offtake Mathematical Modelling | |
| File: | Date: Fri Jul 5 1996 | Simulated Discharge and Sediment transport in Gorai and Ganges, 1. base 2. bar 3. narrowing |
| Scale: | Init: hge | dwg. no. **Figure 7.10.11** |

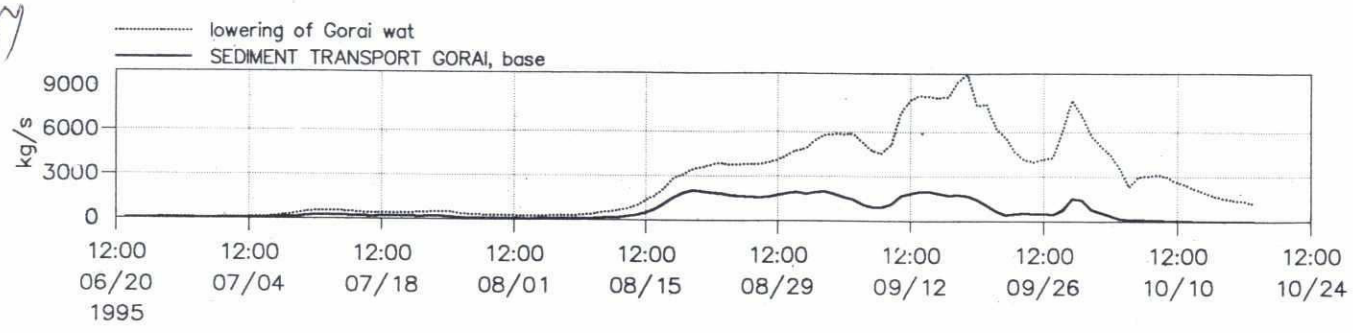


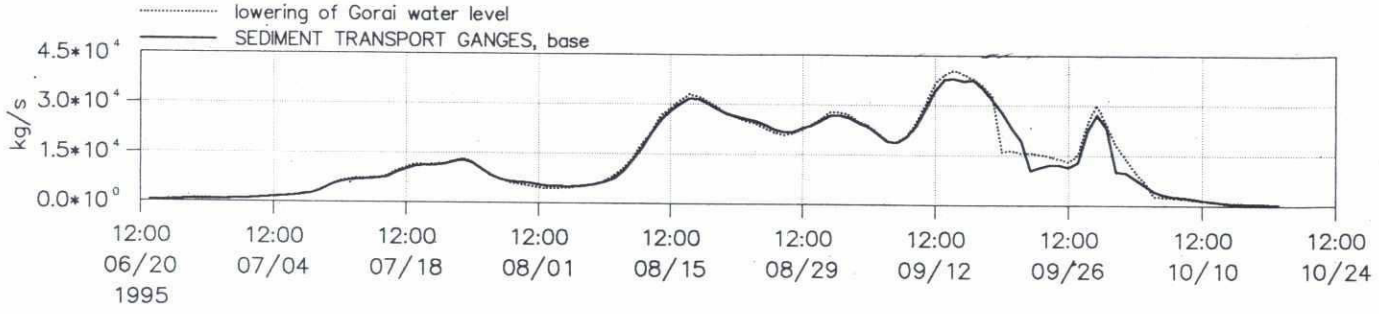


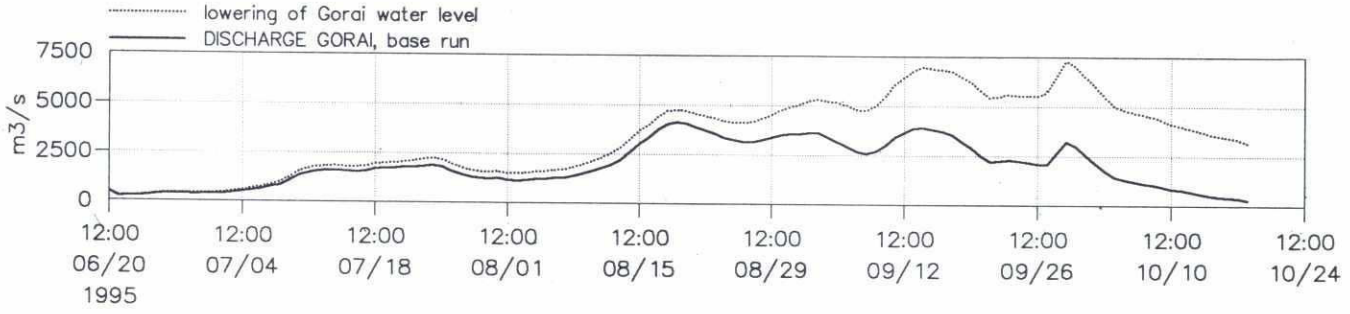


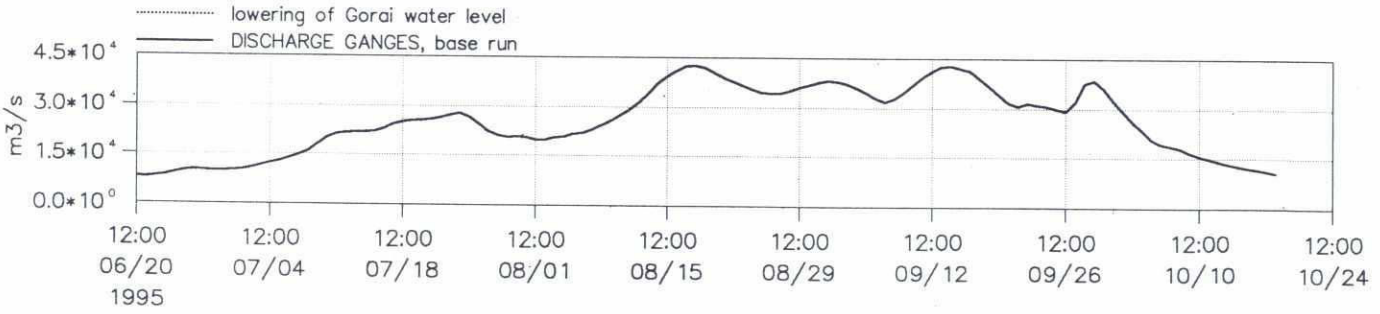


| SWMC | River Survey Project FAP24 | MIKE 21 |
|---|---|---|
| | Gorai Offtake Mathematical Modelling | |
| File: | Date: Fri Jul 5 1996 | Simulated Discharge and Sediment transport in Gorai and Ganges, 1. base 2. lowering of Gorai waterlevel |
| Scale: | Init: hge | dwg. no. **Figure 7.10.12** |

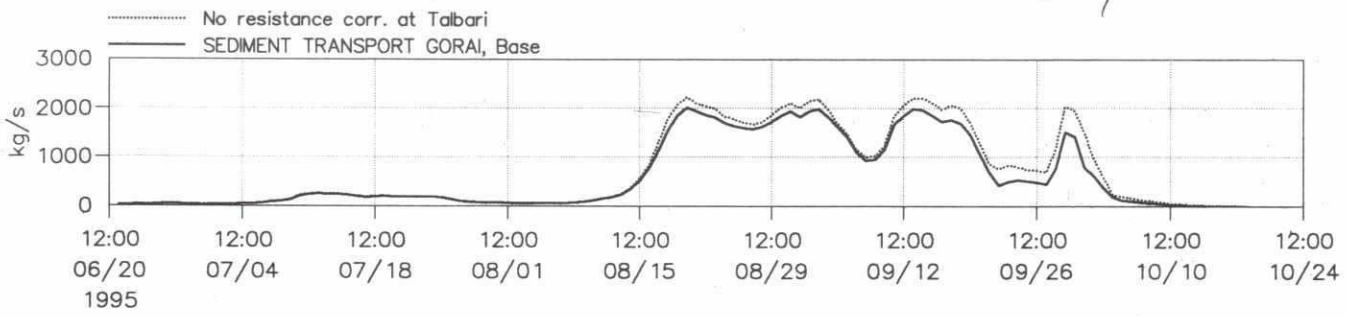


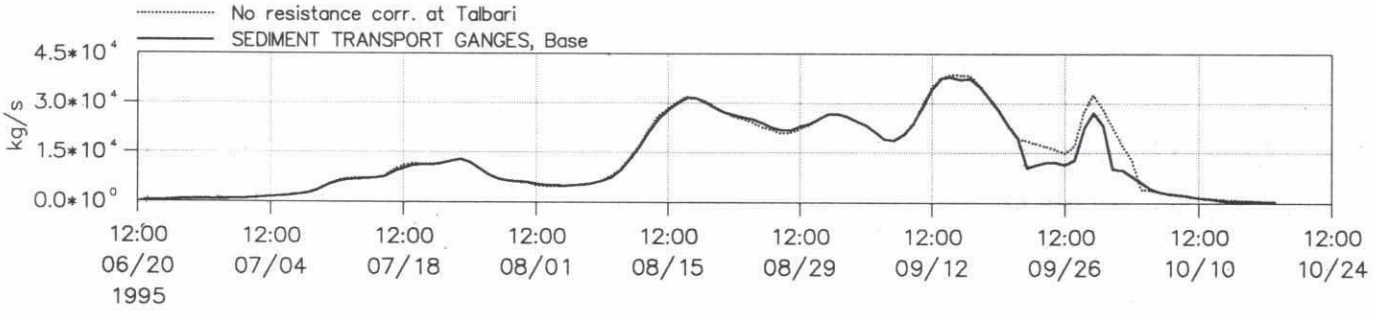


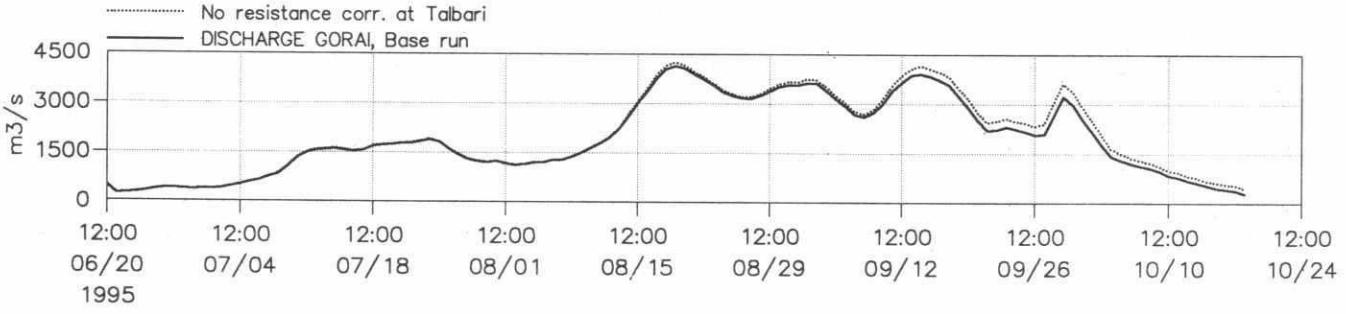


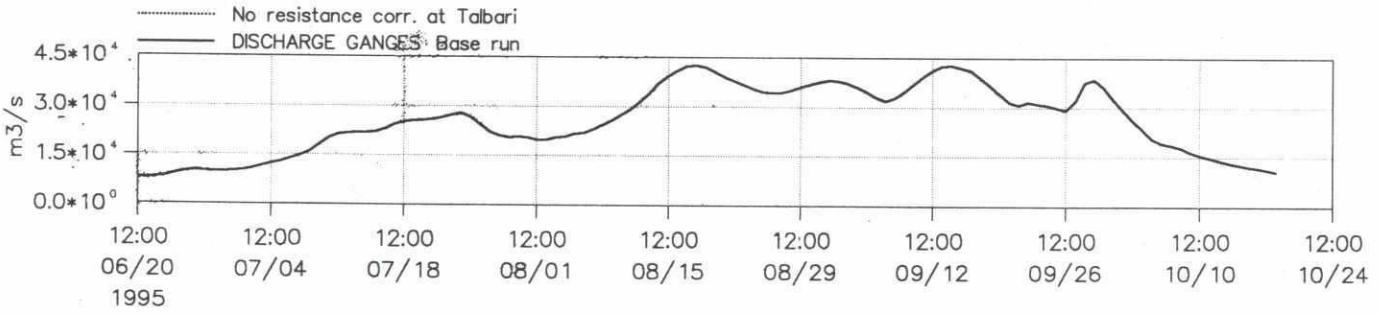


| SWMC | River Survey Project FAP24 | MIKE 21 |
|---|---|---|
| | Gorai Offtake Mathematical Modelling | |
| File: | Date: Thu Jul 11 1996 | Simulated Discharge and Sediment Transp transport in Ganges and Gorai. Sensitivity run. |
| Scale: | Init: hge | dwg. no. **Figure 7.10.13** |

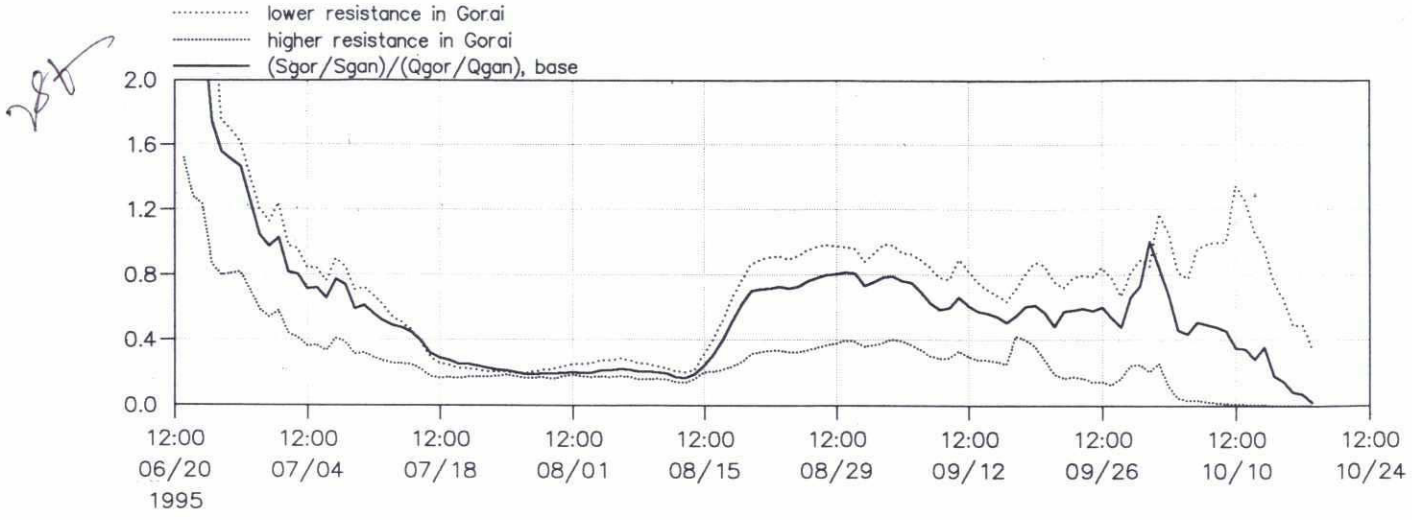


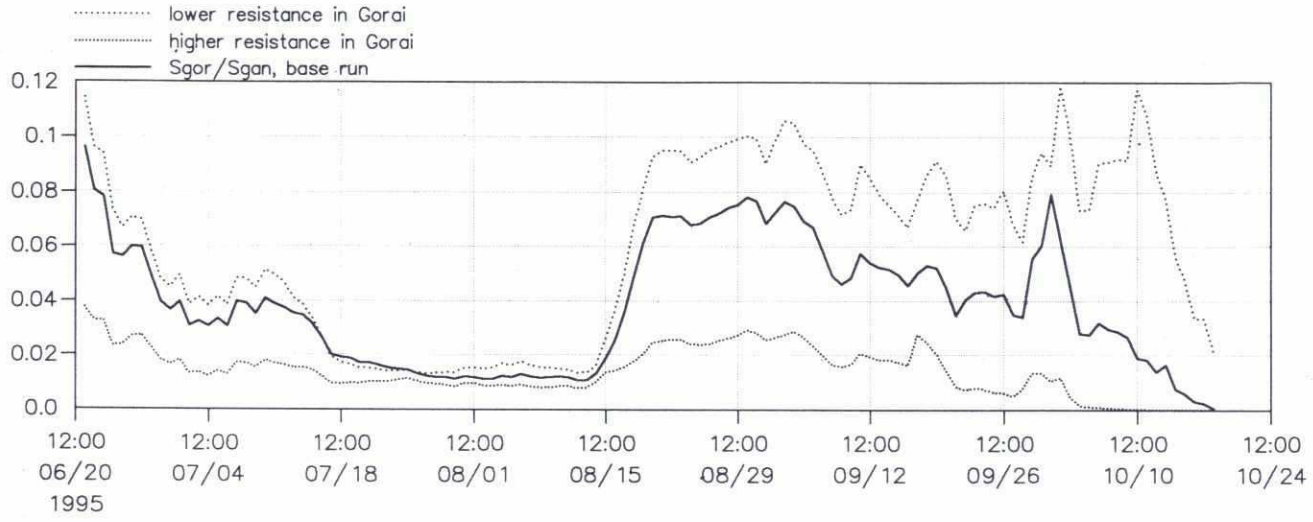


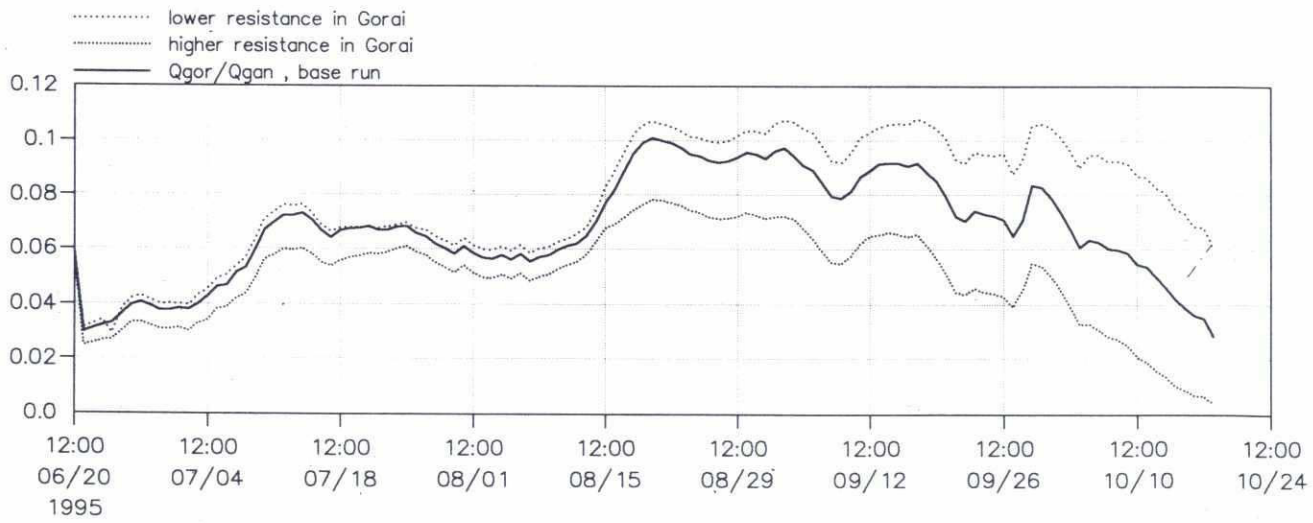


| SWMC | River Survey Project FAP24 | MIKE 21 |
|---|---|---|
| | Gorai Offtake Mathematical Modelling | |
| File: | Date: Fri Jul 5 1996 | Simulated Discharge ratio (Qgor Gorai, Qgan Ganges) and sediment transport ratio (Sgor Gorai, Sgan Ganges) |
| Scale: | Init: hge | dwg. no. **Figure 7.10.14** |

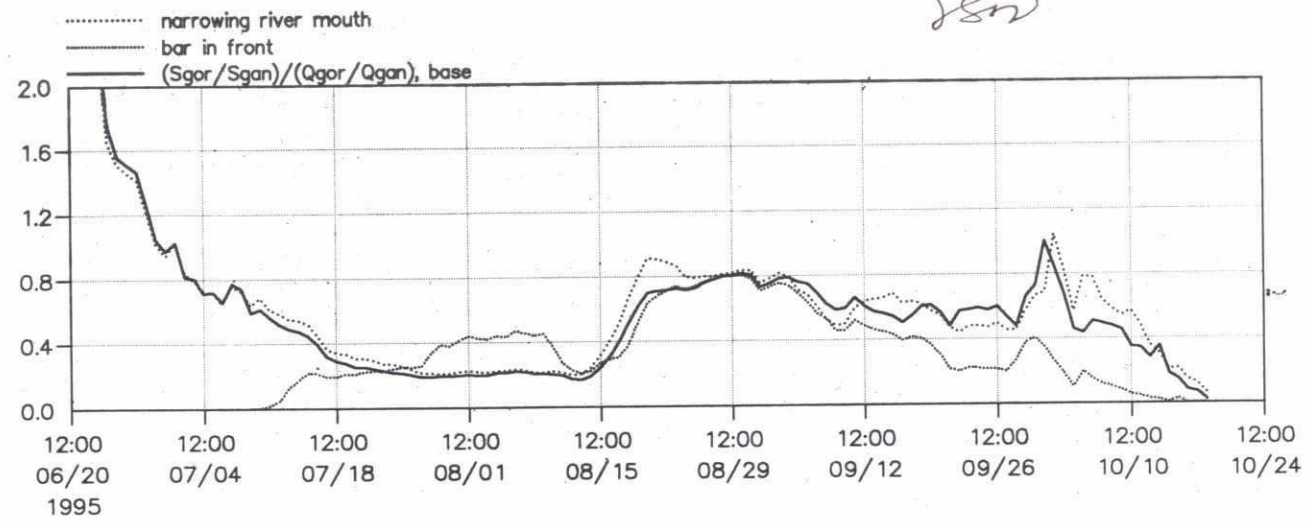


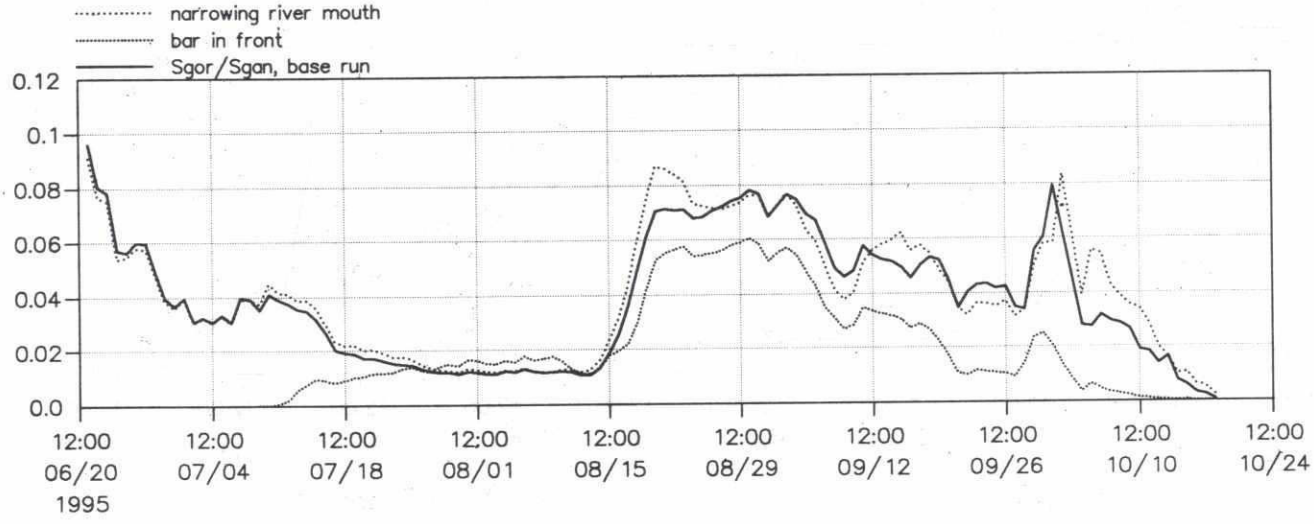


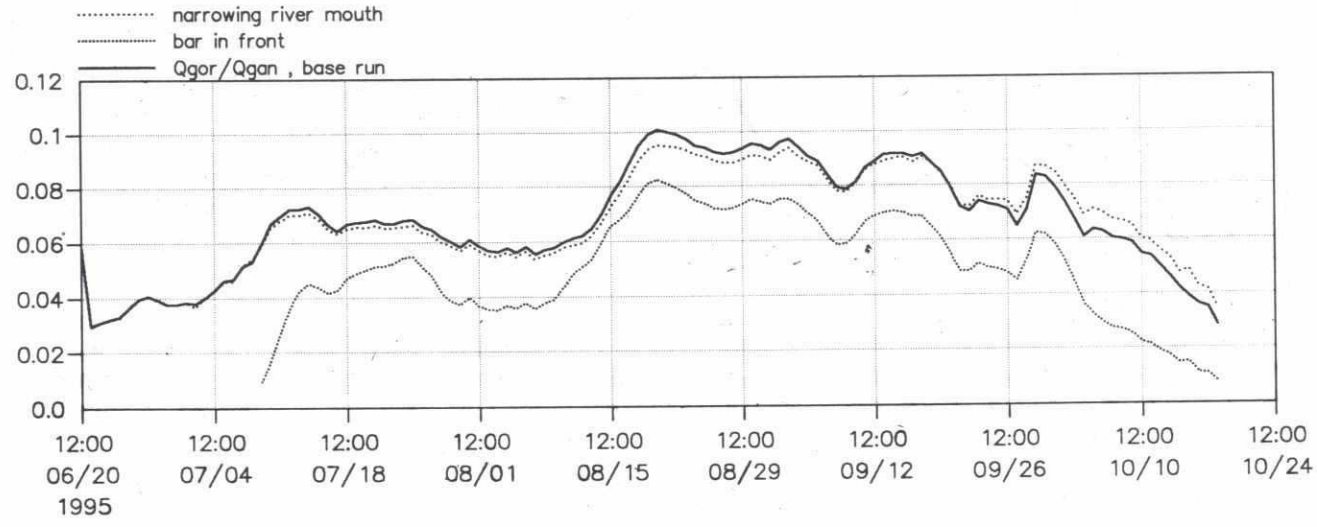


| SWMC | River Survey Project FAP24 | MIKE 21 |
|---|---|---|
| | Gorai Offtake Mathematical Modelling | |
| File: | Date: Fri Jul 5 1996 | Simulated Discharge ratio (Qgor Gorai, Qgan Ganges) and sediment transport ratio (Sgor Gorai, Sgan Ganges) |
| Scale: | Init: hge | dwg. no. **Figure 7.10.15** |

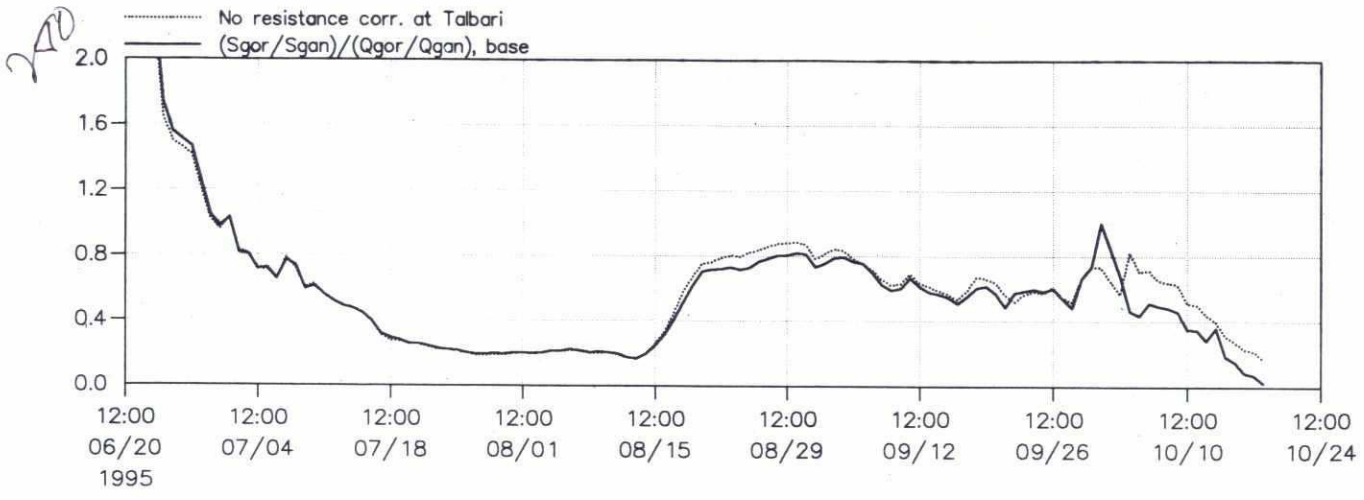


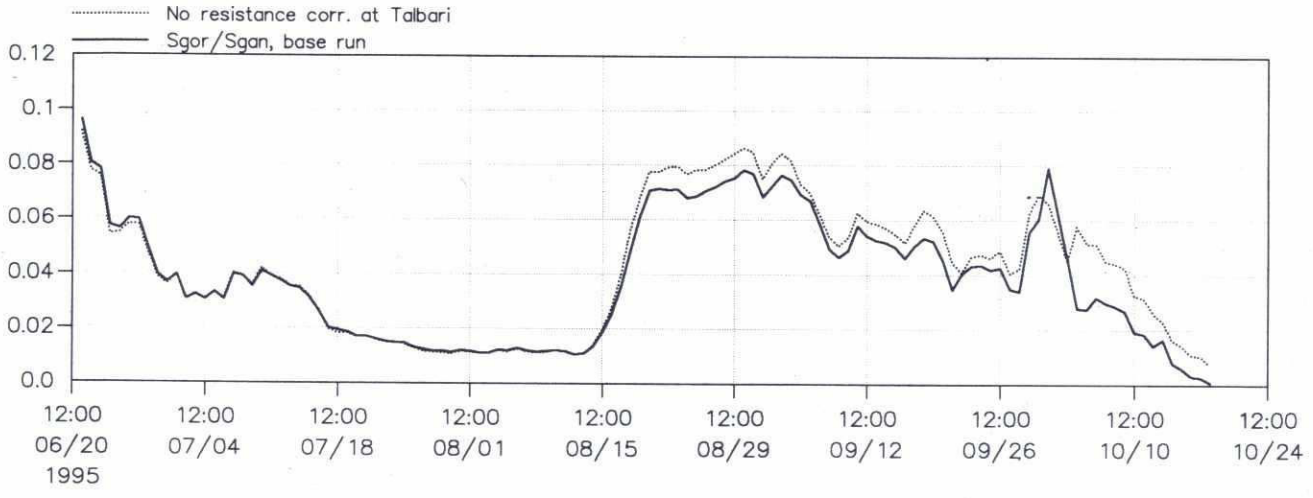


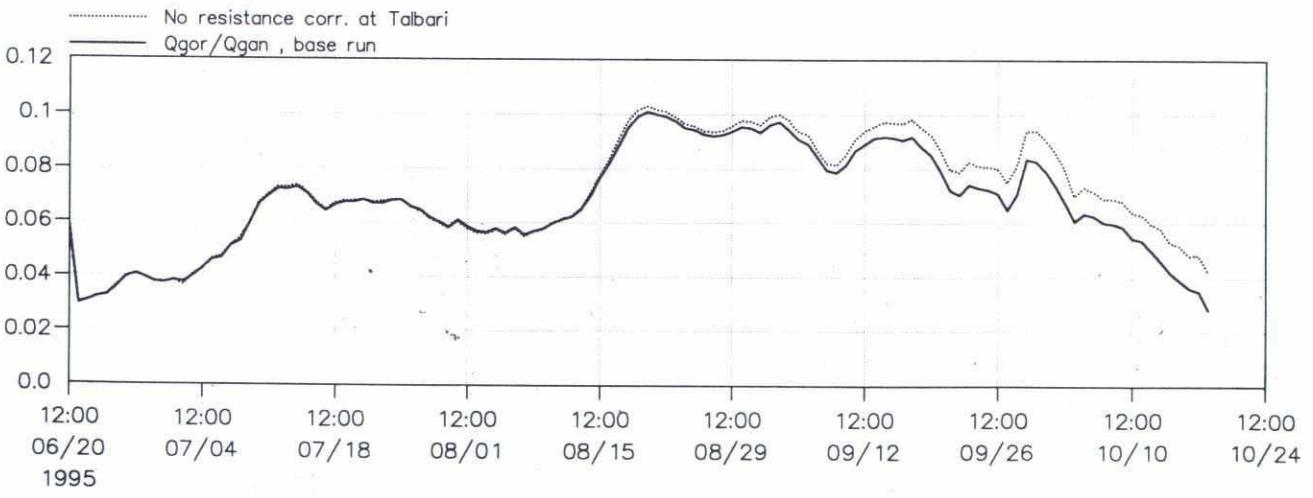


| SWMC | River Survey Project FAP24 | MIKE 21 |
|---|---|---|
| | Gorai Offtake Mathematical Modelling | |
| File: / Date: Thu Jul 11 1996 | Simulated Discharge rátio (Qgor Gorai, Qgan Ganges) and sediment transport ratio (Sgor Gorai, Sgan Ganges) | dwg. no. **Figure 7.10.16** |
| Scale: / Init: hge | | |

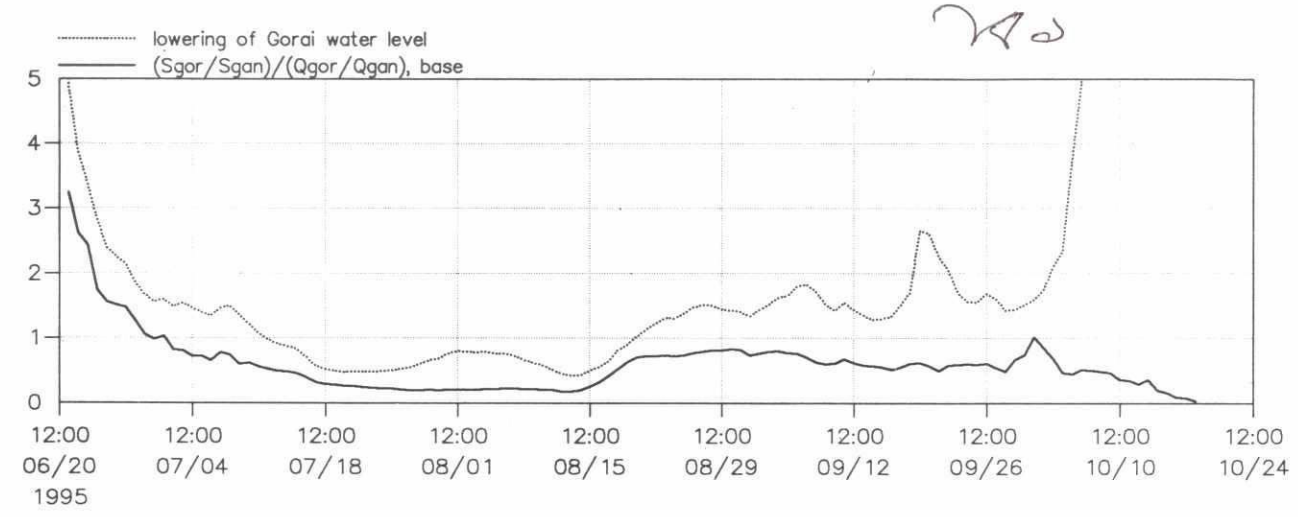


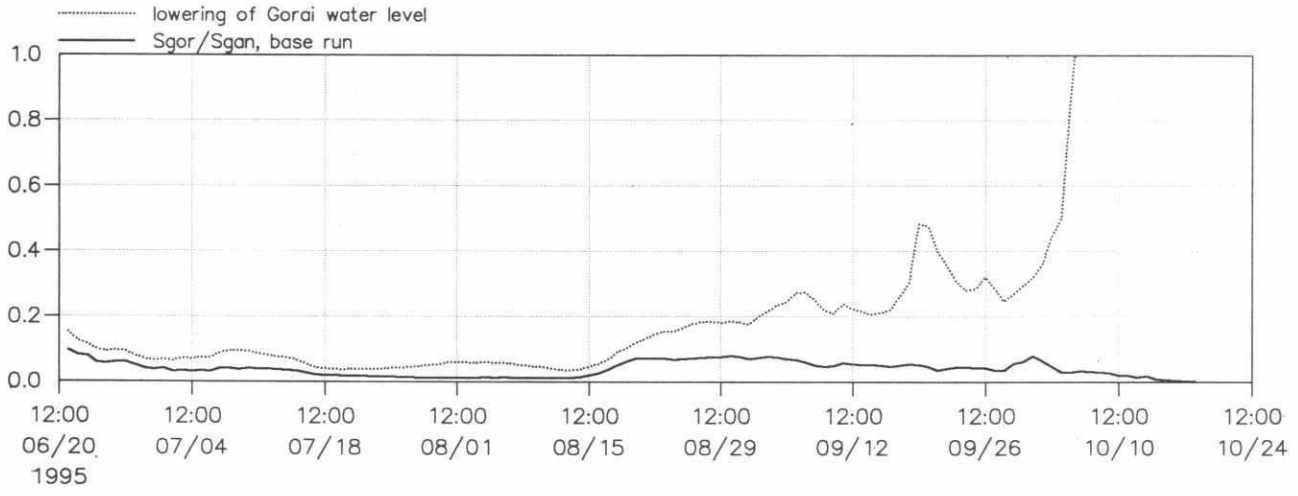


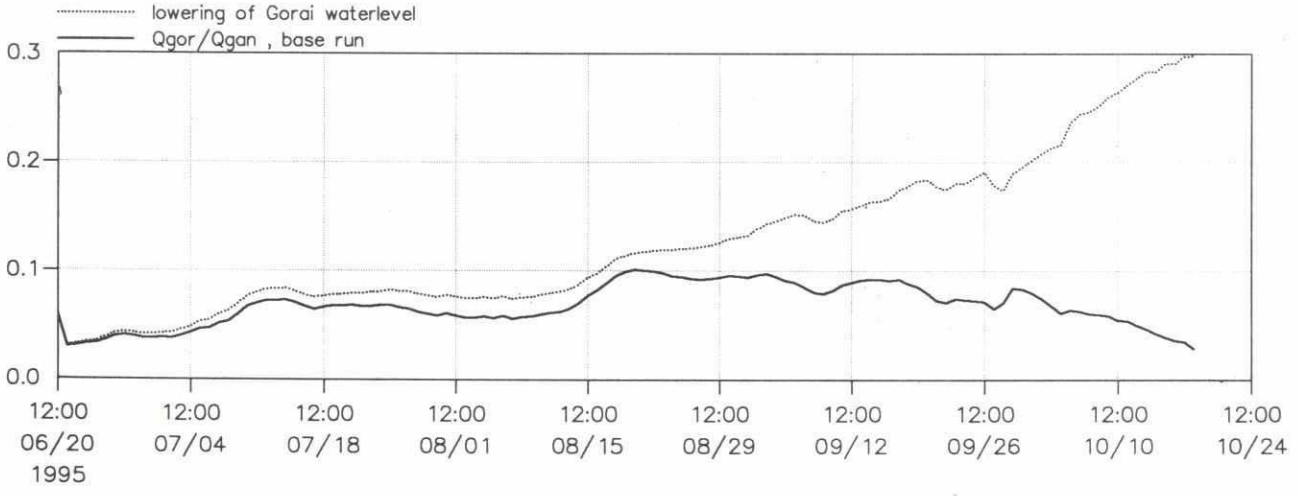


| SWMC | River Survey Project FAP24 | MIKE 21 |
|---|---|---|
| | Gorai Offtake Mathematical Modelling | |
| File: | Date: Fri Jul 5 1996 | Simulated Discharge ratio (Qgor Gorai, Qgan Ganges) and sediment transport ratio (Sgor Gorai, Sgan Ganges) |
| Scale: | Init: hge | dwg. no. **Figure 7.10.17** |

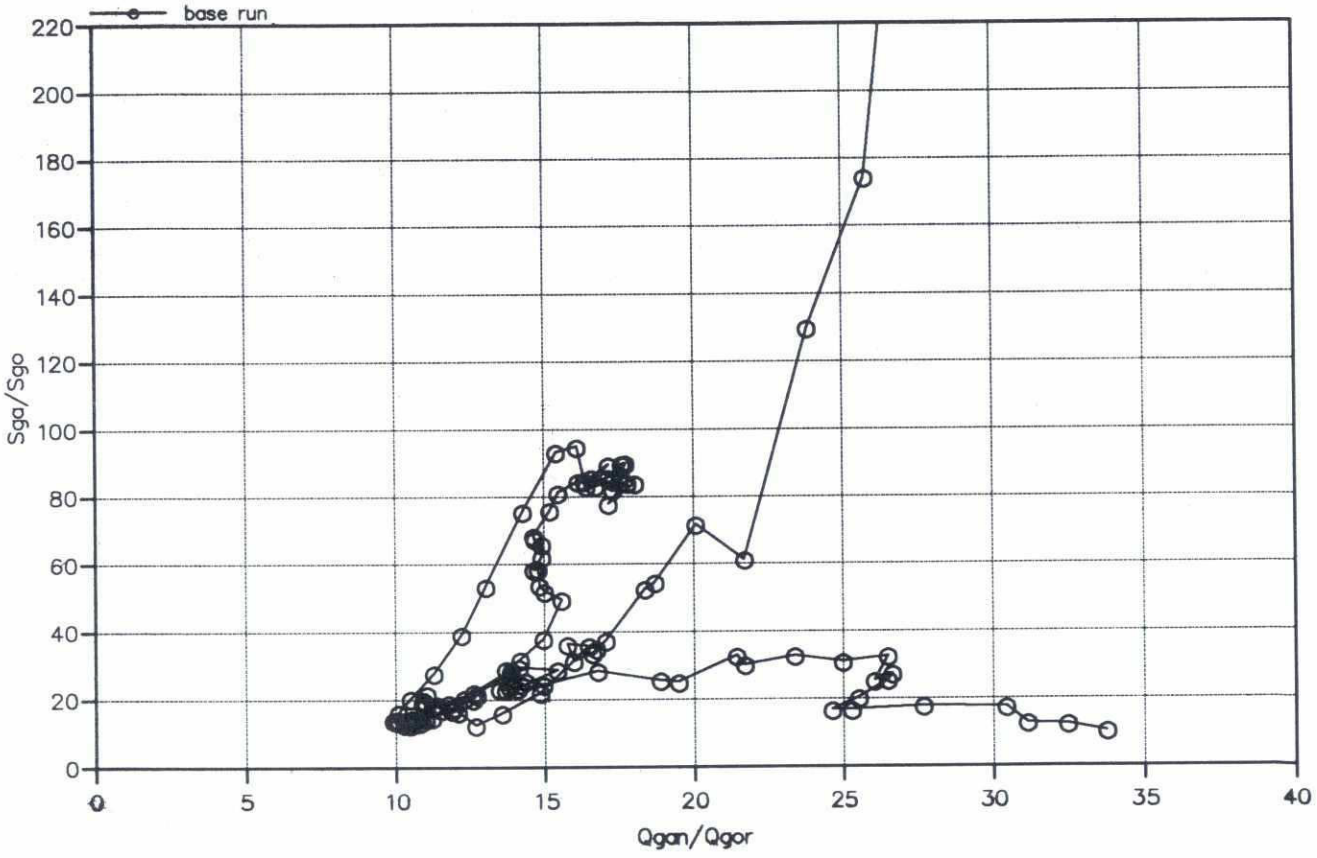


| SWMC | Client: River Survey Project FAP24 | MIKE 21 |
|---|---|---|
| | Project: Gorai Offtake Mathematical Modelling | |
| File: | Date: Fri Jul 5 1996 | Sediment transport ratio (Ganges/Gorai) against Discharge ratio (Ganges/Gorai) | Drawing no. **Figure 7.10.18** |
| Scale: 1:300000 | Init: hge | |

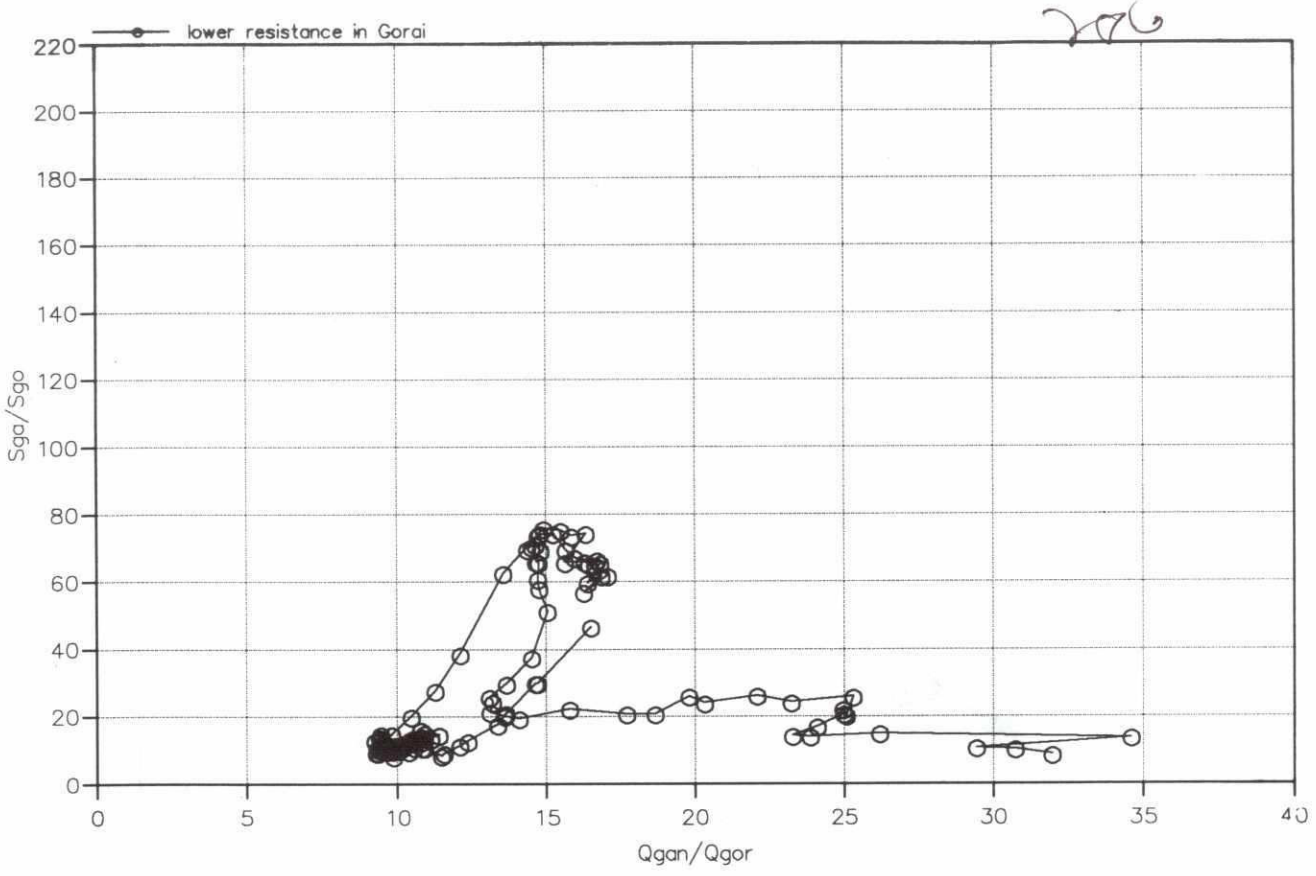


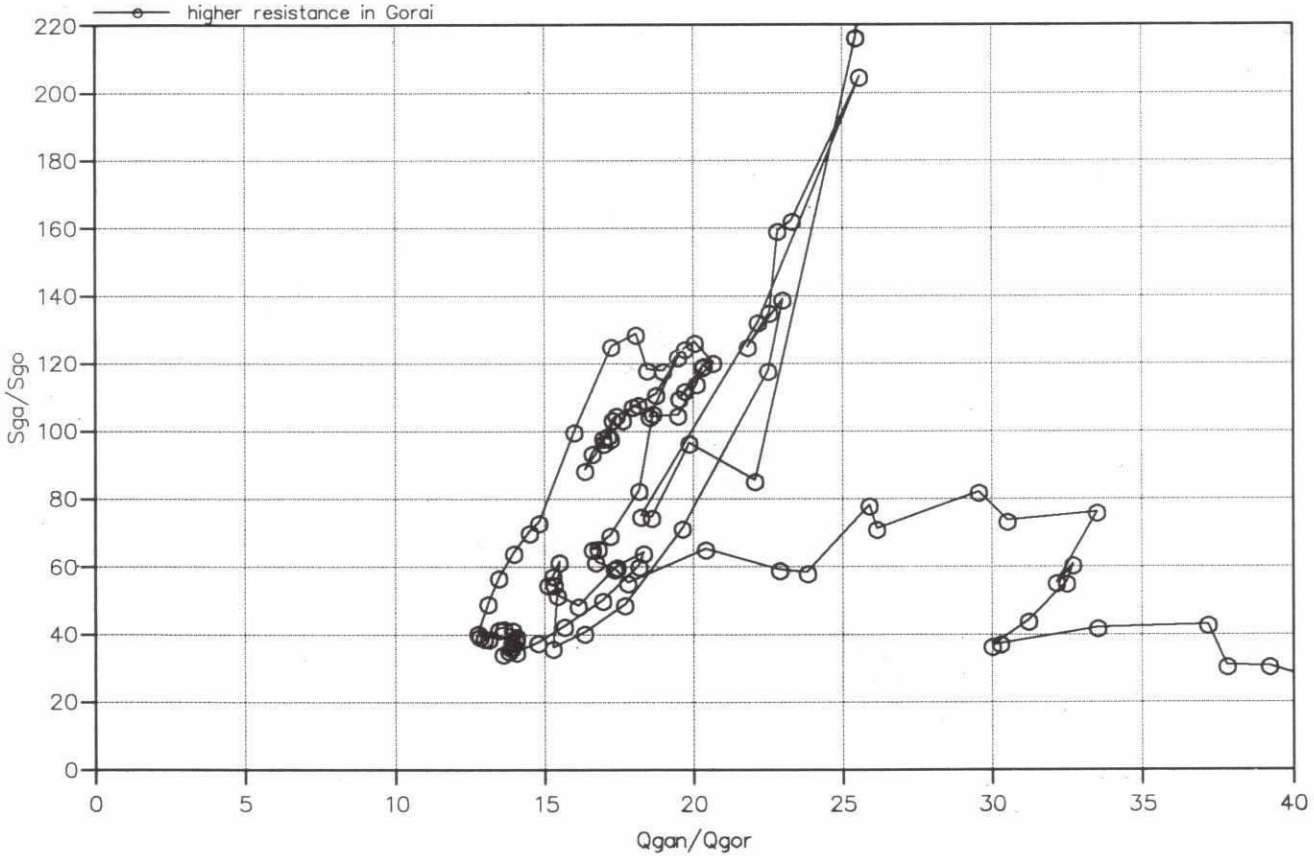


| SWMC | Client: River Survey Project FAP24 | MIKE 21 |
|---|---|---|
| | Project: Gorai Offtake Mathematical Modelling | |
| File: | Date: Fri Jul 5 1996 | Sediment transport ratio (Ganges/Gorai) against Discharge ratio (Ganges/Gorai) |
| Scale: 1:300000 | Init: hge | Drawing no. **Figure 7.10.19** |

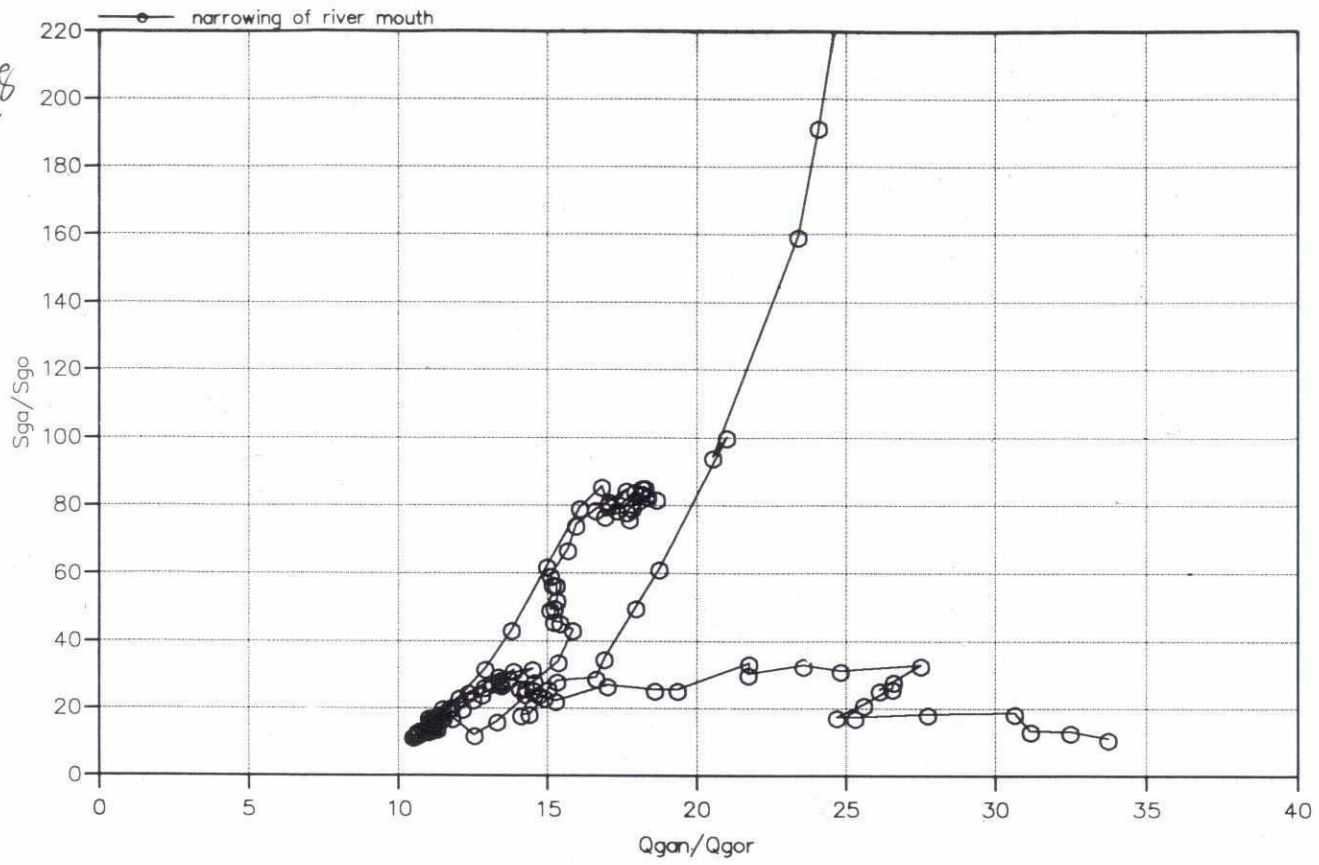


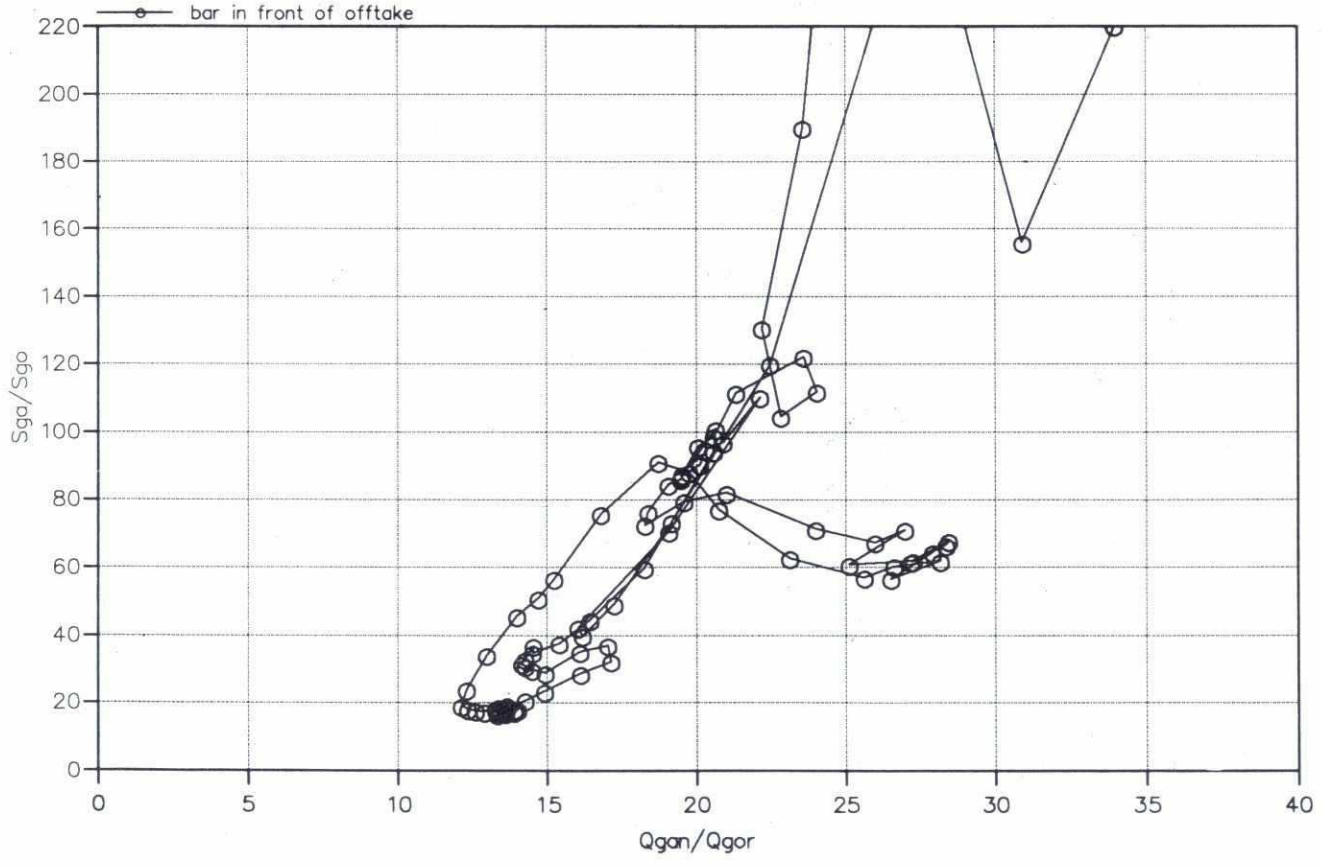


| | | | |
|---|---|---|---|
| SWMC | Client: River Survey Project FAP24 | | MIKE 21 |
| | Project: Gorai Offtake Mathematical Modelling | | |
| File: | Date: Fri Jul 5 1996 | Sediment transport ratio (Ganges/Gorai) against Discharge ratio (Ganges/Gorai) | Drawing no. **Figure 7.10.20** |
| Scale: 1:300000 | Init: hge | | |

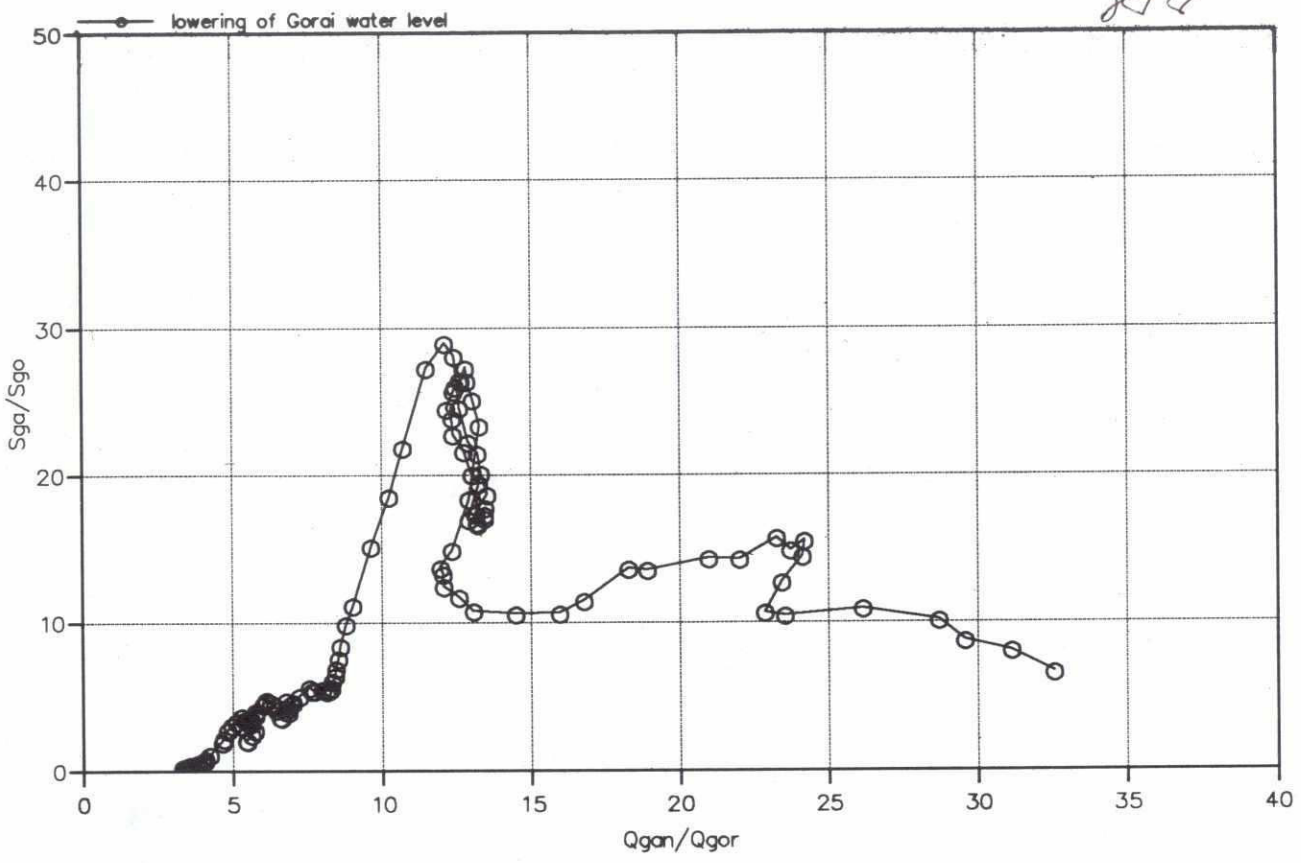


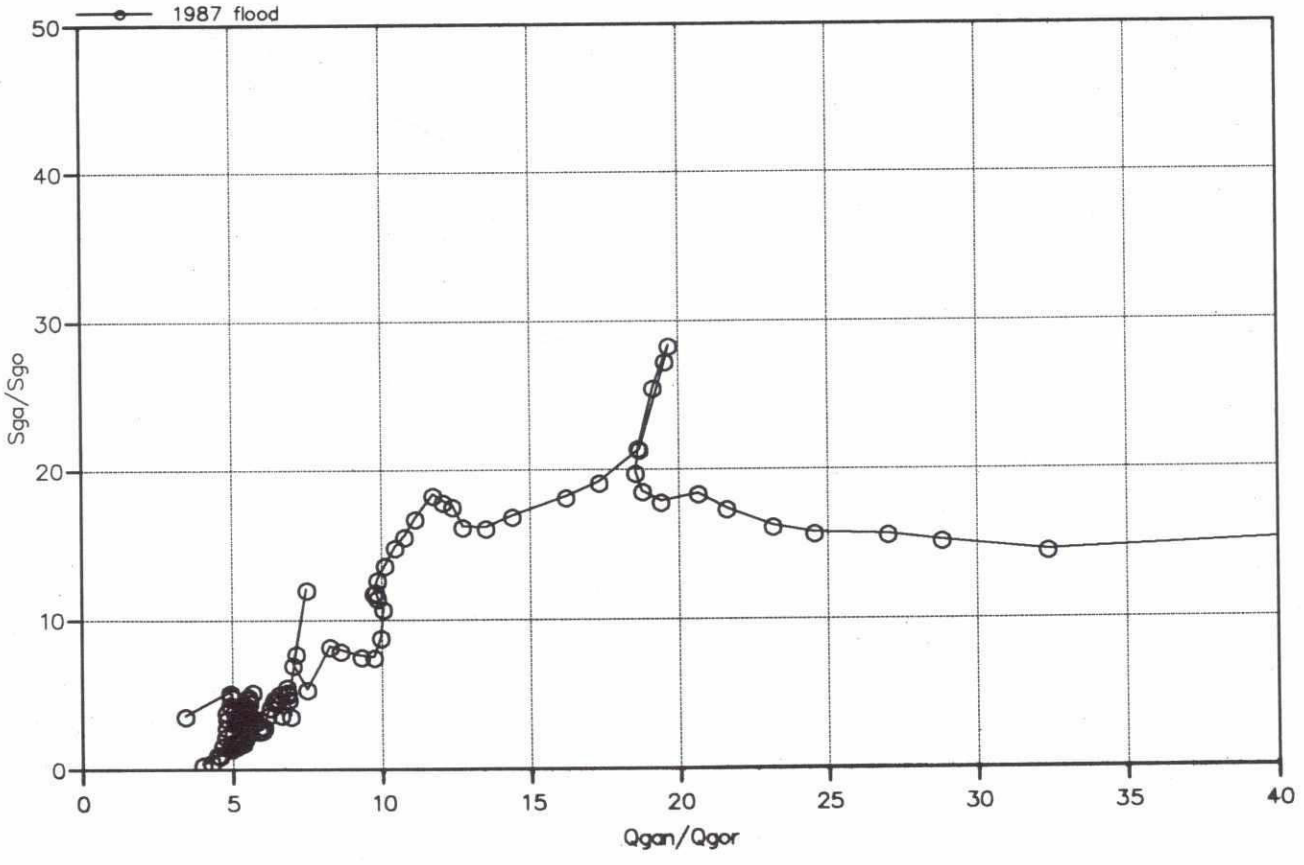


| | | | |
|---|---|---|---|
| SWMC | Client: River Survey Project FAP24 | | MIKE 21 |
| | Project: Gorai Offtake Mathematical Modelling | | |
| File: | Date: Fri Jul 5 1996 | Sediment transport ratio (Ganges/Gorai) against Discharge ratio (Ganges/Gorai) | Drawing no. Figure 7.10.21 |
| Scale: 1:300000 | Init: hge | | |

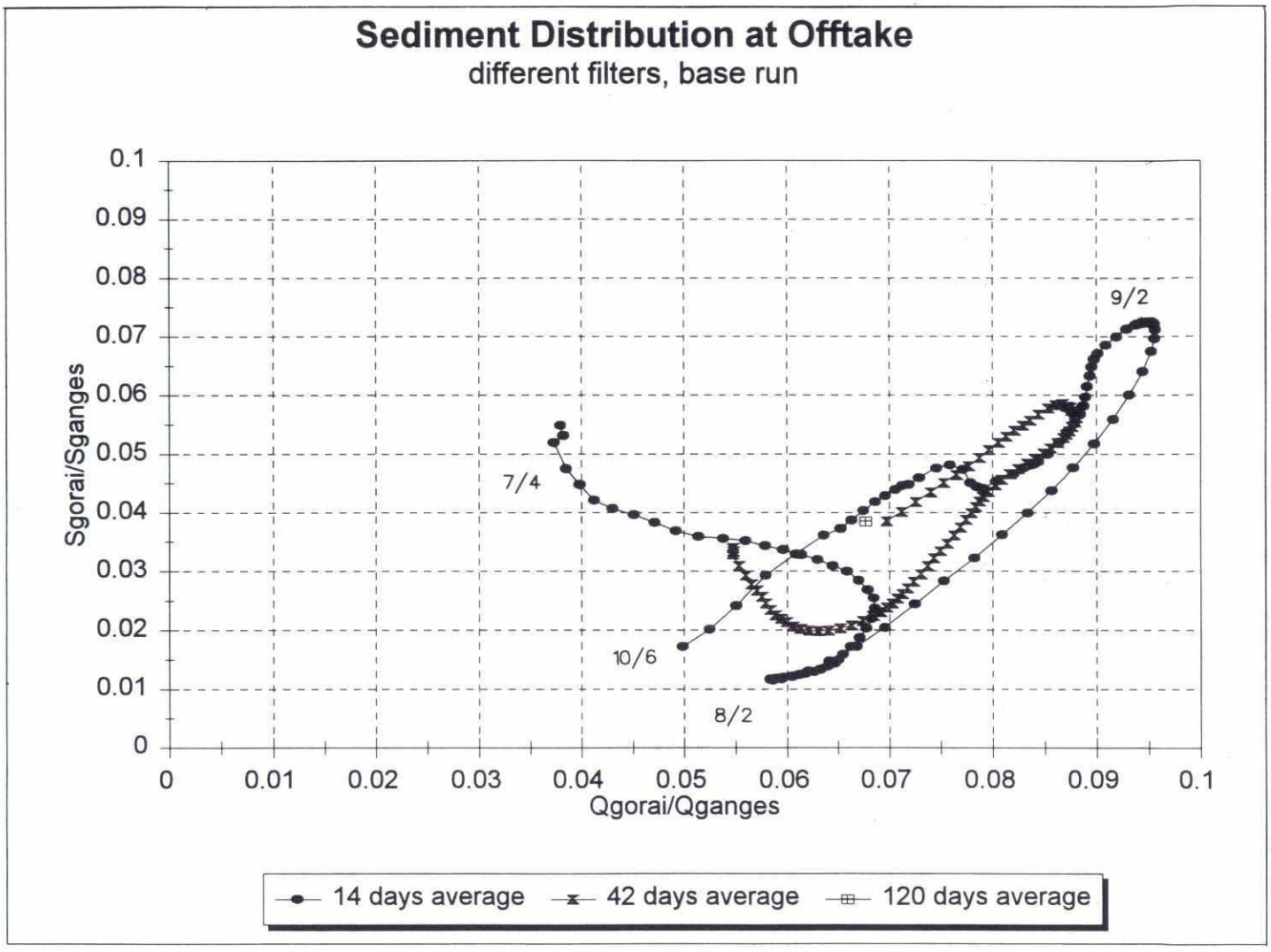


| | | | |
|---|---|---|---|
| SWMC | Client: River Survey Project FAP24 | | MIKE 21 |
| | Project: Gorai Offtake Mathematical Modelling | | |
| File: | Date: Thu Jul 11 1996 | Simulated sediment transport ratio against discharge ratio at offtake. Effect of using running average. | Drawing no. **Figure 7.10.22** |
| Scale: 1:80000 | Init: hge | | |

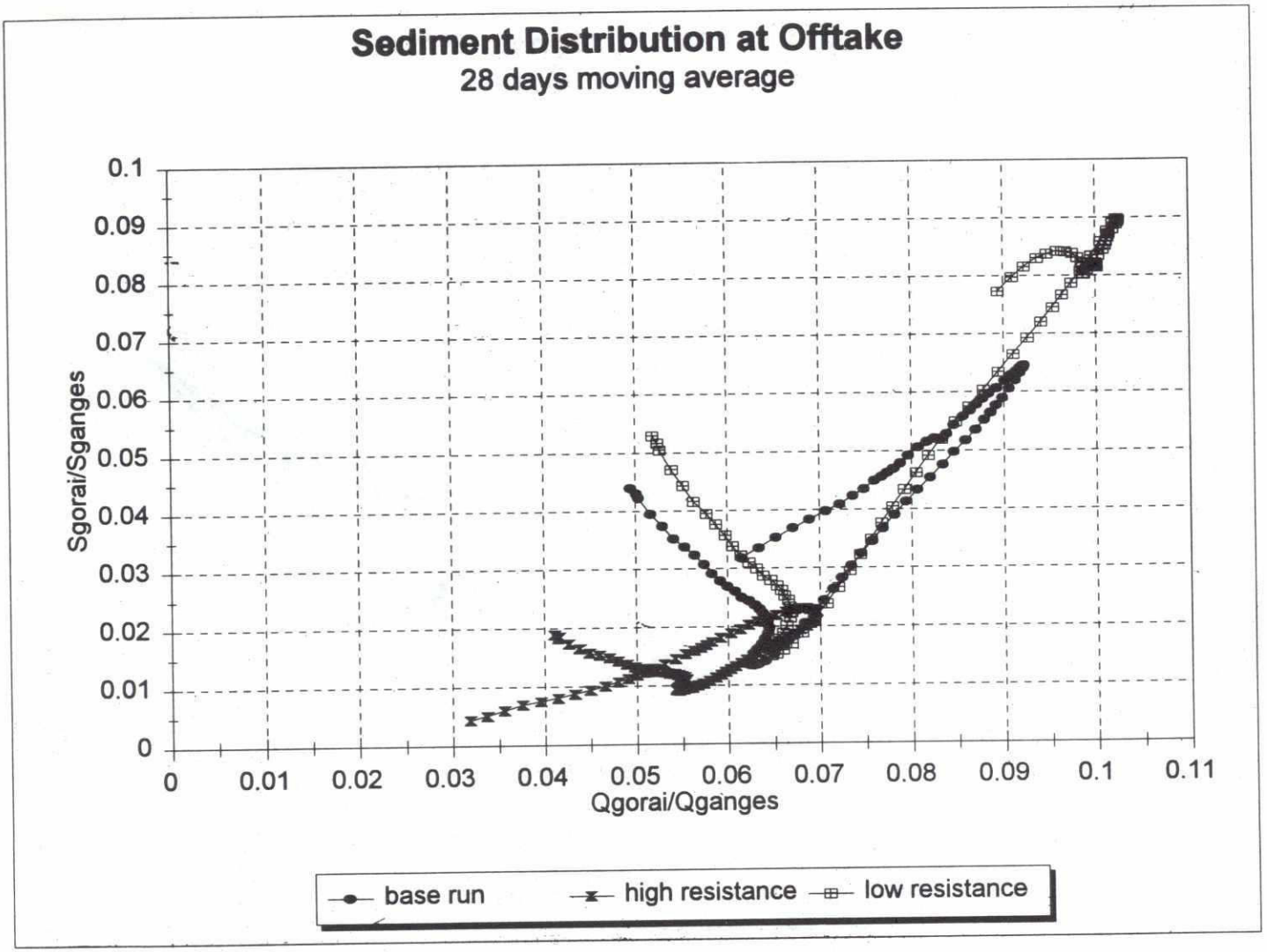


| | | | |
|---|---|---|---|
| SWMC | | Client: River Survey Project FAP24 | MIKE 21 |
| | | Project: Gorai Offtake Mathematical Modelling | |
| File: | Date: Thu Jul 11 1996 | Simulated sediment transport ratio against discharge ratio at offtake. Running average for calibration runs | Drawing no. Figure 7.10.23 |
| Scale: 1:80000 | Init: hge | | |

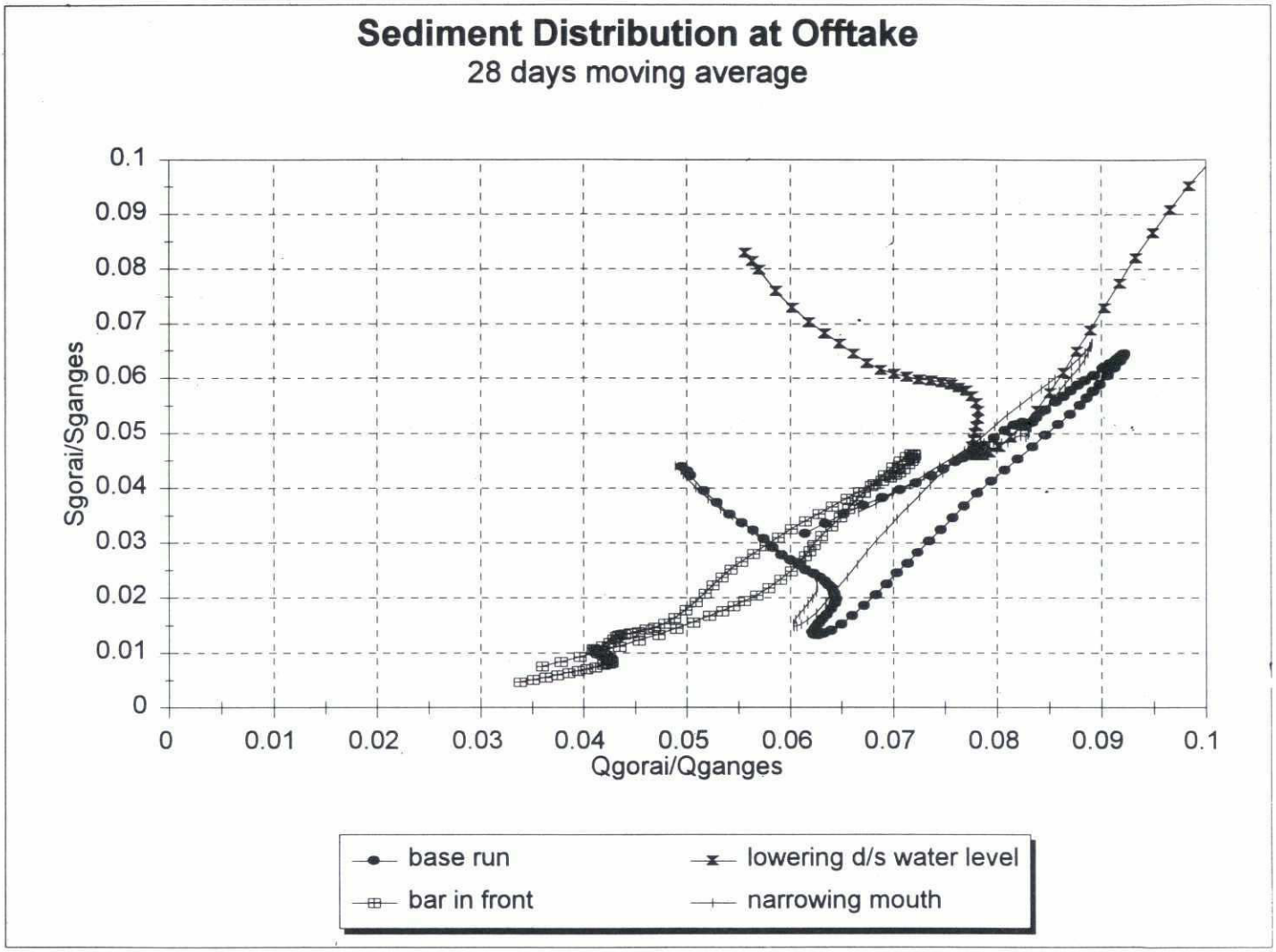


| | | | |
|---|---|---|---|
| SWMC | | Client: River Survey Project FAP24 | MIKE 21 |
| | | Project: Gorai Offtake Mathematical Modelling | |
| File: | Date: Thu Jul 11 1996 | Simulated sediment transport ratio against discharge ratio at offtake. Running average for different scenarios | Drawing no. Figure 7.10.24 |
| Scale: 1:80000 | Init: hge | | |

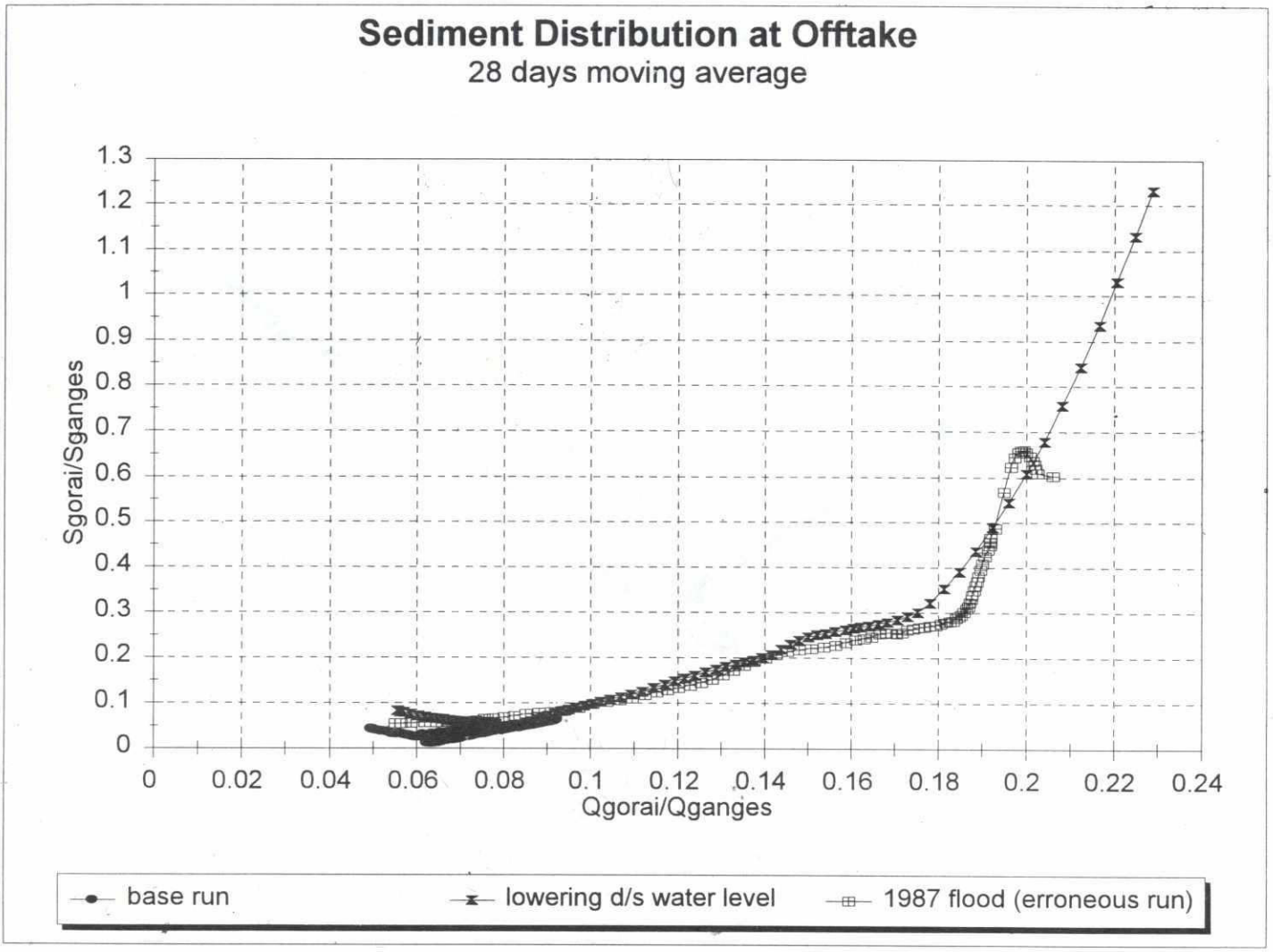


| | | | |
|---|---|---|---|
| SWMC | | Client: River Survey Project FAP24 | MIKE 21 |
| | | Project: Gorai Offtake Mathematical Modelling | |
| File: | Date: Thu Jul 11 1996 | Simulated sediment transport ratio against discharge ratio at offtake. Running average for non-equilib. runs | Drawing no **Figure 7.10.25** |
| Scale: 1:80000 | Init: hge | | |

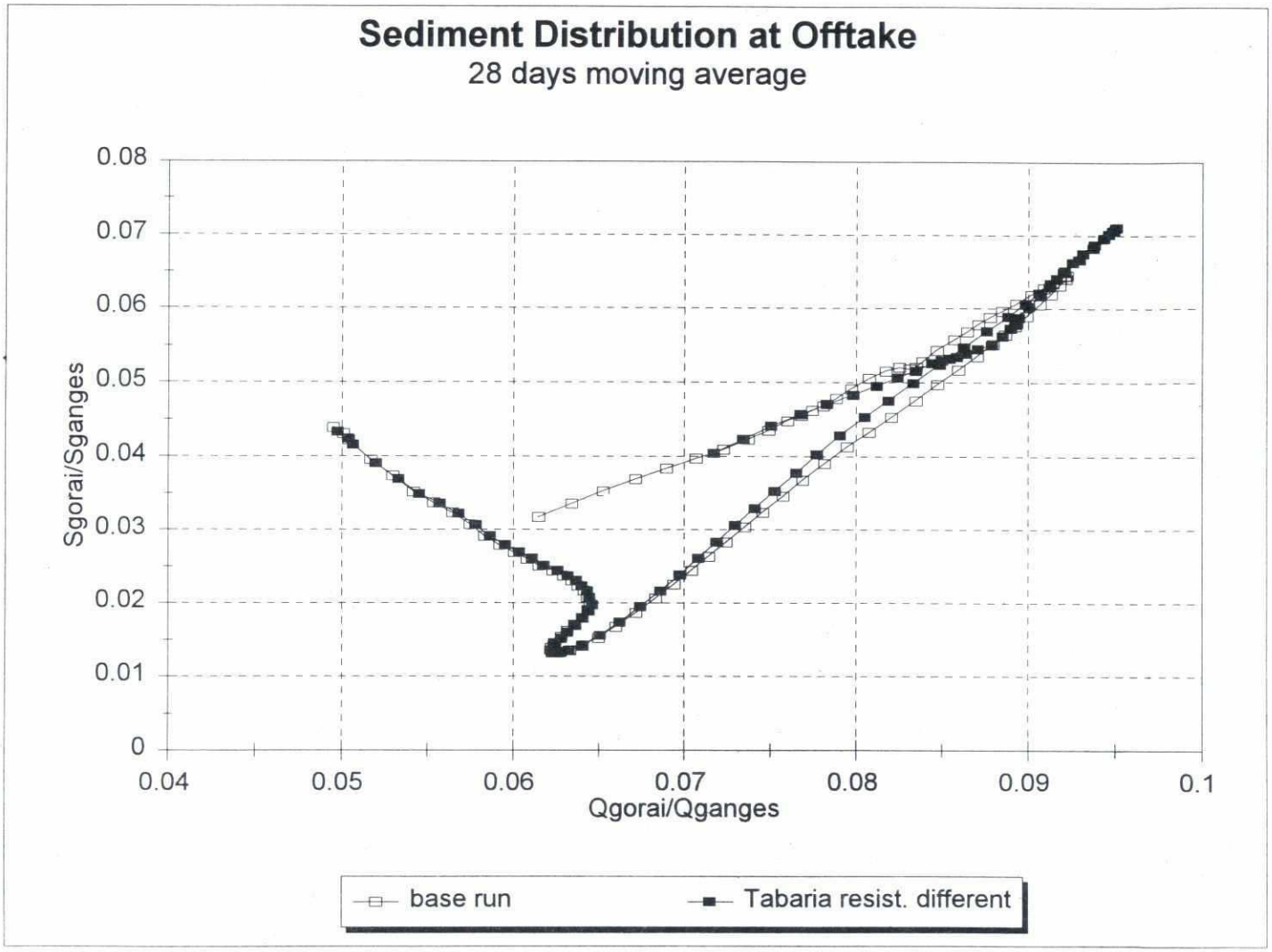


| | | | |
|---|---|---|---|
| SWMC | | Client: River Survey Project FAP24 | MIKE 21 |
| | | Project: Gorai Offtake Mathematical Modelling | |
| File: | Date: Thu Jul 11 1996 | Simulated sediment transport ratio against discharge ratio at offtake. Effect of changing resist. at Talbaria | Drawing no. Figure 7.10.26 |
| Scale: 1:200000 | Init: hge | | |

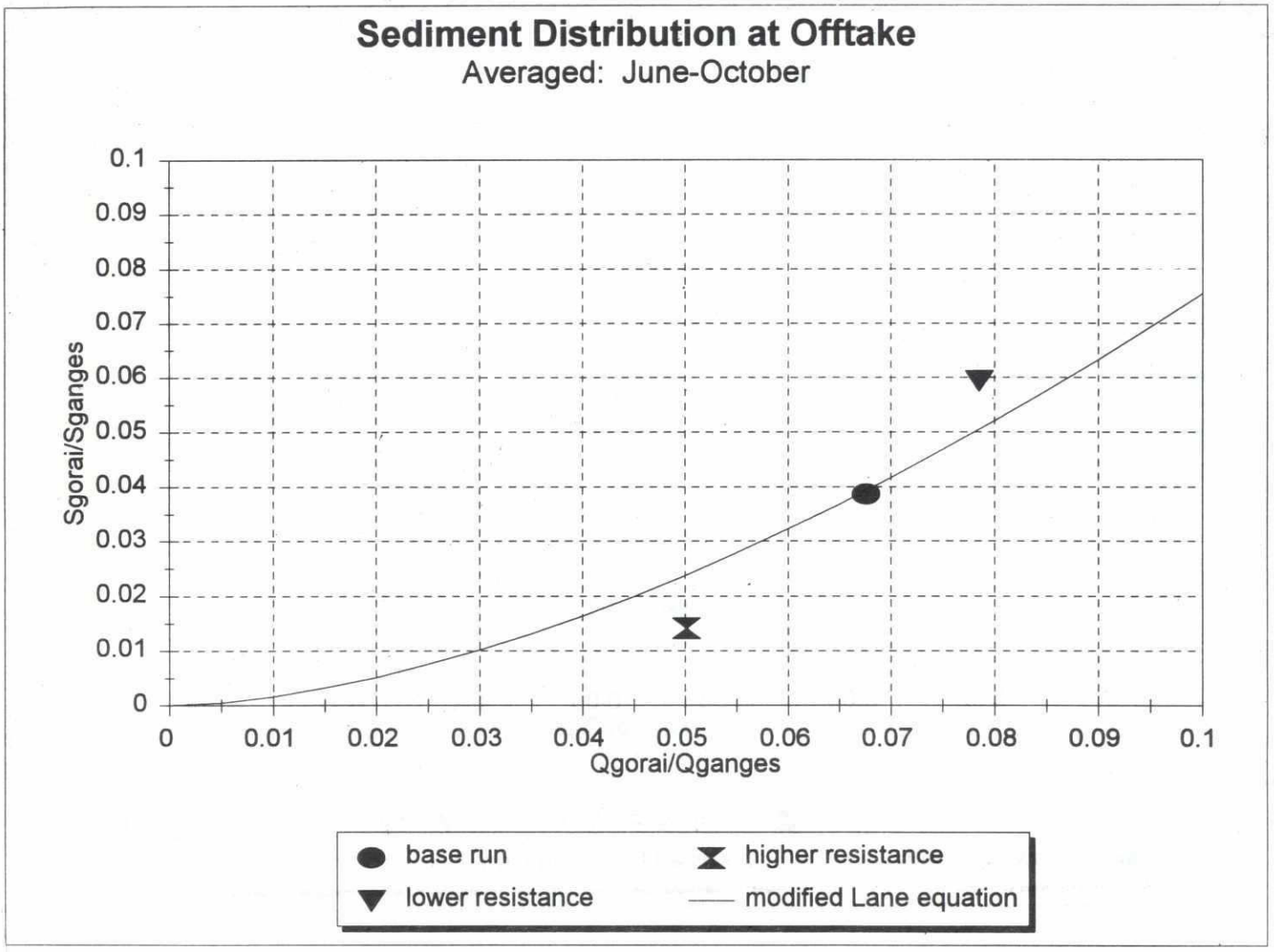


| SWMC | Client: River Survey Project FAP24 | MIKE 21 |
|---|---|---|
| | Project: Gorai Offtake Mathematical Modelling | |
| File: | Date: Thu Jul 11 1996 | Simulated sediment transport ratio against discharge ratio at offtake. Mean value for calibration runs |
| Scale: 1:80000 | Init: hge | Drawing no. **Figure 7.10.27** |

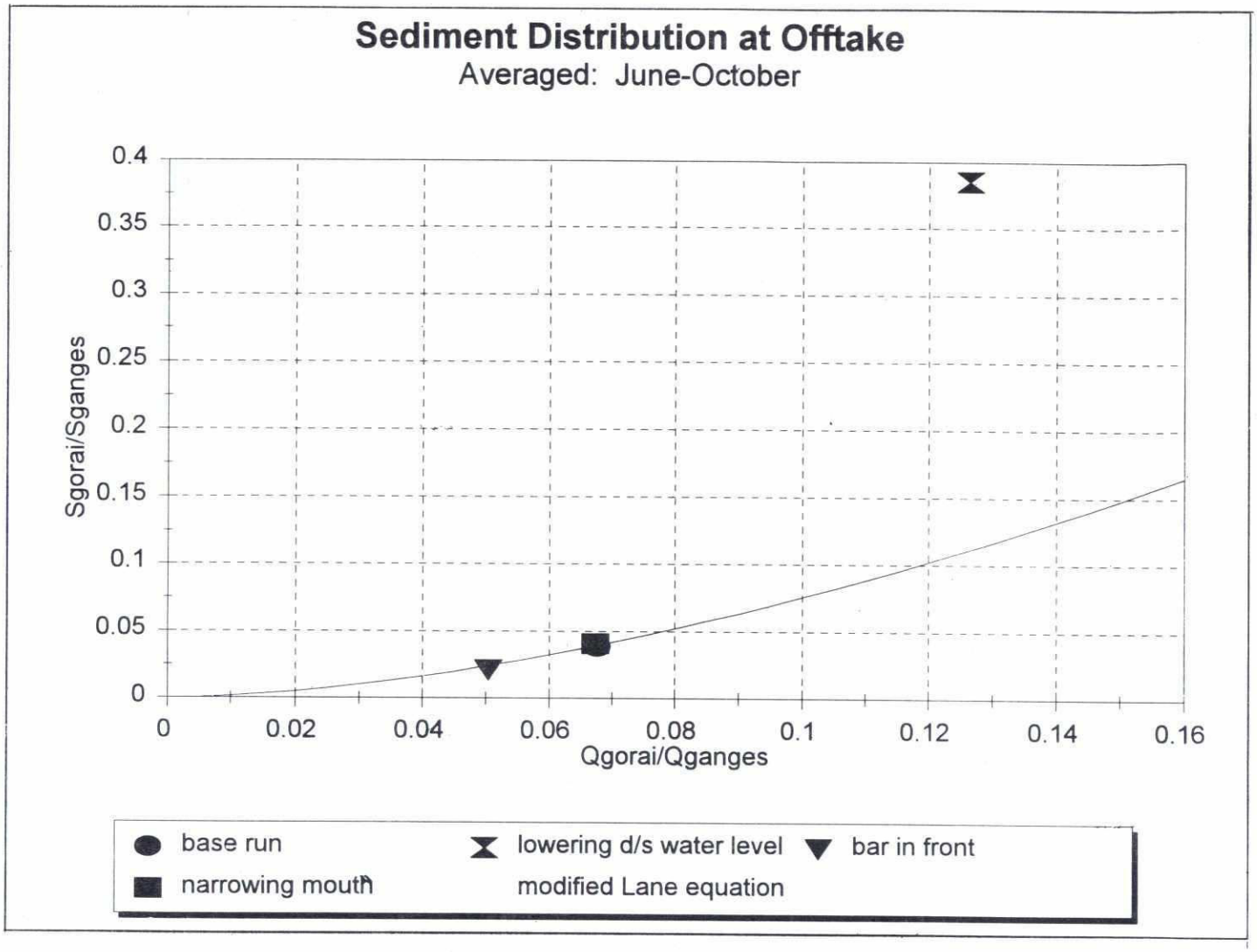


| | | | |
|---|---|---|---|
| SWMC | | Client: River Survey Project FAP24 | MIKE 21 |
| | | Project: Gorai Offtake Mathematical Modelling | |
| File: | Date: Thu Jul 11 1996 | Simulated sediment transport ratio against discharge ratio at offtake. Mean value for different scenarios | Drawing no. Figure 7.10.28 |
| Scale: 1:80000 | Init: hge | | |

**Appendix 1: Water level and discharge data:**

| | | |
|---|---|---|
| - | Hardinge Bridge | 1964-95 |
| - | Talbaria | 1986-95 |
| - | Gorai Railway Bridge | 1964-95 |

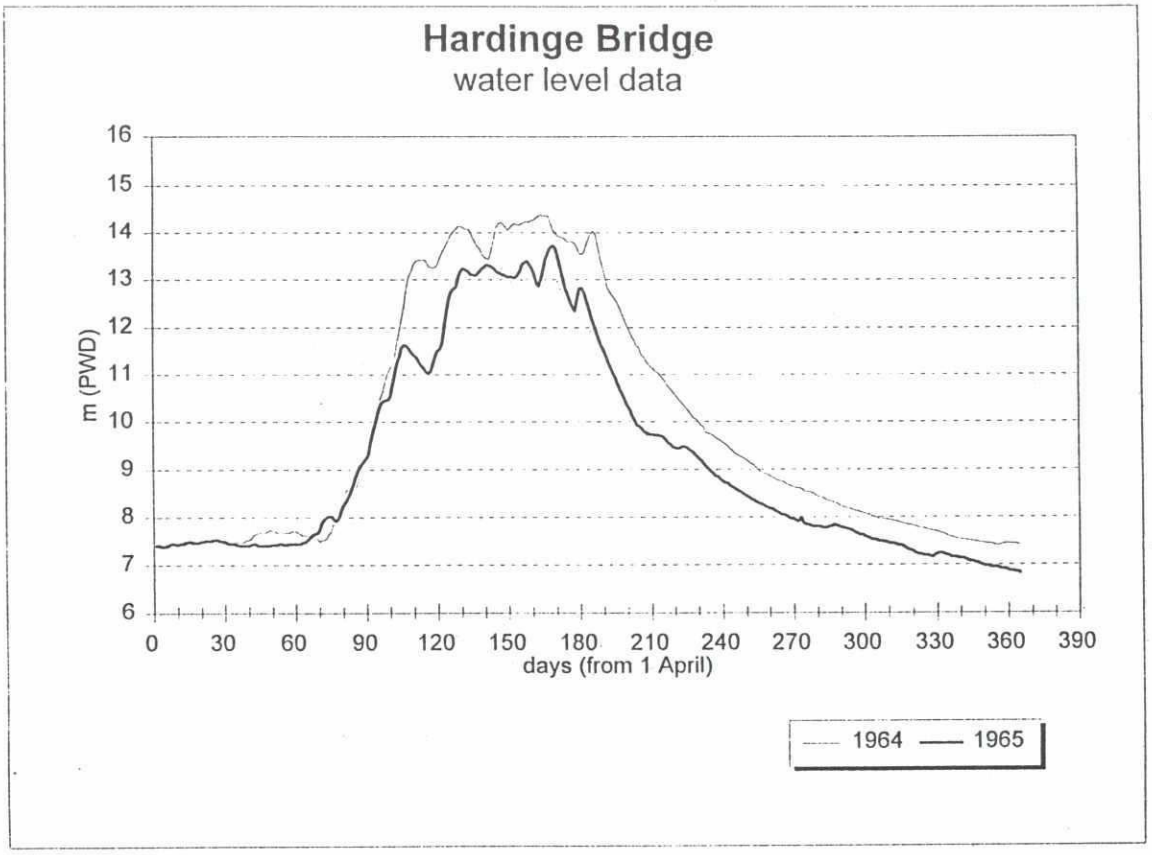
Hardinge Bridge
water level data
m (PWD)
16
15
14
13
12
11
10
9
8
7
6
0 30 60 90 120 150 180 210 240 270 300 330 360 390
days (from 1 April)
1964
1965

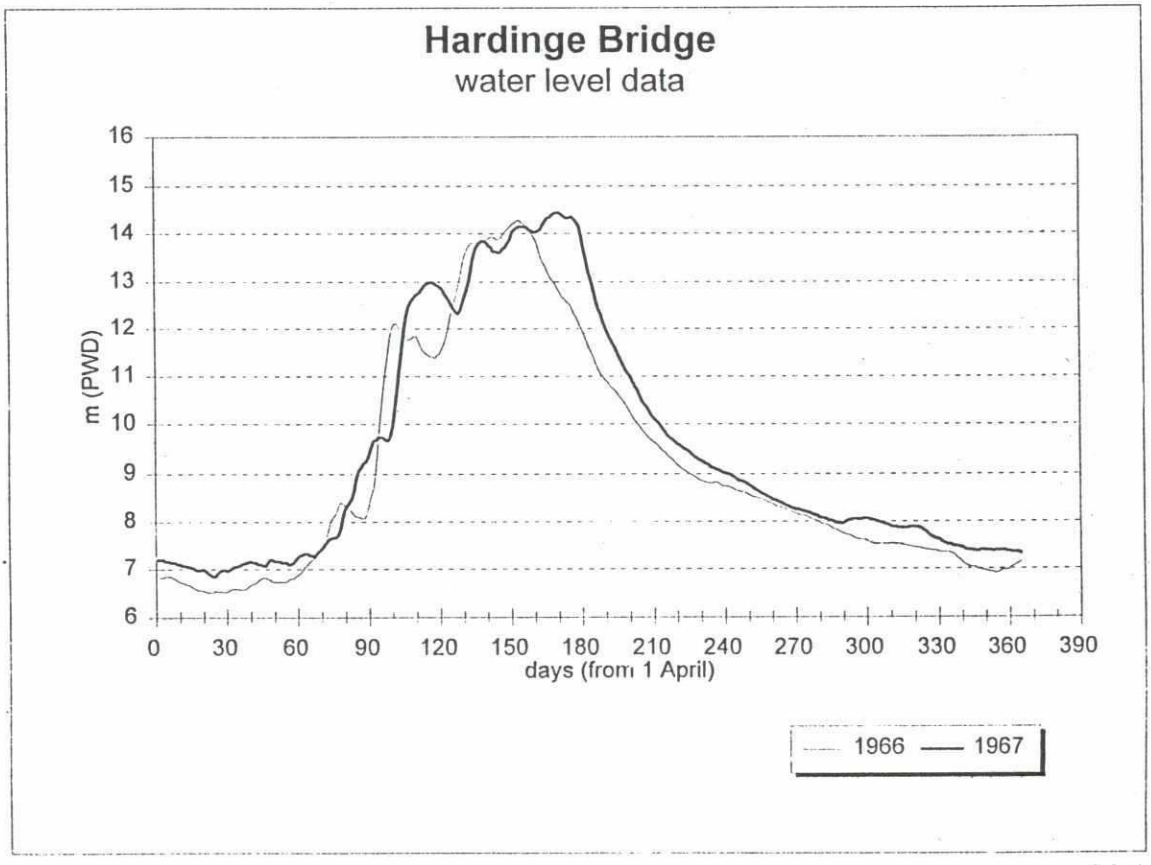
Hardinge Bridge
water level data
m (PWD)
16
15
14
13
12
11
10
9
8
7
6
0 30 60 90 120 150 180 210 240 270 300 330 360 390
days (from 1 April)
1966
1967

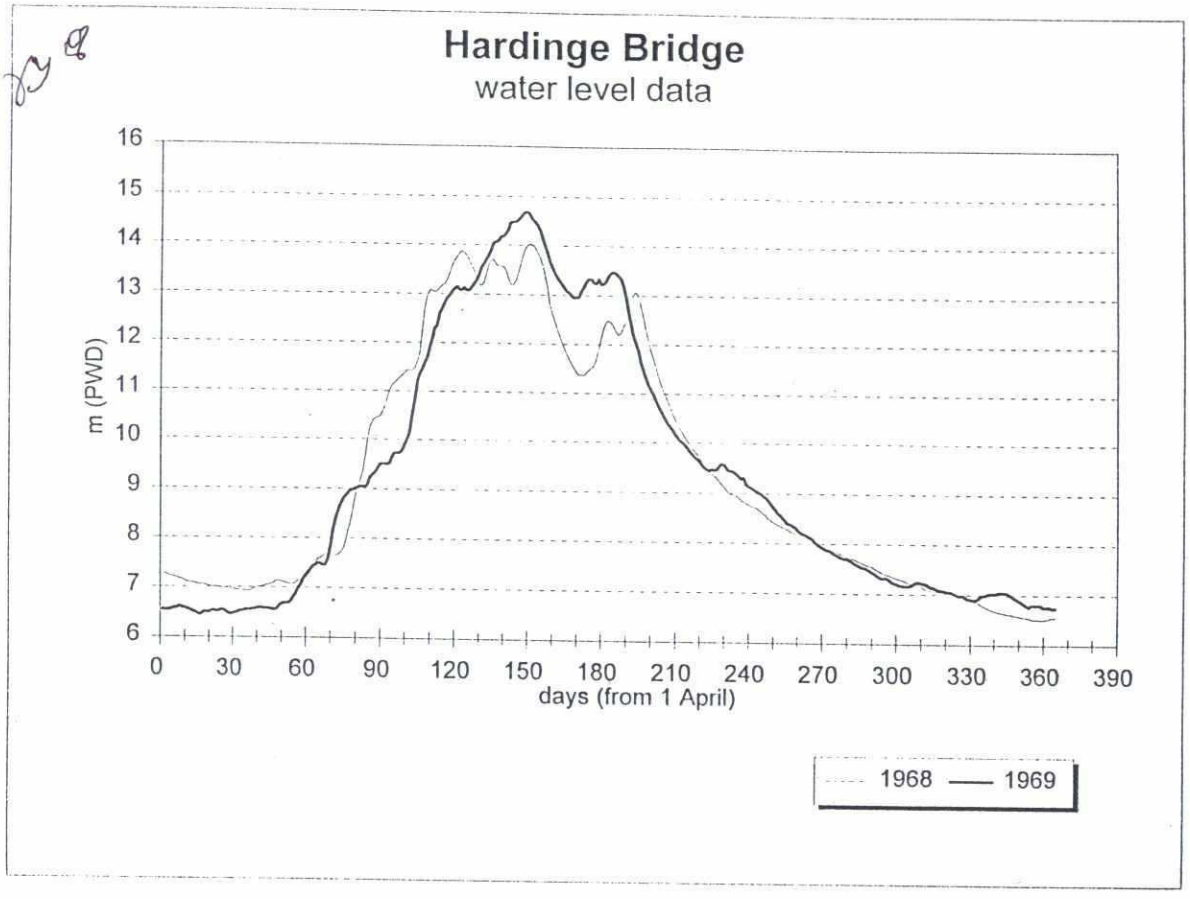
Hardinge Bridge
water level data
m (PWD)
16
15
14
13
12
11
10
9
8
7
6
0 30 60 90 120 150 180 210 240 270 300 330 360 390
days (from 1 April)
1968
1969

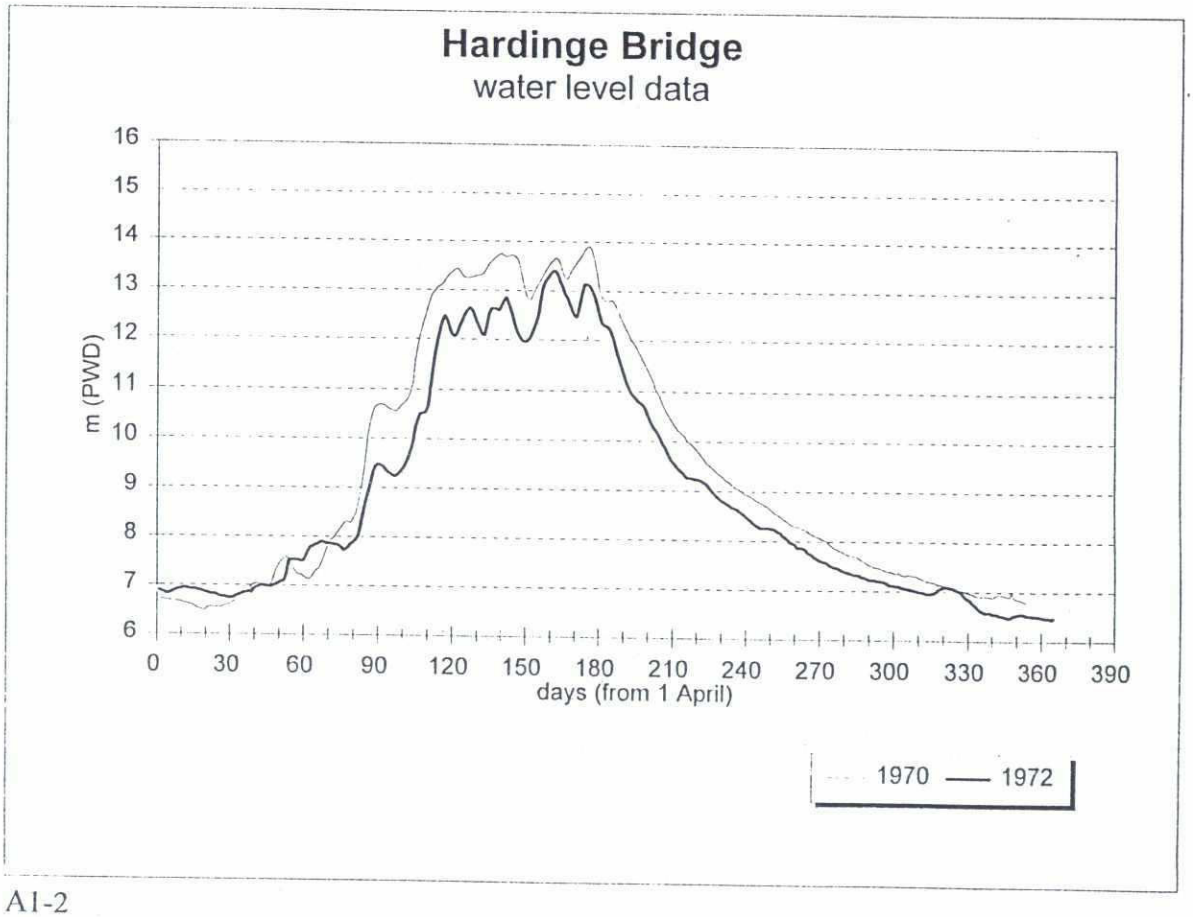
Hardinge Bridge
water level data
m (PWD)
16
15
14
13
12
11
10
9
8
7
6
0 30 60 90 120 150 180 210 240 270 300 330 360 390
days (from 1 April)
1970
1972

## Hardinge Bridge
water level data

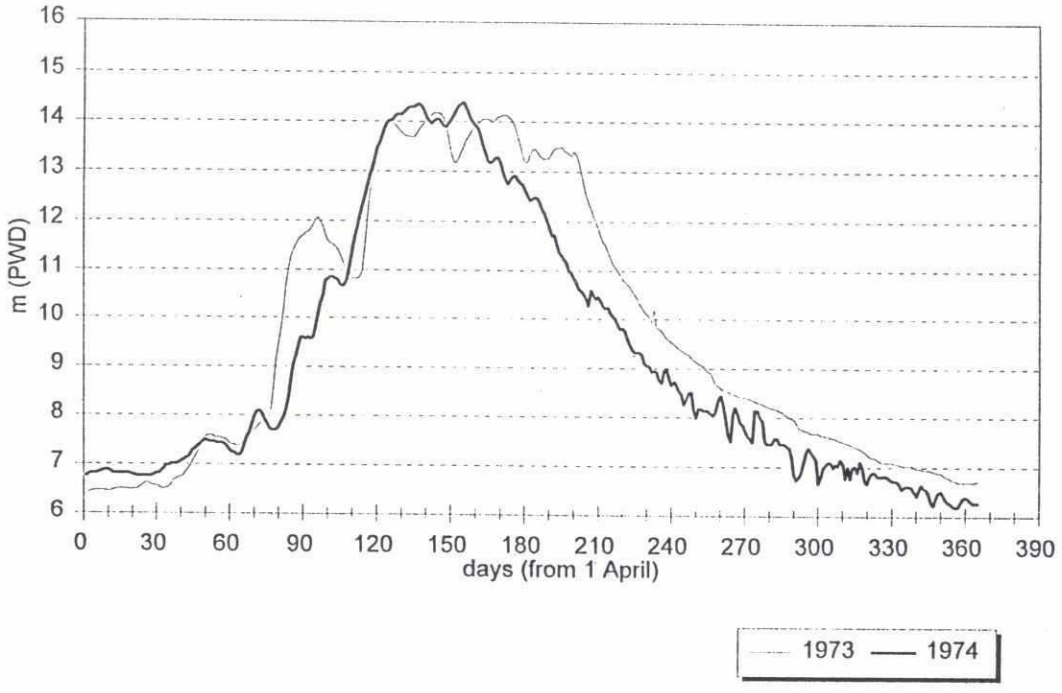


## Hardinge Bridge
water level data

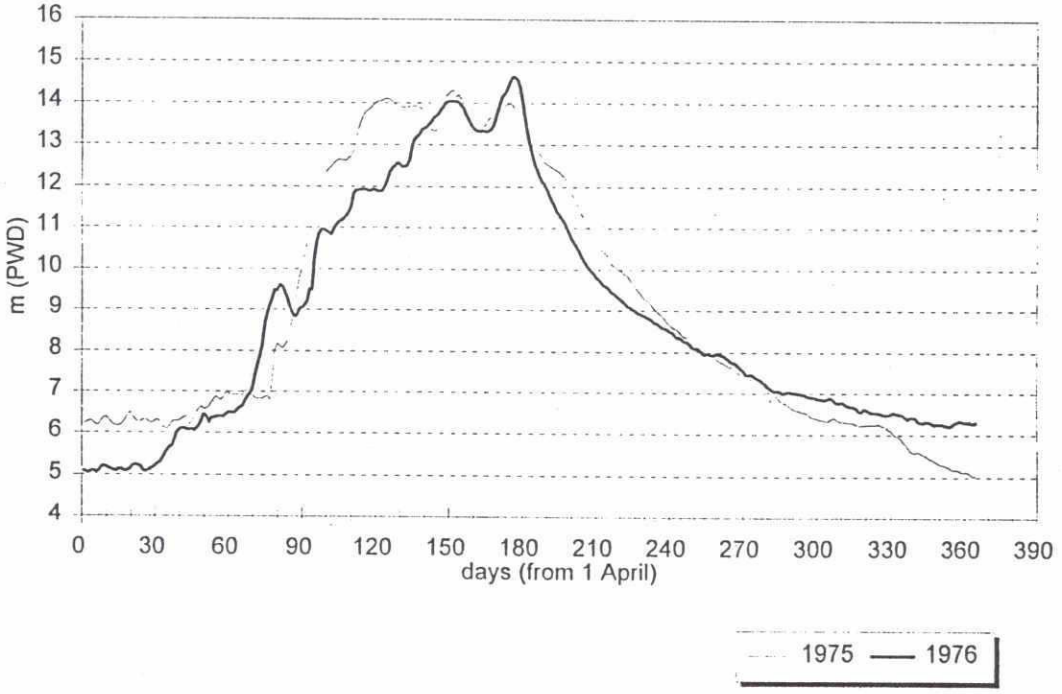

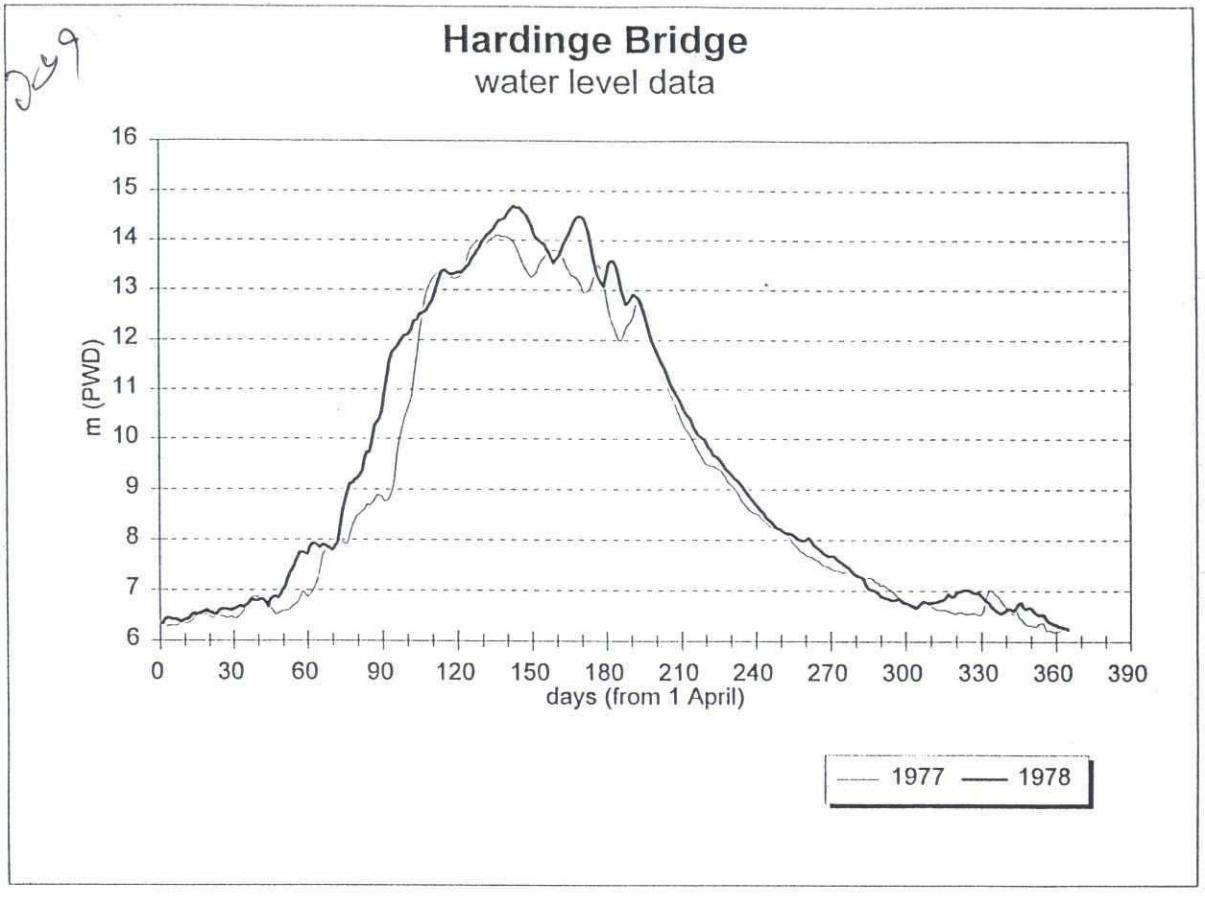
Hardinge Bridge
water level data
m (PWD)
16
15
14
13
12
11
10
9
8
7
6
0 30 60 90 120 150 180 210 240 270 300 330 360 390
days (from 1 April)
1977
1978

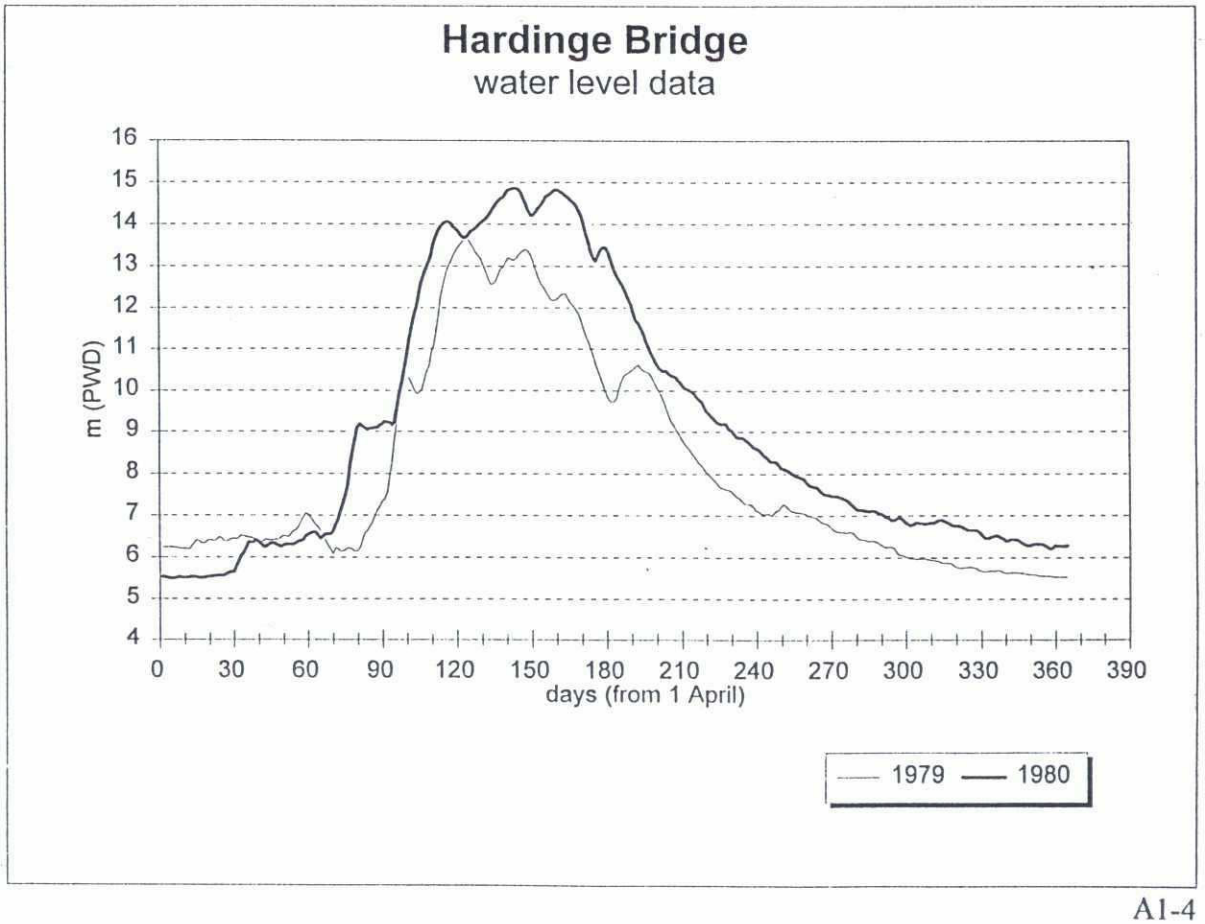
Hardinge Bridge
water level data
m (PWD)
16
15
14
13
12
11
10
9
8
7
6
5
4
0 30 60 90 120 150 180 210 240 270 300 330 360 390
days (from 1 April)
1979
1980

## Hardinge Bridge
water level data

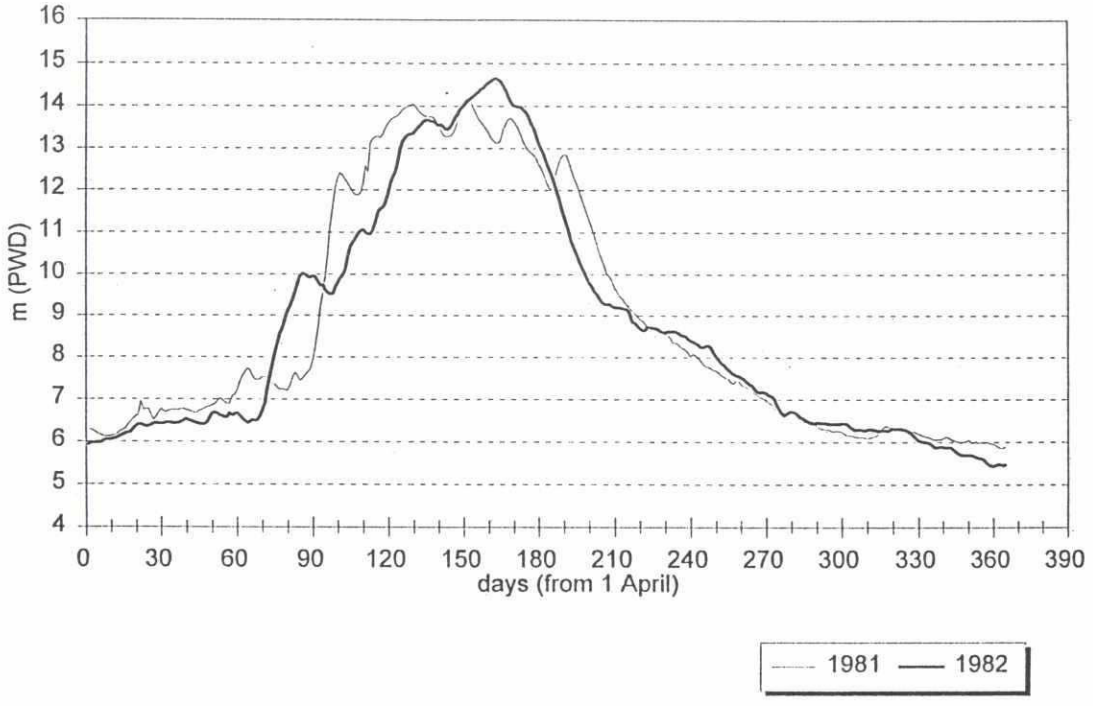


## Hardinge Bridge
water level data

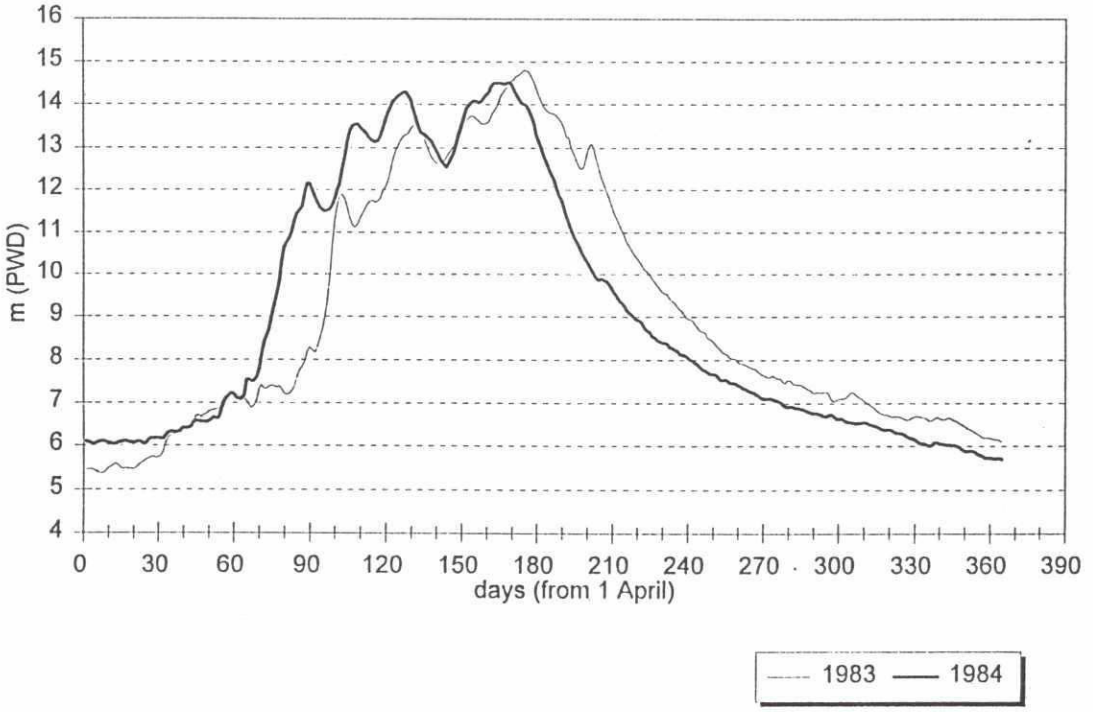

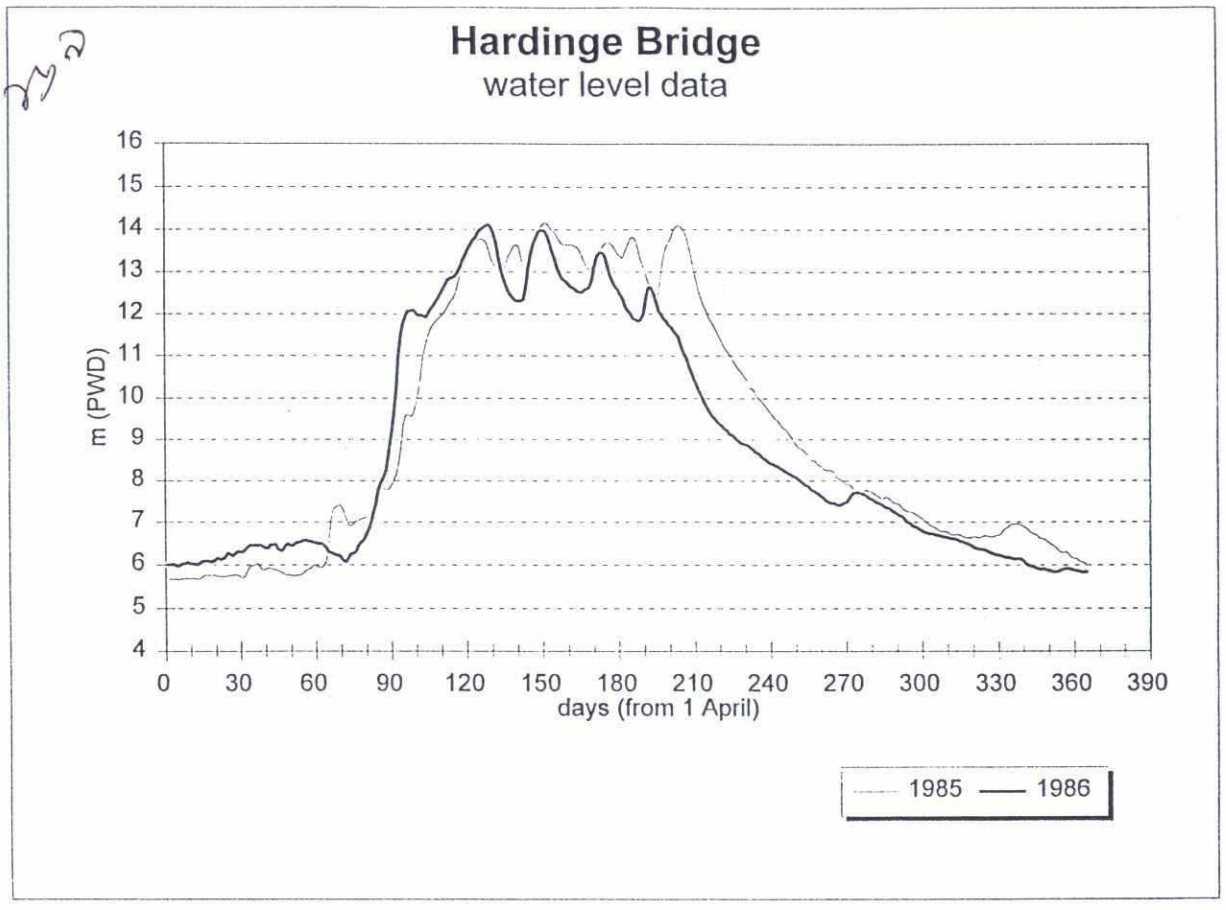
Hardinge Bridge
water level data
m (PWD)
16
15
14
13
12
11
10
9
8
7
6
5
4
0 30 60 90 120 150 180 210 240 270 300 330 360 390
days (from 1 April)
1985
1986

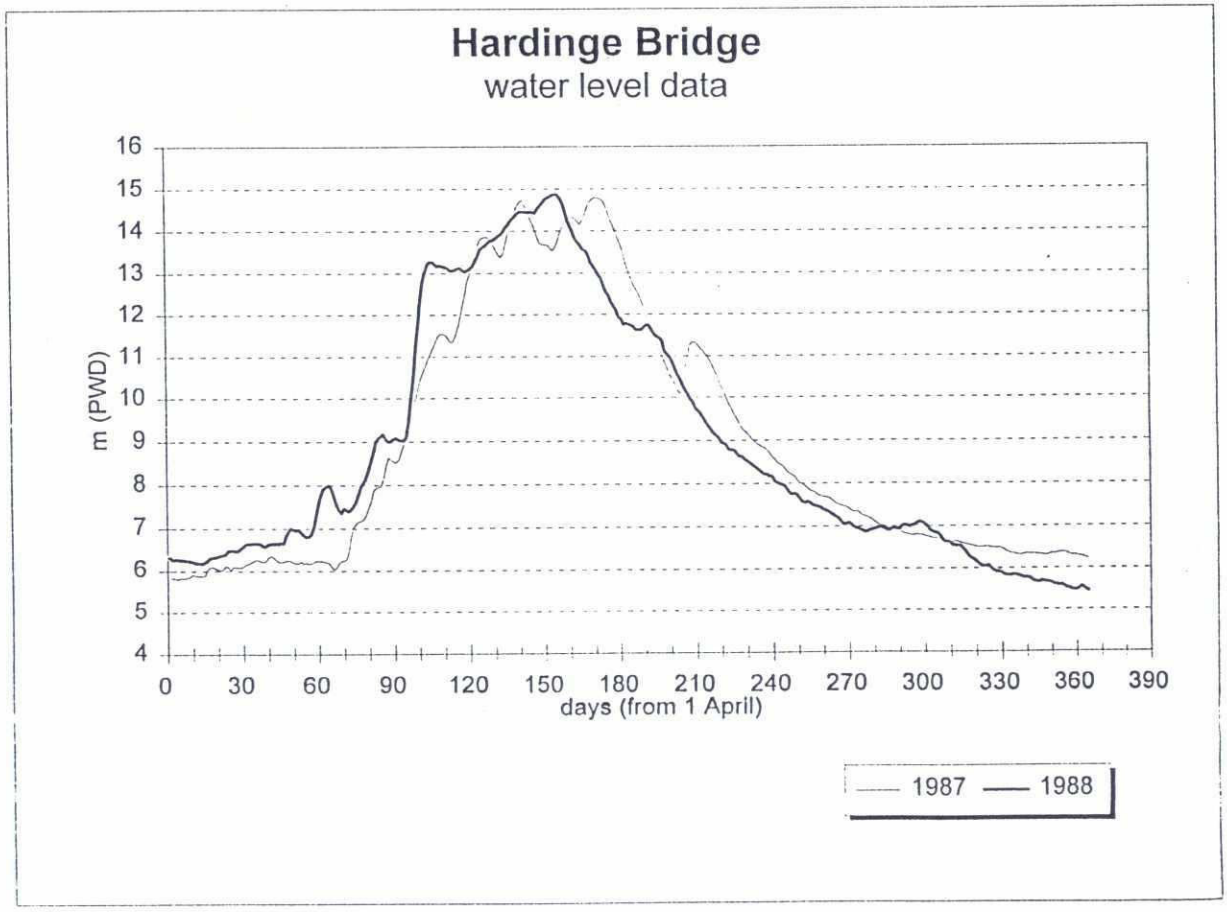
Hardinge Bridge
water level data
m (PWD)
16
15
14
13
12
11
10
9
8
7
6
5
4
0 30 60 90 120 150 180 210 240 270 300 330 360 390
days (from 1 April)
1987
1988

## Hardinge Bridge
water level data

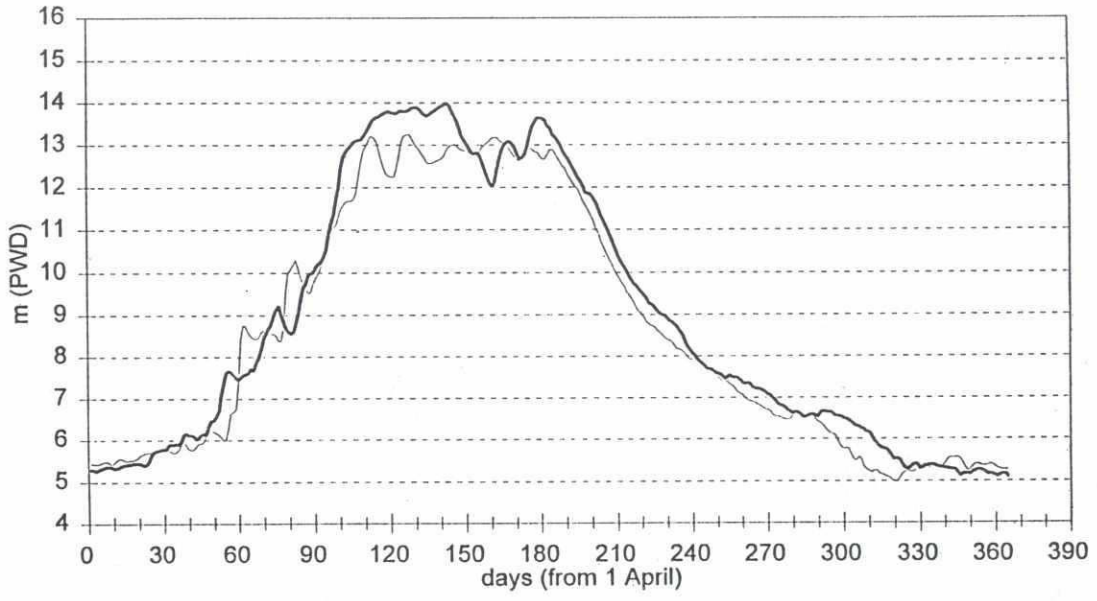


## Hardinge Bridge
water level data

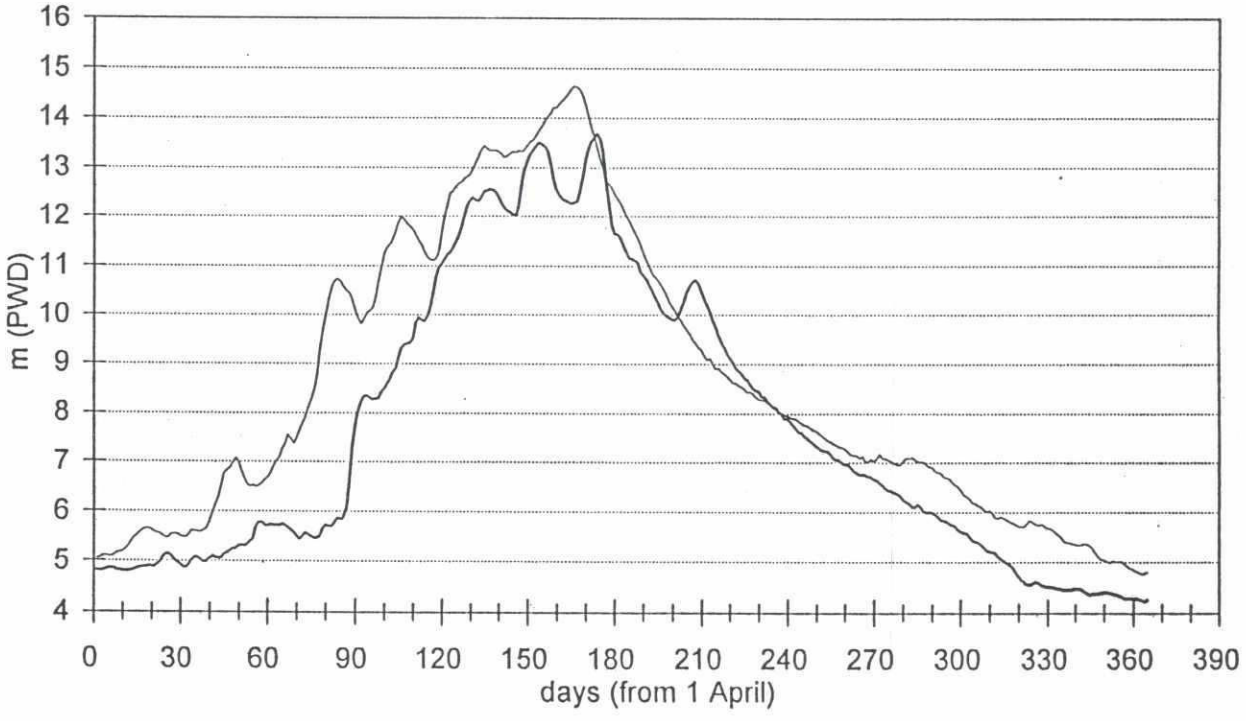

# Hardinge Bridge
water level data

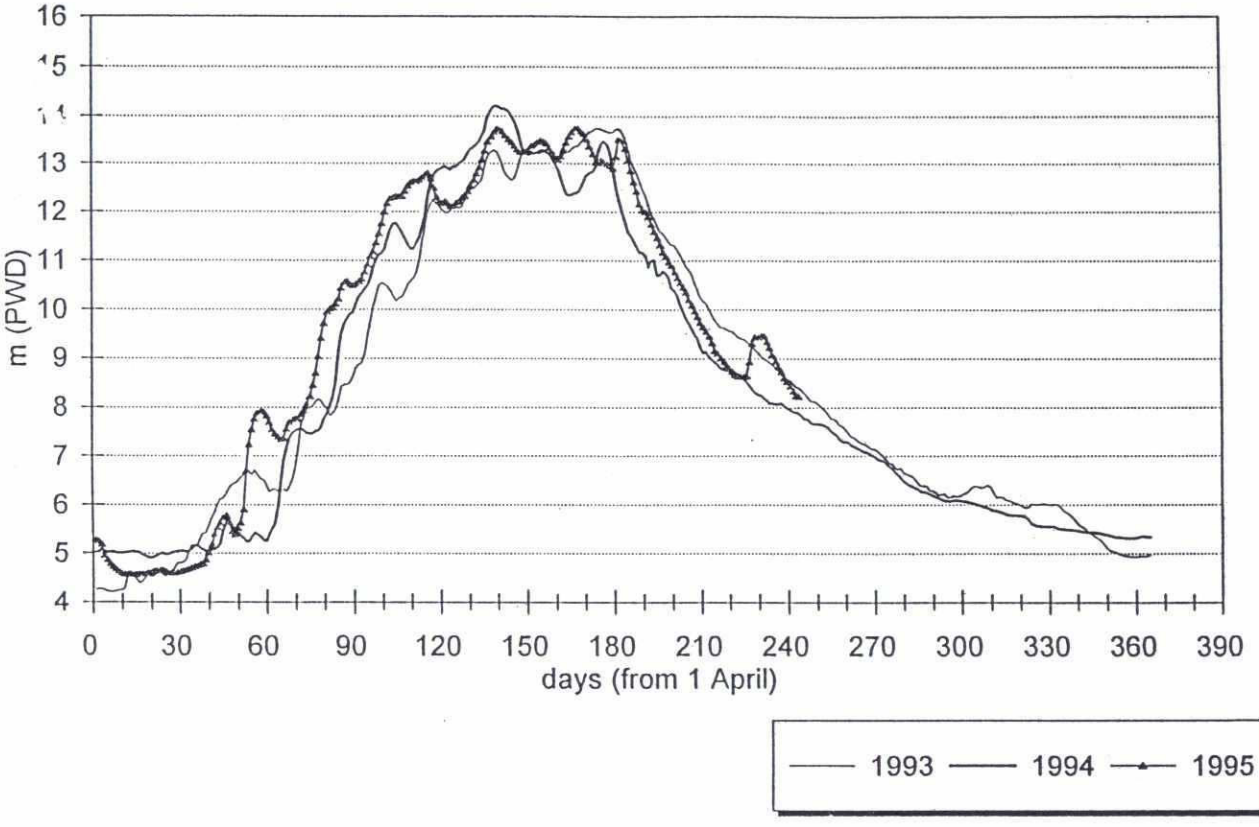

## Talbaria

water level data

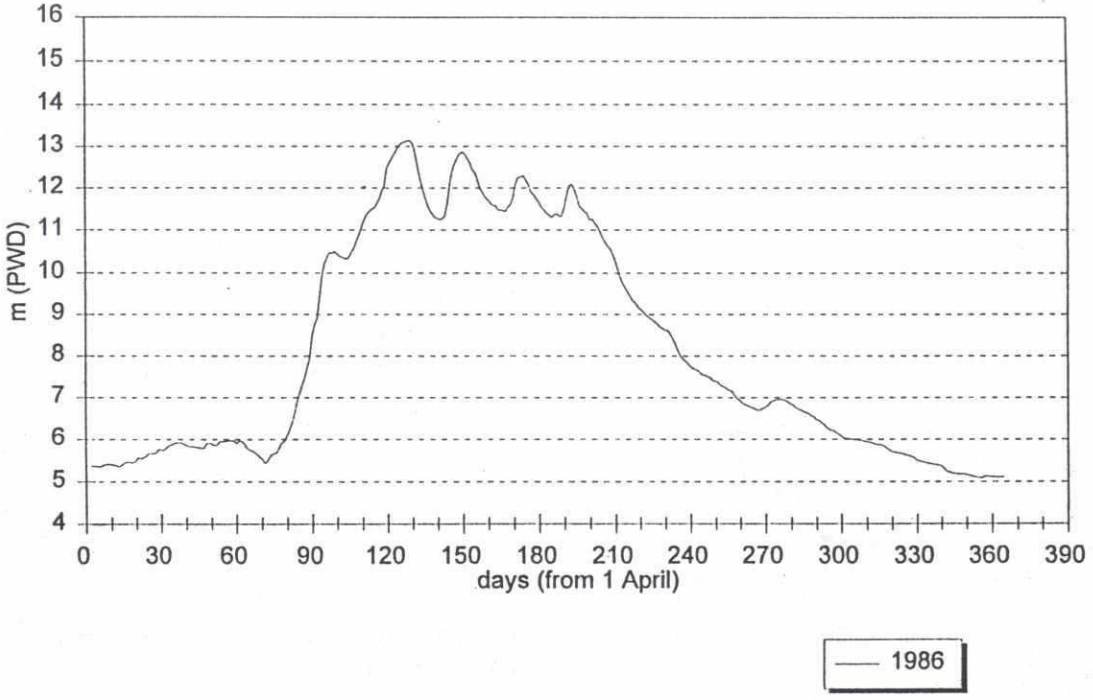


## Talbaria

water level data

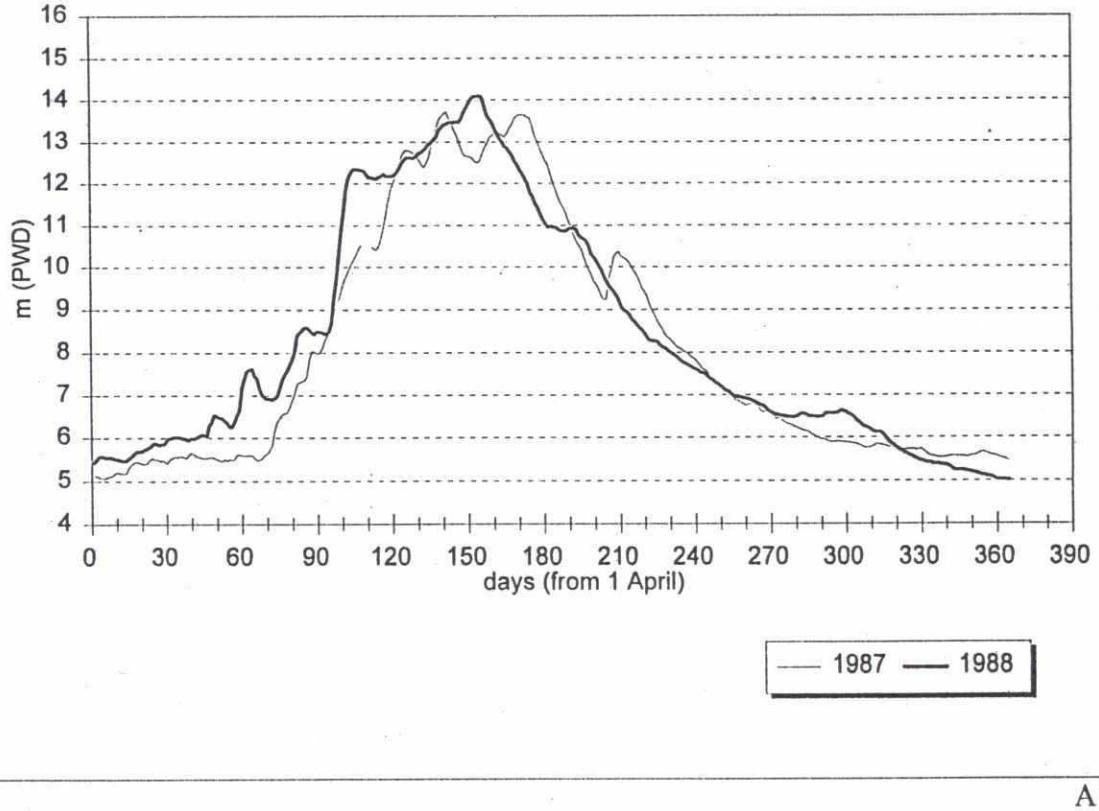

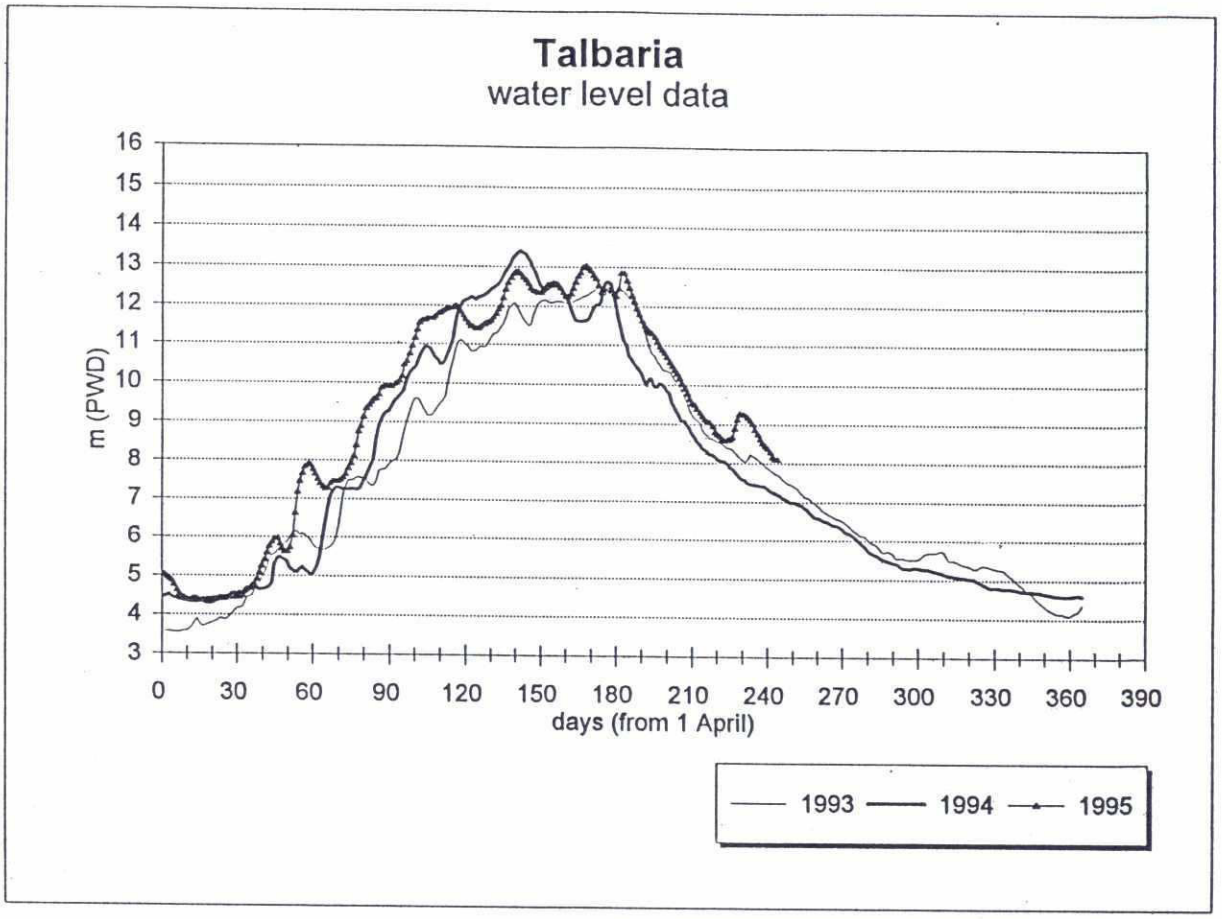
Talbaria
water level data
m (PWD)
16
15
14
13
12
11
10
9
8
7
6
5
4
3
0
30
60
90
120
150
180
210
240
270
300
330
360
390
days (from 1 April)
1993
1994
1995

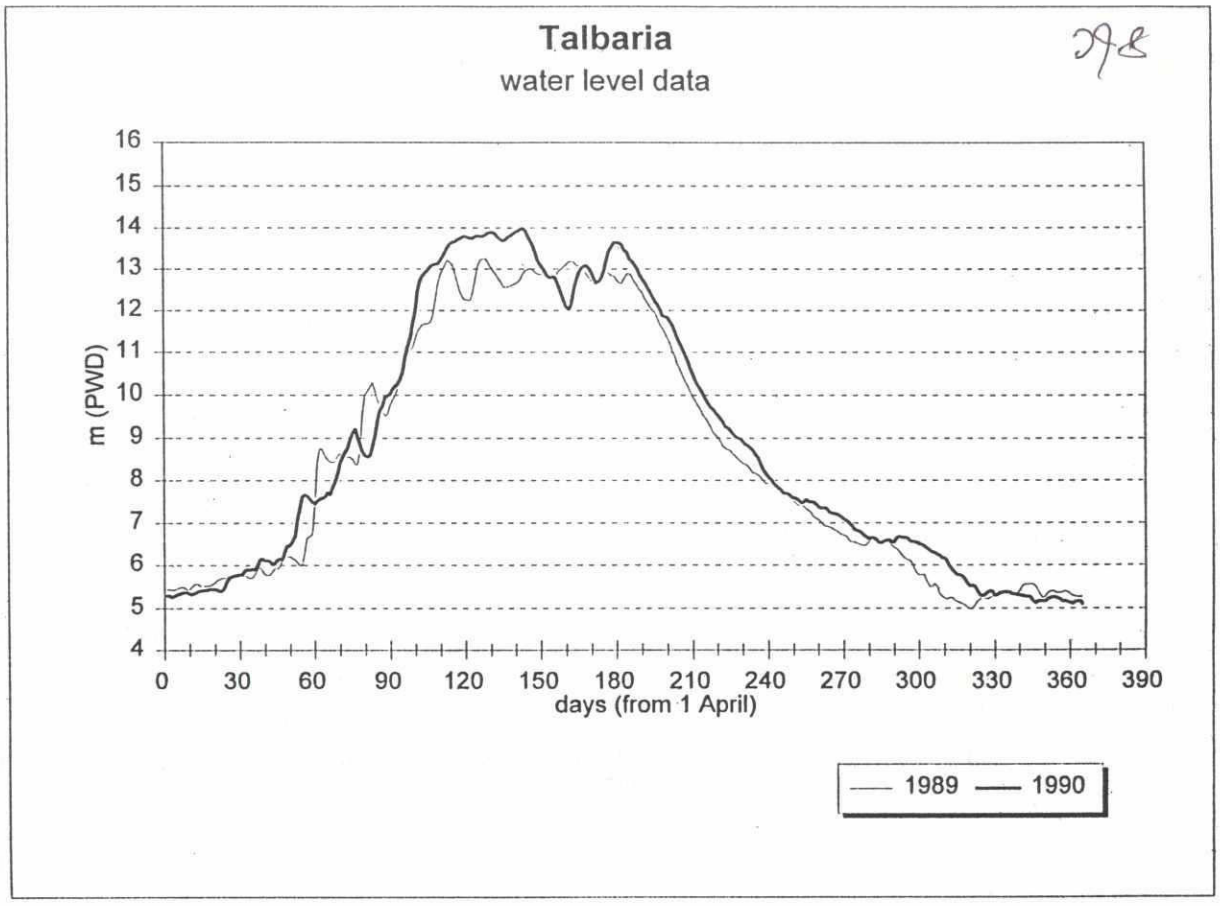
Talbaria
water level data
m (PWD)
days (from 1 April)
1989
1990

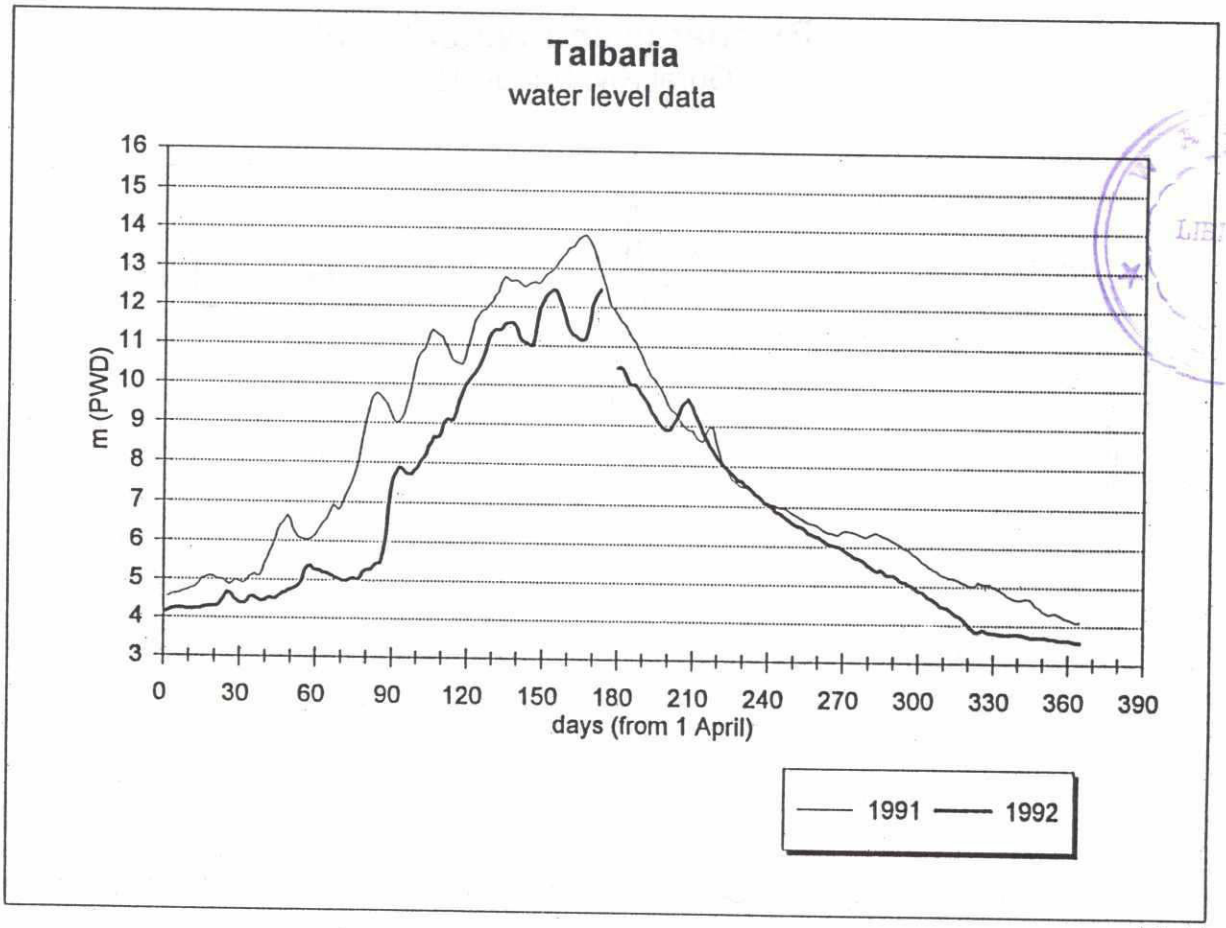
Talbaria
water level data
m (PWD)
days (from 1 April)
1991
1992

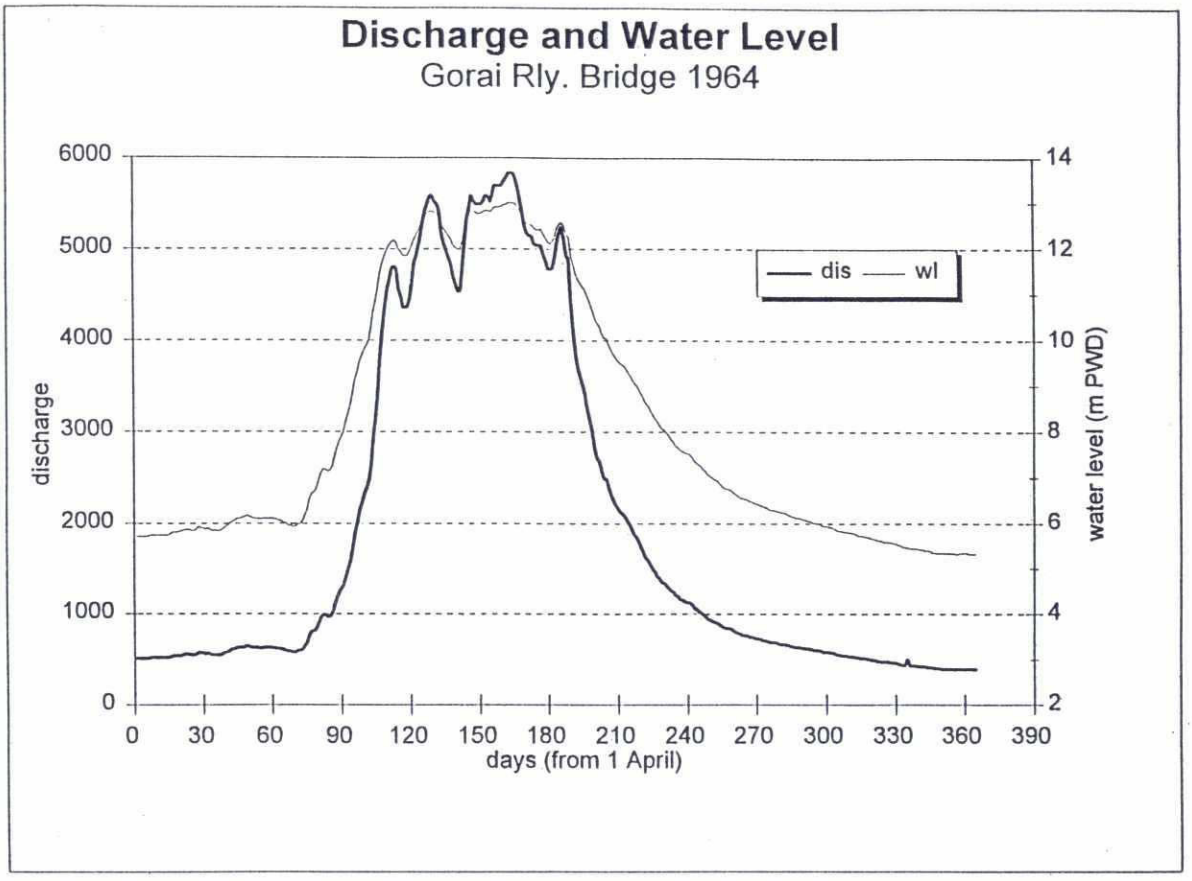
Discharge and Water Level
Gorai Rly. Bridge 1964
discharge
water level (m PWD)
days (from 1 April)
dis
wl
6000
5000
4000
3000
2000
1000
0
14
12
10
8
6
4
2
0 30 60 90 120 150 180 210 240 270 300 330 360 390

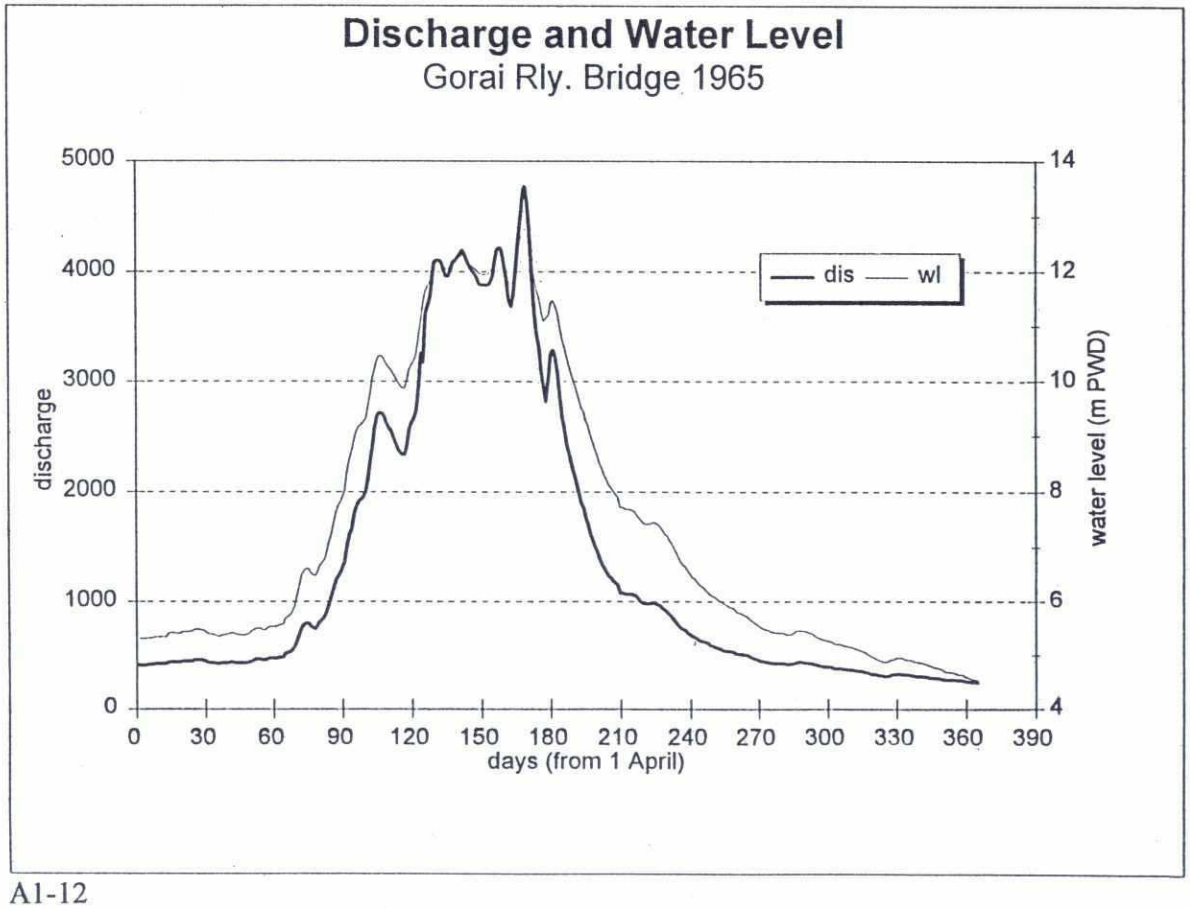
Discharge and Water Level
Gorai Rly. Bridge 1965
discharge
water level (m PWD)
days (from 1 April)
dis
wl
5000
4000
3000
2000
1000
0
14
12
10
8
6
4
0 30 60 90 120 150 180 210 240 270 300 330 360 390

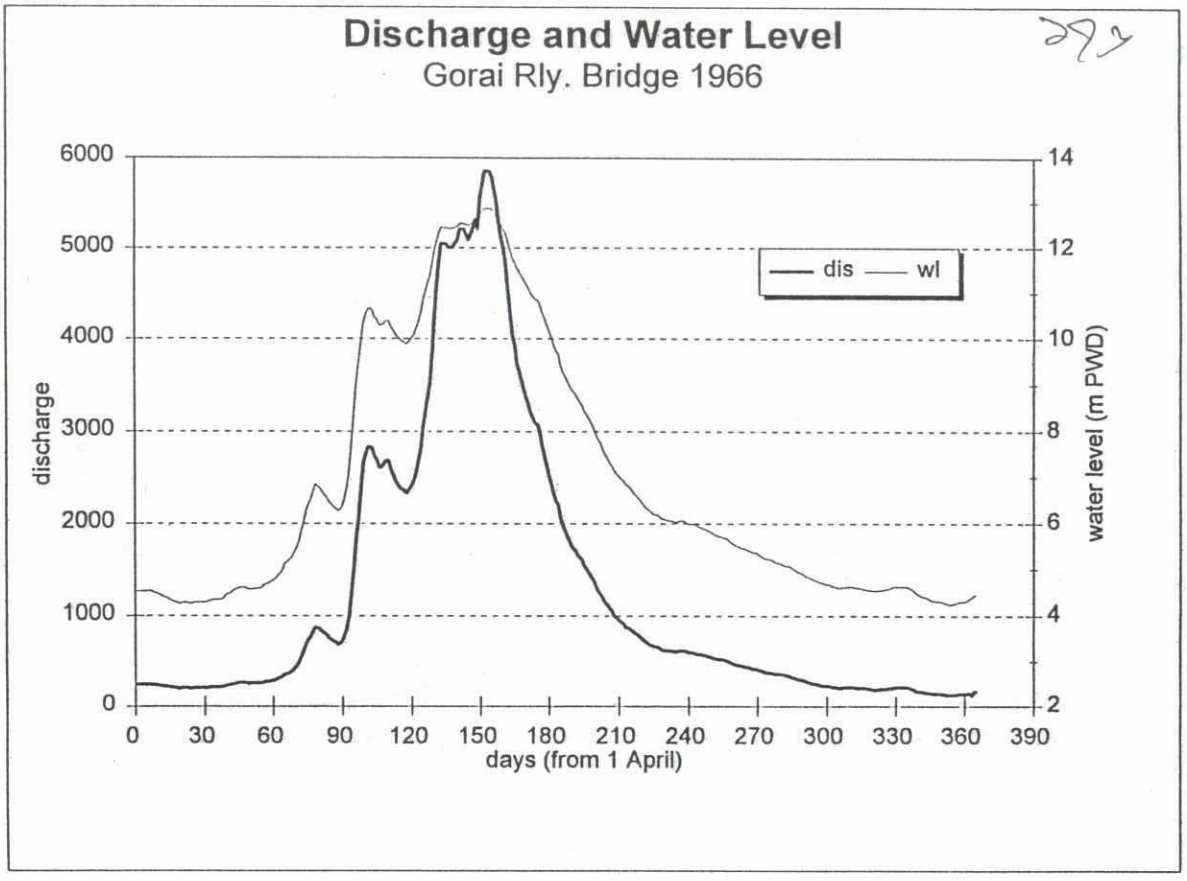
Discharge and Water Level
Gorai Rly. Bridge 1966
6000
5000
4000
3000
2000
1000
0
discharge
14
12
10
8
6
4
2
water level (m PWD)
dis
wl
0 30 60 90 120 150 180 210 240 270 300 330 360 390
days (from 1 April)

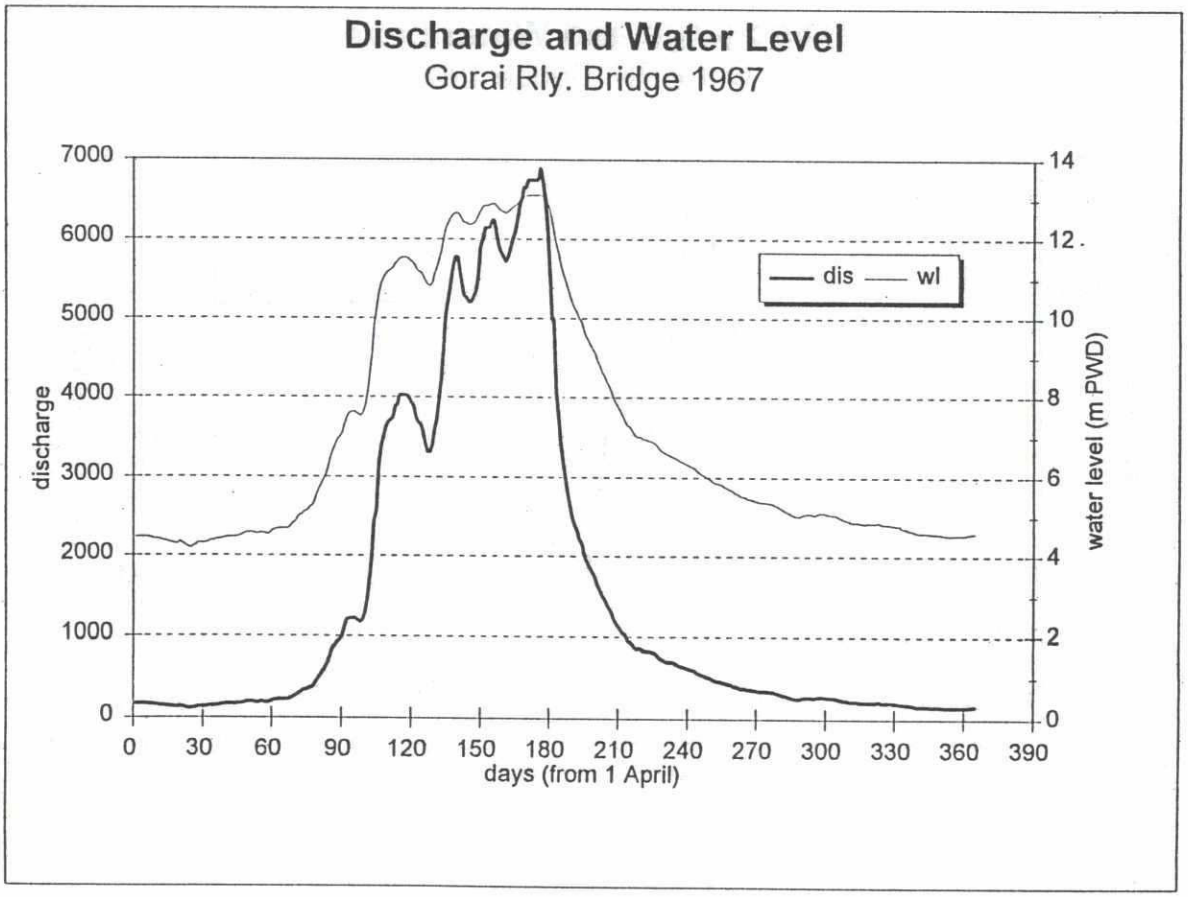
Discharge and Water Level
Gorai Rly. Bridge 1967
7000
6000
5000
4000
3000
2000
1000
0
discharge
14
12
10
8
6
4
2
0
water level (m PWD)
dis
wl
0 30 60 90 120 150 180 210 240 270 300 330 360 390
days (from 1 April)

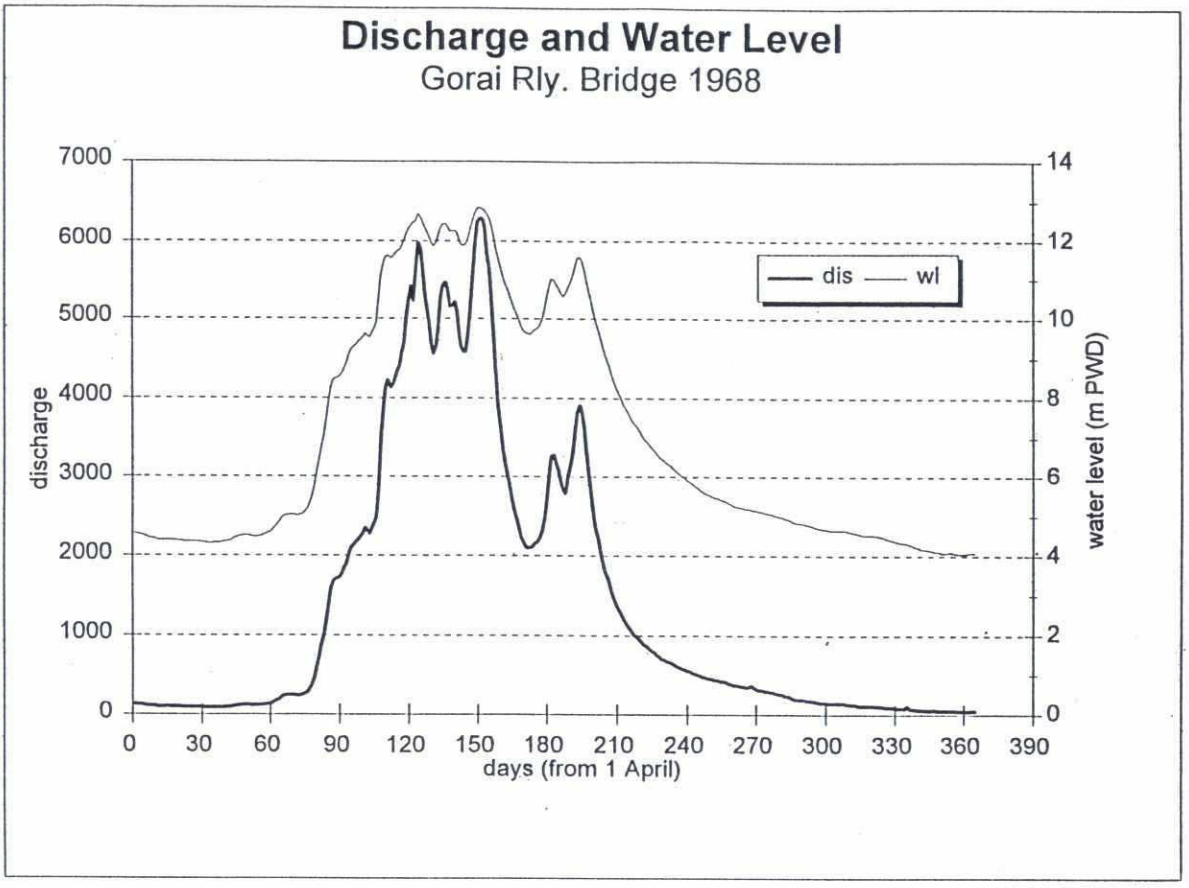
Discharge and Water Level
Gorai Rly. Bridge 1968
discharge
water level (m PWD)
days (from 1 April)
dis
wl
7000
6000
5000
4000
3000
2000
1000
0
14
12
10
8
6
4
2
0
0 30 60 90 120 150 180 210 240 270 300 330 360 390

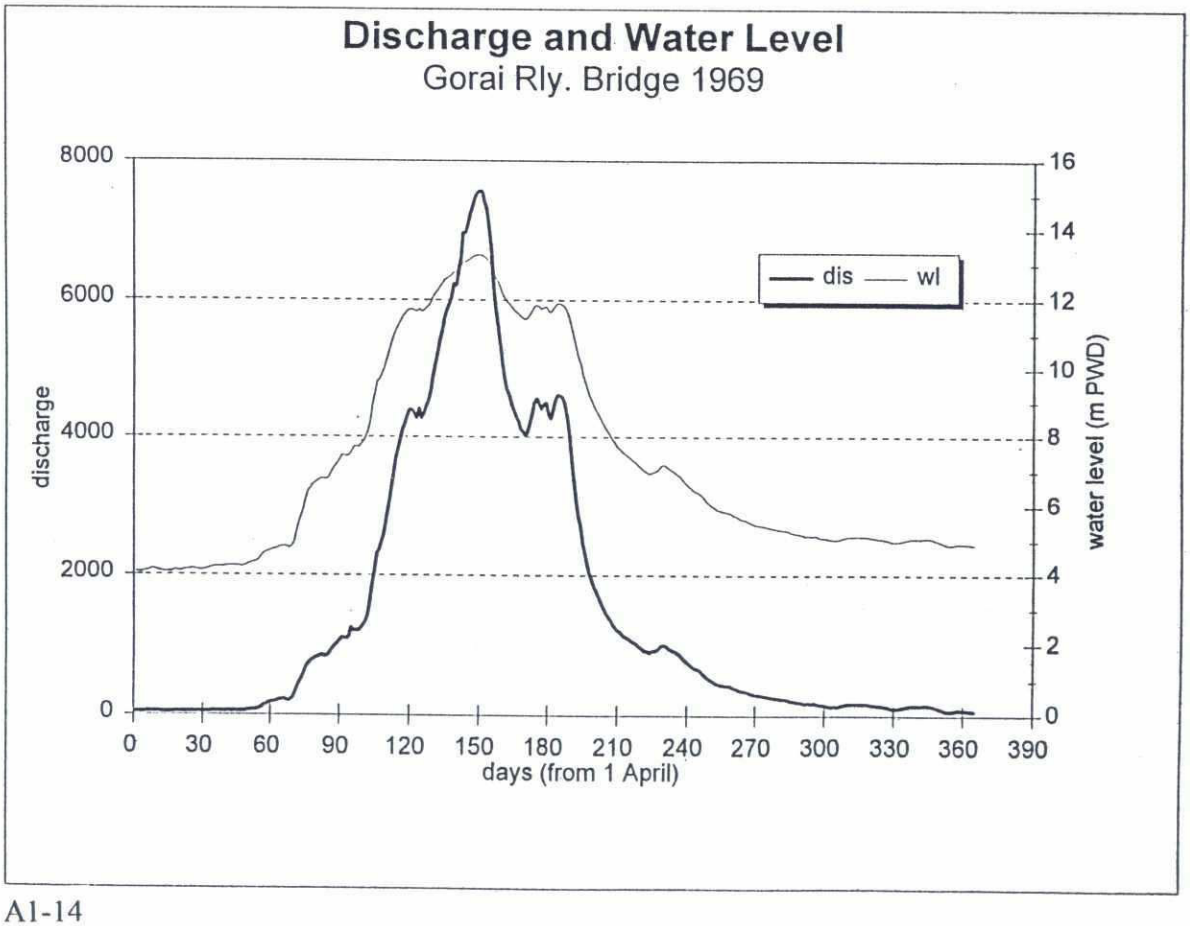
Discharge and Water Level
Gorai Rly. Bridge 1969
discharge
water level (m PWD)
days (from 1 April)
dis
wl
8000
6000
4000
2000
0
16
14
12
10
8
6
4
2
0
0 30 60 90 120 150 180 210 240 270 300 330 360 390

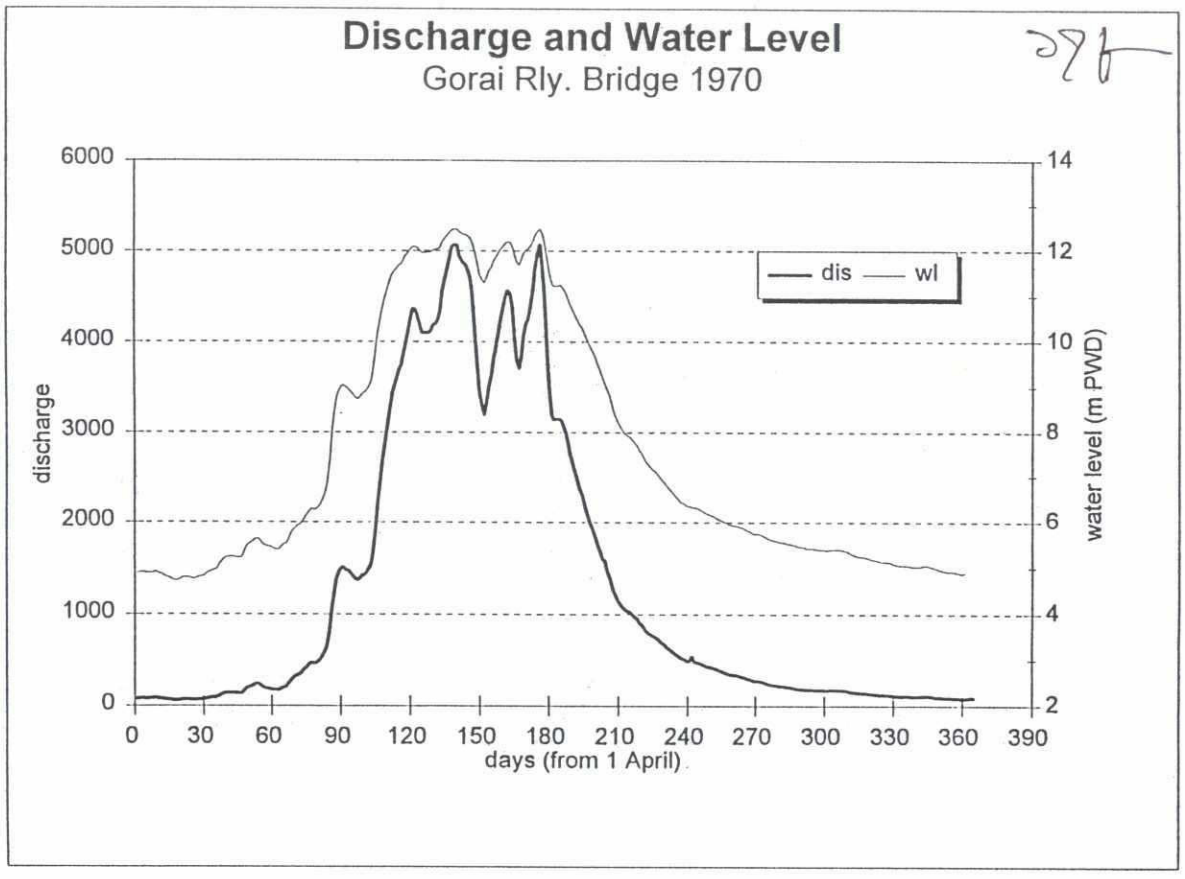
Discharge and Water Level
Gorai Rly. Bridge 1970
6000
5000
4000
3000
2000
1000
0
discharge
14
12
10
8
6
4
2
water level (m PWD)
dis
wl
0
30
60
90
120
150
180
210
240
270
300
330
360
390
days (from 1 April)

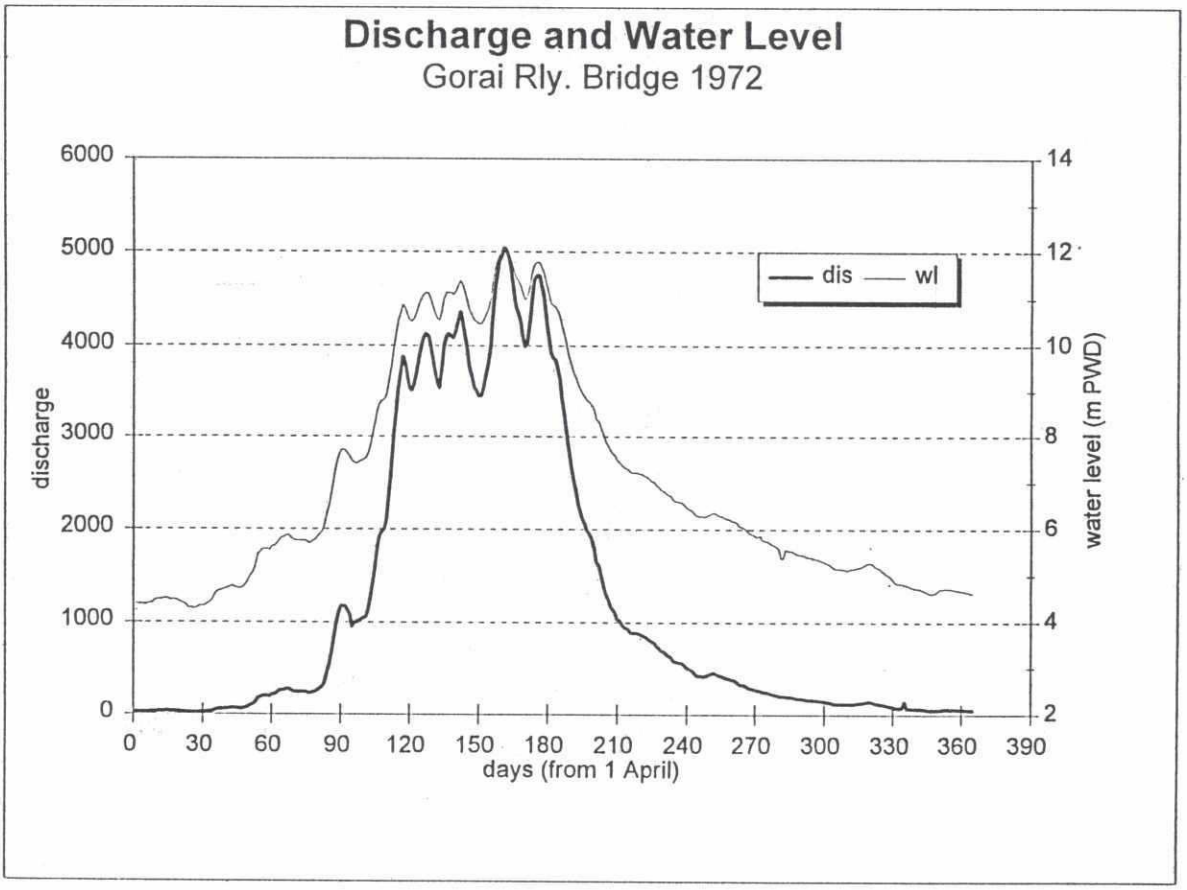
Discharge and Water Level
Gorai Rly. Bridge 1972
6000
5000
4000
3000
2000
1000
0
discharge
14
12
10
8
6
4
2
water level (m PWD)
dis
wl
0
30
60
90
120
150
180
210
240
270
300
330
360
390
days (from 1 April)

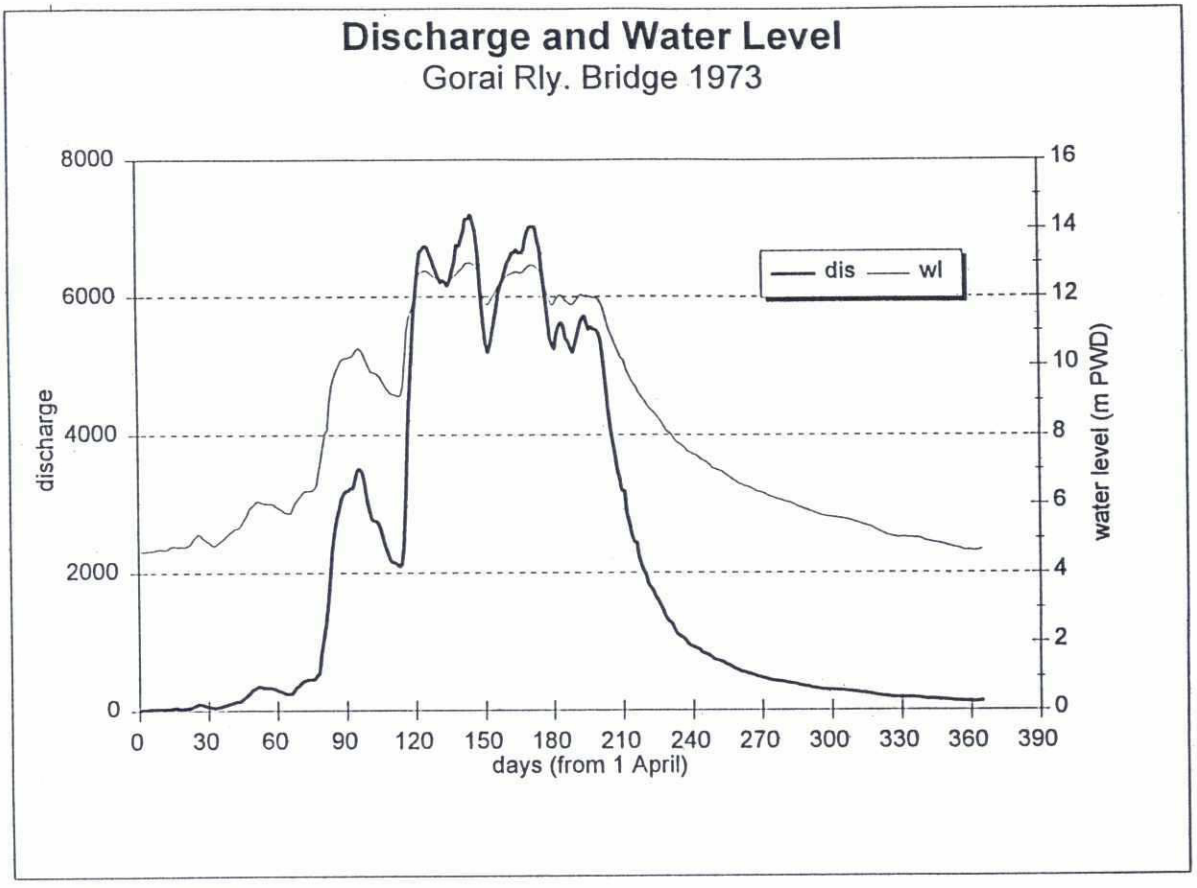
Discharge and Water Level
Gorai Rly. Bridge 1973
discharge
water level (m PWD)
days (from 1 April)
dis
wl
8000
6000
4000
2000
0
16
14
12
10
8
6
4
2
0
0 30 60 90 120 150 180 210 240 270 300 330 360 390

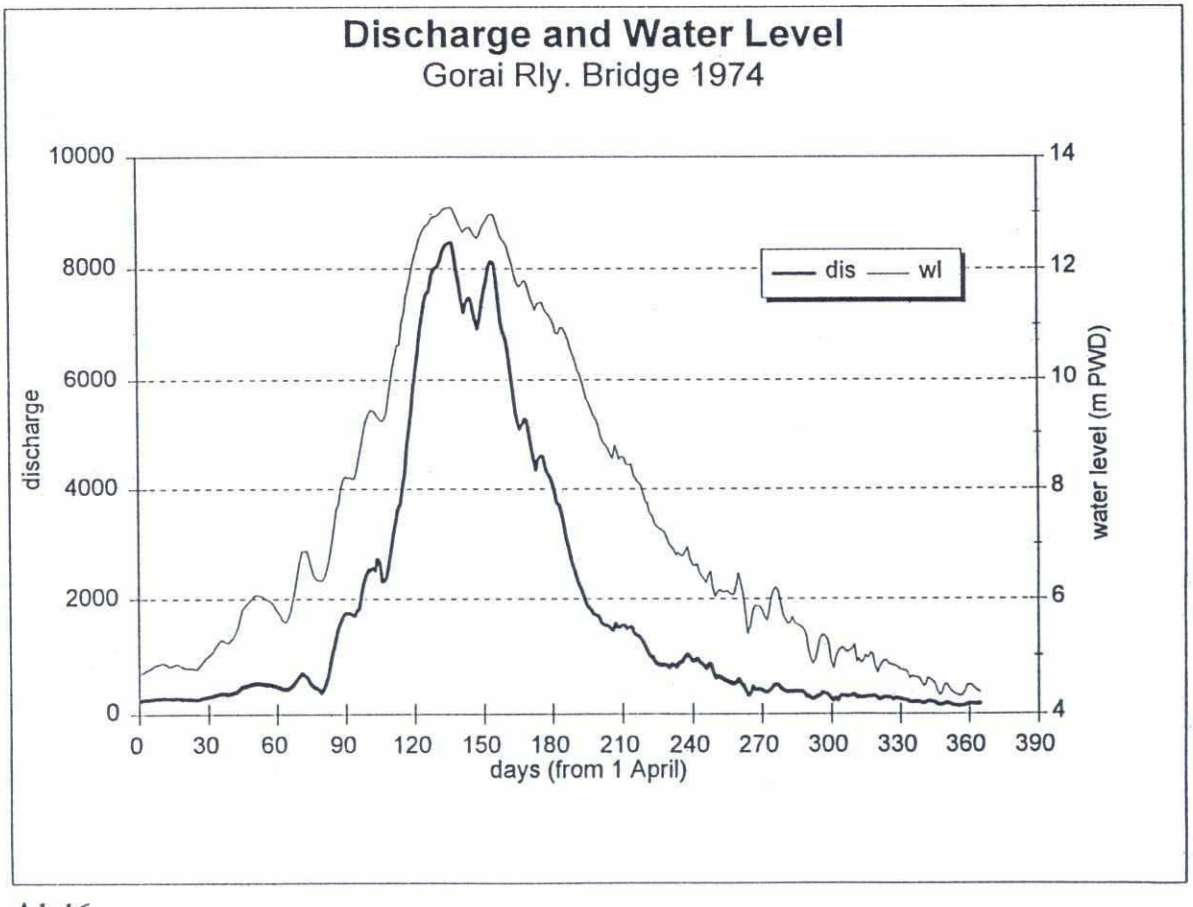
Discharge and Water Level
Gorai Rly. Bridge 1974
discharge
water level (m PWD)
days (from 1 April)
dis
wl
10000
8000
6000
4000
2000
0
14
12
10
8
6
4
0 30 60 90 120 150 180 210 240 270 300 330 360 390

## Discharge and Water Level

Gorai Rly. Bridge 1975

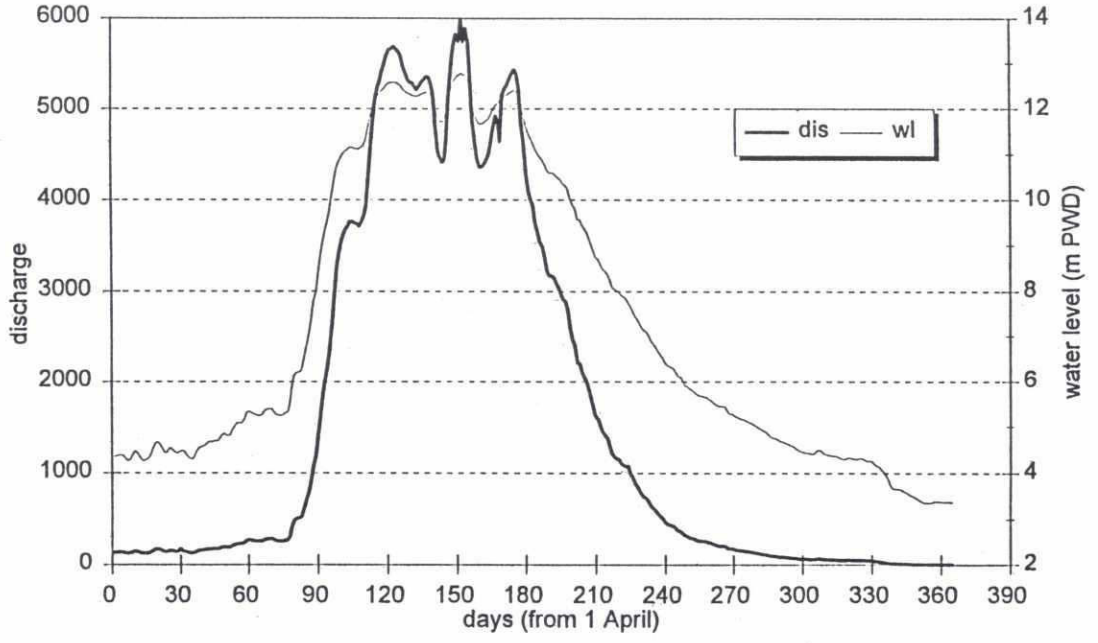


## Discharge and Water Level

Gorai Rly. Bridge 1976

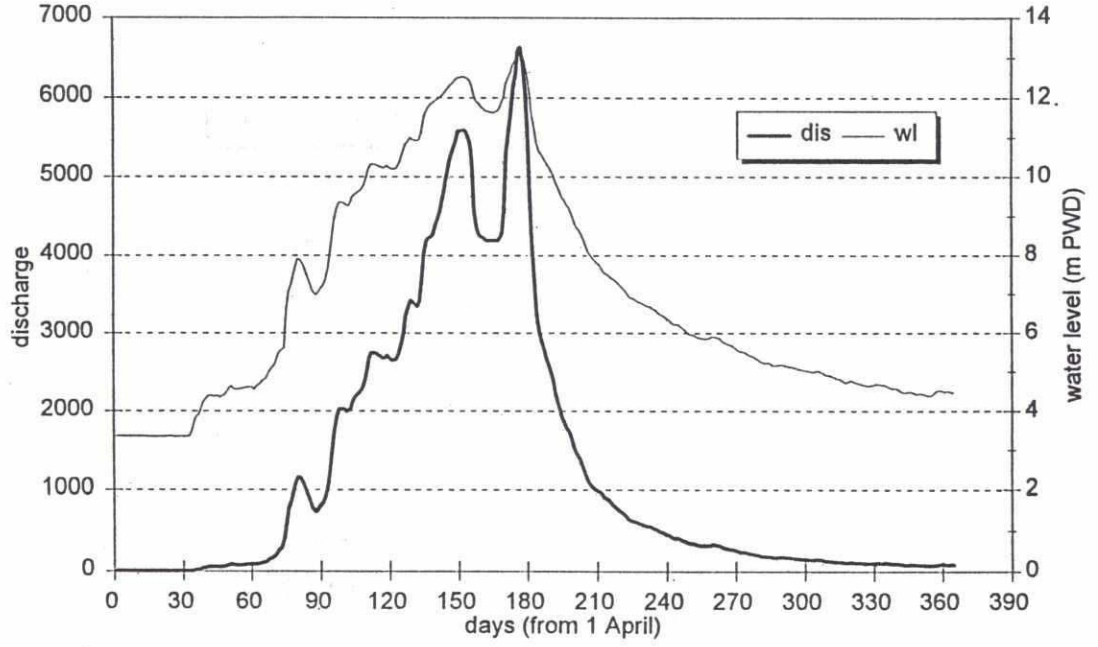

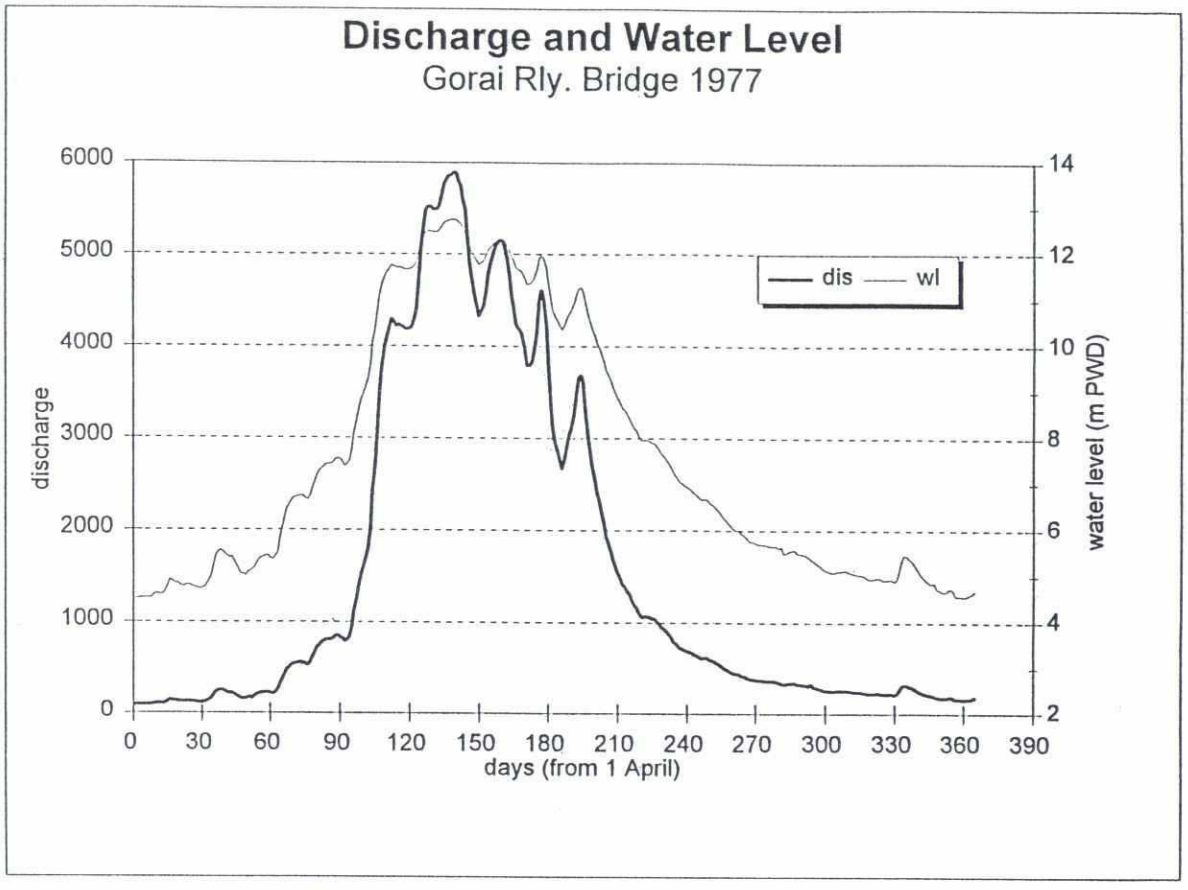
Discharge and Water Level
Gorai Rly. Bridge 1977
discharge
water level (m PWD)
days (from 1 April)
dis
wl
0
1000
2000
3000
4000
5000
6000
2
4
6
8
10
12
14
0
30
60
90
120
150
180
210
240
270
300
330
360
390

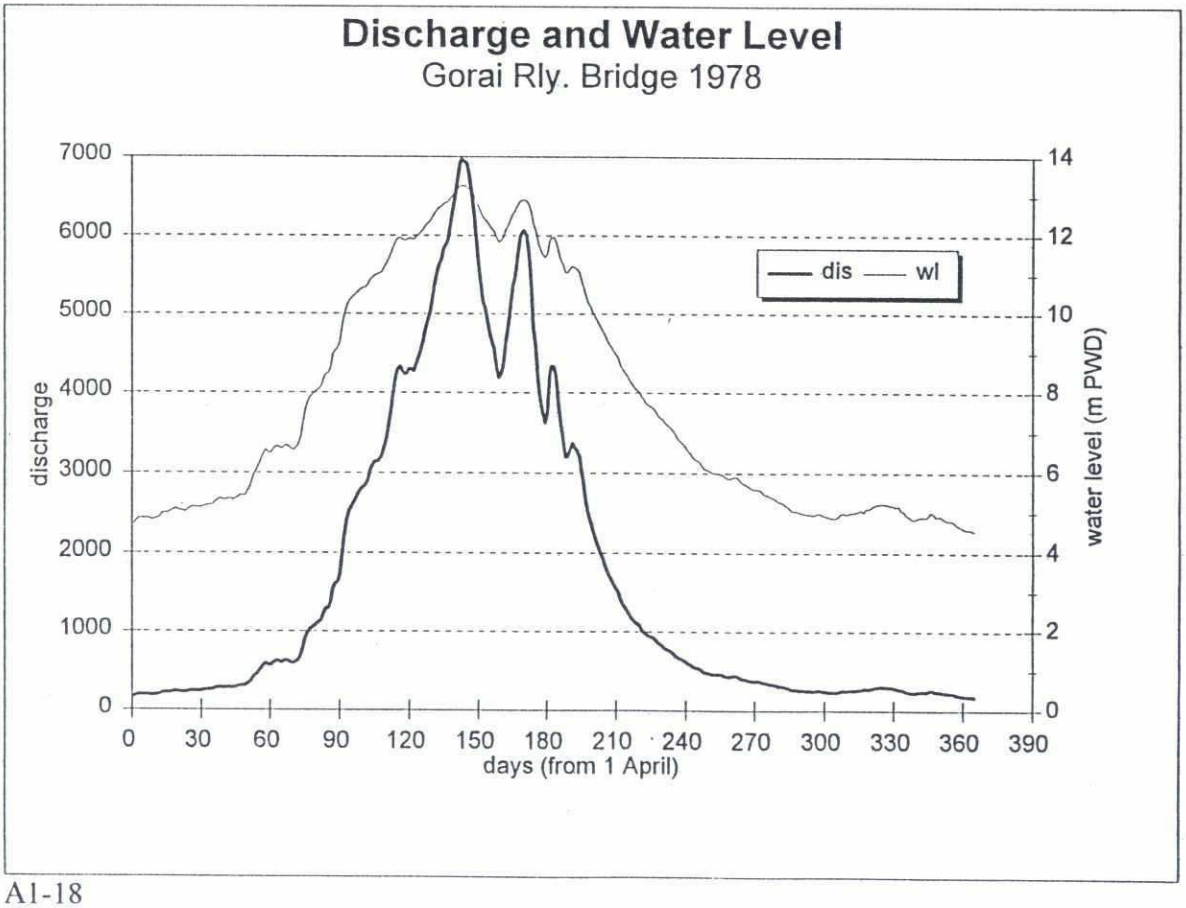
Discharge and Water Level
Gorai Rly. Bridge 1978
discharge
water level (m PWD)
days (from 1 April)
dis
wl
0
1000
2000
3000
4000
5000
6000
7000
0
2
4
6
8
10
12
14
0
30
60
90
120
150
180
210
240
270
300
330
360
390

## Discharge and Water Level

Gorai Rly. Bridge 1979

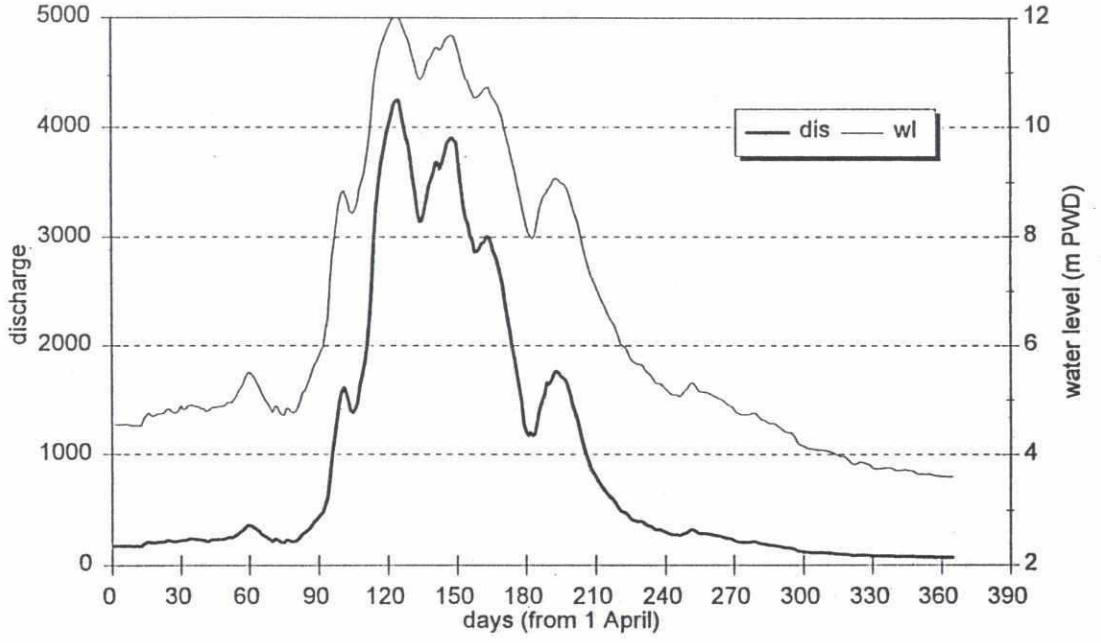


## Discharge and Water Level

Gorai Rly. Bridge 1980

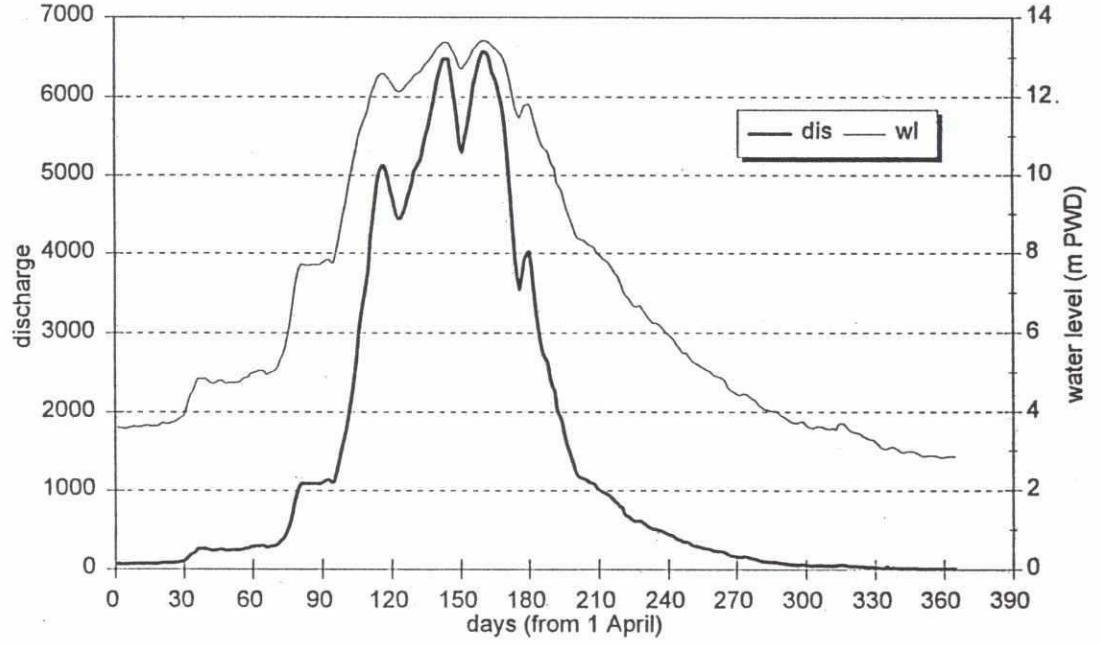

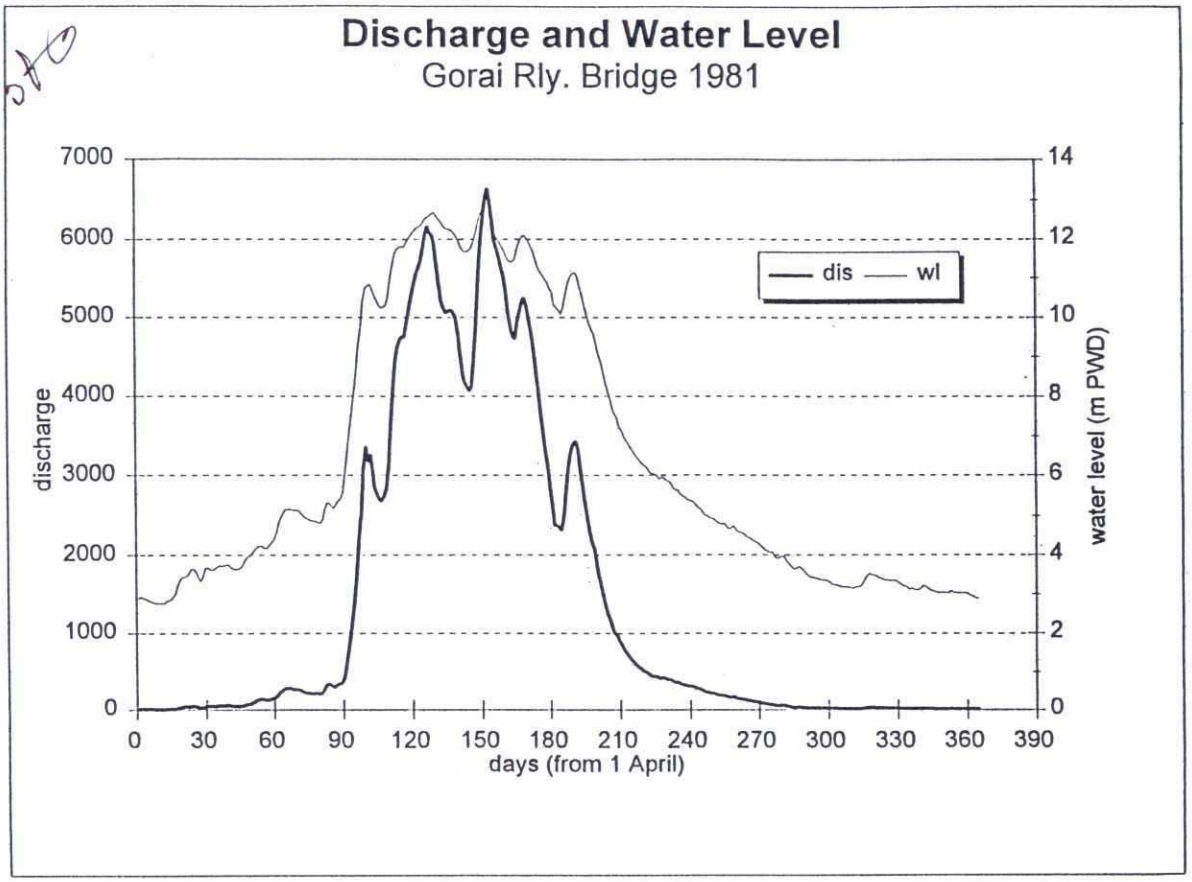
Discharge and Water Level
Gorai Rly. Bridge 1981
discharge
water level (m PWD)
days (from 1 April)
dis
wl
0
1000
2000
3000
4000
5000
6000
7000
0
2
4
6
8
10
12
14
0
30
60
90
120
150
180
210
240
270
300
330
360
390

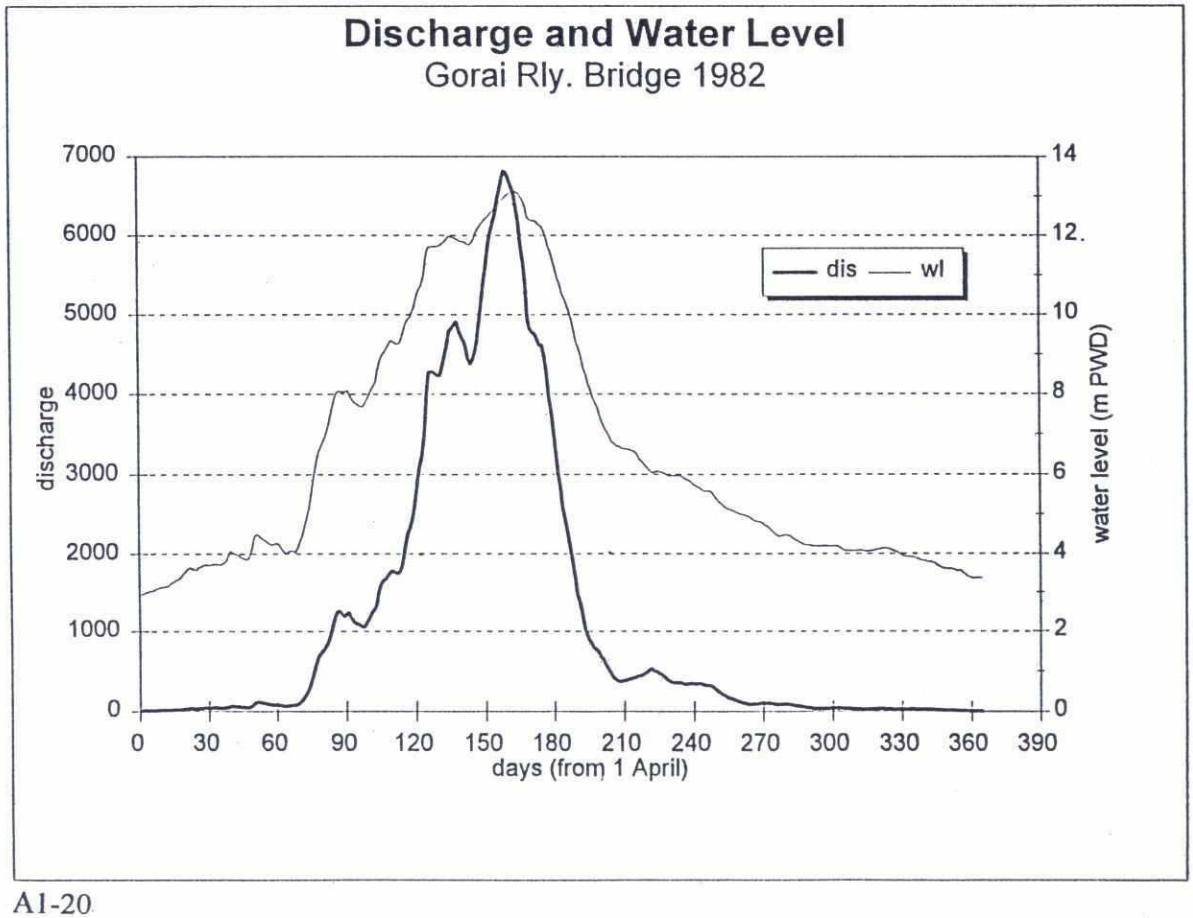
Discharge and Water Level
Gorai Rly. Bridge 1982
discharge
water level (m PWD)
days (from 1 April)
dis
wl
0
1000
2000
3000
4000
5000
6000
7000
0
2
4
6
8
10
12.
14
0
30
60
90
120
150
180
210
240
270
300
330
360
390

## Discharge and Water Level

Gorai Rly. Bridge 1983

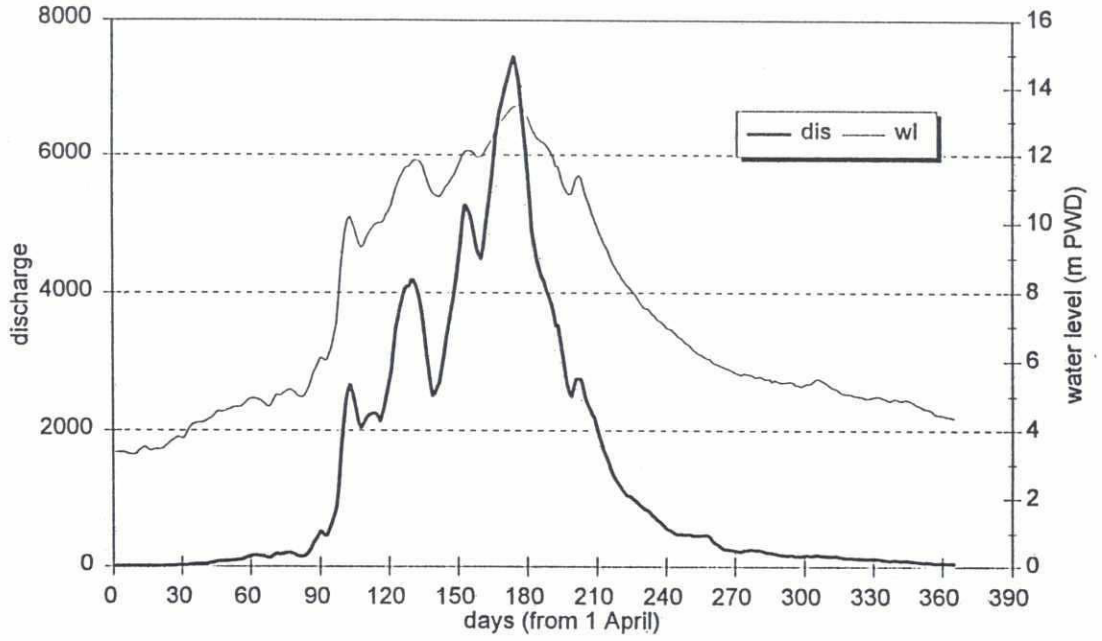


## Discharge and Water Level

Gorai Rly. Bridge 1984

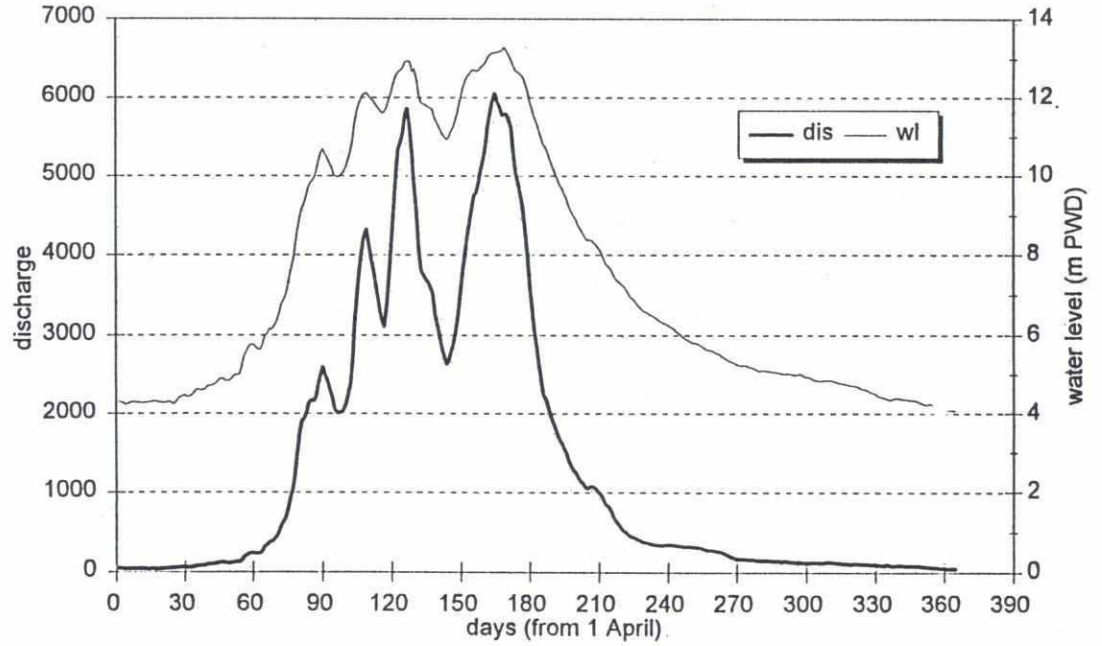

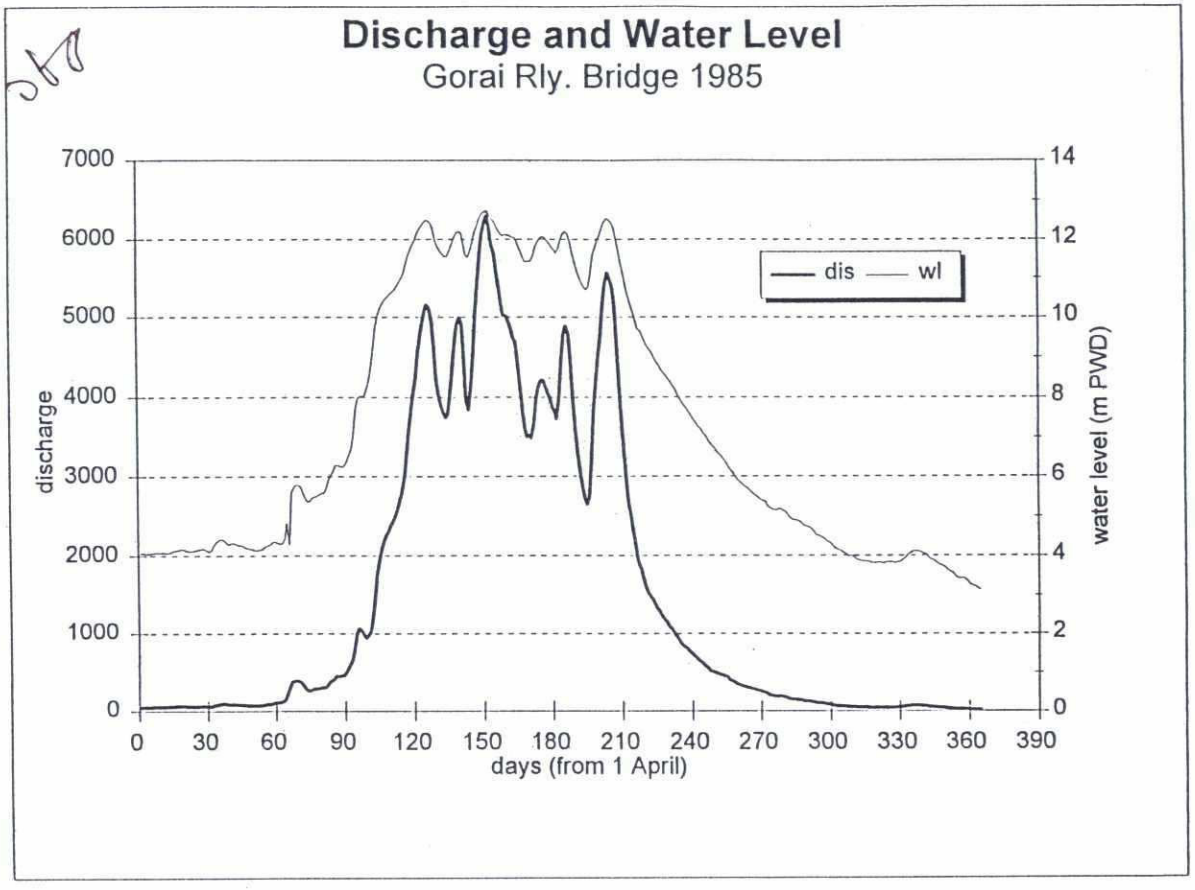
Discharge and Water Level
Gorai Rly. Bridge 1985
7000
6000
5000
4000
3000
2000
1000
0
discharge
14
12
10
8
6
4
2
0
water level (m PWD)
dis
wl
0 30 60 90 120 150 180 210 240 270 300 330 360 390
days (from 1 April)

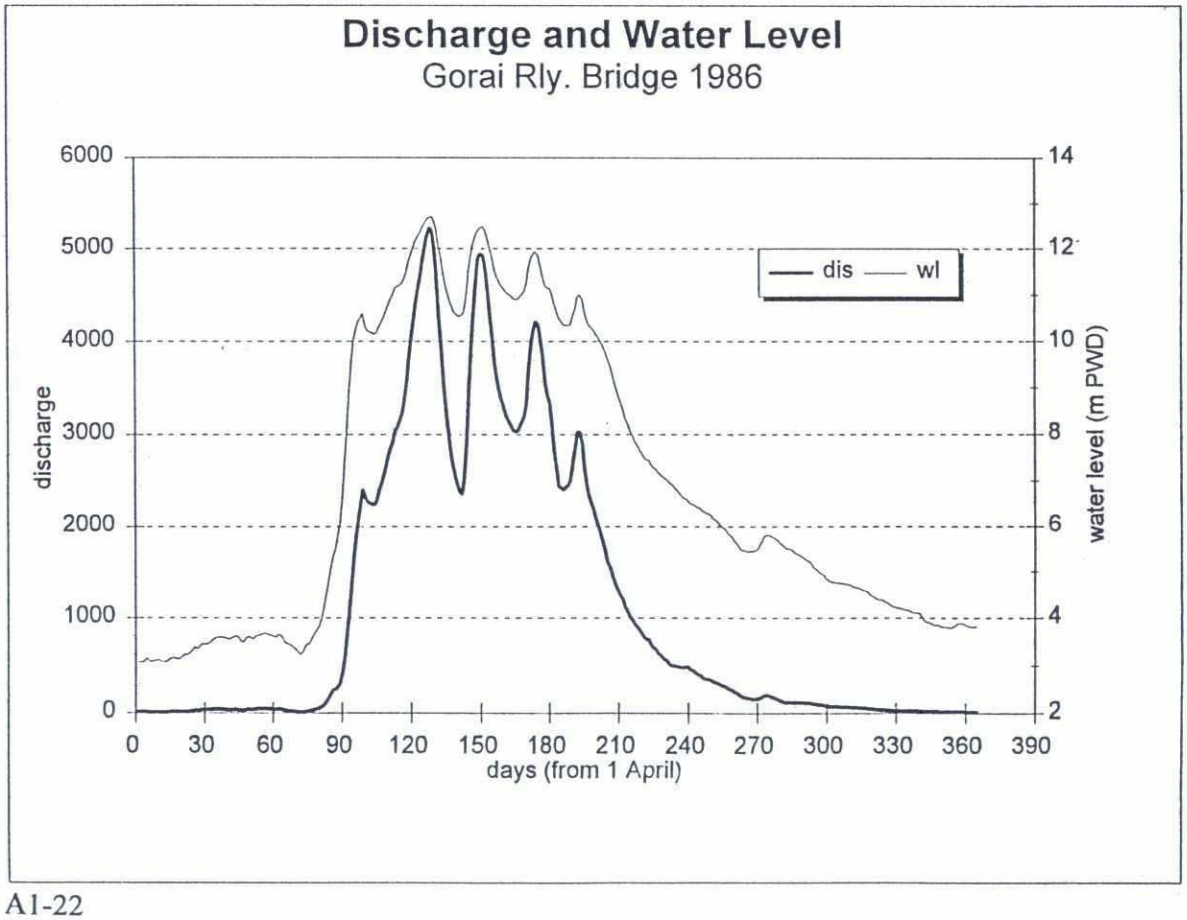
Discharge and Water Level
Gorai Rly. Bridge 1986
6000
5000
4000
3000
2000
1000
0
discharge
14
12
10
8
6
4
2
water level (m PWD)
dis
wl
0 30 60 90 120 150 180 210 240 270 300 330 360 390
days (from 1 April)

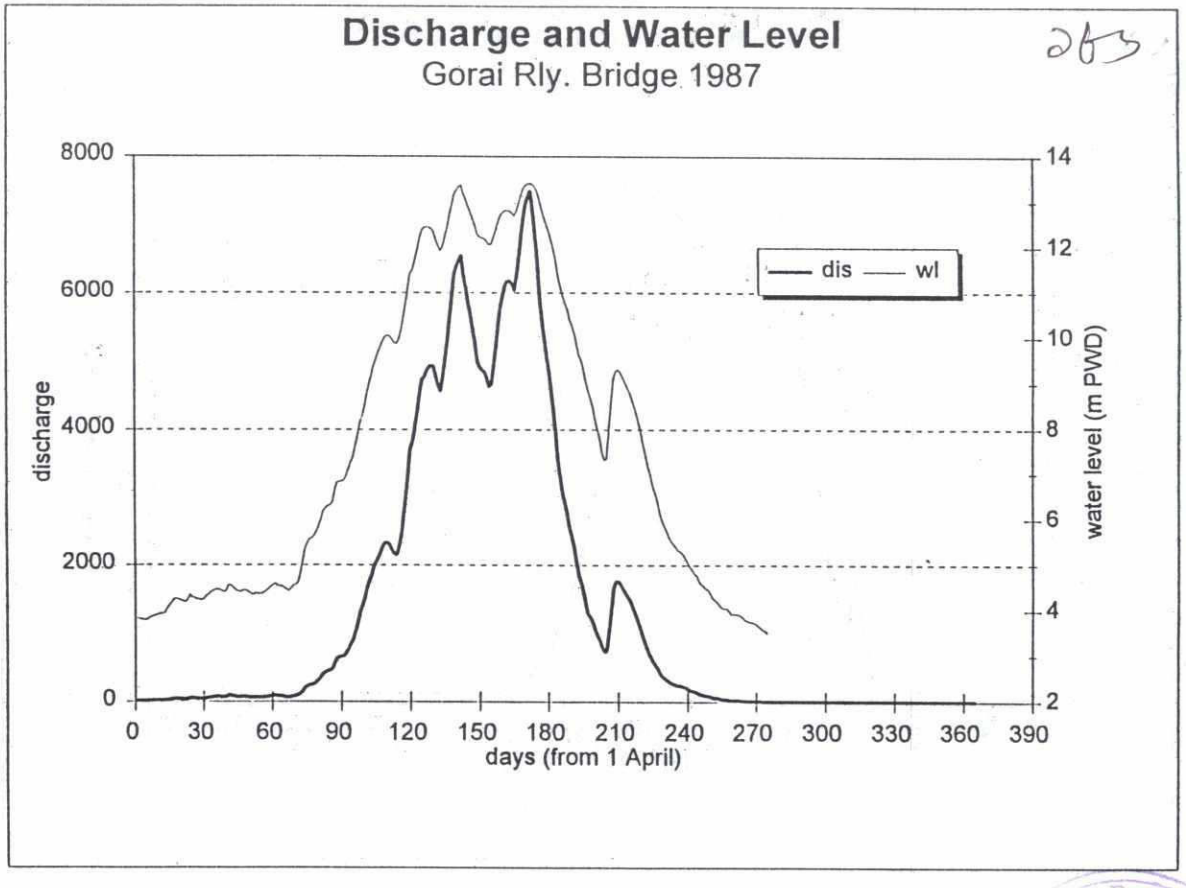




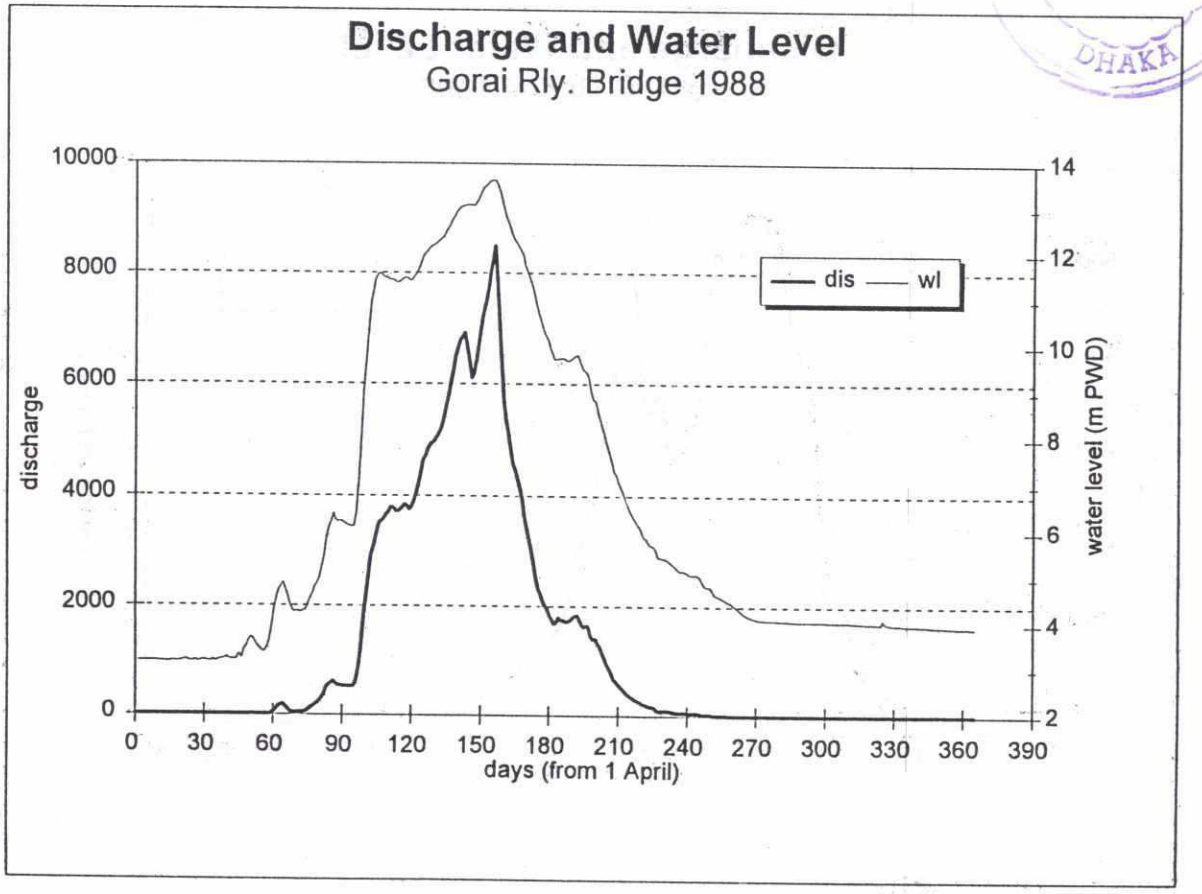

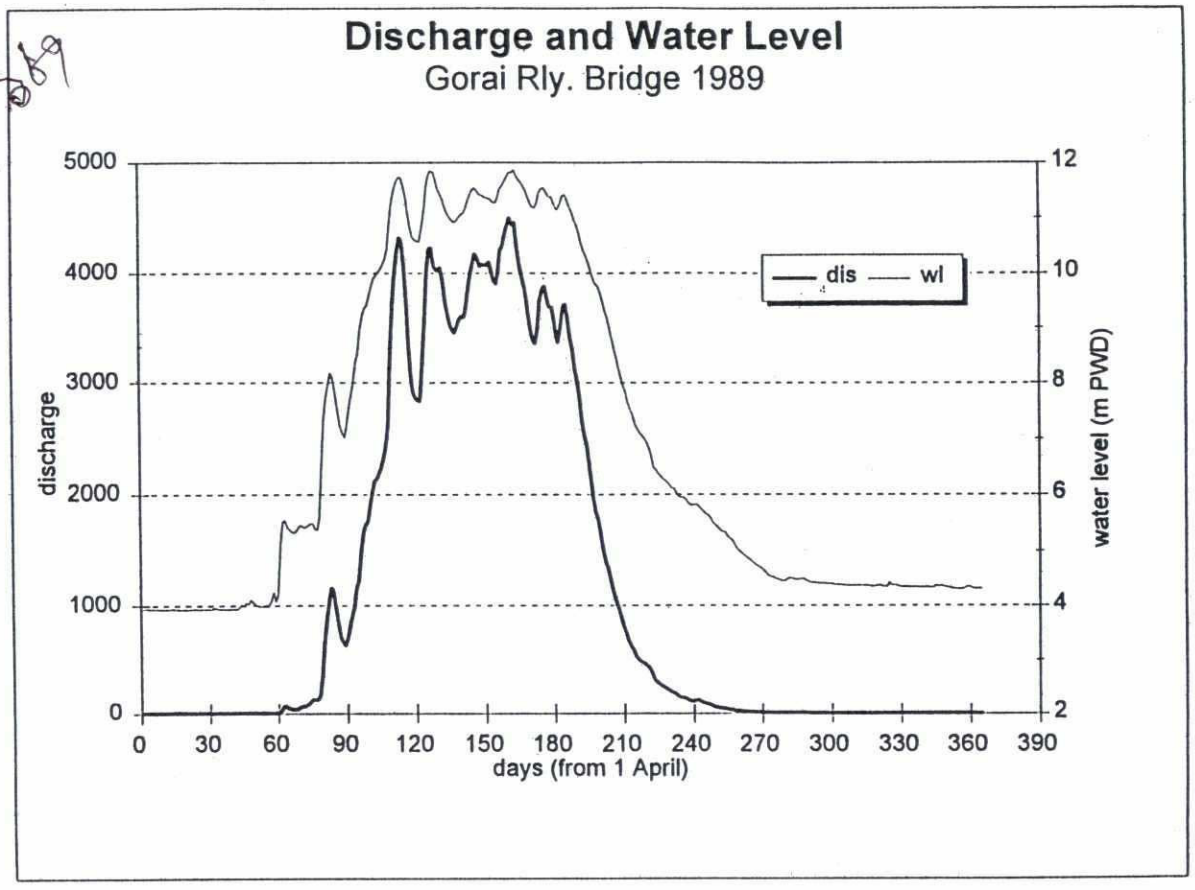
Discharge and Water Level
Gorai Rly. Bridge 1989
dis
wl
discharge
water level (m PWD)
days (from 1 April)
0
1000
2000
3000
4000
5000
2
4
6
8
10
12
0
30
60
90
120
150
180
210
240
270
300
330
360
390

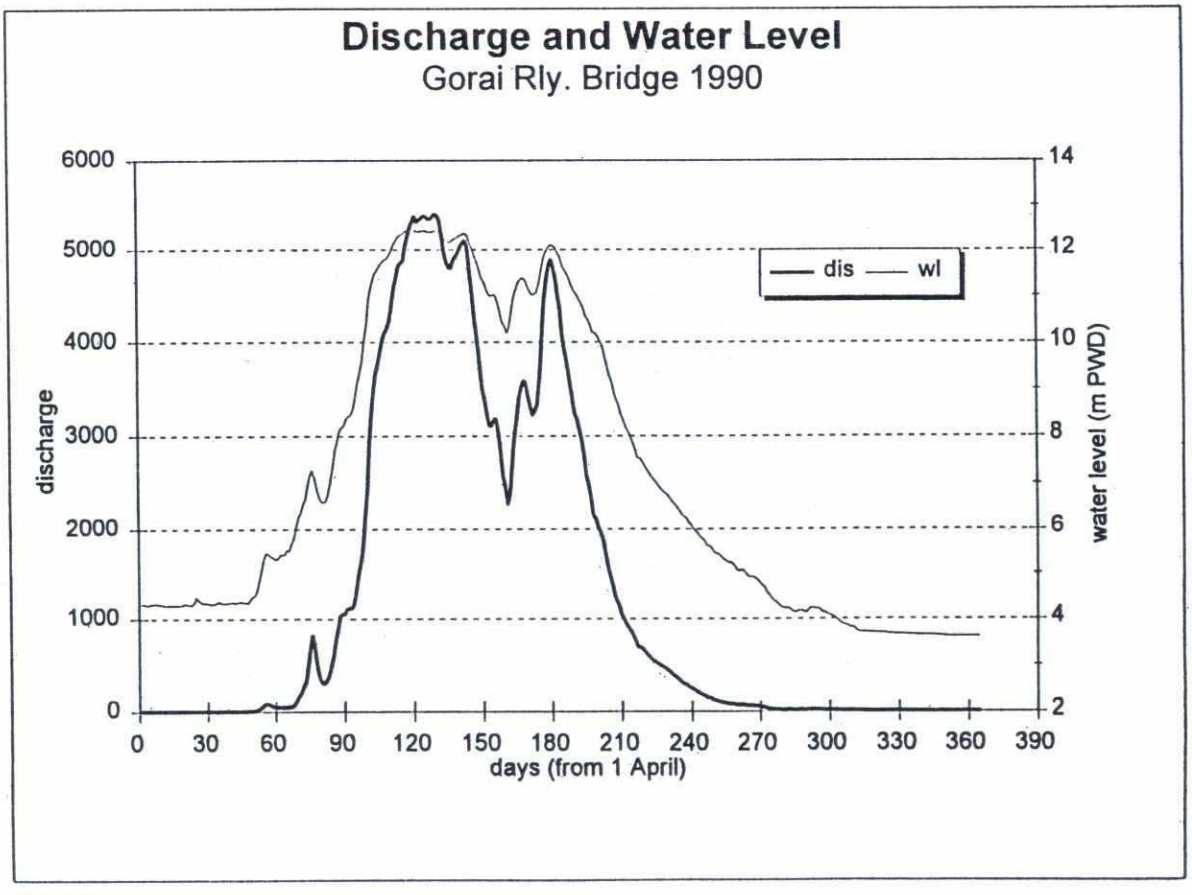
Discharge and Water Level
Gorai Rly. Bridge 1990
dis
wl
discharge
water level (m PWD)
days (from 1 April)
0
1000
2000
3000
4000
5000
6000
2
4
6
8
10
12
14
0
30
60
90
120
150
180
210
240
270
300
330
360
390

## Discharge and Water Level

Gorai Rly. Bridge 1991

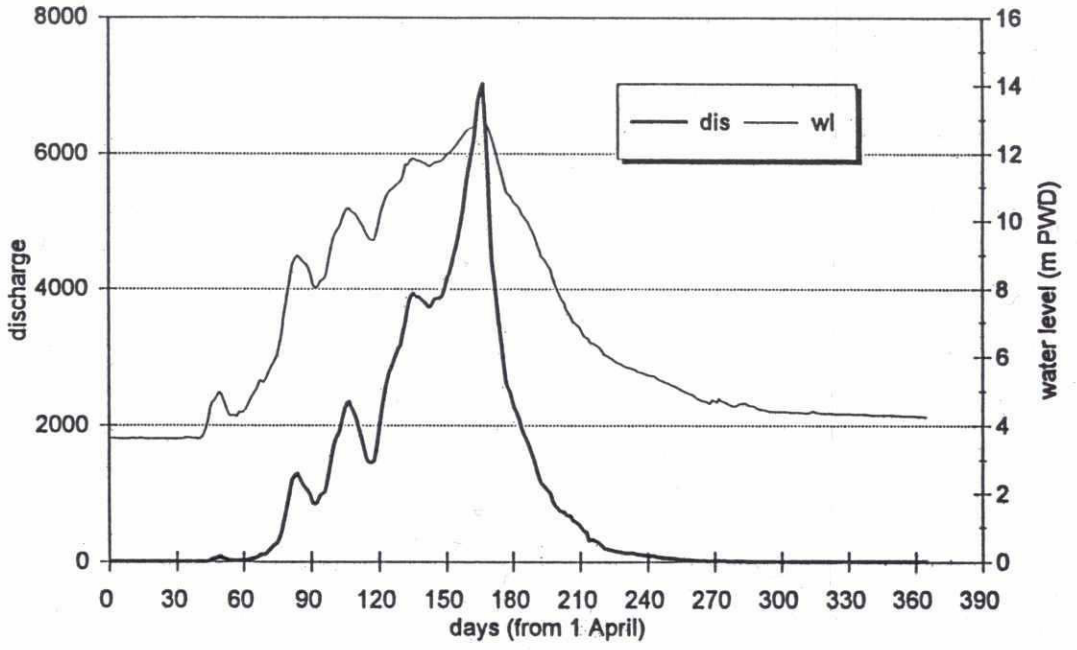


## Discharge and Water Level

Gorai Rly. Bridge 1992

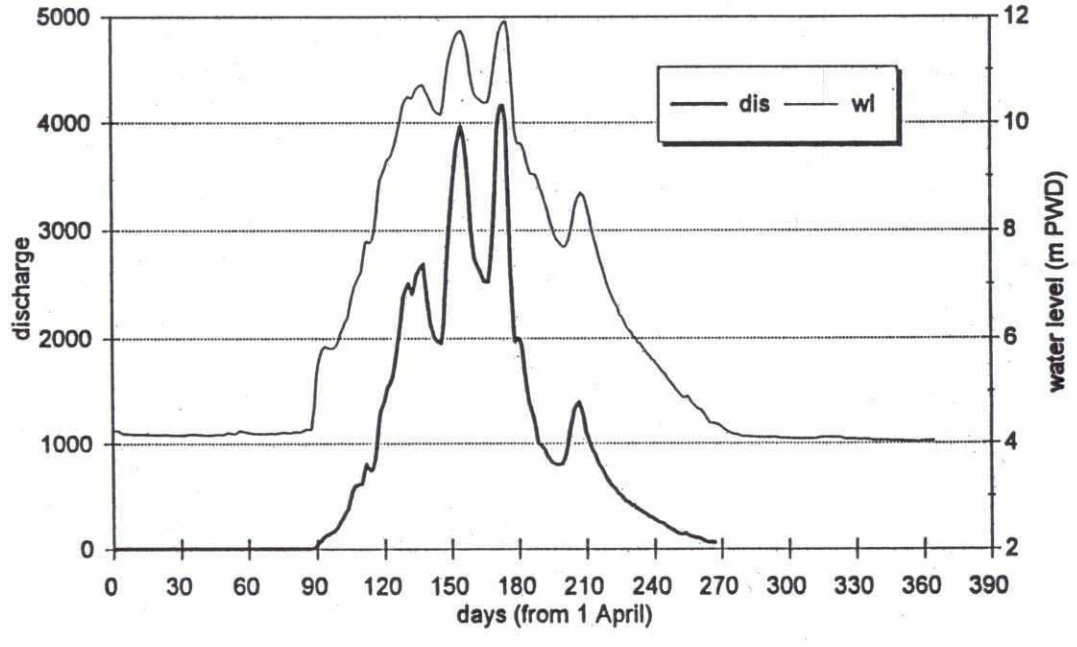

## Discharge and Water Level
Gorai Rly. Bridge 1993

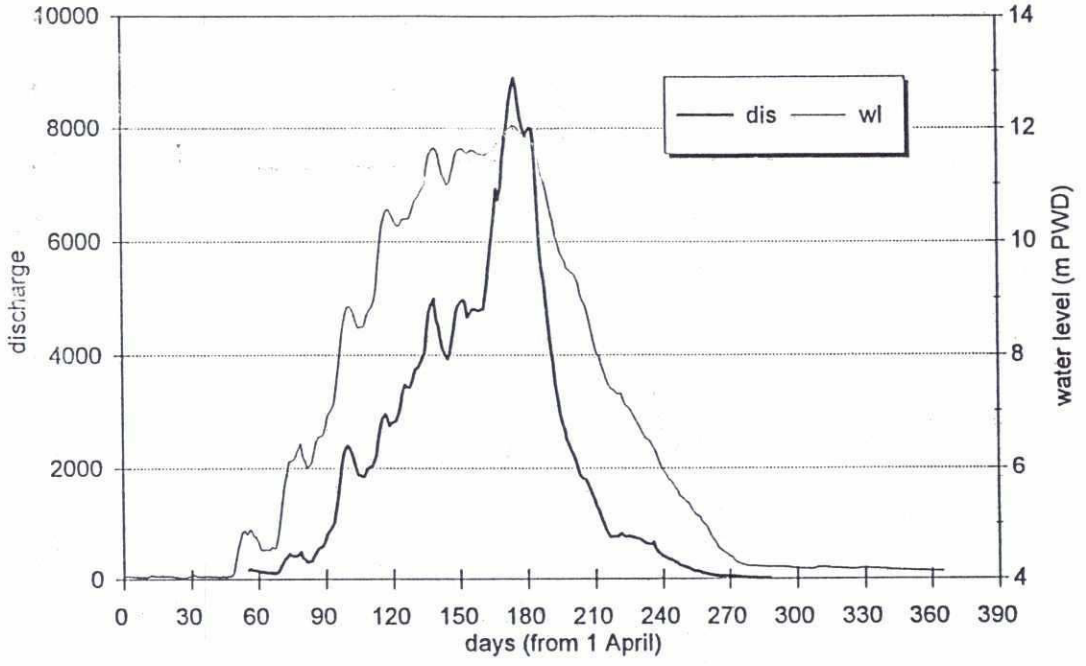


## Discharge and Water Level
Gorai Rly. Bridge 1994

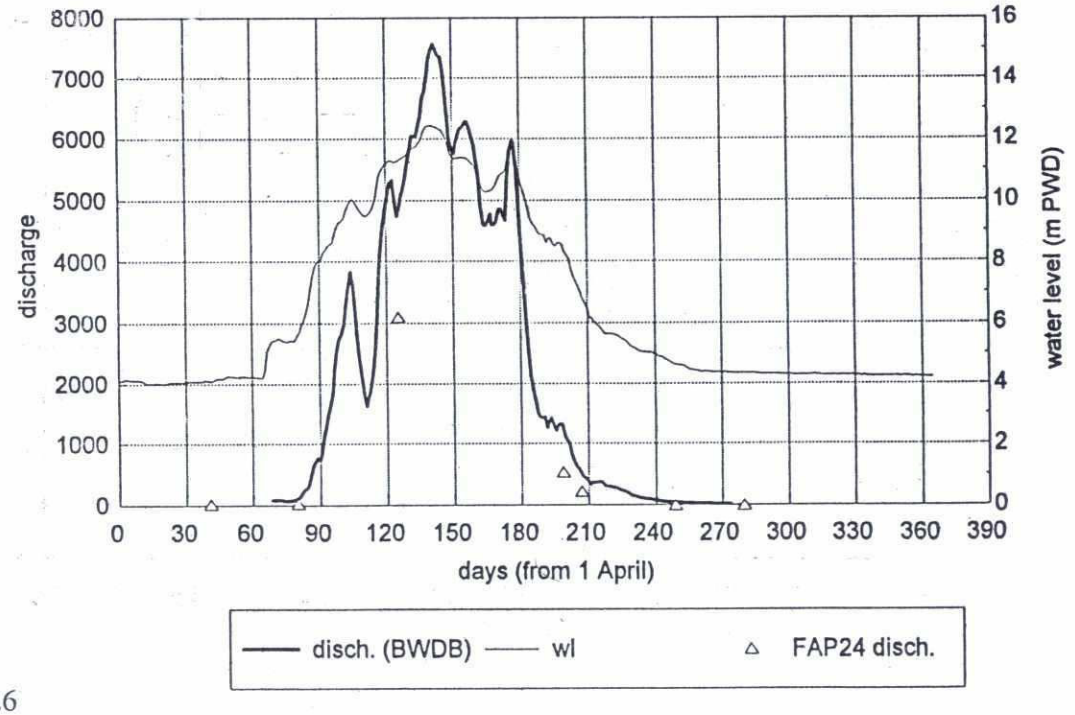

## Discharge and Water Level

Gorai Rly. Bridge 1995

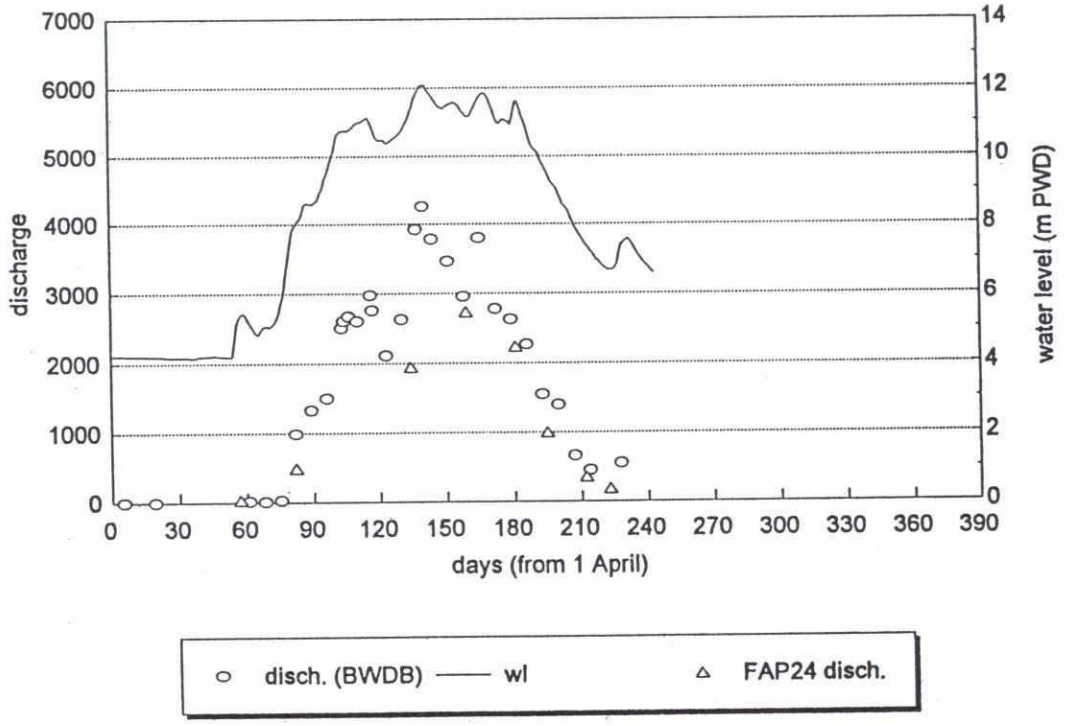

**Appendix 2: Water level slopes:**

- Level difference: Hardinge Bridge to Gorai Railway Br. 1964-95
- Slope: Talbaria to Gorai Railway Bridge 1986-95

## Water level differences

Hardinge Bridge to Gorai Rly. Bridge

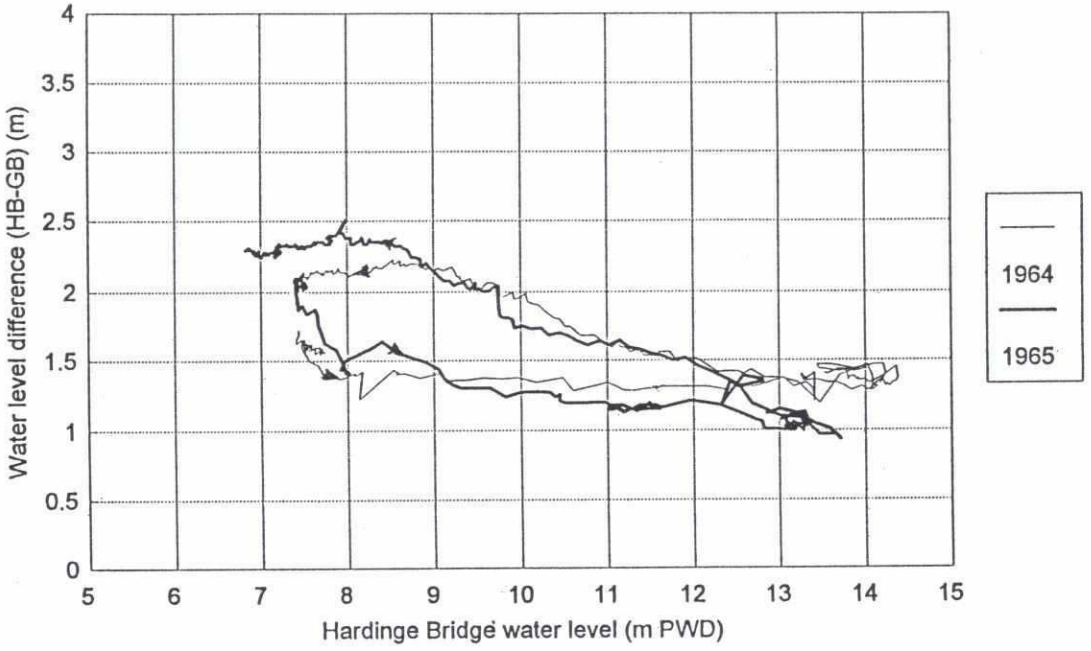


## Water level differences

Hardinge Bridge to Gorai Rly. Bridge

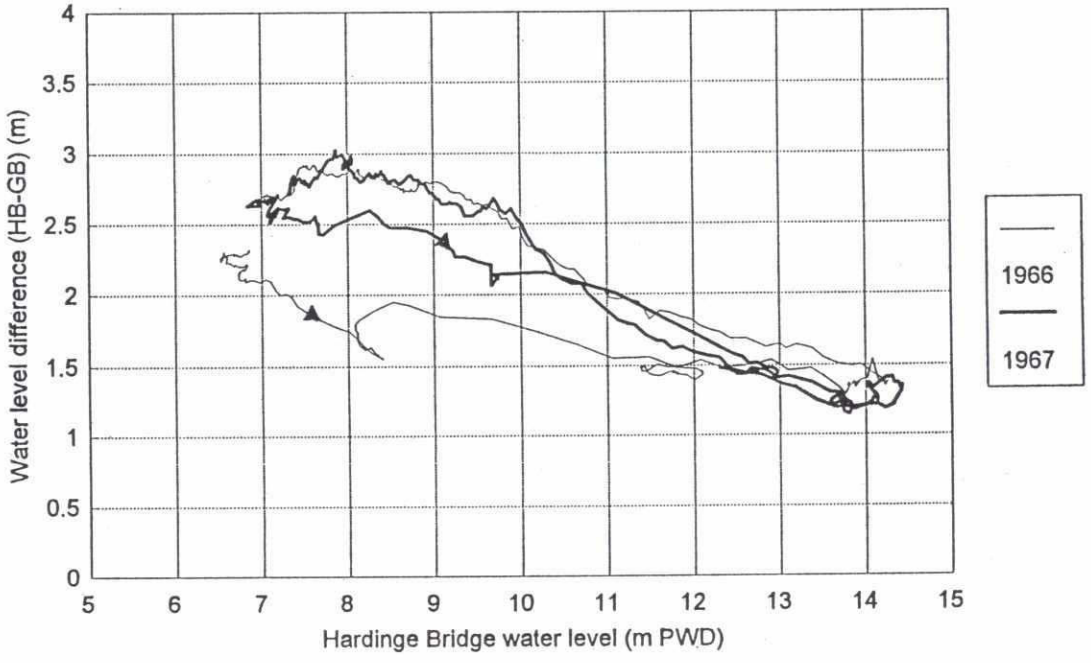

2326

## Water level differences

Hardinge Bridge to Gorai Rly. Bridge

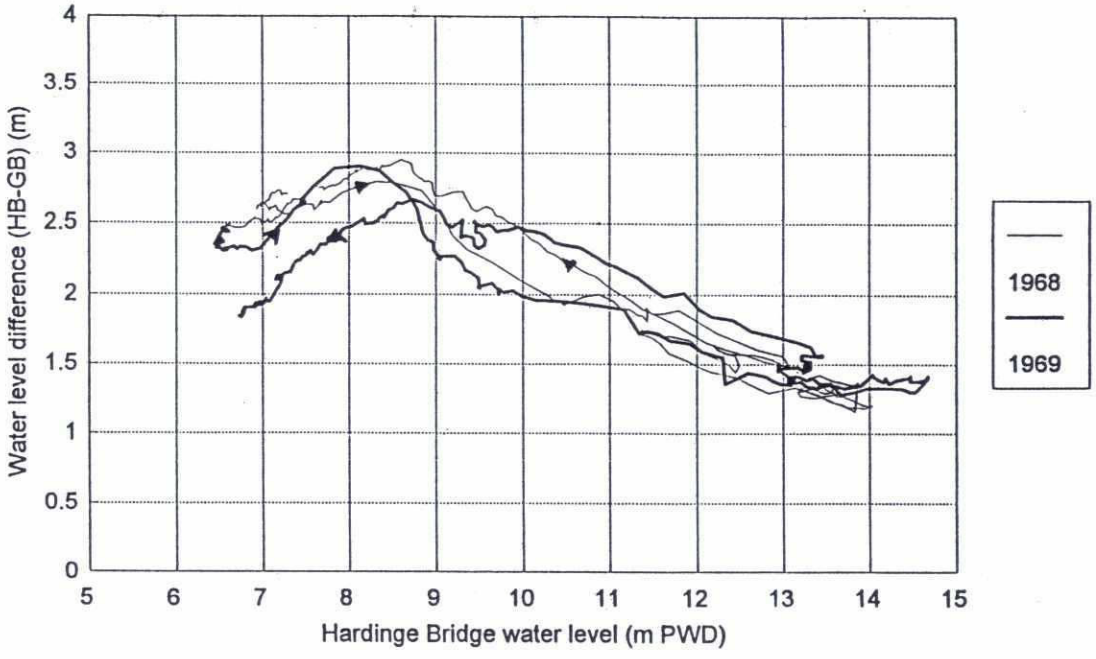


## Water level differences

Hardinge Bridge to Gorai Rly. Bridge

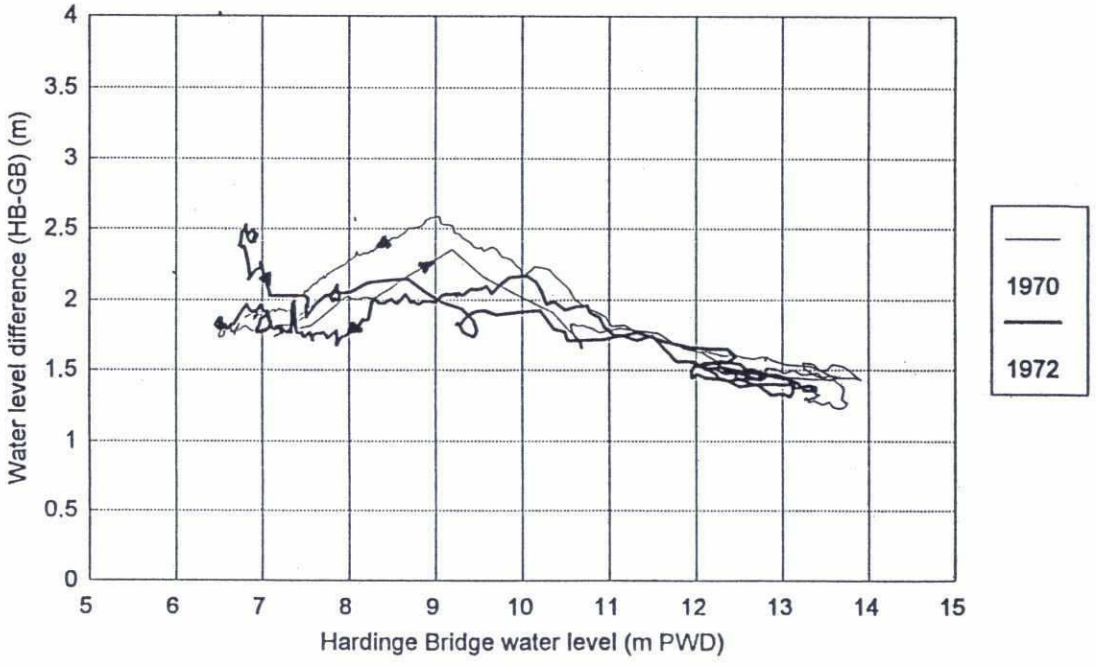

## Water level differences
Hardinge Bridge to Gorai Rly. Bridge

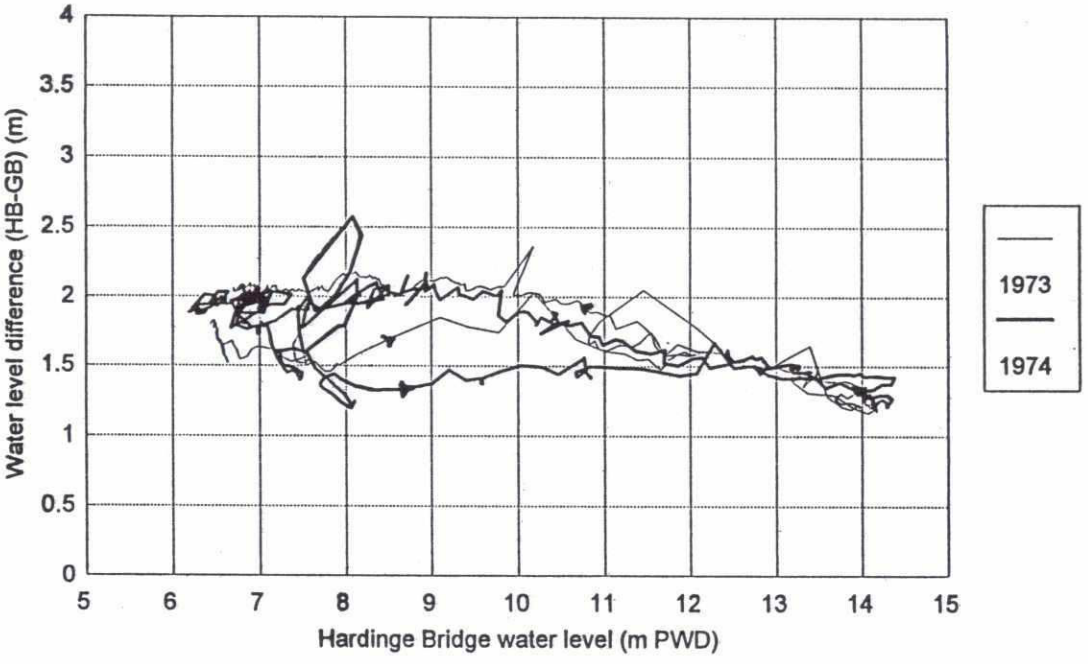


## Water level differences
Hardinge Bridge to Gorai Rly. Bridge

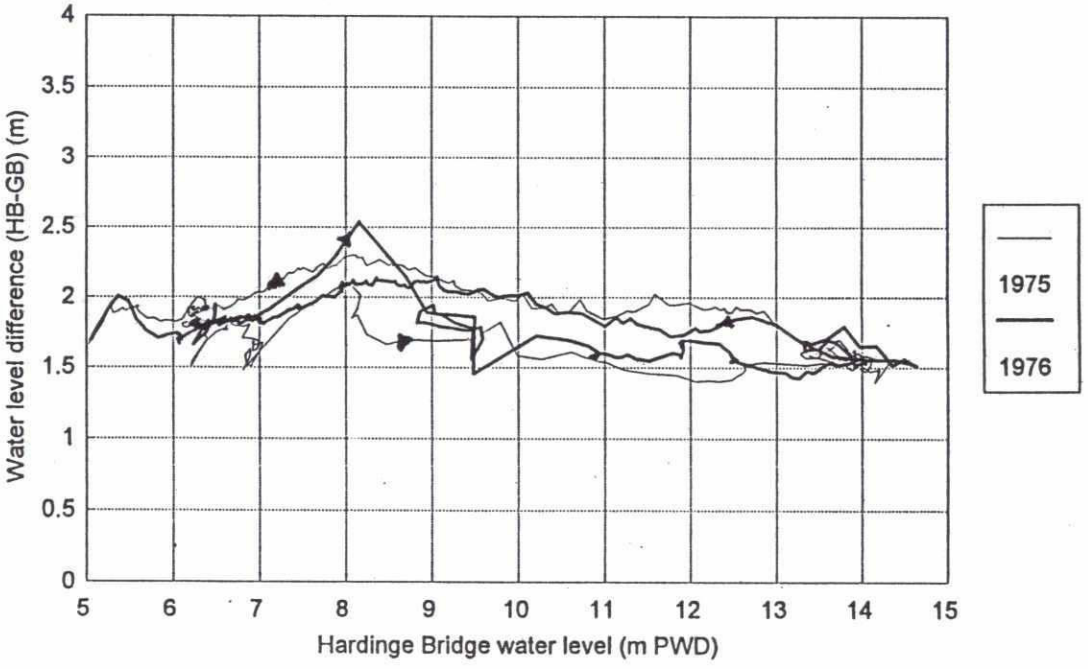

## Water level differences

Hardinge Bridge to Gorai Rly. Bridge

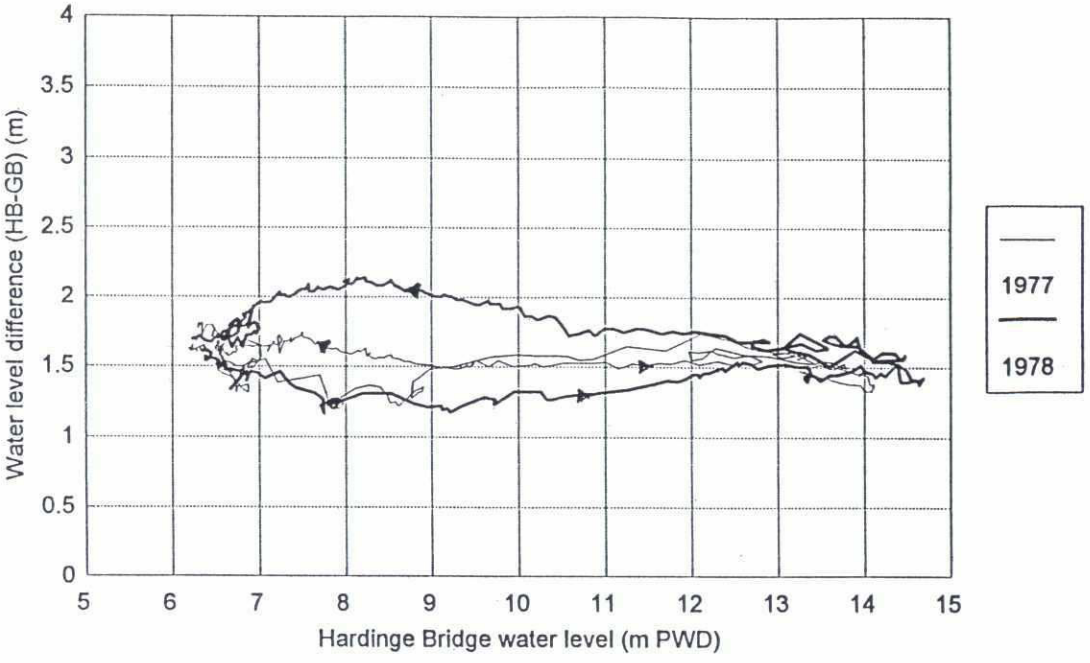


## Water level differences

Hardinge Bridge to Gorai Rly. Bridge

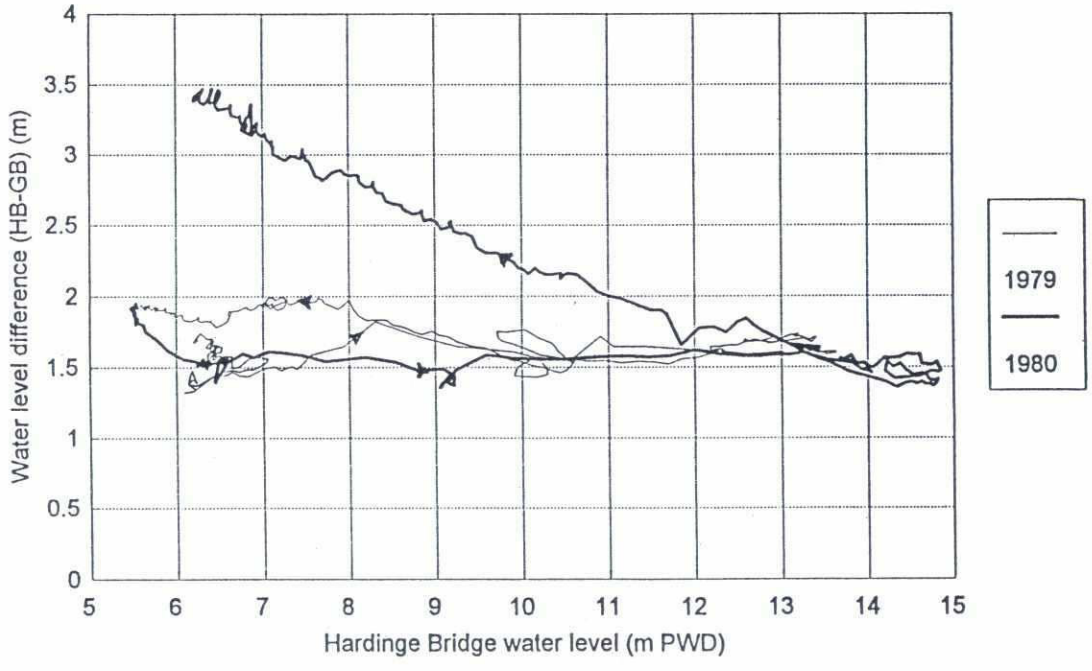

## Water level differences

Hardinge Bridge to Gorai Rly. Bridge

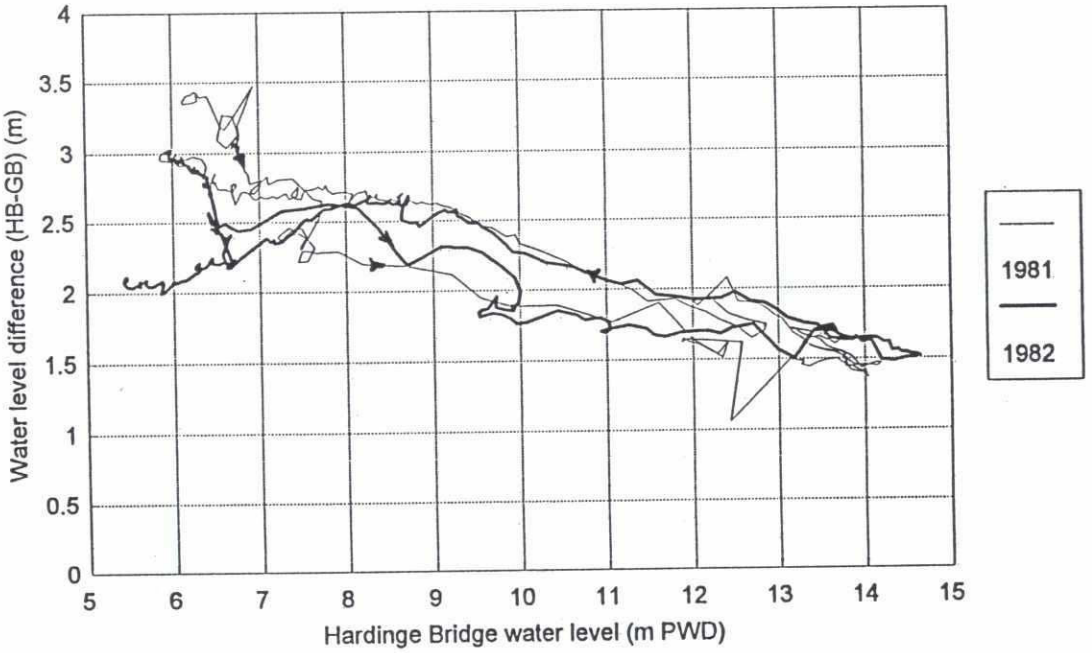




## Water level differences

Hardinge Bridge to Gorai Rly. Bridge

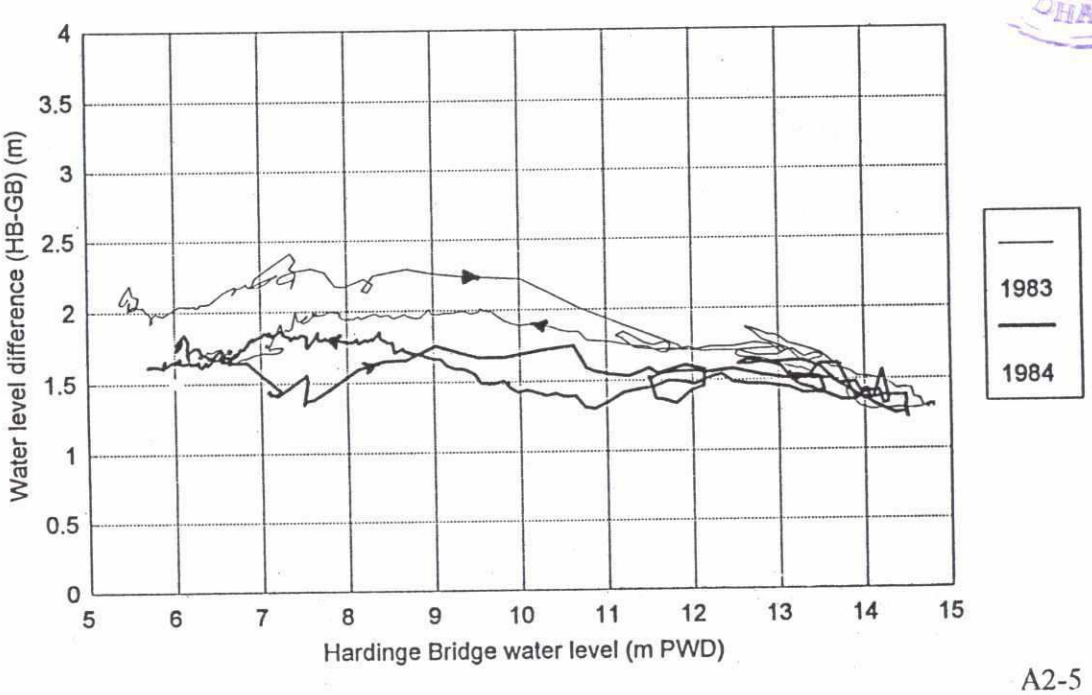

## Water level differences
Hardinge Bridge to Gorai Rly. Bridge

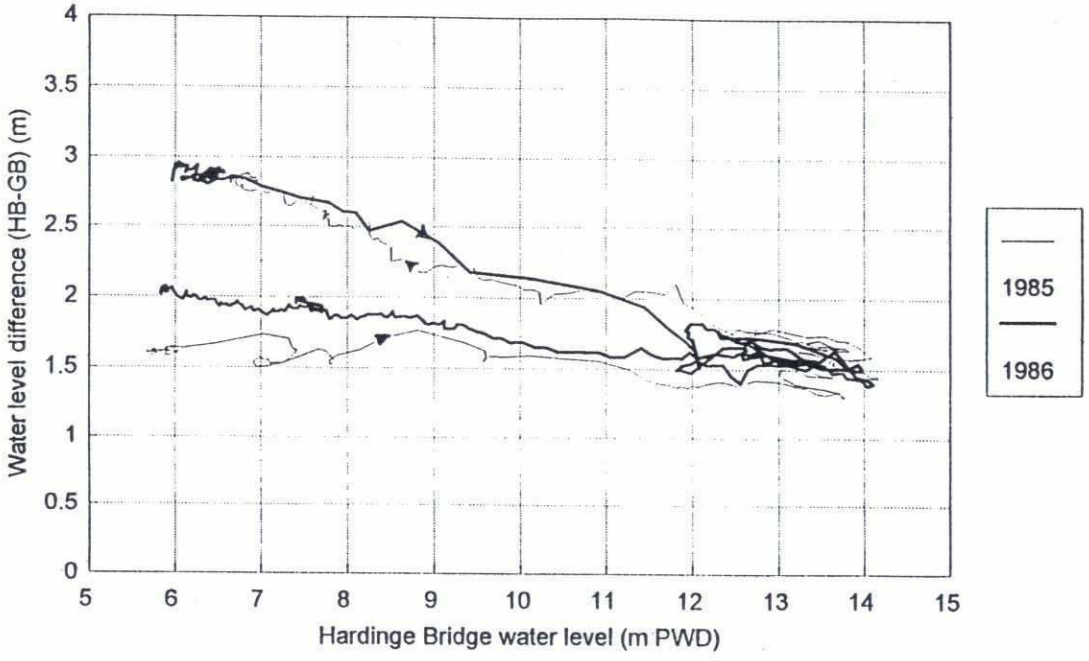


## Water level differences
Hardinge Bridge to Gorai Rly. Bridge

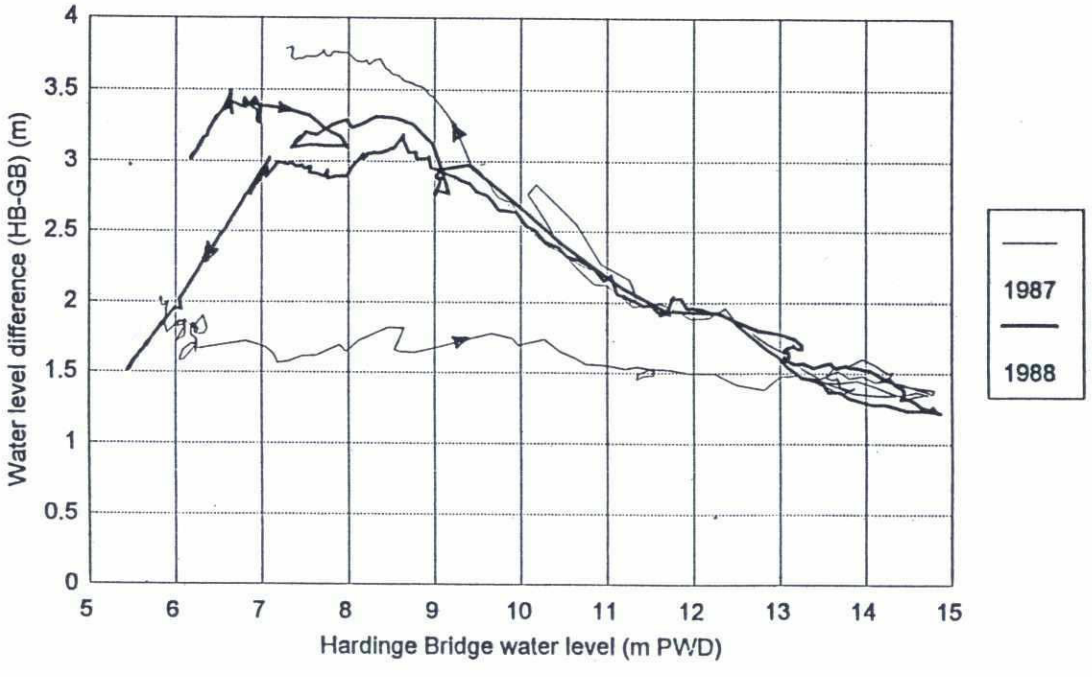

## Water level differences
Hardinge Bridge to Gorai Rly. Bridge

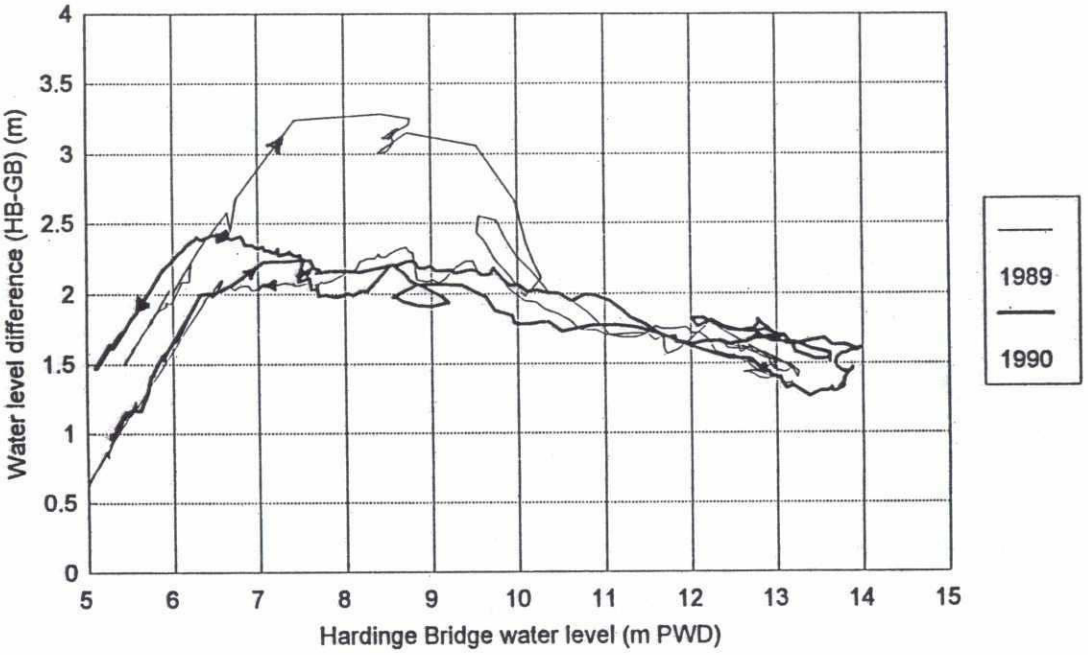


## Water level differences
Hardinge Bridge to Gorai Rly. Bridge

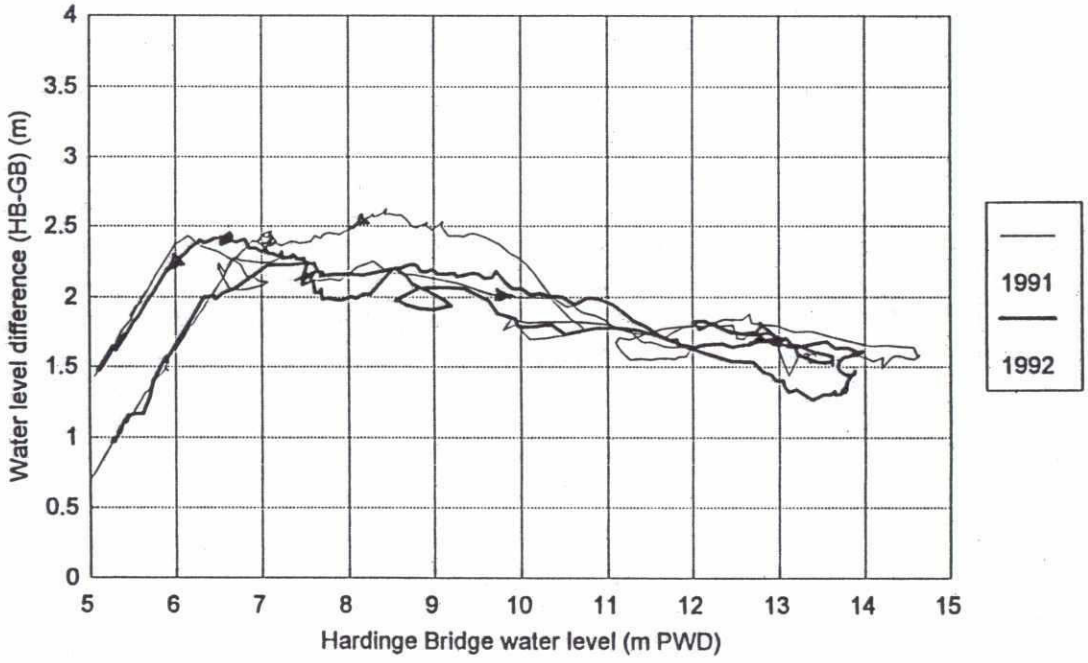

## Water level difference

Hardinge Bridge to Gorai Rly. Bridge

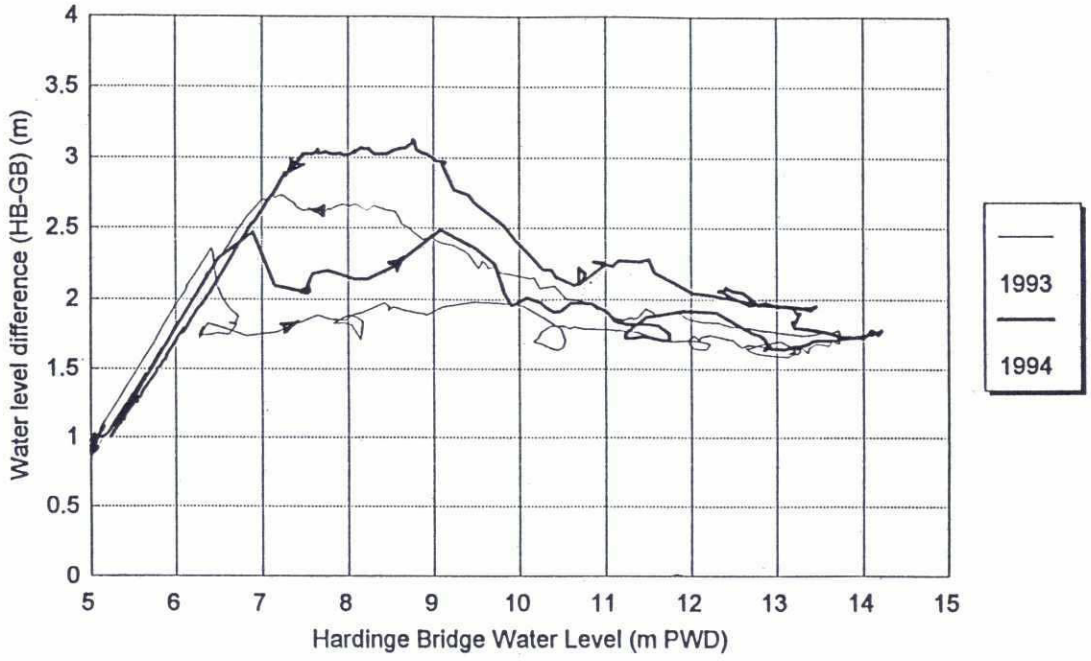


## Water level difference

Hardinge Bridge to Gorai Rly. Bridge

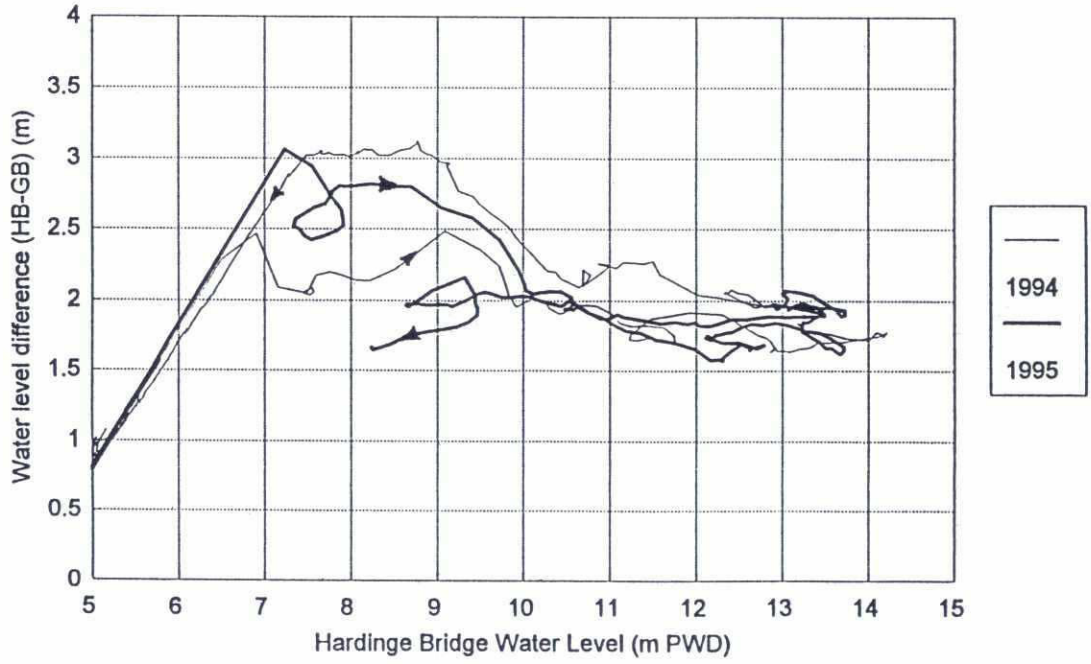

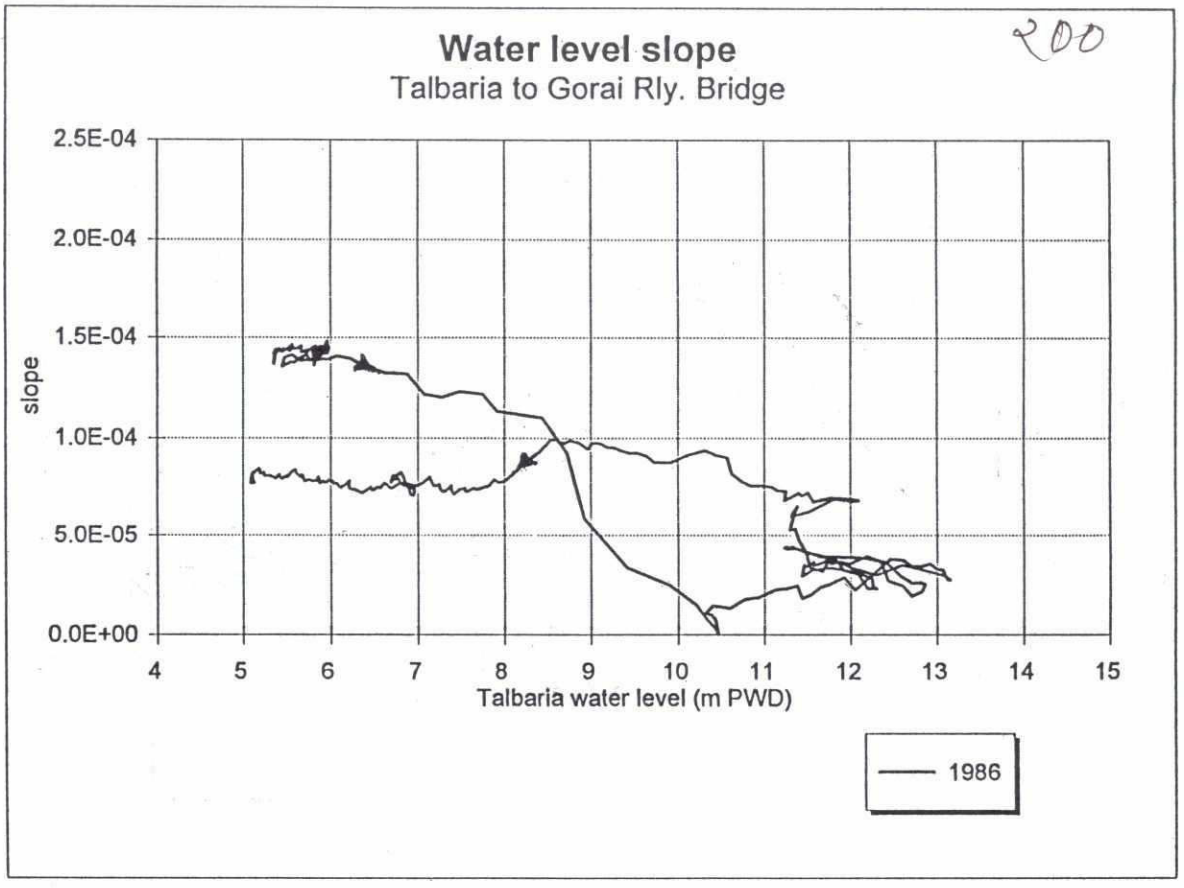
Water level slope
Talbaria to Gorai Rly. Bridge
2.5E-04
2.0E-04
1.5E-04
1.0E-04
5.0E-05
0.0E+00
slope
4
5
6
7
8
9
10
11
12
13
14
15
Talbaria water level (m PWD)
1986

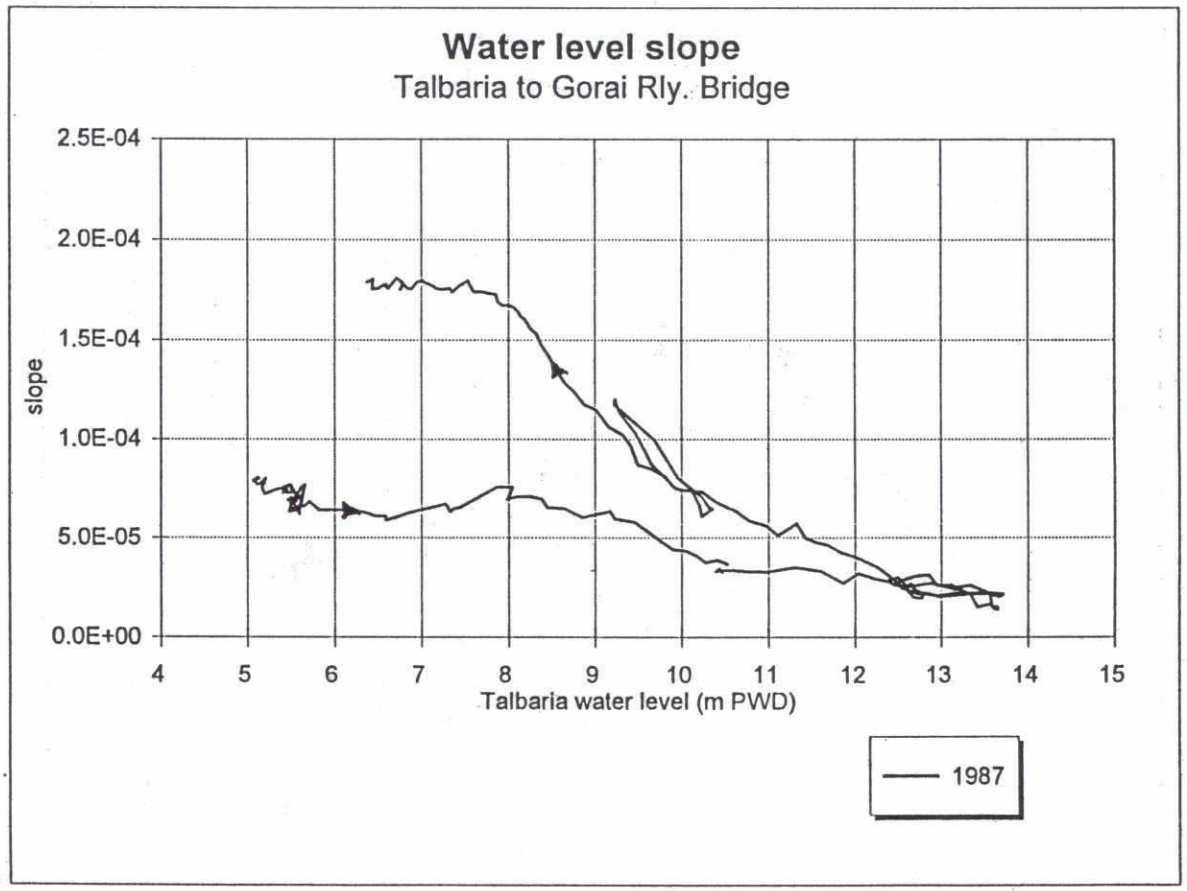
Water level slope
Talbaria to Gorai Rly. Bridge
2.5E-04
2.0E-04
1.5E-04
1.0E-04
5.0E-05
0.0E+00
slope
4
5
6
7
8
9
10
11
12
13
14
15
Talbaria water level (m PWD)
1987

P02

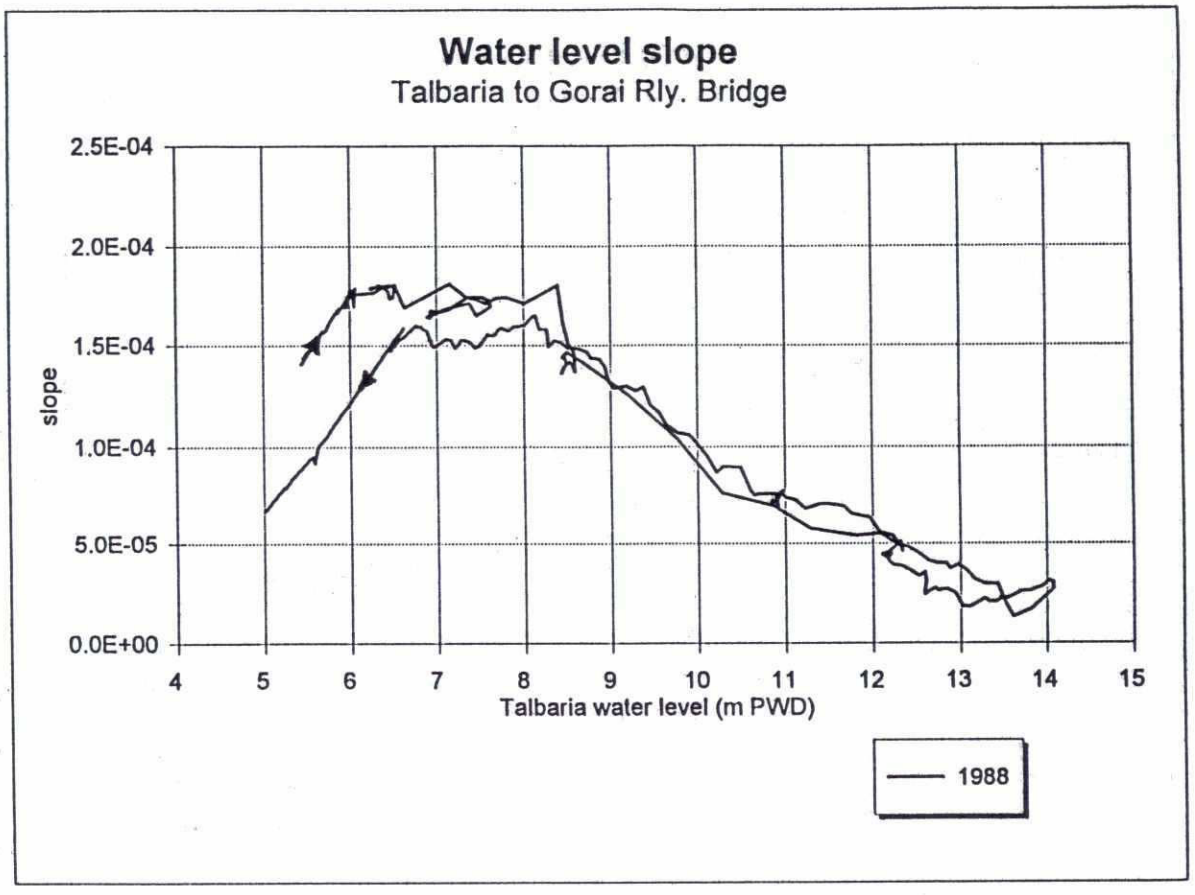
Water level slope
Talbaria to Gorai Rly. Bridge
2.5E-04
2.0E-04
1.5E-04
1.0E-04
5.0E-05
0.0E+00
slope
4
5
6
7
8
9
10
11
12
13
14
15
Talbaria water level (m PWD)
1988

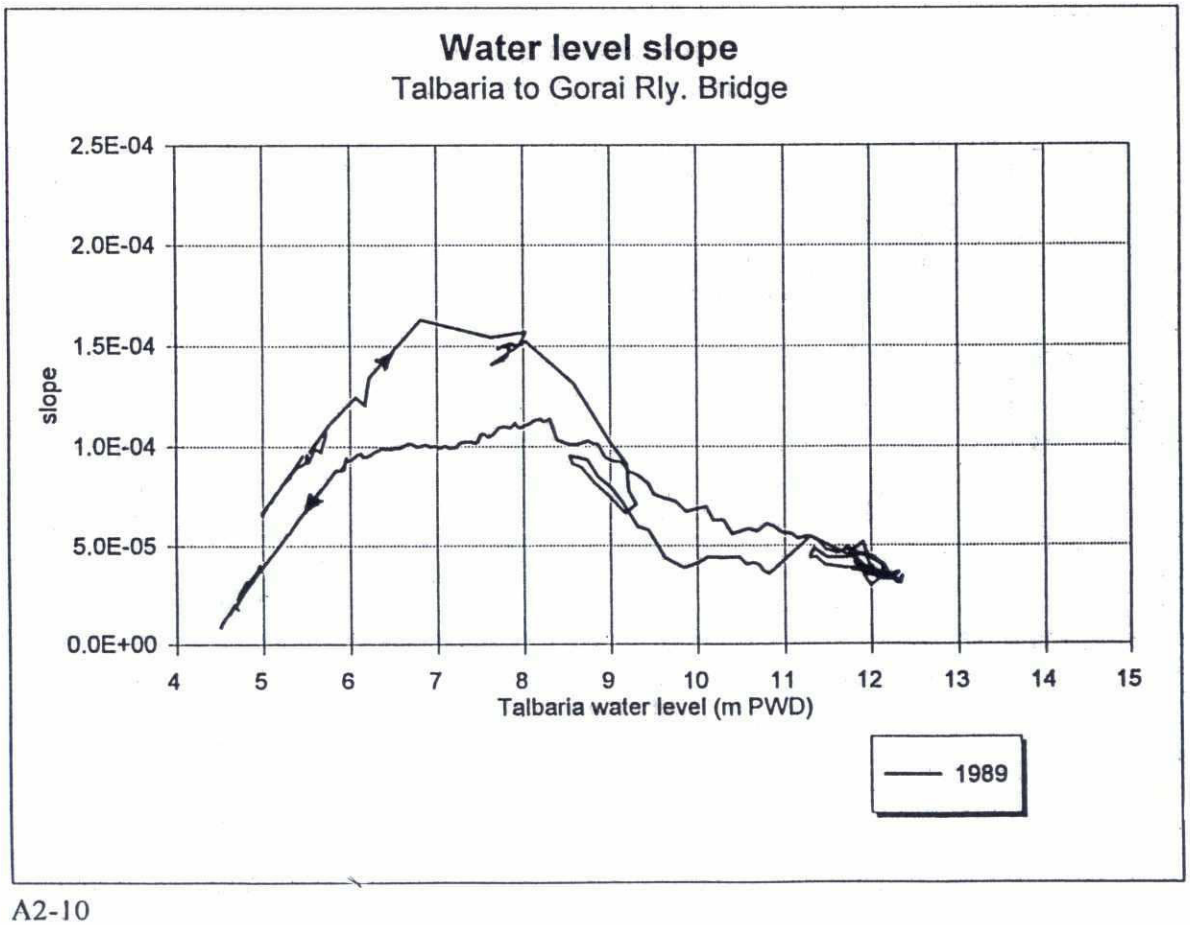
Water level slope
Talbaria to Gorai Rly. Bridge
2.5E-04
2.0E-04
1.5E-04
1.0E-04
5.0E-05
0.0E+00
slope
4
5
6
7
8
9
10
11
12
13
14
15
Talbaria water level (m PWD)
1989

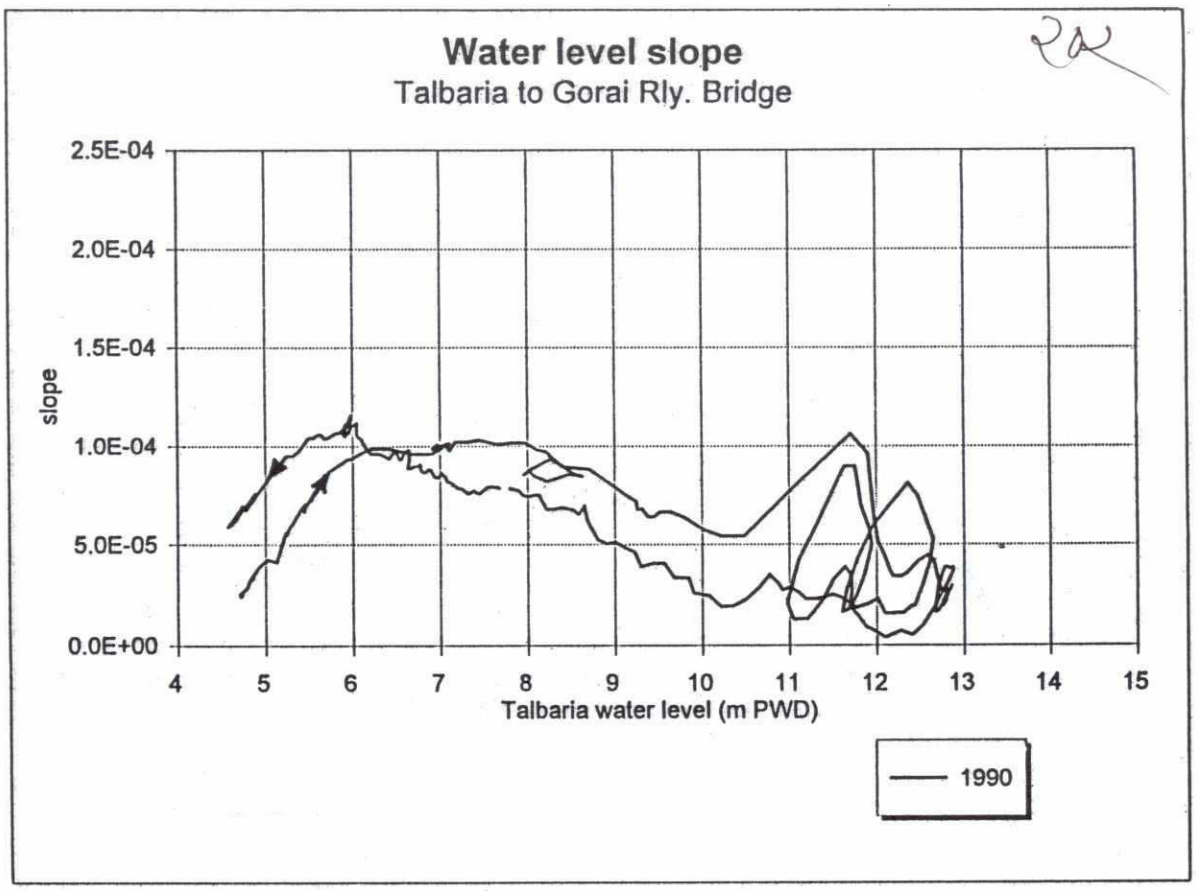
Water level slope
Talbaria to Gorai Rly. Bridge
2.5E-04
2.0E-04
1.5E-04
1.0E-04
5.0E-05
0.0E+00
slope
4
5
6
7
8
9
10
11
12
13
14
15
Talbaria water level (m PWD)
1990

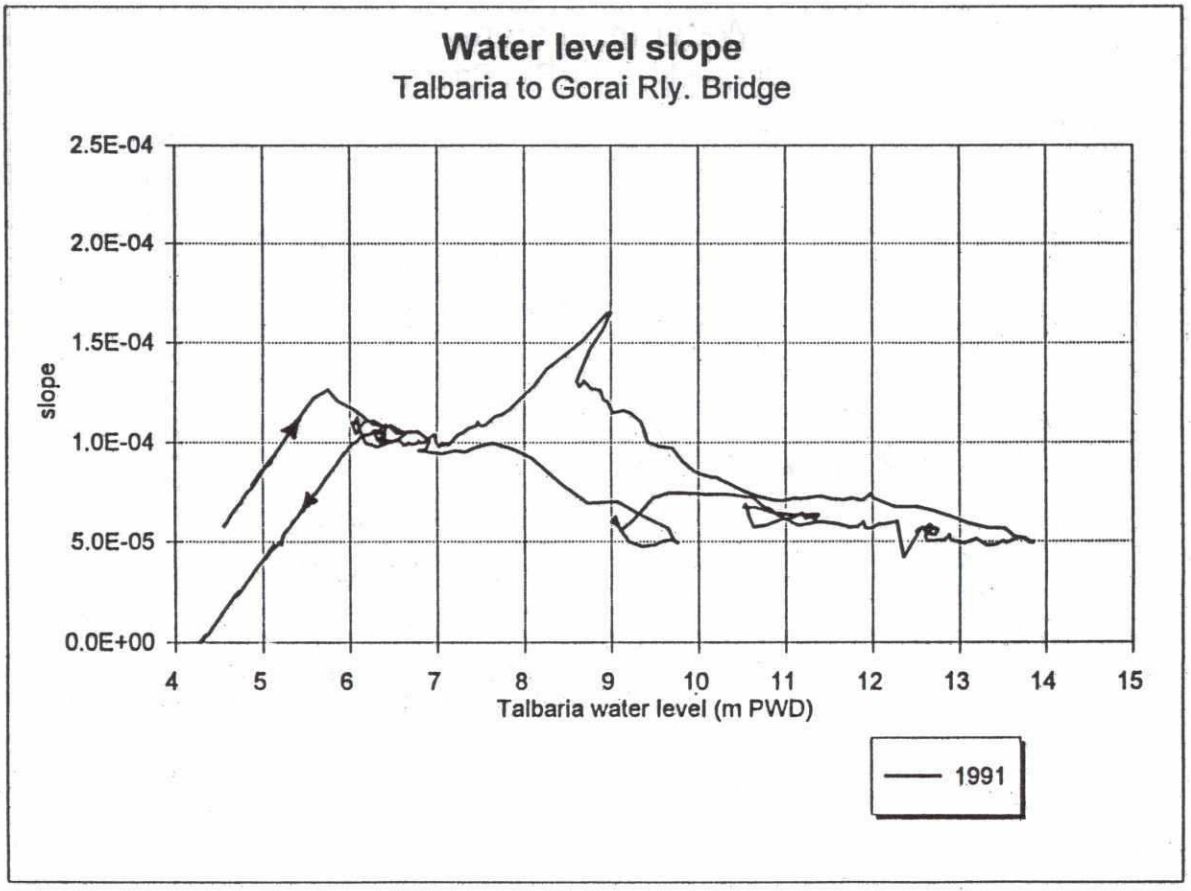
Water level slope
Talbaria to Gorai Rly. Bridge
2.5E-04
2.0E-04
1.5E-04
1.0E-04
5.0E-05
0.0E+00
slope
4
5
6
7
8
9
10
11
12
13
14
15
Talbaria water level (m PWD)
1991

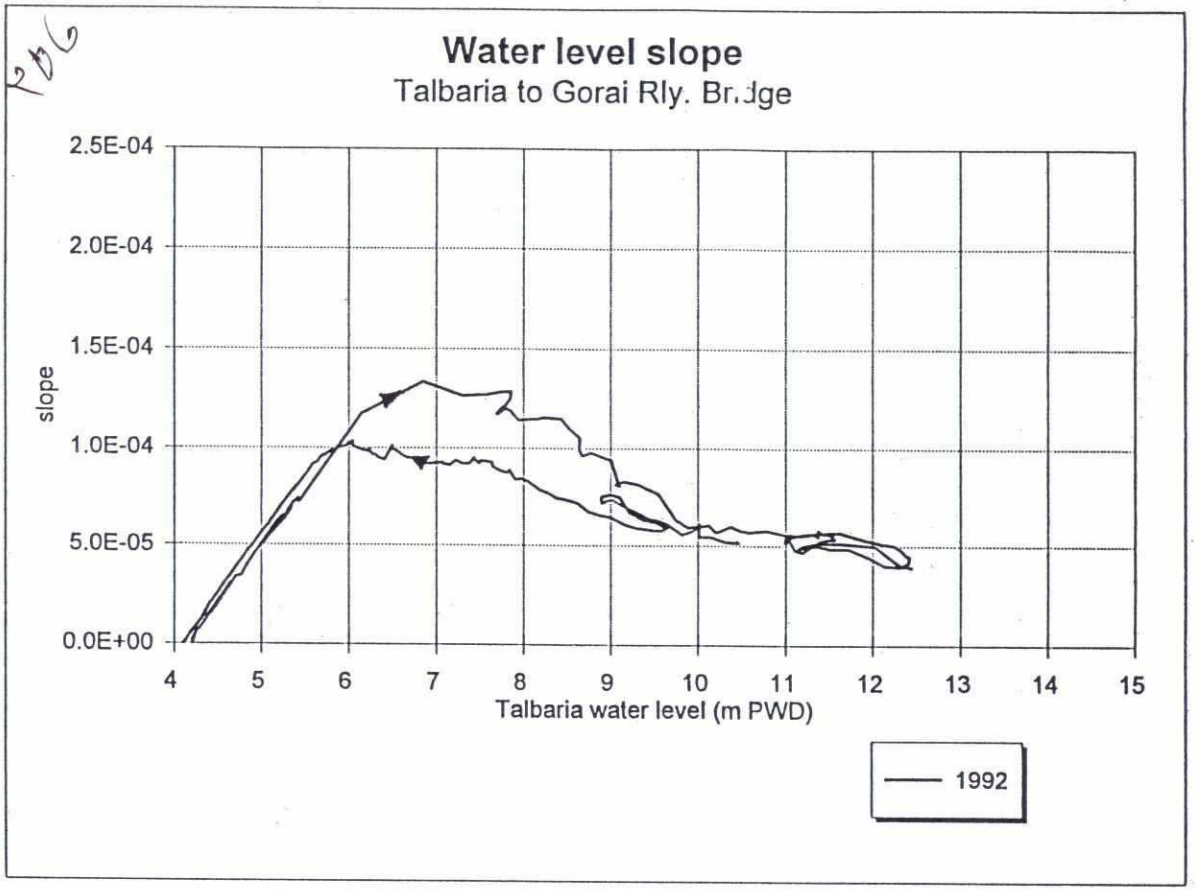
Water level slope
Talbaria to Gorai Rly. Bridge
2.5E-04
2.0E-04
1.5E-04
1.0E-04
5.0E-05
0.0E+00
slope
4
5
6
7
8
9
10
11
12
13
14
15
Talbaria water level (m PWD)
1992

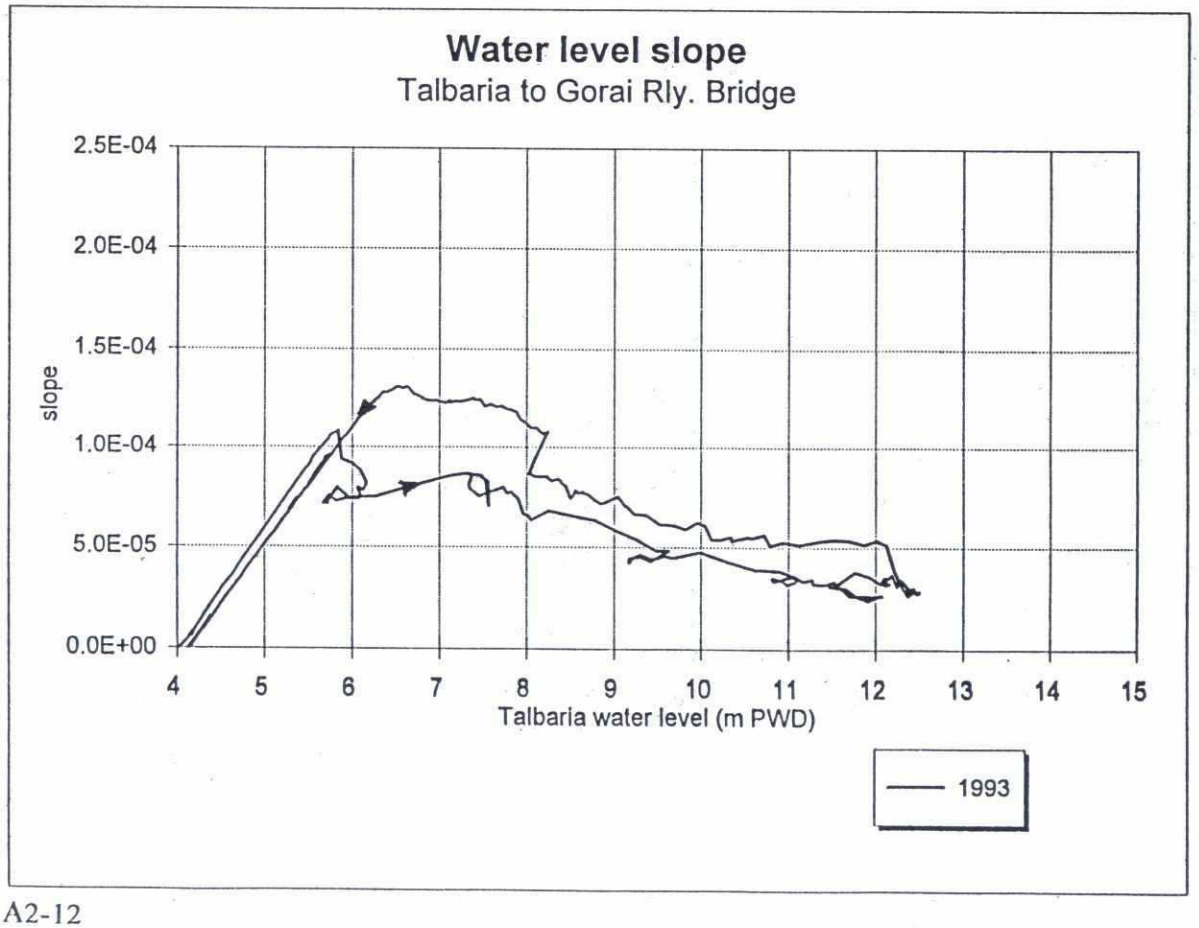
Water level slope
Talbaria to Gorai Rly. Bridge
2.5E-04
2.0E-04
1.5E-04
1.0E-04
5.0E-05
0.0E+00
slope
4
5
6
7
8
9
10
11
12
13
14
15
Talbaria water level (m PWD)
1993

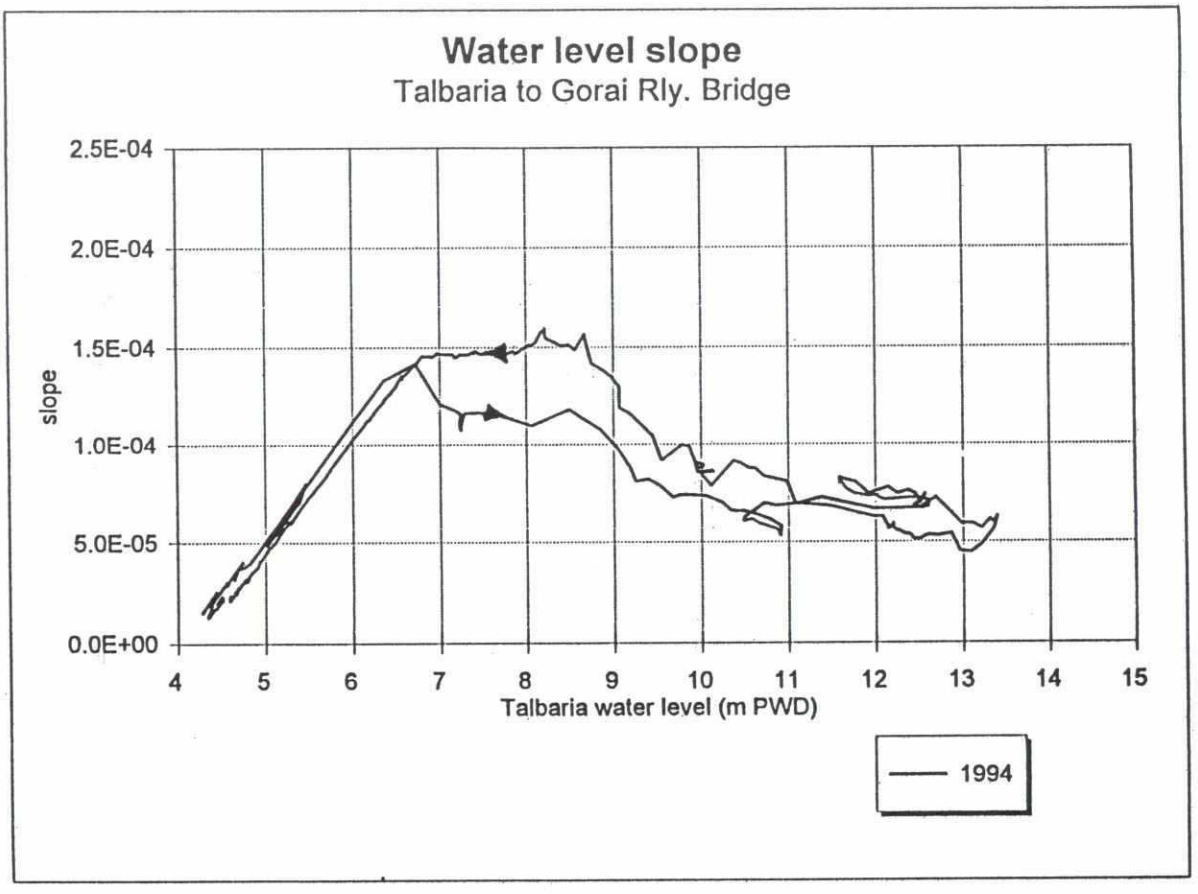
Water level slope
Talbaria to Gorai Rly. Bridge
2.5E-04
2.0E-04
1.5E-04
1.0E-04
5.0E-05
0.0E+00
slope
4
5
6
7
8
9
10
11
12
13
14
15
Talbaria water level (m PWD)
1994

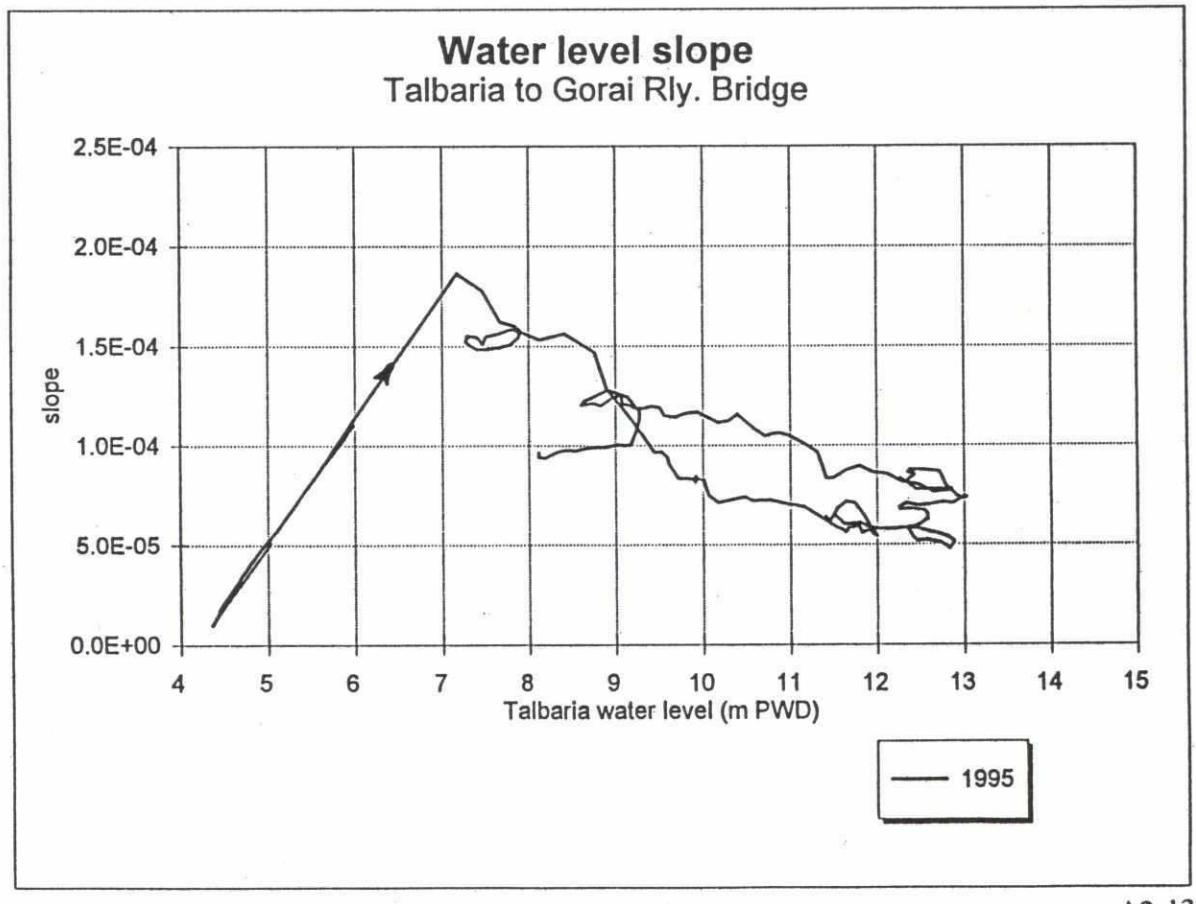
Water level slope
Talbaria to Gorai Rly. Bridge
2.5E-04
2.0E-04
1.5E-04
1.0E-04
5.0E-05
0.0E+00
slope
4
5
6
7
8
9
10
11
12
13
14
15
Talbaria water level (m PWD)
1995

## Appendix 3: Estimated conveyance factors vs. Gorai mouth water level 1964-95

## Estimated conveyance factor

Gorai (Talbaria to Gorai Rly. Bridge)

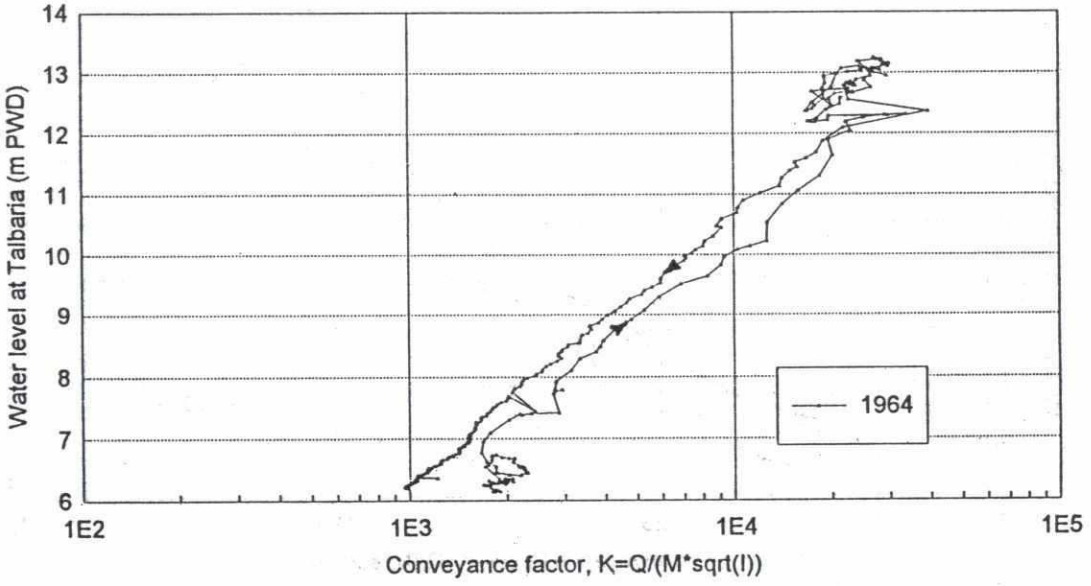


## Estimated conveyance factor

Gorai (Talbaria to Gorai Rly. Bridge)

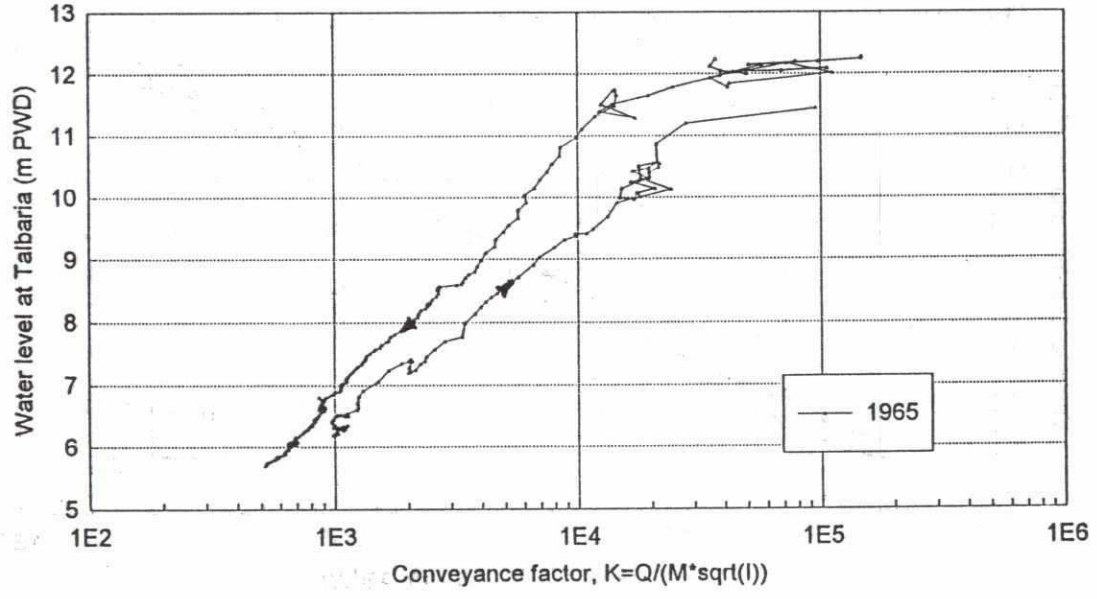

209

## Estimated conveyance factor
Gorai (Talbaria to Gorai Rly. Bridge)

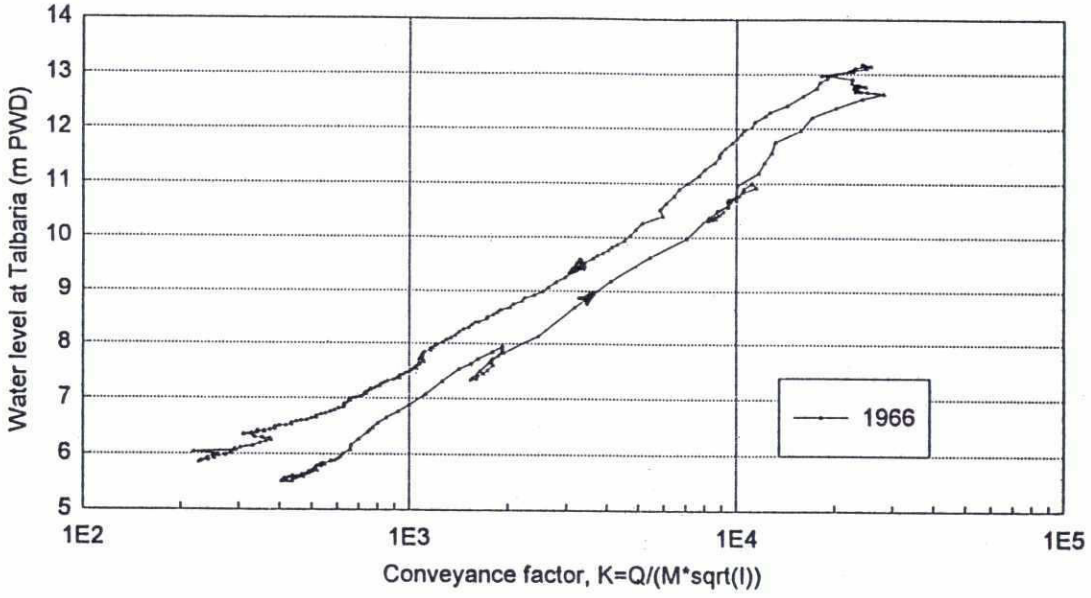


## Estimated conveyance factor
Gorai (Talbaria to Gorai Rly. Bridge)

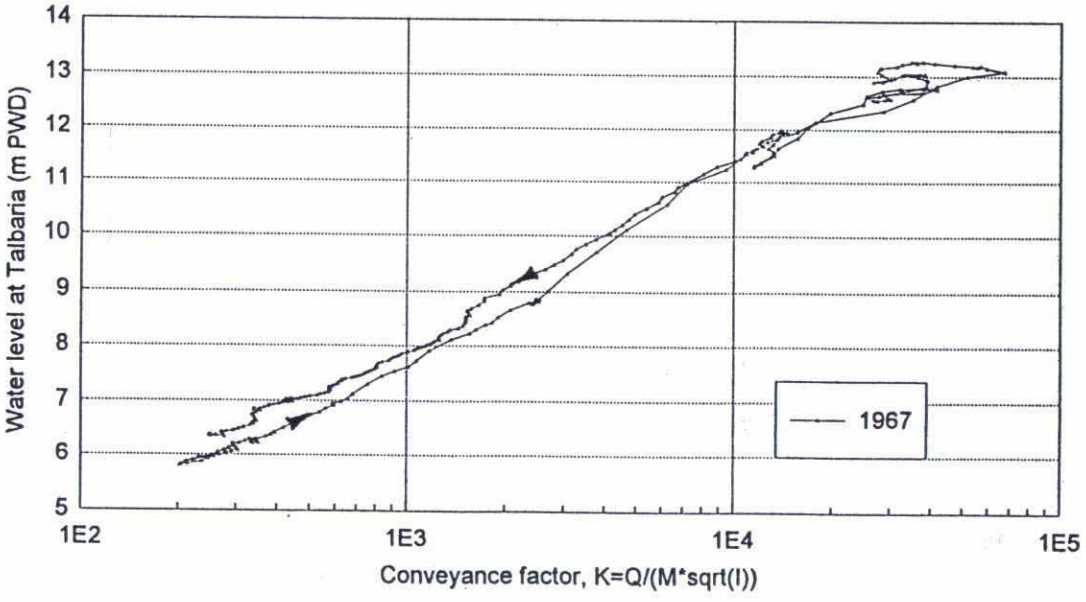

## Estimated conveyance factor
Gorai (Talbaria to Gorai Rly. Bridge)

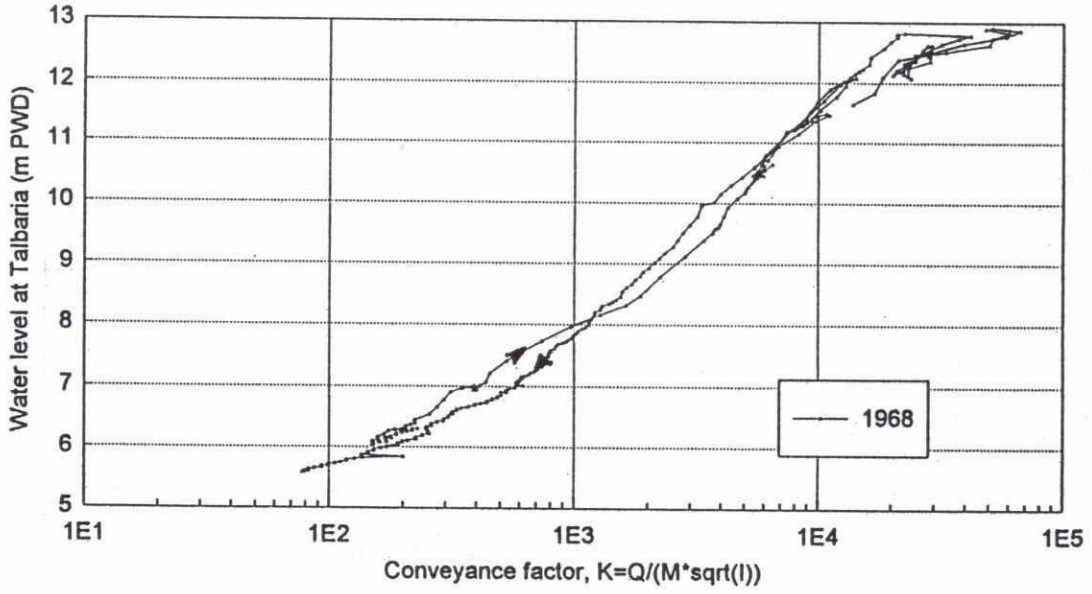


## Estimated conveyance factor
Gorai (Talbaria to Gorai Rly. Bridge)

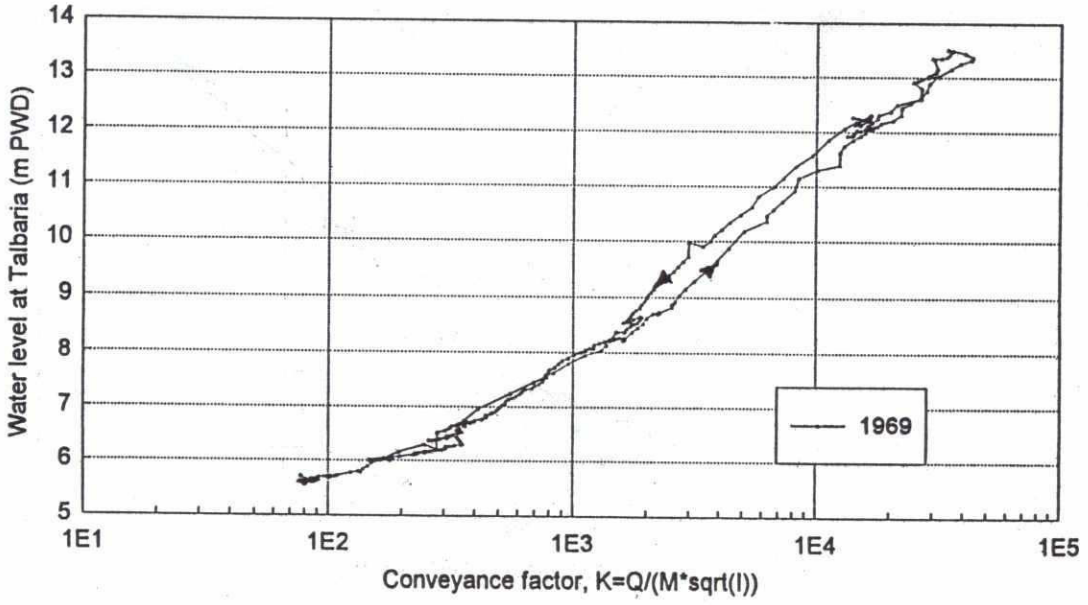

202

## Estimated conveyance factor

Gorai (Talbaria to Gorai Rly. Bridge)

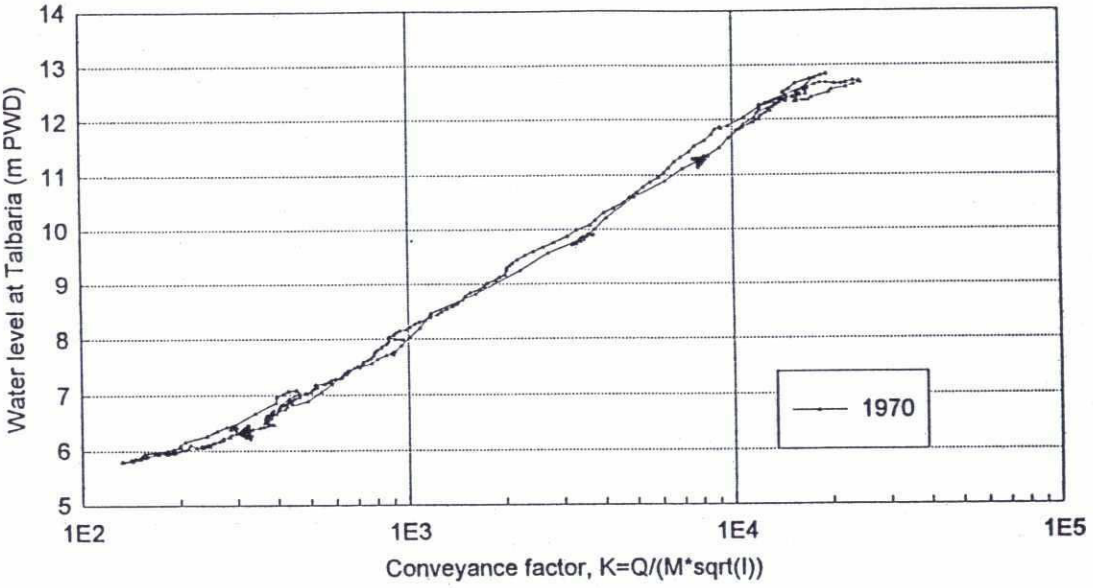


## Estimated conveyance factor

Gorai (Talbaria to Gorai Rly. Bridge)

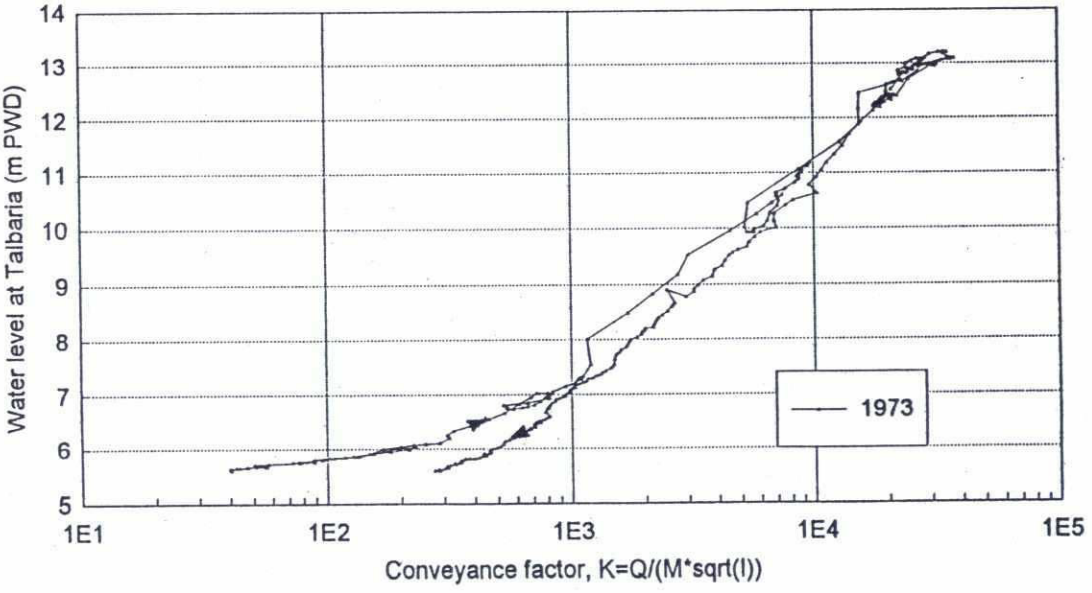

## Estimated conveyance factor
Gorai (Talbaria to Gorai Rly. Bridge)

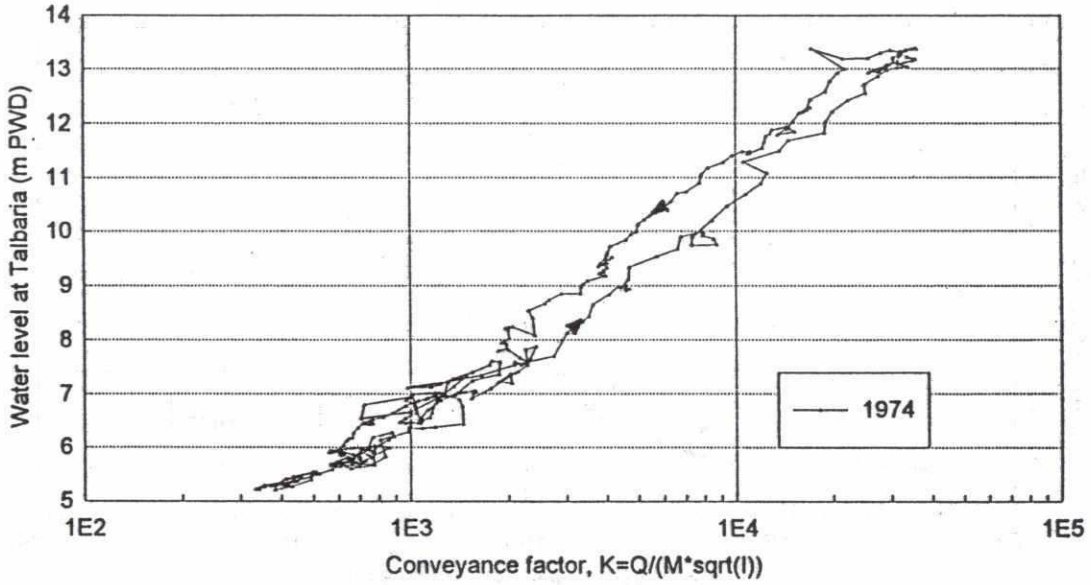


## Estimated conveyance factor
Gorai (Talbaria to Gorai Rly. Bridge)

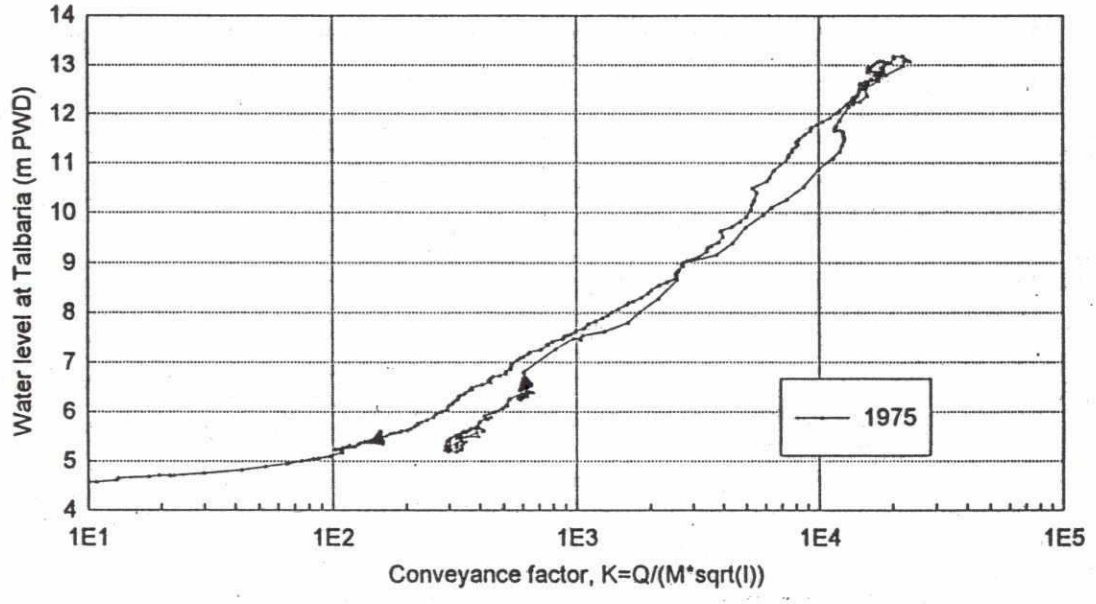

222

## Estimated conveyance factor

Gorai (Talbaria to Gorai Rly. Bridge)

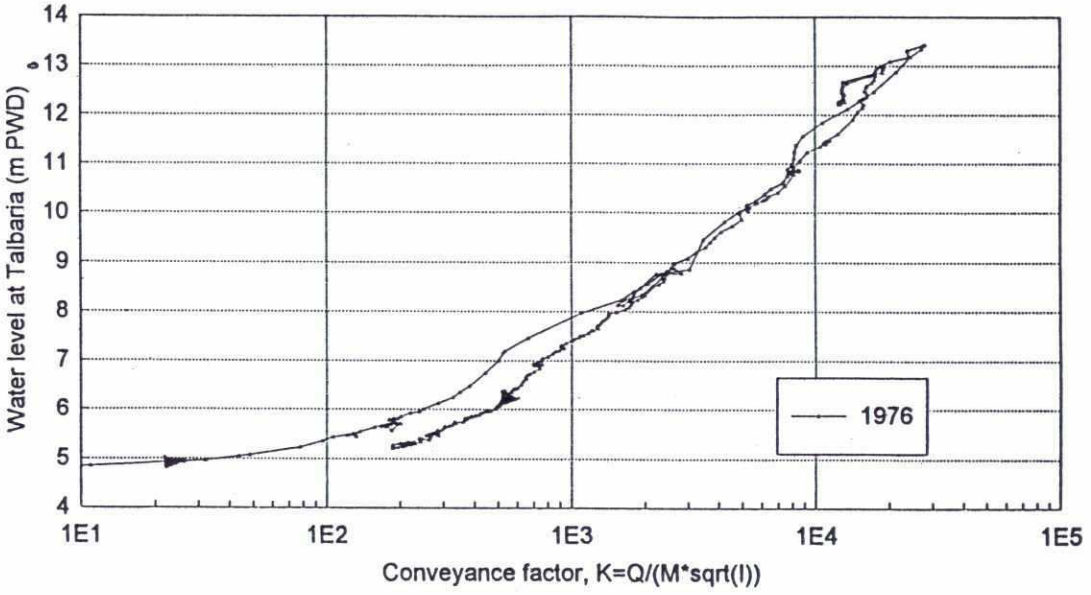


## Estimated conveyance factor

Gorai (Talbaria to Gorai Rly. Bridge)

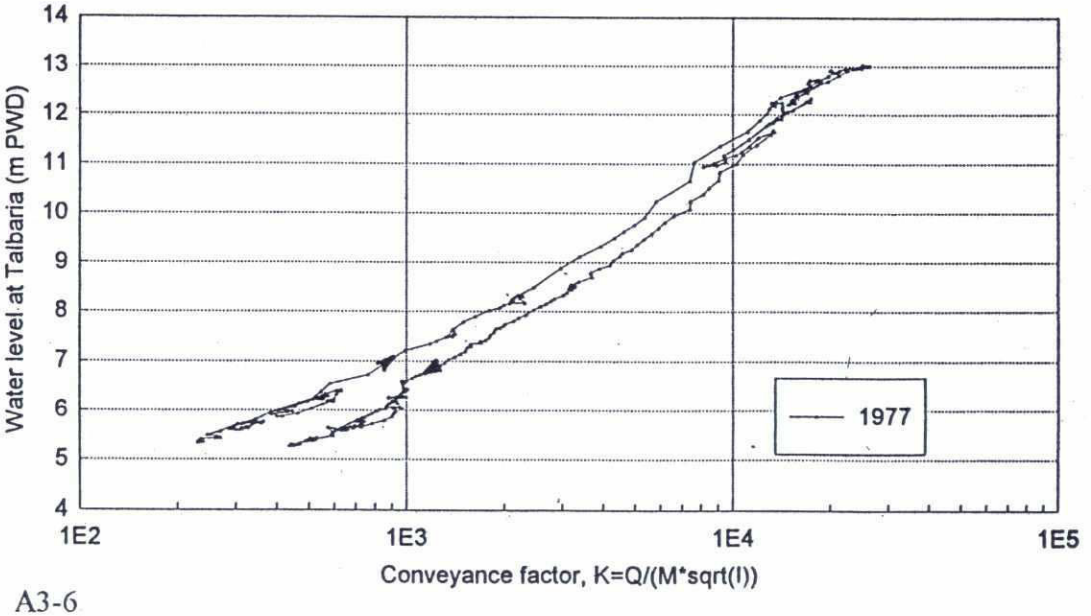

## Estimated conveyance factor

Gorai (Talbaria to Gorai Rly. Bridge)

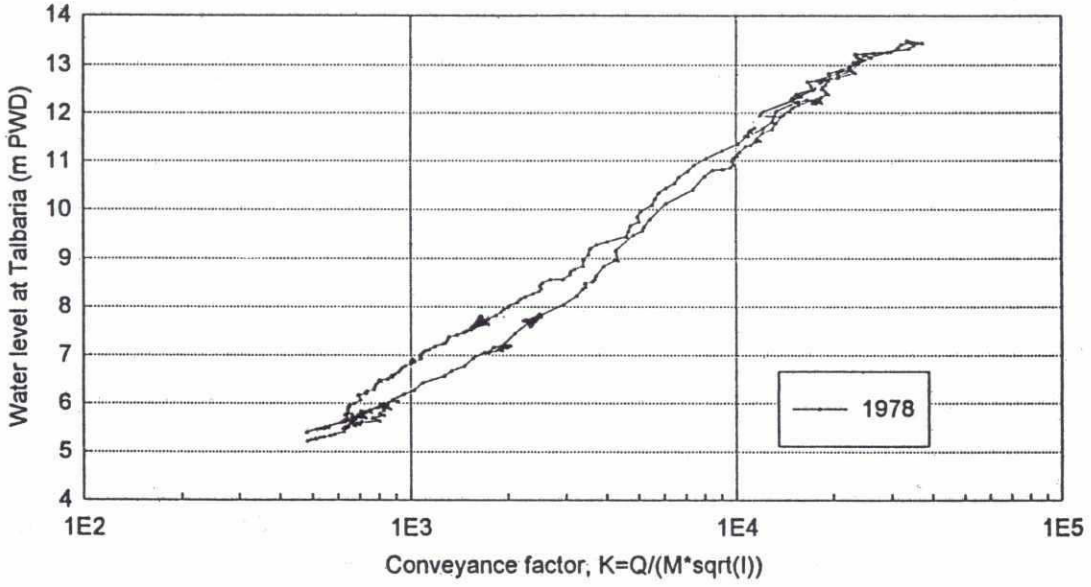


## Estimated conveyance factor

Gorai (Talbaria to Gorai Rly. Bridge)

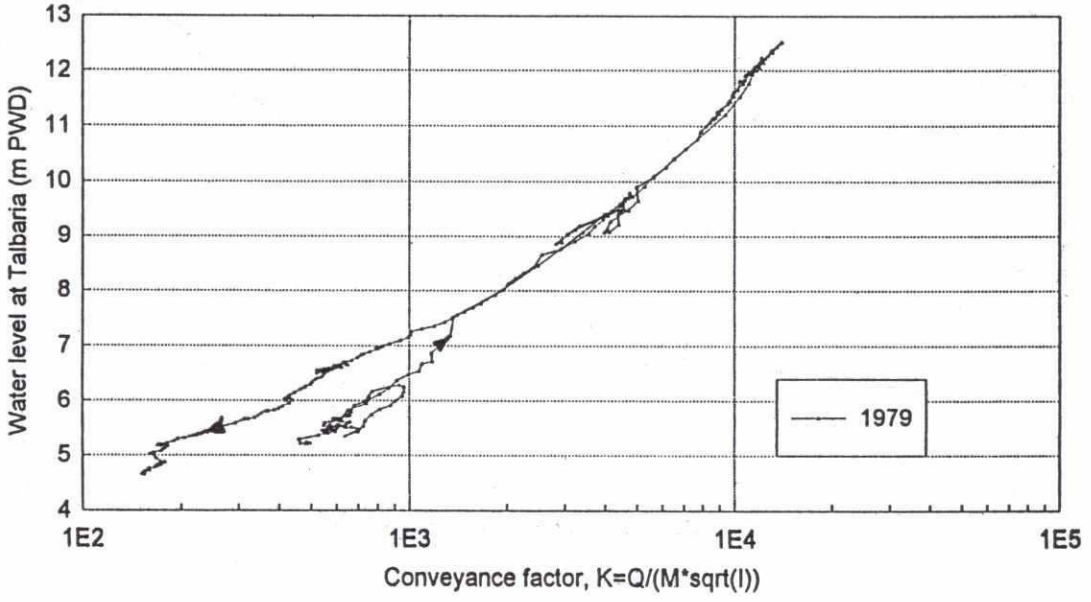

## Estimated conveyance factor
Gorai (Talbaria to Gorai Rly. Bridge)

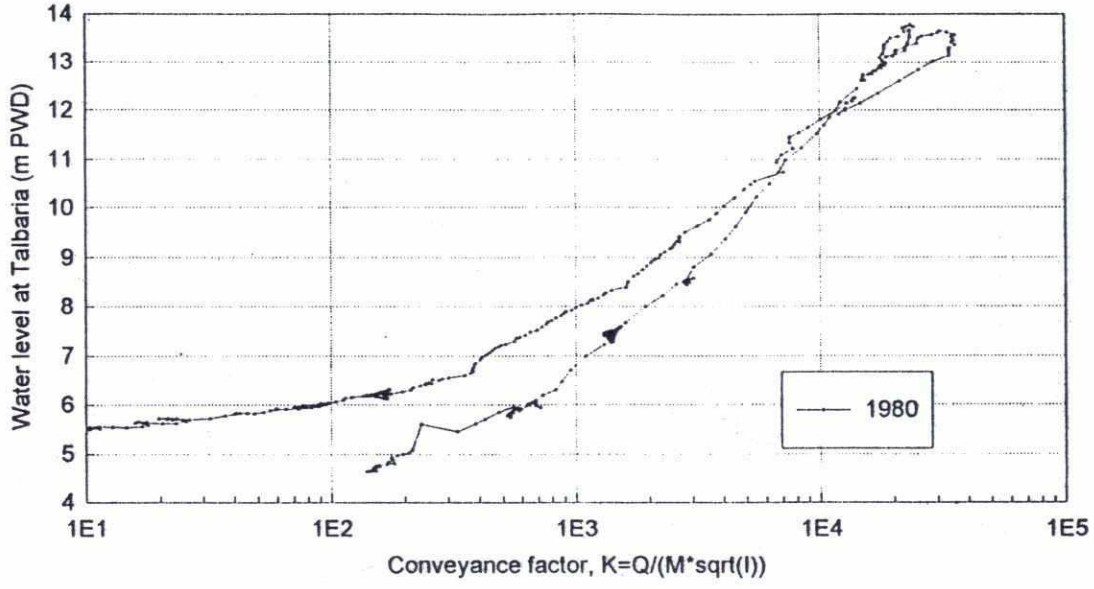


## Estimated conveyance factor
Gorai (Talbaria to Gorai Rly. Bridge)

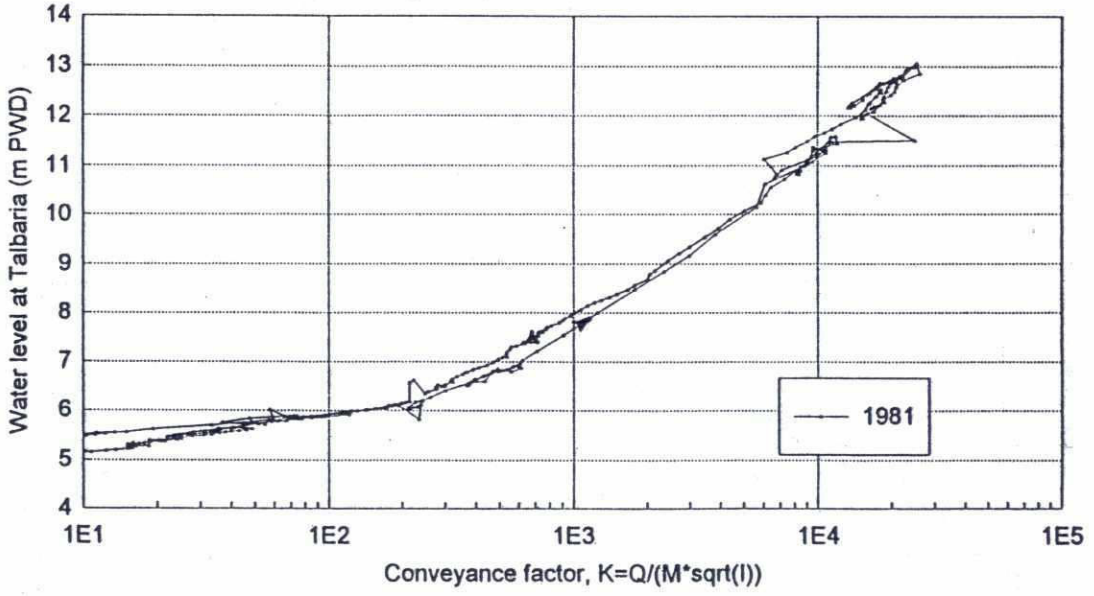

## Estimated conveyance factor

Gorai (Talbaria to Gorai Rly. Bridge)

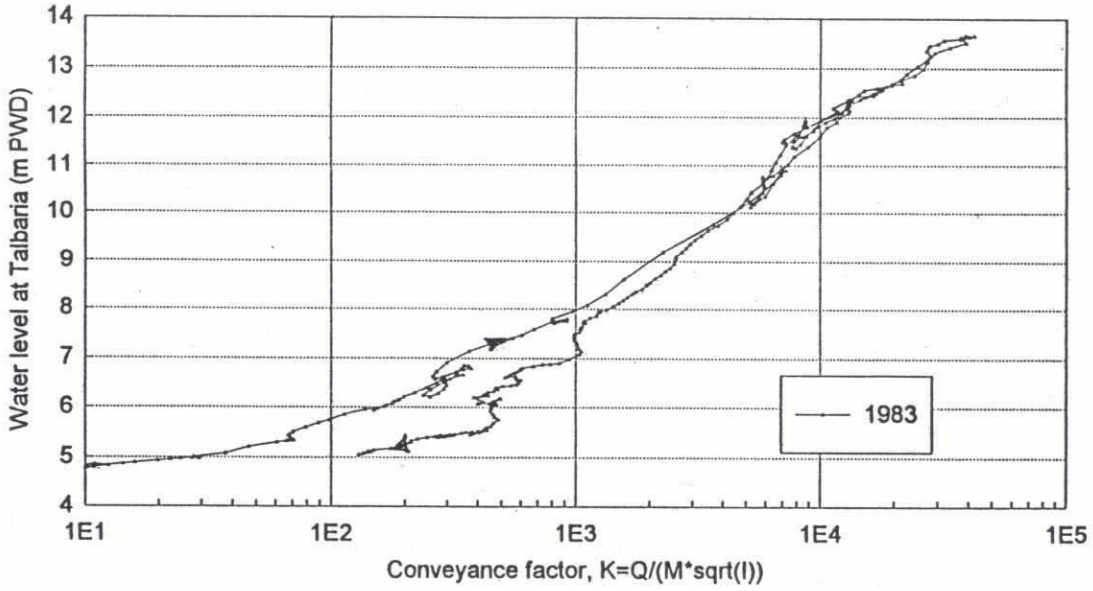


## Estimated conveyance factor

Gorai (Talbaria to Gorai Rly. Bridge)

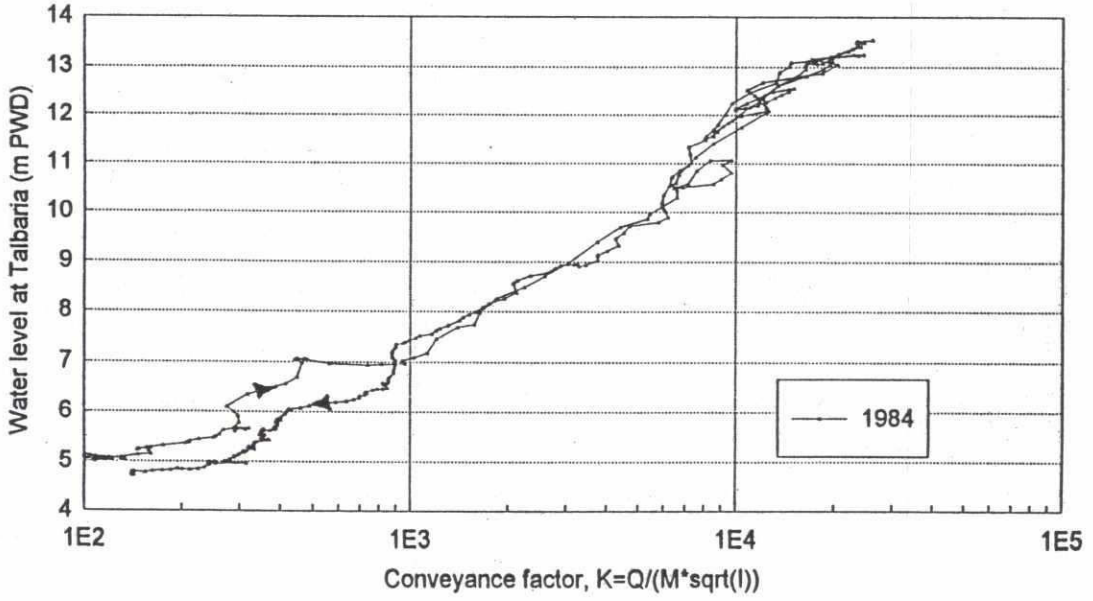

22 a

## Estimated conveyance factor

Gorai (Talbaria to Gorai Rly. Bridge)

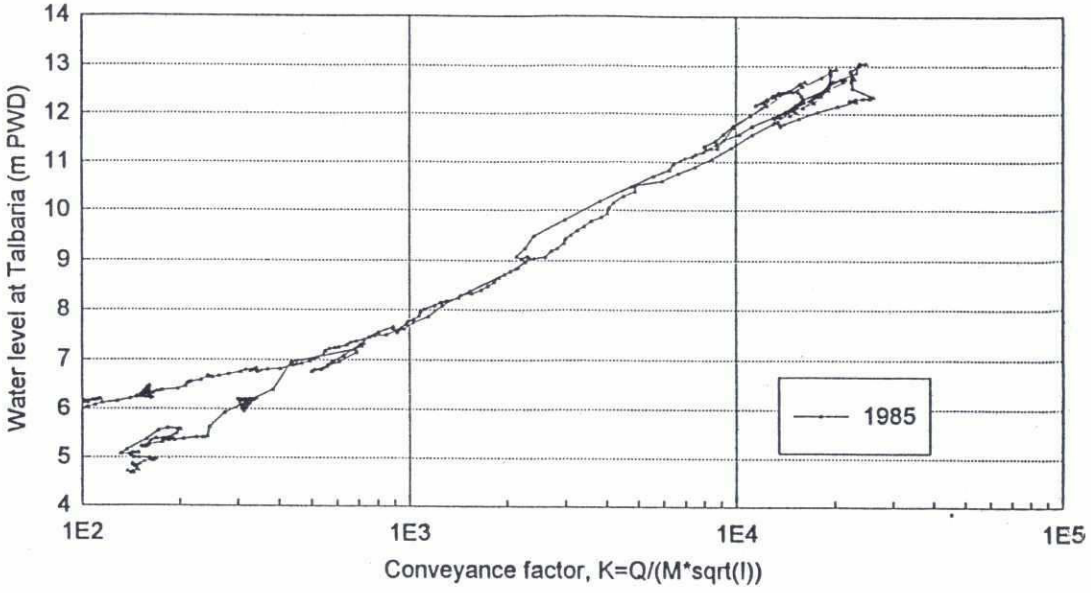


## Estimated conveyance factor

Gorai (Talbaria to Gorai Rly. Bridge)

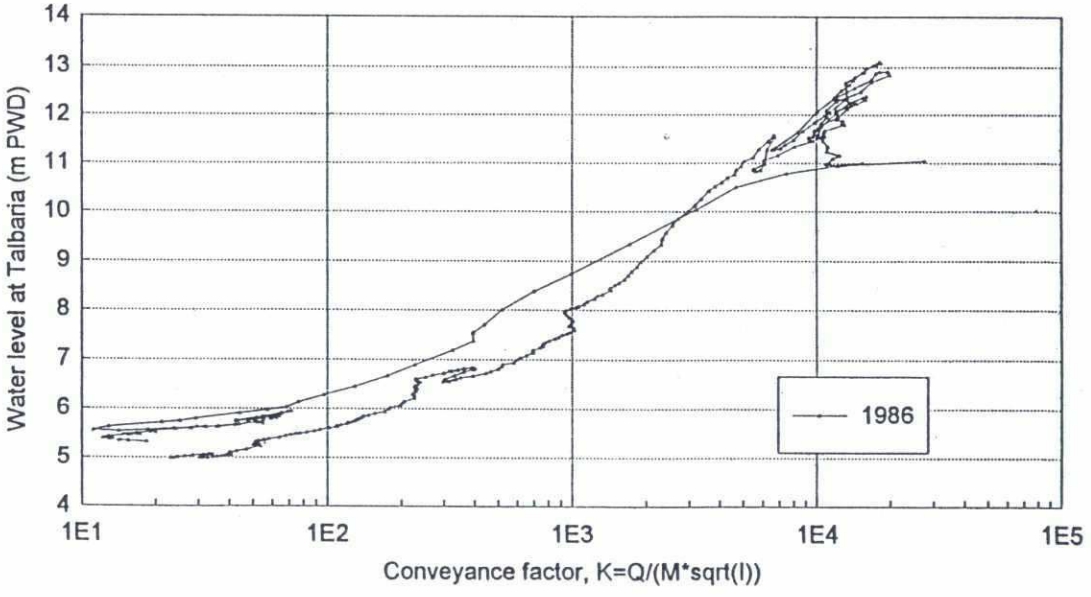

## Estimated conveyance factor
Gorai (Talbaria to Gorai Rly. Bridge)

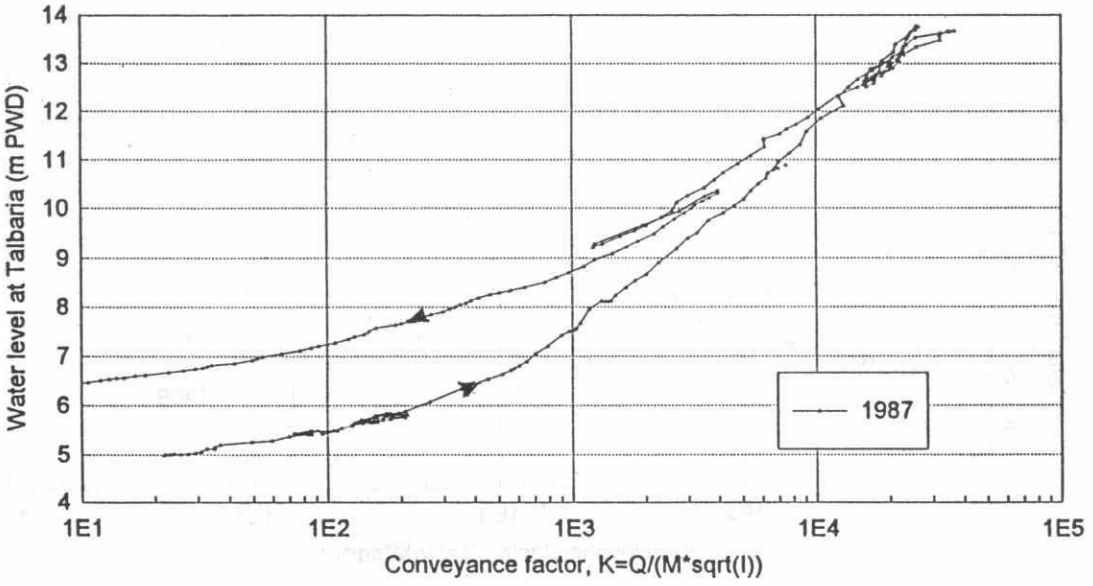


## Estimated conveyance factor
Gorai (Talbaria to Gorai Rly. Bridge)

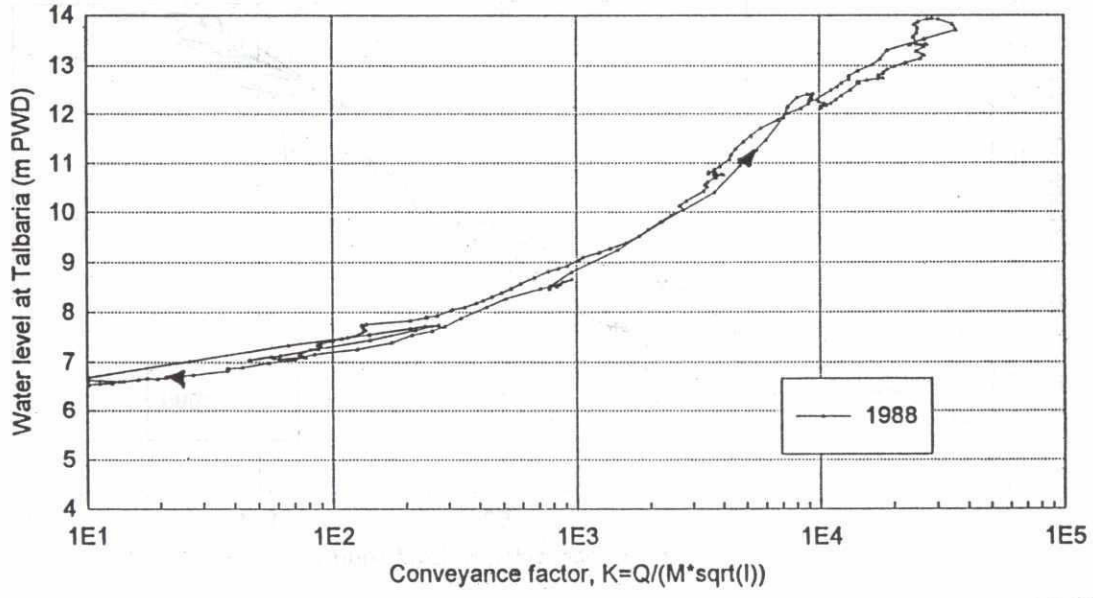

229

## Estimated conveyance factor

Gorai (Talbaria to Gorai Rly. Bridge)

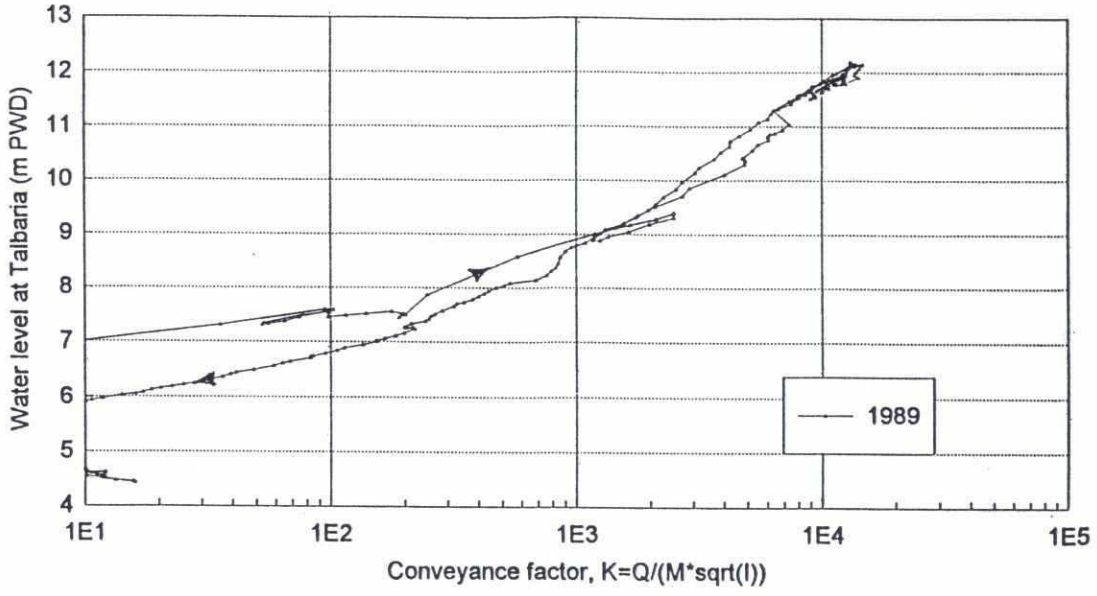


## Estimated conveyance factor

Gorai (Talbaria to Gorai Rly. Bridge)

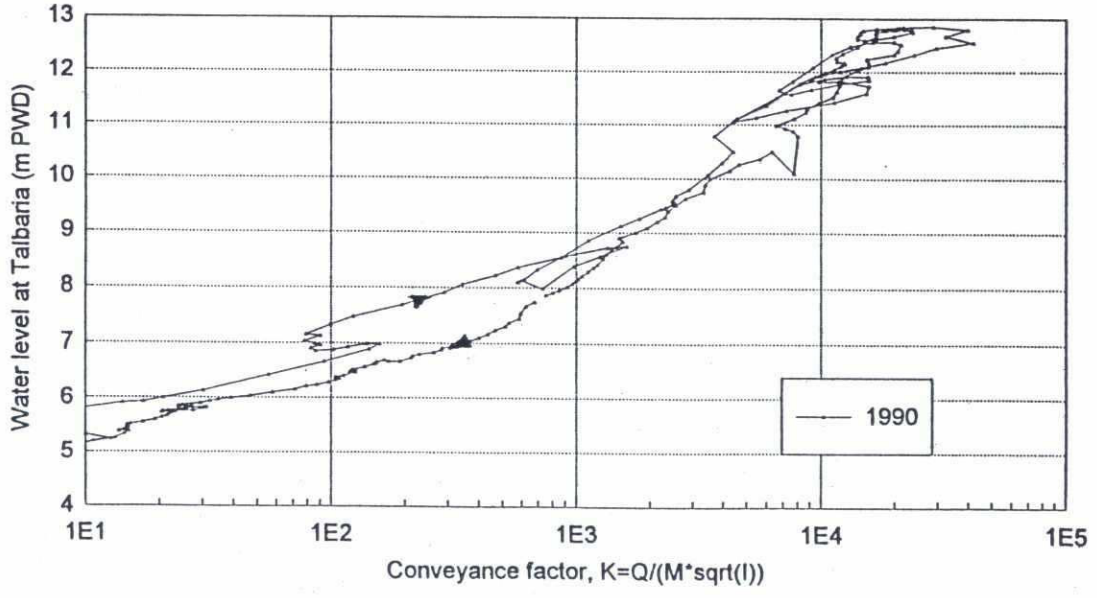

## Estimated conveyance factor
Gorai (Talbaria to Gorai Rly. Bridge)

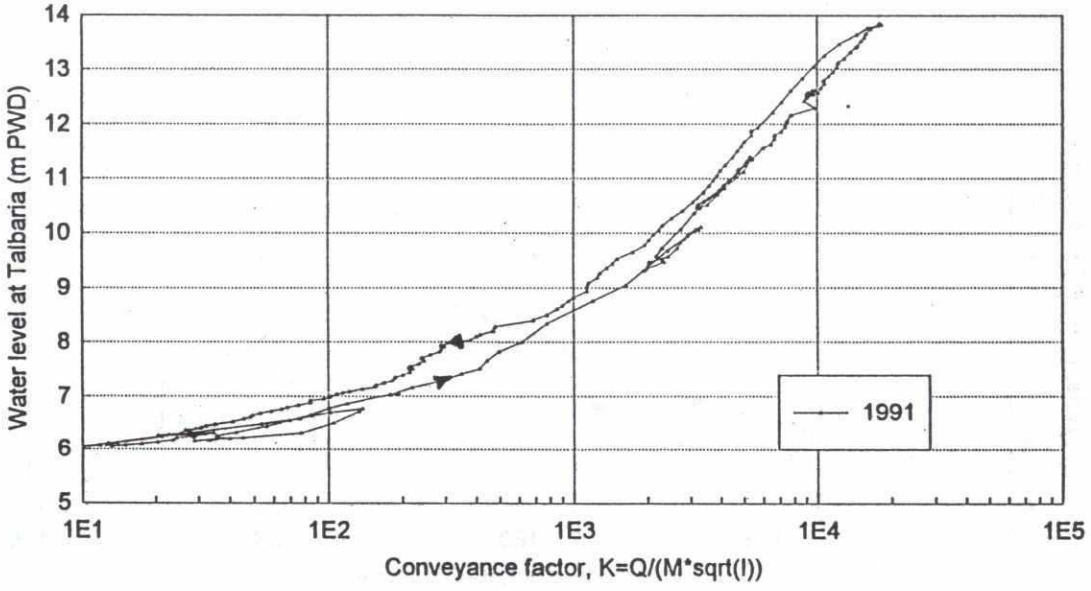


## Estimated conveyance factor
Gorai (Talbaria to Gorai Rly. Bridge)

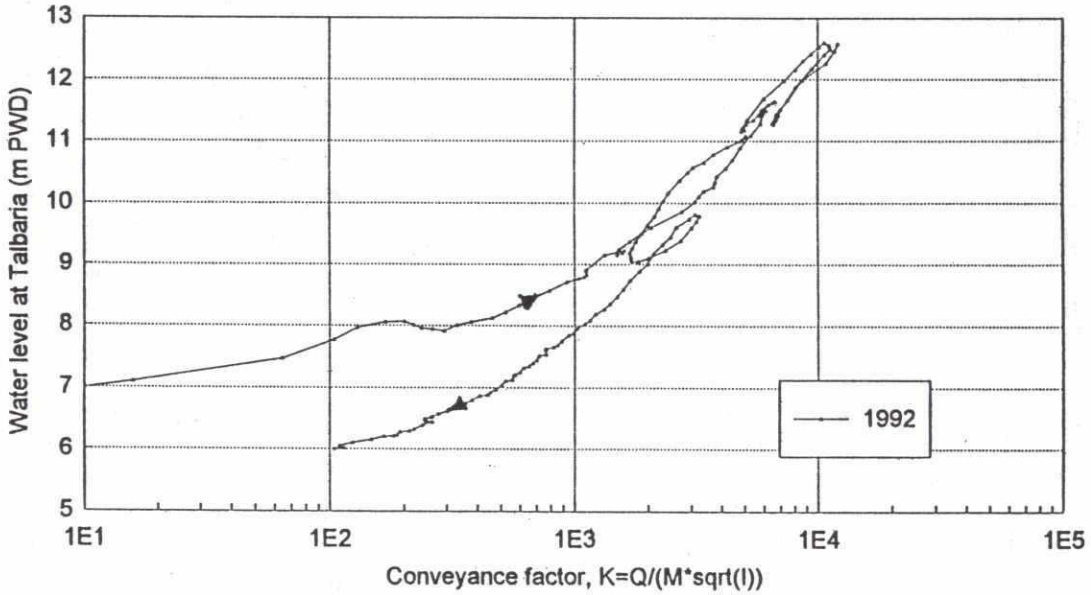

R 12

## Estimated conveyance factor

Gorai (Talbaria to Gorai Rly. Bridge)

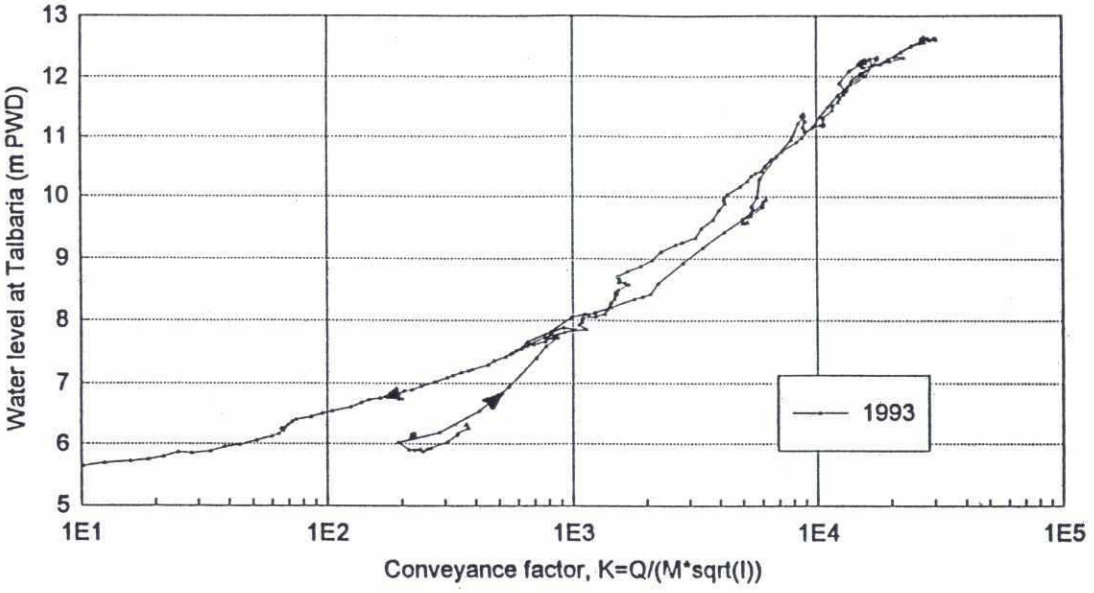


## Estimated conveyance factor

Gorai (Talbaria to Gorai Rly. Bridge)

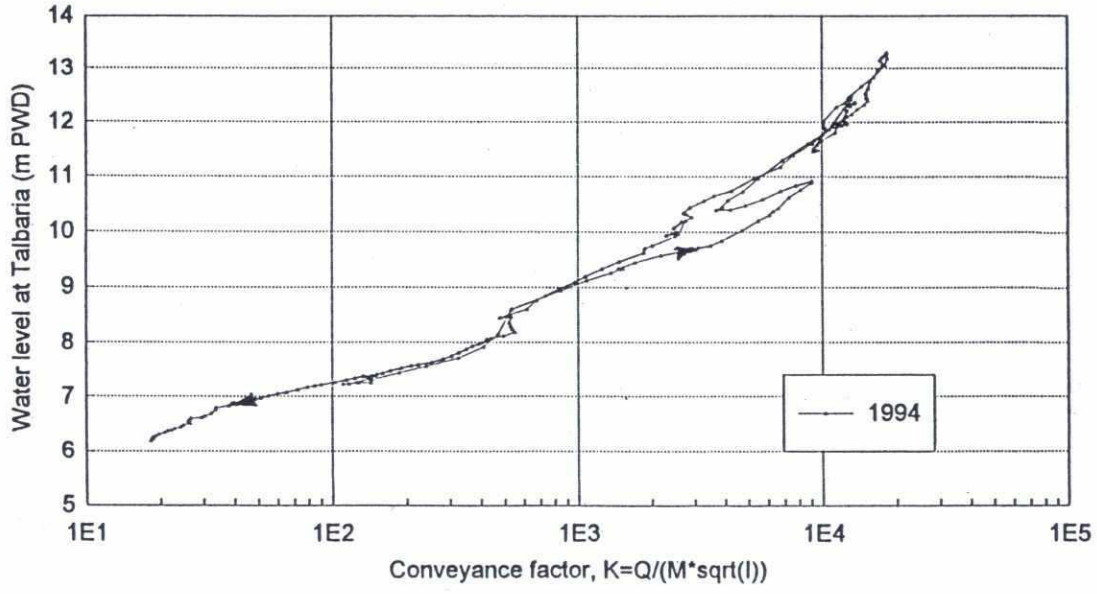

220

## Estimated conveyance factor

Gorai (Talbaria to Gorai Rly. Bridge)

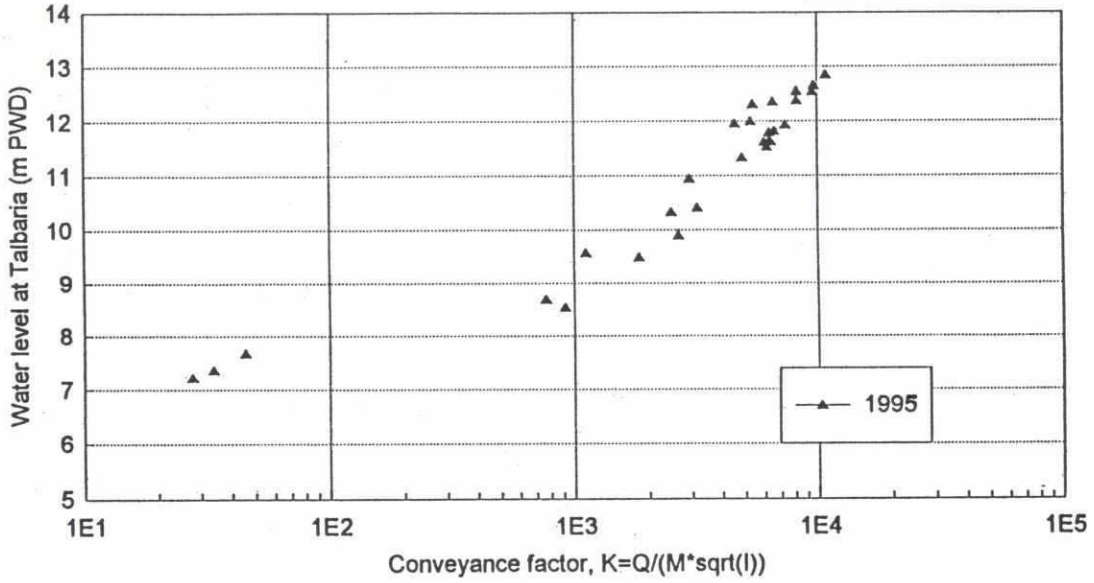

## Appendix 4: MIKE21 Curvilinear, short description

# MIKE 21-C Curvilinear

# Short Description

PRC

List of Contents

# 1. INTRODUCTION TO THE SYSTEM

MIKE 21-C is a generalized mathematical modelling system for the simulation of the hydrodynamics of, and sediment transport in vertically homogenous flows. The modelling system has the capability of utilizing both a rectangular and a curvilinear computational grid.

The modelling system, which is a part of the MIKE 21 software package from the Danish Hydraulic Institute, is composed of a number of modules relevant to sediment and morphology studies in rivers:

- a hydrodynamic model
- a sediment transport model
- a bed form/flow resistance model (small scale morphology)
- a bank erosion model
- a large scale morphological model

These features are described in general terms in the following sections.

The model components can run simultaneously, thus incorporating dynamic feedback from changing hydraulic resistance and bed topography to the hydrodynamic behaviour of the river.

For pre- and post-processing of input and output, the MIKE 21 PP-module (pre- and post-processor) from the MIKE 21 family can be used. Besides from this, special service programs has been developed to handle data in a curvilinear grid format:

- an elliptic curvilinear grid generator
- modified version of the MIKE 21 plot-programme for contour and vector plots

# 2. ELLIPTIC GRID GENERATOR

The standard version of the MIKE 21 utilizes a rectangular computational grid. This may give too poor resolution of curved water/land boundaries and thereby inaccurate flow description in the vicinity of the boundaries. In the open sea, and most estuary and coastal applications of MIKE 21, this does not give rise to significant errors, but for many river application, the poor resolution of the boundaries may have a significant impact on the overall solution.

The application of curvilinear computational grids is especially advantageous in rivers where the often curved bank lines cannot be resolved accurately in a traditional rectangular computational grid. This means that a higher overall accuracy can be

obtained with fewer computational points. In Figure 1, a river reach is discretized in a curvilinear and a rectangular grid. The discretization in the curvilinear grid utilizes 40 computational points, whereas the rectangular discretization uses 75 active (water)points. In the rectangular model, there also has to be sufficient storage in the computer memory for a number of passive (land)points, in the figure 121 points. The time step which can be applied in the curvilinear model will also be much larger, so computational efficiency improves considerably. Moreover, the discretization in the curvilinear grid will provide significantly better modelling accuracy than the rectangular model.

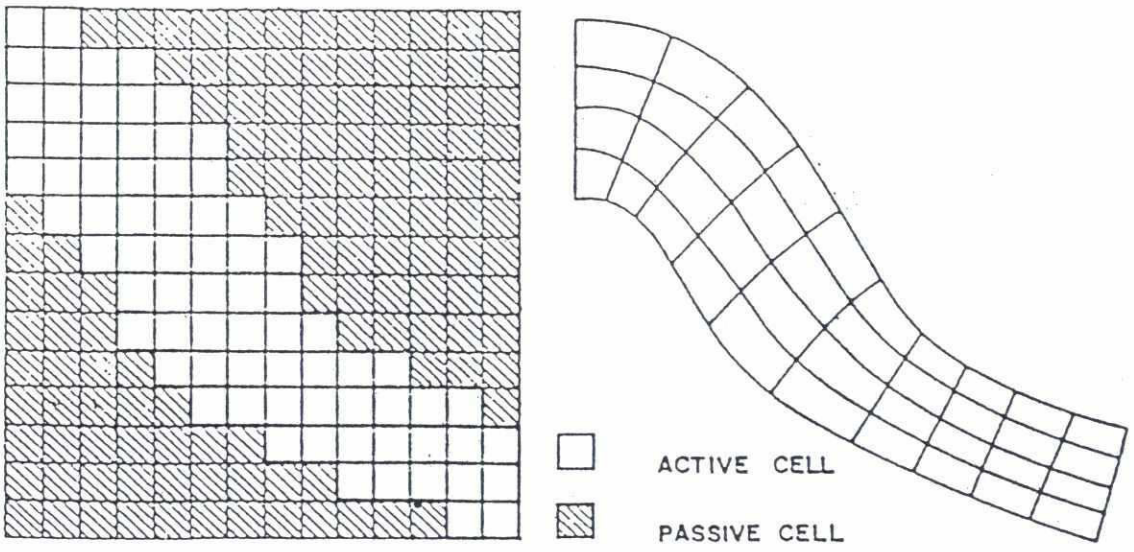


Figure 1 Schematization of river in rectangular and curvilinear grid.

MIKE 21-C requires an orthogonal curvilinear grid. This is obtained with a grid generator which solves a set of elliptic partial differential equations using an implicit alternating direction iteration solution procedure. The advantage of using an orthogonal grid is that the partial differential equations, which describe the two-dimensional flow, and hence, the finite difference approximation, become substantially simpler than if a general (non-orthogonal) curvilinear grid was applied. Thus the truncation errors will be smaller (and accuracy better) in an orthogonal grid.

The orthogonal curvilinear grid used in MIKE 21-C is obtained from the following elliptic partial differential equations:

$$\frac{\partial}{\partial s}\left[g\frac{\partial x}{\partial s}\right]+\frac{\partial}{\partial n}\left[\frac{1}{g}\frac{\partial x}{\partial n}\right]=0$$

$$\frac{\partial}{\partial s}\left[g\frac{\partial y}{\partial s}\right]+\frac{\partial}{\partial n}\left[\frac{1}{g}\frac{\partial y}{\partial n}\right]=0$$

| | | |
|---|---|---|
| where | x,y | Cartesian coordinates |
| | s,n | curvilinear coordinates (anti-clockwise system) |
| | g | "weight" function |

The weight function is a measure of the ratio between the grid cell length in the s- and the n-direction, respectively. It is defined through the following relationships:

$$g=\sqrt{\frac{g_{11}}{g_{22}}}$$

where

$$g_{11}=\frac{\partial x^2}{\partial s}+\frac{\partial y^2}{\partial s}$$

and

$$g_{22}=\frac{\partial x^2}{\partial n}+\frac{\partial y^2}{\partial n}$$

The elliptic grid equations are solved using an implicit finite difference approximation and alternating direction iteration (ADI). The input for the grid generator is the grid weights, g, in every grid point and the boundary conditions in terms of a set of (x,y) coordinates for each of four boundary lines. Figure 2 shows an example of a curvilinear grid obtained with the elliptic grid generator.

The weight function, g, can be linked to the water depth or similar hydraulic parameters in such a way that the grid line density depends on the local hydraulic conditions.

Output from the grid generator comprises the x,y coordinates of the grid line intersection points. In MIKE 21-C, these intersection point coordinates are transformed into grid increments and curvatures which are required for running the

229

core of MIKE 21-C.

Generation of an orthogonal curvilinear grid is an iterative process in which boundaries are smoothened and weight functions are adjusted until the computational grid is judged to be sound, ie. with out too large gradients in grid cell spacings and curvatures. Initial hydrodynamic simulations may still reveal the need for further refinements and adjustments of the grid. The developed graphical facility is an important tool for quick plotting of the computational grid and in assessing the quality of the generated grids.

## 3. HYDRODYNAMIC MODEL

The hydrodynamic model simulates the water level variation and flows. These are resolved on the computational grid covering the area of interest, once this has been provided with the bathymetry, bed resistance coefficients and hydrographic boundary conditions.

The hydrodynamic model has been under continous development at the Danish Hydraulic Institute since 1970. It has undergone many changes and improvements, so that it now constitutes one of the most reliable and accurate mathematical modelling tools available for the modelling of flows in two horizontal directions.

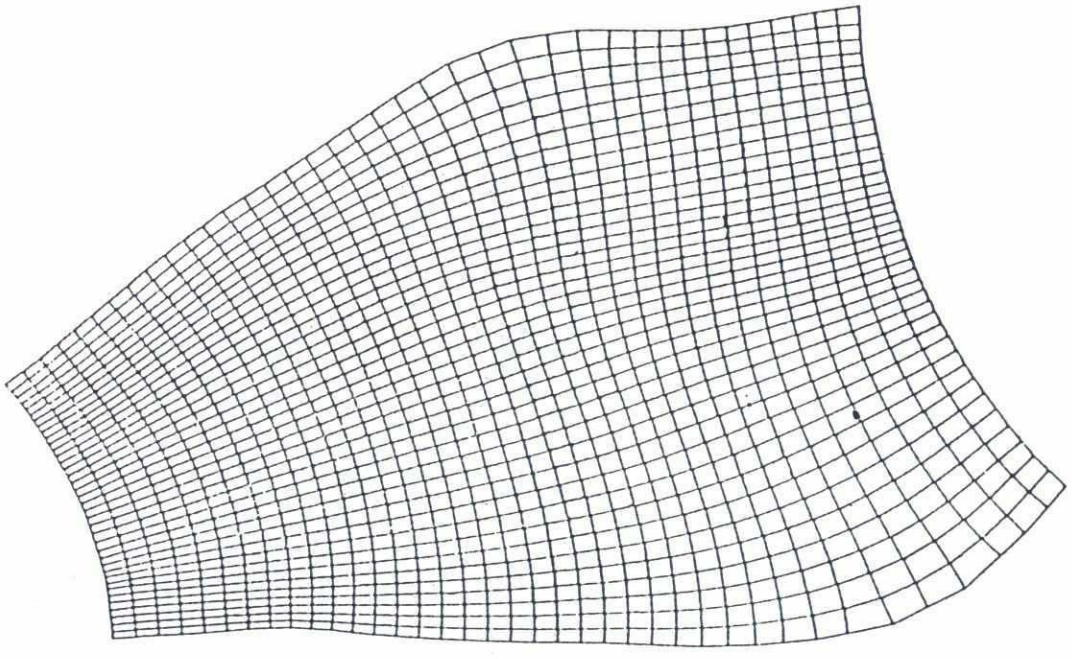

Figure 2 Example of curvilinear grid. The weight function causes the grid to be concentrated in the deeper parts (depth adaptive grid)

The hydrodynamic model solves the vertically integrated equations of continuity and conservation of momentum (the Saint Venant equations) in two directions. The following effects can be included in the equations when used for river applications:

- flow acceleration
- convective and cross-momentum
- pressure gradients (water surface slopes)
- bed shear stress
- momentum dispersion
- Coriolis forces
- wind forces
- flow curvature and helical flow

The curvature of the coordinate lines give rise to additional terms in the partial differential equations for the flow. The equations solved in MIKE 21-C are:

$$\frac{\partial p}{\partial t}+\frac{\partial}{\partial s}\left(\frac{p^2}{h}\right)+\frac{\partial}{\partial n}\left(\frac{pq}{h}\right)+2\frac{pq}{hR_n}+\frac{p^2-q^2}{hR_s}+gh\frac{\partial H}{\partial s}+\frac{g}{C^2}\frac{p\sqrt{p^2+q^2}}{h^2}=RHS$$

$$\frac{\partial q}{\partial t}+\frac{\partial}{\partial s}\left(\frac{pq}{h}\right)+\frac{\partial}{\partial n}\left(\frac{q^2}{h}\right)+2\frac{pq}{hR_s}+\frac{q^2-p^2}{hR_n}+gh\frac{\partial H}{\partial n}+\frac{g}{C^2}\frac{q\sqrt{p^2+q^2}}{h^2}=RHS$$

$$\frac{\partial H}{\partial t}+\frac{\partial p}{\partial s}+\frac{\partial q}{\partial n}-\frac{q}{R_s}+\frac{p}{R_n}=0$$

where

| | |
|---|---|
| s,n | coordinates in the curvilinear coordinate system |
| p,q | mass fluxes in the s- and n-direction, respectively |
| H | water level |
| h | water depth |
| g | gravitational acceleration |
| C | Chezy roughness coefficient |
| $R_s$, $R_n$ | radius of curvature of s- and n-line, respectively. |
| RHS | The right hand side describing a.o. Reynold stresses, Coriolis force, wind friction, atmospheric pressure (see MIKE 21 Hydrodynamic Module) |

Additional terms due to the curvilinear coordiante system also emerge when describing the Reynold stresses. The equations are solved by implicit difference techniques with the variables defined on a space staggered computational grid as shown (in a rectangular grid) in Figure 3.

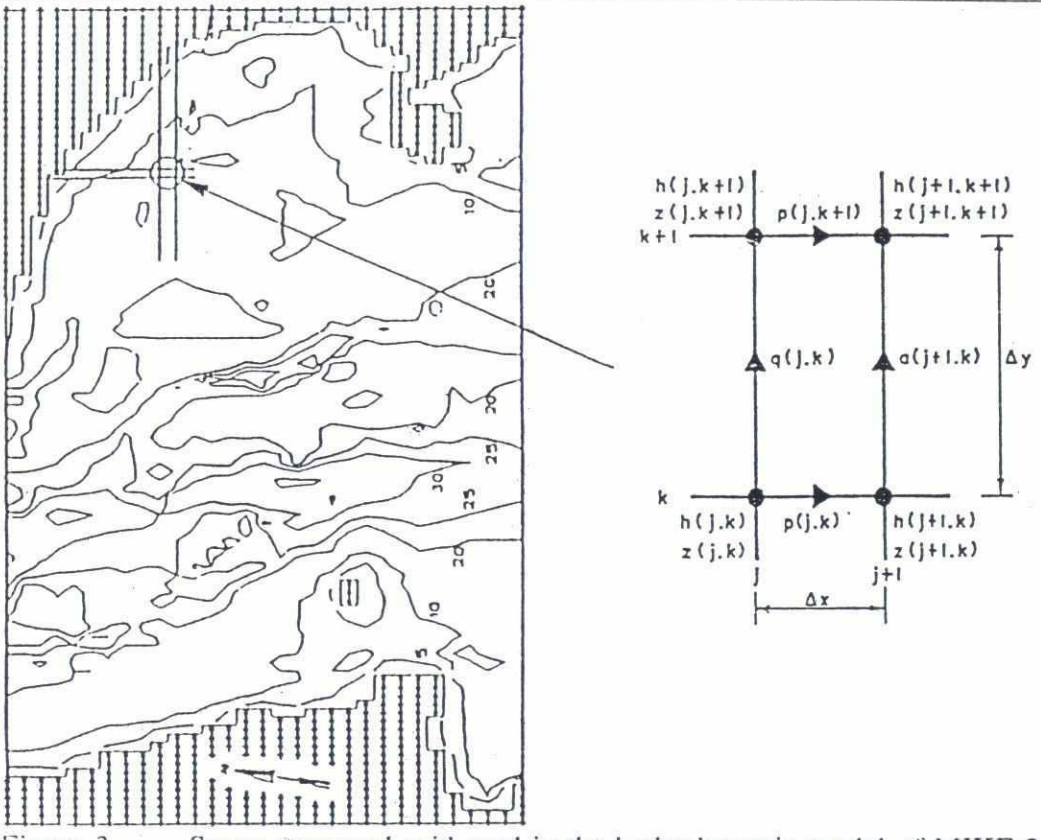


Figure 3 Space staggered grid used in the hydrodynamic model of MIKE 21-C

The setting up of a hydrodynamic river model using MIKE 21-C involves the following three steps:

(i) The extent of the modelling area is determined and the computational grid is selected for the river. If a curvilinear grid is applied, the grid generation described in the previous section is used.

(ii) The bathymetry is entered into the computational grid, ie. a representative bed level is specified in each computational grid point. Various service programmes in MIKE 21-PP performing conversions, interpolation, extrapolation, smoothening etc. are available.

(iii) The specification of the inflow hydrograph, the lateral variation of flow at the inflow boundary, and the temporal variation of water level at the downstream model boundary.

The calibration process for a hydrodynamic model developed with MIKE 21-C involves tuning of a number of calibration factors. All the calibration factors have a physical meaning and should not be arbitrarily given values outside their realistic ranges to obtain agreement with observed data.

The output from a MIKE 21-C hydrodynamic model comprises water flux and flow velocity in two directions, water depth and water surface elevation at all computational points (see Figure 3) at all time steps. In Figures 4 and 5, some computational examples are presented.

## 3.1 Helical Flow

Helical flow is a principal secondary flow phenomenon in rivers. Whilst it does not have any strong influence on the general flow pattern in rivers with large width-depth ratios, it has a significant influence on the sediment transport direction and hence the morphological changes in the river channel ( see Olesen, 1987). The helical flow is, therefore, only calculated when larger scale morphology is modelled, as distinct from the small scale bedform features. It is the cause of bend scour and plays an important role in cnfluence scour, and in char build-up and migration.

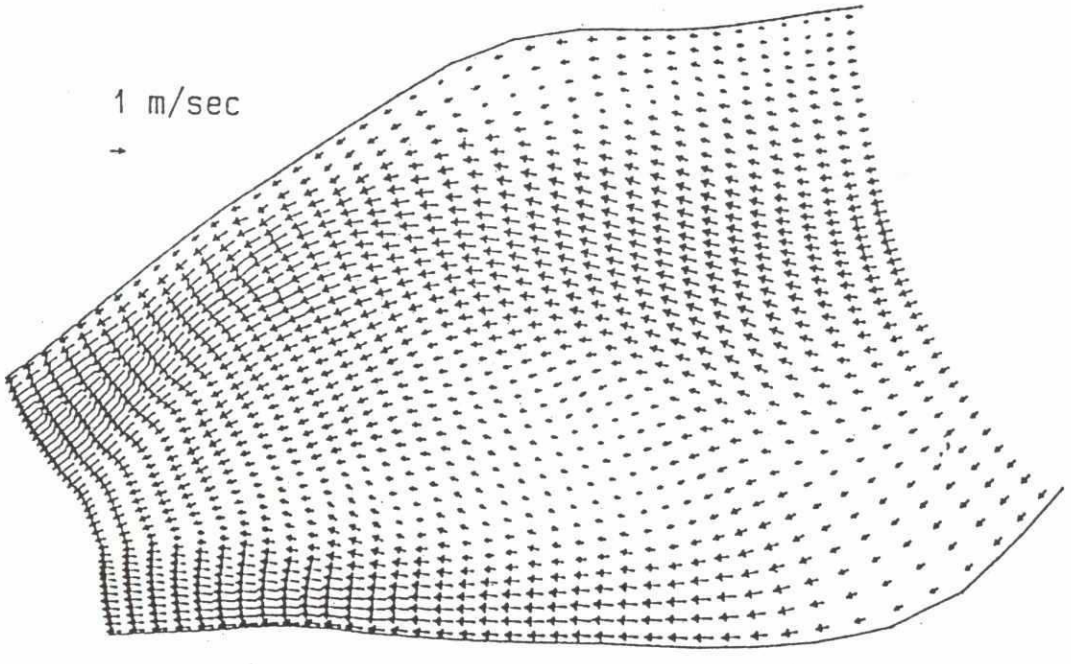


Figure 4 Simulated flow pattern in river. The compuational grid is depicted in Figure 2

The helical flows occur in curved flows, especially in river bends. It arises from the imbalance between the pressure gradient and the centripetal acceleration excerted on the water moving along a curved path. Near the river bed the helical flow is directed towards the centre of flow curvature. The magnitude of the helical flow (i.e. the transverse flow velocity component) rarely exceeds 5-10 % of the main flow velocity in natural rivers. A typical helical flow pattern is shown in Figure 6.

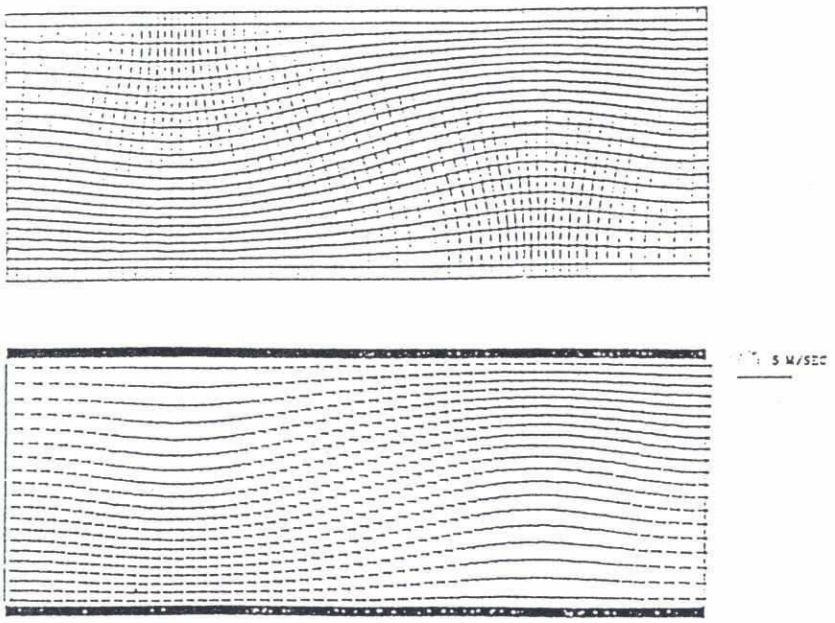


Figure 5 Curvilinear grid and simulated flow distribution in a straight rectangular channel.

Assuming a logarithmic main flow velocity distribution over the vertical and a parabolic eddy viscosity distribution, the magnitude of the secondary flow can be shown to be proportional to the main flow velocity, the depth of flow and the curvature of the main flow stream lines. In MIKE 21-C, the streamline curvature is calculated explicitly from the depth integrated flow field. The gradual adaptation of secondary (helical) flow to changing curvature is accounted for by solving a first order differential equation along the stream lines with the strength of the helical flow as the dependent variable (see also de Vriend, 1981). The strength of the helical flow is used to determine the direction of both bed and suspended load transport.

With streamlines of a constant radius $R_s$ of curvature and depth H, the helical flow

intensity can be expressed as (U is the main flow speed):

$$i_h = \chi_s \cdot U$$

where the helical flow strength was first derived by Rozowsky, 1957:

$$\chi_s = \frac{2}{\kappa^2}\left(1 - \frac{\sqrt{g}}{\kappa \cdot C}\right) \cdot \frac{H}{R_s}$$

## 4. SEDIMENT TRANSPORT

In connection with detailed (two-dimensional) mathematical modelling of sediment transport and morphology in rivers with large suspended load trasnports, it is necessary to distinguish between bed and suspended load in order to:

- simulate the dynamic development of bed form dimensions
- account for the effect of helical flow as well as the bed slope on the sediment transport direction

The relatively simple total load sediment transport formulas, such as Engelund & Hansen, 1967 and Ackers & White, 1973 can therefore not be used for river applications with MIKE 21-C without a separate specification of how the sediment is distributed between bed load and suspended load.

The sediment transport models developed by Engelund & Fredsoe, 1976, and van Rijn, 1984, which distuingish between bed and suspended load form the basis for the sediment transport description in MIKE 21-C. The specification of the sediment transport formulas is, however, very flexible. Specially developed sediment transport formulas (determined from for instance field measurements) can be specified separately for bed load and suspended load, respectively. With this flexible sediment transport formulation, it is also possible to select formulas like Engelund-Hansen, Smart-Jaeggi, and Meyer-Peter.

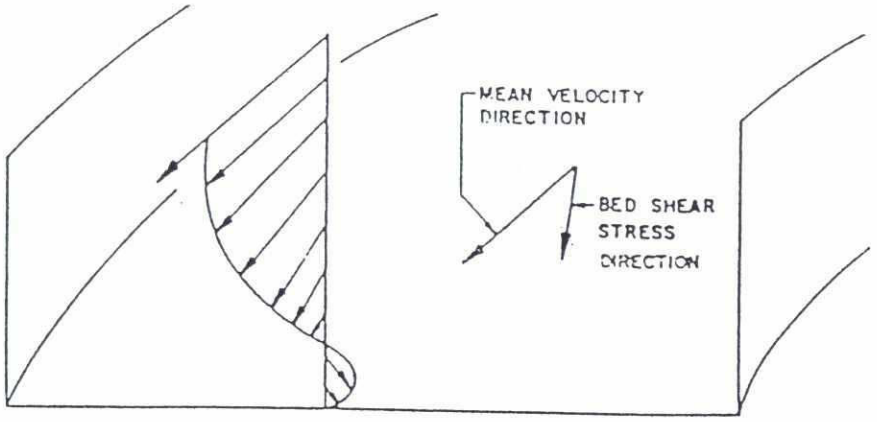


Figure 6 Helical flow in a river bend.

## 4.1 Bed Load Transport

In MIKE 21-C, the bed load transport is calculated explicitly from one of the selected formulas, eg. Engelund-Fredsoe, van Rijn, or Meyer-Peter. These formulas relate the transport rate to the bed shear stress and the grain diameter.

On a horizontal bed, the transport direction will coincide with the direction of the bed shear stress. The direction of the bed shear stress may, however, deviate from the direction of the depth-averaged flow due to the helical flow as described in section 3.1. If $\delta$ is the angle of deviation due to the helical flow and $\chi$ is the helical flow strength, the following relation exists:

$$\tan \delta = \chi$$

On sloping beds, the gravity will have influence on the transport direction as outlined in Figure 7. Several relations for the description of the effect of gravity and bed slope on the transport direction can be implemented in MIKE 21-C, in which the angle of deviation, $\alpha$, due to bed slope effects in its general form is (G and a are coefficients, I transverse bed slope, $\theta$ is non-dimensional bed shear stress):

$$\tan \alpha = G \cdot \theta^{-a} \cdot I$$

Typical values of G and a are 0.66 and 0.5, respectivily. Most of these relations have, however, only been verified against data from laboratory tests and are, therefore, not necessarily applicable to natural rivers with large suspended load transports, see also Talmon/Struiksma/van Mierlo 1995. The applicable relation is therefore often determined via calibration of the model. Corrections in the calculated bed load transport due to sloping river bed in the main flow direction is also done in

MIKE 21-C.

The output from the bed load model is the bed load transport rate and direction at every compitational grid point.

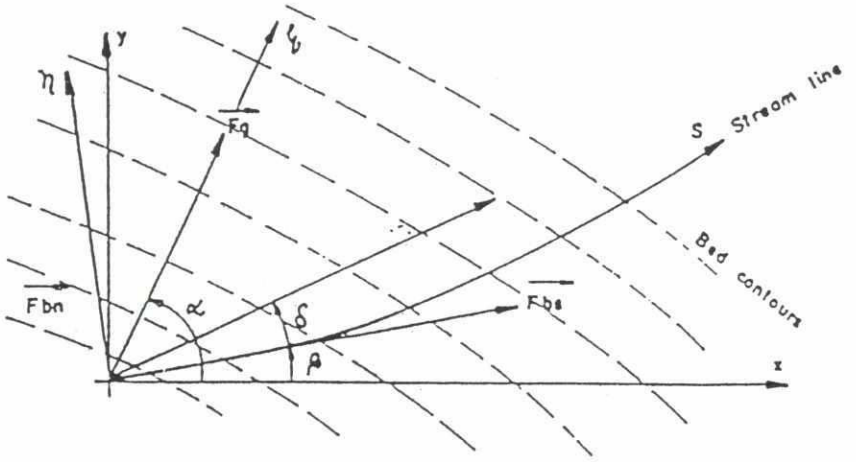


Figure 7 Shear stress on bed load sediment particles.

## 4.2 Suspended Load

Standard methods for calculation of suspended load are not appliable in the case of detailed (ie. high resolution) modelling of rivers. It is necessary to include the time-space lag in the sediment transport response to changes in local hydraulic conditions. Consider, for instance, an increase of flow velocity in a river (eg. a constriction). As flow velocity increases, the entrainment at the river bed will increase correspondingly, but it will take some time (and hence some distance) for the sediment entrained at the bottom to disperse all through the water column. This means that the actual suspended load rate is not only a function of local hydraulic conditions, as it is normally assumed in most mathematical sediment transport models, but it is also a function of what takes place upstream and earlier in time.

A relevant time scale for the time lag (T) is the settling time for a sediment grain in the water column:

$$T = h_s/w_s$$

where $h_s$ is the effective fall height (depends on the shape of the vertical concentration profile and, thus, on the fall velocity and eddy dispersion) and $w_s$ is the fall velocity.

Correspondingly, a length scale for the space lag is

$$L = T\,U$$

where U is the flow velocity. Assuming $h_s$=8 m, $w_s$=0.02 m/s, U =2 m/s, the time and length scales are 400 s and 800 m, respectively. Consequently, the space lag is important for river applications .

The space lag effect is modelled in MIKE 21-C by a depth-averaged convection-dispersion model which represents the transport and the vertical distribution of suspended solids and flow. This model is an extension of the model first developed for one dimension by Galappatti (1983) and later in two dimensions by Wang (1989). The model by Wang, however, was primarily developed for estuarine applications and did not include the effect of helical flow. This effect is essential in the case of river applications because the suspended load transport direction will be different from the main flow direction due to helical flow, as shown in Figure 7.

The secondary flow profile is computed in MIKE 21-C and used together with the primary flow profile and the concentration profile when the suspended load is integrated over the depth. As the concentration is highest near the river bed, the suspended load transport will be deflected towards the centre of flow curvature. In contrast to bed load, the transverse river bed slope does not influence the direction of suspended load transport.

The depth averaged convection-dispersion model requires an expression for the equilibrium concentration. The models by eg. Engelund & Fredsoe (1982) or van Rijn (1984) can be used for that purpose. The emperical formulas implemented in MIKE 21-C can also be used assuming that the equilibrium concentration equals the suspended load transport divided by the water flux.

The output from the suspended load model is the concentration of suspended sediment as well as the suspended load transport and direction at every computational grid point.

## 4.3 Bed Forms and Hydraulic Resistance

It is far more complex to determine the hydraulic resistance in alluvial rivers than in channels with a fixed bed. This is because a large part of the hydraulic resistance in alluvial rivers is caused by bed form drag. The bed forms have a configuration determined by the sediment transport and flow. The hydraulic resistance will therefore exhibit both temporal and spatial variations.

Generally, the hydraulic resistance is divided into that caused by drag on the bed forms (form friction) and due to shear forces on the bed (skin friction). The skin friction is relatively accurately determined from a logaritmic boundary layer equation based on the median grain size of the bed. The form friction, however, can only be determined analytically if the size of the bed forms is known.

Several hydraulic resistance predictors for alluvial rivers have been proposed, including those of Engelund-Hansen and Ackers & White. Both of these models are semi-empirical linking the hydraulic resistance to the local instantaneous flow conditions. However, there can be a significant lag between the form friction (ie. the bed form size) and the hydraulic conditions. For instance, in many tropical rivers, with distinct dry and wet periods, the sand dunes found at the river bed during the dry season have been formed during a receding flood at the end of the flood season. In such rivers, the hydraulic resistance will often be relatively larger during the dry season. It is therefore important to account for this time lag.

In MIKE 21-C, the dynamic development of the bed form size (height and length) is calculated with the model developed by Fredsoe (1979). In a subsequent step, the form friction is calculated using a Carnot type formula for expansion loss. The skin friction is determined from a logarithmic boundary layer equation. In quasi-steady flow, this model suggests that as the flow velocity increases, the dune size and hence the hydraulic resistance increases. As the flow velocity increases further, the bed form height and water depth first increase at more or less the same rate and hence the hydraulic resistance only changes slowly until the sand dunes are washed away relatively abruptly and the hydraulic resistance decreases rapidly. These features are illustrated in Figure 8.

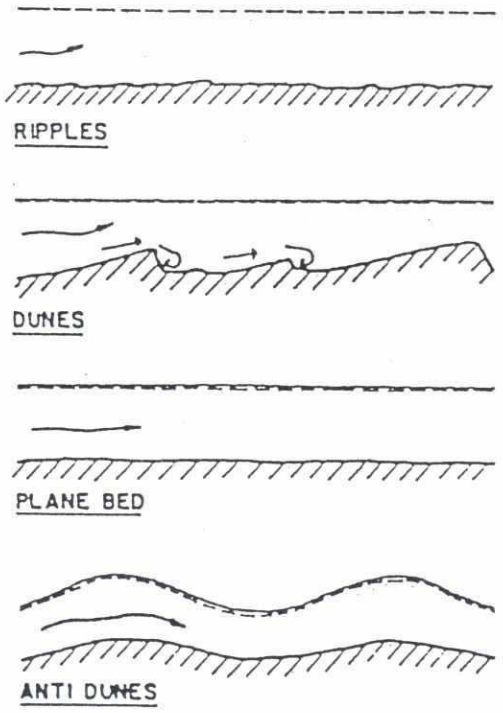


Figure 8 Development of bed forms as the flow velocity increases.

## 4.4 Large Scale Morphology

Large scale in this context means changes in the general bed level within the model boundaries as distinct from bed form changes.

The bed and suspended load sediment transport models described earlier in this section yield transport rates in two directions. The change of bed level is, therefore, easily determined by integrating the net inflow or outflow depositing or eroding within a control volume.

This integration is explicit, due to the non-linear character of the sediment transport relations applied. This implies that the large scale morphological model needs to be subjected to a rigorous stability criteria for the time step. However, a time step substantially larger than the time step in the hydrodynamic model can generally be applied.

Two kinds of boundary conditions can be specified for the morphological model: either sediment transport or specification of bed level changes in space and time at

the upstream boundary. The effect of bank erosion is included in the sediment continuity equation, ie. the eroded bank material is included as a lateral boundary condition.

The output from the large scale morphological model is the bed level and the accumulated erosion/deposition at every grid point and at every time step.

## 5. NEW DEVELOPMENTS

The present mathematical model was first developed in 1990 (System 21-Curvilinear) based on the SYSTEM 21 two-dimensional modelling system, which was created in 1970.

In the early 1990'ties, the SYSTEM 21 was modernized and a more user-friendly MIKE 21 software package was established. Following that, the System 21-Curvilinear was updated in 1995 so that the various tools in the MIKE 21 family could be utilized. In connection with this update, major changes have been and are continously being implemented in the curvilinear model.

### Bank erosion

A simple bank erosion formula relating the near bank sediment transport, transverse slope, river bed scour, and bank erosion rate has been implemented. The sediment supply from the river banks are computed and introduced directly into the equation of sediment continuity in the morphological model. Thus, simulated bank erosion in combination with simulated bend scour is usually observed as a reduction in the maximum simulated river bed scour.

Additional output from the large scale morphological model is the accumulated bank erosion at user-specified boundary grid points at every computational time step.

### Movable grid

In its present state, the computational grid is fixed in time and the curvilinear grid is only generated once prior to the model simulation.

However, when bank erosion is included, the width of the affected computational grid cells along the eroding bank, are updated after each time step. When the bank erosion is modest compared to the width of one grid cell, this is fully sufficient.

For larger bank erosion rates (more than the width of one grid cell), it becomes necessary to update the whole computational grid. A version of MIKE 21-C with fully movable grid is presently (January 1996) under development and will be ready in 1996. The main limitation of such a model is that the computational speed goes down as it has to update the grid at every timestep (or at selected time intervals).

Graded Sediment

The MIKE 21-C is now capable of simulating several fractions of sediment, each with a characteristic grain size. Each grain fraction is simulated separately with due consideration to the interaction between the various grain components at the river bed (shielding, armouring). With this model, it is possible to simulate the sorting im space and time of graded sediment which is essential in many river applications.

If the suspended sediment transport is negligible compared to the bed load transport, the suspended sediment model can be switched off, so only a bed load model (or a total load model) is employed.

Cohesive Sediment

Cohesive sediments have different physical properties than non-cohesive sediment. For cohesive sediment, it is not possible to specify explicitly the sediment transport as a function of local hydraulic conditions. In that sense, the cohesive sediment can be interpreted as suspended load transport as modelled in MIKE 21-C with very large time and space lag. Special erosion and deposition functions for cohesive sediment have been implemented in the MIKE 21-C.

## 6. MODEL VERIFICATION

The MIKE 21-C is specially designed for modelling of river morphology. Therefore, it must be able to simulate the development of bend scour, which is one of the main features of meandering rivers.

By testing against physical scale modelling results, it is possible to follow the development from a flat, horizontal river bed. At Delft University of Technology, an extensive number of mobile bed model tests with a curved laboratory flume has been carried out. The results obtained by Talmon, 1992, have been used for verification of the performance of MIKE 21-C.

The u-shaped flume is shown in Figure 9. The width of the flume is 0.50 m. The inflow section (which is straight) has a length of 11 m, the arc length of the bend is 12.9 m, and the radius of curvature of the centre line along the curved section is 4.1 m. The inflow at the upper boundary is constant (5.7 l/s), the average longitudinal slope is 0.0034, the mean depth is 0.048 m, the mean velocity is 0.24 m/s, and the median grain size of the sand in the flume bottom is 0.088 mm.

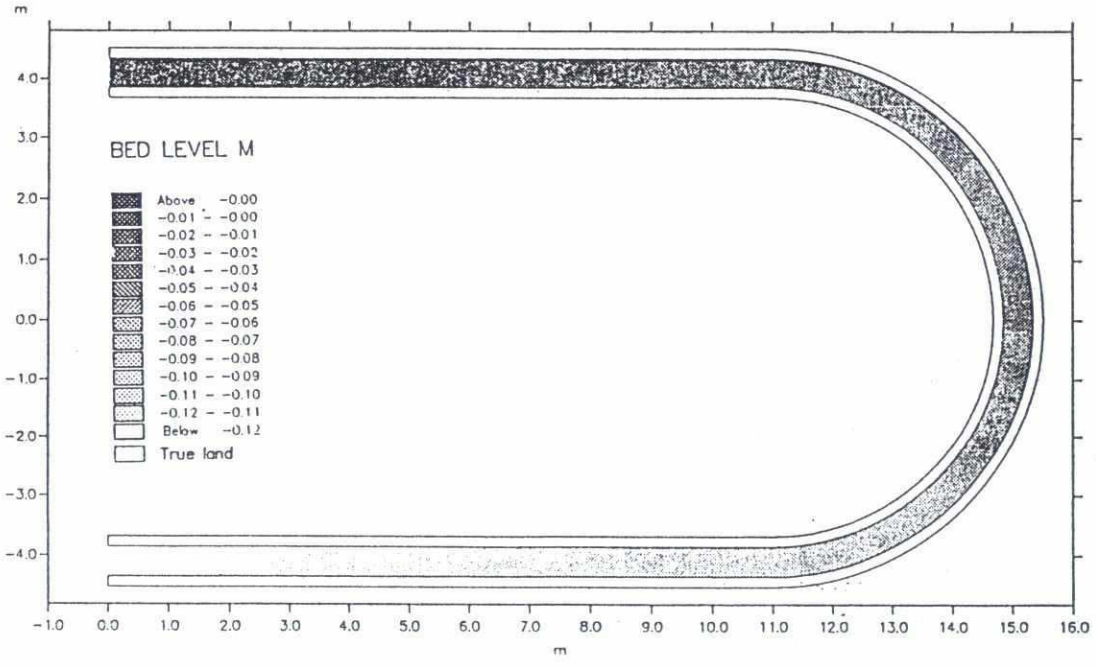


Figure 9 Layout of the laboratory flume as specified in the mathematical MIKE 21-C model. The initial model bathymetry is shown.

After about 200 hours, steady conditions prevail in the physical flume tests. A similar period was simulated with the mathematical MIKE 21-C model. The final equilibrium bathymetry after 200 hours is shown in Figure 10.

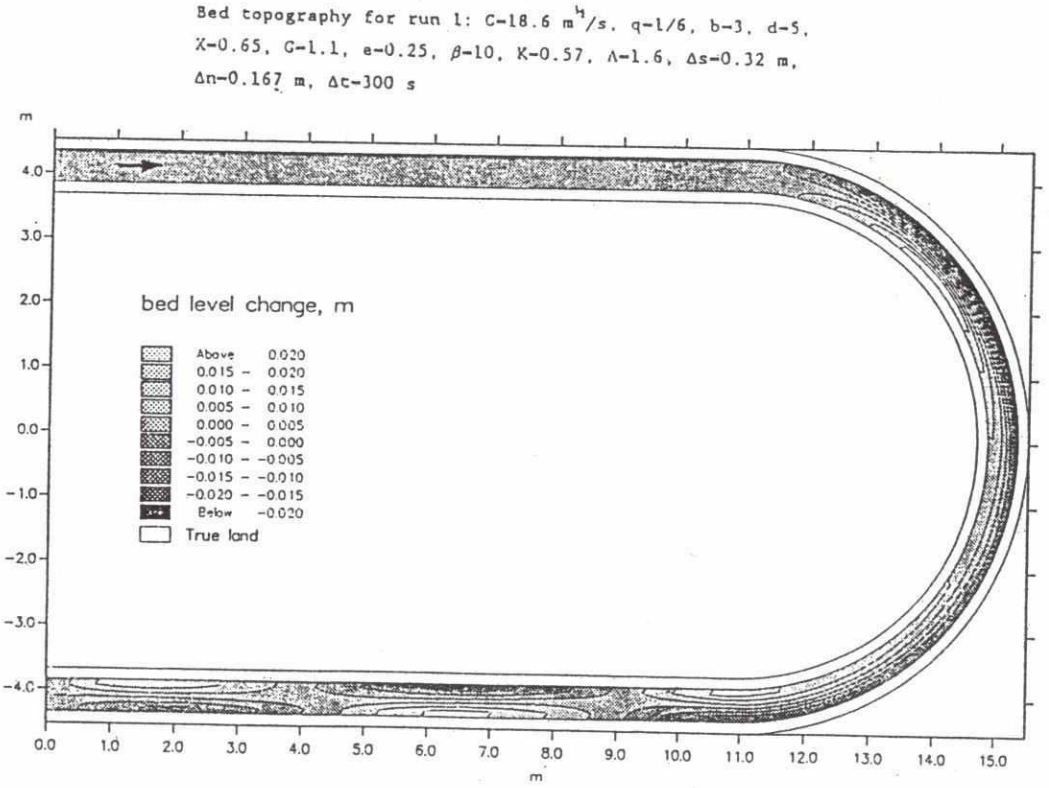


Figure 10 The equilibrium model bathymetry as predicted by the mathematical MIKE 21-C model after 200 hours.

The simulated development of bend scour is clearly seen from Figure 10: Erosion has taken place along the outer bank, and deposition at the inner bank. In the straight reach downstream the curved section, shifting point bars have developed due to the abrupt change in flow (and bank line) curvature.

The observed bed level changes in the physical model test are displayed as longitudinal profiles along the centre line of the flume, along the right (inner) bank and along the left (outer) bank, respectively, in Figure 11. The results obtained by a mathematical model developed at Delft University of Technology (Talmon,1992) are also depicted on this figure (denoted 'computed').

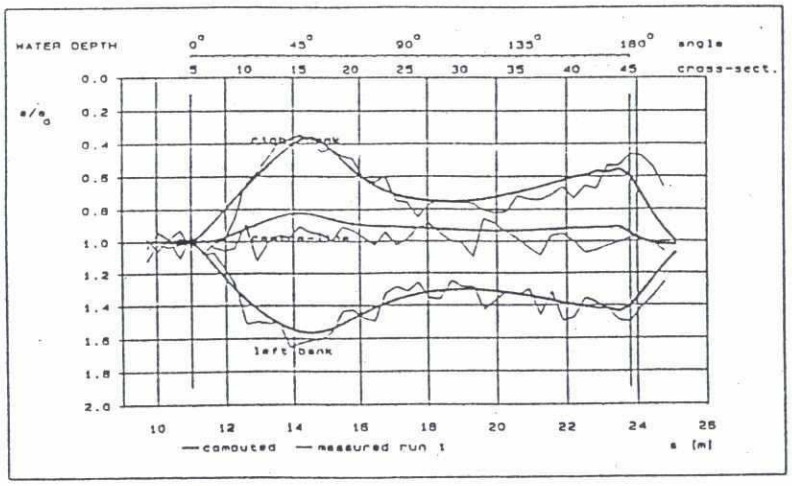


Figure 11 The equilibrium bathymetry as observed in the physical model flume. The relative water depth (actual waterdepth divided by mean water depth) is shown. From Talmon (1992).

The over-shooting phenomenon in bed levels along river bends is very clearly seen from the measurements. The same is simulated with the MIKE 21-C, see Figure 12. This figure shows the development of the mathematical model bathymetry at different times: initial, after 66 hours, after 133 hours, and after 200 hours. The bed profile is seen to be stable after 200 hours. The magnitude of the bed level change is similar to the observed bed level change from the laboratory flume (see Figure 11). Finally, the bed level fluctuations (point bars) downstream of the river bend demonstrate the limited damping in the mathematical model. Unfortunately, the measurements from the physical model do not cover this part.

From the comparison between the laboratory flume results and the mathematical modelling results, it can be concluded that the MIKE 21-C is capable of reproducing the equilibrium river bend scour as well as the dynamic development to its mature state.

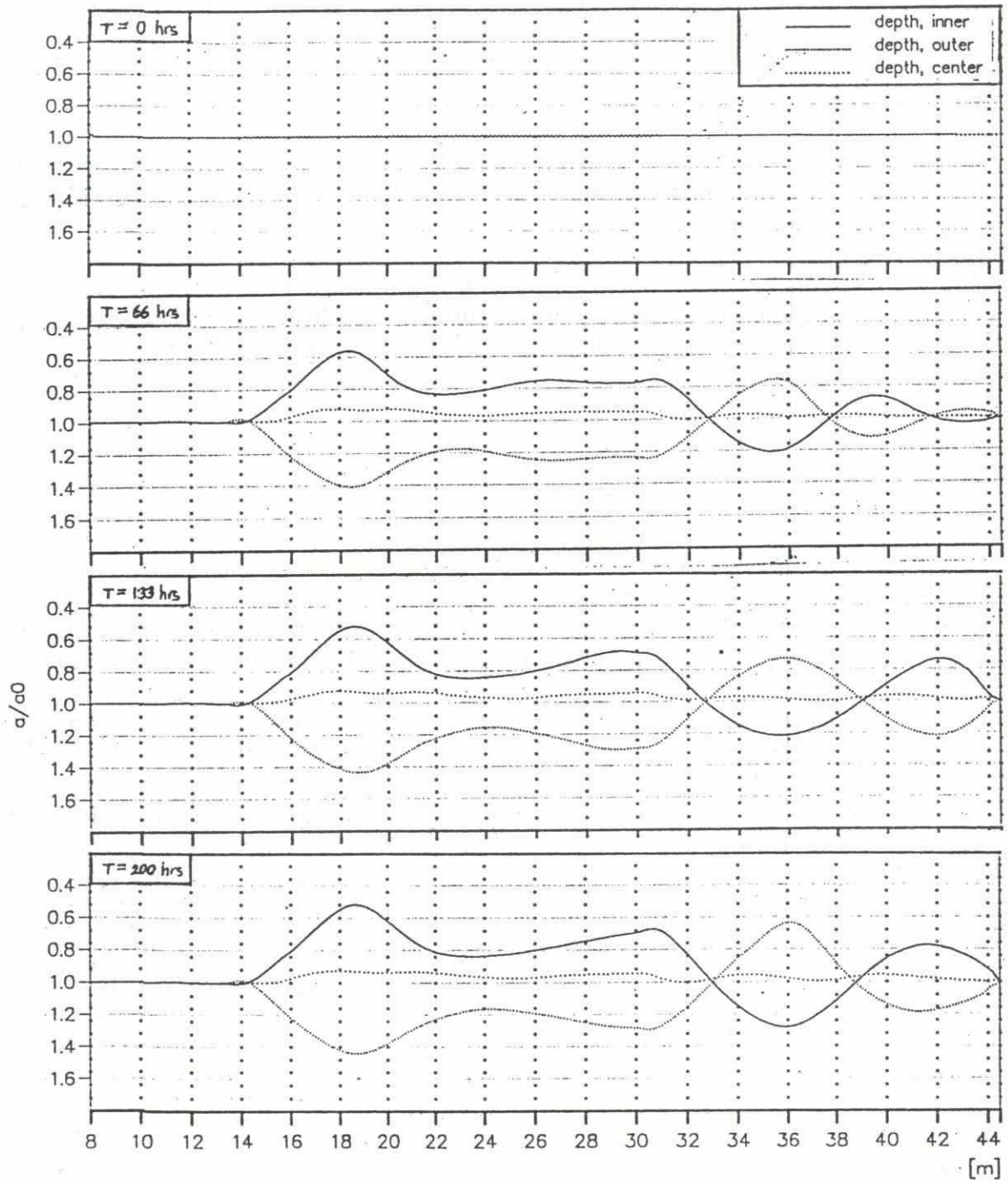


Figure 12 The model bathymetry simulated with MIKE 21-C at different times. The relative water depth (actual waterdepth divided by mean water depth) is shown.

## 6. EXAMPLES OF APPLICATIONS

Sandy, Meandering Rivers

1. Karnafuli River, Mathematical Model Study of Pussur-Sibsa River System and Karnafuli River River Entrance, Client: Government of Bangladesh, Ministry of Shipping, 1990

2. Saripul, Bridge Improvement and Maintenance Project, Phase II, Client: Government of Bangladesh;Consultants: O'Sullivan & Graham, Henry Boot Training, NRSC, Dvelopment Design Consultants, Bangladesh, 1996

Gravel, Braided Rivers

3. River Negro, Argentina, 1995

Sandy, Braided Rivers

4. Brahmaputra, BRTS Brahmaputra River Training Studies, FAP 1, Client: Government of Bangladesh, Bangladesh Water Development Board, 1991

5. Ganges/Gorai Offtake, River Survey Project, FAP 24, Client: Government of Bangladesh, Flood Plan Coordination Organization, 1995

6. Jamuna (Brahmaputra), Mathematical Modelling of Jamuna Bridge Site, Client: Government of Bangladesh, Jamuna Multipurpose Bridge Authority, 1995

## References


/1/ Ackers, P. and Whit, W.R., 1973,"Sediment Transport: New approach and analysis", Proc. ASCE, JHD, 99, HY11 pp. 2041-2060

/2/ Engelund, F. and Fredsoe, J., 1982,"Hydraulic theory of alluvial rivers", Advances in Hydro Science. Vol.13. pp.187-215

/3/ Engelund, F. and Hansen, E./1967,"A monograph on sediment transport in alluvial streams", Teknisk Forlag, Copenhagen

/4/ Fredsoe, J., 1979,"Unsteady flow in straight alluvial streams; modifications of individual dunes", J. Fluid Mech.,Vol. 91, pp 497-512

/5/ Galappatti, R., 1983, "A depth integrated model for suspended load", Communications on Hydraulics 83-7, Dept. Civil Eng. Delft Univ. Tech, The Netherlands

/6/ Olesen, K.W., 1987,"Bed topography in shallow river bends", Faculty of Civil Eng., Delft Univ Tech., Report 87-1

/7/ Ribberink, J.S.,1987,"Mathematical modelling of one-dimensional morphological changes in rivers with non-uniform sediment"

/8/ Rijn, van L.C.,1984a,"Part I: Bed load transport", J. Hydraulic Eng 110, 10, October

/9/ Rijn, van L.C.,1984a,"Part II: Suspended load transport", J. Hyd.Eng, 110, 11, November

/10/ Talmon, A.M.; Struiksma, N.; van Mierlo, M.C.L.M.; "Laboratory Measurements of the Direction of Sediment Transport on Transverse Alluvial-bed Slopes", Journ. of Hydraulic Res., Vol 33, 1995, no.4

/11/ Talmon, A.M.,1992,"Bed topography of river bends with suspended sediment transport", Faculty of Civil Eng., Delft Univ. Tech., Report 92-5

/12/ Vriend, J.J. de, 1981, "Steady flow in shallow river bends", Comm. on Hydraulics 81-3, Dept. Civil Eng..Delft Univ. Tech., The Netherlands

/13/ Wang, Z.B., 1989, "Mathematical Modelling of morphological processes in estuaries", Report No. 89-1, Faculty of Eng.,Delft Univ. Tech., The Netherlands

## Appendix 5: Computer animation of mathematical modelling results

284

## Computer animation of mathematical modelling results

### Introduction

By displaying a sequence of horizontal planplots quickly one after another on a monitor, it is possible to make an animation of the model simulations.

A floppy diskette with animations of the simulated bed levels (in m above PWD) is attached to this report. The contour lines extent from –5 m to +11 m PWD with 4 m interval.

### Users Guide

1 Create a directory on a PC (at least 386, colour monitor) called C:\video

2 Copy the content of the floppy diskette to this directory
copy a:*.* C;\video <return>

3 Start the animation with the following command
video <return>

4 Choose one of the animations in the menu and press <return>. A brief explanation appears. To see the actual animation, press <return> once again.

5 To stop again press <esc>. After 10 repeated loops, the animation will also stop by itself.

### Options

The animation can be started directly by giving the command
v12play [options] 'filename' <return>

where 'filename' is the name of the animation. This way to start the animation may be necessary if your computer does not have a numerical co–processor.

The options are (see also by v12play <return>:

| | | | |
|---|---|---|---|
| -m | memory | : | Allocate mem bytes for picture storage |
| -t | ticks | : | Time between each picture (in 18.6 Hz units) |
| -l | loops | : | Number of times the animation is played |
| -i | video | : | Alternative way to give video file name |
| -c | 1/0 | : | Clear screen after each loop |

During execution:

| | | |
|---|---|---|
| s | : | Toggles between automatic and single step mode |
| spacebar | : | Displays next picture when in single step mode |
| d | : | Dump screen as PCX file |
| ESC | : | Exit |